THEORIES AND COMPUTATION OF SECOND VIRIAL COEFFICIENTS OF ELECTROMAGNETIC PHENOMENA

BY

JEANETTE HOHLS BSC(HONS)(NATAL) MSC(NATAL)

Preface

The work reported in this thesis was carried out in the Department of Physics, University of Natal, Pietermaritzburg, under the supervision of Professor C Graham between January 1993 and April 1997.

I declare this work to be the result of my own research. Where results due to other authors have been used, this is indicated by explicit citations in the text. This thesis has not been submitted in any form for any degree or examination to any other University.

Signed .... on this ...20th... day

of ...March... , 1998.

Acknowledgements

I would like to extend my deepest appreciation and gratitude to all those who have helped and encouraged me during the course of this work. I would especially like to thank the following people:

my supervisor, Professor Clive Graham, for his guidance during this project and for his supervision and critism of this thesis;

my friend and colleague, Dr Vincent Couling, for the helpful discussions about physics, literature and other interesting topics;

Mr Karl Penzhorn, for his assistance with all my computer problems;

Mrs Sandy Diedrichs, for her encouragement and support;

Professor Linda Haines, for her help and advice on using LaTeX 2_ε to typeset this thesis;

the members of the Physics department for their willingness to help when necessary;

the Foundation for Research and Development for a three year Doctoral Bursary;

my family, for their unconditional love and support; and above all

my husband, Trevor, for his tireless patience, interest, support and encouragement, without which I would never have been able to complete this work.

Abstract

Many bulk properties of gases depend linearly on the gas density at lower densities, but as the density increases departures from linearity are observed. The density dependence of a bulk property Q may often be discussed systematically by expanding Q as a power series in $1/V_m$, to yield

$$Q = A_Q + \frac{B_Q}{V_m} + \frac{C_Q}{V_m^2} + \cdots ,$$

where B_Q is known as the second virial coefficient of the property Q. A_Q is the ideal gas value of Q, and B_Q describes the contribution of molecular pair interactions to Q. Theories of Q may be regarded as having two main components, one describing how the presence of a neighbour of a given molecule can enhance or detract from its contribution to Q, and the other the molecular interaction energy which determines the average geometry of a pair encounter. The latter component is common to all theories, and the former requires detailed derivations for each specific bulk property Q. In this work we consider the second virial coefficients of five effects, namely the second pressure virial coefficient $B(T)$, and also the second dielectric, refractivity, Kerr-effect and light-scattering virial coefficients, B_ε, B_R, B_K and B_ρ, respectively. Using a powerful computer algebraic manipulation package we have extended the existing dipole-induced-dipole (DID) theories of the second dielectric, refractivity and Kerr-effect virial coefficients to sufficiently high order to establish convergence in the treatment of both linear and non-linear gases. Together with the established linear theory of the second pressure virial coefficient, the extended theory of the second light-scattering virial coefficient developed by Couling and Graham, and their new non-linear theory of the second pressure and light-scattering virial coefficients, our new theories provide a comprehensive base from which to calculate numerical values for the various effects for comparison with experiment. We have collected as much experimental data of the various second virial coefficients as possible, for a wide range of gases. The ten gases chosen for detailed study comprise a selection of polar and non-polar, linear and non-linear gases: the linear polar gases fluoromethane, trifluoromethane, chloromethane and hydrogen chloride; the non-polar linear gases nitrogen, carbon dioxide and ethane; the non-linear polar gases sulphur dioxide and dimethyl

ether; and the non-linear non-polar gas ethene. Using the best available measured or calculated molecular parameter data for these gases, together with the complete theories for the second virial coefficients, we have attempted to find unique sets of molecular parameters for each gas which explain all the available experimental data. In general, reliable measured or calculated molecular properties are regarded as fixed, and only the Lennard-Jones and shape parameters in the molecular interaction energy are treated as best-fit parameters within the constraints of being physically reasonable.

Many of the apparent failures of second virial coefficient theories have been due to the lack of convergence in the series of terms evaluated. It is essential to work to sufficiently high orders in the polarizabilities and various multipole moments to ensure convergence for meaningful comparison with experiment. This often requires the manipulation of extremely long and complicated expressions, not possible by the manual methods of our recent past. The advent of computer manipulation packages and fast processors for numerical integration have now enabled calculation to high orders, where the degree of convergence can be sensibly followed.

Our efforts to describe all of the effects for which data is available met with mixed success. For four of the gases, fluoromethane, chloromethane, dimethyl ether and ethene, a unique parameter set was found for each which described all of the available effects reasonably well. For the three gases, trifluoromethane, nitrogen and sulphur dioxide, one interaction parameter set explained all but one of the effects for which data was available to within experimental uncertainty. For trifluoromethane the parameter set which yielded good agreement for $B(T)$, B_ε and B_K could not explain the observed values of B_R, while for nitrogen one parameter set produced reasonable agreement for all of the effects except B_ρ and a different set, which yielded good agreement for B_ρ, did not explain the remaining four effects as well as the first set. The parameter set which explained $B(T)$, B_K and B_ρ very well for sulphur dioxide, yielded a value for B_ε which was much larger than the experimental value, although of the correct sign and order of magnitude. Hydrogen chloride posed a special problem as data was only available for two of the effects, $B(T)$ and B_ε. It was possible to find a set of interaction parameters in good agreement with the measured values of $B(T)$, but the experimental data for B_ε was an order of magnitude larger than the largest calculated values. Since the remaining effects have not been measured for this gas it was not possible to test the theory more rigorously. For the remaining gases carbon dioxide and ethane, it was impossible, based on the existing measured values, to select a unique parameter set which explained all of the effects. In many of the cases where definite conclusions could not be drawn, it was not possible to decide whether the disagreement between theory and experiment was due to the large scatter and uncertainty of the experimental data or failure of the theory. However, there were very few instances of complete failure of the theory to explain

experiment, and no one effect showed consistent disagreement, so that in general it may be said that the mechanisms of the second virial coefficients under study are reasonably well understood. It would require more precise measurements of the various effects, as well as more measured or calculated molecular property tensor components, such as the hyperpolarizability and the A- and C-tensors, to test the DID molecular interaction model more stringently.

Contents

List of Tables

xv

List of Figures

Chapter 1

Introduction and Overview

1.1 Second Virial Coefficients

There exists a range of electromagnetic phenomena in gases for which one expects proportionality of the macroscopic observables with the number density of the molecules. This proportionality is exact in a perfect gas, where each molecule is independent of its neighbours.

However, the molecules in a real gas collide and interact with their neighbours, resulting in non-linear density dependence of the bulk properties of the gas. As the density of a gas approaches zero, the bulk properties tend toward ideal gas behaviour. Studies of the deviations in behaviour of real gases from the ideal provide a source of information about the interactions between molecules.

The effects of these interactions can be accounted for with a virial expansion of the relevant macroscopic observable. If Q is a suitably chosen measurable property its observed value may be expanded in terms of the inverse power of V_m, the molar volume, to give [27]

$$Q = A_Q + \frac{B_Q}{V_m} + \frac{C_Q}{V_m^2} + \cdots,$$

(1.1)

where A_Q, B_Q, C_Q, ... are the first, second, third, ... virial coefficients, respectively, and are independent of density. In the limit of infinite dilution ($V_m \to \infty$), when the gas becomes an assembly of independent molecules, Q is equal to A_Q, the ideal gas value. B_Q, C_Q, ... represent the deviations due to pair, triplet, ... interactions respectively.

In a sample of gas containing one mole of non-interacting gas molecules, each molecule contributes an average $\bar{q}$ to the observable Q, so that

$$Q = A_Q = N_A \bar{q}.$$

(1.2)

where N_A is Avagadro's number. However, at higher densities, when the molecules interact with one another, molecule 1 may not always contribute $\bar{q}$ to Q because for some of the time molecule 1 is part of an interacting pair. If τ is the configuration of molecule 2 relative to molecule 1, then at that instant molecule 1 contributes $\frac{1}{2}q_{12}(\tau)$ to Q, where $q_{12}(\tau)$ is the corresponding contribution of the pair. If triplet and higher-order interactions are neglected and $P(\tau)d\tau$ is the probability that molecule 1 has a neighbour in the range $(\tau, \tau + d\tau)$, then [27]

$$Q = N_A \left\{ \bar{q} + \int \left[\frac{1}{2}q_{12}(\tau) - \bar{q} \right] P(\tau)d\tau \right\}. \tag{1.3}$$

$P(\tau)$ is related to the intermolecular potential U_{12} by

$$P(\tau) = \frac{N_A}{\Omega V_m} e^{-\frac{U_{12}(\tau)}{kT}}, \tag{1.4}$$

where $\Omega = \frac{1}{V_m} \int d\tau$ is the integral over the orientational coordinates of the neighbouring molecule, k is Boltzmann's constant and T is the temperature in Kelvin. Now, from equation (1.1)

$$B_Q = \lim_{V_m \to \infty} (Q - A_Q)V_m, \tag{1.5}$$

which, when combined with equations (1.2), (1.3) and (1.4), gives the general expression

$$B_Q = \frac{N_A^2}{\Omega} \int \left[\frac{1}{2}q_{12}(\tau) - \bar{q} \right] e^{-\frac{U_{12}(\tau)}{kT}} d\tau. \tag{1.6}$$

This basic formula can be used to determine the second virial coefficients of various electromagnetic molecular properties, Q.

Several properties of gases have been treated in this way. The pressure-volume-temperature (P-V-T) behaviour of a gas may be described by the virial equation of state [1]:

$$\frac{PV_m}{RT} = 1 + \frac{B(T)}{V_m} + \frac{C(T)}{V_m^2} + \cdots, \tag{1.7}$$

where B, C, ... are called the second, third, ... virial coefficients, or pressure virial coefficients, and are functions of temperature and the nature of the gas. The second pressure virial coefficient $B(T)$ describes the initial deviation from the ideal gas law due to pair interactions in a real gas [1].

2

The total polarization of a gas, or the Clausius-Mossotti function, may be written as a virial expansion [28]:

$$_T P = \frac{\varepsilon_r - 1}{\varepsilon_r + 2} V_m = A_\varepsilon + \frac{B_\varepsilon}{V_m} + \frac{C_\varepsilon}{V_m^2} + \cdots,$$ (1.8)

where ε_r is the static dielectric constant of the gas, and A_ε, B_ε and C_ε are the first, second and third dielectric virial coefficients, respectively. These coefficients are functions of the temperature of the gas.

The density-dependent deviations from the Lorentz-Lorenz equation [29, 30],

$$\frac{n^2 - 1}{n^2 + 2} V_m = \frac{N_A \alpha_0}{3\varepsilon_0},$$ (1.9)

relating the mean polarizability α_0 of an isolated molecule to the refractive index n of the bulk sample at equilibrium, are best described by a virial expansion of the molar refractivity R_m of a gas [31]:

$$R_m = \frac{n^2 - 1}{n^2 + 2} V_m = A_R + \frac{B_R}{V_m} + \frac{C_R}{V_m^2} + \cdots,$$ (1.10)

where A_R, B_R and C_R are the first, second and third refractivity virial coefficients, respectively, and are dependent on the temperature of the gas and the frequency of the refracted light.

When an isotropic gas is placed in a strong uniform electric field, the gas becomes birefringent [32]. This is referred to as the Kerr effect, and the molar Kerr constant $_m K$ of a gas is defined as [33]:

$$_m K = \frac{6n \left(n_{\parallel} - n_{\perp} \right) V_m}{(n^2 + 2)^2 (\varepsilon + 2)^2 E^2},$$ (1.11)

where n is the isotropic refractive index, ε is the dielectric constant of the gas, and $\left(n_{\parallel} - n_{\perp} \right)$ is the difference in refractive index for light polarized parallel and perpendicular to the applied electric field E. The virial expansion of the molar Kerr constant is [34]:

$$_m K = A_K + \frac{B_K}{V_m} + \frac{C_K}{V_m^2} + \cdots,$$ (1.12)

where A_K, B_K and C_K are the first, second and third Kerr-effect virial coefficients, respectively, and are functions temperature and frequency.

3

The depolarization ratio of light scattered by a gas may be expanded in inverse powers of the molar volume [35]:

$$\rho = \rho_0 + \frac{B_\rho}{V_m} + \frac{C_\rho}{V_m^2} + \cdots,$$ (1.13)

where A_ρ, B_ρ and C_ρ are the first, second and third light-scattering virial coefficients, respectively. These coefficients depend on the temperature of the gas and the frequency of the depolarized light.

The second virial coefficients of all these properties describe the contributions of pair interactions to the macroscopic observables. Since, the effect which two interacting molecules have on one another determines the nature of the second virial coefficent of a property, any theory which fully describes the interactions between a pair of molecules must be applicable to all the properties of a gas. If all the effects are considered together, then it should be possible to test the efficacy of the theory. Unfortunately, measurement of second virial coefficents is not always a simple matter, and many gaps exist in the body of experimental data.

In view of the evident success of the theory of the second light-scattering virial coefficient [7, 9, 36], it has become important to establish whether a self-consistent set of molecular parameters coupled with complete theories will serve to obtain agreement between experiment and theory for the full range of second virial coefficients of the different effects. This work sets out to gather second virial coefficient data for the fullest range of molecules with data spanning the various effects, to derive complete theories to the order necessary to ensure convergence in all cases and to evaluate the derived expressions numerically for comparison with experiment. A comprehensive treatment of all effects in this way has only recently become at all feasible through the introduction of computer algebraic manipulation packages, such as Macsyma, which make possible the enormous manipulative task, as well as the greater speed and capacity of the machines which facilitate the extensive numerical integrations.

1.2 Collection of experimental data

1.2.1 Introduction

In order to assess molecular theories of the second virial coefficients it is necessary to have data for the same molecules spanning as wide a range of effects as possible. The data collected below was accumulated in this spirit but, inevitably, gaps remain in places. Nevertheless, the set is as comprehensive as possible for the present purpose.

1.2.2 Tables of experimental values

The simplest and most widely measured effect is the second pressure virial coefficient. Extensive experimental research has been carried out by numerous workers to determine the second and third pressure virial coeffients of a comprehensive range of gases and their mixtures. In 1980, Dymond and Smith [1] published a comprehensive compilation of experimental values of both $B(T)$ and $C(T)$. Where there is good agreement between the results of different authors for the same gas, they present a best-fit of the data over as wide a temperature range as possible. Appendix A contains tables of the experimental values of $B(T)$ for the gases included in this study over a range of temperatures. These values have been taken from Dymond and Smith [1]. Where available, their best-fit data have been used.

The second dielectric virial coefficient has been measured for a variety of molecules by several researchers. Table 1.1 shows experimental values of B_ε for spherical and quasi-spherical gases, Table 1.2 gives values for non-polar gases, and Table 1.3 lists experimental data for polar gases.

The second refractivity virial coefficient data is available for many of the gases under study. In particular, B_R has been measured for a range of wavelengths by several workers for spherical and non-polar gases, as shown in Tables 1.4 and 1.5, respectively. Unfortunately, very little data was found for polar gases. Table 1.6 lists the data available for the polar gases CH_3F and CHF_3.

For the spherical gases, second Kerr-effect virial coefficient data has been measured at several different wavelengths, but each gas usually has only one or two values at different temperatures for the same wavelength. The data available is shown in Table 1.7. The data collected for polar and non-polar gases were all measured at 632 nm, for at least seven different temperatures, as shown in Tables 1.8 to 1.10.

Very little data is available for the second light-scattering virial coefficient as can be seen from Table 1.11, which lists all the measured values available for the gases under study.

The calculations in Chapter 8 of this work will focus on the range of gases: fluoromethane, trifluoromethane, chloromethane, hydrogen chloride, nitrogen, carbon dioxide, ethane, sulphur dioxide, dimethyl ether and ethene, where available data more or less adequately spanned the range of different virial effects.

Table 1.1: Experimental values of B_ε for spherical gases

Gas	Temp. K	$10^{12}B_\varepsilon$ m^6mol^{-2}	Ref.	Gas	Temp. K	$10^{12}B_\varepsilon$ m^6mol^{-2}	Ref.
CH$_4$	242.2	9±0.4	[12]	Ar	242.2	0.6±0.7	[12]
	279.8	8.14±0.29	[37]		242.95	1.84±0.07	[38]
	315.0	7.3±1.8	[12]		296.0	1.6±0.6	[12]
	322.5	7.29±0.32	[37]		298	0.094±0.05	[13]
	373.4	6.75±0.29	[37]			2.06±0.10	[39]
					303.15	1.22±0.09	[38]
CF$_4$	279.8	11.35±0.44	[37]		306.2	1.0±0.7	[12]
	322.5	10.54±0.64	[37]		322.2	0.39±0.20	[13]
	373.4	9.17±0.75	[37]		322.9	0.72±0.12	[40]
					323	2.2±0.2	[41]
SF$_6$	323.3	63.31±2.80	[42]		373	2.9±0.4	[41]
	323.3	64.1	[43]			2.5±0.1	[41]
	348.3	60.54±1.45	[42]		407.6	0.1±0.3	[38]
	373.9	58.89±4.70	[42]		427	2.3±0.1	[41]
						3.1±0.1	[41]
Kr	242.95	8.2±0.4	[38]				
	294	7.49±1.55	[44]	Ne	322	-0.32±0.10	[13]
	298.2	0.90±0.05	[13]				
	322.2	5.6±0.3	[13]	Xe	242.95	35±2	[38]
	323.15	4.3±0.7	[38]		291	24.5±2.9	[44]
	407.6	2.1±0.4	[38]		323.15	32±2	[38]
					407.6	12±2	[38]

Table 1.2: Experimental values of B_ε for non-polar gases

Gas	Temp. K	$10^{12}B_\varepsilon$ m^6mol^{-2}	Ref.	Gas	Temp. K	$10^{12}B_\varepsilon$ m^6mol^{-2}	Ref.
N_2	242.2	4.2±1.0	[12]	H_2	322.2	0.03±0.10	[13]
	296.2	2.0±1.0	[12]				
	306.2	1.8±1.0	[12]	C_2H_4	298.2	31.5	[45]
	322.2	0.60±0.2	[13]		303.2	50.3±1.4	[24]
		1.0±1.0	[12]		304.9	44.3	[45]
	344.2	0.0±0.8	[12]		323.2	48.0	[45]
		1.5±2.5	[12]			30	[46]
						25±7	[47]
CO_2	273.2	35.4±1	[41]			46.4±1.2	[41]
	295.2	64±10	[48]			43.2±1.2	[41]
	302.6	57.6±0.9	[40]			47.5±1.4	[24]
	322.9	49.7±1.0	[45]		348.2	62.2	[45]
		50.7±0.9	[40]		373.2	50.8±0.9	[41]
		41.4±2.4	[41]			51.7±0.8	[41]
	348.2	46.4±1.0	[45]			42.0±2.8	[24]
	369.5	36±3	[49]		423.2	58.8±1.7	[41]
	373.2	35.8±0.7	[41]			60.2±3.5	[41]
		33.5±0.4	[41]			37.6±2.4	[24]
		34.8±0.7	[41]				
	423.2	30.0±0.9	[41]	C_2H_6	298.2	32.2±1.8	[19]

Table 1.3: Experimental values of B_ε for polar gases

Gas	Temp. K	$10^{12}B_\varepsilon$ m^{6}mol^{-2}	Ref.	Gas	Temp. K	$10^{12}B_\varepsilon$ m^{6}mol^{-2}	Ref.
HCl	292.5	4000±1000	[10]	CH$_3$Cl	278.2	-8500±1800	[50]
		3600±1000	[11]		298.2	-10200±1400	[50]
	312.8	3600±1000	[10]		303.2	-6200±1200	[51]
		3200±1000	[11]			-7100±1400	[51]
					318.2	8500±1500	[50]
CH$_3$F	323.2	-1188±50	[52]		323.2	-3550±600	[51]
		-1307±37	[2]			-3800±800	[51]
	348.2	- 701±100	[52]			-4470±200	[2]
	369.5	- 606±30	[2]		343.2	-2650±600	[51]
	416.5	- 331±66	[2]			-2800±800	[51]
					369.5	-2517±50	[2]
CHF$_3$	292.6	3100±2400	[50]		404.8	-1696±60	[2]
		3600±1000	[10]				
	303.2	1330±100	[51]	CHCl$_3$	352.9	-11000±6000	[53]
		1300±160	[51]				
	323.2	1120±200	[51]	(CH$_3$)$_2$O	291.2	2800	[10]
		1100±160	[51]		294.7	4000±1000	[54]
		1125±52	[2]		303.2	2800±1000	[51]
		1090±50	[5]		311.5	2020	[55]
	343.2	980±200	[51]		313.5	2600±1000	[54]
	353.7	1200±1600	[53]		323.2	1600±400	[51]
		-6500±1400	[53]		334.7	2400±1000	[54]
		2000±1400	[56]		340.5	1540	[55]
		4600	[57]		343.2	1600±400	[51]
	369.5	903±20	[2]				
		930±100	[49]	SO$_2$	292.7	1700±1000	[10]
	416.5	704±10	[2]				

Table 1.4: Experimental values of B_R for spherical gases.

Gas	Temp. K	λ nm	$10^{12}B_R$ m^6mol^{-2}	Ref.	Gas	Temp. K	λ nm	$10^{12}B_R$ m^6mol^{-2}	Ref.
CH$_4$	220	546.2	6.1±1.0	[58]	Ar	296.8	325.1	1.81±0.34	[59]
	294.5	543.5	11.72±0.005	[59]	(cont.)	298	633.0	1.49±0.15	[60]
		325.1	11.14±0.005	[59]			577.1	1.44±0.25	[60]
	298	633.0	6.14±0.2	[61]			546.2	1.56±0.15	[60]
	298.2	632.8	7.76±1.32	[62]			514.7	1.56±0.15	[60]
		514.5	6.40±0.83	[62]			501.9	1.49±0.15	[60]
		488.0	8.93±0.57	[62]			488.1	1.47±0.15	[60]
		457.9	7.04±0.78	[62]			476.6	1.51±0.15	[60]
	299	632.8	7.15±0.35	[39]			436.0	1.40±0.25	[60]
	300	546.2	5.5±1.0	[58]		298.2	632.8	1.57±0.58	[62]
	302	632.8	6.6±0.38	[63]			514.5	1.55±0.74	[62]
	323		6.08±0.1	[64]			488.0	1.58±0.69	[62]
	323.2	633.0	5.83±0.15	[65]			457.9	1.53±0.32	[62]
	373.4		6.13±0.15	[64]		299	632.8	2.16±0.34	[39]
						303	633.0	1.75±0.05	[66]
CF$_4$	298.2	632.8	-14±144	[67]		323		1.76±0.05	[64]
			4.27±1.38	[62]					
		514.5	4.65±1.53	[62]	Kr	296.8	612.0	6.46±0.54	[59]
		488.0	4.71±0.67	[62]			594.1	5.83±0.54	[59]
		457.9	4.27±0.84	[62]			543.5	6.24±0.54	[59]
							325.1	6.90±0.54	[59]
SF$_6$	298.2	632.8	27.28±5.18	[62]		289.2	633.0	6.23±1.55	[62]
		514.5	19.48±4.68	[62]			514.5	5.11±1.39	[62]
		488.0	24.93±2.99	[62]			488.0	4.28±1.87	[62]
		457.9	20.32±3.08	[62]			457.9	5.54±0.80	[62]
	299	632.8	29.0±5.4	[39]		303	633.0	5.96±0.06	[66]
	323		36.0±1.8	[68]					
	373		22.7±0.5	[64]	Xe	293.6	543.5	24.58±0.80	[59]
							325.1	23.25±0.80	[59]
Ne	298.2	632.8	-0.14±0.14	[62]		294.1	543.5	25.26±0.80	[59]
			-0.11±0.20	[62]			325.1	23.25±0.80	[59]
	299		-0.06±0.09	[39]		298.2	632.8	25.50±2.85	[62]
	303	633.0	-0.11±0.02	[66]			514.5	18.56±2.36	[62]
							488.0	14.91±2.14	[62]
Ar	296.8	594.1	2.52±0.34	[59]			457.9	16.26±2.55	[62]
		543.5	1.73±0.34	[59]		348	633.0	28.5±0.5	[66]

Table 1.5: Experimental values of B_R for non-polar gases.

Gas	Temp. K	λ nm	$10^{12}B_R$ m^{6}mol^{-2}	Ref.	Gas	Temp. K	λ nm	$10^{12}B_R$ m^{6}mol^{-2}	Ref.
H$_2$	323	632.8	0.13±0.08	[64]	N$_2$	298	632.8	0.74±0.65	[62]
								0.75±0.10	[69]
CO$_2$	243–	632.8	4.6	[70]				1.0±0.31	[39]
	263			[71]		323.2	633.0	0.89±0.06	[64]
	298.2		3.2±1.6	[39]				0.64±0.08	[65]
			4.75±1.30	[62]		298	577.1	0.76±0.10	[69]
	320	633.0	0.0±1.0	[72]			546.2	0.81±0.10	[69]
	323		1.9±0.2	[64]			514.5	0.62±0.78	[62]
		632.8	5.3	[13]				0.81±0.10	[69]
			3.31±3.6	[68]			488.0	0.96±0.68	[62]
	293.8	594.1	7.33±0.53	[59]			488.1	0.85±0.10	[69]
	299.3		5.74±0.53	[59]			476.6	0.92±0.10	[69]
	307.2	546.1	0.4±0.36	[73],			457.9	0.92±0.43	[62]
				[13]			436.0	0.70±0.10	[69]
	293.8	543.5	8.96±0.53	[59]					
	299.3		6.83±0.53	[59]	C$_2$H$_4$	295.5	594.1	17.65±0.85	[59]
	298.2	514.5	0.73±0.66	[62]			543.5	22.83±0.85	[59]
		488.0	1.03±0.66	[62]			325.1	44.10±0.85	[59]
		457.9	1.27±0.85	[62]		303	633.0	17.60±2.2	[74]
	293.8	325.1	4.87±0.53	[59]				40.8±2.0	[75]
	323.2	447.1–	5.23±0.9	[76]				6.0	[24]
		667.8		[13]				17.7±0.4	[77]
	373.2	447.1–	2.7±1.4	[76]				20.3±0.8	[78]
		587.6		[13]				17.4±0.4	[79]
C$_2$H$_6$	348	633.0	22.9±3.0	[72]		373		19.50±0.50	[64]
	373		26.6±0.05	[64]				17.8±0.3	[77]
	"Various"		27.8±1.0	[80]				20.1±0.5	[78]
	"Various"	589.3	23.2±0.6	[80]				17.8±0.3	[79]
	295.5	325.1	31.58±0.90	[59]					

Table 1.6: Experimental values of B_R for polar gases at room temperature

Gas	λ nm	$10^{12}B_R$ m^6mol^{-2}	Ref.	Gas	λ nm	$10^{12}B_R$ m^6mol^{-2}	Ref.
CHF$_3$	632.8	3.4±1.1	[39]	CH$_3$F	632.8	4.32±1.80	[62]
		2.54±1.35	[62]		546.0	7±100	[67]
	514.5	2.44±0.89	[62]		514.5	-0.40±1.28	[62]
	488.0	1.56±0.75	[62]		488.0	-1.02±1.09	[62]
	457.0	1.97±0.86	[62]		451.9	1.12±0.88	[62]

Table 1.7: Experimental values of B_K for spherical gases

Gas	Temp. K	λ nm	$10^{33}B_K$ $C^2m^8J^{-2}mol^{-2}$	Ref.	Gas	Temp. K	λ nm	$10^{33}B_K$ $C^2m^8J^{-2}mol^{-2}$	Ref.
CH$_4$	249.7	632.8	30.5±3.1	[33]	CF$_4$	288.8	632.8	42.2±4.2	[33]
	273.6		28.3±2.8	[33]		293	633.0	42±8	[81]
	303.7		24.5±2.5	[33]		302		40±8	[81]
	302	458.0	37±5	[81]					
					Kr	296	514.5	17±15	[82]
SF$_6$	296	514.5	334±45	[82]		303	458.0	16±2	[81]
	303	633.0	470±90	[81]					
					Xe	296	514.5	72±24	[82]
Ar	296	514.5	4.1±0.7	[82]		302	458.0	98±17	[81]
	305	458.0	3.8±0.7	[81]					

11

Table 1.8: Experimental values of B_K for polar gases at 632.8 nm.

Gas	Temp. K	$10^{30}B_K$ $C^2m^8J^{-2}mol^{-2}$	Ref.	Gas	Temp. K	$10^{30}B_K$ $C^2m^8J^{-2}mol^{-2}$	Ref.
CH$_3$F	250.8	5.6±2.8		CH$_3$Cl	304.1	1.97±0.29	[83]
	252.6	9.3±4.7					
	259.2	3.9±2.0		(CH$_3$)$_2$O	259.0	34.2±6.8	
	275.0	6.1±3.1			269.0	18.8±3.8	
	280.2	4.7±2.4	[33]		278.4	16.1±3.2	
	284.4	6.5±3.3			288.2	13.1±2.6	[23]
	303.1	5.1±2.6			302.4	11.1±2.2	
	312.4	5.1±2.6			318.9	10.2±2.0	
	318.9	4.5±2.3			333.8	5.8±1.2	
	323.0	2.5±0.7	[83]				
	371.3	1.2±0.4	[83]	SO$_2$	298.7	13.8±0.8	
					307.3	11.4±0.5	
CHF$_3$	245.5	9.6±4.8			315.4	10.1±0.5	
	250.3	3.8±1.9			330.7	7.5±0.4	
	252.1	9.5±4.8			348.8	6.5±0.6	
	268.5	4.2±2.1	[33]		370.9	6.5±0.5	
	275.4	6.8±3.4			381.2	4.2±0.9	
	285.9	1.8±0.9			395.7	7.6±1.5	
	303.5	3.7±1.9			423.7	4.7±1.1	[21]
	308.9	3.2±1.6			457.0	2.1±1.3	
	310.1	3.2±1.0	[83]		471.5	3.4±1.8	
	323.0	2.5±0.7	[83]		490.3	1.5±0.6	
	371.3	1.7±0.3	[83]				

Table 1.9: Experimental values of B_K for non-polar gases at 632.8 nm.

Gas	Temp. K	$10^{32}B_K$ $C^2m^8J^{-2}mol^{-2}$	Ref.	Gas	Temp. K	$10^{32}B_K$ $C^2m^8J^{-2}mol^{-2}$	Ref.
CO$_2$	299.2	6±1		C$_2$H$_6$	255	18.2±3.7	
	314.9	0±1			259	17.7±3.6	
	330.9	4±2			269	16.7±3.3	
	348.8	2±1			278	18.0±3.6	
	370.9	-6±2	[15]			15.7±3.1	[14]
	394.5	2±2			287	16.8±3.3	
	422.8	-3±2			299	17.7±3.6	
	455.8	-3±4			304	14.9±3.0	
	489.5	-5±3			309	14.2±2.9	
	252	23±19			318	15.0±3.0	
	259	5±27					
	267	-6±11		N$_2$	248	-0.08±0.28	
	279	-1±13			260	0.07±0.39	
	287	-3±9	[14]		277	-0.21±0.33	
	301	-3±7			286	-0.23±0.45	[14]
	302	0±10			299	-0.30±0.59	
	318	-11±8			315	0.04±0.30	
	337	-9±9			334	-0.41±0.18	

Table 1.10: Experimental values of B_K for non-polar gases at 632.8 nm. (cont.)

Gas	Temp. K	$10^{32}B_K$ $C^2m^8J^{-2}mol^{-2}$	Ref.	Gas	Temp. K	$10^{32}B_K$ $C^2m^8J^{-2}mol^{-2}$	Ref.
C_2H_4	262	34±7		H_2	196.1	0.090±0.011	(4)
	268	26±6				0.129±0.011	(2)
	273	23±5			207.1	0.063±0.009	(4)
	280	18±3				0.100±0.009	(2)
	286	22±5			219.5	0.063±0.005	(4)
	294	24±5				0.100±0.005	(2)
	298	18±3	[14]		232.3	0.074±0.020	(4)
	302	18±3				0.108±0.020	(2)
	313	16±3			247.0	0.025±0.015	(4)
	314	18±3				0.059±0.015	(2)
	333	17±3			259.5	0.103±0.014	(4)
	334	17±3			0.138	0.014±(2)	
	202.4	103.0±7.6	(2)		273.6	0.087±0.021	(4)
		100.0±7.8	(4)			0.120±0.021	(2)
	211.0	90.1±12.2	(2)		288.9	0.068±0.007	(4)
		87.4±12.2	(4)			0.101±0.007	(2)
	214.8	63.3±12.8	(2)		303.7	0.054±0.008	(4)
		60.5±12.8	(4)			0.086±0.008	(2)
	222.2	49.9±2.3	(2)		328.0	0.038±0.006	(4)
		47.2±2.3	(4)			0.069±0.006	(2)
	235.6	44.5±0.8	(2)		350.4	0.063±0.007	(4)
		41.9±0.8	(4)			0.093±0.007	(2)
	250.0	39.6±0.9	(2) [25]		376.5	0.083±0.009	(4)
		37.1±0.9	(4)			0.113±0.009	(2)
	266.6	34.2±1.5	(2)		411.7	0.035±0.010	(4)
		31.9±1.5	(4)			0.063±0.010	(2) [84]
	284.9	32.8±1.5	(2)				
		30.6±1.6	(4)				
	303.2	19.6±2.2	(2)				
		17.6±2.2	(4)				
	333.4	15.9±1.0	(2)				
		14.0±1.0	(4)				
	363.7	28.4±2.7	(2)				
		26.6±2.7	(4)				

(4): values deduced using the usual KE local-field function $f^{(4)}(n,\varepsilon) = \left(\frac{n^2+2}{3}\right)^2\left(\frac{\varepsilon+2}{3}\right)^2$, derived from the Lorentz-Lorenz and Clausius-Mossotti equations [85].

(2): values deduced using an alternative KE local-field function $f^{(2)}(n,\varepsilon) = \frac{n^2+2}{3}\frac{\varepsilon+2}{3}$ [86,87].

14

Table 1.11: Experimental values of B_ρ for various gases.

Gas	Temp. K	λ nm	$10^6 B_\rho$ m^3mol^{-1}	Ref.	Gas	Temp. K	λ nm	$10^6 B_\rho$ m^3mol^{-1}	Ref.
CO	298.2	514.5	0.213±0.016	[7]	Ar	290	488.0	0.21±0.03	[16]
						294		0.34±0.03	[88]
CH_3Cl	299.6	514.5	-3.30±0.26	[7]		298	514.5	< 0.4	[89]
						298	?	0.20±0.01	[90]
SO_2	338.4	514.5	-6.96±0.49	[9]					
					Kr	294	488.0	0.67±0.01	[88]
N_2	295.5	514.5	0.138±0.014	[7]		298	514.5	0.52±0.06	[89]
	310		0.16	[91]					
	290	488.0	0.14	[16]	Xe	294	488.0	1.52±0.04	[88]
CO_2	298.2	514.5	-8.29±0.16	[7]	CH_4	294	488.0	0.59±0.21	[88]
	300	488.0	-10	[16]		298	514.5	0.65±0.09	[89]
						298	?	0.403±0.013	[90]
C_2H_6	295.9	514.5	0.315±0.018	[7]					
					SF_6	294	488.0	1.08±0.10	[88]
C_2H_4	294.9	514.5	-2.384±0.027	[9]		298	514.5	1.37±0.04	[89]
	328.0		-1.78±0.07	[92]					

Chapter 2

The Intermolecular Potential Energy

From the general expression for B_Q in (1.6), it is clear that the explicit form of the intermolecular potential energy $U_{12}(\tau)$ is necessary to perform any calculations of second virial coefficients. It has been shown [93] that $U_{12}(\tau)$ may be regarded as having three components when the intermolecular separation R is large relative to the dimension of the molecules:

(i) the *electrostatic energy*, U_{elec}, which arises from interactions of the zero-field multipole moments (charge, dipole, quadrupole, *et cetera*) of the pair of molecules,

(ii) the *induction energy*, U_{ind}, arising from the distortion of the structure due to the action of the permanent electric moments on the neighbouring molecule, and

(iii) the London *dispersion energy*, U_{disp}, resulting from interactions of the electric moments due to fluctuations in the charge distribution of the molecules.

These three interaction energies are due to well understood long-range forces [34, 93–95], for which it is assumed that negligible overlap of the electron clouds of the interacting molecules occurs. When the intermolecular separation R is small, there is significant overlap of the molecular wavefunctions and prohibitively complex *ab initio* quantum-mechanical calculations are necessary to account for the intermediate-range exchange forces. Instead, it is usually assumed [31, 96, 97] that components (i), (ii), and (iii) of the interaction energy are applicable to short-range interactions if an additional contribution is included to accommodate the repulsive short-range interactions. This term is called U_{overlap}. Thus, the intermolecular potential energy may be written as:

$$U_{12}(\tau) = U_{\text{elec}} + U_{\text{ind}} + U_{\text{disp}} + U_{\text{overlap}}. \tag{2.1}$$

16

Most previous studies of the properties of gases [2, 31, 39, 40, 96–98] use the central-field Lennard-Jones 6:12 potential, U_{LJ}, to represent $(U_{disp} + U_{overlap})$:

$$U_{LJ} = 4\varepsilon \left[\left(\frac{R_0}{R} \right)^{12} - \left(\frac{R_0}{R} \right)^6 \right], \tag{2.2}$$

where the term $4\varepsilon \left(\frac{R_0}{R} \right)^6$ describes the attractive part of the potential, $4\varepsilon \left(\frac{R_0}{R} \right)^{12}$ describes the short-range repulsive contribution, and the symbols ε and R_0 are the Lennard-Jones parameters. It can be seen from (2.2) that U_{LJ} is spherically symmetric. To allow for the angular dependence of the repulsive short-range overlap forces of non-spherical molecules, Buckingham and Pople [96] proposed an additional term, U_{shape}, to be included in the overlap potential, so that:

$$(U_{disp} + U_{overlap}) = U_{LJ} + U_{shape}. \tag{2.3}$$

The form of the shape potential is discussed in detail in Section 2.2.

Thus, substituting (2.3) into (2.1), the intermolecular pair potential is given by:

$$U_{12}(\tau) = U_{LJ} + U_{shape} + U_{elec} + U_{ind}. \tag{2.4}$$

2.1 The relative configuration of a pair of interacting molecules

In order to derive exact expressions for the various parts of the intermolecular potential in (2.4) (except the Lennard-Jones potential), it is necessary to specify the relative configuration τ of the two interacting gas molecules. When describing the configuration of a pair of molecules, three sets of orthogonal axes are required:

(i) The space-fixed axes: O(x,y,z), which are usually chosen to coincide with the direction of the plane of a light wave or the direction of an applied electromagnetic field. In the tensor notation of this work, these axes are denoted by the subscripts α, β, γ;

(ii) The coordinate system of molecule 1: O(1,2,3), with the principal axes chosen to exploit the symmetry of the molecule. These axes are denoted by the tensor subscripts i, j, k; and

(iii) The coordinate system of molecule 2: $O'(1', 2', 3')$, similarly chosen to exploit the symmetry of the molecule. The subscripts i', j', k' are used to denote molecule 2's axes in tensor notation.
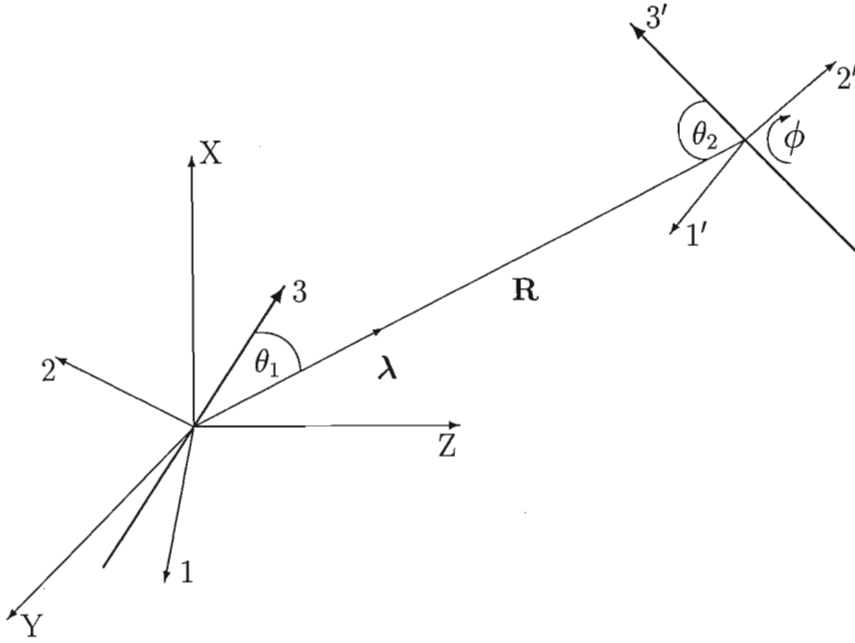
Figure 2.1: The coordinates R, θ_1, θ_2 and ϕ describing the configuration of two linear molecules [26].

2.1.1 Linear molecules

The physical property tensors of a molecule are usually specified relative to a coordinate system of mutually perpendicular axes fixed in the molecule, such that one of the axes co-incides with a symmetry axis of the molecule. A description of the interaction of two identical molecules, each with its own molecular axes, requires a set of interaction parameters. Figure 2.1 shows how the angles θ_1, θ_2 and ϕ and the separation, $\mathbf{R}$, specify the relative configuration τ of a pair of interacting linear molecules [26]. The coordinate systems of molecules 1 and 2 are O(1,2,3) and O$'$(1$'$, 2$'$, 3$'$), with axes 3 and 3$'$ lying along the symmetry axes of molecules 1 and 2 respectively. It can be seen that $\mathbf{R}$ is the distance between the centres of the two molecules, called the line of centres; θ_1 and θ_2 are the angles between the line of centres and the dipole axes of molecules 1 and 2; and ϕ is the angle between the two planes formed by the molecular axes and the line of centres. $\boldsymbol{\lambda}$ is the unit vector along $\mathbf{R}$.

2.1.2 Non-linear molecules

Experimental measurements of macroscopic observables, such as the depolarization ratio, the Kerr constant or the molar refraction of a gas, are carried out in a system of space-fixed axes orientated with respect to the direction of the incident light beam. However, molecular property tensors must be referred to the system of molecule-fixed axes which

18
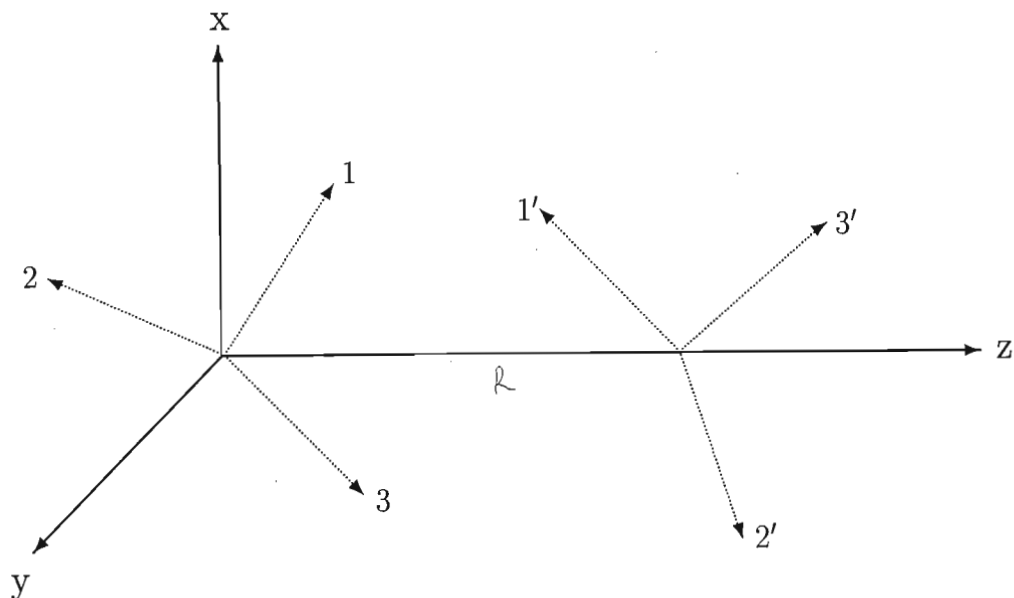
Figure 2.2: The molecule-fixed axes $O(1,2,3)$ and $O'(1',2',3')$ of interacting molecules 1 and 2 respectively, in the space-fixed axes $O(x,y,z)$

exploits the symmetry of the molecule. This set of molecule-fixed axes changes constantly with respect to the space-fixed axes as the molecules move around in the sample. In order to obtain the average projection of the tensor properties of the molecule, it is necessary to refer the molecular property tensors to molecule-fixed axes, then project these tensors into the space-fixed axes of the sample, and finally, average the projection over the orientational motion of the molecule.

Figure 2.2 shows the axes $O(1,2,3)$ of molecule 1, the axes $O'(1',2',3')$ of molecule 2, and the space-fixed axes $O(x,y,z)$. It is possible to specify fully the relative configuration of a pair of interacting non-linear molecules using seven parameters:

(i) The displacement of the two molecular centres is given by the parameter R, which is initially fixed along the z-axis. This choice of direction is possible, since the resultant expressions will be orientationally averaged over all possible configurations, in the absence of any bias.

(ii) The orientation of the molecule-fixed axes of molecule 1 relative to the space-fixed axes may be described by nine direction cosines. However, in order to specify any rotation of a Cartesian system of axes about its origin completely, only three parameters are necessary. The three Euler angles α_1, β_1 and γ_1 are often used to describe such a rotation. Recently, Couling and Graham [36] used the Euler angles in their work on non-linear molecules. Three successive rotations are needed to rotate (1,2,3) into (x,y,z) [99, 100]:

(a) rotation about the 3-axis through an angle α_1 $\quad$ $(0 \leq \alpha_1 \leq 2\pi)$,

(b) rotation about the new 2'-axis through an angle β_1 $\quad$ $(0 \leq \beta_1 \leq \pi)$,

(c) rotation about the new 3"-axis through an angle γ_1 $\quad$ $(0 \leq \gamma_1 \leq 2\pi)$.

The nine direction cosines a_i^α are now expressed as functions of the three Euler angles. Thus, we have [99, 100]:

$$
a_i^\alpha = \begin{bmatrix} \cos\gamma_1 & \sin\gamma_1 & 0 \\ -\sin\gamma_1 & \cos\gamma_1 & 0 \\ 0 & 0 & 1 \end{bmatrix} \begin{bmatrix} \cos\beta_1 & 0 & -\sin\beta_1 \\ 0 & 1 & 0 \\ \sin\beta_1 & 0 & \cos\beta_1 \end{bmatrix} \begin{bmatrix} \cos\alpha_1 & \sin\alpha_1 & 0 \\ -\sin\alpha_1 & \cos\alpha_1 & 0 \\ 0 & 0 & 1 \end{bmatrix} =
$$

$$
\begin{bmatrix} \cos\alpha_1 \cos\beta_1 \cos\gamma_1 - \sin\alpha_1 \sin\gamma_1 & \sin\alpha_1 \cos\beta_1 \cos\gamma_1 + \cos\alpha_1 \sin\gamma_1 & -\sin\beta_1 \cos\gamma_1 \\ -\cos\alpha_1 \cos\beta_1 \sin\gamma_1 - \sin\alpha_1 \cos\gamma_1 & -\sin\alpha_1 \cos\beta_1 \sin\gamma_1 + \cos\alpha_1 \cos\gamma_1 & \sin\beta_1 \sin\gamma_1 \\ \cos\alpha_1 \sin\beta_1 & \sin\alpha_1 \sin\beta_1 & \cos\beta_1 \end{bmatrix}
$$

$$(2.5)$$

(iii) In the same way, the relative orientation of the molecule-fixed axes of molecule 2 and the space-fixed axes is described by nine direction cosines $a_{i'}^\alpha$, which are expressed as functions of the three Euler angles α_2, β_2 and γ_2. The individual components of $a_{i'}^\alpha$ have the same form as those of a_i^α in (2.5), with only the subscripts of the angles changing from 1 to 2:

$$
a_{i'}^\alpha =
$$

$$
\begin{bmatrix} \cos\alpha_2 \cos\beta_2 \cos\gamma_2 - \sin\alpha_2 \sin\gamma_2 & \sin\alpha_2 \cos\beta_2 \cos\gamma_2 + \cos\alpha_2 \sin\gamma_2 & -\sin\beta_2 \cos\gamma_2 \\ -\cos\alpha_2 \cos\beta_2 \sin\gamma_2 - \sin\alpha_2 \cos\gamma_2 & -\sin\alpha_2 \cos\beta_2 \sin\gamma_2 + \cos\alpha_2 \cos\gamma_2 & \sin\beta_2 \sin\gamma_2 \\ \cos\alpha_2 \sin\beta_2 & \sin\alpha_2 \sin\beta_2 & \cos\beta_2 \end{bmatrix}
$$

$$(2.6)$$

2.2 The shape potential

The Lennard-Jones potential used to represent the dispersion and overlap energies is a spherically symmetric central-field potential with an attractive part and a repulsive part, as can be seen from equation (2.2). The parameter R_0 represents the closest approach of two spherical molecules before the resultant force is repulsive. However, for non-spherical molecules the distance of closest approach may differ for different relative orientations. This angular dependence cannot be described by a spherically-symmetric potential. To account for this, Buckingham and Pople [96] proposed the addition of a *shape* potential.

(a) Colliding spheres.

(b) Colliding plates where θ_1 and θ_2 are 0 or π.

(c) Colliding plates where θ_1 and θ_2 are $\pm(\pi/2)$. The **3** axis may be in or out of the page.

(d) Colliding rods where θ_1 and θ_2 are $\pm(\pi/2)$.
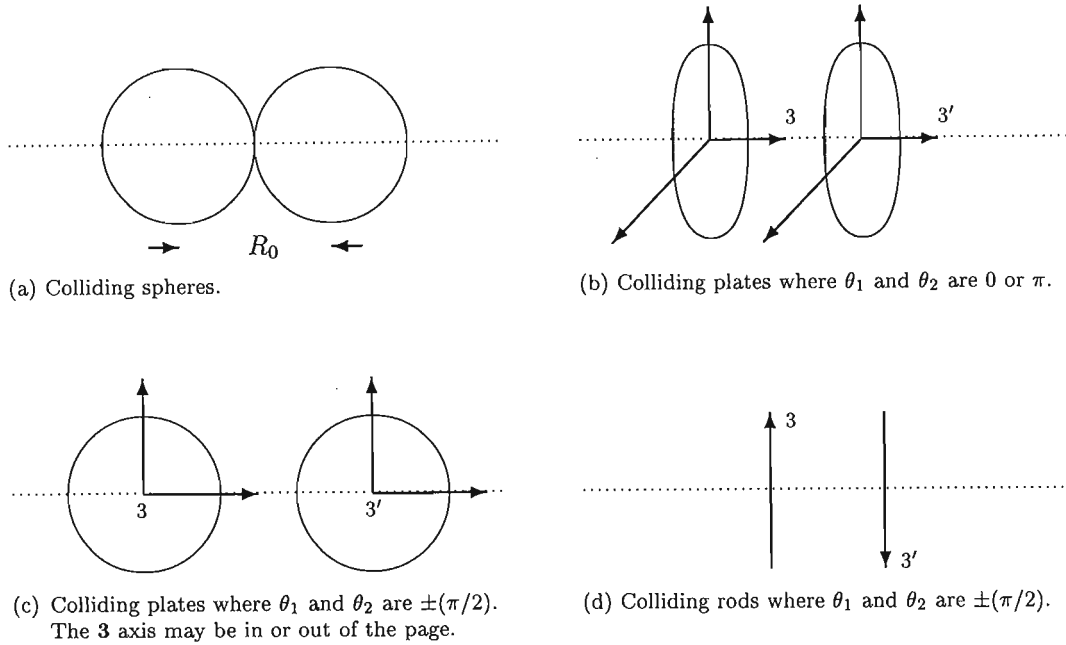
Figure 2.3: Collision configurations for spherical, plate-like and rod-like molecules.

For axially-symmetric molecules, they proposed that U_{shape} be given by:

$$U_{\text{shape}} = 4D\varepsilon \left(\frac{R_0}{R}\right)^{12} \left(3\cos^2\theta_1 + 3\cos^2\theta_2 - 2\right), \tag{2.7}$$

where θ_1 and θ_2 are angles which describe the relative configuration of the colliding molecules (Figure 2.1), and D is a dimensionless parameter called the shape factor with $-0.25 \leq D \leq 0.50$. The form of the angular dependence was chosen as the lowest order of spherical harmonic to give a reasonable variation of range of repulsive force with orientation. For spherical molecules, D is obviously zero, since no correction is necessary. It is argued below that D is positive for rod-like molecules, which are elongated in the direction of the dipole moment axis [2], and negative for plate-like molecules, which are fore-shortened in the direction of the axis of the dipole moment [2]. Rod-like molecules, such as CH_3F, favour an anti-parallel configuration (Figure 2.3 (d)), while plate-like molecules, such as CHF_3, prefer a parallel arrangement, as can be seen in Figure 2.3 (b) [101].

When two spheres of diameter R_0 collide, as in Figure 2.3 (a), U_{LJ} is zero when the approach distance $R = R_0$. If R is less than R_0, U_{LJ} will be positive and, therefore, repulsive. If two plate-like molecules collide in the configuration shown in Figure 2.3 (b), R can be less than R_0 before repulsion occurs. In order to reduce the repulsive R^{-12} term of the Lennard-Jones potential, U_{shape} must be negative and it follows that the shape factor D must be negative. In the limit of infinitely thin plates colliding as in

The ethene molecule. Molecular geometry is taken from [102,103].

The sulphur dioxide molecule. Molecular geometry is taken from [104].

case (i):
α_1 and α_2 can be any angle
β_1 and β_2 can be 0 or π
γ_1 and γ_2 can be any angle

case (ii):
α_1 and α_2 can be any angle
β_1 and β_2 can be $\pi/2$ or $3\pi/2$
γ_1 and γ_2 can be 0 or π

case (iii):
α_1 and α_2 can be any angle
β_1 and β_2 can be $\pi/2$ or $3\pi/2$
γ_1 and γ_2 can be $\pi/2$ or $3\pi/2$
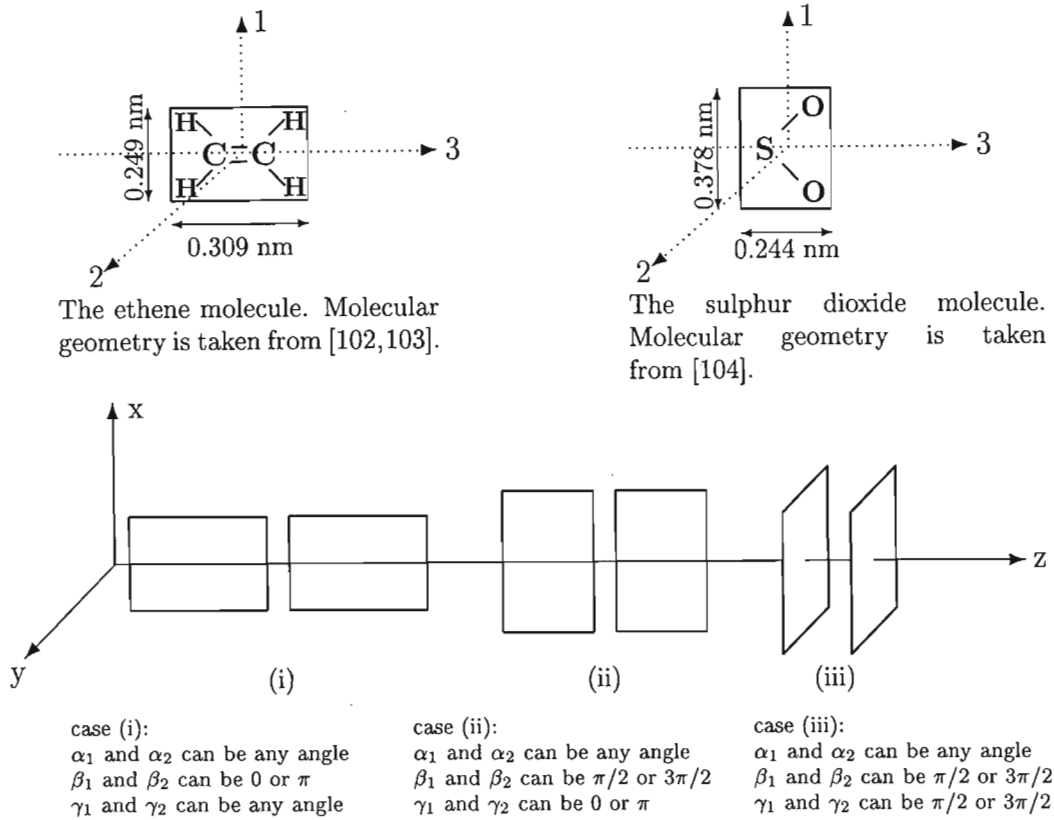
Figure 2.4: The three extreme intermolecular approaches for two colliding ethene molecules. For sulphur dioxide, the ethene molecules must be replaced with the equivalent sulphur dioxide, shown above [9].

Figure 2.3 (b), where θ_1 and θ_2 are 0 or π, the smallest approach distance is zero and there is no repulsive potential. Therefore, it can be seen from (2.2) and (2.7) that $D = -0.25$. Obviously, real plate-like molecules will have non-zero thickness and the shape factor will fall between zero and -0.25. When the two molecules collide as shown in Figure 2.3 (c), then θ_1 and θ_2 are $\pm\frac{\pi}{2}$ and, since D is negative, the shape potential will be positive, increasing the repulsive potential, which results in repulsive forces occurring when $R > R_0$. For infinitely thin rod-like molecules, when θ_1 and θ_2 are $\pm\frac{\pi}{2}$ (Figure 2.3 (d)), the closest approach occurs for $R = 0$. From (2.2) and (2.7) it can be seen that $D = +0.50$. For real molecules with finite thickness, D will lie between zero and 0.5.

Recently, Couling and Graham [36] constructed a shape potential to describe the important role played by the molecular shape in determining interactions between non-linear molecules. They used the force field for axially symmetric molecules of Buckingham and Pople [96], shown in (2.7), as the basis for a new U_{shape} to describe the orientation effects due to short-range overlap repulsive forces for non-linear gases with D_{2h} (eg. ethene) and C_{2v} (eg. sulphur dioxide) symmetry. Figure 2.4 [9] shows how the molecule-fixed axes

(1,2,3) have been chosen so that the 1-3 plane coincides with the plane of the molecule, with the 3 axis along the principal molecular axis. Figure 2.4 also shows the three extreme intermolecular approaches possible. From the figure it can be seen that in all three cases α_1 and α_2 may assume any value from 0 to 2π and, therefore, the shape potential is independent of these angles. The simplest force-field which reproduces the orientation effects of the shape of the non-linear molecules is [36]

$$
U_{\text{shape}} = 4\varepsilon \left(\frac{R_0}{R}\right)^{12} \left\{ D_1 \left[3\cos^2\beta_1 + 3\cos^2\beta_2 - 2\right] \right. \\
\left. + D_2 \left[3\sin^2\beta_1\cos^2\gamma_1 + 3\sin^2\beta_2\cos^2\gamma_2 - 2\right]\right\},
$$

(2.8)

where D_1 and D_2 are dimensionless parameters called the shape factors. If $D_2 = 0$ then (2.8) simplifies to the shape potential for axially symmetric molecules defined in (2.7).

For two planar molecules approaching as in case (iii) of Figure 2.4, the approach distance R can be less than R_0 before contact forces arise. Thus, the repulsive part of the Lennard-Jones potential must be reduced by a negative shape potential. For case (iii), β_1, β_2, γ_1 and γ_2 are all $\pm\frac{\pi}{2}$, therefore, from (2.8) it can be seen that if U_{shape} is negative $(D_1 + D_2)$ must be positive. If the planes were infinitely thin, then the closest possible approach is $R = 0$. For this orientation there is no repulsive potential, so the $4\varepsilon \left(\frac{R_0}{R}\right)^{12}$ term of the Lennard-Jones potential must be completely cancelled by the shape potential, so that $(D_1 + D_2) = 0.50$. Since real planar molecules will have finite thickness, it it likely that $(D_1 + D_2) < 0.50$ [36].

2.3 The electrostatic and induction potentials

According to convention [9, 40, 44, 97, 105], U_{elec} consists of potential energies resulting from the interactions of permanent multipole moments, whereas U_{ind} incorporates those energies arising from interactions between permanent multipole moments of one molecule and the induced moments of the second molecule. To quadrupole order in the permanent moments and to dipole order in the induced moments,

$$
U_{\text{elec}} + U_{\text{ind}} = U_{\mu,\mu} + U_{\mu,\theta} + U_{\theta,\theta} + U_{\mu,\text{ind}\,\mu} + U_{\theta,\text{ind}\,\mu} + U_{\text{ind}\,\mu,\text{ind}\,\mu},
$$

(2.9)

where $U_{\mu,\mu}$, $U_{\mu,\theta}$ and $U_{\theta,\theta}$ are the electrostatic dipole-dipole, dipole-quadrupole and quadrupole-quadrupole interaction energies of the permanent moments of the pair of interacting molecules, while $U_{\mu,\text{ind}\,\mu}$ and $U_{\theta,\text{ind}\,\mu}$ are the dipole-induced-dipole and quadrupole-induced-dipole interaction energies. $U_{\text{ind}\,\mu,\text{ind}\,\mu}$ is the induced-dipole-induced-dipole interaction energy, which Buckingham and Pople [96] were the first to include in their calcu-

lations. This term is frequently omitted, but working to this order in our calculations produced a 7% increase in the second dielectric virial coefficient of hydrogen chloride, so that the effect can be significant, and the term is generally included in this work.

Buckingham [26] shows that:

$$U_{\mu,\mu} = -\mu_\alpha^{(1)} T_{\alpha\beta}^{(1)} \mu_\beta^{(2)}, \tag{2.10}$$

$$U_{\mu,\theta} = \tfrac{1}{3} \left(\mu_\alpha^{(1)} T_{\alpha\beta\gamma}^{(1)} \theta_{\beta\gamma}^{(2)} - \mu_\alpha^{(2)} T_{\alpha\beta\gamma}^{(1)} \theta_{\beta\gamma}^{(1)} \right), \tag{2.11}$$

$$U_{\theta,\theta} = \tfrac{1}{9} \theta_{\alpha\beta}^{(1)} T_{\alpha\beta\gamma\delta}^{(1)} \theta_{\gamma\delta}^{(2)}, \tag{2.12}$$

$$U_{\mu,\text{ind}\,\mu} = -\tfrac{1}{2} a \left(T_{\alpha\beta}^{(1)} \mu_\beta^{(2)} T_{\alpha\gamma}^{(1)} \mu_\gamma^{(2)} + T_{\alpha\beta}^{(1)} \mu_\beta^{(1)} T_{\alpha\gamma}^{(1)} \mu_\gamma^{(1)} \right), \tag{2.13}$$

$$U_{\theta,\text{ind}\,\mu} = -\tfrac{1}{18} a \left(T_{\alpha\beta\gamma}^{(1)} \theta_{\beta\gamma}^{(1)} T_{\alpha\delta\varepsilon}^{(1)} \theta_{\delta\varepsilon}^{(1)} + T_{\alpha\beta\gamma}^{(1)} \theta_{\beta\gamma}^{(2)} T_{\alpha\delta\varepsilon}^{(1)} \theta_{\delta\varepsilon}^{(2)} \right), \tag{2.14}$$

$$U_{\text{ind}\,\mu,\text{ind}\,\mu} = -a^2 T_{\alpha\gamma}^{(1)} \mu_\gamma^{(1)} T_{\alpha\beta}^{(1)} T_{\beta\delta}^{(1)} \mu_\delta^{(2)}, \tag{2.15}$$

where a is the mean static dipole polarizability, and use is made of the powerful T-tensor notation, which was formulated [26] to express the electric field E_α and electric field gradient $E_{\alpha\beta}$ at the origin of one molecule due to the point multipole moments of its neighbour. Thus, for the field and field gradient at molecule 1 due to the multipole moments of molecule 2, we have:

$$E_\alpha^{(1)} = T_{\alpha\beta}^{(1)} \mu_\beta^{(2)} - \tfrac{1}{3} T_{\alpha\beta\gamma}^{(1)} \theta_{\beta\gamma}^{(2)} + \cdots, \tag{2.16}$$

$$E_{\alpha\beta}^{(1)} = T_{\alpha\beta\gamma}^{(1)} \mu_\gamma^{(2)} - \tfrac{1}{3} T_{\alpha\beta\gamma\delta}^{(1)} \theta_{\gamma\delta}^{(2)} + \cdots, \tag{2.17}$$

where $T_{\alpha\beta}^{(1)}$, $T_{\alpha\beta\gamma}^{(1)}$ and $T_{\alpha\beta\gamma\delta}^{(1)}$ are the second, third and fourth rank T-tensors, defined by [26]:

$$T_{\alpha\beta}^{(1)} = \frac{1}{4\pi\varepsilon_0} \nabla_\alpha \nabla_\beta \frac{1}{R} = \frac{1}{4\pi\varepsilon_0} \frac{1}{R^5} \left(3R_\alpha R_\beta - R^2 \delta_{\alpha\beta} \right), \tag{2.18}$$

$$\begin{aligned} T_{\alpha\beta\gamma}^{(1)} &= -\frac{1}{4\pi\varepsilon_0} \nabla_\alpha \nabla_\beta \nabla_\gamma \frac{1}{R} \\ &= \frac{3}{4\pi\varepsilon_0} \frac{1}{R^7} \left[5R_\alpha R_\beta R_\gamma - R^2 \left(R_\alpha \delta_{\beta\gamma} + R_\beta \delta_{\alpha\gamma} + R_\gamma \delta_{\alpha\beta} \right) \right], \end{aligned} \tag{2.19}$$

$$T^{(1)}_{\alpha\beta\gamma\delta} = -\frac{1}{4\pi\varepsilon_0}\nabla_\alpha\nabla_\beta\nabla_\gamma\nabla_\delta\frac{1}{R}$$

$$= \frac{3}{4\pi\varepsilon_0}\frac{1}{R^9}\left[35R_\alpha R_\beta R_\gamma R_\delta - 5R^2\left(R_\alpha R_\beta\delta_{\gamma\delta} + R_\alpha R_\gamma\delta_{\beta\delta}\right.\right.$$

$$\left.+ R_\alpha R_\delta\delta_{\beta\gamma} + R_\beta R_\gamma\delta_{\alpha\delta} + R_\beta R_\delta\delta_{\alpha\gamma} + R_\gamma R_\delta\delta_{\alpha\beta}\right)$$

$$\left.+ R^4\left(\delta_{\alpha\beta}\delta_{\gamma\delta} + \delta_{\alpha\gamma}\delta_{\beta\delta} + \delta_{\alpha\delta}\delta_{\beta\gamma}\right)\right], \tag{2.20}$$

$$\text{where} \quad \nabla_\alpha = \left(\frac{\partial}{\partial R_\alpha}\right), \tag{2.21}$$

and R_α is the vector from the origin of molecule 1 to the origin of the second molecule. The field and field gradient at molecule 2 due to the multipole moments of molecule 1 are defined in the same way:

$$E^{(2)}_\alpha = T^{(2)}_{\alpha\beta}\mu^{(1)}_\beta - \tfrac{1}{3}T^{(2)}_{\alpha\beta\gamma}\theta^{(1)}_{\beta\gamma} + \cdots, \tag{2.22}$$

$$E^{(2)}_{\alpha\beta} = T^{(2)}_{\alpha\beta\gamma}\mu^{(1)}_\gamma - \tfrac{1}{3}T^{(2)}_{\alpha\beta\gamma\delta}\theta^{(1)}_{\gamma\delta} + \cdots, \tag{2.23}$$

$$\text{where} \quad T^{(2)}_{\alpha\ldots} = (-1)^n T^{(1)}_{\alpha\ldots} \quad \text{for the n}^{\text{th}}\text{ rank T-tensor}, \tag{2.24}$$

since the vector R_α always lies in the direction from molecule 1 to molecule 2. It follows from (2.24), that for second and fourth rank T-tensors the superscript may be omitted, but for third rank T-tensors the superscript must be specified to accommodate the change in sign. In this work, for simplicity, we will adopt the following notation for third rank T-tensors:

$$T_{\alpha\beta\gamma} = T^{(1)}_{\alpha\beta\gamma} = -T^{(2)}_{\alpha\beta\gamma}. \tag{2.25}$$

For non-polar molecules, $U_{\mu,\mu}$, $U_{\mu,\theta}$ and $U_{\mu,\text{ind}\,\mu}$ are all identically zero.

2.3.1   Linear molecules

In order to determine the explicit forms of the potentials in equations (2.10) to (2.15) for linear molecules it is necessary to express the molecular property tensors in terms of the angles specifying their relative configurations. Figure 2.1 shows molecules 1 and 2 with their respective systems of axes. As was stated in Section 2.1, molecular properties are usually expressed in terms of molecule fixed axes to exploit the symmetry of the molecule. It is then necessary to project these property tensors into the space fixed axes O(X,Y,Z). Unit vectors, $\ell^{(1)}_\alpha$ and $\ell^{(2)}_\alpha$ along the principal axes of molecules 1 and 2, respectively, and

λ_α along the line of centres $\mathbf{R}$, are related to the angles θ_1, θ_2 and ϕ describing the relative configuration τ of the pair of interacting molecules as follows:

$$\ell_\alpha^{(1)} \lambda_\alpha = \cos \theta_1, \tag{2.26}$$

$$\ell_\alpha^{(2)} \lambda_\alpha = -\cos \theta_2, \tag{2.27}$$

$$\ell_\alpha^{(1)} \ell_\alpha^{(2)} = \cos \theta_{12} = -\cos \theta_1 \cos \theta_2 + \sin \theta_1 \sin \theta_2 \cos \phi. \tag{2.28}$$

Buckingham [26] has demonstrated how the property tensors of an axially symmetric molecule p may be expressed in terms of $\ell_\alpha^{(p)}$:

$$\mu_\alpha^{(p)} = \mu \ell_\alpha^{(p)}, \qquad \text{where} \quad \mu = \mu_3^{(1)} = \mu_{3'}^{(2)}; \tag{2.29}$$

$$\theta_{\alpha\beta}^{(p)} = \tfrac{1}{2} \theta \left(3 \ell_\alpha^{(p)} \ell_\beta^{(p)} - \delta_{\alpha\beta} \right), \qquad \text{where} \quad \theta = \begin{cases} \theta_{33}^{(1)} = -2\theta_{22}^{(1)} = -2\theta_{11}^{(1)} \\ \theta_{3'3'}^{(2)} = -2\theta_{2'2'}^{(2)} = -2\theta_{1'1'}^{(2)} \end{cases}. \tag{2.30}$$

Also, by definition,

$$R_\alpha = R\lambda_\alpha. \tag{2.31}$$

Using the coordinate system in Figure 2.1, the electrostatic and induction potentials for linear molecules are [26]:

$$U_{\mu,\mu} = \frac{1}{4\pi\varepsilon_0} \left\{ \frac{\mu^2}{R^3} \left(2\cos\theta_1 \cos\theta_2 + \sin\theta_1 \sin\theta_2 \cos\phi \right) \right\}, \tag{2.32}$$

$$U_{\mu,\theta} = \frac{1}{4\pi\varepsilon_0} \left\{ \frac{3}{2} \frac{\mu\theta}{R^4} \left[\cos\theta_1 \left(3\cos^2\theta_2 - 1 \right) + \cos\theta_2 \left(3\cos^2\theta_1 - 1 \right) \right. \right.$$
$$\left. \left. +2\sin\theta_1 \sin\theta_2 \cos\theta_2 \cos\phi + 2\sin\theta_1 \cos\theta_1 \sin\theta_2 \cos\phi \right] \right\}, \tag{2.33}$$

$$U_{\theta,\theta} = \frac{1}{4\pi\varepsilon_0} \left\{ \frac{3}{4} \frac{\theta^2}{R^5} \left(1 - 5\cos^2\theta_1 - 5\cos^2\theta_2 + 17\cos^2\theta_1 \cos^2\theta_2 \right. \right.$$
$$\left. \left. +2\sin^2\theta_1 \sin^2\theta_2 \cos^2\phi + 16\sin\theta_1 \cos\theta_1 \sin\theta_2 \cos\theta_2 \cos\phi \right) \right\}, \tag{2.34}$$

$$U_{\mu,\text{ind}\,\mu} = \frac{1}{(4\pi\varepsilon_0)^2} \left\{ -\frac{1}{2} \frac{a\mu^2}{R^6} \left[\left(3\cos^2\theta_1 - 1 \right) + \left(3\cos^2\theta_2 - 1 \right) \right] \right\}, \tag{2.35}$$

$$U_{\theta,\text{ind}\,\mu} = \frac{1}{(4\pi\varepsilon_0)^2} \left\{ -\frac{9}{8} \frac{a\theta^2}{R^8} \left(4\cos^4\theta_1 + 4\cos^4\theta_2 + \sin^4\theta_1 + \sin^4\theta_2 \right) \right\}, \tag{2.36}$$

26

$$U_{\text{ind}\,\mu,\text{ind}\,\mu} = \frac{1}{(4\pi\varepsilon_0)^3} \left\{ \frac{a^2\mu^2}{R^9} \left(8\cos\theta_1\cos\theta_2 + \sin\theta_1\sin\theta_2\cos\phi \right) \right\}. \tag{2.37}$$

It should be noted that $U_{\mu,\text{ind}\,\mu}$ has been written so that its unweighted orientational average is zero (i.e. so that it is purely orientational). The part of $U_{\mu,\text{ind}\,\mu}$ which is independent of orientation is assumed to be incorporated in the $\left(\frac{R_0}{R}\right)^6$ term of the Lennard-Jones potential [96]

2.3.2 Non-linear molecules

For polar molecules of C_2, C_{2v} and higher symmetries with the 3-axis along the principal molecular axis, the dipole moment has only one independent component [26]:

$$\mu_i^{(1)} = \mu_{i'}^{(2)} = \begin{bmatrix} 0 & 0 & \mu \end{bmatrix}, \tag{2.38}$$

while for molecules with C_{2v}, D_2 and D_{2h} and higher symmetries, the traceless quadrupole moment has two independent components [26]:

$$\theta_{ij}^{(1)} = \theta_{i'j'}^{(2)} = \begin{bmatrix} \theta_1 & 0 & 0 \\ 0 & \theta_2 & 0 \\ 0 & 0 & -(\theta_1 + \theta_2) \end{bmatrix}. \tag{2.39}$$

Referring the T-Tensors to the space-fixed axes (x,y,z) is simple, since R is fixed along the z-axis initially. Thus the second-rank tensor, defined in (2.18), becomes

$$T_{\alpha\beta} = \frac{1}{4\pi\varepsilon_0} \frac{1}{R^3} \begin{bmatrix} -1 & 0 & 0 \\ 0 & -1 & 0 \\ 0 & 0 & 2 \end{bmatrix}. \tag{2.40}$$

Similarly, the third-rank T-tensor becomes

$$T_{1\beta\gamma} = \frac{3}{4\pi\varepsilon_0} \frac{1}{R^3} \begin{bmatrix} 0 & 0 & -1 \\ 0 & 0 & 0 \\ -1 & 0 & 0 \end{bmatrix}, \quad T_{2\beta\gamma} = \frac{3}{4\pi\varepsilon_0} \frac{1}{R^3} \begin{bmatrix} 0 & 0 & 0 \\ 0 & 0 & -1 \\ 0 & -1 & 0 \end{bmatrix}, \quad T_{3\beta\gamma} = \frac{3}{4\pi\varepsilon_0} \frac{1}{R^3} \begin{bmatrix} -1 & 0 & 0 \\ 0 & -1 & 0 \\ 0 & 0 & 2 \end{bmatrix}.$$
$$\tag{2.41}$$

The components of the electrostatic and induction potentials are referred to the space-fixed axes. Thus, the dipole and quadrupole moments need to be projected from their respective molecule-fixed axes to the space-fixed axes as follows:

$$\mu_\alpha^{(1)} = a_i^\alpha \mu_i^{(1)}, \qquad\qquad \mu_\alpha^{(2)} = a_{i'}^\alpha \mu_{i'}^{(2)}; \tag{2.42}$$

$$\theta_{\alpha\beta}^{(1)} = a_i^\alpha a_j^\beta \theta_{ij}^{(1)}, \qquad\qquad \theta_{\alpha\beta}^{(2)} = a_{i'}^\alpha a_{j'}^\beta \theta_{i'j'}^{(2)}. \qquad (2.43)$$

To simplify the resulting expressions, the direction cosines may be written as

$$a_i^\alpha = \begin{bmatrix} A_1 & A_2 & A_3 \\ A_4 & A_5 & A_6 \\ A_7 & A_8 & A_9 \end{bmatrix}, \qquad\qquad a_{i'}^\alpha = \begin{bmatrix} B_1 & B_2 & B_3 \\ B_4 & B_5 & B_6 \\ B_7 & B_8 & B_9 \end{bmatrix}, \qquad (2.44)$$

where

$$A_1 = \cos\alpha_1 \cos\beta_1 \cos\gamma_1 - \sin\alpha_1 \sin\gamma_1,$$
$$(2.45)$$
$$B_1 = \cos\alpha_2 \cos\beta_2 \cos\gamma_2 - \sin\alpha_2 \sin\gamma_2,$$

$$A_2 = \sin\alpha_1 \cos\beta_1 \cos\gamma_1 + \cos\alpha_1 \sin\gamma_1,$$
$$(2.46)$$
$$B_2 = \sin\alpha_2 \cos\beta_2 \cos\gamma_2 + \cos\alpha_2 \sin\gamma_2,$$

$$A_3 = -\sin\beta_1 \cos\gamma_1,$$
$$(2.47)$$
$$B_3 = -\sin\beta_2 \cos\gamma_2,$$

$$A_4 = -\cos\alpha_1 \cos\beta_1 \sin\gamma_1 - \sin\alpha_1 \cos\gamma_1,$$
$$(2.48)$$
$$B_4 = -\cos\alpha_2 \cos\beta_2 \sin\gamma_2 - \sin\alpha_2 \cos\gamma_2,$$

$$A_5 = -\sin\alpha_1 \cos\beta_1 \sin\gamma_1 + \cos\alpha_1 \cos\gamma_1,$$
$$(2.49)$$
$$B_5 = -\sin\alpha_2 \cos\beta_2 \sin\gamma_2 + \cos\alpha_2 \cos\gamma_2,$$

$$A_6 = \sin\beta_1 \sin\gamma_1,$$
$$(2.50)$$
$$B_6 = \sin\beta_2 \sin\gamma_2,$$

$$A_7 = \cos\alpha_1 \sin\beta_1,$$
$$(2.51)$$
$$B_7 = \cos\alpha_2 \sin\beta_2,$$

$$A_8 = \sin\alpha_1 \sin\beta_1,$$
$$(2.52)$$
$$B_8 = \sin\alpha_2 \sin\beta_2,$$

$$A_9 = \cos\beta_1,$$
$$(2.53)$$
$$B_9 = \cos\beta_2.$$

Hence, for interacting non-linear C_{2v} and D_{2h} molecules in the coordinate system shown in Figure 2.2 [9]:

$$U_{\mu,\mu} = \frac{\mu_3^2}{(4\pi\varepsilon_0)R^3}\left\{A_3B_3 + A_6B_6 - 2A_9B_9\right\}, \tag{2.54}$$

$$
\begin{aligned}
U_{\mu,\theta} = \frac{\mu_3}{(4\pi\varepsilon_0)R^4}\Big\{&\theta_1\left[A_9(-B_1^2 + B_3^2 - B_4^2 + B_6^2 + 2B_7^2 - 2B_9^2)\right.\\
&+ 2B_3(A_1A_7 - A_3A_9) + 2B_6(A_4A_7 - A_6A_9) - 2B_7(A_3B_1 + A_6B_4)\\
&+ \left.B_9(A_1^2 - A_3^2 + A_4^2 - A_6^2 - 2A_7^2 + 2A_9^2 + 2A_3B_3 + 2A_6B_6)\right]\\
&+ \theta_2\left[A_9(-B_2^2 + B_3^2 - B_5^2 + B_6^2 + 2B_8^2 - 2B_9^2) + 2B_3(A_2A_8 - A_3A_9)\right.\\
&+ 2B_6(A_5A_8 - A_6A_9) - 2B_8(A_3B_2 + A_6B_5)\\
&+ \left.B_9(A_2^2 - A_3^2 + A_5^2 - A_6^2 - 2A_8^2 + 2A_9^2 + 2A_3B_3 + 2A_6B_6)\right]\Big\},
\end{aligned}
\tag{2.55}
$$

$$
\begin{aligned}
U_{\theta,\theta} = \frac{1}{3(4\pi\varepsilon_0)R^5}\Big\{&\theta_1^2\left[B_1^2(3A_1^2 - 3A_3^2 + A_4^2 - A_6^2 - 4A_7^2 + 4A_9^2) + B_3^2(-3A_1^2\right.\\
&+ 3A_3^2 - A_4^2 + A_6^2 + 4A_7^2 - 4A_9^2) + B_4^2(A_1^2 - A_3^2 + 3A_4^2 - 3A_6^2 - 4A_7^2 + 4A_9^2)\\
&+ 4(A_3A_6 - A_1A_4)(B_3B_6 - B_1B_4) + B_6^2(-A_1^2 + A_3^2 - 3A_4^2 + 3A_6^2 + 4A_7^2\\
&- 4A_9^2) + 4(A_1^2 - A_3^2 + A_4^2 - A_6^2 - 2A_7^2 + 2A_9^2)(B_9 - B_7)(B_9 + B_7)\\
&- \left.16(A_3A_9 - A_1A_7)(B_3B_9 - B_1B_7) - 16(A_6A_9 - A_4A_7)(B_6B_9 - B_4B_7)\right]\\
&+ \theta_2^2\left[B_2^2(3A_2^2 - 3A_3^2 + A_5^2 - A_6^2 - 4A_8^2 + 4A_9^2) + B_3^2(-3A_2^2 + 3A_3^2\right.\\
&- A_5^2 + A_6^2 + 4A_8^2 - 4A_9^2) + B_5^2(A_2^2 - A_3^2 + 3A_5^2 - 3A_6^2 - 4A_8^2 + 4A_9^2)\\
&+ 4(A_3A_6 - A_2A_5)(B_3B_6 - B_2B_5) + B_6^2(-A_2^2 + A_3^2 - 3A_5^2 + 3A_6^2 + 4A_8^2\\
&- 4A_9^2) + 4(A_2^2 - A_3^2 + A_5^2 - A_6^2 - 2A_8^2 + 2A_9^2)(B_9 - B_8)(B_9 + B_8)\\
&- \left.16(A_3A_9 - A_2A_8)(B_3B_9 - B_2B_8) - 16(A_6A_9 - A_5A_8)(B_6B_9 - B_5B_8)\right]\\
&+ \theta_1\theta_2\left[B_1^2(3A_2^2 - 3A_3^2 + A_5^2 - A_6^2 - 4A_8^2 + 4A_9^2) + B_2^2(3A_1^2 - 3A_3^2 + A_4^2\right.\\
&- A_6^2 - 4A_7^2 + 4A_9^2) + B_3^2\left(-3(A_1^2 + A_2^2) + 6A_3^2 - A_4^2 - A_5^2 + 2A_6^2\right.\\
&+ \left.4(A_7^2 + A_8^2) - 8A_9^2\right) - 4B_1B_4(A_3A_6 - A_2A_5) + B_4^2(A_2^2 - A_3^2 + 3A_5^2\\
&- 3A_6^2 - 4A_8^2 + 4A_9^2) - 4B_2B_5(A_3A_6 - A_1A_4) + B_5^2(A_1^2 - A_3^2 + 3A_4^2 - 3A_6^2
\end{aligned}
$$

29

$$-4A_7^2 + 4A_9^2) + 4B_3B_6(2A_3A_6 - A_2A_5 - A_1A_4) + B_6^2\left(-A_1^2 - A_2^2 + 2A_3^2\right.$$

$$-3(A_4^2 + A_5^2) + 6A_6^2 + 4(A_7^2 + A_8^2) - 8A_9^2) + 16B_1B_7(A_3A_9 - A_2A_8)$$

$$+16B_4B_7(A_6A_9 - A_5A_8) - 4B_7^2(A_2^2 - A_3^2 + A_5^2 - A_6^2 - 2A_8^2 + 2A_9^2)$$

$$+16B_2B_8(A_3A_9 - A_1A_7) + 16B_5B_8(A_6A_9 - A_4A_7) - 4B_8^2(A_1^2 - A_3^2 + A_4^2$$

$$-A_6^2 - 2A_7^2 + 2A_9^2) - 16B_3B_9(2A_3A_9 - A_2A_8 - A_1A_7) - 16B_6B_9(2A_6A_9$$

$$-A_5A_8 - A_4A_7) + 4B_9^2\left(A_1^2 + A_2^2 + A_4^2 + A_5^2 - 2(A_3^2 + A_6^2 + A_7^2 + A_8^2)\right.$$

$$\left.\left.+4A_9^2)\right]\right\},\tag{2.56}$$

$$U_{\mu,\mathrm{ind}\,\mu} = \frac{a\mu_3^2}{2(4\pi\varepsilon_0)^2R^6}\left\{3A_9^2 + 3B_9^2 - 2\right\},\tag{2.57}$$

$$U_{\mathrm{ind}\,\mu,\mathrm{ind}\,\mu} = \frac{a}{2(4\pi\varepsilon_0)^2R^8}\left\{\theta_1^2\left[A_1^4 - 2A_1^2A_3^2 + A_3^4 + 2A_4^2(A_1^2 - A_3^2) + A_4^4 + 2A_6^2(-A_1^2\right.\right.$$

$$+A_3^2 - A_4^2) + A_6^4 + 4A_7^2(A_3^2 + A_6^2) + 4A_7^4 - 8A_7A_9(A_1A_3 + A_4A_6)$$

$$+4A_9^2(A_1^2 + A_4^2 - 2A_7^2) + 4A_9^4\big] + \theta_2^2\left[A_2^4 - 2A_2^2A_3^2 + A_3^4 + 2A_5^2(A_2^2 - A_3^2)\right.$$

$$+A_5^4 + 2A_6^2(-A_2^2 + A_3^2 - A_5^2) + A_6^4 + 4A_8^2(A_3^2 + A_6^2) + 4A_8^4$$

$$-8A_8A_9(A_2A_3 + A_5A_6) + 4A_9^2(A_2^2 + A_5^2 - 2A_8^2) + 4A_9^4\big]$$

$$+2\theta_1\theta_2\left[A_1^2A_2^2 - A_3^2(A_1^2 + A_2^2) + A_3^4 + A_4^2(A_2^2 - A_3^2) + A_5^2(A_1^2 - A_3^2\right.$$

$$+A_4^2) - A_6^2(A_1^2 + A_2^2 - 2A_3^2 + A_4^2 + A_5^2) + A_6^4 + 2A_7^2(-A_2^2 + A_3^2$$

$$-A_5^2 + A_6^2) + 4A_7A_8(A_1A_2 + A_4A_5) + 2A_8^2(-A_1^2 + A_3^2 - A_4^2 + A_6^2$$

$$+2A_7^2) - 4A_9\left[A_7(A_1A_3 + A_4A_6) + A_8(A_2A_3 + A_5A_6)\right]$$

$$\left.\left.+2A_9^2(A_1^2 + A_2^2 + A_4^2 + A_5^2 - 2A_7^2 - 2A_8^2) + 4A_9^4\big]\right\}.\tag{2.58}$$

Here, as for linear molecules (Section 2.3.1), the unweighted orientational average of $U_{\mu,\mathrm{ind}\,\mu}$ is zero, with the orientation-independent part assumed to be accounted for in U_{LJ}. The tensor facilities of the Macsyma algebraic manipulation package were used to determine the terms above. When used in numerical integration, the resulting expressions were converted directly to Fortran by Macsyma, eliminating the typographical errors possible when programming manually.

These expressions describe the interactions of molecules with C_{2v} and higher symme-

tries and are generally applicable to linear or spherical molecules by appropriate simplification of the multipole moment components. A powerful test of the computer programs used later is to check that both sets of equations yield the same results when the simple tensor forms for axially symmetric molecules are used in the more general expressions. Agreement to within at least four significant figures was always obtained.

Now that exact expressions have been determined for all the components of the intermolecular potential energy, they may be used to calculate all of the second virial coefficients. The second pressure virial coefficient will be considered first, since it has the simplest form and the largest volume of experimental data of proven accuracy available for any second virial coefficient. For these reasons, it has historically been employed to fit the Lennard-Jones and shape parameters used in U_{LJ} and U_{shape}.

Chapter 3

The Second Pressure Virial Coefficient, $B(T)$

The ideal gas law, $PV = nRT$, decribes the relationship between pressure, volume and temperature (P-V-T) for a sample of n moles of an ideal gas. For one mole of an ideal gas $PV_m = RT$. The virial equation of state describes the departure from this ideal behaviour of a real gas [1]:

$$\frac{PV_m}{RT} = 1 + \frac{B(T)}{V_m} + \frac{C(T)}{V_m^2} + \cdots , \tag{3.1}$$

where B, C, ... are called the second, third, ... virial coefficients, or pressure virial coefficients. In order to describe the P-V-T behaviour of a particular gas completely it is necessary to know the values of these virial coefficients.

It can be shown [95] that

$$B(T) = -\frac{N_A}{2V_m} \left[\int_{r_1} \int_{r_2} e^{-\frac{U_{12}(\tau)}{kT}} dr_1 dr_2 - V_m^2 \right], \tag{3.2}$$

where dr_1 is the volume element in space at the position of molecule 1 in a Cartesian coordinate system, and dr_2 is the corresponding volume element for molecule 2. Now,

$$\int_{r_1} \int_{r_2} dr_1 dr_2 = V.V = V_m^2. \tag{3.3}$$

Therefore, equation (3.2) may be written as:

$$B(T) = \frac{N_A}{V_m} \int_{r_1} \int_{r_2} \left(1 - e^{-\frac{U_{12}(\tau)}{kT}} \right) dr_1 dr_2 \tag{3.4}$$

or, in terms of τ, the relative configuration of molecules 1 and 2,

$$B(T) = \frac{N_A}{2} \int_\tau \left(1 - e^{-\frac{U_{12}(\tau)}{kT}}\right) d\tau, \tag{3.5}$$

which is the general form of the integral. Note that the factor $\frac{1}{V_m}$ has been cancelled out because $\int d\boldsymbol{r}_1 = V_m$.

3.1 $B(T)$ for spherical molecules

For spherical molecules, the pair interaction energy, U_{12}, depends only on the separation, $R = |\boldsymbol{r}_1 - \boldsymbol{r}_2|$, of the molecules so the integral $\int d\tau$ can be replaced by $4\pi R^2 dR$. As R approaches infinity, U_{12} tends towards zero and $e^{-\frac{U_{12}}{kT}}$ approaches unity. Therefore, the integrand in equation (3.5) becomes zero for large separations and the upper limit of the integral may be set to infinity. The expression for $B(T)$ for spherical molecules becomes

$$B(T) = 2\pi N_A \int_{R=0}^{\infty} \left(1 - e^{-\frac{U_{12}(\tau)}{kT}}\right) R^2 dR. \tag{3.6}$$

In practice, for all gases treated here, numerical calculation of $B(T)$ shows that for separations larger than 3 nm the integrand is negligible.

3.2 $B(T)$ for linear molecules

In order to describe the relative configuration, τ, between two interacting non-spherical molecules, it is necessary to consider angular coordinates defining the orientation of the two molecules, as well as the separation between them. When these angular coordinates are included in the integral for $B(T)$ a normalisation factor, Ω, must be introduced, resulting in the following expression for the second pressure coefficient [95]:

$$B(T) = \frac{2\pi N_A}{\Omega^2} \iiint \left(1 - e^{-\frac{U_{12}(\tau)}{kT}}\right) R^2 \, dR \, d\boldsymbol{\omega}_1 \, d\boldsymbol{\omega}_2, \tag{3.7}$$

where $\boldsymbol{\omega}_1$ and $\boldsymbol{\omega}_2$ are the angular configurations of molecule 1 and molecule 2, respectively. The value of the normalisation factor, Ω, is determined by the number of angular variables required to specify completely the orientation of a molecule relative to fixed axes. For linear molecules, the molecular orientation can be described fully by two angles, θ_i and ϕ_i, therefore [95]

$$d\boldsymbol{\omega}_i = \sin\theta_i \, d\theta_i \, d\phi_i \qquad \text{and} \qquad \Omega = 4\pi. \tag{3.8}$$

Substituting (3.8) into (3.7) yields [96]

$$B(T) = \frac{N_A}{8\pi} \int\limits_{R=0}^{\infty} \int\limits_{\theta_1=0}^{\pi} \int\limits_{\theta_2=0}^{\pi} \int\limits_{\phi_1=0}^{2\pi} \int\limits_{\phi_2=0}^{2\pi} \left(1 - e^{-\frac{U_{12}}{kT}}\right) R^2 \sin\theta_1 \sin\theta_2 \, dR \, d\theta_1 d\theta_2 d\phi_1 d\phi_2, \quad (3.9)$$

where $U_{12} \equiv U_{12}(\tau)$.

However, it is unnecessary to retain both ϕ_1 and ϕ_2 separately, and they may be replaced by a single angle $\phi = \phi_1 - \phi_2$. Figure 2.1 [26] on page 18 shows how the angles, θ_1, θ_2 and ϕ, and the separation, $\mathbf{R}$, specify the relative configuration, τ, of a pair of interacting linear molecules [26].

By replacing ϕ_1 and ϕ_2 with ϕ in equation (3.9), the 5-variable integral simplifies to a 4-variable integral, which must be multiplied by 2π. Thus, (3.9) becomes the well known expression for the second pressure virial coefficient for linear molecules [56, 95, 106]

$$B(T) = \frac{N_A}{8\pi} \int\limits_{R=0}^{\infty} \int\limits_{\theta_1=0}^{\pi} \int\limits_{\theta_2=0}^{\pi} \int\limits_{\phi=0}^{2\pi} \left(1 - e^{-\frac{U_{12}(\tau)}{kT}}\right) R^2 \sin\theta_1 \sin\theta_2 \, dR \, d\theta_1 \, d\theta_2 \, d\phi. \quad (3.10)$$

It can be seen from equations (3.6) and (3.10) that the second pressure virial coefficient of a gas depends on U_{12}. In order to calculate $B(T)$, it is necessary to know the pair interaction energy. On the other hand, measurements of $B(T)$ yield information about the nature of U_{12}. The explicit form of the intermolecular potential energy has been discussed in Chapter 2.

3.3 $B(T)$ for non-linear molecules

In (3.7), which gives $B(T)$ for non-spherical molecules, $\boldsymbol{\omega}_i$ is the angular configuration of molecule i and the value of the normalisation factor, Ω, is determined by the number of angular variables required to specify the orientation of a molecule completely. For non-linear molecules, the molecular orientation can be described fully by three angles, α, β and γ (Section 2.1.2), therefore [95]

$$d\boldsymbol{\omega} = \sin\beta \, d\alpha \, d\beta \, d\gamma, \qquad \text{and} \qquad \Omega = 8\pi^2. \quad (3.11)$$

Substituting (3.11) into (3.7) yields [9]

$$B(T) = \frac{N_A}{32\pi^2} \int\limits_{R=0}^{\infty} \int\limits_{\alpha_1=0}^{2\pi} \int\limits_{\beta_1=0}^{\pi} \int\limits_{\gamma_1=0}^{2\pi} \int\limits_{\alpha_2=0}^{2\pi} \int\limits_{\beta_2=0}^{\pi} \int\limits_{\gamma_2=0}^{2\pi} \left(1 - e^{-\frac{U_{12}(\tau)}{kT}}\right)$$

$$\times R^2 \sin\beta_1 \sin\beta_2 \, dR \, d\alpha_1 d\beta_1 d\gamma_1 d\alpha_2 d\beta_2 d\gamma_2. \qquad (3.12)$$

3.4 Summary of experimental work on the second pressure virial coefficient

Extensive experimental research has been carried out by numerous workers to determine the second and third pressure virial coeffients of a comprehensive range of gases and their mixtures. In 1980, Dymond and Smith [1] published a comprehensive compilation of experimental values of both $B(T)$ and $C(T)$. Where there is good agreement between the results of different authors for the same gas, they present a best-fit of the data over as wide a temperature range as possible. Tables A.1, A.2 and A.3 in Appendix A show experimental values of $B(T)$ for various gases over a range of temperatures, taken from Dymond and Smith's [1] best-fit data. This tabulation is limited to gases which are to be investigated in this study.

It can be seen from Tables A.1 to A.3 that values for $B(T)$ are predominantly negative. It is also apparent that $B(T)$ becomes less negative (and in some cases becomes positive) as the temperature increases. It is possible to explain this tendency through the intermolecular potential [106]. When the temperature is low, the mean energies of the molecules in the gas are of the same order of magnitude as the depth of the potential energy well, resulting in an increase in the attractive forces between interacting molecules. This increase in attraction causes a corresponding decrease in pressure, giving rise to a negative value for the second pressure virial coefficient. At high temperatures the average energies of the molecules increase and become large in comparison with the maximum energy of attraction and so the predominant contribution to the second virial coefficient is that due to the repulsive portion of the potential [95, 106, 107]. The increased repulsion between molecules results in an increase in pressure and consequently, $B(T)$ becomes positive.

Sometimes, at high temperatures, molecules may collide with such great force that some interpenetration is possible. When this occurs the effective molecular volume decreases. At very high temperatures, the number of such collisions may become significant, and the resultant decrease in the molar volume causes a decrease in $B(T)$ [106]. An example of a molecule where this behaviour is observed is Helium [108], as can be

seen in Table A.1.

There are several different experimental methods for measuring $B(T)$ of gases and their mixtures. Pool *et al.* [109] and Orcutt and Cole [13], amongst others, have described methods which make use of the direct measurements of P, V and T. Orcutt and Cole's cyclic expansion method [13] has subsequently been used by Sutter and Cole [2], Bose and Cole [40] and Copeland and Cole [110]. Another method of measuring $B(T)$ is the differential method, described by McGlashan and Potter [111]. In this procedure, the behaviour of the relevant gas is compared with that of another appropriate gas with almost ideal properties. $B(T)$ may also be measured using gas adsorption, or it may be derived from other measured properties of the gas; for example, the Joule-Thomson coefficient [95].

It was shown in Section 3.2, that the value of $B(T)$ is determined by the intermolecular potential energy U_{12}. Thus, an important application of the second pressure virial coefficient is in the study of the pair interaction potential [27,106]. Unfortunately, second pressure virial coefficients on their own are not sufficient to evaluate all the parameters involved in pair interactions unambiguously, since they are not very sensitive to non-spherical potentials [97]. Many authors seeking to evaluate molecular interaction parameters investigate the second dielectric virial coefficient, B_ε, and $B(T)$ simultaneously [2, 3, 37, 40, 42, 97, 110, 112], because B_ε is extremely sensitive to the form of the intermolecular potential [2,3,11,49]. In order to determine the most reliable model of the intermolecular potential, B_ε and $B(T)$ are calculated for a variety of potentials and the results are compared with experimental values [2, 3, 12, 13, 40, 56, 96, 97, 110, 113–115].

Chapter 4

The Second Dielectric Virial Coefficient, B_ε

The pressure dependence of the static dielectric constant of a compressed gas is a potential source of information about molecular interactions. As with other equilibrium properties, a theory can be developed to relate the second and higher-order virial coefficients to the molecular interaction energy. The second, third, ... virial coefficients can be related to the properties of a group of one, two, three, ... molecules respectively [101]

The theory of the second dieletric virial coefficient was first examined in detail by Buckingham and Pople [28, 101] in 1955. Prior to that Harris and Alder [116–118] had developed formulae for the density-dependence of the dielectric constant for polar substances from some simple force fields, using the Onsager [119] model for estimating the mean dipole moment of a molecule. This equation was not yet in the virial form which has since become the preferred method for treating molecular interaction effects. Buckingham and Pople [101] were the first to show that it was possible to draw more general and systematic conclusions about molecular interactions if one dealt only with the initial deviation from ideal gas behaviour. In the first approximation they considered a rigid dipole model for polar molecules with a Stockmayer [120] type potential, consisting of the Lennard-Jones potential and the dipole-dipole interaction energy (See Chapter 2) . The role of molecular polarizability was then estimated by comparing the earlier results with those attained by extending the theory to consider a polarizable dipole model [101]. They also examined separately the effect of including the permanent quadrupole moment of the molecules in the intermolecular potential, as well as considering the effect of its shape. The various effects were considered separately due to the difficulty involved in performing the integration of the algebraic expressions, but the relative importance of the various contributions was established.

In the comprehensive treatment which follows, the most general intermolecular potential to quadrupole order and including polarizability and shape effects is used, dipole-

induced-dipole contributions are taken to the highest orders necessary to establish convergence, whilst the field gradient effects in the interactions are also included.

If we consider an assembly of N_A identical molecules placed in a uniform external field, $\boldsymbol{E}_0$, then the electric displacement, $\boldsymbol{D}_i$, inside the sample is related to the macroscopic internal field, $\boldsymbol{E}_i$, and the dipole moment per unit volume, $\boldsymbol{P}_i$, as follows:

$$\boldsymbol{D}_i = \varepsilon_0 \boldsymbol{E}_i + \boldsymbol{P}_i, \tag{4.1}$$

where ε_0 is the permittivity of a vacuum. Now, since $\boldsymbol{D}_i = \varepsilon_r \varepsilon_0 \boldsymbol{E}_i$, where ε_r is the dielectric constant, (4.1) can be written as:

$$\varepsilon_0 \left(\varepsilon_r - 1 \right) = \frac{\boldsymbol{P}_i}{\boldsymbol{E}_i}. \tag{4.2}$$

In order to develop the theory of dielectric virial coefficients, it is necessary to evaluate $\frac{\boldsymbol{P}_i}{\boldsymbol{E}_i}$ using statistical mechanics. However, because $\boldsymbol{E}_i$ is an averaged quantity it is not suitable as a statistical-mechanical parameter, and it is usually expressed in terms of the external field, $\boldsymbol{E}_0$, which is an independent variable. The relationship between $\boldsymbol{E}_i$ and $\boldsymbol{E}_0$ is determined by the sample shape under consideration, so it is necessary to specify the shape of the sample. Fortunately, since ε_r is a shape-independent property of a gas, it is possible to consider the simplest case of a spherical sample [121] without loss of generality. From classical electrostatics, the general result for an isolated spherical sample is

$$\boldsymbol{E}_i = \frac{3}{\varepsilon_r + 2} \boldsymbol{E}_0. \tag{4.3}$$

Substituting (4.3) into (4.2) yields

$$\frac{\varepsilon_r - 1}{\varepsilon_r + 2} = \frac{1}{3\varepsilon_0} \left(\frac{\boldsymbol{P}_i}{\boldsymbol{E}_0} \right). \tag{4.4}$$

Since saturation effects are usually negliglible under experimental conditions, it is possible to evaluate $\left(\frac{\boldsymbol{P}_i}{\boldsymbol{E}_0} \right)$ in the limit of zero field, and

$$\lim_{E_0 \to 0} \left(\frac{\boldsymbol{P}_i}{\boldsymbol{E}_0} \right) = \frac{1}{V_m} \left(\frac{\partial \overline{\boldsymbol{M}}}{\partial E_0} \right)_{E_0 = 0}, \tag{4.5}$$

where $\overline{\boldsymbol{M}}(E_0)$ is the total mean moment of the sample. In an isotropic fluid, $\overline{\boldsymbol{M}}(E_0)$ is parallel to $\boldsymbol{E}_0$. When (4.5) is substituted into (4.4), we get the total polarization, or

Claussius-Mossotti function [28],

$$_T P = \frac{\varepsilon_r - 1}{\varepsilon_r + 2} V_m = \frac{1}{3\varepsilon_0} \left(\frac{\partial \overline{M}}{\partial E_0} \right)_{E_0=0}. \tag{4.6}$$

The average moment is given by the statistical mechanical expression

$$\overline{M}(E_0) = \frac{\int M(\Gamma, E_0).e \, e^{-\frac{V(\Gamma, E_0)}{kT}} d\Gamma}{\int e^{-\frac{V(\Gamma, E_0)}{kT}} d\Gamma}, \tag{4.7}$$

where e is a unit vector in the direction of E_0 and Γ represents all the coordinates (translational and rotational) of all the molecules. $V(\Gamma, E_0)$ is the potential energy of the system and $\left(\frac{\partial V(\Gamma, E_0)}{\partial E_0} \right)_{E_0=0} = -M(\Gamma, 0).e$.

Carrying out the differentiation of (4.7) and letting $E_0 \to 0$ yields

$$\left(\frac{\partial \overline{M}}{\partial E_0} \right)_{E_0=0} = \left\langle \frac{\partial M(\Gamma, E_0)}{\partial E_0}.e \right\rangle + \frac{1}{kT} \left\langle \{M(\Gamma, 0).e\} \{M(\Gamma, 0).e\} \right\rangle$$

$$- \frac{1}{kT} \left\langle M(\Gamma, 0).e \right\rangle \left\langle M(\Gamma, 0).e \right\rangle, \tag{4.8}$$

where $\langle X \rangle$ represents the statistical-mechanical average of X in the absence of an external field. Now, since the sample under consideration is isotropic [122],

$$\left\langle \{M(\Gamma, 0).e\} \{M(\Gamma, 0).e\} \right\rangle = \tfrac{1}{3} \left\langle M(\Gamma, 0)^2 \right\rangle$$

$$\text{and} \quad \left\langle M(\Gamma, 0).e \right\rangle = 0, \tag{4.9}$$

so that (4.8) simplifies to

$$\left(\frac{\partial \overline{M}}{\partial E_0} \right)_{E_0=0} = \left\langle \frac{\partial M(\Gamma, E_0)}{\partial E_0}.e \right\rangle + \frac{1}{3kT} \left\langle M(\Gamma, 0)^2 \right\rangle. \tag{4.10}$$

If (4.10) is substituted into (4.6), we obtain

$$_T P = \frac{\varepsilon_r - 1}{\varepsilon_r + 2} V_m = \frac{1}{3\varepsilon_0} \left\{ \left\langle \frac{\partial M(\Gamma, E_0)}{\partial E_0}.e \right\rangle + \frac{1}{3kT} \left\langle M(\Gamma, 0)^2 \right\rangle \right\}, \tag{4.11}$$

which, since the sample is composed of identical molecules, may be written as follows:

$$_T P = \frac{\varepsilon_r - 1}{\varepsilon_r + 2} V_m = \frac{N_A}{3\varepsilon_0} \left\{ \left\langle \frac{\partial \mu^{(1)}}{\partial E_0}.e \right\rangle + \frac{1}{3kT} \sum_{i=1}^{N_A} \left\langle \mu^{(1)}.\mu^{(i)} \right\rangle \right\}, \tag{4.12}$$

where $\boldsymbol{\mu}^{(i)}$ is the dipole moment of the ith molecule.

The two terms on the right-hand side of equation (4.12) each have a distinct physical interpretation. The first term is a result of polarization of the molecules by the applied field. The second term originates from the natural inclination of the molecular dipole moments to align themselves spontaneously in the direction of the external field, in order to assume lower energy positions. For molecules with permanent dipole moments, the second term is the most significant. However, this second term is not necessarily zero for non-polar molecules, since it is possible for moments to be induced in individual molecules.

The Claussius-Mossotti function may be expanded in inverse powers of the molar volume [28] to yield

$$_{T}P = \frac{\varepsilon_r - 1}{\varepsilon_r + 2}V_m = A_\varepsilon + \frac{B_\varepsilon}{V_m} + \frac{C_\varepsilon}{V_m^2} + \cdots , \qquad (4.13)$$

where A_ε, B_ε and C_ε are the first, second and third dielectric virial coefficients, respectively. The value of A_ε is obtained by allowing V_m to tend to zero. Therefore, from (4.12),

$$A_\varepsilon = \frac{N_A}{3\varepsilon_0}\left(a_0 + \frac{\mu_0^2}{3kT}\right), \qquad (4.14)$$

where a_0 is the mean static polarizability of an isolated molecule and μ_0 is the permanent dipole moment of an isolated molecule. From equations (4.12), (4.13) and (4.14), it follows that the second virial coefficient is given by

$$B_\varepsilon = \lim_{V_m \to \infty} \left\{ V_m \left[\frac{\varepsilon_r - 1}{\varepsilon_r + 2}V_m - A_\varepsilon \right] \right\}$$

$$= \frac{N_A^2}{3\varepsilon_0\Omega} \int_\tau \left\{ \left[\frac{\partial \boldsymbol{\mu}^{(1)}}{\partial E_0}.e - a_0 \right] + \frac{1}{3kT}\left[\boldsymbol{\mu}^{(1)}.(\boldsymbol{\mu}^{(1)} + \boldsymbol{\mu}^{(2)}) - \mu_0^2 \right] \right\} e^{-\frac{U_{12}(\tau)}{kT}} d\tau$$

$$= \frac{N_A^2}{3\varepsilon_0\Omega} \int_\tau \left\{ \left[\frac{1}{2}\frac{\partial(\boldsymbol{\mu}^{(1)} + \boldsymbol{\mu}^{(2)})}{\partial E_0}.e - a_0 \right] + \frac{1}{3kT}\left[\tfrac{1}{2}(\boldsymbol{\mu}^{(1)} + \boldsymbol{\mu}^{(2)})^2 - \mu_0^2 \right] \right\} e^{-\frac{U_{12}(\tau)}{kT}} d\tau,$$

$$(4.15)$$

where $\boldsymbol{\mu}_0$ is the permanent dipole moment of an isolated molecule, and $(\boldsymbol{\mu}^{(1)} + \boldsymbol{\mu}^{(2)})$ is the dipole moment of an interacting pair of molecules in the absence of a field.

In order to perform the integration in (4.15) to calculate B_ε, it is necessary to evaluate both the first distortion term (Section 4.1) and the second temperature-dependent orientation term (Section 4.2). Unfortunately, no simple general theory, which is applicable to all molecules at all intermolecular separations, exists for either term [122].

40

The theory of both terms is understood for large intermolecular separations (long-range limit), but complicated *ab initio* quantum mechanical calculations are required at very short range, where the the charge distributions of the molecules begin to overlap and they can no longer be treated as individual entities. In view of this difficulty, it is usual to assume [9, 28, 105, 122] that the two molecules preserve their individual identities, even where overlap occurs. The resulting expressions are used for the entire interaction range, including the overlap regions, and the interaction is described in terms of the properties of molecules 1 and 2. The effect of short-range contact forces on the intermolecular potential are handled separately, as discussed in Chapter 2.

4.1 Expression for $\left(\frac{\partial \boldsymbol{\mu}^{(1)}}{\partial E_0}.\boldsymbol{e} - a_0\right)$

The expression for $\left(\frac{\partial \mu^{(1)}}{\partial E_0}.\boldsymbol{e} - a_0\right)$ has been derived by various authors [122–124]. The treatment of Graham [122] is followed here because it is the most general.

The dipole moment $\mu_i^{(1)}$ of molecule 1 is partly due to the direct effect of the external field E_0, and partly a result of the fields and field gradients at molecule 1 due to the electric moments on molecule 2. Thus, the dipole moment of molecule 1 may be written as [26]:

$$\mu_i^{(1)} = \mu_{0i}^{(1)} + a_{ij}^{(1)}\left(E_{0j} + E_j^{(1)}\right) + \tfrac{1}{3}A_{ijk}^{(1)}E_{jk}^{(1)}, \tag{4.16}$$

where $\mu_{0i}^{(1)}$ is the permanent dipole moment of molecule 1, $E_j^{(1)}$ and $E_{jk}^{(1)}$ are the field and field gradient at molecule 1 due to molecule 2, $a_{ij}^{(1)}$ is the static polarizability of molecule 1, and $A_{ijk}^{(1)}$ is the property tensor which describes the dipole induced by an electric field gradient or the quadrupole induced by an electric field [26]. Since $\mu_i^{(1)}e_i$ will be differentiated with respect to E_0, only those components of (4.16) due to E_0 need be considered. For molecules with permanent moments the field $F_i^{(1)}$ at molecule 1 due to the permanent moments of molecule 2 may be strong enough to modify the effective polarizability of the first molecule. These modifications may be accounted for by including the static hyperpolarizability tensors b_{ijk} and g_{ijkl} [26, 34, 125]. In addition, the field gradient $F_{ij}^{(1)}$ at molecule 1 due to permanent moments on molecule 2 may modify the polarizability of molecule 1. In order to describe this effect, the term $\phi_{ijkl}^{(1)}F_{kl}^{(1)}$ is included in the effective polarizability. This modified polarizability, which may be referred to as the differential polarizability $p_{ij}^{(1)}$, is given by:

$$p_{ij}^{(1)} = a_{ij}^{(1)} + b_{ijk}^{(1)}F_k^{(1)} + \tfrac{1}{2}g_{ijkl}^{(1)}F_k^{(1)}F_l^{(1)} + \phi_{ijkl}^{(1)}F_{kl}^{(1)} + \cdots. \tag{4.17}$$

Thus, the dipole moment induced on molecule 1 may be written as:

$$\mu_i^{(1)}(E_0) = \left(a_{ij}^{(1)} + b_{ijk}^{(1)} F_k^{(1)} + \tfrac{1}{2} g_{ijkl}^{(1)} F_k^{(1)} F_l^{(1)} + \phi_{ijkl}^{(1)} F_{kl}^{(1)} + \cdots \right) \left(E_{0j} + \mathcal{F}_j^{(1)} \right)$$

$$+ \tfrac{1}{3} A_{ijk}^{(1)} \mathcal{F}_{jk}^{(1)} + \cdots , \tag{4.18}$$

where $\mathcal{F}_j^{(1)}$ and $\mathcal{F}_{jk}^{(1)}$ are the field and field gradient at molecule 1 due to the moments induced on molecule 2 by the external field E_0. The dipole moment $\mu_i^{(2)}$ induced on molecule 2 is given by an analogous expression.

Now, using the T-tensor notation described in equations (2.18) to (2.24) of Section 2.3, we can write:

$$\mathcal{F}_i^{(1)} = T_{ij}\mu_j^{(2)}(E_0) - \tfrac{1}{3} T_{ijk}\theta_{jk}^{(2)}(E_0) + \cdots , \tag{4.19}$$

$$\mathcal{F}_{ij}^{(1)} = T_{ijk}\mu_k^{(2)}(E_0) - \tfrac{1}{3} T_{ijkl}\theta_{kl}^{(2)}(E_0) + \cdots , \tag{4.20}$$

where $\theta_{jk}^{(2)}(E_0)$ is given by:

$$\theta_{jk}^{(2)}(E_0) = A_{ljk}^{(2)} \left(E_{0l} + \mathcal{F}_l^{(2)} \right) + \cdots + C_{jklm}^{(2)} \mathcal{F}_{lm}^{(2)} + \cdots , \tag{4.21}$$

$$\text{where} \quad \mathcal{F}_l^{(2)} = T_{lm}\mu_m^{(1)}(E_0) + \tfrac{1}{3} T_{lmn}\theta_{mn}^{(1)}(E_0) + \cdots , \tag{4.22}$$

$$\text{and} \quad \mathcal{F}_{lm}^{(2)} = -T_{lmn}\mu_n^{(1)}(E_0) - \tfrac{1}{3} T_{lmnp}\theta_{np}^{(1)}(E_0) + \cdots . \tag{4.23}$$

$\theta_{mn}^{(1)}(E_0)$ is given by an expression analogous to (4.21).

Substituting $\mu_j^{(2)}$ and $\theta_{jk}^{(2)}$ into $\mathcal{F}_i^{(1)}$ in (4.19), then substituting $\mathcal{F}_k^{(2)}$ and $\mathcal{F}_{kl}^{(2)}$ into the resultant equation, and finally substituting for $\mu_l^{(1)}$ and $\theta_{lm}^{(1)}$ yields the following expression for $\mathcal{F}_i^{(1)}$, where only the simplest terms are retained:

$$\mathcal{F}_j^{(1)} = T_{jk}p_{kl}^{(2)} E_{0l} + T_{jk}p_{kl}^{(2)} T_{lm}p_{mn}^{(1)} E_{0n} + \cdots$$

$$+ T_{jk}p_{kl}^{(2)} T_{lmn} A_{pmn}^{(1)} E_{0p} + \cdots - \tfrac{1}{3} T_{jk} A_{klm}^{(2)} T_{lmn} p_{np}^{(1)} E_{0p} + \cdots \tag{4.24}$$

$$- \tfrac{1}{3} T_{jkl} A_{mkl}^{(2)} E_{0m} + \cdots + \tfrac{1}{3} T_{jkl} C_{klmn}^{(2)} T_{mnp} p_{pq}^{(1)} E_{0q} + \cdots .$$

A simple physical interpretation of some of the terms in this expression follows:

(i) The first term represents the field at molecule 1 due to the dipole moment $p_{kl}^{(2)} E_{0l}$ induced on molecule 2 by the external field E_0.

(ii) The second term represents the field at molecule 1 arising from the dipole moment

42

$p_{lm}^{(2)}T_{mn}p_{np}^{(1)}E_{0p}$ on molecule 2, initiated by the field $T_{mn}p_{np}^{(1)}E_{0p}$ due to the dipole moment $p_{np}^{(1)}E_{0p}$ induced on molecule 1 by the external field.

(iii) The third term describes the field at molecule 1 due to the dipole moment on molecule 2 $(p_{kl}^{(2)}T_{lmn}A_{pmn}^{(1)}E_{0p})$ arising from the field $T_{lmn}A_{pmn}^{(1)}E_{0p}$, which is due in turn to the quadrupole moment on molecule 1 $(A_{pmn}^{(1)}E_{0p})$ produced by E_0.

(iv) The last term describes the field at molecule 1 due to the quadrupole moment induced on molecule 2 $(-C_{klmn}^{(2)}T_{mnp}p_{pq}^{(1)}E_{0q})$ by the field *gradient* $-T_{mnp}p_{pq}^{(1)}E_{0q}$ arising from the dipole moment $p_{pq}^{(1)}E_{0q}$ on molecule 1 produced by E_0.

Only a few of the possible terms have been illustrated here, but the relay effect described above results in an infinite series of progressively higher-order terms. Unfortunately, until the individual terms are calculated it is impossible to be sure that convergence has been reached. In the past the point of termination of the series was determined by the practical constraints of calculating the terms by hand, or with limited computing facilities. As computer capablilties have improved, it has become possible to add as many terms as necessary to ensure convergence. This is achieved by calculating sucessive terms in the series until the point of convergence is reached. In previous work by Burns, Graham and Weller [62], the series was arbitrarily truncated when the terms have fourteen or more indices. In this work, all the terms considered in the past by Buckingham [31], Kielich [124], Graham [122] and Burns, Graham and Weller [62] have been included, as well as some terms of comparable order which were excluded by Burns, Graham and Weller.

Thus, substituting (4.17) into (4.24), we now write [105]:

$$
\begin{aligned}
\mathcal{F}_j^{(1)} = {}& T_{jk}a_{kl}^{(2)}E_{0l} + T_{jk}b_{klm}^{(2)}F_m^{(2)}E_{0l} + \tfrac{1}{2}T_{jk}g_{klmn}^{(2)}F_m^{(2)}F_n^{(2)}E_{0l} + T_{jk}a_{kl}^{(2)}T_{lm}a_{mn}^{(1)}E_{0n} \\
& + T_{jk}a_{kl}^{(2)}T_{lm}a_{mn}^{(1)}T_{np}a_{pq}^{(2)}E_{0q} + \tfrac{1}{3}T_{jk}a_{kl}^{(2)}T_{lmn}A_{pmn}^{(1)}E_{0p} - \tfrac{1}{3}T_{jk}A_{klm}^{(2)}T_{lmn}a_{np}^{(1)}E_{0p} \\
& - \tfrac{1}{3}T_{jkl}A_{mkl}^{(2)}E_{0m} - \tfrac{1}{3}T_{jkl}A_{mkl}^{(2)}T_{mn}a_{np}^{(1)}E_{0p} - \tfrac{1}{9}T_{jk}A_{klm}^{(2)}T_{lmnp}A_{qnp}^{(1)}E_{0q} \\
& - \tfrac{1}{9}T_{jkl}A_{mkl}^{(2)}T_{mnp}A_{qnp}^{(1)}E_{0q} + \tfrac{1}{3}T_{jkl}C_{klmn}^{(2)}T_{mnp}a_{pq}^{(1)}E_{0q} + \cdots,
\end{aligned}
\tag{4.25}
$$

$$
\begin{aligned}
\mathcal{F}_{jk}^{(1)} = {}& T_{jkl}a_{lm}^{(2)}E_{0m} + T_{jkl}a_{lm}^{(2)}T_{mn}a_{np}^{(1)}E_{0p} + \tfrac{1}{3}T_{jkl}a_{lm}^{(2)}T_{mnp}A_{qnp}^{(1)}E_{0q} \\
& - \tfrac{1}{3}T_{jkl}A_{lmn}^{(2)}T_{mnp}a_{pq}^{(1)}E_{0q} - \tfrac{1}{3}T_{jklm}A_{nlm}^{(2)}E_{0n} - \tfrac{1}{3}T_{jklm}A_{nlm}^{(2)}T_{np}a_{pq}^{(1)}E_{0q} + \cdots.
\end{aligned}
\tag{4.26}
$$

Substituting (4.25) and (4.26) into (4.18) results in the following expression for the

dipole moment induced on molecule 1 by the external field E_0, in the presence of molecule 2:

$$\mu_i^{(1)}(E_0) = a_{ij}^{(1)} E_{0j} + a_{ij}^{(1)} T_{jk} a_{kl}^{(2)} E_{0l} + a_{ij}^{(1)} T_{jk} a_{kl}^{(2)} T_{lm} a_{mn}^{(1)} E_{0n}$$

$$+ a_{ij}^{(1)} T_{jk} a_{kl}^{(2)} T_{lm} a_{mn}^{(1)} T_{np} a_{pq}^{(2)} E_{0q} + \cdots$$

$$+ b_{ijk}^{(1)} F_k^{(1)} E_{0j} + b_{ijk}^{(1)} F_k^{(1)} T_{jl} a_{lm}^{(2)} E_{0m} + a_{ij}^{(1)} T_{jk} b_{klm}^{(2)} F_m^{(2)} E_{0l} + \cdots$$

$$+ \tfrac{1}{2} g_{ijkl}^{(1)} F_k^{(1)} F_l^{(1)} E_{0j} + \cdots + \phi_{ijkl}^{(1)} F_{kl}^{(1)} E_{0j} + \cdots$$

$$- \tfrac{1}{3} a_{ij}^{(1)} T_{jkl} A_{mkl}^{(2)} E_{0m} + \tfrac{1}{3} A_{ijk}^{(1)} T_{jkl} a_{lm}^{(2)} E_{0m}$$

$$+ \tfrac{1}{3} a_{ij}^{(1)} T_{jk} a_{kl}^{(2)} T_{lmn} A_{pmn}^{(1)} E_{0p} - \tfrac{1}{3} a_{ij}^{(1)} T_{jk} A_{klm}^{(2)} T_{lmn} a_{np}^{(1)} E_{0p}$$

$$- \tfrac{1}{3} a_{ij}^{(1)} T_{jkl} A_{mkl}^{(2)} T_{mn} a_{np}^{(1)} E_{0p} + \tfrac{1}{3} A_{ijk}^{(1)} T_{jkl} a_{lm}^{(2)} T_{mn} a_{np}^{(1)} E_{0p}$$

$$- \tfrac{1}{9} A_{ijk}^{(1)} T_{jklm} A_{nlm}^{(2)} E_{0n} - \tfrac{1}{9} a_{ij}^{(1)} T_{jk} A_{klm}^{(2)} T_{lmnp} A_{qnp}^{(1)} E_{0q}$$

$$- \tfrac{1}{9} a_{ij}^{(1)} T_{jkl} A_{mkl}^{(2)} T_{mnp} A_{qnp}^{(1)} E_{0q} + \tfrac{1}{9} A_{ijk}^{(1)} T_{jkl} a_{lm}^{(2)} T_{mnp} A_{qnp}^{(1)} E_{0q}$$

$$- \tfrac{1}{9} A_{ijk}^{(1)} T_{jkl} A_{lmn}^{(2)} T_{mnp} a_{pq}^{(1)} E_{0q} - \tfrac{1}{9} A_{ijk}^{(1)} T_{jklm} A_{nlm}^{(2)} T_{np} a_{pq}^{(1)} E_{0q} + \cdots$$

$$+ \tfrac{1}{3} a_{ij}^{(1)} T_{jkl} C_{klmn}^{(2)} T_{mnp} a_{pq}^{(1)} E_{0q} + \cdots . \tag{4.27}$$

When the differentiation $\frac{\partial \mu_i^{(1)}(E_0)}{\partial E_{0j}} e_i$ is carried out on (4.27), terms containing the product $e_i e_j$ of unit vectors in the direction of the applied field are produced. Since, we require the derivative in the limit of zero field, all orientations of the molecules are equally probable and $e_i e_j$ may be replaced by its isotropic average $\tfrac{1}{3} \delta_{ij}$. Thus, differentiating (4.27) and subtracting a_0, we get:

$$\left(\frac{\partial \mu_i^{(1)}}{\partial E_0} e_i - a_0 \right)_{E=0} = \alpha_1 + \alpha_2 + \alpha_3 + \alpha_4 + \cdots + \beta_1 + \alpha_1 \beta_1 + \cdots + \gamma_1 + \cdots + \phi_1 + \cdots$$

$$+ \alpha_1 \mathcal{A}_1 + \alpha_2 \mathcal{A}_1 + \cdots + \mathcal{A}_2 + \alpha_1 \mathcal{A}_2 + \cdots \alpha_2 C_1 + \cdots , \tag{4.28}$$

where

$$\alpha_1 = \tfrac{1}{3} a_{ii}^{(1)} - a_0, \tag{4.29}$$

$$\alpha_2 = \tfrac{1}{3} a_{ij}^{(1)} T_{jk} a_{ki}^{(2)}, \tag{4.30}$$

$$\alpha_3 = \tfrac{1}{3} a_{ij}^{(1)} T_{jk} a_{kl}^{(2)} T_{lm} a_{mi}^{(1)}, \tag{4.31}$$

44

$$\alpha_4 = \tfrac{1}{3} a_{ij}^{(1)} T_{jk} a_{kl}^{(2)} T_{lm} a_{mn}^{(1)} T_{np} a_{pi}^{(2)} , \tag{4.32}$$

$$\beta_1 = \tfrac{1}{3} b_{iik}^{(1)} F_k^{(1)} , \tag{4.33}$$

$$\alpha_1 \beta_1 = \tfrac{1}{3} \left(b_{ijk}^{(1)} F_k^{(1)} T_{jl} a_{li}^{(2)} + a_{ij}^{(1)} T_{jk} b_{kil}^{(2)} F_l^{(2)} \right) , \tag{4.34}$$

$$\gamma_1 = \tfrac{1}{6} g_{iikl}^{(1)} F_k^{(1)} F_l^{(1)} , \tag{4.35}$$

$$\phi_1 = \tfrac{1}{3} \phi_{iikl}^{(1)} F_{kl}^{(1)} , \tag{4.36}$$

$$\alpha_1 \mathcal{A}_1 = -\tfrac{1}{9} \left(a_{ij}^{(1)} T_{jkl} A_{ikl}^{(2)} - A_{ijk}^{(1)} T_{jkl} a_{li}^{(2)} \right) , \tag{4.37}$$

$$\alpha_2 \mathcal{A}_1 = \tfrac{1}{9} \left(a_{ij}^{(1)} T_{jk} a_{kl}^{(2)} T_{lmn} A_{imn}^{(1)} - a_{ij}^{(1)} T_{jk} A_{klm}^{(2)} T_{lmn} a_{ni}^{(1)} \right.$$
$$\left. - a_{ij}^{(1)} T_{jkl} A_{mkl}^{(2)} T_{mn} a_{ni}^{(1)} + A_{ijk}^{(1)} T_{jkl} a_{lm}^{(2)} T_{mn} a_{ni}^{(1)} \right) , \tag{4.38}$$

$$\mathcal{A}_2 = -\tfrac{1}{27} A_{ijk}^{(1)} T_{jklm} A_{ilm}^{(2)} , \tag{4.39}$$

$$\alpha_1 \mathcal{A}_2 = -\tfrac{1}{27} \left(a_{ij}^{(1)} T_{jk} A_{klm}^{(2)} T_{lmnp} A_{inp}^{(1)} + a_{ij}^{(1)} T_{jkl} A_{mkl}^{(2)} T_{mnp} A_{inp}^{(1)} \right.$$
$$- A_{ijk}^{(1)} T_{jkl} a_{lm}^{(2)} T_{mnp} A_{inp}^{(1)} + A_{ijk}^{(1)} T_{jkl} A_{lmn}^{(2)} T_{mnp} a_{pi}^{(1)}$$
$$\left. + A_{ijk}^{(1)} T_{jklm} A_{nlm}^{(2)} T_{np} a_{pi}^{(1)} \right) , \tag{4.40}$$

$$\alpha_2 C_1 = \tfrac{1}{9} a_{ij}^{(1)} T_{jkl} C_{klmn}^{(2)} T_{mnp} a_{pi}^{(1)} . \tag{4.41}$$

To proceed, one must introduce the explicit forms of the parameters T_{ij}, T_{ijk}, T_{ijkl}, $F_i^{(i)}$ and $F_{ij}^{(i)}$.

4.2 Expression for $\frac{1}{3kT} \left[\frac{1}{2} (\boldsymbol{\mu}^{(1)} + \boldsymbol{\mu}^{(2)})^2 - \boldsymbol{\mu}_0^2 \right]$

For the second term in B_ε, we must consider the total dipole moment on each molecule. That is, the combination of the permanent dipole moment of the molecule and the dipole moment induced on it by fields and field gradients due to the total moments on the second molecule, permanent and induced. Thus we write:

$$\mu_i^{(1)} = \mu_{0i}^{(1)} + a_{ij}^{(1)} F_j^{(1)} + b_{ijk}^{(1)} F_j^{(1)} F_k^{(1)} + \tfrac{1}{3} A_{ijk}^{(1)} F_{jk}^{(1)} , \tag{4.42}$$

$$\mu_i^{(2)} = \mu_{0i}^{(2)} + a_{ij}^{(2)} F_j^{(2)} + b_{ijk}^{(2)} F_j^{(2)} F_k^{(2)} + \tfrac{1}{3} A_{ijk}^{(2)} F_{jk}^{(2)} , \tag{4.43}$$

45

where

$$F_j^{(1)} = T_{jk}\mu_k^{(2)} - \tfrac{1}{3}T_{jkl}\theta_{kl}^{(2)} + \cdots, \qquad F_j^{(2)} = T_{jk}\mu_k^{(1)} + \tfrac{1}{3}T_{jkl}\theta_{kl}^{(1)} + \cdots, \qquad (4.44)$$

$$F_{jk}^{(1)} = T_{jkl}\mu_l^{(2)} - \tfrac{1}{3}T_{jklm}\theta_{lm}^{(2)} + \cdots, \qquad F_{jk}^{(2)} = -T_{jkl}\mu_l^{(1)} - \tfrac{1}{3}T_{jklm}\theta_{lm}^{(1)} + \cdots \qquad (4.45)$$

and

$$\theta_{kl}^{(1)} = \theta_{0kl}^{(1)} + A_{mkl}^{(1)}F_m^{(1)} + \tfrac{1}{2}B_{mnkl}^{(1)}F_m^{(1)}F_n^{(1)} + C_{klmn}^{(1)}F_{mn}^{(1)}, \qquad (4.46)$$

$$\theta_{kl}^{(2)} = \theta_{0kl}^{(2)} + A_{mkl}^{(2)}F_m^{(2)} + \tfrac{1}{2}B_{mnkl}^{(2)}F_m^{(2)}F_n^{(2)} + C_{klmn}^{(2)}F_{mn}^{(2)}. \qquad (4.47)$$

To obtain and expression for $\mu_i^{(1)}$, one must first substitute (4.45) for $F_j^{(1)}$ and $F_{jk}^{(1)}$ in (4.42), then substitute (4.43) for $\mu_k^{(2)}$ and (4.47) for $\theta_{kl}^{(2)}$ into the resulting equation, as follows:

$$\mu_i^{(1)} = \mu_{0i}^{(1)} + a_{ij}^{(1)}(T_{jk}\mu_k^{(2)} - \tfrac{1}{3}T_{jkl}\theta_{kl}^{(2)}) + b_{ijk}^{(1)}(T_{jl}\mu_l^{(2)} - \tfrac{1}{3}T_{jlm}\theta_{lm}^{(2)})(T_{kn}\mu_n^{(2)} - \tfrac{1}{3}T_{knp}\theta_{np}^{(2)})$$

$$+ \tfrac{1}{3}A_{ijk}^{(1)}(T_{jkl}\mu_l^{(2)} - \tfrac{1}{3}T_{jklm}\theta_{lm}^{(2)})$$

$$= \mu_{0i}^{(1)} + a_{ij}^{(1)}T_{jk}(\mu_{0k}^{(2)} + a_{kl}^{(2)}F_l^{(2)} + b_{klm}^{(2)}F_l^{(2)}F_m^{(2)} + \tfrac{1}{3}A_{klm}^{(2)}F_{lm}^{(2)})$$

$$- \tfrac{1}{3}a_{ij}^{(1)}T_{jkl}(\theta_{0kl}^{(1)} + A_{mkl}^{(1)}F_m^{(1)} + \tfrac{1}{2}B_{mnkl}^{(1)}F_m^{(1)}F_n^{(1)} + C_{klmn}^{(1)}F_{mn}^{(1)})$$

$$+ b_{ijk}^{(1)}T_{jl}(\mu_{0l}^{(2)} + a_{lm}^{(2)}F_m^{(2)} + \cdots)T_{kn}(\mu_{0n}^{(2)} + a_{np}^{(2)}F_p^{(2)} + \cdots)$$

$$- \tfrac{1}{3}b_{ijk}^{(1)}T_{jl}(\mu_{0l}^{(2)} + a_{lm}^{(2)}F_m^{(2)} + \cdots)T_{knp}(\theta_{0np}^{(2)} + \cdots)$$

$$- \tfrac{1}{3}b_{ijk}^{(1)}T_{jlm}(\theta_{0lm}^{(2)} + \cdots)T_{kn}(\mu_{0n}^{(2)} + a_{np}^{(2)}F_p^{(2)} + \cdots)$$

$$+ \tfrac{1}{9}b_{ijk}^{(1)}T_{jlm}(\theta_{0lm}^{(2)} + \cdots)T_{knp}(\theta_{0np}^{(2)} + \cdots)$$

$$+ \tfrac{1}{3}A_{ijk}^{(1)}T_{jkl}(\mu_{0l}^{(2)} + a_{lm}^{(2)}F_m^{(2)} + \cdots + \tfrac{1}{3}A_{lmn}^{(2)}F_{mn}^{(2)})$$

$$- \tfrac{1}{9}A_{ijk}^{(1)}T_{jklm}(\theta_{0lm}^{(2)} + A_{nlm}^{(2)}F_n^{(2)} + \cdots). \qquad (4.48)$$

Continuing in this way, by substituting first for $F_l^{(2)}$ and $F_{lm}^{(2)}$, then for $\mu_m^{(1)}$ and $\theta_{mn}^{(1)}$, and so on, neglecting all terms with sixteen or more subscripts, or with more than one hyperpolarizability tensor and all terms with the g_{ijkl} or B_{ijkl} tensors, yields the following expression for the dipole moment of molecule 1:

$$\mu_i^{(1)} = \mu_{0i}^{(1)} + a_{ij}^{(1)}T_{jk}\mu_{0k}^{(2)} + a_{ij}^{(1)}T_{jk}a_{kl}^{(2)}T_{lm}\mu_{0m}^{(1)} + a_{ij}^{(1)}T_{jk}a_{kl}^{(2)}T_{lm}a_{mn}^{(1)}T_{np}\mu_{0p}^{(2)} + \cdots$$

$$- \tfrac{1}{3}a_{ij}^{(1)}T_{jkl}\theta_{0kl}^{(2)} + \tfrac{1}{3}a_{ij}^{(1)}T_{jk}a_{kl}^{(2)}T_{lmn}\theta_{0mn}^{(1)} - \tfrac{1}{3}a_{ij}^{(1)}T_{jk}a_{kl}^{(2)}T_{lm}a_{mn}^{(1)}T_{npq}\theta_{0q}^{(2)} + \cdots$$

$$+ b^{(1)}_{ijk}T_{jl}\mu^{(2)}_{0l}T_{km}\mu^{(2)}_{0m} + a^{(1)}_{ij}T_{jk}b^{(2)}_{klm}T_{ln}\mu^{(1)}_{0n}T_{mp}\mu^{(1)}_{0p} + b^{(1)}_{ijk}T_{jl}\mu^{(2)}_{0l}T_{km}a^{(2)}_{mn}T_{np}\mu^{(1)}_{0p}$$

$$+ b^{(1)}_{ijk}T_{jl}a^{(2)}_{ln}T_{np}\mu^{(1)}_{0p}T_{km}\mu^{(2)}_{0m} + \cdots$$

$$- \tfrac{1}{3}b^{(1)}_{ijk}T_{jl}\mu^{(2)}_{0l}T_{kmn}\theta^{(2)}_{0mn} - \tfrac{1}{3}b^{(1)}_{ijk}T_{jlm}\theta^{(2)}_{0lm}T_{kn}\mu^{(2)}_{0n}$$

$$+ \tfrac{1}{3}a^{(1)}_{ij}T_{jk}b^{(2)}_{klm}T_{ln}\mu^{(1)}_{0n}T_{mpq}\theta^{(1)}_{0pq} + \tfrac{1}{3}a^{(1)}_{ij}T_{jk}b^{(2)}_{klm}T_{lnp}\theta^{(1)}0pT_{mq}\mu^{(1)}_{0q}$$

$$+ \tfrac{1}{3}b^{(1)}_{ijk}T_{jl}\mu^{(2)}_{0l}T_{km}a^{(2)}_{mn}T_{npq}\theta^{(1)}_{0pq} + \tfrac{1}{3}b^{(1)}_{ijk}T_{jl}a^{(2)}_{ln}T_{npq}\theta^{(1)}_{0pq}T_{km}\mu^{(2)}_{0m}$$

$$- \tfrac{1}{3}b^{(1)}_{ijk}T_{jl}a^{(2)}_{lp}T_{pq}\mu^{(1)}_{0q}T_{kmn}\theta^{(2)}_{0mn} - \tfrac{1}{3}b^{(1)}_{ijk}T_{jlm}\theta^{(2)}_{0lm}T_{kn}a^{(2)}_{np}T_{pq}\mu^{(1)}_{0q} + \cdots$$

$$+ \tfrac{1}{9}b^{(1)}_{ijk}T_{jlm}\theta^{(2)}_{0lm}T_{knp}\theta^{(2)}_{0np} + \cdots$$

$$+ \tfrac{1}{3}A^{(1)}_{ijk}T_{jkl}\mu^{(2)}_{0l} - \tfrac{1}{3}a^{(1)}_{ij}T_{jk}A^{(2)}_{klm}T_{lmn}\mu^{(1)}_{0n} - \tfrac{1}{3}a^{(1)}_{ij}T_{jkl}A^{(2)}_{mkl}T_{mn}\mu^{(1)}_{0n}$$

$$+ \tfrac{1}{3}A^{(1)}_{ijk}T_{jkl}a^{(2)}_{lm}T_{mn}\mu^{(1)}_{0n} + \tfrac{1}{3}a^{(1)}_{ij}T_{jk}a^{(2)}_{kl}T_{lm}A^{(1)}_{mnp}T_{npq}\mu^{(2)}_{0q}$$

$$+ \tfrac{1}{3}a^{(1)}_{ij}T_{jk}a^{(2)}_{kl}T_{lmn}A^{(1)}_{pmn}T_{pq}\mu^{(2)}_{0q} - \tfrac{1}{3}a^{(1)}_{ij}T_{jk}A^{(2)}_{klm}T_{lmn}a^{(1)}_{np}T_{pq}\mu^{(2)}_{0q}$$

$$- \tfrac{1}{3}a^{(1)}_{ij}T_{jkl}A^{(2)}_{mkl}T_{mn}a^{(1)}_{np}T_{pq}\mu^{(2)}_{0q} + \tfrac{1}{3}A^{(1)}_{ijk}T_{jkl}a^{(2)}_{lm}T_{mn}a^{(1)}_{ni}T_{pq}\mu^{(2)}_{0q} + \cdots$$

$$- \tfrac{1}{9}A^{(1)}_{ijk}T_{jklm}\theta^{(2)}_{0lm} + \tfrac{1}{9}a^{(1)}_{ij}T_{jk}A^{(2)}_{klm}T_{lmnp}\theta^{(1)}_{0np} + \tfrac{1}{9}a^{(1)}_{ij}T_{jkl}A^{(2)}_{mkl}T_{mnp}\theta^{(1)}_{0np}$$

$$+ \tfrac{1}{9}A^{(1)}_{ijk}T_{jkl}a^{(2)}_{lm}T_{mnp}\theta^{(1)}_{0np} + \cdots$$

$$\tfrac{1}{3}a^{(1)}_{ij}T_{jkl}C^{(2)}_{klmn}T_{mnp}\mu^{(1)}_{0p} + \cdots + \tfrac{1}{9}a^{(1)}_{ij}T_{jkl}C^{(2)}_{klmn}T_{mnpq}\theta^{(1)}_{0pq} + \cdots . \tag{4.49}$$

The order to which equation (4.49) has been expanded is partially justified in retrospect through studies of convergence of the terms. The exclusion of terms in the hyperpolarizability g_{ijkl} is based on observations that the lower-order third-rank hyperpolarizability tensor b_{ijk} (which may be expected to make the leading hyperpolarizability contribution) plays an insignificant role. The expression for $\mu^{(2)}_i$ is determined by the same procedure to yield an analogous expression. Thus:

$$\frac{1}{3kT}\left[\tfrac{1}{2}(\mu^{(1)}_i + \mu^{(2)}_i)^2 - \mu^2_0\right] = \frac{1}{3kT}[\mu_2 + \alpha_1\mu_2 + \alpha_2\mu_2 + \alpha_3\mu_2 + \cdots$$

$$+ \alpha_1\mu_1\theta_1 + \alpha_2\mu_1\theta_1 + \cdots + \alpha_2\theta_2 + \alpha_3\theta_2 + \alpha_4\theta_2 + \cdots$$

$$+ \beta_1\mu_3 + \alpha_1\beta_1\mu_3 + \cdots + \beta_1\mu_2\theta_1 + \cdots$$

$$+ \mathcal{A}_1\mu_2 + \alpha_1\mathcal{A}_1\mu_2 + \cdots + \mathcal{A}_1\mu_1\theta_1 + \cdots + \alpha_1\mathcal{A}_1\theta_2 + \cdots$$

$$+ \alpha_1 C_1\mu_2 + \cdots + \alpha_1 C_1\mu_1\theta_1 + \cdots + \alpha_2 C_1\theta_2], \tag{4.50}$$

where

$$\mu_2 = \mu_{0i}^{(1)}\mu_{0i}^{(2)}, \tag{4.51}$$

$$\alpha_1\mu_2 = \left(\mu_{0i}^{(1)} + \mu_{0i}^{(2)}\right)\left(a_{ij}^{(1)}T_{jk}\mu_{0k}^{(2)} + a_{ij}^{(2)}T_{jk}\mu_{0k}^{(1)}\right)$$

$$= 2\mu_{0i}^{(1)}\left(a_{ij}^{(1)}T_{jk}\mu_{0k}^{(2)} + a_{ij}^{(2)}T_{jk}\mu_{0k}^{(1)}\right), \tag{4.52}$$

$$\alpha_2\mu_2 = \left(\mu_{0i}^{(1)} + \mu_{0i}^{(2)}\right)\left(a_{ij}^{(1)}T_{jk}a_{kl}^{(2)}T_{lm}\mu_{0m}^{(1)} + a_{ij}^{(2)}T_{jk}a_{kl}^{(1)}T_{lm}\mu_{0m}^{(2)}\right)$$

$$+ \tfrac{1}{2}\left(a_{ij}^{(1)}T_{jk}\mu_{0k}^{(2)} + a_{ij}^{(2)}T_{jk}\mu_{0k}^{(1)}\right)\left(a_{il}^{(1)}T_{lm}\mu_{0m}^{(2)} + a_{il}^{(2)}T_{lm}\mu_{0m}^{(1)}\right)$$

$$= 2\mu_{0i}^{(1)}\left(a_{ij}^{(1)}T_{jk}a_{kl}^{(2)}T_{lm}\mu_{0m}^{(1)} + a_{ij}^{(2)}T_{jk}a_{kl}^{(1)}T_{lm}\mu_{0m}^{(2)}\right)$$

$$+ a_{ij}^{(1)}T_{jk}\mu_{0k}^{(2)}\left(a_{il}^{(1)}T_{lm}\mu_{0m}^{(2)} + a_{il}^{(2)}T_{lm}\mu_{0m}^{(1)}\right), \tag{4.53}$$

$$\alpha_3\mu_2 = \left(\mu_{0i}^{(1)} + \mu_{0i}^{(2)}\right)\left(a_{ij}^{(1)}T_{jk}a_{kl}^{(2)}T_{lm}a_{mn}^{(1)}T_{np}\mu_{0p}^{(2)} + a_{ij}^{(2)}T_{jk}a_{kl}^{(1)}T_{lm}a_{mn}^{(2)}T_{np}\mu_{0p}^{(1)}\right)$$

$$+ \left(a_{ij}^{(1)}T_{jk}\mu_{0k}^{(2)} + a_{ij}^{(2)}T_{jk}\mu_{0k}^{(1)}\right)\left(a_{il}^{(1)}T_{lm}a_{mn}^{(2)}T_{np}\mu_{0p}^{(1)} + a_{il}^{(2)}T_{lm}a_{mn}^{(1)}T_{np}\mu_{0p}^{(2)}\right)$$

$$= 2\left[\mu_{0i}^{(1)}\left(a_{ij}^{(1)}T_{jk}a_{kl}^{(2)}T_{lm}a_{mn}^{(1)}T_{np}\mu_{0p}^{(2)} + a_{ij}^{(2)}T_{jk}a_{kl}^{(1)}T_{lm}a_{mn}^{(2)}T_{np}\mu_{0p}^{(1)}\right)\right.$$

$$\left. + a_{ij}^{(1)}T_{jk}\mu_{0k}^{(2)}\left(a_{il}^{(1)}T_{lm}a_{mn}^{(2)}T_{np}\mu_{0p}^{(1)} + a_{il}^{(2)}T_{lm}a_{mn}^{(1)}T_{np}\mu_{0p}^{(2)}\right)\right], \tag{4.54}$$

$$\alpha_1\mu_1\theta_1 = -\tfrac{1}{3}\left(\mu_{0i}^{(1)} + \mu_{0i}^{(2)}\right)\left(a_{ij}^{(1)}T_{jkl}\theta_{0kl}^{(2)} - a_{ij}^{(2)}T_{jkl}\theta_{0kl}^{(1)}\right)$$

$$= -\tfrac{2}{3}\mu_{0i}^{(1)}\left(a_{ij}^{(1)}T_{jkl}\theta_{0kl}^{(2)} - a_{ij}^{(2)}T_{jkl}\theta_{0kl}^{(1)}\right), \tag{4.55}$$

$$\alpha_2\mu_1\theta_1 = \tfrac{1}{3}\left[\left(\mu_{0i}^{(1)} + \mu_{0i}^{(2)}\right)\left(a_{ij}^{(1)}T_{jk}a_{kl}^{(2)}T_{lmn}\theta_{0mn}^{(1)} - a_{ij}^{(2)}T_{jk}a_{kl}^{(1)}T_{lmn}\theta_{0mn}^{(2)}\right)\right.$$

$$\left. - \left(a_{ij}^{(1)}T_{jk}\mu_{0k}^{(2)} + a_{ij}^{(2)}T_{jk}\mu_{0k}^{(1)}\right)\left(a_{il}^{(1)}T_{lmn}\theta_{0mn}^{(2)} - a_{il}^{(2)}T_{lmn}\theta_{0mn}^{(1)}\right)\right]$$

$$= \tfrac{2}{3}\left[\mu_{0i}^{(1)}\left(a_{ij}^{(1)}T_{jk}a_{kl}^{(2)}T_{lmn}\theta_{0mn}^{(1)} - a_{ij}^{(2)}T_{jk}a_{kl}^{(1)}T_{lmn}\theta_{0mn}^{(2)}\right)\right.$$

$$\left. - a_{ij}^{(1)}T_{jk}\mu_{0k}^{(2)}\left(a_{il}^{(1)}T_{lmn}\theta_{0mn}^{(2)} - a_{il}^{(2)}T_{lmn}\theta_{0mn}^{(1)}\right)\right], \tag{4.56}$$

$$\alpha_2\theta_2 = \tfrac{1}{18}\left(a_{ij}^{(1)}T_{jkl}\theta_{0kl}^{(2)} - a_{ij}^{(2)}T_{jkl}\theta_{0kl}^{(1)}\right)\left(a_{im}^{(1)}T_{mnp}\theta_{0np}^{(2)} - a_{im}^{(2)}T_{mnp}\theta_{0np}^{(1)}\right)$$

$$= \tfrac{1}{9}a_{ij}^{(1)}T_{jkl}\theta_{0kl}^{(2)}\left(a_{im}^{(1)}T_{mnp}\theta_{0np}^{(2)} - a_{im}^{(2)}T_{mnp}\theta_{0np}^{(1)}\right) \tag{4.57}$$

$$\alpha_3\theta_2 = -\frac{1}{9}\left(a^{(1)}_{ij}T_{jkl}\theta^{(2)}_{0kl} - a^{(2)}_{ij}T_{jkl}\theta^{(1)}_{0kl}\right)\left(a^{(1)}_{im}T_{mn}a^{(2)}_{np}T_{pqr}\theta^{(1)}_{0qr}\right.$$

$$\left. - a^{(2)}_{im}T_{mn}a^{(1)}_{np}T_{pqr}\theta^{(2)}_{0qr}\right)$$

$$= -\frac{2}{9}a^{(1)}_{ij}T_{jkl}\theta^{(2)}_{0kl}\left(a^{(1)}_{im}T_{mn}a^{(2)}_{np}T_{pqr}\theta^{(1)}_{0qr} - a^{(2)}_{im}T_{mn}a^{(1)}_{np}T_{pqr}\theta^{(2)}_{0qr}\right), \tag{4.58}$$

$$\alpha_4\theta_2 = \frac{1}{18}\left[2\left(a^{(1)}_{ij}T_{jkl}\theta^{(2)}_{0kl} - a^{(2)}_{ij}T_{jkl}\theta^{(1)}_{0kl}\right)\left(a^{(1)}_{im}T_{mn}a^{(2)}_{np}T_{pq}a^{(1)}_{qr}T_{rst}\theta^{(2)}_{0st}\right.\right.$$

$$\left. - a^{(2)}_{im}T_{mn}a^{(1)}_{np}T_{pq}a^{(2)}_{qr}T_{rst}\theta^{(1)}_{0st}\right) + \left(a^{(1)}_{ij}T_{jk}a^{(2)}_{kl}T_{lmn}\theta^{(1)}_{0mn}\right.$$

$$\left.\left. - a^{(2)}_{ij}T_{jk}a^{(1)}_{kl}T_{lmn}\theta^{(2)}_{0mn}\right)\left(a^{(1)}_{ip}T_{pq}a^{(2)}_{qr}T_{rst}\theta^{(1)}_{0st} - a^{(2)}_{ip}T_{pq}a^{(1)}_{qr}T_{rst}\theta^{(2)}_{0st}\right)\right]$$

$$= \frac{1}{9}\left[2a^{(1)}_{ij}T_{jkl}\theta^{(2)}_{0kl}\left(a^{(1)}_{im}T_{mn}a^{(2)}_{np}T_{pq}a^{(1)}_{qr}T_{rst}\theta^{(2)}_{0st} - a^{(2)}_{im}T_{mn}a^{(1)}_{np}T_{pq}a^{(2)}_{qr}T_{rst}\theta^{(1)}_{0st}\right)\right.$$

$$\left. + a^{(1)}_{ij}T_{jk}a^{(2)}_{kl}T_{lmn}\theta^{(1)}_{0mn}\left(a^{(1)}_{ip}T_{pq}a^{(2)}_{qr}T_{rst}\theta^{(1)}_{0st} - a^{(2)}_{ip}T_{pq}a^{(1)}_{qr}T_{rst}\theta^{(2)}_{0st}\right)\right], \tag{4.59}$$

$$\beta_1\mu_3 = \left(\mu^{(1)}_{0i} + \mu^{(2)}_{0i}\right)\left(b^{(1)}_{ijk}T_{jl}\mu^{(2)}_{0l}T_{km}\mu^{(2)}_{0m} + b^{(2)}_{ijk}T_{jl}\mu^{(1)}_{0l}T_{km}\mu^{(1)}_{0m}\right)$$

$$= 2\mu^{(1)}_{0i}\left(b^{(1)}_{ijk}T_{jl}\mu^{(2)}_{0l}T_{km}\mu^{(2)}_{0m} + b^{(2)}_{ijk}T_{jl}\mu^{(1)}_{0l}T_{km}\mu^{(1)}_{0m}\right), \tag{4.60}$$

$$\alpha_1\beta_1\mu_3 = \left(\mu^{(1)}_{0i} + \mu^{(2)}_{0i}\right)\left(a^{(1)}_{ij}T_{jk}b^{(2)}_{klm}T_{ln}\mu^{(1)}_{0n}T_{mp}\mu^{(1)}_{0p} + a^{(2)}_{ij}T_{jk}b^{(1)}_{klm}T_{ln}\mu^{(2)}_{0n}T_{mp}\mu^{(2)}_{0p}\right)$$

$$+ 2\left(\mu^{(1)}_{0i} + \mu^{(2)}_{0i}\right)\left(b^{(1)}_{ijk}T_{jl}\mu^{(2)}_{0l}T_{km}a^{(2)}_{mn}T_{np}\mu^{(1)}_{0p} + b^{(2)}_{ijk}T_{jl}\mu^{(1)}_{0l}T_{km}a^{(1)}_{mn}T_{np}\mu^{(2)}_{0p}\right)$$

$$+ \left(a^{(1)}_{ij}T_{jk}\mu^{(2)}_{0k} + a^{(2)}_{ij}T_{jk}\mu^{(1)}_{0k}\right)\left(b^{(1)}_{ilm}T_{ln}\mu^{(2)}_{0n}T_{mp}\mu^{(2)}_{0p} + b^{(2)}_{ilm}T_{ln}\mu^{(1)}_{0n}T_{mp}\mu^{(1)}_{0p}\right)$$

$$= 2\mu^{(1)}_{0i}\left(a^{(1)}_{ij}T_{jk}b^{(2)}_{klm}T_{ln}\mu^{(1)}_{0n}T_{mp}\mu^{(1)}_{0p} + a^{(2)}_{ij}T_{jk}b^{(1)}_{klm}T_{ln}\mu^{(2)}_{0n}T_{mp}\mu^{(2)}_{0p}\right)$$

$$+ 4\mu^{(1)}_{0i}\left(b^{(1)}_{ijk}T_{jl}\mu^{(2)}_{0l}T_{km}a^{(2)}_{mn}T_{np}\mu^{(1)}_{0p} + b^{(2)}_{ijk}T_{jl}\mu^{(1)}_{0l}T_{km}a^{(1)}_{mn}T_{np}\mu^{(2)}_{0p}\right) \tag{4.61}$$

$$+ 2a^{(1)}_{ij}T_{jk}\mu^{(2)}_{0k}\left(b^{(1)}_{ilm}T_{ln}\mu^{(2)}_{0n}T_{mp}\mu^{(2)}_{0p} + b^{(2)}_{ilm}T_{ln}\mu^{(1)}_{0n}T_{mp}\mu^{(1)}_{0p}\right),$$

$$\beta_1\mu_2\theta_1 = -\frac{2}{3}\left(\mu^{(1)}_{0i} + \mu^{(2)}_{0i}\right)\left(b^{(1)}_{ijk}T_{jl}\mu^{(2)}_{0l}T_{kmn}\theta^{(2)}_{0mn} - b^{(1)}_{ijk}T_{jl}\mu^{(2)}_{0l}T_{kmn}\theta^{(2)}_{0mn}\right)$$

$$= -\frac{4}{3}\mu^{(1)}_{0i}\left(b^{(1)}_{ijk}T_{jl}\mu^{(2)}_{0l}T_{kmn}\theta^{(2)}_{0mn} - b^{(1)}_{ijk}T_{jl}\mu^{(2)}_{0l}T_{kmn}\theta^{(2)}_{0mn}\right), \tag{4.62}$$

$$\mathcal{A}_1\mu_2 = -\frac{1}{3}\left(\mu^{(1)}_{0i} + \mu^{(2)}_{0i}\right)\left(A^{(1)}_{ijk}T_{jkl}\mu^{(2)}_{0l} - A^{(2)}_{ijk}T_{jkl}\mu^{(1)}_{0l}\right)$$

$$= -\frac{2}{3}\mu^{(1)}_{0i}\left(A^{(1)}_{ijk}T_{jkl}\mu^{(2)}_{0l} - A^{(2)}_{ijk}T_{jkl}\mu^{(1)}_{0l}\right), \tag{4.63}$$

$$\alpha_1 \mathcal{A}_1 \mu_2 = -\frac{1}{3} \left[\left(\mu_{0i}^{(1)} + \mu_{0i}^{(2)} \right) \left(a_{ij}^{(1)} T_{jk} A_{klm}^{(2)} T_{lmn} \mu_{0n}^{(1)} - a_{ij}^{(2)} T_{jk} A_{klm}^{(1)} T_{lmn} \mu_{0n}^{(2)} \right) \right.$$

$$+ \left(\mu_{0i}^{(1)} + \mu_{0i}^{(2)} \right) \left(a_{ij}^{(1)} T_{jkl} A_{mkl}^{(2)} T_{mn} \mu_{0n}^{(1)} - a_{ij}^{(2)} T_{jkl} A_{mkl}^{(1)} T_{mn} \mu_{0n}^{(2)} \right)$$

$$- \left(\mu_{0i}^{(1)} + \mu_{0i}^{(2)} \right) \left(A_{ijk}^{(1)} T_{jkl} a_{lm}^{(2)} T_{mn} \mu_{0n}^{(1)} - A_{ijk}^{(2)} T_{jkl} a_{lm}^{(1)} T_{mn} \mu_{0n}^{(2)} \right)$$

$$- \left(a_{ij}^{(1)} T_{jk} \mu_{0k}^{(2)} + a_{ij}^{(2)} T_{jk} \mu_{0k}^{(1)} \right) \left(A_{ilm}^{(1)} T_{lmn} \mu_{0n}^{(2)} - A_{ilm}^{(2)} T_{lmn} \mu_{0n}^{(1)} \right) \Bigg]$$

$$= -\frac{2}{3} \left[\mu_{0i}^{(1)} \left(a_{ij}^{(1)} T_{jk} A_{klm}^{(2)} T_{lmn} \mu_{0n}^{(1)} - a_{ij}^{(2)} T_{jk} A_{klm}^{(1)} T_{lmn} \mu_{0n}^{(2)} \right) \right.$$

$$+ \mu_{0i}^{(1)} \left(a_{ij}^{(1)} T_{jkl} A_{mkl}^{(2)} T_{mn} \mu_{0n}^{(1)} - a_{ij}^{(2)} T_{jkl} A_{mkl}^{(1)} T_{mn} \mu_{0n}^{(2)} \right)$$

$$\quad (4.64)$$

$$- \mu_{0i}^{(1)} \left(A_{ijk}^{(1)} T_{jkl} a_{lm}^{(2)} T_{mn} \mu_{0n}^{(1)} - A_{ijk}^{(2)} T_{jkl} a_{lm}^{(1)} T_{mn} \mu_{0n}^{(2)} \right)$$

$$- a_{ij}^{(1)} T_{jk} \mu_{0k}^{(2)} \left(A_{ilm}^{(1)} T_{lmn} \mu_{0n}^{(2)} - A_{ilm}^{(2)} T_{lmn} \mu_{0n}^{(1)} \right) \Bigg],$$

$$\mathcal{A}_1 \mu_1 \theta_1 = -\frac{1}{9} \left(\mu_{0i}^{(1)} + \mu_{0i}^{(2)} \right) \left(A_{ijk}^{(1)} T_{jklm} \theta_{0lm}^{(2)} + A_{ijk}^{(2)} T_{jklm} \theta_{0lm}^{(1)} \right)$$

$$= -\frac{2}{9} \mu_{0i}^{(1)} \left(A_{ijk}^{(1)} T_{jklm} \theta_{0lm}^{(2)} + A_{ijk}^{(2)} T_{jklm} \theta_{0lm}^{(1)} \right), \quad (4.65)$$

$$\alpha_1 \mathcal{A}_1 \theta_2 = \frac{1}{27} \left(a_{ij}^{(1)} T_{jkl} \theta_{0kl}^{(2)} - a_{ij}^{(1)} T_{jkl} \theta_{0kl}^{(2)} \right) \left(A_{imn}^{(1)} T_{mnpq} \theta_{0pq}^{(2)} + A_{imn}^{(2)} T_{mnpq} \theta_{0pq}^{(2)} \right)$$

$$= \frac{2}{27} a_{ij}^{(1)} T_{jkl} \theta_{0kl}^{(2)} \left(A_{imn}^{(1)} T_{mnpq} \theta_{0pq}^{(2)} + A_{imn}^{(2)} T_{mnpq} \theta_{0pq}^{(2)} \right), \quad (4.66)$$

$$\alpha_1 C_1 \mu_2 = \frac{1}{3} \left(\mu_{0i}^{(1)} + \mu_{0i}^{(2)} \right) \left(a_{ij}^{(1)} T_{jkl} C_{klmn}^{(2)} T_{mnp} \mu_{0p}^{(1)} + a_{ij}^{(2)} T_{jkl} C_{klmn}^{(1)} T_{mnp} \mu_{0p}^{(2)} \right)$$

$$= \frac{2}{3} \mu_{0i}^{(1)} \left(a_{ij}^{(1)} T_{jkl} C_{klmn}^{(2)} T_{mnp} \mu_{0p}^{(1)} + a_{ij}^{(2)} T_{jkl} C_{klmn}^{(1)} T_{mnp} \mu_{0p}^{(2)} \right), \quad (4.67)$$

$$\alpha_1 C_1 \mu_1 \theta_1 = \frac{1}{9} \left(\mu_{0i}^{(1)} + \mu_{0i}^{(2)} \right) \left(a_{ij}^{(1)} T_{jkl} C_{klmn}^{(2)} T_{mnpq} \theta_{0pq}^{(1)} - a_{ij}^{(2)} T_{jkl} C_{klmn}^{(1)} T_{mnpq} \theta_{0pq}^{(2)} \right)$$

$$= \frac{2}{9} \mu_{0i}^{(1)} \left(a_{ij}^{(1)} T_{jkl} C_{klmn}^{(2)} T_{mnpq} \theta_{0pq}^{(1)} - a_{ij}^{(2)} T_{jkl} C_{klmn}^{(1)} T_{mnpq} \theta_{0pq}^{(2)} \right), \quad (4.68)$$

$$\alpha_2 C_1 \theta_2 = -\frac{1}{27} \left(a_{ij}^{(1)} T_{jkl} \theta_{0kl}^{(2)} - a_{ij}^{(2)} T_{jkl} \theta_{0kl}^{(1)} \right) \left(a_{im}^{(1)} T_{mnp} C_{npqr}^{(2)} T_{qrst} \theta_{0st}^{(1)} \right.$$

$$- a_{im}^{(2)} T_{mnp} C_{npqr}^{(1)} T_{qrst} \theta_{0st}^{(2)} \Bigg)$$

$$= -\frac{1}{27} a_{ij}^{(1)} T_{jkl} \theta_{0kl}^{(2)} \left(a_{im}^{(1)} T_{mnp} C_{npqr}^{(2)} T_{qrst} \theta_{0st}^{(1)} - a_{im}^{(2)} T_{mnp} C_{npqr}^{(1)} T_{qrst} \theta_{0st}^{(2)} \right). \quad (4.69)$$

4.3 B_ε for spherical molecules

The general form of the second dielectric virial coefficient is given by:

$$B_\varepsilon = \frac{N_A^2}{3\varepsilon_0\Omega} \int_\tau \left\{ \left[\frac{1}{2}\frac{\partial\boldsymbol{\mu}^{(1)}+\boldsymbol{\mu}^{(1)}}{\partial E_0}.\boldsymbol{e} - a_0 \right] + \frac{1}{3kT}\left[\frac{1}{2}(\boldsymbol{\mu}^{(1)}+\boldsymbol{\mu}^{(2)})^2 - \boldsymbol{\mu}_0^2 \right] \right\} e^{-\frac{U_{12(\tau)}}{kT}} d\tau.$$

(4.70)

Three effects contribute to B_ε [28]. Firstly, if the mean polarizability is altered by the presence of a neighbour, then $\left\langle \frac{\partial(\boldsymbol{\mu}^{(1)}+\boldsymbol{\mu}^{(2)})}{\partial E_0}.\boldsymbol{e} \right\rangle$ will not equal $2a_0$, and the first term will be non-zero. If the polarizability is reduced as in the calculations of de Groot and ten Seldam [126], then the contribution of this term to B_ε will be negative. Secondly, when a pair of molecules interact, the induced moment of one molecule may in turn induce an additional moment on its neighbour, by dipole-induced-dipole interaction. When this is averaged over all configurations, it may contribute to $\left\langle \frac{\partial(\boldsymbol{\mu}^{(1)}+\boldsymbol{\mu}^{(2)})}{\partial E_0}.\boldsymbol{e} \right\rangle$. This is the effect first investigated in terms of a simple model by Kirkwood [127]. Thirdly, if a pair of interacting molecules possess a resultant dipole, whether permanent or induced, in the absence of an external field, then a contribution will arise from the second term in equation (4.70). It is possible, for example, for the quadrupole moment of a non-polar molecule to induce a dipole moment on a neighbouring molecule, resulting in a non-zero moment for the pair. These transient moments may be orientated by the external field, thereby contributing to the second term in B_ε, which must obviously be positive. For inert gases, however, $(\boldsymbol{\mu}^{(1)} + \boldsymbol{\mu}^{(2)})$ is always zero because, by symmetry, atomic gases have no multipole moments of any order. Therefore, the second term in B_ε must be zero. Quasi-spherical molecules, such as CH_4, CF_4 and SF_6, may have octopole, or higher, moments, but the contribution of these to the second term is assumed to be negligible.

Thus, for spherical and quasi-spherical molecules, the second virial coefficient is given by

$$B_\varepsilon = \frac{N_A^2}{3\varepsilon_0\Omega} \int_\tau \left\{ \left[\frac{\partial\boldsymbol{\mu}^{(1)}}{\partial E_0}.\boldsymbol{e} - a_0 \right] \right\} e^{-\frac{U_{12(\tau)}}{kT}} d\tau$$

$$= \frac{4\pi N_A^2}{3\varepsilon_0} \int_0^\infty \left\{ \left[\frac{\partial\boldsymbol{\mu}^{(1)}}{\partial E_0}.\boldsymbol{e} - a_0 \right] \right\} e^{-\frac{U_{12(R)}}{kT}} R^2 dR,$$

(4.71)

since τ is completely specified by the distance, R, between two interacting molecules.

Now, for spherically symmetric molecules equation (4.28) is greatly simplified, since they possess no permanent multipole moments in their ground state, A_{ijk} and b_{ijk} are both zero, and C_{ijkl} has only one independent component [26]. The static polarizability

tensor a_{ij} is isotropic and may be written as:

$$a_{ij} = a\delta_{ij}, \tag{4.72}$$

where a is the static polarizability of the gas. Thus for a spherical molecule it can be shown that [62, 128]:

$$\left(\frac{\partial \boldsymbol{\mu}^{(1)}}{\partial E_0} . e - a_0 \right) = \alpha_1 + \alpha_3 + \alpha_4 + \alpha_2 C_1, \tag{4.73}$$

$$\text{where} \quad \alpha_1 = a^{(1)} - a_0, \qquad \alpha_3 = \frac{2a^3}{(4\pi\varepsilon_0)^2 R^6}, \qquad \alpha_4 = \frac{2a^4}{(4\pi\varepsilon_0)^3 R^9}, \tag{4.74}$$

$$\text{and} \quad \alpha_2 C_1 = \frac{10a^2 C}{(4\pi\varepsilon_0)^2 R^8}. \tag{4.75}$$

The first term is the amount by which the mean intrinsic polarizability of a molecule is modified by the presence of a neighbour. However, the classical molecular theory adopted in this work does not account for this difference and the term $(a^{(1)} - a_0)$ is assumed to be zero. *Ab initio* quantum-mechanical calculations carried out by Buckingham and Watts [129], and O'Brien *et al.* [130] for helium show that the polarizability of a molecule decreases at short range. The second term is the Kirkwood "fluctuation" term [127], and is usually the largest contribution to B_ε for spherical molecules. In the past, this was often the only term considered in classical theories of of B_ε. However, in 1982 Logan and Madden demonstrated the importance of the C-tensor term [131]. Unfortunately, there is a lack of measured values for the C-tensor components.

4.4 B_ε for linear molecules

For linear gases the second virial coefficient is given by

$$B_\varepsilon = \frac{N_A^2}{3\varepsilon_0 \Omega} \int\limits_\tau \left\{ \left[\frac{\partial \boldsymbol{\mu}^{(1)}}{\partial E_0} . e - a_0 \right] + \frac{1}{3kT} \left[\tfrac{1}{2}(\boldsymbol{\mu}^{(1)} + \boldsymbol{\mu}^{(2)})^2 - \mu_0^2 \right] \right\} e^{-\frac{U_{12}(\tau)}{kT}} d\tau$$

$$= \frac{N_A}{3\varepsilon_0} \int\limits_{R=0}^{\infty} \int\limits_{\theta_1=0}^{\pi} \int\limits_{\theta_2=0}^{\pi} \int\limits_{\phi=0}^{2\pi} \left\{ \left[\frac{\partial \boldsymbol{\mu}^{(1)}}{\partial E_0} . e - a_0 \right] + \frac{1}{3kT} \left[\tfrac{1}{2}(\boldsymbol{\mu}^{(1)} + \boldsymbol{\mu}^{(2)})^2 - \mu_0^2 \right] \right\} e^{-\frac{U_{12}}{kT}}$$

$$\times R^2 \sin\theta_1 \sin\theta_2 \, dR \, d\theta_1 \, d\theta_2 \, d\phi, \tag{4.76}$$

where the general forms of the two terms are given by equations (4.28) and (4.50)

In order to determine the explicit forms of these expressions, it is necessary to express

the molecular property tensors in terms of the angles specifying their relative configuration, τ. The method for describing τ is described in Section 2.1.1.

In 1967 Buckingham [26] demonstrated how the property tensors of an linear molecule p may be expressed in terms of $\ell_i^{(p)}$, where $\ell_i^{(1)}$ and $\ell_i^{(2)}$ are the unit vectors along the principal axes of molecules 1 and 2, respectively:

$$\mu_i^{(p)} = \mu \ell_i^{(p)}, \tag{4.77}$$

where $\mu = \mu_3^{(1)} = \mu_{3'}^{(2)}$;

$$\theta_{ij}^{(p)} = \tfrac{1}{2}\theta \left(3\ell_i^{(p)}\ell_j^{(p)} - \delta_{ij} \right), \tag{4.78}$$

where $\theta = \theta_{33}^{(1)} = -2\theta_{22}^{(1)} = -2\theta_{11}^{(1)} = \theta_{3'3'}^{(2)} = -2\theta_{2'2'}^{(2)} = -2\theta_{1'1'}^{(2)}$;

$$a_{ij}^{(p)} = a\delta_{ij} + \kappa a \left(3\ell_i^{(p)}\ell_j^{(p)} - \delta_{ij} \right), \tag{4.79}$$

where $a = \tfrac{1}{3}a_{ii}^{(1)} = \tfrac{1}{3}a_{i'i'}^{(2)}$ and $\kappa = \dfrac{a_{33}^{(1)} - a_{11}^{(1)}}{3a} = \dfrac{a_{\parallel} - a_{\perp}}{3a} = \dfrac{\Delta a}{3a}$;

$$b_{ijk}^{(p)} = b_{\perp} \left(\ell_i^{(p)}\delta_{jk} + \ell_j^{(p)}\delta_{ki} + \ell_k^{(p)}\delta_{ij} \right) + (b_{\parallel} - 3b_{\perp}) \, \ell_i^{(p)}\ell_j^{(p)}\ell_k^{(p)}, \tag{4.80}$$

where $b_{\parallel} = b_{333}^{(1)} = b_{3'3'3'}^{(2)}$ and $b_{\perp} = b_{113}^{(1)} = b_{131}^{(1)} = b_{311}^{(1)} = b_{1'1'3'}^{(2)} = b_{1'3'1'}^{(2)} = b_{3'1'1'}^{(2)}$;

$$g_{iikl}^{(p)} = \left(g_{3311}^{(1)} + \tfrac{4}{3}g_{1111}^{(1)} \right) \delta_{kl} + \left(g_{3333}^{(1)} + g_{3311}^{(1)} - \tfrac{4}{3}g_{1111}^{(1)} \right) \ell_k^{(p)}\ell_l^{(p)}; \tag{4.81}$$

$$\phi_{iikl}^{(i)} = \left(\phi_{1111}^{(1)} + \phi_{2211}^{(1)} + \phi_{3311}^{(1)} \right) \delta_{kl} + \left(\phi_{3333}^{(1)} + 2\phi_{1133}^{(1)} - \phi_{1111}^{(1)} \right.$$
$$\left. -\phi_{2211}^{(1)} - \phi_{3311}^{(1)} \right) \ell_k^{(p)}\ell_l^{(p)}; \tag{4.82}$$

$$A_{ijk}^{(p)} = \tfrac{1}{2}A_{\parallel}\ell_i^{(p)} \left(3\ell_j^{(p)}\ell_k^{(p)} - \delta_{jk} \right) + A_{\perp} \left(\ell_j^{(p)}\delta_{ik} + \ell_k^{(p)}\delta_{ij} - 2\ell_i^{(p)}\ell_j^{(p)}\ell_k^{(p)} \right), \tag{4.83}$$

where $A_{\parallel} = A_{333}^{(1)} = -2A_{322}^{(1)} = -2A_{311}^{(1)} = A_{3'3'3'}^{(2)} = -2A_{3'2'2'}^{(2)} = -2A_{3'1'1'}^{(2)}$

and $A_{\perp} = A_{113}^{(1)} = A_{223}^{(1)} = A_{131}^{(1)} = A_{232}^{(1)} = A_{1'1'3'}^{(2)} = A_{2'2'3'}^{(2)} = A_{1'3'1'}^{(2)} = A_{2'3'2'}^{(2)}$;

and $\quad C_{ijkl}^{(p)} = \frac{1}{10} \left(C_{3333}^{(1)} + 8C_{1313}^{(1)} + 8C_{1111}^{(1)} \right) \left[\frac{1}{2}(\delta_{ik}\delta_{jl} + \delta_{il}\delta_{jk}) - \frac{1}{3}\delta_{ij}\delta_{kl} \right]$

$$+ \frac{1}{28} \left(5C_{3333}^{(1)} + 4C_{1313}^{(1)} - 8C_{1111}^{(1)} \right) \left[(3\ell_i^{(p)}\ell_k^{(p)} - \delta_{ik})\delta_{jl} \right.$$

$$+ (3\ell_i^{(p)}\ell_l^{(p)} - \delta_{il})\delta_{jk} + (3\ell_j^{(p)}\ell_k^{(p)} - \delta_{jk})\delta_{il} + (3\ell_j^{(p)}\ell_l^{(p)} - \delta_{jl})\delta_{ik}$$

$$\left. - \frac{4}{3}(3\ell_i^{(p)}\ell_j^{(p)} - \delta_{ij})\delta_{kl} - \frac{4}{3}(3\ell_k^{(p)}\ell_l^{(p)} - \delta_{kl})\delta_{ij} \right] \quad (4.84)$$

$$+ \frac{1}{35} \left(2C_{3333}^{(1)} - 4C_{1313}^{(1)} + C_{1111}^{(1)} \right) \left[35\ell_i^{(p)}\ell_j^{(p)}\ell_k^{(p)}\ell_l^{(p)} \right.$$

$$- 5(\ell_i^{(p)}\ell_j^{(p)}\delta_{kl} + \ell_i^{(p)}\ell_k^{(p)}\delta_{jl} + \ell_i^{(p)}\ell_l^{(p)}\delta_{jk} + \ell_j^{(p)}\ell_k^{(p)}\delta_{il}$$

$$\left. + \ell_j^{(p)}\ell_l^{(p)}\delta_{ik} + \ell_k^{(p)}\ell_l^{(p)}\delta_{ij}) + \delta_{ij}\delta_{kl} + \delta_{ik}\delta_{jl} + \delta_{il}\delta_{jk} \right] .$$

Also,

$$T_{ij} = \frac{1}{4\pi\varepsilon_0} \frac{1}{R^3} \left(3\lambda_i\lambda_j - \delta_{\alpha\beta} \right), \quad (4.85)$$

$$T_{ijk} = \frac{3}{4\pi\varepsilon_0} \frac{1}{R^4} \left[5\lambda_i\lambda_j\lambda_k - (\lambda_i\delta_{jk} + \lambda_j\delta_{i\gamma} + \lambda_k\delta_{\alpha\beta}) \right], \quad (4.86)$$

$$T_{ijkl} = \frac{3}{4\pi\varepsilon_0} \frac{1}{R^5} \left[35\lambda_i\lambda_j\lambda_k\lambda_l - 5 \left(\lambda_i\lambda_j\delta_{kl} + \lambda_i\lambda_k\delta_{jl} + \lambda_i\lambda_l\delta_{jk} \right. \right.$$
$$\left. \left. + \lambda_j\lambda_k\delta_{il} + \lambda_j\lambda_l\delta_{ik} + \lambda_k\lambda_l\delta_{ij} \right) + (\delta_{ij}\delta_{kl} + \delta_{ik}\delta_{jl} + \delta_{il}\delta_{jk}) \right]. \quad (4.87)$$

Explicit forms of $F_i^{(p)}$ and $F_{ij}^{(p)}$ are also required. These are obtained by substituting (4.77) and (4.78) into (4.45), yielding:

$$F_i^{(1)} = \frac{1}{4\pi\varepsilon_0} \left[\frac{\mu}{R^3} \left(3\lambda_i\lambda_j - \delta_{ij} \right) \ell_j^{(2)} - \frac{\theta}{2R^4} \left(5\lambda_i\lambda_j\lambda_k \right. \right.$$

$$\left. \left. -\lambda_i\delta_{jk} - \lambda_j\delta_{ik} - \lambda_k\delta_{ij} \right) \left(3\ell_j^{(2)}\ell_k^{(2)} - \delta_{jk} \right) + \cdots \right], \quad (4.88)$$

$$F_i^{(2)} = \frac{1}{4\pi\varepsilon_0} \left[\frac{\mu}{R^3} \left(3\lambda_i\lambda_j - \delta_{ij} \right) \ell_j^{(1)} + \frac{\theta}{2R^4} \left(5\lambda_i\lambda_j\lambda_k \right. \right.$$

$$\left. \left. -\lambda_i\delta_{jk} - \lambda_j\delta_{ik} - \lambda_k\delta_{ij} \right) \left(3\ell_j^{(1)}\ell_k^{(1)} - \delta_{jk} \right) + \cdots \right], \quad (4.89)$$

$$F_{ij}^{(1)} = \frac{1}{4\pi\varepsilon_0} \left[\frac{3\mu}{R^4} \left(5\lambda_i\lambda_j\lambda_k - \lambda_i\delta_{jk} - \lambda_j\delta_{ik} - \lambda_k\delta_{ij} \right) \ell_k^{(2)} + \cdots \right], \quad (4.90)$$

where $F_{ij}^{(1)}$ includes only dipole effects.

The unit vectors $\ell_\alpha^{(1)}$ and $\ell_\alpha^{(2)}$, and λ_α, which is the unit vector along the line of centres $\mathbf{R}$, are related to the angles θ_1, θ_2 and ϕ as shown in equations (2.26) to (2.28). These equations are the dot products of the unit vectors expressed in terms of the space-fixed axes, but the results are applicable to any set of axes. In particular, they apply to the molecule-fixed axes of molecule 1. Since the unit vector $\ell_i^{(1)}$ lies along the 3 axis, the expressions in equations (2.26) to (2.28) may be simplified as follows:

$$a_i^{3'} = \ell_i^{(2)}, \tag{4.91}$$

$$\ell_i^{(1)}\ell_i^{(2)} = \ell_3^{(2)} = \cos\theta_{12} = -\cos\theta_1\cos\theta_2 + \sin\theta_1\sin\theta_2\cos\phi, \tag{4.92}$$

$$\ell_i^{(1)}\lambda_i = \lambda_3 = \cos\theta_1, \tag{4.93}$$

$$\ell_i^{(2)}\lambda_i = -\cos\theta_2. \tag{4.94}$$

Substituting equations (4.77) to (4.90) into equations (4.29) to (4.41) yields terms containing $\ell_i^{(p)}$ and λ_i, which are eliminated using equations (4.92) to (4.94). This yields the following expressions for the induction term of B_ε:

$$\alpha_1 = a^{(1)} - a_0, \tag{4.95}$$

$$\alpha_2 = \frac{a^2}{4\pi\varepsilon_0 R^3}\left[\kappa(1-\kappa)\left(3\cos^2\theta_1 + 3\cos^2\theta_2 - 2\right) + 3\kappa^2\left(2\cos^2\theta_1\cos^2\theta_2\right.\right.$$
$$\left.\left. - \sin\theta_1\cos\theta_1\sin\theta_2\cos\theta_2\cos\phi - \sin^2\theta_1\sin^2\theta_2\cos^2\phi\right)\right], \tag{4.96}$$

$$\alpha_3 = \frac{a^3}{(4\pi\varepsilon_0)^2 R^6}\left[2(1-\kappa)^3 + \kappa(2+\kappa)(1-\kappa)\left(3\cos^2\theta_1 + 1\right) + \kappa(1-\kappa)^2\right.$$
$$\left. \times \left(3\cos^2\theta_2 + 1\right) + 3\kappa^2(2+\kappa)\left(2\cos\theta_1\cos\theta_2 + \sin\theta_1\sin\theta_2\cos\phi\right)^2\right], \tag{4.97}$$

$$\alpha_4 = \frac{a^4}{(4\pi\varepsilon_0)^3 R^9}\left\{2 + 6\kappa\left(3\cos^2\theta_1 + 3\cos^2\theta_2 - 2\right) + \kappa^2\left[18 - 54\left(\cos^2\theta_1 + \cos^2\theta_2\right)\right.\right.$$

$$\left. + 27\left(\cos^4\theta_1 + \cos^4\theta_2 - \cos\theta_1\cos\theta_2\cos\theta_{12}\right) + 81\cos^2\theta_1\cos^2\theta_2 - 12\cos^2\theta_{12}\right]$$

$$+ \kappa^3\left[54\left(\cos^2\theta_1 + \cos^2\theta_2 - \cos^4\theta_1 - \cos^4\theta_2\right) - 324\cos^2\theta_1\cos^2\theta_2\right.$$

$$+ 243\left(\cos^2\theta_1\cos^4\theta_2 + \cos^4\theta_1\cos^2\theta_2\right) - 8 + 81\cos\theta_{12}\left(\cos\theta_1\cos^3\theta_2\right.$$

$$\left. + \cos^3\theta_1\cos\theta_2\right) - 108\cos\theta_1\cos\theta_2\cos\theta_{12} - 12\cos^2\theta_{12}\right]$$

$$+ \kappa^4\left[27\left(\cos^4\theta_1 + \cos^4\theta_2\right) - 18\left(\cos^2\theta_1 + \cos^2\theta_2\right)\right.$$

$$- 243 \left(\cos^2 \theta_1 \cos^4 \theta_2 + \cos^4 \theta_1 \cos^2 \theta_2 - \cos^2 \theta_1 \cos^2 \theta_2\right)$$

$$- 81 \cos \theta_{12} \left(9 \cos^3 \theta_1 \cos^3 \theta_2 + \cos \theta_1 \cos^3 \theta_2 + \cos^3 \theta_1 \cos \theta_2\right)$$

$$+ 135 \cos \theta_1 \cos \theta_2 \cos \theta_{12} - 729 \cos^2 \theta_1 \cos^2 \theta_2 \cos^2 \theta_{12} + 24 \cos^2 \theta_{12}$$

$$\left. -243 \cos \theta_1 \cos \theta_2 \cos^3 \theta_{12} - 27 \cos^4 \theta_{12}\right] \Big\} , \tag{4.98}$$

$$\beta_1 = -\frac{5}{9} \frac{\mu b}{4\pi\varepsilon_0 R^3} \left(2 \cos \theta_1 \cos \theta_2 + \sin \theta_1 \sin \theta_2 \cos \phi\right)$$
$$- \frac{5}{6} \frac{\theta b}{4\pi\varepsilon_0 R^4} \left(3 \cos \theta_1 \cos^2 \theta_2 + 2 \sin \theta_1 \sin \theta_2 \cos \theta_2 \cos \phi - \cos \theta_1\right) , \tag{4.99}$$

$$\alpha_1 \beta_1 = -\frac{1}{3} \frac{a\mu}{(4\pi\varepsilon_0)^2 R^6} \Big\{ b_\perp \left[4(1 - \kappa) \left(3 \cos \theta_1 \cos \theta_2 - \cos \theta_{12}\right)\right.$$

$$\left. +9\kappa \left(\left(6 \cos \theta_1 \cos \theta_2 + \cos \theta_{12}\right) \left(\cos^2 \theta_1 + \cos^2 \theta_2\right) - 4 \cos \theta_1 \cos \theta_2 - 2 \cos \theta_{12}\right)\right]$$

$$+ \left(b_\parallel - 3b_\perp\right) \left[(1 - k) \left(3 \cos^2 \theta_2 + 3 \cos^2 \theta_1 - 2\right) \left(3 \cos \theta_1 \cos \theta_2 + \cos \theta_{12}\right)\right.$$

$$\left.\left. +6\kappa \left(-9 \cos^2 \theta_1 \cos^2 \theta_2 \cos \theta_{12} - 6 \cos \theta_1 \cos \theta_2 \cos^2 \theta_{12} - \cos^3 \theta_{12}\right)\right]\right\}$$

$$+ \frac{1}{2} \frac{a\theta}{(4\pi\varepsilon_0)^2 R^7} \Big\{ b_\perp \left[4(1 - \kappa) \left(\cos \theta_1 + \cos \theta_2\right) \left(1 - 2 \cos \theta_1 \cos \theta_2 + \cos \theta_{12}\right)\right.$$

$$- 3\kappa \left(\cos \theta_{12} \left(\cos \theta_2 (7 \cos^2 \theta_2 - 5) + \cos \theta_1 (7 \cos^2 \theta_1 - 5)\right)\right.$$

$$+ \cos \theta_1 \left(2 \cos^2 \theta_1 - 1\right) \left(15 \cos^2 \theta_1 - 1\right) + \cos \theta_2 \left(2 \cos^2 \theta_2 - 1\right)$$

$$\left.\left. \times \left(15 \cos^2 \theta_2 - 1\right)\right)\right] + \left(b_\parallel - 3b_\perp\right) \left[(1 - \kappa) \left(3(\cos^3 \theta_1 + \cos^3 \theta_2)\right.\right.$$

$$\left. +(\cos \theta_1 + \cos \theta_2) \left((1 - 3 \cos \theta_1 \cos \theta_2)(5 \cos \theta_1 \cos \theta_2 + 2 \cos \theta_{12}) - 1\right)\right)$$

$$+ 3\kappa(\cos \theta_1 + \cos \theta_2) \left(3 \cos \theta_1 \cos \theta_2 \cos \theta_{12}(5 \cos \theta_1 \cos \theta_2 - 1)\right.$$

$$\left.\left.\left. + \cos^2 \theta_{12}(11 \cos \theta_1 \cos \theta_2 - 1) + 2 \cos^3 \theta_{12}\right)\right]\right\} , \tag{4.100}$$

$$\gamma_1 = \frac{1}{18} \frac{\mu^2}{(4\pi\varepsilon_0) R^6} \Big\{ (3g_{3311} + 4g_{1111}) \left(3 \cos^2 \theta_2 + 1\right)$$
$$+ (3g_{3333} + 3g_{3311} - 4g_{1111}) \left(3 \cos \theta_1 \cos \theta_2 + \cos \theta_{12}\right)^2 \Big\} , \tag{4.101}$$

$$\phi_1 = -\frac{\mu}{(4\pi\varepsilon_0) R^4} \left(\phi_{3333} + 2\phi_{1133} - \phi_{1111} - \phi_{2211} - \phi_{3311}\right)$$
$$\times \left(5 \cos^2 \theta_1 \cos \theta_2 + 2 \cos \theta_1 \cos \theta_{12} - \cos \theta_2\right) , \tag{4.102}$$

$$\alpha_1\mathcal{A}_1 = \frac{2}{3}\frac{a}{4\pi\varepsilon_0 R^4}\left\{\left(\tfrac{3}{2}A_\parallel - 2A_\perp\right)\left[(1-\kappa)\left(5\cos^3\theta_1 - 3\cos\theta_1\right)\right.\right.$$

$$\left.-3\kappa\left(5\cos^2\theta_1\cos\theta_2\cos\theta_{12} - \cos\theta_2\cos\theta_{12}\right] + 2\cos\theta_1\cos^2\theta_{12}\right)\right] \tag{4.103}$$

$$\left.+6A_\perp\left(5\cos\theta_1\cos^2\theta_2 - \cos\theta_1 + 2\cos\theta_2\cos\theta_{12}\right)\right\},$$

$$\alpha_2\mathcal{A}_1 = \frac{2}{3}\frac{a^2}{(4\pi\varepsilon_0)^2 R^7}\left\{\left(\tfrac{3}{2}A_\parallel - 2A_\perp\right)\left[(1-\kappa)^2\left(4\cos^3\theta_1 + 4\cos^3\theta_2\right)\right.\right.$$

$$+ 3\kappa(2+\kappa)\left(15\cos^2\theta_1\cos^3\theta_2 - 3\cos^2\theta_1\cos\theta_2 + 11\cos\theta_1\cos^2\theta_2\cos\theta_{12}\right.$$

$$\left.- \cos\theta_1\cos\theta_{12} + 2\cos\theta_2\cos^2\theta_{12}\right) + 3\kappa(1+2\kappa)\left(15\cos^3\theta_1\cos^2\theta_2\right.$$

$$\left.+11\cos^2\theta_1\cos\theta_2\cos\theta_{12} - 3\cos\theta_1\cos^2\theta_2 + 2\cos\theta_1\cos^2\theta_{12} - \cos\theta_2\cos\theta_{12}\right)$$

$$\left.+12\kappa(1-\kappa)\cos^3\theta_1\right] + 2A_\perp\left[6(1-\kappa)^2(\cos\theta_1 + \cos\theta_2)\right.$$

$$+ \kappa(2+\kappa)\left(4\cos^2\theta_1\cos\theta_2 + \cos\theta_1\cos\theta_{12} - \cos\theta_2\right)$$

$$+ 3\kappa(1-\kappa)\left(4\cos^3\theta_1 + 4\cos\theta_1\cos^2\theta_2 + \cos\theta_2\cos\theta_{12} + \cos\theta_1\right)$$

$$9\kappa^2\left(15\cos^3\theta_1\cos^2\theta_2 + 11\cos^2\theta_1\cos\theta_2\cos\theta_{12} - 3\cos\theta_1\cos^2\theta_2\right.$$

$$\left.\left.+2\cos\theta_1\cos^2\theta_{12} - \cos\theta_2\cos\theta_{12}\right)\right]\right\}, \tag{4.104}$$

$$\mathcal{A}_2 = -\frac{1}{9}\frac{1}{4\pi\varepsilon_0 R^5}\left\{\left(\tfrac{3}{2}A_\parallel - 2A_\perp\right)^2\left(35\cos^2\theta_1\cos^2\theta_2\cos\theta_{12} - 5\cos^2\theta_1\cos\theta_{12}\right.\right.$$

$$\left.-5\cos^2\theta_2\cos\theta_{12} + 20\cos\theta_1\cos\theta_2\cos^2\theta_{12} + 2\cos^3\theta_{12} + \cos\theta_{12}\right)$$

$$- \left(3A_\parallel A_\perp - 4A_\perp^2\right)\left(35\cos^3\theta_1\cos\theta_2 + 35\cos\theta_1\cos^3\theta_2 + 15\cos^2\theta_1\cos\theta_{12}\right.$$

$$\left.\left.+15\cos^2\theta_2\cos\theta_{12} - 30\cos\theta_1\cos\theta_2 - 6\cos\theta_{12}\right)\right\}, \tag{4.105}$$

$$\alpha_1\mathcal{A}_2 = \frac{1}{9}\frac{a}{(4\pi\varepsilon_0)R^8}\left\{2\left[\left((1+2\kappa)\left(\tfrac{3}{2}A_\parallel - 2A_\perp\right)^2 + 3\kappa\left(3A_\parallel A_\perp - 4A_\perp^2\right)\right)\right.\right.$$

$$\times\left(180\cos^3\theta_1\cos^3\theta_2 - 30\cos^3\theta_1\cos\theta_2 - 30\cos\theta_1\cos^3\theta_2 + 6\cos\theta_1\cos\theta_2\right.$$

$$\left.+155\cos^2\theta_1\cos^2\theta_2\cos\theta_{12} + 38\cos\theta_1\cos\theta_2\cos^2\theta_{12} - 11\cos^2\theta_1\cos\theta_{12}\right.$$

$$\left.-11\cos^2\theta_2\cos\theta_{12} + 2\cos^3\theta_{12} + \cos\theta_{12}\right)$$

$$+ \left((1+2\kappa)\left(3A_\parallel A_\perp - 4A_\perp^2\right) + 12\kappa A_\perp^2\right)\left(40\cos^3\theta_1\cos\theta_2 + 12\cos^2\theta_1\cos\theta_{12}\right)$$

$$+ (1-\kappa)\left(3A_\parallel A_\perp - 4A_\perp^2\right)\left(40\cos\theta_1\cos\theta_23 + 12\cos^2\theta_1\cos\theta_{12}\right)$$

$$+4(1 - \kappa)A_\perp^2 \left(48 \cos\theta_1 \cos\theta_2 + 6 \cos\theta_{12}\right)\big]$$

$$+ 3\left[\left(\tfrac{9}{4}A_\parallel^2 - 4A_\perp^2\right)\left((1 - \kappa)\left(5 \cos^4\theta_1 - 2 \cos^2\theta_1 + 1\right)\right.\right.$$

$$+ 3\kappa\left(25 \cos^4\theta_1 \cos^2\theta_2 + 20 \cos^3\theta_1 \cos\theta_2 \cos\theta_{12} - 10 \cos^2\theta_1 \cos^2\theta_2\right.$$

$$\left.-4 \cos\theta_1 \cos\theta_2 \cos\theta_{12} + 4 \cos^2\theta_1 \cos^2\theta_{12} + \cos^2\theta_2\right))$$

$$+ 4A_\perp^2 \left(2(1 - \kappa)\left(2 \cos^2\theta_1 + 1\right) + 3\kappa\left(5 \cos^2\theta_1 \cos^2\theta_2\right.\right.$$

$$\left.\left.\left.+ 4 \cos\theta_1 \cos\theta_2 \cos\theta_{12} + \cos^2\theta_1 + \cos^2\theta_2 + \cos^2\theta_{12}\right)\right)\right]\right\}, \tag{4.106}$$

$$\alpha_2 C_1 = \frac{a^2}{(4\pi\varepsilon_0)R^8} \left\{\left(C_{3333} + 8C_{1313} + 8C_{1111}\right)\left[1 + 2\kappa^2 + \tfrac{2}{5}\kappa(2 + \kappa)\left(3 \cos^2\theta_1 - 1\right)\right]\right.$$

$$+ \tfrac{1}{28}\left(5C_{3333} + 4C_{1313} - 8C_{1111}\right)\left[16(1 + 2\kappa)^2\left(3 \cos^2\theta_2 - 1\right) + 12\kappa(2 + \kappa)\right.$$

$$\left.\times \left(15 \cos^2\theta_1 \cos^2\theta_2 + 12 \cos\theta_1 \cos\theta_2 \cos\theta_{12} + 3 \cos^2\theta_{12} - \cos^2\theta_1 - 1\right)\right]$$

$$+ \tfrac{1}{35}\left(2C_{3333} - 4C_{1313} + C_{1111}\right)\left[(1 - \kappa)^2\left(175 \cos^4\theta_2 - 150 \cos^2\theta_2 + 15\right)\right.$$

$$+ 3\kappa(2 + \kappa)\left(875 \cos^2\theta_1 \cos^4\theta_2 + 700 \cos\theta_1 \cos^3\theta_2 \cos\theta_{12}\right.$$

$$+ 140 \cos^2\theta_2 \cos^2\theta_{12} - 450 \cos^2\theta_1 \cos^2\theta_2 - 220 \cos\theta_1 \cos\theta_2 \cos\theta_{12}$$

$$\left.\left.\left.-20 \cos^2\theta_2 - 20 \cos^2\theta_{12} + 23 \cos^2\theta_1 + 4\right)\right]\right\}. \tag{4.107}$$

Substituting equations (4.77) to (4.90) into equations (4.51) to (4.69) yields the following expressions for the orientation term of B_ε:

$$\mu_2 = \mu_0^2 \cos\theta_{12}, \tag{4.108}$$

$$\alpha_1 \mu_2 = \frac{2a\mu}{4\pi\varepsilon_0 R^3} \left\{(1 - \kappa)\left(3 \cos^2\theta_1 - 1\right)\right.$$

$$\left.-(1 + 2\kappa + 3\kappa \cos\theta_{12})\left(3 \cos\theta_1 \cos\theta_2 + \cos\theta_{12}\right)\right\}, \tag{4.109}$$

$$\alpha_2 \mu_2 = \frac{3a^2\mu^2}{(4\pi\varepsilon_0)^2 R^6} \left\{(1 - \kappa)^2\left(2 \cos^2\theta_1 + \cos^2\theta_2 - 3 \cos\theta_1 \cos\theta_2 + \cos\theta_{12} + 1\right)\right.$$

$$+ \kappa(1 - \kappa)\left[2\left(3 \cos^2\theta_1 + 1\right) + 3 \cos\theta_{12}\left(2 - 3 \cos^2\theta_1 + \cos^2\theta_2\right)\right.$$

$$\left.+4\left(3 \cos\theta_1 \cos\theta_2 + \cos\theta_{12}\right)^2 + 3 \cos\theta_1 \cos\theta_2\left(4 - 9 \cos^2\theta_1 - 3 \cos^2\theta_2\right)\right]$$

$$\left.+9\kappa^2(1 + \cos\theta_{12})\left(3 \cos\theta_1 \cos\theta_2 + \cos\theta_{12}\right)^2\right\}, \tag{4.110}$$

$$\alpha_3\mu_2 = \frac{2a^3\mu^2}{(4\pi\varepsilon_0)^3 R^9} \left\{ (1-\kappa)^3 \left[3\left(\cos\theta_1 + \cos\theta_2\right)^2 - 2\left(\cos\theta_{12} + 1\right) \right] + 3\kappa(1-\kappa)^2 \right.$$

$$\times \left[9\cos^4\theta_1 + 9\cos^4\theta_2 - 27\cos^3\theta_1\cos\theta_2 + 18\cos\theta_1\cos^3\theta_2 - 4\cos^2\theta_{12} \right.$$

$$\left. -3\cos\theta_{12}\left(3\cos^2\theta_1 + 2\cos^2\theta_2 + 3\cos\theta_1\cos\theta_2 - 2\right) - 24\cos\theta_1\cos\theta_2 \right]$$

$$+ 27\kappa^2(1-\kappa) \left[18\cos^4\theta_1\cos^2\theta_2 + 9\cos^2\theta_1\cos^4\theta_2 - 27\cos^3\theta_1\cos^3\theta_2 \right.$$

$$- 9\cos^3\theta_1\cos\theta_2 - 3\cos\theta_1\cos^3\theta_2 - 9\cos^2\theta_1\cos^2\theta_2 - 3\cos\theta_1\cos\theta_2$$

$$- \cos\theta_{12}\left(27\cos^2\theta_1\cos^2\theta_2 - 9\cos^3\theta_1 + 9\cos\theta_1\cos\theta_2 + 2\cos^2\theta_1\right.$$

$$\left. + \cos^2\theta_2 + 1\right) + \cos^2\theta_{12}\left(\cos^2\theta_1 - \cos^2\theta_2 - 9\cos\theta_1\cos\theta_2 - 2\right) - \cos^3\theta_{12}\right]$$

$$- 54\kappa^3 \left(27\cos^3\theta_1\cos\theta_2 2 + 27\cos^2\theta_1\cos^2\theta_2\cos\theta_{12}\left(1 - \cos\theta_1\cos\theta_2\right)\right.$$

$$+ 9\cos\theta_1\cos\theta_2\cos^2\theta_{12}\left[1 + 3\cos\theta_1\cos\theta_2\right) + \cos^3\theta_{12}\left(1 + 9\cos\theta_1\cos\theta_2\right)$$

$$\left. \left. + \cos^4\theta_{12}\right] \right\}, \tag{4.111}$$

$$\alpha_1\mu_1\theta_1 = -\frac{3a\mu\theta}{4\pi\varepsilon_0 R^4} \left\{ (1 + \kappa(3\cos\theta_{12} - 1))\left(5\cos^2\theta_1\cos\theta_2 - \cos\theta_2 + 2\cos\theta_1\cos\theta_{12}\right) \right.$$

$$\left. + (1 + 2\kappa)\left(5\cos\theta_1\cos^2\theta_2 - \cos\theta_1 + 2\cos\theta_2\cos\theta_{12}\right) \right\}, \tag{4.112}$$

$$\alpha_2\mu_1\theta_1 = \frac{3a^2\mu\theta}{(4\pi\varepsilon_0)R^7} \left\{ 2(1-\kappa)^2 \left[(\cos\theta_1 + \cos\theta_2)\left(1 - 2\cos\theta_1\cos\theta_2 + \cos\theta_{12}\right) \right. \right.$$

$$\left. + 2\left(\cos^3\theta_1 + \cos^3\theta_2\right) \right] + 3\kappa(1-\kappa)\left[7\cos^3\theta_1 + 3\cos^3\theta_2 - \cos\theta_1 \right.$$

$$- \cos\theta_2 - 15\cos^4\theta_1\cos\theta_2 + 15\cos^2\theta_1\cos^3\theta_2 + 8\cos^2\theta_1\cos\theta_2$$

$$+ 2\cos\theta_1\cos^2\theta_2 + \cos\theta_{12}\left(3\cos\theta_1 + \cos\theta_2 - 5\cos^3\theta_1 + 4\cos^3\theta_2\right.$$

$$\left. + 5\cos^2\theta_1\cos\theta_2 + 16\cos\theta_1\cos^2\theta_2\right) + 2\cos^2\theta_{12}\left(\cos\theta_1 + 2\cos\theta_2\right)\right]$$

$$+ 9\kappa^2\left(\cos\theta_1 + \cos\theta_2\right)\left[15\cos^2\theta_1\cos^2\theta_2 - 3\cos\theta_1\cos\theta_2 \right.$$

$$+ \cos\theta_{12}\left(15\cos^2\theta_1\cos^2\theta_2 + 8\cos\theta_1\cos\theta_2 - 1\right)$$

$$\left. \left. + \cos^2\theta_{12}\left(11\cos\theta_1\cos\theta_2 + 1\right) + 2\cos^3\theta_{12}\right] \right\}, \tag{4.113}$$

$$\alpha_2\theta_2 = \frac{9}{4}\frac{a^2\theta^2}{(4\pi\varepsilon_0)^2 R^8}\left\{(1-\kappa)^2\left(5\cos^4\theta_2 + 3\cos^2\theta_1 + \cos^2\theta_2 - 5\cos^2\theta_1\cos^2\theta_2\right.\right.$$

$$\left.+4\cos\theta_1\cos\theta_2\cos\theta_{12}\right) + 3\kappa(1-\kappa)\left[5\cos^4\theta_1 + 5\cos^4\theta_2 - \cos^2\theta_1\right.$$

$$-3\cos^2\theta_2 - 25\cos^4\theta_1\cos^2\theta_2 + 25\cos^2\theta_1\cos^4\theta_2 + 10\cos^2\theta_1\cos^2\theta_2$$

$$+2\cos\theta_1\cos\theta_2\cos\theta_{12}\left(15\cos^2\theta_2 - 5\cos^2\theta_1 + 2\right) + 8\cos^2\theta_2\cos^2\theta_{12}\Big]$$

$$+9\kappa^2\left[\cos^2\theta_1\left(5\cos^2\theta_2 - 1\right)^2 + \cos\theta_1\cos\theta_2\cos\theta_{12}\left(25\cos^2\theta_1\cos^2\theta_2\right.\right.$$

$$+15\cos^2\theta_2 - 5\cos^2\theta_1 - 3\Big) + 2\cos^2\theta_{12}\left(10\cos^2\theta_1\cos^2\theta_2 + \cos^2\theta_2\right.$$

$$\left.\left.\left.-\cos^2\theta_1\right) + 4\cos\theta_1\cos\theta_2\cos^3\theta_{12}\right]\right\}, \tag{4.114}$$

$$\alpha_3\theta_2 = \frac{9}{2}\frac{a^3\theta^2}{(4\pi\varepsilon_0)^3 R^{11}}\left\{2(1-\kappa)^3\left(11\cos^4\theta_2 + 3\cos^2\theta_1 - 5\cos^2\theta_2\right.\right.$$

$$\left.-11\cos^2\theta_1\cos^2\theta_2 - 2\cos\theta_1\cos\theta_2\cos\theta_{12}\right) + 12\kappa(1-\kappa)^2\left[5\cos^6\theta_2\right.$$

$$+2\cos^4\theta_1 - 2\cos^4\theta_2 + \cos^2\theta_1 - 10\cos^4\theta_1\cos^2\theta_2 + 5\cos^2\theta_1\cos^4\theta_2$$

$$-7\cos^2\theta_1\cos^2\theta_2 - \cos\theta_1\cos\theta_2\cos\theta_{12}\left(4\cos^2\theta_1 + 3\cos^2\theta_2 + 1\right)$$

$$\left.-2\cos^2\theta_2\cos^2\theta_{12}\right] + 9\kappa^2(1-\kappa)\left[7\cos^4\theta_1 - \cos^2\theta_1 + 75\cos^2\theta_1\cos^6\theta_2\right.$$

$$-75\cos^4\theta_1\cos^4\theta_2 - 20\cos^4\theta_1\cos^2\theta_2 - 55\cos^2\theta_1\cos^4\theta_2$$

$$+13\cos^2\theta_1\cos^2\theta_2 + \cos\theta_1\cos\theta_2\cos\theta_{12}\left(35\cos^4\theta_2 + 2\cos^2\theta_1 - 32\cos^2\theta_2\right.$$

$$-110\cos^2\theta_1\cos^2\theta_2 + 5\Big) + 2\cos^2\theta_{12}\left(\cos^4\theta_2 + 2\cos^2\theta_1 - 3\cos^2\theta_2\right.$$

$$\left.-26\cos^2\theta_1\cos^2\theta_2\right) - 8\cos\theta_1\cos\theta_2\cos^3\theta_{12}\Big] + 27\kappa^3\left[3\cos^2\theta_1\cos^2\theta_2\right.$$

$$\times\left(5\cos^2\theta_1 + 5\cos^2\theta_2 - 25\cos^2\theta_1\cos^2\theta_2 - 1\right) + \cos\theta_1\cos\theta_2\cos\theta_{12}$$

$$\times\left(8\cos^2\theta_1 + 11\cos^2\theta_2 - 75\cos^2\theta_1\cos^4\theta_2 - 55\cos^2\theta_1\cos^2\theta_2 - 1\right)$$

$$+\cos^2\theta_{12}\left(\cos^2\theta_1 + 2\cos^2\theta_2 - 85\cos^2\theta_1\cos^4\theta_2 - 10\cos^2\theta_1\cos^2\theta_2\right)$$

$$\left.\left.-32\cos\theta_1\cos^3\theta_2\cos^3\theta_{12} - 4\cos^2\theta_2\cos^4\theta_{12}\right]\right\}, \tag{4.115}$$

$$\beta_1\mu_3 = 2\frac{\mu^3}{(4\pi\varepsilon_0)^2 R^9}\left\{\left(2b_\perp + (b_\parallel - 3b_\perp)(1 - \cos\theta_{12})\right)(3\cos\theta_1\cos\theta_2 + \cos\theta_{12})^2\right.$$

$$+ b_\perp\left[3\cos\theta_{12}\left(1 - \cos^2\theta_1\right) + 6\cos\theta_1\cos\theta_2\left(1 - 3\cos^2\theta_1\right)\right.$$

$$\left.\left.+3\cos^2\theta_2 + 1\right]\right\}, \tag{4.116}$$

$$\alpha_1\beta_1\mu_3 = -2\frac{a\mu^3}{(4\pi\varepsilon_0)^3 R^9}\left\{b_\perp\left[(1-\kappa)\left(\cos\theta_1\cos\theta_2(63\cos^2\theta_1 + 27\cos^2\theta_2 + 48\right.\right.\right.$$

$$- 90\cos\theta_1\cos\theta_2) - 6\cos^2\theta_1 + 6\cos^2\theta_2 + 4 + 3\cos\theta_{12}(7\cos^2\theta_1 + 3\cos^2\theta_2$$

$$+6\cos\theta_1\cos\theta_2 + 4) + 8\cos^2\theta_{12}\big) + 9\kappa\left(3\cos\theta_1\cos\theta_2(2 + 3\cos^2\theta_1)\right.$$

$$+ 18\cos^2\theta_1\cos^2\theta_2(1 - 3\cos^2\theta_1) + \cos\theta_1\cos^3\theta_2(1 + 6\cos^2\theta_1)$$

$$+ \cos\theta_{12}\left(3\cos^2\theta_1 + 3\cos^2\theta_2 + 2 + 9\cos\theta_1\cos\theta_2(\cos^2\theta_2 - 3\cos^2\theta_1\right.$$

$$+6\cos\theta_1\cos\theta_2 + 2)\big) + \cos^2\theta_{12}\left(3\cos^2\theta_2 - 3\cos^2\theta_1 + 18\cos\theta_1\cos\theta_2 + 4\right)$$

$$+2\cos^3\theta_{12}\big)\big] + (b_\parallel - 3b_\perp)\left[(1-\kappa)\left(6\cos\theta_1\cos\theta_2(1 + 3\cos\theta_1\cos\theta_2\right.\right.$$

$$+ 3\cos^2\theta_1) - 27\cos^2\theta_1\cos^2\theta_2(\cos\theta_1 - \cos\theta_2)^2 + 2\cos\theta_{12}\left(1 + 3\cos^2\theta_1\right.$$

$$+9\cos\theta_1\cos\theta_2(3\cos\theta_1\cos\theta_2 - \cos^2\theta_1 + 1)\big) + \cos^2\theta_{12}\left(4 + 3\cos^2\theta_2\right.$$

$$-3\cos^2\theta_1 + 18\cos\theta_1\cos\theta_2\big) + 2\cos^3\theta_{12}\big) + 12\kappa\left(27\cos^3\theta_1\cos^3\theta_2\right.$$

$$+ 27\cos^2\theta_1\cos^2\theta_2\cos\theta_{12}(1 + \cos\theta_1\cos\theta_2) + 9\cos\theta_1\cos\theta_2\cos^2\theta_{12}$$

$$\left.\left.\times(1 + 3\cos\theta_1\cos\theta_2) + \cos^3\theta_{12}(1 + 9\cos\theta_1\cos\theta_2) + \cos^4\theta_{12}\big)\right]\right\}, \tag{4.117}$$

$$\beta_1\mu_2\theta_1 = -6\frac{\mu^2\theta}{(4\pi\varepsilon_0)^2 R^7}\left\{b_\perp\left[\cos\theta_2\left(1 - 11\cos^2\theta_1 + 3\cos^4\theta_1\right) - 4\cos\theta_2\cos^2\theta_{12}\right.\right.$$

$$-2\cos^3\theta_2\left(2 + 15\cos^2\theta_1\right) - \cos\theta_1\cos\theta_{12}\left(3 - 7\cos^2\theta_1 + 22\cos^2\theta_2\right)\big]$$

$$+ (b_\parallel - 3b_\perp)\left[3\cos^2\theta_1\cos\theta_2\left(1 - 5\cos^2\theta_2\right) + \cos\theta_1\cos\theta_{12}\right.$$

$$\left(1 - \cos^2\theta_2(8 + 15\cos^2\theta_1)\right) - \cos\theta_2\cos^2\theta_{12}\left(1 + 11\cos^{12}\theta_1\right)$$

$$\left.\left.-2\cos\theta_1\cos^3\theta_2\right]\right\}, \tag{4.118}$$

$$\mathcal{A}_1\mu_2 = -\frac{\mu^2}{4\pi\varepsilon_0 R^4}\left(3A_\parallel - 4A_\perp\right)\left[\cos\theta_2\left(5\cos^2\theta_1 + 2\cos^2\theta_{12} - 1\right)\right.$$
$$\left. + \cos\theta_1\cos\theta_{12}\left(5\cos^2\theta_2 + 1\right)\right], \tag{4.119}$$

$$\alpha_1\mathcal{A}_1\mu_2 = -\frac{a\mu^2}{(4\pi\varepsilon_0)^2 R^7}\left\{\left(3A_\parallel - 4A_\perp\right)\left[(1-\kappa)\left(15\cos\theta_1\cos^3\theta_2(\cos\theta_2 - 2\cos\theta_1)\right.\right.\right.$$
$$-5\cos\theta_1\cos^2\theta_2(3\cos^2\theta_1+1) + \cos\theta_2(5\cos^2\theta_1-1)(6\cos^2\theta_1-1) + \cos\theta_1$$
$$-4\cos^3\theta_1 - \cos\theta_{12}(3\cos\theta_1 + \cos\theta_2 - 11\cos^3\theta_1 - 2\cos^3\theta_2 + (2\cos\theta_{12}$$
$$+11\cos\theta_1\cos\theta_2)(\cos\theta_1 + 2\cos\theta_2))) + 6\kappa(\cos\theta_1+\cos\theta_2)\left(3\cos\theta_1\cos\theta_2\right.$$
$$-15\cos^2\theta_1\cos^2\theta_2 + \cos\theta_{12}(1 - 8\cos\theta_1\cos\theta_2 - 15\cos^2\theta_1\cos^2\theta_2)$$
$$\left.\left. -\cos^2\theta_{12}(11\cos\theta_1\cos\theta_2 + 1) - 2\cos^3\theta_{12}\right)\right] + 4A_\perp\left[(1-\kappa)\left(\cos\theta_1\right.\right.$$
$$-3\cos\theta_2 + 4\cos\theta_1(\cos^2\theta_2 - \cos^2\theta_1) + \cos\theta_{12}(\cos\theta_2 - 3\cos\theta_1))$$
$$-6\kappa\left(\cos\theta_2(4\cos^2\theta_1 + 1) + 2\cos\theta_1\cos\theta_{12}(2\cos^2\theta_2 + 1)\right.,$$
$$\left.\left.\left. +\cos\theta_2\cos^2\theta_{12}\right)\right]\right\}, \tag{4.120}$$

$$\mathcal{A}_1\mu_1\theta_1 = -\frac{1}{2}\frac{\mu\theta}{4\pi\varepsilon_0 R^5}\left\{\left[3A_\parallel(1+\cos\theta_{12}) - 4A_\perp\cos\theta_{12}\right]\left[1 - 5\cos^2\theta_1\right.\right.$$
$$\left. -5\cos^2\theta_2(1 - 7\cos^2\theta_1) + 20\cos\theta_1\cos\theta_2\cos\theta_{12} + 2\cos^2\theta_{12}\right]$$
$$\left. +4A_\perp\left[5\cos\theta_1\cos\theta_2(3 - 7\cos^2\theta_1)\right] + 3\cos\theta_{12}(1 - 5\cos^2\theta_1)\right]\right\}, \tag{4.121}$$

$$\alpha_1\mathcal{A}_1\theta_2 = \frac{3}{4}\frac{a\theta^2}{(4\pi\varepsilon_0)^2 R^9}\left\{\left[3A_\parallel(1+2\kappa) - 4A_\perp(1-\kappa)\right]\left[5\cos^3\theta_1 - \cos\theta_1\right.\right.$$
$$+ 5\cos\theta_1\cos^2\theta_2\left(2(1 - 6\cos^2\theta_1) - 5\cos^2\theta_2(1 - 7\cos^2\theta_1)\right)$$
$$+ 2\cos\theta_2\cos\theta_{12}\left(1 - 15\cos^2\theta_1 - 5\cos^2\theta_2(1 - 17\cos^2\theta_1)\right)$$
$$\left. -2\cos\theta_1\cos^2\theta_{12}(1 - 25\cos^2\theta_2) + 4\cos\theta_2\cos^3\theta_{12}\right]$$
$$+ 8A_\perp(1-\kappa)\left[2\cos\theta_1 - 5\cos\theta_1\cos^2\theta_2(1 - 3\cos^2\theta_2)\right.$$
$$\left.\left. -\cos\theta_2\cos\theta_{12}(1 - 5\cos^2\theta_2)\right]\right\}, \tag{4.122}$$

$$\alpha_1 C_1 \mu_2 = 6 \frac{a\mu^2}{(4\pi\varepsilon_0)^2 R^8} \left\{ \tfrac{1}{5}(C_{3333} + 8C_{1313} + 8C_{1111}) \left[(1 + 2\kappa)\left(2\cos^2\theta_1 + 1 \right. \right. \right.$$

$$\left. + \cos\theta_{12}\right) - 2(1-\kappa)\cos\theta_1\cos\theta_2 + 6\kappa\cos^2\theta_2\cos\theta_{12}\big]$$

$$+ \tfrac{1}{7}(5C_{3333} + 4C_{1313} - 8C_{1111}) \left[(1 + 2\kappa)\left(3\cos^2\theta_2(1 + 5\cos^2\theta_1) - 2 \right. \right.$$

$$- \cos^2\theta_1\big) + 3\left(1 + \kappa(2 + 3\cos\theta_{12})\right)\cos\theta_{12}(4\cos\theta_1\cos\theta_2 + \cos\theta_{12})$$

$$+ (1-\kappa)\left(\cos\theta_1\cos\theta_2(7 - 15\cos^2\theta_1) + \cos\theta_{12}(1 - 3\cos^2\theta_1)\right)$$

$$+ 3\kappa\cos\theta_{12}\left(\cos^2\theta_2(15\cos^2\theta_1 - 1) + 3\cos^2\theta_1 - 2)\right]$$

$$+ \tfrac{1}{35}(2C_{3333} - 4C_{1313} + C_{1111}) \left[(1 + 2\kappa)\left(23\cos^2\theta_1 - 20\cos^2\theta_2 + 4 \right. \right.$$

$$+ 25\cos^2\theta_1\cos^2\theta_2(35\cos^2\theta_2 - 18) + 20\cos\theta_1\cos\theta_2\cos\theta_{12}(35\cos^2\theta_2 - 11)$$

$$+ 20\cos^2\theta_{12}(7\cos^2\theta_2 - 1)\big) - (1-\kappa)\left(\cos\theta_1\cos\theta_2(875\cos^4\theta_1 + 133 \right.$$

$$- 800\cos^2\theta_1) + \cos\theta_{12}(350\cos^4\theta_2 + 16 - 230\cos^2\theta_2)\big) + 3\kappa\cos\theta_{12}$$

$$\times \left(23\cos^2\theta_2 - 20\cos^2\theta_1 + 4 + 20\cos\theta_1\cos\theta_2\cos\theta_{12}(35\cos^2\theta_1 - 11)\right.$$

$$+ 25\cos^2\theta_1\cos^2\theta_2(35\cos^2\theta_1 - 18) + 20\cos^2\theta_{12}(7\cos^2\theta_1 - 1))\big] \right\}, \quad (4.123)$$

$$\alpha_1 C_1 \mu_1 \theta_1 = 3 \frac{a\mu\theta}{(4\pi\varepsilon_0)^2 R^9} \left\{ \tfrac{2}{5}(C_{3333} + 8C_{1313} + 8C_{1111}) \left[(1 - \kappa)\left(5\cos^3\theta_1 + 4\cos\theta_1 \right. \right. \right.$$

$$- 5\cos\theta_1\cos^2\theta_2 + 4\cos\theta_2\cos\theta_{12}\big) + 3\kappa\left(5\cos^3\theta_1 + \cos\theta_1 + \cos\theta_2\cos\theta_{12}\right.$$

$$+ 5\cos^3\theta_2\cos\theta_{12}\big) + \tfrac{1}{7}(5C_{3333} + 4C_{1313} - 8C_{1111}) \left[5(1 - \kappa)\left(5\cos^3\theta_1 \right. \right.$$

$$- 5\cos\theta_1 + 10\cos\theta_1\cos^2\theta_2 + \cos\theta_2\cos\theta_{12}(1 + 15\cos^2\theta_1)$$

$$+ 6\cos\theta_1\cos^2\theta_{12}\big) + 3\kappa\left(90\cos^3\theta_1\cos^2\theta_2 - 5\cos^3\theta_1 - 7\cos\theta_1\right.$$

$$+ 5\cos\theta_2\cos\theta_{12}(15\cos^2\theta_1 - 2 + \cos^2\theta_2(18\cos^2\theta_1 - 1))$$

$$+ 15\cos\theta_1\cos^2\theta_{12}(1 + 5\cos^2\theta_2) + 18\cos\theta_2\cos^3\theta_{12})\big]$$

$$+ \tfrac{3}{35}(2C_{3333} - 4C_{1313} + C_{1111}) \left[(1 - \kappa)\left(875\cos^5\theta_1 - 785\cos^3\theta_1 \right. \right.$$

$$+ 162\cos\theta_1 - 5\cos\theta_1\cos^2\theta_2(1225\cos^4\theta_1 - 490\cos^2\theta_1 + 83)$$

$$+ 875\cos\theta_1\cos^4\theta_2(7\cos^2\theta_1 - 1) - \cos\theta_2\cos\theta_{12}(3500\cos^4\theta_1 - 55\cos^2\theta_1$$

$$+ 38 - 350\cos^2\theta_2(17\cos^2\theta_1 - 1)) + 10\cos\theta_1\cos^2\theta_{12}(175\cos^2\theta_2$$

$$-35\cos^2\theta_1 - 6) + 140\cos\theta_2\cos^3\theta_{12}) + 3\kappa\left(115\cos^3\theta_1 - 7\cos\theta_1\right.$$

$$+ 50\cos\theta_1\cos^2\theta_2(7 - 54\cos^2\theta_1) + 875\cos\theta_1\cos^4\theta_2(7\cos^2\theta_1 - 1)$$

$$- \cos\theta_2\cos\theta_{12}(875\cos^4\theta_1 + 1200\cos^2\theta_1 - 83 - 5\cos^2\theta_2(1225\cos^4\theta_1$$

$$+ 650\cos^2\theta_1 - 47)) - 50\cos\theta_1\cos^2\theta_{12}(7\cos^2\theta_1 + 2 - \cos^2\theta_2(119\cos^2\theta_1$$

$$\left.+4)) + 50\cos\theta_2\cos^3\theta_{12}(35\cos^2\theta_1 - 1) + 140\cos\theta_1\cos^4\theta_2)\right]\Big\}. \qquad (4.124)$$

The explicit expressions for $\alpha_4\theta_2$ and $\alpha_2C_1\theta_2$ are too long to give here. In order to eliminate programming errors, Macsyma's Fortran conversion facility was used to convert the expressions directly into Fortran.

If the molecules are assumed to be isotropic and, therefore, the molecular anisotropy κ to be zero, then the terms for μ_2, $\alpha_1\mu_2$ and $\alpha_2\mu_2$ in equations (4.108) to (4.111) reduce to the familiar expressions derived by Buckingham and Pople [101].

4.5 B_ε for non-linear molecules

For non-linear gases the second virial coefficient is given by

$$B_\varepsilon = \frac{N_A^2}{3\varepsilon_0\Omega}\int_\tau \left\{\left[\frac{\partial\boldsymbol{\mu}^{(1)}}{\partial E_0}.\boldsymbol{e} - a_0\right] + \frac{1}{3kT}\left[\tfrac{1}{2}(\boldsymbol{\mu}^{(1)} + \boldsymbol{\mu}^{(2)})^2 - \mu_0^2\right]\right\}e^{-\frac{U_{12}(\tau)}{kT}}d\tau$$

$$= \frac{N_A^2}{48\pi^3\varepsilon_0}\int\limits_{R=0}^{\infty}\int\limits_{\alpha_1=0}^{2\pi}\int\limits_{\beta_1=0}^{\pi}\int\limits_{\gamma_1=0}^{2\pi}\int\limits_{\alpha_2=0}^{2\pi}\int\limits_{\beta_2=0}^{\pi}\int\limits_{\gamma_2=0}^{2\pi}\left\{\left[\frac{\partial\boldsymbol{\mu}^{(1)}}{\partial E_0}.\boldsymbol{e} - a_0\right]\right.$$

$$\left.+ \frac{1}{3kT}\left[\tfrac{1}{2}(\boldsymbol{\mu}^{(1)} + \boldsymbol{\mu}^{(2)})^2 - \mu_0^2\right]\right\}e^{-\frac{U_{12}}{kT}}\ R^2\ \sin\beta_1\sin\beta_2\ dR\ d\alpha_1 d\beta_1 d\gamma_1 d\alpha_2, d\beta_2 d\gamma_2,$$

$$(4.125)$$

where general expressions for the two terms are given by equations (4.28) and (4.50). For the non-linear gases under consideration, experimental values for some of the molecular properties, such as the hyperpolarizabilities and the A- and C-tensors, are not available. For this reason, and because of estimations of the relative importance of these terms based on the results for the linear gases, terms containing hyperpolarizabilities and the A- and C-tensors were neglected for the non-linear gases. The remaining terms in the dipole moment, quadrupole moment and the molecular polarizabilities, were calculated

to an order high enough to establish convergence.

The general formulae for these terms must now be expressed in terms of the elements of the seven interaction parameters R, α_1, β_1, γ_1, α_2, β_2 and γ_2, described in Section 2.1.2.

Since the terms in equations (4.28) and (4.50) are referred to O(1,2,3), the property tensors of molecule 2 must be projected into the axes of molecule 1. This is achieved by first rotating the tensor from $O'(1', 2', 3')$ into O(x,y,z) using the direction cosine $a_{i'}^\alpha$, and then rotating the resultant tensor into O(1,2,3) by means of a_i^α. Thus, the dipole moment of molecule 2 referred to molecule 1's axes is given by:

$$\mu_i^{(2)} = a_\alpha^i \mu_\alpha^{(2)} = a_\alpha^i a_{i'}^\alpha \mu_{i'}^{(2)}, \tag{4.126}$$

where $\mu_{i'}^{(2)} = \mu_i^{(1)} = [0 \quad 0 \quad \mu]$, and a_α^i may be viewed as the transpose of equation (2.5). Using equation (2.44) we get:

$$\mu_i^{(2)} = \mu[\mathcal{D}_1 \quad \mathcal{D}_2 \quad \mathcal{D}_3], \tag{4.127}$$

where

$$\mathcal{D}_1 = A_7 B_9 + A_4 B_6 + A_1 B_3,$$

$$\mathcal{D}_2 = A_8 B_9 + A_5 B_6 + A_2 B_3, \tag{4.128}$$

$$\mathcal{D}_3 = A_9 B_9 + A_6 B_6 + A_3 B_3,$$

where A_1 to A_9 and B_1 to B_9 are defined in equations (2.45) to (2.53).

Similarly, the quadrupole moment of molecule 2 referred to O(1,2,3) is given by:

$$\theta_{ij}^{(2)} = a_\alpha^i a_\beta^j a_{i'}^\alpha a_{j'}^\beta \theta_{i'j'}^{(2)} = \begin{bmatrix} Q_{11} & Q_{12} & Q_{13} \\ Q_{12} & Q_{22} & Q_{23} \\ Q_{13} & Q_{23} & Q_{33} \end{bmatrix}, \tag{4.129}$$

where

$$\theta_{i'j'}^{(2)} = \theta_{ij}^{(1)} = \begin{bmatrix} \theta_1 & 0 & 0 \\ 0 & \theta_2 & 0 \\ 0 & 0 & -(\theta_1 + \theta_2) \end{bmatrix} \tag{4.130}$$

65

and

$$Q_{11} = \theta_1 \left[A_7^2(B_7^2 - B_9^2) + A_4^2(B_4^2 - B_6^2) + A_1^2(B_1^2 - B_3^2) - 2A_7B_9(A_4B_6 \right.$$
$$\left. + A_1B_3) + 2A_7B_7(A_4B_4 + A_1B_1) + 2A_1A_4(B_1B_4 - B_3B_6) \right]$$
$$+ \theta_2 \left[A_7^2(B_8^2 - B_9^2) + A_4^2(B_5^2 - B_6^2) + A_1^2(B_2^2 - B_3^2) - 2A_7B_9(A_4B_6 \right.$$
$$\left. + A_1B_3) + 2A_7B_8(A_4B_5 + A_1B_2) + 2A_1A_4(B_2B_5 - B_3B_6) \right],$$

(4.131)

$$Q_{22} = \theta_1 \left[A_8^2(B_7^2 - B_9^2) + A_5^2(B_4^2 - B_6^2) + A_2^2(B_1^2 - B_3^2) - 2A_8B_9(A_5B_6 \right.$$
$$\left. + A_2B_3) + 2A_8B_7(A_5B_4 + A_2B_1) + 2A_2A_5(B_1B_4 - B_3B_6) \right]$$
$$+ \theta_2 \left[A_8^2(B_8^2 - B_9^2) + A_5^2(B_5^2 - B_6^2) + A_2^2(B_2^2 - B_3^2) - 2A_8B_9(A_5B_6 \right.$$
$$\left. + A_2B_3) + 2A_8B_8(A_5B_5 + A_2B_2) + 2A_2A_5(B_2B_5 - B_3B_6) \right],$$

(4.132)

$$Q_{33} = \theta_1 \left[A_9^2(B_7^2 - B_9^2) + A_6^2(B_4^2 - B_6^2) + A_3^2(B_1^2 - B_3^2) - 2A_9B_9(A_6B_6 \right.$$
$$\left. + A_3B_3) + 2A_9B_9(A_6B_4 + A_3B_1) + 2A_3A_6(B_1B_4 - B_3B_6) \right]$$
$$+ \theta_2 \left[A_9^2(B_8^2 - B_9^2) + A_6^2(B_5^2 - B_6^2) + A_3^2(B_2^2 - B_3^2) - 2A_9B_9(A_6B_6 \right.$$
$$\left. + A_3B_3) + 2A_9B_8(A_6B_5 + A_3B_2) + 2A_3A_6(B_2B_5 - B_3B_6) \right],$$

(4.133)

$$Q_{12} = -(\theta_1 + \theta_2)[(A_4A_8 + A_5A_7)B_6 + (A_1A_8 + A_2A_7)B_3]B_9$$
$$+ \theta_1 \left[A_7A_8(B_7^2 - B_9^2) + A_4A_5(B_4^2 - B_6^2) + A_1A_2(B_1^2 - B_3^2) + [(A_4A_8 \right.$$
$$\left. + A_5A_7)B_4 + (A_1A_8 + A_2A_7)B_1]B_7 + (A_1A_5 + A_2A_4)(B_1B_4 - B_3B_6) \right]$$
$$+ \theta_2 \left[A_7A_8(B_8^2 - B_9^2) + A_4A_5(B_5^2 - B_6^2) + A_1A_2(B_2^2 - B_3^2) + [(A_4A_8 \right.$$
$$\left. + A_5A_7)B_5 + (A_1A_8 + A_2A_7)B_2]B_8 + (A_1A_5 + A_2A_4)(B_2B_5 - B_3B_6) \right],$$

(4.134)

$$Q_{13} = -(\theta_1 + \theta_2)[(A_4A_9 + A_6A_7)B_6 + (A_1A_9 + A_3A_7)B_3]B_9$$
$$+ \theta_1 \left[A_7A_9(B_7^2 - B_9^2) + A_4A_6(B_4^2 - B_6^2) + A_1A_3(B_1^2 - B_3^2) + [(A_4A_9 \right.$$
$$\left. + A_6A_7)B_4 + (A_1A_9 + A_3A_7)B_1]B_7 + (A_1A_6 + A_3A_4)(B_1B_4 - B_3B_6) \right]$$
$$+ \theta_2 \left[A_7A_9(B_8^2 - B_9^2) + A_4A_6(B_5^2 - B_6^2) + A_1A_3(B_2^2 - B_3^2) + [(A_4A_9 \right.$$
$$\left. + A_6A_7)B_5 + (A_1A_9 + A_3A_7)B_2]B_8 + (A_1A_6 + A_3A_4)(B_2B_5 - B_3B_6) \right],$$

(4.135)

$$Q_{23} = -(\theta_1 + \theta_2)[(A_5 A_9 + A_6 A_8)B_6 + (A_2 A_9 + A_3 A_8)B_3]B_9$$

$$+ \theta_1 \left[A_8 A_9 (B_7^2 - B_9^2) + A_5 A_6 (B_4^2 - B_6^2) + A_2 A_3 (B_1^2 - B_3^2) + [(A_5 A_9 \right.$$

$$\left. + A_6 A_8)B_4 + (A_2 A_9 + A_3 A_8)B_1]B_7 + (A_2 A_6 + A_3 A_5)(B_1 B_4 - B_3 B_6)] \right. \quad (4.136)$$

$$+ \theta_2 \left[A_8 A_9 (B_8^2 - B_9^2) + A_5 A_6 (B_5^2 - B_6^2) + A_2 A_3 (B_2^2 - B_3^2) + [(A_5 A_9 \right.$$

$$\left. + A_6 A_8)B_5 + (A_2 A_9 + A_3 A_8)B_2]B_8 + (A_2 A_6 + A_3 A_5)(B_2 B_5 - B_3 B_6)] \right. .$$

The static polarizability, $a_{ij}^{(2)}$ is given by:

$$a_{ij}^{(2)} = \mathrm{a}_\alpha^i \mathrm{a}_\beta^j \mathrm{a}_{i'}^\alpha \mathrm{a}_{j'}^\beta a_{i'j'}^{(2)} = \begin{bmatrix} W_{11} & W_{12} & W_{13} \\ W_{12} & W_{22} & W_{23} \\ W_{13} & W_{23} & W_{33} \end{bmatrix}, \quad (4.137)$$

where

$$a_{i'j'}^{(2)} = a_{ij}^{(1)} = \begin{bmatrix} a_{11} & 0 & 0 \\ 0 & a_{22} & 0 \\ 0 & 0 & a_{33} \end{bmatrix} \quad (4.138)$$

and

$$W_{11} = a_{11} \left[A_1^2 B_1^2 + A_4^2 B_4^2 + A_7^2 B_7^2 + 2A_1 A_4 B_1 B_4 + 2A_7 B_7 (A_4 B_4 + A_1 B_1) \right]$$

$$+ a_{22} \left[A_1^2 B_2^2 + A_4^2 B_5^2 + A_7^2 B_8^2 + 2A_1 A_4 B_2 B_5 + 2A_7 B_8 (A_4 B_5 + A_1 B_2) \right] \quad (4.139)$$

$$+ a_{33} \left[A_1^2 B_3^2 + A_4^2 B_6^2 + A_7^2 B_9^2 + 2A_1 A_4 B_3 B_6 + 2A_7 B_9 (A_4 B_6 + A_1 B_3) \right],$$

$$W_{22} = a_{11} \left[A_2^2 B_1^2 + A_5^2 B_4^2 + A_8^2 B_7^2 + 2A_2 A_5 B_1 B_4 + 2A_8 B_7 (A_5 B_4 + A_2 B_1) \right]$$

$$+ a_{22} \left[A_2^2 B_2^2 + A_5^2 B_5^2 + A_8^2 B_8^2 + 2A_2 A_5 B_2 B_5 + 2A_8 B_8 (A_5 B_5 + A_2 B_2) \right] \quad (4.140)$$

$$+ a_{33} \left[A_2^2 B_3^2 + A_5^2 B_6^2 + A_8^2 B_9^2 + 2A_2 A_5 B_3 B_6 + 2A_8 B_9 (A_5 B_6 + A_2 B_3) \right],$$

$$W_{33} = a_{11} \left[A_3^2 B_1^2 + A_6^2 B_4^2 + A_9^2 B_7^2 + 2A_3 A_6 B_1 B_4 + 2A_9 B_7 (A_6 B_4 + A_3 B_1) \right]$$

$$+ a_{22} \left[A_3^2 B_2^2 + A_6^2 B_5^2 + A_9^2 B_8^2 + 2A_3 A_6 B_2 B_5 + 2A_9 B_8 (A_6 B_5 + A_3 B_2) \right] \quad (4.141)$$

$$+ a_{33} \left[A_3^2 B_3^2 + A_6^2 B_6^2 + A_9^2 B_9^2 + 2A_3 A_6 B_3 B_6 + 2A_9 B_9 (A_6 B_6 + A_3 B_3) \right],$$

$$W_{12} = a_{11} \left[A_1 A_2 B_1^2 + A_4 A_5 B_4^2 + A_7 A_8 B_7^2 + B_1 B_4 (A_1 A_5 + A_2 A_4) \right.$$

$$\left. + B_7 \left(B_4 (A_4 A_8 + A_5 A_7) + B_1 (A_1 A_8 + A_2 A_7) \right) \right] + a_{22} \left[A_1 A_2 B_2^2 \right.$$

$$+ A_4 A_5 B_5^2 + A_7 A_8 B_8^2 + B_2 B_5 (A_1 A_5 + A_2 A_4) + B_8 \left(B_5 (A_4 A_8 + A_5 A_7) \right. \quad (4.142)$$

$$\left. + B_2 (A_1 A_8 + A_2 A_7) \right) \right] + a_{33} \left[A_1 A_2 B_3^2 + A_4 A_5 B_6^2 + A_7 A_8 B_9^2 \right.$$

$$\left. + B_3 B_6 (A_1 A_5 + A_2 A_4) + B_9 \left(B_6 (A_4 A_8 + A_5 A_7) + B_3 (A_1 A_8 + A_2 A_7) \right) \right],$$

$$W_{13} = a_{11} \left[A_1 A_3 B_1^2 + A_4 A_6 B_4^2 + A_7 A_9 B_7^2 + B_1 B_4 (A_1 A_6 + A_3 A_4) \right.$$

$$\left. + B_7 \left(B_4 (A_4 A_9 + A_6 A_7) + B_1 (A_1 A_9 + A_3 A_7) \right) \right] + a_{22} \left[A_1 A_3 B_2^2 \right.$$

$$+ A_4 A_6 B_5^2 + A_7 A_9 B_8^2 + B_2 B_5 (A_1 A_6 + A_3 A_4) + B_8 \left(B_5 (A_4 A_9 + A_6 A_7) \right. \quad (4.143)$$

$$\left. + B_2 (A_1 A_9 + A_3 A_7) \right) \right] + a_{33} \left[A_1 A_3 B_3^2 + A_4 A_6 B_6^2 + A_7 A_9 B_9^2 \right.$$

$$\left. + B_3 B_6 (A_1 A_6 + A_3 A_4) + B_9 \left(B_6 (A_4 A_9 + A_6 A_7) + B_3 (A_1 A_9 + A_3 A_7) \right) \right],$$

$$W_{23} = a_{11} \left[A_2 A_3 B_1^2 + A_5 A_6 B_4^2 + A_8 A_9 B_7^2 + B_1 B_4 (A_2 A_6 + A_3 A_5) \right.$$

$$\left. + B_7 \left(B_4 (A_5 A_9 + A_6 A_8) + B_1 (A_2 A_9 + A_3 A_8) \right) \right] + a_{22} \left[A_2 A_3 B_2^2 \right.$$

$$+ A_5 A_6 B_5^2 + A_8 A_9 B_8^2 + B_2 B_5 (A_2 A_6 + A_3 A_5) + B_8 \left(B_5 (A_5 A_9 + A_6 A_8) \right. \quad (4.144)$$

$$\left. + B_2 (A_2 A_9 + A_3 A_8) \right) \right] + a_{33} \left[A_2 A_3 B_3^2 + A_5 A_6 B_6^2 + A_8 A_9 B_9^2 \right.$$

$$\left. + B_3 B_6 (A_2 A_6 + A_3 A_5) + B_9 \left(B_6 (A_5 A_9 + A_6 A_8) + B_3 (A_2 A_9 + A_3 A_8) \right) \right].$$

The expressions for the second and third rank T-tensors referred to space-fixed axes are given in equations (2.40) and (2.41). These must be projected into molecule 1's axes as follows:

$$T_{ij} = a_\alpha^i a_\beta^j T_{\alpha\beta} = \frac{1}{4\pi\varepsilon_0} \frac{1}{R^3} \begin{bmatrix} T_{11} & T_{12} & T_{13} \\ T_{12} & T_{22} & T_{23} \\ T_{13} & T_{23} & T_{33} \end{bmatrix}, \quad (4.145)$$

where

$$
\left.\begin{aligned}
T_{11} &= 2A_7^2 - A_4^2 - A_1^2, \\
T_{22} &= 2A_8^2 - A_5^2 - A_2^2, \\
T_{33} &= 2A_9^2 - A_6^2 - A_3^2, \\
T_{12} &= 2A_7A_8 - A_4A_5 - A_1A_2, \\
T_{13} &= 2A_7A_9 - A_4A_6 - A_1A_3, \\
T_{23} &= 2A_8A_9 - A_5A_6 - A_2A_3.
\end{aligned}\right\}
\tag{4.146}
$$

$$
T_{ijk} = \mathrm{a}_\alpha^i \mathrm{a}_\beta^j \mathrm{a}_\gamma^k T_{\alpha\beta\gamma},
\tag{4.147}
$$

therefore,

$$
\begin{aligned}
T_{1jk} &= \tfrac{3}{4\pi\varepsilon_0 R^4}
\begin{bmatrix}
T_{111} & T_{112} & T_{113} \\
T_{112} & T_{122} & T_{123} \\
T_{113} & T_{123} & T_{133}
\end{bmatrix}, \\[2mm]
T_{2jk} &= \tfrac{3}{4\pi\varepsilon_0 R^4}
\begin{bmatrix}
T_{112} & T_{122} & T_{123} \\
T_{122} & T_{222} & T_{223} \\
T_{123} & T_{223} & T_{233}
\end{bmatrix}, \\[2mm]
T_{3jk} &= \tfrac{3}{4\pi\varepsilon_0 R^4}
\begin{bmatrix}
T_{113} & T_{123} & T_{133} \\
T_{123} & T_{223} & T_{233} \\
T_{133} & T_{233} & T_{333}
\end{bmatrix},
\end{aligned}
\tag{4.148}
$$

where

$$
\left.\begin{aligned}
T_{111} &= 2A_7^3 - 3A_7(A_4^2 + A_1^2), \\
T_{222} &= 2A_8^3 - 3A_8(A_5^2 + A_2^2), \\
T_{333} &= 2A_9^3 - 3A_9(A_6^2 + A_3^2), \\
T_{112} &= 2A_7(A_7A_8 - A_4A_5 - A_1A_2) - A_8(A_4^2 + A_1^2), \\
T_{113} &= 2A_7(A_7A_9 - A_4A_6 - A_1A_3) - A_9(A_4^2 + A_1^2), \\
T_{122} &= 2A_8(A_7A_8 - A_4A_5 - A_1A_2) - A_7(A_5^2 + A_2^2), \\
T_{133} &= 2A_9(A_7A_9 - A_4A_6 - A_1A_3) - A_7(A_6^2 + A_3^2), \\
T_{223} &= 2A_8(A_8A_9 - A_5A_6 - A_2A_3) - A_9(A_5^2 + A_2^2), \\
T_{233} &= 2A_9(A_8A_9 - A_5A_6 - A_2A_3) - A_8(A_6^2 + A_3^2), \\
T_{123} &= A_9(2A_7A_8 - A_4A_5 - A_1A_2) - A_8(A_4A_6 + A_1A_3) \\
&\quad - A_7(A_5A_6 + A_2A_3).
\end{aligned}\right\}
\tag{4.149}
$$

In order to simplify the final expressions for the terms, we define an additional tensor:

$$
G_{il} = a_{ij}^{(1)} T_{jk} a_{kl}^{(2)} = \begin{bmatrix} G_{11} & G_{12} & G_{13} \\ G_{21} & G_{22} & G_{23} \\ G_{31} & G_{32} & G_{33} \end{bmatrix},
\tag{4.150}
$$

where

$$
\left.
\begin{aligned}
G_{11} &= a_{11}(W_{11}T_{11} + W_{12}T_{12} + W_{13}T_{13}), \\
G_{12} &= a_{11}(W_{12}T_{11} + W_{22}T_{12} + W_{23}T_{13}), \\
G_{13} &= a_{11}(W_{13}T_{11} + W_{23}T_{12} + W_{33}T_{13}), \\
G_{21} &= a_{22}(W_{11}T_{12} + W_{12}T_{22} + W_{13}T_{23}), \\
G_{22} &= a_{22}(W_{12}T_{12} + W_{22}T_{22} + W_{23}T_{23}), \\
G_{23} &= a_{22}(W_{13}T_{12} + W_{23}T_{22} + W_{33}T_{23}), \\
G_{31} &= a_{33}(W_{11}T_{13} + W_{12}T_{23} + W_{13}T_{33}), \\
G_{32} &= a_{33}(W_{12}T_{13} + W_{22}T_{23} + W_{23}T_{33}), \\
G_{31} &= a_{33}(W_{13}T_{13} + W_{23}T_{23} + W_{33}T_{33}).
\end{aligned}
\right\}
\tag{4.151}
$$

With these tensors defined it is now possible to use Macsyma's tensor manipulation facilities to evaluate the relevant terms in the integration. Thus, substituting equations (4.126) to (4.149) into equations (4.30) to (4.32), (4.51) to (4.55) and (4.57) yields:

$$
\alpha_2 = \frac{1}{3(4\pi\varepsilon_0)R^3}(G_{11} + G_{22} + G_{33}),
\tag{4.152}
$$

$$
\alpha_3 = \frac{1}{3(4\pi\varepsilon_0)^2 R^6}\left\{ a_{11}(G_{13}T_{13} + G_{12}T_{12} + G_{11}T_{11}) + a_{22}(G_{23}T_{23} + G_{22}T_{22} \right.
$$
$$
\left. + G_{21}T_{12}) + a_{33}(G_{33}T_{33} + G_{32}T_{23} + G_{31}T_{13}) \right\},
\tag{4.153}
$$

$$
\alpha_4 = \frac{1}{3(4\pi\varepsilon_0)^3 R^9}\left\{ T_{11}(G_{11}^2 + G_{12}G_{21} + G_{13}G_{31}) + T_{22}(G_{12}G_{21} + G_{22}^2 \right.
$$
$$
+ G_{23}G_{32}) + T_{33}(G_{13}G_{31} + G_{23}G_{32} + G_{33}^2) + T_{12}[(G_{11} + G_{22})(G_{12}
$$
$$
+ G_{21}) + G_{13}G_{32} + G_{23}G_{31}] + T_{13}[(G_{11} + G_{33})(G_{13} + G_{31}) + G_{12}G_{23}
$$
$$
\left. + G_{21}G_{32}] + T_{23}[(G_{22} + G_{33})(G_{23} + G_{32}) + G_{12}G_{31} + G_{13}G_{21}] \right\},
\tag{4.154}
$$

$$
\mu_2 = \mu^2 \mathcal{D}_3,
\tag{4.155}
$$

$$\alpha_1\mu_2 = \frac{2\mu_2}{(4\pi\varepsilon_0)R^3}\left\{a_{33}(1+\mathcal{D}_3)(\mathcal{D}_1T_{13}+\mathcal{D}_2T_{23}+\mathcal{D}_3T_{33})+W_{13}T_{13}+W_{23}T_{23}+W_{33}T_{33}\right\},$$

$$(4.156)$$

$$\alpha_2\mu_2 = \frac{\mu_2}{(4\pi\varepsilon_0)^2R^6}\left\{a_{11}^2[2(\mathcal{D}_1\mathcal{D}_2T_{11}T_{12}+\mathcal{D}_1\mathcal{D}_3T_{11}T_{13}+\mathcal{D}_2\mathcal{D}_3T_{12}T_{13})+\mathcal{D}_1^2T_{11}^2\right.$$

$$+\mathcal{D}_2^2T_{12}^2+\mathcal{D}_3^2T_{13}^2]+a_{22}^2[2(\mathcal{D}_1\mathcal{D}_2T_{12}T_{22}+\mathcal{D}_1\mathcal{D}_3T_{12}T_{23}+\mathcal{D}_2\mathcal{D}_3T_{22}T_{23})+\mathcal{D}_1^2T_{12}^2$$

$$+\mathcal{D}_2^2T_{22}^2+\mathcal{D}_3^2T_{23}^2]+a_{33}^2[2(\mathcal{D}_1\mathcal{D}_2T_{13}T_{23}+\mathcal{D}_1\mathcal{D}_3T_{13}T_{33}+\mathcal{D}_2\mathcal{D}_3T_{23}T_{33})+\mathcal{D}_1^2T_{13}^2$$

$$+\mathcal{D}_2^2T_{23}^2+\mathcal{D}_3^2T_{33}^2]+a_{11}(\mathcal{D}_1T_{11}+\mathcal{D}_2T_{12}+\mathcal{D}_3T_{13})[2(W_{13}T_{11}+W_{23}T_{12}$$

$$+W_{33}T_{13})+W_{11}T_{13}+W_{12}T_{23}+W_{13}T_{33}]+a_{22}(\mathcal{D}_1T_{12}+\mathcal{D}_2T_{22}+\mathcal{D}_3T_{23})$$

$$\times[2(W_{13}T_{12}+W_{23}T_{22}+W_{33}T_{23})+W_{12}T_{13}+W_{22}T_{23}+W_{23}T_{33}]+a_{33}(\mathcal{D}_1T_{13}$$

$$+\mathcal{D}_2T_{23}+\mathcal{D}_3T_{33})[3(W_{13}T_{13}+W_{23}T_{23}+W_{33}T_{33})+2(W_{11}T_{13}^2+W_{22}T_{23}^2$$

$$\left.+W_{33}T_{33}^2+2(W_{12}T_{13}T_{23}+W_{13}T_{13}T_{33}+W_{23}T_{23}T_{33}))]\right\},$$

$$(4.157)$$

$$\alpha_3\mu_2 = \frac{2\mu_2}{(4\pi\varepsilon_0)^3R^9}\left\{a_{11}(\mathcal{D}_1T_{11}+\mathcal{D}_2T_{12}+\mathcal{D}_3T_{13})[G_{31}T_{11}+G_{32}T_{12}+G_{33}T_{13}+G_{11}T_{13}\right.$$

$$+G_{12}T_{23}+G_{13}T_{33}]+a_{22}(\mathcal{D}_1T_{12}+\mathcal{D}_2T_{22}+\mathcal{D}_3T_{23})[G_{32}T_{12}+G_{32}T_{22}+G_{33}T_{23}$$

$$+G_{21}T_{13}+G_{22}T_{23}+G_{23}T_{33}]+2a_{33}(\mathcal{D}_1T_{13}+\mathcal{D}_2T_{23}+\mathcal{D}_3T_{33})[G_{31}T_{13}$$

$$+G_{32}T_{23}+G_{33}T_{33}]+W_{11}T_{13}(G_{11}T_{13}+G_{12}T_{23}+G_{13}T_{33})+W_{22}T_{23}(G_{21}T_{13}$$

$$+G_{22}T_{23}+G_{23}T_{33})+W_{33}[T_{33}(G_{31}T_{13}+G_{32}T_{23}+G_{33}T_{33})+T_{13}T_{23}(G_{12}+G_{21})$$

$$+T_{13}T_{33}(G_{13}+G_{31})+T_{23}T_{33}(G_{23}+G_{32})+G_{11}T_{13}^2+G_{22}T_{23}^2+G_{33}T_{33}^2]$$

$$+W_{12}[T_{33}(G_{23}T_{13}+G_{13}T_{23})+T_{23}(G_{22}T_{13}+G_{12}T_{23})+T_{13}(G_{21}T_{13}+G_{11}T_{23})]$$

$$+W_{13}[T_{33}(G_{13}T_{11}+G_{23}T_{12}+2G_{33}T_{13}+G_{13}T_{33})+T_{23}(G_{12}T_{11}+G_{22}T_{12}$$

$$+2G_{32}T_{13}+G_{12}T_{33})+T_{13}(G_{11}T_{11}+G_{21}T_{12}+2G_{31}T_{13}+G_{11}T_{33})]$$

$$+W_{23}[T_{33}(G_{13}T_{12}+G_{23}T_{22}+2G_{33}T_{23}+G_{23}T_{33})+T_{23}(G_{12}T_{12}+G_{22}T_{22}$$

$$\left.+2G_{32}T_{23}+G_{22}T_{33})+T_{13}(G_{11}T_{12}+G_{21}T_{22}+2G_{31}T_{23}+G_{21}T_{33})]\right\},$$

$$(4.158)$$

$$\alpha_1\mu_1\theta_1 = -\frac{2\mu^2}{(4\pi\varepsilon_0)R^4}\left\{a_{33}[Q_{11}T_{113} + Q_{22}T_{223} + Q_{33}T_{333} + 2(Q_{12}T_{123} + Q_{13}T_{133}\right.$$

$$+ Q_{23}T_{233})] - \theta_1[W_{33}T_{113} + W_{23}T_{112} + W_{13}T_{111}] - \theta_2[W_{33}T_{223}$$

$$\left.+W_{23}T_{222} + W_{13}T_{122}] + (\theta_1 + \theta_2)[W_{33}T_{333} + W_{23}T_{233} + W_{13}T_{133}]\right\},$$

(4.159)

$$\alpha_2\theta_2 = \frac{1}{(4\pi\varepsilon_0)^2 R^8}\left\{a_{11}^2[Q_{11}T_{111} + Q_{22}T_{122} + Q_{33}T_{133} + 2(Q_{12}T_{112} + Q_{13}T_{113}\right.$$

$$+ Q_{23}T_{123})]^2 + a_{22}^2[Q_{11}T_{112} + Q_{22}T_{222} + Q_{33}T_{233} + 2(Q_{12}T_{122} + Q_{13}T_{123}$$

$$+ Q_{23}T_{223})]^2 + a_{33}^2[Q_{11}T_{113} + Q_{22}T_{223} + Q_{33}T_{333} + 2(Q_{12}T_{123} + Q_{13}T_{133}$$

$$+ Q_{23}T_{233})]^2 - a_{11}[Q_{11}T_{111} + Q_{22}T_{122} + Q_{33}T_{133} + 2(Q_{12}T_{112} + Q_{13}T_{113}$$

$$+ Q_{23}T_{123})][\theta_1(W_{11}T_{111} + W_{12}T_{112} + W_{13}T_{113}) + \theta_2(W_{11}T_{122} + W_{12}T_{222}$$

$$+ W_{13}T_{223}) - (\theta_1 + \theta_2)(W_{11}T_{133} + W_{12}T_{233} + W_{13}T_{333})] - a_{22}[Q_{11}T_{112}$$

$$+ Q_{22}T_{222} + Q_{33}T_{233} + 2(Q_{12}T_{122} + Q_{13}T_{123} + Q_{23}T_{223})][\theta_1(W_{12}T_{111}$$

$$+ W_{22}T_{112} + W_{23}T_{113}) + \theta_2(W_{12}T_{122} + W_{22}T_{222} + W_{23}T_{223})$$

$$- (\theta_1 + \theta_2)(W_{12}T_{133} + W_{22}T_{233} + W_{23}T_{333})] - a_{33}[Q_{11}T_{113} + Q_{22}T_{223}$$

$$+ Q_{33}T_{333} + 2(Q_{12}T_{123} + Q_{13}T_{133} + Q_{23}T_{233})][\theta_1(W_{13}T_{111} + W_{23}T_{112}$$

$$+ W_{33}T_{113}) + \theta_2(W_{13}T_{122} + W_{23}T_{222} + W_{33}T_{223}) - (\theta_1 + \theta_2)(W_{13}T_{133}$$

$$\left.+ W_{23}T_{233} + W_{33}T_{333})].$$

(4.160)

It can be seen from the above equations, that in spite of the methods employed to abbreviate the expressions, they become increasingly complicated. The terms $\alpha_2\mu_1\theta_1$ and $\alpha_3\theta_2$ have been evaluated, but are not quoted here since they are very long and it is preferable to generate the expressions using an algebraic manipulation package such as Macsyma, which can convert them directly into Fortran for integration, eliminating the introduction of typographical errors. These terms were necessary to establish convergence. The computer programs to calculate each term are time-consuming. For a polar gas, calculating all the terms necessary to determine B_ε takes more than 24 hours on a Pentium 133 MHz PC with 64 Mb of RAM.

4.6 Summary of experimental work on the second dielectric virial coefficient

Tables 1.1 to 1.3 contain a comprehensive summary of the experimental second dielectric virial coefficient data available, for the molecules under study. For many of the values the experimental errors quoted are substantial, and the results of different workers vary considerably. Thus, it is often difficult to distinguish a trend over the range of temperatures for which data is available. Apart from some recent work by Huot and Bose in 1991 [38] on noble gases, the majority of the data was measured in the 1960's and 1970's.

The earliest measurements [10, 12, 45, 46, 53] were made using Burnett's expansion method [132]. This was later modified by Orcutt and Cole [13] in 1967, to provide more accurate density measurements, and therefore, more accurate values of B_ε, using a cyclic expansion technique. This method has been used extensively in the measurement of the second dielectric virial coefficient [2, 24, 42, 43, 51, 110, 133]. However, in both these methods the second dielectric virial coefficient is not determined directly, but as a ratio of $\frac{B_\varepsilon}{A_\varepsilon^2}$, with A_ε determined in a separate experiment. In 1970, Buckingham, Cole and Sutter [49] reported on a simple differential technique for the direct determination of B_ε, which involved the use of almost identical cells, one of which is evacuated. The sum of the capacitances in both cells was measured, the gas was allowed to expand to fill both cells, and the the change in the sum was measured. The same principle was used by Buckingham and Graham [39], and later by Burns and Graham [44], to measure B_R for a range of gases. This method was also used by St-Arnaud and Bose [68] in 1979 to measure the second refractivity virial coefficient of carbon dioxide and sulfur hexafluoride, by Bose *et al* [74] in 1988 to measure B_R for ethylene-argon mixtures, and by Huot [38] to measure dielectric virial coefficients of atomic gases. Koschine and Lehman [134] measured B_ε for 1,1-difluoroethylene using a modification of the cyclic expansion method. In 1995 St-Arnaud *et al.* [135] designed a computer-controlled measuring system which employs the differential expansion technique of Buckingham *et al.* [49] to measure the dielectric constant as a function of pressure and temperature. They showed that the computer-controlled system can improve the efficiency of the experimental procedures.

It can be seen from comparison of Table 1.2 and 1.3 that the second virial coefficients for dipolar molecules are much larger than those for molecules without a permanent dipole. This can be understood by considering the contribution of the two terms in equation (4.15). The first term, which represents the polarization due to the moments induced in the molecules, is sometimes referred to as $B_{\varepsilon_{ind}}$. The second term, which represents the polarization due to the dipoles orientating themselves in the direction of

the field, is called $B_{\varepsilon_{\mathrm{or}}}$. Therefore, B_ε may be written as [40]:

$$B_\varepsilon = B_{\varepsilon_{\mathrm{ind}}} + B_{\varepsilon_{\mathrm{or}}}. \tag{4.161}$$

For atomic gases, only the first term contributes to B_ε, while for other non-polar gases, there is some contribution from the second term, but the first term usually dominates. For polar gases, $B_{\varepsilon_{\mathrm{ind}}}$ is usually assumed to be negligible in comparison with $B_{\varepsilon_{\mathrm{or}}}$ [2,3,27]. There have been some attempts to separate the contributions of $B_{\varepsilon_{\mathrm{ind}}}$ and $B_{\varepsilon_{\mathrm{or}}}$ [136], so that mulitpole moments may be evaluated from $B_{\varepsilon_{\mathrm{or}}}$, but the methods are unreliable and there are few results available.

4.7 Summary of theoretical calculations of the second dielectric virial coefficient

The deviations of real gases from the Clausius-Mossotti formula in (4.6) have been discussed by many workers. In the 1930's various models of dielectrics were proposed in an attempt to explain the Clausius-Mossoti formula [119, 121]. Harris and Alder [116] later expanded Kirkwood's correlation factor g in powers of $\frac{1}{V}$ in an attempt to model the density-dependence of the Clausius-Mossotti equation, and developed formulae for the dielectric polarization from some simple force fields, using the Onsager relation [119] for estimating the mean dipole moment of a molecule. Their model, like Kirkwood's, excluded induction effects.

Later, Buckingham and Pople [28, 101] considered a virial type expansion of the Clausius-Mossotti formula and presented a general statistical mechanical derivation of the second dielectric virial coefficient by considering a macroscopic spherical volume of gas. This generally accepted formula for B_ε is given in equation (4.15). They showed that it was unnecessary to make the approximation of using the Onsager relation if one considered only the initial deviation from the ideal gas behaviour. They introduced a shape factor D, discussed in Section 2.2, into the intermolecular potential to account for the orientation effects of the shape of a molecule, such as the large positive values of B_ε for CHF_3 and negative values for CH_3F (Table 1.3). Much of the subsequent work on the subject has been based on their model, with mixed results [3,45,97]. In order to perform the necessary integration they used H_k functions introduced by Lennard-Jones [137], which they tabulated [96]. This method involves expansion of the orientation-dependent part of the Boltzmann factor $e^{-\frac{U_{12}}{kT}}$ in powers of $\frac{1}{kT}$ which leads to increasingly complex functions from higher powers of U_{12} and problems with convergence. Due to the difficulties involved in the integration, only the leading terms in the integrands were evaluated. As numerical integration using computers became practical, it was possible to include

more terms and consider quadrupole-quadrupole and quadrupole-induced-dipole potentials together with the Lennard-Jones, dipole-dipole and shape potentials. In our work we have included as many terms as was necessary to ensure convergence, as well as the full DID potential model, as described in Chapter 2.

The second dielectric virial coefficients of spherical and quasi-spherical gases have been studied by various workers. Isnard, Robert and Galatry [112] calculated B_ε for the quasi-spherical CH_4 and CF_4 by including the dipole-induced-dipole contribution for the distortion term and the octopolar and hexadecapolar fields for the orientation term, and found good agreement with experimental data. Logan and Madden [131] calculated B_ε for CH_4 and the inert gases by considering the induced quadrupole contribution to the induction component. They showed [138] that the induced quadrupole made a significant contribution to B_ε of argon, demonstrating the importance of the C-tensor term in $B_{\varepsilon_{\text{ind}}}$.

More recently, Huot and Bose [38] calculated B_ε for atomic gases from *ab initio* calculations incorporating quantum short-range corrections. These were determined by the Hartree-Fock self-consistent field (HF-SCF) method, but apart from helium the calculated values were not in agreement with their measured values.

In 1994, Bulanin, Hohm and Ladvischchenko [139] calculated B_ε for rare gases using accurate HFD-type interatomic interaction potentials. They compared their calculations with experimental data and previous calculations of Hohm [140] based on a Lennard-Jones potential, and found that improving the accuracy of the potential did not improve the overall agreement with experiment.

The treatment of spherical and quasi-spherical gases is complex and requires consideration of high-order multipoles as well as long and short-range corrections. This type of treatment is beyond the scope of this work and shall not be considered here.

The second dielectric virial coefficient of polar and non-polar gases has been investigated by many workers. Johnston and Cole [45] generalised Buckingham and Pople's theory for $B_{\varepsilon_{\text{or}}}$ of linear non-polar molecules to include molecules of lower symmetry, such as ethene, including only the leading term in the quadrupole moment. They noted, however, that the approximation adopted by Buckingham and Pople [141] of retaining only the leading term in the expansion of the Boltzmann factor might be inadequate, but were unable to improve the model due to the complex angular dependence of the quadrupole-quadrupole interaction energy, defined in equation (2.12). Later, Bose and Cole [40] included the quadrupole-induced-dipole interaction energy into the potential energy and found that it made a small but significant contribution.

In 1963, Lawley and Smith [142] suggested an off-centre hard sphere dipole model for polar molecules to account for the negative experimental values of B_ε for some polar gases. Dymond and Smith [56] expanded on this model by considering a soft Lennard-Jones spherical molecule. Spurling and Mason [143] showed that this off-centre dipole model

can be replaced by an equivalent central dipole-quadrupole model including Buckingham and Pople's shape factor. The calculations for this model are simpler than for the off-centre dipole model.

In 1969, Sutter [3] measured the first and second dielectric virial coefficients and the second pressure virial coefficient at three temperatures for five polar linear halogenated methanes. He used his values of A_ε to determine the permanent dipole moments and static molecular polarizabilies of the gases. He then fitted Lennard-Jones parameters to his data for $B(T)$. A surprising result was that the value of R_0 fitted for CHF_3 was smaller than the fitted value for CH_3F. Using the fitted Lennard-Jones parameters and his values for μ and a he fitted Buckingham and Pople's [101] B_ε model to his experimental data to obtain a value for the shape factor of each molecule. In the model he omitted the effects of the quadrupole moment and molecular polarizability anisotropy, as well as the $B_{\varepsilon_{ind}}$ contribution. He obtained reasonable values of the shape factor for CH_3F, CH_3Cl and $CClF_3$, but the value of D for CHF_3 was positive, erroneously indicating a rod-shaped molecule. He concluded that although the measured values of B_ε showed differences in sign, magnitude and temperature dependence which appear to be correlated with deviations from the spherical shape, attempts to account for them using the model for molecular shape proposed by Buckingham and Pople [28] were unsatisfactory. However, since the model used neglects the effects of the quadrupole moment and anisotropy of the molecular polarizability, which may have a significant effect on the value of B_ε, these findings are inconclusive. In this work we have included the effects of the quadrupole moment, anisotropy and hyperpolarizabilities on the effective polarizability and dipole moment, as well as including quadrupole effects on the intermolecular potential. We have also included the $B_{\varepsilon_{ind}}$ contribution, resulting in a more complete model.

In general, researchers use $B(T)$, which is less sensitive to non-central potentials, to fit the Lennard-Jones parameters, R_0 and $\frac{\varepsilon}{k}$. These are then used in the calculations for B_ε and the resultant equations used to fit the shape parameter, D. It has been noted that fitting R_0 and $\frac{\varepsilon}{k}$ to $B(T)$ sometimes results in unrealistically small values for R_0 [3, 51, 142, 144]. In this work we have included the shape potential when evaluating $B(T)$ and have attempted to optimize the Lennard-Jones parameters and the shape factor for both $B(T)$ and B_ε simultaneously.

In order to address the problem of physically unreasonable fitted values for R_0, Copeland and Cole [97] calculated B_ε for CHF_3 and CH_3F, by fitting R_0 and $\frac{\varepsilon}{k}$ to Casparian and Cole's [145] viscosity data, using these with a known dipole moment to fit the quadrupole moment from $B(T)$, and finally fitting the shape factor to experimental values of the second dielectric virial coefficient. They used methods similar to that of Sutter [3], but included the $\alpha_2\theta_2$ term in $B_{\varepsilon_{or}}$ and the effects of the quadrupole moment on the potential energy. This method yielded values of D for CHF_3 and CH_3F in fair

agreement with Buckingham and Pople's model.

In 1974, Hosticka, Bose and Sochanski [146] included the quadrupole-quadrupole interaction energy in the potential in a model for $B_{\varepsilon_{or}}$ of ethylene, taking into account its low symmetry. Only the leading quadrupole term in the integrand was considered and the anisotropy of the polarizability was not included in the model. The intermolecular potential was taken to be the sum of the Lennard-Jones central potential and the quadrupole-quadrupole interaction energy with no shape potential. They used this model to reanalyze the experimental results of Bose and Cole [24], in order to estimate the mean quadrupole moment. From their results they concluded that ethylene can be treated as an linear molecule without significant error. However, Couling and Graham [36] showed that treating ethylene as a non-linear molecule improved the calculated values of both the second light-scattering and Kerr-effect virial coefficients. Thus, we will use the non-linear model which we have developed to calculate B_ε for ethylene, including as many terms as are necessary to ensure convergence, and the shape potential introduced by Couling and Graham [9, 36].

Powles and McGrath [11] calculated B_ε for HCl using several different models for the intermolecular potential, but were unable to obtain agreement with the experimental data of Lawley and Sutton [10], which are almost an order of magnitude larger than the calculated values. However, in their models they consider only the two leading terms, μ_2 and $\alpha\mu_2$, of the dipole series of $B_{\varepsilon_{or}}$, and include no induction terms in the intermolecular potentials. For their model using the Lennard-Jones potential they include only the dipole-dipole potential, with no shape potential and performed the integration using the H_k functions tabulated by Buckingham and Pople [96]. In our calculations of B_ε for HCl we include as many terms as necessary to ensure convergence of both $B_{\varepsilon_{ind}}$ and $B_{\varepsilon_{or}}$ and the full DID potential described in Chapter 2.

In 1987 Kielpinski and Murad [147] studied the effects of isotropic and anisotropic polarizability on properties of dilute gases, including the second dielectric virial coefficient. They showed that polarizability makes a significant contribution to B_ε, while the contribution of the polarizability anisotropy, although smaller is still significant. Although many earlier workers omitted the anisotropy of linear molecules [3, 11, 28, 97, 146], we have included it in all our calculations, since we have found that it can be significant.

Joslin and Goldman [148] considered the numerical calculations of Powles and McGrath [11] and Kielpinski and Murad [147] to be unsatisfactory because $B_{\varepsilon_{ind}}$ was omitted, and Powles and McGrath also excluded induction effects in the intermolecular potential. Joslin and Goldman calculated B_ε and B_R numerically for anisotropically polarizable dipolar hard spheres using a simple intermolecular potential, claiming their method to be essentially exact, although it does not include any quadrupole or shape. They applied this method to CHF_3 and found their results agreed with available experimental data.

Chapter 5

The Second Refractivity Virial Coefficient, B_R

The molar refraction R_m of a medium is defined as follows:

$$R_m = \frac{n^2 - 1}{n^2 + 2} V_m, \tag{5.1}$$

where n is the refractive index and V_m is the molar volume of the medium. An equation relating the mean polarizability α_0 of an isolated molecule to the molar refraction of a bulk sample at equilibrium was derived independently by L. Lorenz [30] and J. A. Lorentz [29] in 1880. This formula later became known as the Lorenz-Lorentz equation:

$$\frac{n^2 - 1}{n^2 + 2} V_m = \frac{N_A \alpha_0}{3 \varepsilon_0}, \tag{5.2}$$

where N_A is Avogadro's number and ε_0 is the permittivity of a vacuum. If α_0 is assumed to be independent of density, the Lorenz-Lorentz equation implies that the molar refraction is independent of density. Early values of R_m for many gases appeared to be constant within the experimental error for a wide range of pressure and temperature. However, more precise experimental techniques used by subsequent workers [76,80,149–151] showed significant variations of the molar refractivity with density. To account for this variation Buckingham [152] wrote R_m in the form of a virial expansion:

$$R_m = \frac{n^2 - 1}{n^2 + 2} V_m = A_R + \frac{B_R}{V_m} + \frac{C_R}{V_m^2} + \cdots, \tag{5.3}$$

where $A_R, B_R, C_R, \ldots$ are called the first, second, third, ... refractivity virial coefficients. In the limit of infinite dilution, the first refractivity virial coefficient A_R is the only contribution to R_m, and equation (5.3) reduces to the Lorenz-Lorentz formula. Thus,

A_R, which describes the ideal gas contribution, is given by:

$$A_R = \lim_{V_m \to \infty} R_m = \frac{N_A \alpha_0}{3\varepsilon_0}. \qquad (5.4)$$

The second and third refractivity virial coefficients describe the mean contribution to R_m of interacting pairs and triplets, respectively. B_R describes the inital deviation from ideal gas behaviour and has been the subject of many experimental [13, 39, 44, 58, 60, 63, 67, 68, 80, 122, 150, 151] and theoretical [44, 105, 122, 124, 152] investigations.

5.1   Theory of B_R

Buckingham [152] presented a general theory of the second refractivity virial coefficient B_R for pure gas systems, which was later extended by Kielich [124] to mixtures of gases. These theories are closely analogous to the treatment of the second dielectric virial coefficient presented in Section 4. The two theories are associated through the relationship between the refractive index and the dielectric constant of a gas:

$$n^2 = \varepsilon_r \mu_r, \qquad (5.5)$$

where n and ε_r are the refractive index and dielectric constant of the gas at the same frequency, and μ_r is the relative permeability, which for dilute non-magnetic gases is assumed to be negligibly different from unity.

In Chapter 4 the following equation was obtained for the total polarization of a dielectric gas in the presence of a static external field:

$$_T P = \frac{\varepsilon_r - 1}{\varepsilon_r + 2} V_m = \frac{N_A}{3\varepsilon_0} \left\{ \left\langle \frac{\partial \boldsymbol{\mu}^{(1)}}{\partial E_0} . \boldsymbol{e} \right\rangle + \frac{1}{3kT} \sum_{i=1}^{N_A} \left\langle \boldsymbol{\mu}^{(1)} . \boldsymbol{\mu}^{(i)} \right\rangle \right\}, \qquad (5.6)$$

where $\boldsymbol{\mu}^{(i)}$ is the dipole moment of the ith molecule. The first term on the right-hand side of (5.6) is due to the distortion of the molecules by the external field, while the second term is due to the tendency of the dipole moments (permanent or induced) to align themselves in the direction of the static applied field. For alternating external fields, equation (5.6) is only strictly correct if the molecular orientations are able to follow the alternations exactly. For alternating fields of optical frequency, the orientation of the dipoles is completely suppressed by the inertia of the molecules, so that the second, temperature-dependent term of (5.6) reduces to zero. Thus, at optical frequencies ω,

equation (5.6) becomes:

$$_TP = \frac{\varepsilon_r(\omega) - 1}{\varepsilon_r(\omega) + 2} V_m = \frac{N_A}{3\varepsilon_0} \left\langle \frac{\partial \boldsymbol{\mu}^{(1)}}{\partial \mathcal{E}_0} . \boldsymbol{e} \right\rangle, \tag{5.7}$$

where $\mathcal{E}_0$ is an electric field alternating at optical frequency ω.

If $\mu_r \approx 1$, then from (5.5) it follows that:

$$\frac{\varepsilon_r(\omega) - 1}{\varepsilon_r(\omega) + 2} = \frac{n^2 - 1}{n^2 + 2}, \tag{5.8}$$

therefore, from (5.7):

$$\frac{n^2 - 1}{n^2 + 2} V_m = \frac{N_A}{3\varepsilon_0} \left\langle \frac{\partial \boldsymbol{\mu}^{(1)}}{\partial \mathcal{E}_0} . \boldsymbol{e} \right\rangle. \tag{5.9}$$

From equations (5.3), (5.4) and (5.9), it follows that the second refractivity virial coefficient is given by:

$$B_R = \lim_{V_m \to \infty} [(R_m - A_R) V_m] = \frac{N_A}{3\varepsilon_0} \lim_{V_m \to \infty} \left[\left\langle \frac{\partial \boldsymbol{\mu}^{(1)}}{\partial \mathcal{E}_0} . \boldsymbol{e} - \alpha_0 \right\rangle V_m \right]$$

$$= \frac{N_A^2}{3\varepsilon_0 \Omega} \int_\tau \left[\frac{\partial \boldsymbol{\mu}^{(1)}}{\partial \mathcal{E}_0} . \boldsymbol{e} - \alpha_0 \right] e^{-\frac{U_{12}(\tau)}{kT}} d\tau, \tag{5.10}$$

where τ describes the relative configuration of the pair of molecules.

In general four distinct contributions to $\left(\frac{\partial \boldsymbol{\mu}^{(1)}}{\partial \mathcal{E}_0} . \boldsymbol{e} - \alpha_0 \right)$ can be identified:

(i) The 'fluctuation' contribution of Kirkwood [127] and Yvon [153] is a classical effect first investigated by Silberstein [154]. The effective polarizability of each molecule of an interacting pair is modified by the extra field at one due to the induced dipole on the other. Silberstein [154] showed that if the molecules have an intrinsic isotropic polarizability α_0 and are separated by R, then

$$\tfrac{1}{2} \alpha_{12}(R) - \alpha_0 = \tfrac{1}{3} \alpha_0 \left[\left(1 - \frac{2\alpha_0}{4\pi\varepsilon_0 R^3} \right)^{-1} + 2 \left(1 + \frac{\alpha_0}{4\pi\varepsilon_0 R^3} \right)^{-1} - 3 \right].$$

The expression diverges at separation $R = \sqrt[3]{\frac{2\alpha_0}{4\pi\varepsilon_0}}$, and for large R

$$\tfrac{1}{2} \alpha_{12}(R) - \alpha_0 = \frac{2\alpha_0^3}{(4\pi\varepsilon_0)^2 R^6}.$$

The divergence is unimportant since it occurs at a separation where the electron clouds overlap extensively, so that the model is inappropriate at this distance. The effect makes a positive contribution to B_R which can easily be determined if U_{12} is known.

(ii) When the separation R is large the intrinsic molecular polarizability changes as a result of dispersion-type interactions. Jansen and Mazur [155] first investigated these effects and showed that they lead to a significant positive contribution to α_{12} that varies as R^{-6} at large R. Other workers [123, 128, 156, 157] have studied the effect, which is attributed to the distortion of the electronic structure of the pair of molecules due to dispersion interactions.

(iii) α_{12} is modified by overlap of the electron clouds at short range. Theoretical investigations of this effect [129, 130, 158–160] indicate that the contribution to B_R is probably negative and this may be attributed to the additional electron-nuclear attraction associated with an increase in the effective nuclear charge.

(iv) Non-linear polarization effects may result from the strong intermolecular electric fields produced by permanent electric moments. These effects are described by the molecular hyperpolarizabilities [34, 125].

The distortion terms in B_R and B_ε are similar in form, but the molecular polarizabilities in B_ε are the static polarizabilities, while those in B_R are the dynamic polarizabilities and depend on the frequency, ω. For pure samples of the inert gases the second term in B_ε is always zero (Section 4.3). Therefore, since the absorption frequencies for the inert gases are found in the far ultra-violet range, dispersion effects should be small, and B_R and B_ε should be almost equal for these gases.

To evaluate B_R, the specific form of $\left(\frac{\partial \mu^{(1)}}{\partial \varepsilon_0} . e - \alpha_0 \right)$ is required. The derivation of the general expression is described in detail in Section 4.1, with the specific forms for spherical, linear and non-linear molecules given in Sections 4.3, 4.4 and 4.5, respectively. The only change necessary is to substitute dynamic polarizabilities for the static polarizabilities.

5.2 Summary of experimental work on the second refractivity virial coefficient

Tables 1.4 to 1.6 contain a comprehensive summary of the experimental second refractivity virial coefficient data available.

In almost all the work carried out before 1974, the absolute method for the determination of the second refractivity virial coefficient was employed. In this method, B_R is determined from refractive index measurements made at varying gas densities, and the accuracy of the calculated values is limited by the accuracy of the density data. Since the contribution $\frac{B_R}{V_m}$ due to pair interactions is only a small fraction (typically 1 part in

10^4 at 10^5Pa) of the molar refractivity,

$$\frac{B_R}{V_m} = \frac{n^2 - 1}{n^2 + 2}V_m - A_R \qquad (5.11)$$

is a small difference between two large quantities and small errors in the density lead to large errors in B_R. Errors reported by workers using this technique are often 100% or more [13, 67, 150, 151].

In 1974, Buckingham and Graham [39] introduced a new direct determination method, now often referred to as the differential method, based on a technique first used by Buckingham, Cole and Sutter [49] for the direct determination of of the second dielectric virial coefficient. This differential-interferometric method measures directly the effects of molecular interactions on the refractivity of gases, and consists of measuring differentially the total optical path when a gas is decompressed from one cell into a similar evacuated cell. This measurement, together with measurements of A_R, yields values of B_R of much greater precision than previously possible. Buckingham and Graham [39, 122] used this new technique to measure B_R for a wide range of gases. This method has subsequently been used by St-Arnaud and Bose [63, 68, 75], Burns, Graham and Weller [44, 62], and Bose *et al.* [74].

More recently, Achtermann *et al.* [65, 77] improved the differential-interferometric technique by developing a device consisting of two coupled interferometers. One interferometer, with two similar cells in series, measures differentially the the excess contribution to R_m due to gas imperfections, while the second interferometer, with two similar cells in parallel, measures the absolute value of the refractive index at the same time. This technique allowed measurements to be carried out to much higher pressures (up to 40 MPa) than had previously been practical. The accuracy of the measured values was estimated to be between 2-5% for the second refractivity virial coefficient.

There is some evidence [62, 151] that B_R may depend on the wavelength of the incident light, but the large experimental errors render the results inconclusive. In 1991 Hohm [161] developed a low pressure experimental method to determine the second refractivity virial coefficient $b_R(\lambda) = B_R/A_R$ relative to a given fixed value $b_R(\lambda_1)$ for various wavelengths λ. The results of the measurements for Ar, Kr and CO_2 were found to be in fair agreement with the higher pressure results of Burns, Graham and Weller [62]. In the case of CO_2 dispersion effects were larger than those predicted by the small dispersion of the molecular polarizabilities which enter B_R. Hohm [59] later used this method to measure the frequency dependence of B_R for a much wider range of gases, and presented a simple theory to account for the observed dependence.

5.3 Summary of theoretical work on the second refractivity virial coefficient

There have been several theoretical approaches to the density-dependence of the molecular polarizability by Kirkwood [127], Yvon [153], Michels, de Boer and Bijl [158], Brown [162], Jansen and Mazur [155], Buckingham and Pople [31,96] and Levine and McQuarrie [163].

The classical statistical-mechanical theory of the second refractivity virial coefficient presented by Buckingham and Pople [31,96] has been used by many workers [63,66,68,69, 74,75,80] to calculate values for B_R to compare with their measured values. Kielich [124] developed the theory to consider mixtures of gases. The pure gas theory of Buckingham and Pople [31,96] was later expanded by Graham [122] to include the effects of polariz-ability anisotropy, quadrupole moments and field-gradients. This work was continued by Burns, Graham and Weller [62,105] to include more terms in order to establish conver-gence. Several workers have modified these theories for large quasi-spherical molecules by substituting a generalized Lennard-Jones (7-28) potential for the more common (6-12) potential with some success [62,68,164].

These classical theories do not include quantum-mechanical long-range or short-range effects. Long-range dispersion-type interactions have been investigated by Jansen and Mazur [155], Buckingham [123], Heinrichs [156], Certain and Fortune [157], Buckingham, Martin and Watts [128] and Buckingham and Clarke [165]. Short-range overlap effects have been studied by Michels *et al.* [158], ten Seldam and de Groot [159], Lim *et al.* [160], O'Brien *et al.* [130], and Buckingham and Watts [129]. Until recently, complete calcula-tions which include both these considerations were only available for the lightest gases, helium and neon [166]. For these atoms, B_R is negative, while the classical DID model al-ways gives a positive value for the second refractivity virial coefficient. Thus, Achtermann *et al.* [66] adopted a semiclassical approach of adding the positive classical DID contribu-tion to the negative short-range *ab initio* calculations of Dacre [166–169], using potentials presented by Aziz *et al.* [170–172]. Similarly, in 1994, Meinander [173] presented a the-ory for spherical and quasi-spherical atoms and molecules using empirical intermolecular potentials and a model for the pair polarizaibility trace which includes both long and short-range effects. The short-range contribution is modelled with an exponential func-tion derived from Dacre's polarizabilities [166,168,169], while the potentials are those of Aziz *et al.* [170–172]. The work on spherical gases shows that especially for the lighter atoms, the short-range effects are significant. For non-spherical molecules, however, the classical theory is usually adopted. In this work, we will not consider the spherical and quasi-spherical gases and all our calculations are based on the classical theory presented earlier in this chapter.

Chapter 6

The Second Kerr-Effect Virial Coefficient, B_K

In 1875, Kerr observed that when a strong electric field is applied across an isotropic medium, the medium becomes birefringent [32]. In this work we will consider only gases, where the anisotropy in the molecular distribution due to an applied field is the result of the intrinsic anisotropy of the molecules or the anisotropy induced in the molecules by the applied field.
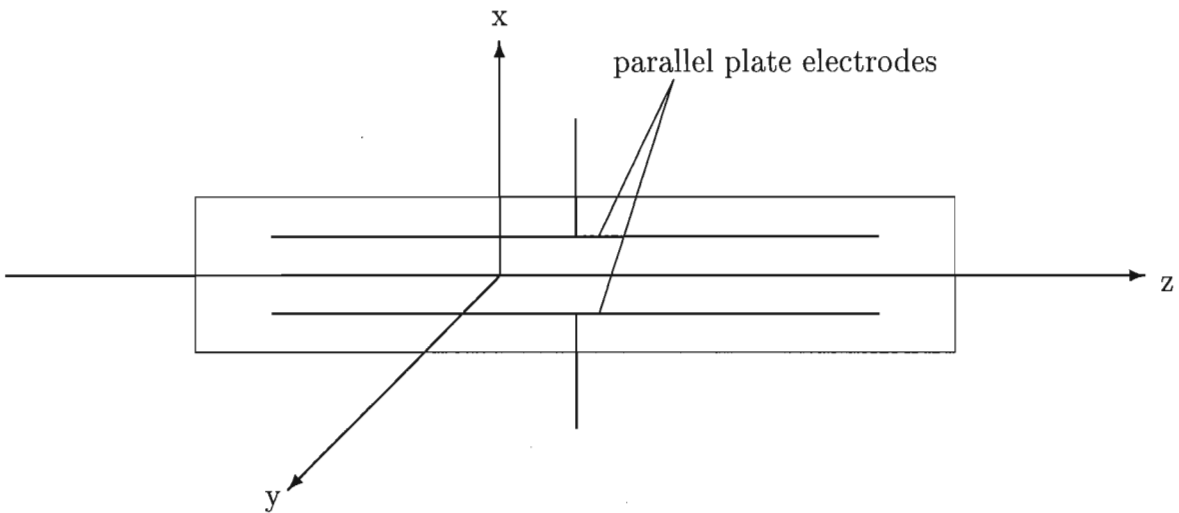
Figure 6.1: The Kerr cell, with space-fixed axes O(x,y,z) where z is in the direction of propagation of the light beam, x is in the direction of the applied electric field, and y is perpendicular to the field.

In the arrangement shown in Figure 6.1, the space-fixed system of axes O(x,y,z) is fixed in the Kerr cell with the z-axis in the direction of propagation of the incident light wave, the x-axis in the direction of the applied static electric field, and the y-axis perpendicular to the applied field. If a gas is introduced into the cell and a uniform electric field is

applied in the x direction using the pair of parallel plates, then a light wave, polarized in the xz plane and propagating in the z direction, experiences a refractive index n_x. If, however the light wave is polarized in the yz plane, it will experience a refractive index n_y, which differs from n_x. This phenomenon is known as the Kerr effect. In order to develop a theory of the Kerr effect, it is necessary to relate the macroscopically observable quantity $(n_x - n_y)$ to the molecular property tensors of the individual molecules in the gas. Buckingham and Pople [34] developed such a theory in 1955 for gases at low pressures. For an ideal gas, $(n_x - n_y)$ is independent of density, but for real gases the density-dependence is described by a virial expansion, with the contribution of pairs of interacting molecules given by the second Kerr-effect virial coefficient.

In 1995, Couling and Graham [9] extended the theory first developed by Buckingham and Pople [34] to include the case of non-linear gases and included many high-order terms to ensure convergence. They did not present the specific form for linear gases, but used the non-linear equations, for which linear gases are a special case. In this work we shall follow the treatment of Couling and Graham, but shall include the equations for linear gases, as these are less complex and require less time to integrate numerically.

6.1 Non-interacting molecules

For a sample of non-interacting molecules, the oscillating dipole moment $\mu_i^{(p)}$ of molecule p is due only to the polarizing action of the alternating electric field $\mathcal{E}_0$ of the light wave, since there are no molecules close enough to cause fields and field gradients at molecule p due to their oscillating moments. However, the strong static electric field E_i applied to the sample may modify the optical-frequency polarizability α_{ij}, resulting in a new effective polarizability tensor π_{ij}, called the differential polarizability, which is written as:

$$\pi_{ij} = \frac{\partial \mu_i}{\partial \mathcal{E}_{0j}} = \alpha_{ij} + \beta_{ijk} E_k + \tfrac{1}{2} \gamma_{ijkl} E_k E_l + \cdots , \qquad (6.1)$$

where all the tensors are referred to the molecule fixed axes O(1,2,3). The polarizability α_{ij}, and the first and second hyperpolarizabilities β_{ijk} and γ_{ijkl} respectively, depend on the frequency ω of the light wave propagating through the medium.

In order to compare the refractive indices n_x and n_y the direction cosines a_i^x between the space-fixed x axis and the molecule-fixed i axis, and a_i^y between the space-fixed y axis and the molecule-fixed i axis are required. For a specific *fixed* configuration σ of the molecule, the difference between the differential polarizabilities is given by:

$$\pi(\sigma, E) = \pi_{ij} \left(a_i^x a_j^x - a_i^y a_j^y \right) . \qquad (6.2)$$

Now, by substituting (6.1) into (6.2) and writing $E a_i^x$ for E_i, a full expression for $\pi(\sigma, E)$ is obtained:

$$\pi(\sigma, E) = \left(\alpha_{ij} + \beta_{ijk} E\, a_k^x + \tfrac{1}{2} \gamma_{ijkl} E^2\, a_k^x a_l^x + \cdots \right) \left(a_i^x a_j^x - a_i^y a_j^y \right). \tag{6.3}$$

This quantity must be averaged over all possible configurations of the molecule *in the presence of the biasing influence of* E_i. By making the assumptions that the period of oscillation of the light wave is much smaller than the time for the molecule to rotate, and that the rotational energy levels are close enough for the orientation to be considered continuous, a Boltzmann-type weighting factor may be used to average over the configurations:

$$\bar{\pi} = \frac{\int \pi(\sigma, E)\, e^{-\frac{U(\sigma, E)}{kT}}\, d\tau}{\int e^{-\frac{U(\sigma, E)}{kT}}\, d\tau}, \tag{6.4}$$

where $U(\sigma, E)$ is the energy of the molecule in a specific configuration σ in the presence of the applied field E_i. In molecule-fixed axes this is given by:

$$U(\sigma, E) = U_0 - \mu_{0i} E_i - \tfrac{1}{2} a_{ij} E_i E_j - \tfrac{1}{6} b_{ijk} E_i E_j E_k - \cdots, \tag{6.5}$$

where U_0 is the energy of the molecule in the absence of the external field, μ_{0i} is the permanent dipole moment of the molecule, a_{ij} is the static polarizability and b_{ijk} is the static first-order hyperpolarizability. Thus, the difference between the refractive indices is given by:

$$n_x - n_y = \frac{2\pi N_A}{(4\pi \varepsilon_0) V_m} \bar{\pi}. \tag{6.6}$$

In order to perform the biased average of π in (6.4), it is converted into isotropic averages by Taylor expansion in powers of E. It is important to note that $\bar{\pi}$ depends on E through both $\pi(\sigma, E)$ and $U(\sigma, E)$. Since the distortion and orientation effects of E_i on gas molecules is very small, it is safe to assume that the Taylor series will converge rapidly. Thus, we can write:

$$\bar{\pi} = A + BE + CE^2 + \cdots, \tag{6.7}$$

where

$$A = (\bar{\pi})_{E=0}, \tag{6.8}$$

$$B = \left(\frac{\partial \bar{\pi}}{\partial E} \right)_{E=0}, \tag{6.9}$$

$$C = \tfrac{1}{2} \left(\frac{\partial^2 \bar{\pi}}{\partial E^2} \right)_{E=0}. \tag{6.10}$$

Buckingham [174] has shown that $(\bar{\pi})_{E=0}$ is zero. Differentiating equation (6.4) and then setting E equal to zero, yields the following expressions for the coefficients B and C:

$$B = \left(\frac{\partial \bar{\pi}}{\partial E} \right)_{E=0} = \left\langle \frac{\partial \pi}{\partial E} \right\rangle - \frac{1}{kT} \left\langle \pi \frac{\partial U}{\partial E} \right\rangle, \tag{6.11}$$

$$C = \tfrac{1}{2} \left(\frac{\partial^2 \bar{\pi}}{\partial E^2} \right)_{E=0} = \tfrac{1}{2} \left\langle \frac{\partial^2 \pi}{\partial E^2} \right\rangle - \frac{1}{2kT} \left\langle 2 \frac{\partial \pi}{\partial E} \frac{\partial U}{\partial E} + \pi \frac{\partial^2 U}{\partial E^2} \right\rangle + \frac{1}{2(kT)^2} \left\langle \pi \left(\frac{\partial U}{\partial E} \right)^2 \right\rangle, \tag{6.12}$$

where $\langle X \rangle$ represents the isotropic average of any quantity $X(\sigma, E)$ in the absence of an external field, so that:

$$\langle X \rangle = \frac{\int X(\sigma, 0) \, e^{-\frac{U(\sigma,0)}{kT}} \, d\tau}{\int e^{-\frac{U(\sigma,0)}{kT}} \, d\tau}. \tag{6.13}$$

Differentiating (6.5) and (6.3) and setting the field to zero, yields:

$$\left(\frac{\partial \pi}{\partial E} \right)_{E=0} = \beta_{ijk} \, \mathrm{a}_k^x \left(\mathrm{a}_i^x \mathrm{a}_j^x - \mathrm{a}_i^y \mathrm{a}_j^y \right), \tag{6.14}$$

$$\left(\frac{\partial U}{\partial E} \right)_{E=0} = -\mu_{0i} \, \mathrm{a}_i^x, \tag{6.15}$$

$$\left(\frac{\partial^2 \pi}{\partial E^2} \right)_{E=0} = \gamma_{ijkl} \, \mathrm{a}_k^x \mathrm{a}_l^x \left(\mathrm{a}_i^x \mathrm{a}_j^x - \mathrm{a}_i^y \mathrm{a}_j^y \right) \tag{6.16}$$

and $\qquad \left(\frac{\partial^2 U}{\partial E^2} \right)_{E=0} = -a_{ij} \, \mathrm{a}_i^x \mathrm{a}_j^x. \tag{6.17}$

From (6.14) and (6.15) it can be seen that both of the terms in (6.11) will average to zero over all directions of a_i^x. Thus, since Buckingham [174] has shown that $(\bar{\pi})_{E=0}$ is zero, the leading non-vanishing term in (6.7) is CE^2. The standard isotropic averages [34, 175] are given by:

$$\langle \mathrm{a}_i^x \mathrm{a}_j^x \mathrm{a}_k^x \mathrm{a}_l^x \rangle = \tfrac{1}{15} \left(\delta_{ij}\delta_{kl} + \delta_{ik}\delta_{jl} + \delta_{il}\delta_{jk} \right), \tag{6.18}$$

$$\langle \mathrm{a}_i^y \mathrm{a}_j^y \mathrm{a}_k^x \mathrm{a}_l^x \rangle = \tfrac{1}{30} \left(4\delta_{ij}\delta_{kl} - \delta_{ik}\delta_{jl} - \delta_{il}\delta_{jk} \right). \tag{6.19}$$

Therefore,

$$\langle a_i^x a_j^x a_k^x a_l^x - a_i^y a_j^y a_k^x a_l^x \rangle = \tfrac{1}{30}\left(-2\delta_{ij}\delta_{kl} + 3\delta_{ik}\delta_{jl} + 3\delta_{il}\delta_{jk}\right). \tag{6.20}$$

Using equation (6.20) for the isotropic averages and equations (6.3) and (6.14) to (6.17), yields the following expressions for the terms of (6.12):

$$\tfrac{1}{2}\left\langle \frac{\partial^2 \pi}{\partial E^2} \right\rangle = \tfrac{1}{2}\gamma_{ijkl}\left\langle a_i^x a_j^x a_k^x a_l^x - a_i^y a_j^y a_k^x a_l^x \right\rangle$$

$$= \tfrac{2}{30}\gamma_{iijj}, \tag{6.21}$$

$$-\frac{1}{2kT}\left\langle 2\frac{\partial\pi}{\partial E}\frac{\partial U}{\partial E} + \pi\frac{\partial^2 U}{\partial E^2} \right\rangle = \frac{1}{kT}\beta_{ijk}\mu_{0l}\left\langle a_i^x a_j^x a_k^x a_l^x - a_i^y a_j^y a_k^x a_l^x \right\rangle$$

$$+ \frac{1}{2kT}\alpha_{ij}a_{kl}\left\langle a_i^x a_j^x a_k^x a_l^x - a_i^y a_j^y a_k^x a_l^x \right\rangle$$

$$= \frac{2}{15kT}\beta_{iij}\mu_{0j} + \frac{1}{15kT}\left(\alpha_{ij}a_{ij} - 3\alpha a\right), \tag{6.22}$$

$$\frac{1}{2(kT)^2}\left\langle \pi\left(\frac{\partial U}{\partial E}\right)^2 \right\rangle = \frac{1}{2(kT)^2}\alpha_{ij}\mu_{0k}\mu_{0l}\left\langle a_i^x a_j^x a_k^x a_l^x - a_i^y a_j^y a_k^x a_l^x \right\rangle$$

$$= \frac{3}{15(kT)^2}\left(\alpha_{ij}\mu_{0i}\mu_{0j} - \alpha\mu_0^2\right), \tag{6.23}$$

where $\alpha = \alpha_{ii}$ and $a = a_{ii}$. Thus,

$$\left(\frac{\partial^2 \bar{\pi}}{\partial E^2}\right)_{E=0} = \tfrac{4}{30}\gamma_{iijj} + \frac{4}{15kT}\beta_{iij}\mu_{0j} + \frac{2}{15kT}\left(\alpha_{ij}a_{ij} - 3\alpha a\right) + \frac{6}{15(kT)^2}\left(\alpha_{ij}\mu_{0i}\mu_{0j} - \alpha\mu_0^2\right) \tag{6.24}$$

and equation (6.7) becomes:

$$\bar{\pi} = \left\{ \tfrac{2}{30}\gamma_{iijj} + \frac{2}{15kT}\beta_{iij}\mu_{0j} + \frac{1}{15kT}\left(\alpha_{ij}a_{ij} - 3\alpha a\right) + \frac{3}{15(kT)^2}\left(\alpha_{ij}\mu_{0i}\mu_{0j} - \alpha\mu_0^2\right) \right\} E^2. \tag{6.25}$$

In the low density limit, the definition of the molecular Kerr constant proposed by Otterbein [176] becomes:

$$K_m = \lim_{V_m \to \infty}\left\{ \frac{2(n_x - n_y)V_m}{27(4\pi\varepsilon_0)E^2} \right\}_{E\to 0} = \frac{2\pi N_A}{27(4\pi\varepsilon_0)}\left(\frac{\partial^2 \bar{\pi}}{\partial E^2}\right)_{E=0}. \tag{6.26}$$

88

Taking the second derivative of $\bar{\pi}$ in (6.25) with respect to E, setting $E = 0$ and substituting the resulting expression into (6.26) yields:

$$K_m = \frac{2\pi N_A}{405(4\pi\varepsilon_0)} \left\{ 2\gamma_{iijj} + \frac{1}{kT} \left[4\beta_{iij}\mu_{0j} + 3\left(\alpha_{ij}a_{ij} - 3\alpha a\right) \right] + \frac{3}{(kT)^2} \left(\alpha_{ij}\mu_{0i}\mu_{0j} - \alpha\mu_0^2 \right) \right\}.$$

(6.27)

First derived by Buckingham and Pople [34] in 1955, this equation is a generalization of the well-known Langevin-Born equation to include the effects of high field strengths on the polarizability.

In the special case of a gas consisting of non-interacting spherical molecules, (6.27) simplifies to:

$$K_m = \frac{4\pi N_A}{81(4\pi\varepsilon_0)}\gamma,$$

(6.28)

where $\gamma = \frac{1}{5}\gamma_{ijij}$. Thus, the hyperpolarizability constant γ can be determined directly from low pressure measurements of the molecular Kerr constant. Although the measured value of γ will depend on the frequency ω of the incident light, it should not be significantly different from the static value if ω lies well below the electronic absorption band of the gas [9].

6.2 Interacting molecules

For gas densities where interactions between the molecules in the sample become significant, Buckingham and Pople argued that the average contribution of a molecule 1 to $(n_x - n_y)$ is not necessarily equal to $\frac{2\pi}{(4\pi\varepsilon_0)V_m}\bar{\pi}$ as shown in (6.26). If molecule 1 comes into contact with a second molecule, then it must be treated as half of an interacting pair. When molecules 1 and 2 are in the relative configuration τ at a particular instant, then molecule 1 contributes $\frac{1}{2}\left\{\frac{2\pi}{(4\pi\varepsilon_0)V_m}\pi^{(12)}(\tau, E)\right\}$ to $(n_x - n_y)$. If $\pi_{ij}^{(12)}$ is the differential polarizability of the interacting pair, then the difference between the differential polarizabilities $\pi_{ij}^{(12)}a_i^x a_j^x$ and $\pi_{ij}^{(12)}a_i^y a_j^y$ of an interacting pair in a specific relative interaction configuration τ in the presence of the applied field may be written as:

$$\pi^{(12)}(\tau, E) = \pi_{ij}^{(12)}(a_i^x a_j^x - a_i^y a_j^y).$$

(6.29)

To obtain the biased orientational average $\overline{\pi^{(12)}(\tau, E)}$ for a pair of molecules, they are held fixed in the relative configuration τ and allowed to rotate as a rigid whole in the presence of E_i. As for an isolated molecule, the biased average may be converted to

isotropic averages by Taylor expansion in powers of E, and the leading term is given by:

$$\overline{\pi^{(12)}(\tau, E)} = \tfrac{1}{2}\left(\frac{\partial^2 \overline{\pi^{(12)}(\tau, E)}}{\partial E^2}\right)_{E=0} E^2 \tag{6.30}$$

$$= \tfrac{1}{2}\left\{\left\langle\frac{\partial^2 \pi^{(12)}}{\partial E^2}\right\rangle - \frac{1}{kT}\left\langle 2\frac{\partial \pi^{(12)}}{\partial E}\frac{\partial U^{(12)}}{\partial E} + \pi^{(12)}\frac{\partial^2 U^{(12)}}{\partial E^2}\right\rangle\right.$$

$$\left. + \frac{1}{(kT)^2}\left\langle\pi^{(12)}\left(\frac{\partial U^{(12)}}{\partial E}\right)^2\right\rangle\right\} E^2, \tag{6.31}$$

where the angular brackets indicate averages in the absence of any field. Note, $U^{(12)}(\tau, E)$ is the pair interaction energy in the presence of the external field E_i. Initially, all the quantities in the angular brackets are referred to the molecule-fixed axes $O(1,2,3)$ because, for a given τ, the tensor product in $O(1,2,3)$ is fixed. By allowing the pair of molecules to rotate isotropically as a rigid whole in the space-fixed axes $O(x,y,z)$, the average projection of pair properties referred to $O(1,2,3)$ may be averaged into $O(x,y,z)$ over all orientations. Finally, the average over the interaction parameters τ of the pair may be performed.

The density dependence of K_m may be written as a virial expansion in powers of density [34]:

$$K_m = A_K + \frac{B_K}{V_m} + \frac{C_K}{V_m^2} + \cdots, \tag{6.32}$$

where A_K, B_K, C_K ... are the first, second, third, ... Kerr-effect virial coefficients, respectively. The definition of the molecular Kerr constant in the low density limit is given by equation (6.26) in Section 6.1. Thus, since the first Kerr-effect virial coeffiecient is the contribution of non-interacting molecules to K_m, we have:

$$A_K = \lim_{V_m \to \infty}(K_m) = \frac{2\pi N_A}{27(4\pi\varepsilon_0)}\left(\frac{\partial^2 \bar{\pi}}{\partial E^2}\right)_{E=0}. \tag{6.33}$$

The second Kerr-effect virial coefficient B_K describes the deviations from A_K due to pair interactions and is given by:

$$B_K = \lim_{V_m \to \infty}(K_m - A_K)V_m. \tag{6.34}$$

From (6.31) and (6.32) to (6.34), we have:

$$K_m = A_K + \frac{2\pi N_A}{27(4\pi\varepsilon_0)}\int_\tau\left\{\tfrac{1}{2}\left(\frac{\partial^2 \overline{\pi^{(12)}(\tau, E)}}{\partial E^2}\right)_{E=0} - \left(\frac{\partial^2 \bar{\pi}}{\partial E^2}\right)_{E=0}\right\}P(\tau)d\tau, \tag{6.35}$$

where $P(\tau)d\tau$ is the probability of molecule 1 having a neighbour in the range $(\tau, \tau + d\tau)$, and is related to the intermolecular potential as shown in equation (1.4) in Chapter 1. Combining (6.26), (6.35) and (1.4), yields the following expression for the second Kerr-effect virial coefficient:

$$B_K = \frac{2\pi N_A^2}{27\Omega(4\pi\varepsilon_0)} \int_\tau \left\{ \frac{1}{2}\left(\frac{\partial^2 \overline{\pi^{(12)}(\tau, E)}}{\partial E^2} \right)_{E=0} - \left(\frac{\partial^2 \bar{\pi}}{\partial E^2} \right)_{E=0} \right\} e^{-\frac{U^{(12)}(\tau)}{kT}} \, d\tau. \quad (6.36)$$

In order to calculate B_K, explicit expressions for the terms in the integral must be derived, and the integrals are then evaluated numerically. Expressions for the second term in the integral have been derived in Section 6.1. The first term must now be evaluated.

6.3 Expression for $\frac{1}{2}\left(\dfrac{\partial^2 \overline{\pi^{(12)}(\tau, E)}}{\partial E^2} \right)_{E=0}$

From equations (6.30) and (6.31) we have:

$$\frac{1}{2}\left(\frac{\partial^2 \overline{\pi^{(12)}(\tau, E)}}{\partial E^2} \right)_{E=0} = \frac{1}{2}\left\langle \frac{\partial^2 \pi^{(12)}}{\partial E^2} \right\rangle - \frac{1}{2kT}\left\langle 2\frac{\partial \pi^{(12)}}{\partial E}\frac{\partial U^{(12)}}{\partial E} + \pi^{(12)}\frac{\partial^2 U^{(12)}}{\partial E^2} \right\rangle$$

$$+ \frac{1}{2(kT)^2}\left\langle \pi^{(12)}\left(\frac{\partial U^{(12)}}{\partial E} \right)^2 \right\rangle. \quad (6.37)$$

Thus, in order to evaluate the components of this term, we need to determine $\pi^{(12)}(\tau, E)$ and $U^{(12)}(\tau, E)$. The relationship between $\pi^{(12)}(\tau, E)$ and the differential polarizability of the pair is given by (6.29). Now, the differential polarizability of the pair is:

$$\pi_{ij}^{(12)} = \frac{\partial \mu_i^{(12)}}{\partial \mathcal{E}_{0j}}, \quad (6.38)$$

where $\mu_i^{(12)}(\mathcal{E}_{0j})$ is the total oscillating dipole induced in the pair of interacting molecules by the alternating field of the light wave. In order to proceed, it is necessary to assume that the interacting molecules retain their separate identities. While this assumption is always valid for large separations, it probably remains adequate at short range in most cases and we join past workers [9, 44, 62, 122, 177] in treating the interacting molecules as though they remain separate, even in the region of overlap, so that we have:

$$\mu_i^{(12)} = \mu_i^{(1)} + \mu_i^{(2)}, \quad (6.39)$$

and equation (6.38) becomes:

$$\pi_{ij}^{(12)} = \frac{\partial(\mu_i^{(1)} + \mu_i^{(2)})}{\partial \mathcal{E}_{0j}}. \tag{6.40}$$

Thus, from (6.29):

$$\pi^{(12)}(\tau, E) = \frac{\partial(\mu_i^{(1)} + \mu_i^{(2)})}{\partial \mathcal{E}_{0j}}(\mathrm{a}_i^x \mathrm{a}_j^x - \mathrm{a}_i^y \mathrm{a}_j^y)$$

$$= \left(\frac{\partial \mu_i^{(1)}}{\partial \mathcal{E}_{0j}} + \frac{\partial \mu_i^{(2)}}{\partial \mathcal{E}_{0j}}\right)(\mathrm{a}_i^x \mathrm{a}_j^x - \mathrm{a}_i^y \mathrm{a}_j^y)$$

$$= \left(\pi_{ij}^{(1)} + \pi_{ij}^{(2)}\right)(\mathrm{a}_i^x \mathrm{a}_j^x - \mathrm{a}_i^y \mathrm{a}_j^y)$$

$$= \pi^{(1)}(\tau, E) + \pi^{(2)}(\tau, E), \tag{6.41}$$

since $\pi_{ij}^{(p)} = \frac{\partial \mu_i^{(p)}}{\partial \mathcal{E}_{0j}}$ and $\pi^{(p)}(\tau, E) = \pi_{ij}^{(p)}(\mathrm{a}_i^x \mathrm{a}_j^x - \mathrm{a}_i^y \mathrm{a}_j^y)$. Thus, to determine $\pi^{(12)}(\tau, E)$, it is necessary to evaluate the total oscillating dipole moment induced on molecule p by the light wave field $\mathcal{E}_{0j}$ and by the field $\mathcal{F}_j^{(p)}$ arising at molecule p due to the oscillating moments of molecule q.

The pair interaction potential in the presence of E_i may be written as follows [177]:

$$U^{(12)}(\tau, E) = U^{(12)}(\tau, 0) - \int_0^E \mu_i^{(12)}(\tau, E)\mathrm{a}_i^x \, dE, \tag{6.42}$$

where $\mu_i^{(12)}$ is the total dipole moment of the pair in the presence of $E\mathrm{a}_i^x$. Since, as in equation (6.39), $\mu_i^{(12)}$ is equal to the sum of the total dipole moments on molecules 1 and 2, in the presence of the external field and each other, (6.42) becomes [9]:

$$U^{(12)}(\tau, E) = U^{(12)}(\tau, 0) + U^{(1)}(\tau, E) + U^{(2)}(\tau, E), \tag{6.43}$$

where the potential energy at molecule p in the presence of the external field and molecule q, is given by:

$$U^{(p)}(\tau, E) = \int_0^E \mu_i^{(p)}\mathrm{a}_i^x \, dE. \tag{6.44}$$

Thus, we need to determine the total dipole moment $\mu_i^{(p)}(\tau, E)$ on molecule p due to the static applied field E_j and to the static field $F_j^{(p)}$ at molecule p due to the permanent and

92

induced multipole moments of its neighbour, molecule q.

Since molecules 1 and 2 are identical, use of equations (6.41) and (6.43) in equation (6.37) yields [9]:

$$
\frac{1}{2}\left(\frac{\partial^2 \overline{\pi^{(12)}(\tau, E)}}{\partial E^2}\right)_{E=0} = \left\langle\frac{\partial^2 \pi^{(1)}}{\partial E^2}\right\rangle - \frac{2}{kT}\left\{\left\langle\frac{\partial \pi^{(1)}}{\partial E}\frac{\partial U^{(1)}}{\partial E}\right\rangle + \left\langle\frac{\partial \pi^{(1)}}{\partial E}\frac{\partial U^{(2)}}{\partial E}\right\rangle\right\}
$$

$$
- \frac{1}{kT}\left\{\left\langle\pi^{(1)}\frac{\partial^2 U^{(1)}}{\partial E^2}\right\rangle + \left\langle\pi^{(1)}\frac{\partial^2 U^{(2)}}{\partial E^2}\right\rangle\right\} + \frac{1}{(kT)^2}\left\{\left\langle\pi^{(1)}\left(\frac{\partial U^{(1)}}{\partial E}\right)^2\right\rangle\right.
$$

$$
\left. + \left\langle\pi^{(1)}\left(\frac{\partial U^{(2)}}{\partial E}\right)^2\right\rangle + \left\langle\pi^{(1)}\frac{\partial U^{(1)}}{\partial E}\frac{\partial U^{(2)}}{\partial E}\right\rangle\right\}. \tag{6.45}
$$

Now, it remains to determine explicit expressions for $\pi^{(1}(\tau, E)$ and $U^{(p)}(\tau, E)$.

6.3.1 Expression for $\pi^{(1)}(\tau, E)$

In a dense medium, the total oscillating dipole moment induced in a molecule 1 may be due not only to the oscillating electric field $\mathcal{E}_{0i}$ of the incident light, but also to the oscillating field $\mathcal{F}_i^{(1)}$ and field gradient $\mathcal{F}_{ij}^{(1)}$ at molecule 1 due to the oscillating moments of a neighbouring molecule 2. In addition, the polarizability of the molecule may be distorted by the presence of the static electric field E_i. Similarly, the oscillating dipole moment of molecule 2 is induced by the light wave field, as well as by the field and field gradients due to the oscillating moments of molecule 1. Thus, for the oscillating dipole moments of molecules 1 and 2, we have:

$$
\mu_i^{(1)}(\mathcal{E}_0) = \left(\alpha_{ij}^{(1)} + \beta_{ijk}^{(1)}E_k + \tfrac{1}{2}\gamma_{ijkl}^{(1)}E_kE_l\right)\left(\mathcal{E}_{0j} + \mathcal{F}_j^{(1)}\right) + \tfrac{1}{3}A_{ijk}^{(1)}\mathcal{F}_{jk}^{(1)} + \cdots, \tag{6.46}
$$

$$
\mu_i^{(2)}(\mathcal{E}_0) = \left(\alpha_{ij}^{(2)} + \beta_{ijk}^{(2)}E_k + \tfrac{1}{2}\gamma_{ijkl}^{(2)}E_kE_l\right)\left(\mathcal{E}_{0j} + \mathcal{F}_j^{(2)}\right) + \tfrac{1}{3}A_{ijk}^{(2)}\mathcal{F}_{jk}^{(2)} + \cdots, \tag{6.47}
$$

where, using the T-tensor notation described in Section 2.3,

$$
\mathcal{F}_j^{(1)} = T_{jk}\mu_k^{(2)} - \tfrac{1}{3}T_{jkl}\theta_{kl}^{(2)} + \cdots, \qquad \mathcal{F}_j^{(2)} = T_{jk}\mu_k^{(1)} + \tfrac{1}{3}T_{jkl}\theta_{kl}^{(1)} + \cdots, \tag{6.48}
$$

$$
\mathcal{F}_{jk}^{(1)} = T_{jkl}\mu_l^{(2)} - \tfrac{1}{3}T_{jklm}\theta_{lm}^{(2)} + \cdots, \qquad \mathcal{F}_{jk}^{(2)} = -T_{jkl}\mu_l^{(1)} - \tfrac{1}{3}T_{jklm}\theta_{lm}^{(1)} + \cdots. \tag{6.49}
$$

The oscillating quadrupole moments are given by:

$$
\theta_{kl}^{(1)}(\mathcal{E}_0) = A_{mkl}^{(1)}\left(\mathcal{E}_{0m} + \mathcal{F}_m^{(1)}\right) + \cdots, \tag{6.50}
$$

$$
\theta_{kl}^{(2)}(\mathcal{E}_0) = A_{mkl}^{(2)}\left(\mathcal{E}_{0m} + \mathcal{F}_m^{(2)}\right) + \cdots. \tag{6.51}
$$

The field gradient $\mathcal{E}_{0ij}$ of the light wave has been neglected in these equations since the molecular dimensions of the gases under study are very small compared to the wavelength.

Repeated substitution of $\mathcal{F}_i^{(1)}$, $\mathcal{F}_{jk}^{(1)}$, $\mu_k^{(2)}$, $\theta_{kl}^{(2)}$, $\mathcal{F}_j^{(2)}$, $\mathcal{F}_{jk}^{(2)}$, $\mu_k^{(1)}$ and $\theta_{kl}^{(1)}$ into (6.46) results in a final expression for the total oscillating dipole moment induced on molecule 1 by the light wave field in the presence of molecule 2:

$$
\begin{aligned}
\mu_i^{(1)}(\mathcal{E}_0) =\ & \alpha_{ij}^{(1)}\mathcal{E}_{0j} + \alpha_{ik}^{(1)}T_{kl}\alpha_{lj}^{(2)}\mathcal{E}_{0j} + \alpha_{ik}^{(1)}T_{kl}\alpha_{lm}^{(2)}T_{mn}\alpha_{nj}^{(1)}\mathcal{E}_{0j} \\
& + \alpha_{ik}^{(1)}T_{kl}\alpha_{lm}^{(2)}T_{mn}\alpha_{np}^{(1)}T_{pq}\alpha_{qj}^{(2)}\mathcal{E}_{0j} + \cdots \\
& - \tfrac{1}{3}\alpha_{ik}^{(1)}T_{klm}A_{jlm}^{(2)}\mathcal{E}_{0j} + \tfrac{1}{3}A_{ikl}^{(1)}T_{klm}\alpha_{mj}^{(2)}\mathcal{E}_{0j} \\
& + \tfrac{1}{3}\alpha_{ik}^{(1)}T_{kl}\alpha_{lm}^{(2)}T_{mnp}A_{jnp}^{(1)}\mathcal{E}_{0j} - \tfrac{1}{3}\alpha_{ik}^{(1)}T_{kl}A_{lmn}^{(2)}T_{mnp}\alpha_{pj}^{(1)}\mathcal{E}_{0j} \\
& - \tfrac{1}{3}\alpha_{ik}^{(1)}T_{klm}A_{nlm}^{(2)}T_{np}\alpha_{pj}^{(1)}\mathcal{E}_{0j} + \tfrac{1}{3}A_{ikl}^{(1)}T_{klm}\alpha_{mn}^{(2)}T_{np}\alpha_{pj}^{(1)}\mathcal{E}_{0j} \\
& + \beta_{ijk}^{(1)}E_k\mathcal{E}_{0j} + \alpha_{il}^{(1)}T_{lm}\beta_{mjk}^{(2)}E_k\mathcal{E}_{0j} + \beta_{ilk}^{(1)}E_kT_{lm}\alpha_{mj}^{(2)}\mathcal{E}_{0j} \\
& + \alpha_{il}^{(1)}T_{lm}\alpha_{mn}^{(2)}T_{np}\beta_{pjk}^{(1)}E_k\mathcal{E}_{0j} + \alpha_{il}^{(1)}T_{lm}\beta_{mnk}^{(2)}E_kT_{np}\alpha_{pj}^{(1)}\mathcal{E}_{0j} \\
& + \beta_{ilk}^{(1)}E_kT_{lm}\alpha_{mn}^{(2)}T_{np}\alpha_{pj}^{(1)}\mathcal{E}_{0j} + \cdots \\
& + \tfrac{1}{2}\gamma_{ijkl}^{(1)}E_kE_l\mathcal{E}_{0j} + \tfrac{1}{2}\alpha_{im}^{(1)}T_{mn}\gamma_{njkl}^{(2)}E_kE_l\mathcal{E}_{0j} + \tfrac{1}{2}\gamma_{imkl}^{(1)}E_kE_lT_{mn}\alpha_{nj}^{(2)}\mathcal{E}_{0j} \\
& + \tfrac{1}{2}\alpha_{im}^{(1)}T_{mn}\alpha_{np}^{(2)}T_{pq}\gamma_{qjkl}^{(1)}E_kE_l\mathcal{E}_{0j} + \tfrac{1}{2}\alpha_{im}^{(1)}T_{mn}\gamma_{npkl}^{(2)}E_kE_lT_{pq}\alpha_{qj}^{(1)}\mathcal{E}_{0j} \\
& + \tfrac{1}{2}\gamma_{imkl}^{(1)}E_kE_lT_{mn}\alpha_{np}^{(2)}T_{pq}\alpha_{qj}^{(1)}\mathcal{E}_{0j} + \cdots .
\end{aligned} \tag{6.52}
$$

When (6.52) is differentiated with respect to $\mathcal{E}_{0j}$, the resulting expression gives the differential polarizability of molecule 1 in the presence of the applied field and molecule 2, in a specific relative configuration τ:

$$
\begin{aligned}
\pi_{ij}^{(1)} = \frac{\partial \mu_i^{(1)}}{\partial \mathcal{E}_{0j}} =\ & \alpha_{ij}^{(1)} + \alpha_{ik}^{(1)}T_{kl}\alpha_{lj}^{(2)} + \alpha_{ik}^{(1)}T_{kl}\alpha_{lm}^{(2)}T_{mn}\alpha_{nj}^{(1)} + \alpha_{ik}^{(1)}T_{kl}\alpha_{lm}^{(2)}T_{mn}\alpha_{np}^{(1)}T_{pq}\alpha_{qj}^{(2)} + \cdots \\
& - \tfrac{1}{3}\alpha_{ik}^{(1)}T_{klm}A_{jlm}^{(2)} + \tfrac{1}{3}A_{ikl}^{(1)}T_{klm}\alpha_{mj}^{(2)} + \tfrac{1}{3}\alpha_{ik}^{(1)}T_{kl}\alpha_{lm}^{(2)}T_{mnp}A_{jnp}^{(1)} \\
& - \tfrac{1}{3}\alpha_{ik}^{(1)}T_{kl}A_{lmn}^{(2)}T_{mnp}\alpha_{pj}^{(1)} - \tfrac{1}{3}\alpha_{ik}^{(1)}T_{klm}A_{nlm}^{(2)}T_{np}\alpha_{pj}^{(1)} + \tfrac{1}{3}A_{ikl}^{(1)}T_{klm}\alpha_{mn}^{(2)}T_{np}\alpha_{pj}^{(1)} \\
& + \Big(\beta_{ijk}^{(1)} + \alpha_{il}^{(1)}T_{lm}\beta_{mjk}^{(2)} + \beta_{ilk}^{(1)}T_{lm}\alpha_{mj}^{(2)} + \alpha_{il}^{(1)}T_{lm}\alpha_{mn}^{(2)}T_{np}\beta_{pjk}^{(1)} \\
& + \alpha_{il}^{(1)}T_{lm}\beta_{mnk}^{(2)}T_{np}\alpha_{pj}^{(1)} + \beta_{ilk}^{(1)}T_{lm}\alpha_{mn}^{(2)}T_{np}\alpha_{pj}^{(1)} + \cdots \Big)E a_k^x
\end{aligned}
$$

$$+ \tfrac{1}{2} \left(\gamma_{ijkl}^{(1)} + \alpha_{im}^{(1)} T_{mn} \gamma_{njkl}^{(2)} + \gamma_{imkl}^{(1)} T_{mn} \alpha_{nj}^{(2)} + \alpha_{im}^{(1)} T_{mn} \alpha_{np}^{(2)} T_{pq} \gamma_{qjkl}^{(1)} \right.$$

$$\left. + \alpha_{im}^{(1)} T_{mn} \gamma_{npkl}^{(2)} T_{pq} \alpha_{qj}^{(1)} + \gamma_{imkl}^{(1)} T_{mn} \alpha_{np}^{(2)} T_{pq} \alpha_{qj}^{(1)} + \cdots \right) E^2 \mathrm{a}_k^x \mathrm{a}_l^x + \cdots . \tag{6.53}$$

Recall that

$$\pi^{(1)}(\tau, E) = \pi_{ij}^{(1)} (\mathrm{a}_i^x \mathrm{a}_j^x - \mathrm{a}_i^y \mathrm{a}_j^y). \tag{6.54}$$

Differentiating equation (6.53), multiplied by $(\mathrm{a}_i^x \mathrm{a}_j^x - \mathrm{a}_i^y \mathrm{a}_j^y)$, with respect to E and then setting $E = 0$ yields the following expressions:

$$\left(\pi^{(1)} \right)_{E=0} = \left(\alpha_{ij}^{(1)} + \alpha_{ik}^{(1)} T_{kl} \alpha_{lj}^{(2)} + \alpha_{ik}^{(1)} T_{kl} \alpha_{lm}^{(2)} T_{mn} \alpha_{nj}^{(1)} + \alpha_{ik}^{(1)} T_{kl} \alpha_{lm}^{(2)} T_{mn} \alpha_{np}^{(1)} T_{pq} \alpha_{qj}^{(2)} + \cdots \right.$$

$$- \tfrac{1}{3} \alpha_{ik}^{(1)} T_{klm} A_{jlm}^{(2)} + \tfrac{1}{3} A_{ikl}^{(1)} T_{klm} \alpha_{mj}^{(2)} + \tfrac{1}{3} \alpha_{ik}^{(1)} T_{kl} \alpha_{lm}^{(2)} T_{mnp} A_{jnp}^{(1)}$$

$$\left. - \tfrac{1}{3} \alpha_{ik}^{(1)} T_{kl} A_{lmn}^{(2)} T_{mnp} \alpha_{pj}^{(1)} - \tfrac{1}{3} \alpha_{ik}^{(1)} T_{klm} A_{nlm}^{(2)} T_{np} \alpha_{pj}^{(1)} + \tfrac{1}{3} A_{ikl}^{(1)} T_{klm} \alpha_{mn}^{(2)} T_{np} \alpha_{pj}^{(1)} \right)$$

$$\times \left(\mathrm{a}_i^x \mathrm{a}_j^x - \mathrm{a}_i^y \mathrm{a}_j^y \right), \tag{6.55}$$

$$\left(\frac{\partial \pi^{(1)}}{\partial E} \right)_{E=0} = \left(\beta_{ijk}^{(1)} + \alpha_{il}^{(1)} T_{lm} \beta_{mjk}^{(2)} + \beta_{ilk}^{(1)} T_{lm} \alpha_{mj}^{(2)} + \alpha_{il}^{(1)} T_{lm} \alpha_{mn}^{(2)} T_{np} \beta_{pjk}^{(1)} \right.$$

$$\left. + \alpha_{il}^{(1)} T_{lm} \beta_{mnk}^{(2)} T_{np} \alpha_{pj}^{(1)} + \beta_{ilk}^{(1)} T_{lm} \alpha_{mn}^{(2)} T_{np} \alpha_{pj}^{(1)} + \cdots \right) \mathrm{a}_k^x \left(\mathrm{a}_i^x \mathrm{a}_j^x - \mathrm{a}_i^y \mathrm{a}_j^y \right), \tag{6.56}$$

$$\left(\frac{\partial^2 \pi^{(1)}}{\partial E^2} \right)_{E=0} = \left(\gamma_{ijkl}^{(1)} + \alpha_{im}^{(1)} T_{mn} \gamma_{njkl}^{(2)} + \gamma_{imkl}^{(1)} T_{mn} \alpha_{nj}^{(2)} + \alpha_{im}^{(1)} T_{mn} \alpha_{np}^{(2)} T_{pq} \gamma_{qjkl}^{(1)} \right.$$

$$\left. + \alpha_{im}^{(1)} T_{mn} \gamma_{npkl}^{(2)} T_{pq} \alpha_{qj}^{(1)} + \gamma_{imkl}^{(1)} T_{mn} \alpha_{np}^{(2)} T_{pq} \alpha_{qj}^{(1)} + \cdots \right) \mathrm{a}_k^x \mathrm{a}_l^x \left(\mathrm{a}_i^x \mathrm{a}_j^x - \mathrm{a}_i^y \mathrm{a}_j^y \right). \tag{6.57}$$

6.3.2   Expression for $U^{(p)}(\tau, E)$

The total dipole moment $\mu_i^{(p)}$ of molecule p in the presence of the static applied field E_i and molecule q, is given by:

$$\mu_i^{(p)} = \mu_{0i}^{(p)} + a_{ij}^{(p)} \left(E_j + F_j^{(p)} \right) + \tfrac{1}{3} A_{ijk}^{(p)} F_{jk}^{(p)} + \cdots , \tag{6.58}$$

where $\mu_{0i}^{(p)}$ is the permanent dipole moment of the molecule, and $F_j^{(p)}$ and $F_{jk}^{(p)}$ are the static field and field gradient at molecule p due to the permanent and induced dipole and

quadrupole moments of molecule q, such that:

$$F_j^{(p)} = T_{jk}\mu_k^{(q)} - \tfrac{1}{3}T_{jkl}^{(p)}\theta_{kl}^{(q)},$$ (6.59)

$$F_{jk}^{(p)} = T_{jkl}^{(p)}\mu_l^{(q)} - \tfrac{1}{3}T_{jklm}\theta_{lm}^{(q)},$$ (6.60)

where the total quadrupole moment of molecule q due to the external field and the field due to the permanent and induced multipole moments of molecule p is given by:

$$\theta_{kl}^{(q)} = \theta_{0kl}^{(q)} + A_{mkl}^{(q)}\left(E_m + F_m^{(q)}\right) + \cdots.$$ (6.61)

Substituting repeatedly for $F_i^{(p)}$, $F_{ij}^{(p)}$, $\mu_i^{(q)}$ and $\theta_{ij}^{(q)}$ into equation (6.58), yields the following expression:

$$\begin{aligned}
\mu_i^{(p)} &= \mu_{0i}^{(p)} + a_{ij}^{(p)}T_{jk}\mu_{0k}^{(q)} + a_{ij}^{(p)}T_{jk}a_{kl}^{(q)}T_{lm}\mu_{0m}^{(p)} + a_{ij}^{(p)}T_{jk}a_{kl}^{(q)}T_{lm}a_{mn}^{(p)}T_{np}\mu_{0p}^{(q)} \\
&\quad + a_{ij}^{(p)}T_{jk}a_{kl}^{(q)}T_{lm}a_{mn}^{(p)}T_{np}a_{pq}^{(q)}T_{pr}\mu_{0r}^{(p)} + \cdots \\
&\quad + \tfrac{1}{3}A_{ijk}^{(p)}T_{jkl}^{(p)}\mu_{0l}^{(q)} + \tfrac{1}{3}a_{ij}^{(p)}T_{jk}A_{klm}^{(q)}T_{lmn}^{(q)}\mu_{0n}^{(p)} - \tfrac{1}{3}a_{ij}^{(p)}T_{jkl}^{(p)}A_{mkl}^{(q)}T_{mn}\mu_{0n}^{(p)} \\
&\quad + \tfrac{1}{3}A_{ijk}^{(p)}T_{jkl}^{(p)}a_{lm}^{(q)}T_{mn}\mu_{0n}^{(p)} + \cdots \\
&\quad - \tfrac{1}{3}a_{ij}^{(p)}T_{jkl}^{(p)}\theta_{kl}^{(q)} - \tfrac{1}{3}a_{ij}^{(p)}T_{jk}a_{kl}^{(q)}T_{lmn}^{(q)}\theta_{mn}^{(p)} + \cdots - \tfrac{1}{9}A_{ijk}^{(p)}T_{jklm}\theta_{lm}^{(q)} + \cdots \\
&\quad + a_{ij}^{(p)}E_j + a_{ik}^{(p)}T_{kl}a_{lj}^{(q)}E_j + a_{ik}^{(p)}T_{kl}a_{lm}^{(q)}T_{mn}a_{nj}^{(p)}E_j \\
&\quad + a_{ik}^{(p)}T_{kl}a_{lm}^{(q)}T_{mn}a_{np}^{(p)}T_{pq}a_{qj}^{(q)}E_j + a_{ik}^{(p)}T_{kl}a_{lm}^{(q)}T_{mn}a_{np}^{(p)}T_{pq}a_{qr}^{(q)}T_{rs}a_{sj}^{(p)}E_j + \cdots \\
&\quad - \tfrac{1}{3}a_{ik}^{(p)}T_{klm}^{(p)}A_{jlm}^{(q)}E_j + \tfrac{1}{3}A_{ikl}^{(p)}T_{klm}^{(p)}a_{mj}^{(q)}E_j - \tfrac{1}{3}a_{ik}^{(p)}T_{kl}a_{lm}^{(q)}T_{mnp}^{(q)}A_{jnp}^{(p)}E_j \\
&\quad + \tfrac{1}{3}a_{ik}^{(p)}T_{kl}A_{lmn}^{(q)}T_{mnp}^{(q)}a_{pj}^{(p)}E_j - \tfrac{1}{3}a_{ik}^{(p)}T_{klm}^{(p)}A_{nlm}^{(q)}T_{np}a_{pj}^{(p)}E_j \\
&\quad + \tfrac{1}{3}A_{ikl}^{(p)}T_{klm}^{(p)}a_{mn}^{(q)}T_{np}a_{pj}^{(p)}E_j + \cdots - \tfrac{1}{9}A_{ikl}^{(p)}T_{klmn}A_{jmn}^{(q)}E_j + \cdots + O(E^2) + \cdots.
\end{aligned}$$ (6.62)

Therefore, from equations (6.44) and (6.62), the potential energy at molecule p in the presence of the external field and molecule q, is:

$$\begin{aligned}
U^{(p)}(\tau, E) &= -\Big(\mu_{0i}^{(p)} + a_{ij}^{(p)}T_{jk}\mu_{0k}^{(q)} + a_{ij}^{(p)}T_{jk}a_{kl}^{(q)}T_{lm}\mu_{0m}^{(p)} + a_{ij}^{(p)}T_{jk}a_{kl}^{(q)}T_{lm}a_{mn}^{(p)}T_{np}\mu_{0p}^{(q)} \\
&\quad + a_{ij}^{(p)}T_{jk}a_{kl}^{(q)}T_{lm}a_{mn}^{(p)}T_{np}a_{pq}^{(q)}T_{pr}\mu_{0r}^{(p)} + \cdots \\
&\quad + \tfrac{1}{3}A_{ijk}^{(p)}T_{jkl}^{(p)}\mu_{0l}^{(q)} + \tfrac{1}{3}a_{ij}^{(p)}T_{jk}A_{klm}^{(q)}T_{lmn}^{(q)}\mu_{0n}^{(p)} - \tfrac{1}{3}a_{ij}^{(p)}T_{jkl}^{(p)}A_{mkl}^{(q)}T_{mn}\mu_{0n}^{(p)}
\end{aligned}$$

$$+ \tfrac{1}{3} A_{ijk}^{(p)} T_{jkl}^{(p)} a_{lm}^{(q)} T_{mn} \mu_{0n}^{(p)} + \cdots$$

$$- \tfrac{1}{3} a_{ij}^{(p)} T_{jkl}^{(p)} \theta_{kl}^{(q)} \quad - \tfrac{1}{3} a_{ij}^{(p)} T_{jk} a_{kl}^{(q)} T_{lmn}^{(q)} \theta_{mn}^{(p)} + \cdots - \tfrac{1}{9} A_{ijk}^{(p)} T_{jklm} \theta_{lm}^{(q)} + \cdots \Bigg) E \mathrm{a}_i^x$$

$$- \tfrac{1}{2} \left(a_{ij}^{(p)} + a_{ik}^{(p)} T_{kl} a_{lj}^{(q)} + a_{ik}^{(p)} T_{kl} a_{lm}^{(q)} T_{mn} a_{nj}^{(p)} \right.$$

$$+ a_{ik}^{(p)} T_{kl} a_{lm}^{(q)} T_{mn} a_{np}^{(p)} T_{pq} a_{qj}^{(q)} + a_{ik}^{(p)} T_{kl} a_{lm}^{(q)} T_{mn} a_{np}^{(p)} T_{pq} a_{qr}^{(q)} T_{rs} a_{sj}^{(p)} + \cdots$$

$$- \tfrac{1}{3} a_{ik}^{(p)} T_{klm}^{(p)} A_{jlm}^{(q)} + \tfrac{1}{3} A_{ikl}^{(p)} T_{klm}^{(p)} a_{mj}^{(q)} - \tfrac{1}{3} a_{ik}^{(p)} T_{kl} a_{lm}^{(q)} T_{mnp}^{(q)} A_{jnp}^{(p)}$$

$$+ \tfrac{1}{3} a_{ik}^{(p)} T_{kl} A_{lmn}^{(q)} T_{mnp}^{(q)} a_{pj}^{(p)} - \tfrac{1}{3} a_{ik}^{(p)} T_{klm}^{(p)} A_{nlm}^{(q)} T_{np} a_{pj}^{(p)}$$

$$+ \tfrac{1}{3} A_{ikl}^{(p)} T_{klm}^{(p)} a_{mn}^{(q)} T_{np} a_{pj}^{(p)} + \cdots \; - \tfrac{1}{9} A_{ikl}^{(p)} T_{klmn} A_{jmn}^{(q)} + \cdots \Bigg) E^2 \mathrm{a}_i^x \mathrm{a}_j^x. \qquad (6.63)$$

Differentiating this equation with respect to E and then setting E to zero, yields the following expressions:

$$\left(\frac{\partial U^{(p)}}{\partial E} \right)_{E=0} = - \left(\mu_{0i}^{(p)} + a_{ij}^{(p)} T_{jk} \mu_{0k}^{(q)} + a_{ij}^{(p)} T_{jk} a_{kl}^{(q)} T_{lm} \mu_{0m}^{(p)} + a_{ij}^{(p)} T_{jk} a_{kl}^{(q)} T_{lm} a_{mn}^{(p)} T_{np} \mu_{0p}^{(q)} \right.$$

$$+ a_{ij}^{(p)} T_{jk} a_{kl}^{(q)} T_{lm} a_{mn}^{(p)} T_{np} a_{pq}^{(q)} T_{pr} \mu_{0r}^{(p)} + \cdots + \tfrac{1}{3} A_{ijk}^{(p)} T_{jkl}^{(p)} \mu_{0l}^{(q)}$$

$$+ \tfrac{1}{3} a_{ij}^{(p)} T_{jk} A_{klm}^{(q)} T_{lmn}^{(q)} \mu_{0n}^{(p)} - \tfrac{1}{3} a_{ij}^{(p)} T_{jkl}^{(p)} A_{mkl}^{(q)} T_{mn} \mu_{0n}^{(p)}$$

$$+ \tfrac{1}{3} A_{ijk}^{(p)} T_{jkl}^{(p)} a_{lm}^{(q)} T_{mn} \mu_{0n}^{(p)} + \cdots - \tfrac{1}{3} a_{ij}^{(p)} T_{jkl}^{(p)} \theta_{kl}^{(q)}$$

$$- \tfrac{1}{3} a_{ij}^{(p)} T_{jk} a_{kl}^{(q)} T_{lmn}^{(q)} \theta_{mn}^{(p)} + \cdots - \tfrac{1}{9} A_{ijk}^{(p)} T_{jklm} \theta_{lm}^{(q)} + \cdots \Bigg) \mathrm{a}_i^x, \qquad (6.64)$$

$$\left(\frac{\partial^2 U^{(p)}}{\partial E^2} \right)_{E=0} = - \left(a_{ij}^{(p)} + a_{ik}^{(p)} T_{kl} a_{lj}^{(q)} + a_{ik}^{(p)} T_{kl} a_{lm}^{(q)} T_{mn} a_{nj}^{(p)} \right.$$

$$+ a_{ik}^{(p)} T_{kl} a_{lm}^{(q)} T_{mn} a_{np}^{(p)} T_{pq} a_{qj}^{(q)} + a_{ik}^{(p)} T_{kl} a_{lm}^{(q)} T_{mn} a_{np}^{(p)} T_{pq} a_{qr}^{(q)} T_{rs} a_{sj}^{(p)} + \cdots$$

$$- \tfrac{1}{3} a_{ik}^{(p)} T_{klm}^{(p)} A_{jlm}^{(q)} + \tfrac{1}{3} A_{ikl}^{(p)} T_{klm}^{(p)} a_{mj}^{(q)} - \tfrac{1}{3} a_{ik}^{(p)} T_{kl} a_{lm}^{(q)} T_{mnp}^{(q)} A_{jnp}^{(p)}$$

$$+ \tfrac{1}{3} a_{ik}^{(p)} T_{kl} A_{lmn}^{(q)} T_{mnp}^{(q)} a_{pj}^{(p)} - \tfrac{1}{3} a_{ik}^{(p)} T_{klm}^{(p)} A_{nlm}^{(q)} T_{np} a_{pj}^{(p)}$$

$$+ \tfrac{1}{3} A_{ikl}^{(p)} T_{klm}^{(p)} a_{mn}^{(q)} T_{np} a_{pj}^{(p)} + \cdots \; - \tfrac{1}{9} A_{ikl}^{(p)} T_{klmn} A_{jmn}^{(q)} + \cdots \Bigg) \mathrm{a}_i^x \mathrm{a}_j^x. \qquad (6.65)$$

6.3.3 General expression for B_K

Substituting equations (6.55) to (6.57), (6.64) and (6.65), into equation (6.45), and subtracting (6.24), yields the following expression for the integrand in (6.36):

$$\left\{ \frac{1}{2} \left(\frac{\partial^2 \overline{\pi^{(12)}(\tau, E)}}{\partial E^2} \right)_{E=0} - \left(\frac{\partial^2 \bar{\pi}}{\partial E^2} \right)_{E=0} \right\} = \alpha_2 + \alpha_3 + \alpha_4 + \alpha_5 + \alpha_6 + \cdots$$

$$+ \mathcal{A}_1 \alpha_2 + \mathcal{A}_1 \alpha_3 + \cdots + \gamma_1 \alpha_1 + \gamma_1 \alpha_2 + \cdots$$

$$+ \mu_2 \alpha_1 + \mu_2 \alpha_2 + \mu_2 \alpha_3 + \mu_2 \alpha_4 + \cdots$$

$$+ \mu_2 \mathcal{A}_1 \alpha_1 + \mu_2 \mathcal{A}_1 \alpha_2 + \cdots$$

$$+ \mu_1 \beta_1 + \mu_1 \beta_1 \alpha_1 + \cdots + \mu_1 \beta_1 \mathcal{A}_1 + \cdots$$

$$+ \mu_1 \theta_1 \alpha_2 + \mu_1 \theta_1 \alpha_3 + \cdots + \mu_1 \theta_1 \mathcal{A}_1 \alpha_1 + \cdots$$

$$+ \theta_2 \alpha_3 + \theta_2 \alpha_4 + \theta_2 \alpha_5 + \cdots + \theta_1 \beta_1 \alpha_1 + \cdots,$$

$$(6.66)$$

where

$$\alpha_2 = \frac{1}{kT} \left\{ \alpha_{ab}^{(1)} a_{pq}^{(2)} \right\} \left\langle \mathrm{a}_a^x \mathrm{a}_b^x \mathrm{a}_p^x \mathrm{a}_q^x - \mathrm{a}_a^y \mathrm{a}_b^y \mathrm{a}_p^x \mathrm{a}_q^x \right\rangle, \tag{6.67}$$

$$\alpha_3 = \frac{1}{kT} \left\{ \alpha_{ad}^{(1)} a_{pq}^{(1)} T_{qr} a_{rs}^{(2)} + \alpha_{ad}^{(1)} a_{pq}^{(2)} T_{qr} a_{rs}^{(1)} + \alpha_{ab}^{(1)} T_{bc} \alpha_{cd}^{(2)} a_{ps}^{(1)} + \alpha_{ab}^{(1)} T_{bc} \alpha_{cd}^{(2)} a_{ps}^{(1)} \right\}$$

$$\times \left\langle \mathrm{a}_a^x \mathrm{a}_d^x \mathrm{a}_p^x \mathrm{a}_s^x - \mathrm{a}_a^y \mathrm{a}_d^y \mathrm{a}_p^x \mathrm{a}_s^x \right\rangle, \tag{6.68}$$

$$\alpha_4 = \frac{1}{kT} \left\{ \alpha_{af}^{(1)} a_{pq}^{(1)} T_{qr} a_{rs}^{(2)} T_{st} a_{tu}^{(1)} + \alpha_{af}^{(1)} a_{pq}^{(2)} T_{qr} a_{rs}^{(1)} T_{st} a_{tu}^{(2)} + \alpha_{ab}^{(1)} T_{bc} \alpha_{cf}^{(2)} a_{pq}^{(1)} T_{qr} a_{ru}^{(2)} \right.$$

$$\left. + \alpha_{ab}^{(1)} T_{bc} \alpha_{cf}^{(2)} a_{pq}^{(2)} T_{qr} a_{ru}^{(1)} + \alpha_{ab}^{(1)} T_{bc} \alpha_{cd}^{(2)} T_{de} \alpha_{ef}^{(1)} a_{pu}^{(1)} + \alpha_{ab}^{(1)} T_{bc} \alpha_{cd}^{(2)} T_{de} \alpha_{ef}^{(1)} a_{pu}^{(2)} \right\}$$

$$\times \left\langle \mathrm{a}_a^x \mathrm{a}_f^x \mathrm{a}_p^x \mathrm{a}_u^x - \mathrm{a}_a^y \mathrm{a}_f^y \mathrm{a}_p^x \mathrm{a}_u^x \right\rangle, \tag{6.69}$$

$$\alpha_5 = \frac{1}{kT} \left\{ \alpha_{ah}^{(1)} a_{pq}^{(1)} T_{qr} a_{rs}^{(2)} T_{st} a_{tu}^{(1)} T_{uv} a_{vw}^{(2)} + \alpha_{ah}^{(1)} a_{pq}^{(2)} T_{qr} a_{rs}^{(1)} T_{st} a_{tu}^{(2)} T_{uv} a_{vw}^{(1)} \right.$$

$$+ \alpha_{ab}^{(1)} T_{bc} \alpha_{ch}^{(2)} a_{pq}^{(1)} T_{qr} a_{rs}^{(2)} T_{st} a_{tw}^{(1)} + \alpha_{ab}^{(1)} T_{bc} \alpha_{ch}^{(2)} a_{pq}^{(2)} T_{qr} a_{rs}^{(1)} T_{st} a_{tw}^{(2)}$$

$$+ \alpha_{ab}^{(1)} T_{bc} \alpha_{cd}^{(2)} T_{de} \alpha_{eh}^{(1)} a_{pq}^{(1)} T_{qr} a_{rw}^{(2)} + \alpha_{ab}^{(1)} T_{bc} \alpha_{cd}^{(2)} T_{de} \alpha_{eh}^{(1)} a_{pq}^{(2)} T_{qr} a_{rw}^{(1)}$$

$$+ \alpha_{ab}^{(1)} T_{bc} \alpha_{cd}^{(2)} T_{de} \alpha_{ef}^{(1)} T_{fg} \alpha_{gh}^{(2)} a_{pw}^{(1)} + \alpha_{ab}^{(1)} T_{bc} \alpha_{cd}^{(2)} T_{de} \alpha_{ef}^{(1)} T_{fg} \alpha_{gh}^{(2)} a_{pw}^{(2)} \Big\}$$

$$\times \left\langle \mathrm{a}_a^x \mathrm{a}_h^x \mathrm{a}_p^x \mathrm{a}_w^x - \mathrm{a}_a^y \mathrm{a}_h^y \mathrm{a}_p^x \mathrm{a}_w^x \right\rangle, \tag{6.70}$$

$$\mathcal{A}_1 \alpha_2 = \frac{1}{3kT} \Big\{ -\alpha_{ae}^{(1)} a_{pq}^{(1)} T_{qrs} A_{trs}^{(2)} + \alpha_{ae}^{(1)} a_{pq}^{(2)} T_{qrs} A_{trs}^{(1)} + \alpha_{ae}^{(1)} A_{pqr}^{(1)} T_{qrs} a_{st}^{(2)} - \alpha_{ae}^{(1)} A_{pqr}^{(2)} T_{qrs} a_{st}^{(1)}$$

$$- \alpha_{ab}^{(1)} T_{bcd} A_{ecd}^{(2)} a_{pt}^{(1)} + \alpha_{ab}^{(1)} T_{bcd} A_{ecd}^{(2)} a_{pt}^{(2)} + A_{abc}^{(1)} T_{bcd} \alpha_{de}^{(2)} a_{pt}^{(1)} + A_{abc}^{(1)} T_{bcd} \alpha_{de}^{(2)} a_{pt}^{(2)} \Big\}$$

$$\times \left\langle \mathrm{a}_a^x \mathrm{a}_e^x \mathrm{a}_p^x \mathrm{a}_t^x - \mathrm{a}_a^y \mathrm{a}_e^y \mathrm{a}_p^x \mathrm{a}_t^x \right\rangle, \tag{6.71}$$

$$\gamma_1 \alpha_1 = \Big\{ \gamma_{abcd}^{(1)} T_{be} \alpha_{ef}^{(2)} + \alpha_{ab}^{(1)} T_{be} \gamma_{efcd}^{(2)} \Big\} \left\langle \mathrm{a}_a^x \mathrm{a}_f^x \mathrm{a}_c^x \mathrm{a}_d^x - \mathrm{a}_a^y \mathrm{a}_f^y \mathrm{a}_c^x \mathrm{a}_d^x \right\rangle, \tag{6.72}$$

$$\gamma_1 \alpha_2 = \Big\{ \gamma_{abcd}^{(1)} T_{be} \alpha_{ef}^{(2)} T_{fg} \alpha_{gh}^{(1)} + \alpha_{ab}^{(1)} T_{be} \gamma_{efcd}^{(2)} T_{fg} \alpha_{gh}^{(1)} + \alpha_{ab}^{(1)} T_{be} \alpha_{ef}^{(2)} T_{fg} \gamma_{ghcd}^{(1)} \Big\}$$

$$\times \left\langle \mathrm{a}_a^x \mathrm{a}_h^x \mathrm{a}_c^x \mathrm{a}_d^x - \mathrm{a}_a^y \mathrm{a}_h^y \mathrm{a}_c^x \mathrm{a}_d^x \right\rangle, \tag{6.73}$$

$$\mu_2 \alpha_1 = \frac{1}{(kT)^2} \Big\{ \alpha_{ab}^{(1)} \mu_{0i}^{(2)} \mu_{0p}^{(2)} + 2\alpha_{ab}^{(1)} \mu_{0i}^{(1)} \mu_{0p}^{(2)} \Big\} \left\langle \mathrm{a}_a^x \mathrm{a}_b^x \mathrm{a}_i^x \mathrm{a}_p^x - \mathrm{a}_a^y \mathrm{a}_b^y \mathrm{a}_i^x \mathrm{a}_p^x \right\rangle, \tag{6.74}$$

$$\mu_2 \alpha_2 = \frac{1}{(kT)^2} \Big\{ 2\alpha_{ad}^{(1)} \mu_{0i}^{(1)} a_{pq}^{(1)} T_{qr} \mu_{0r}^{(2)} + 2\alpha_{ad}^{(1)} \mu_{0i}^{(2)} a_{pq}^{(2)} T_{qr} \mu_{0r}^{(1)} + 2\alpha_{ad}^{(1)} \mu_{0i}^{(1)} a_{pq}^{(2)} T_{qr} \mu_{0r}^{(1)}$$

$$+ 2\alpha_{ad}^{(1)} \mu_{0i}^{(2)} a_{pq}^{(1)} T_{qr} \mu_{0r}^{(2)} + \alpha_{ab}^{(1)} T_{bc} \alpha_{cd}^{(2)} \mu_{0i}^{(1)} \mu_{0p}^{(1)} + \alpha_{ab}^{(1)} T_{bc} \alpha_{cd}^{(2)} \mu_{0i}^{(2)} \mu_{0p}^{(2)}$$

$$+ 2\alpha_{ab}^{(1)} T_{bc} \alpha_{cd}^{(2)} \mu_{0i}^{(1)} \mu_{0p}^{(2)} \Big\} \left\langle \mathrm{a}_a^x \mathrm{a}_d^x \mathrm{a}_i^x \mathrm{a}_p^x - \mathrm{a}_a^y \mathrm{a}_d^y \mathrm{a}_i^x \mathrm{a}_p^x \right\rangle, \tag{6.75}$$

$$\mu_2 \alpha_3 = \frac{1}{(kT)^2} \Big\{ \alpha_{af}^{(1)} a_{ij}^{(1)} T_{jk} \mu_{0k}^{(2)} a_{pq}^{(1)} T_{qr} \mu_{0r}^{(2)} + \alpha_{af}^{(1)} a_{ij}^{(2)} T_{jk} \mu_{0k}^{(1)} a_{pq}^{(2)} T_{qr} \mu_{0r}^{(1)}$$

$$+ 2\alpha_{af}^{(1)} a_{ij}^{(1)} T_{jk} \mu_{0k}^{(2)} a_{pq}^{(2)} T_{qr} \mu_{0r}^{(1)} + 2\alpha_{af}^{(1)} \mu_{0i}^{(1)} a_{pq}^{(1)} T_{qr} a_{rs}^{(2)} T_{st} \mu_{0t}^{(1)}$$

$$+ 2\alpha_{af}^{(1)} \mu_{0i}^{(2)} a_{pq}^{(2)} T_{qr} a_{rs}^{(1)} T_{st} \mu_{0t}^{(2)} + 2\alpha_{af}^{(1)} \mu_{0i}^{(1)} a_{pq}^{(2)} T_{qr} a_{rs}^{(1)} T_{st} \mu_{0t}^{(2)}$$

$$+ 2\alpha_{af}^{(1)} \mu_{0i}^{(2)} a_{pq}^{(1)} T_{qr} a_{rs}^{(2)} T_{st} \mu_{0t}^{(1)} + 2\alpha_{ab}^{(1)} T_{bc} \alpha_{cf}^{(2)} \mu_{0i}^{(1)} a_{pq}^{(1)} T_{qr} \mu_{0r}^{(2)}$$

$$+ 2\alpha_{ab}^{(1)} T_{bc} \alpha_{cf}^{(2)} \mu_{0i}^{(2)} a_{pq}^{(2)} T_{qr} \mu_{0r}^{(1)} + 2\alpha_{ab}^{(1)} T_{bc} \alpha_{cf}^{(2)} \mu_{0i}^{(1)} a_{pq}^{(2)} T_{qr} \mu_{0r}^{(1)}$$

$$+ 2\alpha_{ab}^{(1)} T_{bc} \alpha_{cf}^{(2)} \mu_{0i}^{(2)} a_{pq}^{(1)} T_{qr} \mu_{0r}^{(2)} + \alpha_{ab}^{(1)} T_{bc} \alpha_{cd}^{(2)} T_{de} \alpha_{ef}^{(1)} \mu_{0i}^{(1)} \mu_{0p}^{(1)}$$

$$+ \alpha_{ab}^{(1)} T_{bc} \alpha_{cd}^{(2)} T_{de} \alpha_{ef}^{(1)} \mu_{0i}^{(2)} \mu_{0p}^{(2)} + 2\alpha_{ab}^{(1)} T_{bc} \alpha_{cd}^{(2)} T_{de} \alpha_{ef}^{(1)} \mu_{0i}^{(1)} \mu_{0p}^{(2)} \Big\}$$

$$\times \left\langle \mathrm{a}_a^x \mathrm{a}_f^x \mathrm{a}_i^x \mathrm{a}_p^x - \mathrm{a}_a^y \mathrm{a}_f^y \mathrm{a}_i^x \mathrm{a}_p^x \right\rangle, \tag{6.76}$$

$$\mu_2\alpha_4 = \frac{1}{(kT)^2}\left\{2\alpha_{ah}^{(1)}\mu_{0i}^{(1)}a_{pq}^{(1)}T_{qr}a_{rs}^{(2)}T_{st}a_{tu}^{(1)}T_{uv}\mu_{0v}^{(2)} + 2\alpha_{ah}^{(1)}\mu_{0i}^{(2)}a_{pq}^{(2)}T_{qr}a_{rs}^{(1)}T_{st}a_{tu}^{(2)}T_{uv}\mu_{0v}^{(1)}\right.$$

$$+ 2\alpha_{ah}^{(1)}\mu_{0i}^{(1)}a_{pq}^{(2)}T_{qr}a_{rs}^{(1)}T_{st}a_{tu}^{(2)}T_{uv}\mu_{0v}^{(1)} + 2\alpha_{ah}^{(1)}\mu_{0i}^{(2)}a_{pq}^{(1)}T_{qr}a_{rs}^{(2)}T_{st}a_{tu}^{(1)}T_{uv}\mu_{0v}^{(2)}$$

$$+ 2\alpha_{ah}^{(1)}a_{ij}^{(1)}T_{jk}\mu_{0k}^{(2)}a_{pq}^{(1)}T_{qr}a_{rs}^{(2)}T_{st}\mu_{0t}^{(1)} + 2\alpha_{ah}^{(1)}a_{ij}^{(2)}T_{jk}\mu_{0k}^{(1)}a_{pq}^{(2)}T_{qr}a_{rs}^{(1)}T_{st}\mu_{0t}^{(2)}$$

$$+ 2\alpha_{ah}^{(1)}a_{ij}^{(1)}T_{jk}\mu_{0k}^{(2)}a_{pq}^{(2)}T_{qr}a_{rs}^{(1)}T_{st}\mu_{0t}^{(2)} + 2\alpha_{ah}^{(1)}a_{ij}^{(2)}T_{jk}\mu_{0k}^{(1)}a_{pq}^{(1)}T_{qr}a_{rs}^{(2)}T_{st}\mu_{0t}^{(1)}$$

$$+ 2\alpha_{ab}^{(1)}T_{bc}\alpha_{ch}^{(2)}\mu_{0i}^{(1)}a_{pq}^{(1)}T_{qr}a_{rs}^{(2)}T_{st}\mu_{0t}^{(1)} + 2\alpha_{ab}^{(1)}T_{bc}\alpha_{ch}^{(2)}\mu_{0i}^{(2)}a_{pq}^{(2)}T_{qr}a_{rs}^{(1)}T_{st}\mu_{0t}^{(2)}$$

$$+ 2\alpha_{ab}^{(1)}T_{bc}\alpha_{ch}^{(2)}\mu_{0i}^{(1)}a_{pq}^{(2)}T_{qr}a_{rs}^{(1)}T_{st}\mu_{0t}^{(2)} + 2\alpha_{ab}^{(1)}T_{bc}\alpha_{ch}^{(2)}\mu_{0i}^{(2)}a_{pq}^{(1)}T_{qr}a_{rs}^{(2)}T_{st}\mu_{0t}^{(1)}$$

$$+ \alpha_{ab}^{(1)}T_{bc}\alpha_{ch}^{(2)}a_{ij}^{(1)}T_{jk}\mu_{0k}^{(2)}a_{pq}^{(1)}T_{qr}\mu_{0r}^{(2)} + \alpha_{ab}^{(1)}T_{bc}\alpha_{ch}^{(2)}a_{ij}^{(2)}T_{jk}\mu_{0k}^{(1)}a_{pq}^{(2)}T_{qr}\mu_{0r}^{(1)}$$

$$+ 2\alpha_{ab}^{(1)}T_{bc}\alpha_{ch}^{(2)}a_{ij}^{(1)}T_{jk}\mu_{0k}^{(2)}a_{pq}^{(2)}T_{qr}\mu_{0r}^{(1)} + 2\alpha_{ab}^{(1)}T_{bc}\alpha_{cd}^{(2)}T_{de}\alpha_{eh}^{(1)}\mu_{0i}^{(1)}a_{pq}^{(2)}T_{qr}\mu_{0r}^{(2)}$$

$$+ 2\alpha_{ab}^{(1)}T_{bc}\alpha_{cd}^{(2)}T_{de}\alpha_{eh}^{(1)}\mu_{0i}^{(2)}a_{pq}^{(2)}T_{qr}\mu_{0r}^{(1)} + 2\alpha_{ab}^{(1)}T_{bc}\alpha_{cd}^{(2)}T_{de}\alpha_{eh}^{(1)}\mu_{0i}^{(1)}a_{pq}^{(1)}T_{qr}\mu_{0r}^{(2)}$$

$$+ 2\alpha_{ab}^{(1)}T_{bc}\alpha_{cd}^{(2)}T_{de}\alpha_{eh}^{(1)}\mu_{0i}^{(2)}a_{pq}^{(1)}T_{qr}\mu_{0r}^{(2)} + \alpha_{ab}^{(1)}T_{bc}\alpha_{cd}^{(2)}T_{de}\alpha_{ef}^{(1)}T_{fg}\alpha_{gh}^{(2)}\mu_{0i}^{(1)}\mu_{0p}^{(1)}$$

$$\left. + \alpha_{ab}^{(1)}T_{bc}\alpha_{cd}^{(2)}T_{de}\alpha_{ef}^{(1)}T_{fg}\alpha_{gh}^{(2)}\mu_{0i}^{(2)}\mu_{0p}^{(2)} + 2\alpha_{ab}^{(1)}T_{bc}\alpha_{cd}^{(2)}T_{de}\alpha_{ef}^{(1)}T_{fg}\alpha_{gh}^{(2)}\mu_{0i}^{(1)}\mu_{0p}^{(2)}\right\}$$

$$\times \left\langle \mathrm{a}_a^x \mathrm{a}_h^x \mathrm{a}_i^x \mathrm{a}_p^x - \mathrm{a}_a^y \mathrm{a}_h^y \mathrm{a}_i^x \mathrm{a}_p^x \right\rangle, \tag{6.77}$$

$$\mu_2\mathcal{A}_1\alpha_1 = \frac{1}{3(kT)^2}\left\{2\alpha_{ae}^{(1)}\mu_{0i}^{(1)}A_{pqr}^{(1)}T_{qrs}\mu_{0s}^{(2)} - 2\alpha_{ae}^{(1)}\mu_{0i}^{(2)}A_{pqr}^{(2)}T_{qrs}\mu_{0s}^{(1)} - 2\alpha_{ae}^{(1)}\mu_{0i}^{(1)}A_{pqr}^{(2)}T_{qrs}\mu_{0s}^{(1)}\right.$$

$$+ 2\alpha_{ae}^{(1)}\mu_{0i}^{(2)}A_{pqr}^{(1)}T_{qrs}\mu_{0s}^{(2)} - \alpha_{ab}^{(1)}T_{bcd}A_{ecd}^{(2)}\mu_{0i}^{(1)}\mu_{0p}^{(1)} - \alpha_{ab}^{(1)}T_{bcd}A_{ecd}^{(2)}\mu_{0i}^{(2)}\mu_{0p}^{(2)}$$

$$- 2\alpha_{ab}^{(1)}T_{bcd}A_{ecd}^{(2)}\mu_{0i}^{(1)}\mu_{0p}^{(2)} + A_{abc}^{(1)}T_{bcd}\alpha_{de}^{(2)}\mu_{0i}^{(1)}\mu_{0p}^{(1)} + A_{abc}^{(1)}T_{bcd}\alpha_{de}^{(2)}\mu_{0i}^{(2)}\mu_{0p}^{(2)}$$

$$\left. + 2A_{abc}^{(1)}T_{bcd}\alpha_{de}^{(2)}\mu_{0i}^{(1)}\mu_{0p}^{(2)}\right\}\left\langle \mathrm{a}_a^x \mathrm{a}_e^x \mathrm{a}_i^x \mathrm{a}_p^x - \mathrm{a}_a^y \mathrm{a}_e^y \mathrm{a}_i^x \mathrm{a}_p^x \right\rangle, \tag{6.78}$$

$$\mu_2\mathcal{A}_1\alpha_2 = \frac{1}{3(kT)^2}\left\{-2\alpha_{ag}^{(1)}\mu_{0i}^{(1)}a_{pq}^{(1)}T_{qr}A_{rst}^{(2)}T_{stu}\mu_{0u}^{(1)} + 2\alpha_{ag}^{(1)}\mu_{0i}^{(2)}a_{pq}^{(2)}T_{qr}A_{rst}^{(1)}T_{stu}\mu_{0u}^{(2)}\right.$$

$$+ 2\alpha_{ag}^{(1)}\mu_{0i}^{(1)}a_{pq}^{(2)}T_{qr}A_{rst}^{(1)}T_{stu}\mu_{0u}^{(2)} - 2\alpha_{ag}^{(1)}\mu_{0i}^{(2)}a_{pq}^{(1)}T_{qr}A_{rst}^{(2)}T_{stu}\mu_{0u}^{(1)}$$

$$- 2\alpha_{ag}^{(1)}\mu_{0i}^{(1)}a_{pq}^{(1)}T_{qrs}A_{trs}^{(2)}T_{tu}\mu_{0u}^{(1)} + 2\alpha_{ag}^{(1)}\mu_{0i}^{(2)}a_{pq}^{(2)}T_{qrs}A_{trs}^{(1)}T_{tu}\mu_{0u}^{(2)}$$

$$+ 2\alpha_{ag}^{(1)}\mu_{0i}^{(1)}a_{pq}^{(2)}T_{qrs}A_{trs}^{(1)}T_{tu}\mu_{0u}^{(2)} - 2\alpha_{ag}^{(1)}\mu_{0i}^{(2)}a_{pq}^{(1)}T_{qrs}A_{trs}^{(2)}T_{tu}\mu_{0u}^{(1)}$$

$$+ 2\alpha_{ag}^{(1)}\mu_{0i}^{(1)}A_{pqr}^{(1)}T_{qrs}a_{st}^{(2)}T_{tu}\mu_{0u}^{(1)} - 2\alpha_{ag}^{(1)}\mu_{0i}^{(2)}A_{pqr}^{(2)}T_{qrs}a_{st}^{(1)}T_{tu}\mu_{0u}^{(2)}$$

$$- 2\alpha_{ag}^{(1)}\mu_{0i}^{(1)}A_{pqr}^{(2)}T_{qrs}a_{st}^{(1)}T_{tu}\mu_{0u}^{(2)} + 2\alpha_{ag}^{(1)}\mu_{0i}^{(2)}A_{pqr}^{(1)}T_{qrs}a_{st}^{(2)}T_{tu}\mu_{0u}^{(1)}.$$

$$+ 2\alpha_{ag}^{(1)}a_{ij}^{(1)}T_{jk}\mu_{0k}^{(2)}A_{pqr}^{(1)}T_{qrs}\mu_{0s}^{(2)} - 2\alpha_{ag}^{(1)}a_{ij}^{(2)}T_{jk}\mu_{0k}^{(1)}A_{pqr}^{(2)}T_{qrs}\mu_{0s}^{(1)}$$

$$- 2\alpha_{ag}^{(1)}a_{ij}^{(1)}T_{jk}\mu_{0k}^{(2)}A_{pqr}^{(2)}T_{qrs}\mu_{0s}^{(1)} + 2\alpha_{ag}^{(1)}a_{ij}^{(2)}T_{jk}\mu_{0k}^{(1)}A_{pqr}^{(1)}T_{qrs}\mu_{0s}^{(2)}$$

$$+ 2\alpha_{ab}^{(1)}T_{bc}\alpha_{cg}^{(2)}\mu_{0i}^{(1)}A_{pqr}^{(1)}T_{qrs}\mu_{0s}^{(2)} - 2\alpha_{ab}^{(1)}T_{bc}\alpha_{cg}^{(2)}\mu_{0i}^{(2)}A_{pqr}^{(2)}T_{qrs}\mu_{0s}^{(1)}$$

$$- 2\alpha_{ab}^{(1)}T_{bc}\alpha_{cg}^{(2)}\mu_{0i}^{(1)}A_{pqr}^{(2)}T_{qrs}\mu_{0s}^{(1)} + 2\alpha_{ab}^{(1)}T_{bc}\alpha_{cg}^{(2)}\mu_{0i}^{(2)}A_{pqr}^{(1)}T_{qrs}\mu_{0s}^{(2)}$$

$$- 2\alpha_{ab}^{(1)}T_{bcd}A_{gcd}^{(2)}\mu_{0i}^{(1)}a_{pq}^{(1)}T_{qr}\mu_{0r}^{(2)} - 2\alpha_{ab}^{(1)}T_{bcd}A_{gcd}^{(2)}\mu_{0i}^{(2)}a_{pq}^{(2)}T_{qr}\mu_{0r}^{(1)}$$

$$- 2\alpha_{ab}^{(1)}T_{bcd}A_{gcd}^{(2)}\mu_{0i}^{(1)}a_{pq}^{(2)}T_{qr}\mu_{0r}^{(1)} - 2\alpha_{ab}^{(1)}T_{bcd}A_{gcd}^{(2)}\mu_{0i}^{(2)}a_{pq}^{(1)}T_{qr}\mu_{0r}^{(2)}$$

$$+ 2A_{abc}^{(1)}T_{bcd}\alpha_{dg}^{(2)}\mu_{0i}^{(1)}a_{pq}^{(1)}T_{qr}\mu_{0r}^{(2)} + 2A_{abc}^{(1)}T_{bcd}\alpha_{dg}^{(2)}\mu_{0i}^{(2)}a_{pq}^{(2)}T_{qr}\mu_{0r}^{(1)}$$

$$+ 2A_{abc}^{(1)}T_{bcd}\alpha_{dg}^{(2)}\mu_{0i}^{(1)}a_{pq}^{(2)}T_{qr}\mu_{0r}^{(1)} + 2A_{abc}^{(1)}T_{bcd}\alpha_{dg}^{(2)}\mu_{0i}^{(2)}a_{pq}^{(1)}T_{qr}\mu_{0r}^{(2)}$$

$$+ \alpha_{ab}^{(1)}T_{bc}\alpha_{cd}^{(2)}T_{def}A_{gef}^{(1)}\mu_{0i}^{(1)}\mu_{0p}^{(1)} + \alpha_{ab}^{(1)}T_{bc}\alpha_{cd}^{(2)}T_{def}A_{gef}^{(1)}\mu_{0i}^{(2)}\mu_{0p}^{(2)}$$

$$+ 2\alpha_{ab}^{(1)}T_{bc}\alpha_{cd}^{(2)}T_{def}A_{gef}^{(1)}\mu_{0i}^{(1)}\mu_{0p}^{(2)} - \alpha_{ab}^{(1)}T_{bc}A_{cde}^{(2)}T_{def}\alpha_{fg}^{(1)}\mu_{0i}^{(1)}\mu_{0p}^{(1)}$$

$$- \alpha_{ab}^{(1)}T_{bc}A_{cde}^{(2)}T_{def}\alpha_{fg}^{(1)}\mu_{0i}^{(2)}\mu_{0p}^{(2)} - 2\alpha_{ab}^{(1)}T_{bc}A_{cde}^{(2)}T_{def}\alpha_{fg}^{(1)}\mu_{0i}^{(1)}\mu_{0p}^{(2)}$$

$$- \alpha_{ab}^{(1)}T_{bcd}A_{ecd}^{(2)}T_{ef}\alpha_{fg}^{(1)}\mu_{0i}^{(1)}\mu_{0p}^{(1)} - \alpha_{ab}^{(1)}T_{bcd}A_{ecd}^{(2)}T_{ef}\alpha_{fg}^{(1)}\mu_{0i}^{(2)}\mu_{0p}^{(2)}$$

$$- 2\alpha_{ab}^{(1)}T_{bcd}A_{ecd}^{(2)}T_{ef}\alpha_{fg}^{(1)}\mu_{0i}^{(1)}\mu_{0p}^{(2)} + A_{abc}^{(1)}T_{bcd}\alpha_{de}^{(2)}T_{ef}\alpha_{fg}^{(1)}\mu_{0i}^{(1)}\mu_{0p}^{(1)}$$

$$+ A_{abc}^{(1)}T_{bcd}\alpha_{de}^{(2)}T_{ef}\alpha_{fg}^{(1)}\mu_{0i}^{(2)}\mu_{0p}^{(2)} + 2\,A_{abc}^{(1)}T_{bcd}\alpha_{de}^{(2)}T_{ef}\alpha_{fg}^{(1)}\mu_{0i}^{(1)}\mu_{0p}^{(2)}\Big\}$$

$$\times \left\langle \mathrm{a}_a^x \mathrm{a}_g^x \mathrm{a}_i^x \mathrm{a}_p^x - \mathrm{a}_a^y \mathrm{a}_h^y \mathrm{a}_i^x \mathrm{a}_p^x \right\rangle, \tag{6.79}$$

$$\mu_1\beta_1 = \frac{2}{kT}\left\{\beta_{abc}^{(1)}\mu_{0p}^{(2)}\right\}\left\langle \mathrm{a}_a^x \mathrm{a}_b^x \mathrm{a}_c^x \mathrm{a}_p^x - \mathrm{a}_a^y \mathrm{a}_b^y \mathrm{a}_c^x \mathrm{a}_p^x \right\rangle, \tag{6.80}$$

$$\mu_1\beta_1\alpha_1 = \frac{2}{kT}\left\{\beta_{abc}^{(1)}a_{pq}^{(1)}T_{qr}\mu_{0r}^{(2)} + \beta_{abc}^{(1)}a_{pq}^{(2)}T_{qr}\mu_{0r}^{(1)} + \alpha_{ad}^{(1)}T_{de}\beta_{ebc}^{(2)}\mu_{0p}^{(1)} + \alpha_{ad}^{(1)}T_{de}\beta_{ebc}^{(2)}\mu_{0p}^{(2)}\right.$$

$$\left. + \beta_{adc}^{(1)}T_{de}\alpha_{eb}^{(2)}\mu_{0p}^{(1)} + \beta_{adc}^{(1)}T_{de}\alpha_{eb}^{(2)}\mu_{0p}^{(2)}\right\}\left\langle \mathrm{a}_a^x \mathrm{a}_b^x \mathrm{a}_c^x \mathrm{a}_p^x - \mathrm{a}_a^y \mathrm{a}_b^y \mathrm{a}_c^x \mathrm{a}_p^x \right\rangle, \tag{6.81}$$

$$\mu_1\theta_1\alpha_2 = \frac{2}{3(kT)^2}\left\{-\alpha_{ab}^{(1)}\mu_{0i}^{(1)}a_{pq}^{(1)}T_{qrs}\theta_{0rs}^{(2)} + \alpha_{ab}^{(1)}\mu_{0i}^{(2)}a_{pq}^{(2)}T_{qrs}\theta_{0rs}^{(1)} + \alpha_{ab}^{(1)}\mu_{0i}^{(1)}a_{pq}^{(2)}T_{qrs}\theta_{0rs}^{(1)}\right.$$

$$\left. - \alpha_{ab}^{(1)}\mu_{0i}^{(2)}a_{pq}^{(1)}T_{qrs}\theta_{0rs}^{(2)}\right\}\left\langle \mathrm{a}_a^x \mathrm{a}_b^x \mathrm{a}_i^x \mathrm{a}_p^x - \mathrm{a}_a^y \mathrm{a}_b^y \mathrm{a}_i^x \mathrm{a}_p^x \right\rangle, \tag{6.82}$$

$$\mu_1\theta_1\alpha_3 = \frac{2}{3(kT)^2}\left\{\alpha_{ab}^{(1)}\mu_{0i}^{(1)}a_{pq}^{(1)}T_{qr}a_{rs}^{(2)}T_{stu}\theta_{0tu}^{(1)} - \alpha_{ab}^{(1)}\mu_{0i}^{(1)}a_{pq}^{(2)}T_{qr}a_{rs}^{(1)}T_{stu}\theta_{0tu}^{(2)}\right.$$

$$+ \alpha_{ab}^{(1)}\mu_{0i}^{(2)}a_{pq}^{(1)}T_{qr}a_{rs}^{(2)}T_{stu}\theta_{0tu}^{(1)} - \alpha_{ab}^{(1)}\mu_{0i}^{(2)}a_{pq}^{(2)}T_{qr}a_{rs}^{(1)}T_{stu}\theta_{0tu}^{(2)}$$

$$- \alpha_{ab}^{(1)}a_{ij}^{(1)}T_{jk}\mu_{0k}^{(2)}a_{pq}^{(1)}T_{qrs}\theta_{0rs}^{(2)} + \alpha_{ab}^{(1)}a_{ij}^{(1)}T_{jk}\mu_{0k}^{(2)}a_{pq}^{(2)}T_{qrs}\theta_{0rs}^{(1)}$$

$$- \alpha_{ab}^{(1)}a_{ij}^{(2)}T_{jk}\mu_{0k}^{(1)}a_{pq}^{(1)}T_{qrs}\theta_{0rs}^{(2)} + \alpha_{ab}^{(1)}a_{ij}^{(2)}T_{jk}\mu_{0k}^{(1)}a_{pq}^{(2)}T_{qrs}\theta_{0rs}^{(1)}$$

$$\left.- 2\alpha_{ac}^{(1)}T_{cd}\alpha_{db}^{(2)}\mu_{0i}^{(1)}a_{pq}^{(1)}T_{qrs}\theta_{0rs}^{(2)} + 2\alpha_{ac}^{(1)}T_{cd}\alpha_{db}^{(2)}\mu_{0i}^{(1)}a_{pq}^{(2)}T_{qrs}\theta_{0rs}^{(1)}\right\}$$

$$\times \left\langle a_a^x a_b^x a_i^x a_p^x - a_a^y a_b^y a_i^x a_p^x\right\rangle, \tag{6.83}$$

$$\mu_1\theta_1\mathcal{A}_1\alpha_1 = \frac{2}{9(kT)^2}\left\{\alpha_{ab}^{(1)}\mu_{0i}^{(1)}A_{pqr}^{(1)}T_{qrst}\theta_{0st}^{(2)} + \alpha_{ab}^{(1)}\mu_{0i}^{(2)}A_{pqr}^{(2)}T_{qrst}\theta_{0st}^{(1)} + \alpha_{ab}^{(1)}\mu_{0i}^{(1)}A_{pqr}^{(2)}T_{qrst}\theta_{0st}^{(1)}\right.$$

$$\left.+ \alpha_{ab}^{(1)}\mu_{0i}^{(2)}A_{pqr}^{(1)}T_{qrst}\theta_{0st}^{(2)}\right\}\left\langle a_a^x a_b^x a_i^x a_p^x - a_a^y a_b^y a_i^x a_p^x\right\rangle, \tag{6.84}$$

$$\theta_2\alpha_3 = \frac{1}{9(kT)^2}\left\{\alpha_{ab}^{(1)}a_{ij}^{(1)}T_{jkl}\theta_{0kl}^{(2)}a_{pq}^{(1)}T_{qrs}\theta_{0rs}^{(2)} + \alpha_{ab}^{(1)}a_{ij}^{(2)}T_{jkl}\theta_{0kl}^{(1)}a_{pq}^{(2)}T_{qrs}\theta_{0rs}^{(1)}\right.$$

$$\left.+ 2\alpha_{ab}^{(1)}a_{ij}^{(1)}T_{jkl}\theta_{0kl}^{(2)}a_{pq}^{(2)}T_{qrs}\theta_{0rs}^{(1)}\right\}\left\langle a_a^x a_b^x a_i^x a_p^x - a_a^y a_b^y a_i^x a_p^x\right\rangle, \tag{6.85}$$

$$\theta_2\alpha_4 = \frac{2}{9(kT)^2}\left\{-\alpha_{ab}^{(1)}a_{ij}^{(1)}T_{jkl}\theta_{0kl}^{(2)}a_{pq}^{(1)}T_{qr}a_{rs}^{(2)}T_{stu}\theta_{0tu}^{(1)} + \alpha_{ab}^{(1)}a_{ij}^{(1)}T_{jkl}\theta_{0kl}^{(2)}a_{pq}^{(2)}T_{qr}a_{rs}^{(1)}T_{stu}\theta_{0tu}^{(2)}\right.$$

$$+ \alpha_{ab}^{(1)}a_{ij}^{(2)}T_{jkl}\theta_{0kl}^{(1)}a_{pq}^{(1)}T_{qr}a_{rs}^{(2)}T_{stu}\theta_{0tu}^{(1)} - \alpha_{ab}^{(1)}a_{ij}^{(2)}T_{jkl}\theta_{0kl}^{(1)}a_{pq}^{(2)}T_{qr}a_{rs}^{(1)}T_{stu}\theta_{0tu}^{(2)}$$

$$\left.+ \alpha_{ac}^{(1)}T_{cd}\alpha_{db}^{(2)}a_{ij}^{(1)}T_{jkl}\theta_{0kl}^{(2)}a_{pq}^{(1)}T_{qrs}\theta_{0rs}^{(2)} - \alpha_{ac}^{(1)}T_{cd}\alpha_{db}^{(2)}a_{ij}^{(1)}T_{jkl}\theta_{0kl}^{(2)}a_{pq}^{(2)}T_{qrs}\theta_{0rs}^{(1)}\right\}$$

$$\times \left\langle a_a^x a_b^x a_i^x a_p^x - a_a^y a_b^y a_i^x a_p^x\right\rangle, \tag{6.86}$$

$$\theta_2\alpha_5 = \frac{1}{9(kT)^2}\left\{2\alpha_{ab}^{(1)}a_{ij}^{(1)}T_{jkl}\theta_{0kl}^{(2)}a_{pq}^{(1)}T_{qr}a_{rs}^{(2)}T_{st}a^{(1)}tuT_{uvw}\theta_{0vw}^{(2)}\right.$$

$$- 2\alpha_{ab}^{(1)}a_{ij}^{(1)}T_{jkl}\theta_{0kl}^{(2)}a_{pq}^{(2)}T_{qr}a_{rs}^{(1)}T_{st}a^{(2)}tuT_{uvw}\theta_{0vw}^{(1)}$$

$$- 2\alpha_{ab}^{(1)}a_{ij}^{(2)}T_{jkl}\theta_{0kl}^{(1)}a_{pq}^{(1)}T_{qr}a_{rs}^{(2)}T_{st}a^{(1)}tuT_{uvw}\theta_{0vw}^{(2)}$$

$$+ 2\alpha_{ab}^{(1)}a_{ij}^{(2)}T_{jkl}\theta_{0kl}^{(1)}a_{pq}^{(2)}T_{qr}a_{rs}^{(1)}T_{st}a^{(2)}tuT_{uvw}\theta_{0vw}^{(1)}$$

$$+ \alpha_{ab}^{(1)}a_{ij}^{(1)}T_{jk}a_{kl}^{(2)}T_{lmn}\theta_{0mn}^{(1)}a_{pq}^{(1)}T_{qr}a_{rs}^{(2)}T_{stu}\theta_{0tu}^{(1)}$$

$$- 2\alpha_{ab}^{(1)}a_{ij}^{(1)}T_{jk}a_{kl}^{(2)}T_{lmn}\theta_{0mn}^{(1)}a_{pq}^{(2)}T_{qr}a_{rs}^{(1)}T_{stu}\theta_{0tu}^{(2)}$$

$$+ \alpha_{ab}^{(1)}a_{ij}^{(2)}T_{jk}a_{kl}^{(1)}T_{lmn}\theta_{0mn}^{(2)}a_{pq}^{(2)}T_{qr}a_{rs}^{(1)}T_{stu}\theta_{0tu}^{(2)}$$

$$- 4\alpha_{ac}^{(1)}T_{cd}\alpha_{db}^{(2)}a_{ij}^{(1)}T_{jkl}\theta_{0kl}^{(2)}a_{pq}^{(1)}T_{qr}a_{rs}^{(2)}T_{stu}\theta_{0tu}^{(1)}$$

$$+ 4\alpha_{ac}^{(1)}T_{cd}\alpha_{db}^{(2)}a_{ij}^{(1)}T_{jkl}\theta_{0kl}^{(2)}a_{pq}^{(2)}T_{qr}a_{rs}^{(1)}T_{stu}\theta_{0tu}^{(2)}$$

$$+ \alpha_{ac}^{(1)}T_{cd}\alpha_{de}^{(2)}T_{ef}\alpha_{fb}^{(1)}a_{ij}^{(1)}T_{jkl}\theta_{0kl}^{(2)}a_{pq}^{(1)}T_{qrs}\theta_{0rs}^{(2)}$$

$$- 2\alpha_{ac}^{(1)}T_{cd}\alpha_{de}^{(2)}T_{ef}\alpha_{fb}^{(1)}a_{ij}^{(1)}T_{jkl}\theta_{0kl}^{(2)}a_{pq}^{(2)}T_{qrs}\theta_{0rs}^{(1)}$$

$$+ \alpha_{ac}^{(1)}T_{cd}\alpha_{de}^{(2)}T_{ef}\alpha_{fb}^{(1)}a_{ij}^{(2)}T_{jkl}\theta_{0kl}^{(1)}a_{pq}^{(2)}T_{qrs}\theta_{0rs}^{(1)}\Big\}$$

$$\times \left\langle \mathrm{a}_a^x \mathrm{a}_b^x \mathrm{a}_i^x \mathrm{a}_p^x - \mathrm{a}_a^y \mathrm{a}_b^y \mathrm{a}_i^x \mathrm{a}_p^x \right\rangle. \tag{6.87}$$

The isotropic averages in equations (6.67) to (6.87) are given by equation (6.20). Thus, for example, the term α_2 in (6.67) becomes:

$$\alpha_2 = \frac{1}{kT} \left\{ \alpha_{ab}^{(1)} a_{pq}^{(2)} \right\} \left\langle \mathrm{a}_a^x \mathrm{a}_b^x \mathrm{a}_p^x \mathrm{a}_q^x - \mathrm{a}_a^y \mathrm{a}_b^y \mathrm{a}_p^x \mathrm{a}_q^x \right\rangle$$

$$= \frac{1}{kT} \left\{ \alpha_{ab}^{(1)} a_{pq}^{(2)} \right\} \tfrac{1}{30} \left(-2\delta_{ab}\delta_{pq} + 3\delta_{ap}\delta_{bq} + 3\delta_{aq}\delta_{bp} \right)$$

$$= \frac{1}{5kT} \left\{ \alpha_{ap}^{(1)} a_{ap}^{(2)} - \alpha a \right\}, \tag{6.88}$$

where $\alpha_{ap}^{(1)}$ is the optical frequency polarizability tensor of molecule 1 referred to the molecule-fixed axes O(1,2,3), $a_{ap}^{(2)}$ is the static polarizability tensor of molecule 2 referred to molecule 1's axes, and α and a are the mean dynamic and static polarizabilities, respectively.

In order to calculate B_K, the exact forms of the tensors in equations (6.67) to (6.87) are required. The specific cases of spherical, linear and non-linear molecules are treated separately.

6.4 B_K for spherical molecules

For spherical or quasi-spherical gases, the second Kerr-effect virial coefficient given in (6.36) becomes:

$$B_K = \frac{8\pi^2 N_A^2}{27\Omega(4\pi\varepsilon_0)} \int_0^\infty \left\{ \frac{1}{2}\left(\frac{\partial^2 \overline{\pi^{(12)}(\tau, E)}}{\partial E^2}\right)_{E=0} - \left(\frac{\partial^2 \bar{\pi}}{\partial E^2}\right)_{E=0} \right\} e^{-\frac{U^{(12)}(R)}{kT}} R^2\, dR, \quad (6.89)$$

where $U^{(12)}(R) = U_{\text{LJ}}$, and the integrand is given by (6.66), the terms of which simplify considerably due to molecular symmetry.

Spherical molecules possess no permanent dipole or quadrupole moments, and A_{ijk} and β_{ijk} are both zero, so that all terms containing these property tensors are zero. The integrand in (6.89) becomes:

$$\left\{ \frac{1}{2}\left(\frac{\partial^2 \overline{\pi^{(12)}(\tau, E)}}{\partial E^2}\right)_{E=0} - \left(\frac{\partial^2 \bar{\pi}}{\partial E^2}\right)_{E=0} \right\} = \alpha_2 + \alpha_3 + \alpha_4 + \alpha_5 + \alpha_6 + \cdots$$

$$+ \gamma_1\alpha_1 + \gamma_1\alpha_2 + \cdots,$$

$$(6.90)$$

where the terms on the right are given by equations (6.67) to (6.70), (6.72) and (6.73). The static and dynamic polarizability tensors have only one independent component each, and are given by:

$$a_{ij} = a\delta_{ij} \qquad \text{and} \qquad \alpha_{ij} = \alpha\delta_{ij}, \quad (6.91)$$

where a and α are the static and dynamic polarizailities, respectively. Thus, both α_2 and α_3 become zero and the leading term is α_4:

$$\alpha_4 = \frac{12\alpha^2 a^2}{5kT(4\pi\varepsilon_0)^2 R^6}. \quad (6.92)$$

The next term is:

$$\alpha_5 = \frac{12(\alpha^2 a^3 + \alpha^3 a^2)}{5kT(4\pi\varepsilon_0)^3 R^9}. \quad (6.93)$$

If one considers only the leading term, then substituting (6.92) into (6.89) yields:

$$B_K = \frac{32\pi^2 \alpha^2 a^2}{45kT(4\pi\varepsilon_0)^3} \int_0^\infty \frac{1}{R^4} e^{-\frac{U_{\text{LJ}}}{kT}}\, dR. \quad (6.94)$$

This is exactly the same expression used by Buckingham and Dunmur [82] in 1968 to calculate the second Kerr-effect virial coefficients for the spherical atomic gases argon, krypton and xenon, and the quasi-spherical molecule sulphur hexafluoride, for comparison with their measured values.

It is useful to note that the second Kerr-effect and light-scattering virial coefficients of atoms and spherical molecules are related by the following expression [178]

$$B_\rho = \frac{27\varepsilon_0 kT}{N_A a^2} B_K. \tag{6.95}$$

If equation (6.94) is used to calculate B_K for atoms and spherical molecules and the results compared with measured values, then the ratio $B_K^{\text{exp}}/B_K^{\text{calc}}$ displays a definite trend. The ratio is less than one for the rare gases and increases above unity as the molecular size increases [9]. Not surprisingly, Watson and Rowell [89] found a similar trend in the ratio of calculated and measured values of the second light scattering virial coefficient of atoms and spherical molecules. They concluded that the point-dipole approximation of the DID model for molecular interactions is inadequate for the large quasi-spherical molecules. However, in 1983, Dunmur *et al.* [88] attributed the inconsistencies between theoretical and experimental values for B_ρ to insufficient allowance for the effects of three-body interactions at higher pressures. They showed that for the atomic gases and methane the DID model for the collision-induced polarizability of pairs of atoms or spherical molecules works well for argon, krypton, xenon and methane, although it appears to be inadequate for sulphur hexafluoride. They suggest that the excessive collision-induced scattering and electric birefringence from sulphur hexafluoride may be a result of contributions from many-body interactions, which have not been determined. This seems quite probable, due to the low vapour pressure of sulphur hexafluoride, which is a very large molecule. It should be noted that the molecules studied in this work are much smaller than sulphur hexafluoride and the measurements of the second virial coefficients are carried out at pressures well below their saturation vapour pressures, so that the number of interactions between three or more molecules should be negligible.

6.5 B_K for linear molecules

For linear molecules, the second Kerr-effect virial coefficient is given by:

$$B_K = \frac{N_A^2}{54\varepsilon_0} \int\limits_{R=0}^{\infty} \int\limits_{\theta_1=0}^{\pi} \int\limits_{\theta_2=0}^{\pi} \int\limits_{\phi=0}^{\pi} \left\{ \frac{1}{2} \left(\frac{\partial^2 \overline{\pi^{(12)}(\tau, E)}}{\partial E^2} \right)_{E=0} - \left(\frac{\partial^2 \bar{\pi}}{\partial E^2} \right)_{E=0} \right\} e^{-\frac{U^{(12)}}{kT}}$$

$$\times R^2 \sin\theta_1 \sin\theta_2 \, dRd\theta_1 d\theta_2 d\phi. \tag{6.96}$$

The terms of the integrand are given by equations (6.67) to (6.87).

In order to determine the explicit forms of these terms, it is necessary to express the molecular property tensors in terms of the angles specifying their relative configuration, τ, as described in Section 2.1.1.

The property tensors of an linear molecule p may be expressed in terms of $\ell_i^{(p)}$, where $\ell_i^{(1)}$ and $\ell_i^{(2)}$ are the unit vectors along the principal axes of molecules 1 and 2, respectively [26].

Expressions for the dipole and quadrupole moment tensors, the static polarizability tensor, the A-tensor and the T-tensors are given in equations (4.77), (4.78), (4.79), (4.83), and equations (4.85) to (4.87) of Section 4.4, respectively. The dynamic polarizability and hyperpolarizability tensors are expressed in the same way:

$$\alpha_{ij}^{(p)} = \alpha\delta_{ij} + \kappa\alpha \left(3\ell_i^{(p)}\ell_j^{(p)} - \delta_{ij} \right), \tag{6.97}$$

where $\alpha = \frac{1}{3}\alpha_{ii}^{(1)} = \frac{1}{3}\alpha_{i'i'}^{(2)}$ and $\kappa = \dfrac{\alpha_{33}^{(1)} - \alpha_{11}^{(1)}}{3\alpha} = \dfrac{\alpha_\parallel - \alpha_\perp}{3\alpha} = \dfrac{\Delta\alpha}{3\alpha}$;

$$\beta_{ijk}^{(p)} = \beta_\perp \left(\ell_i^{(p)}\delta_{jk} + \ell_j^{(p)}\delta_{ki} + \ell_k^{(p)}\delta_{ij} \right) + (\beta_\parallel - 3\beta_\perp) \ell_i^{(p)}\ell_j^{(p)}\ell_k^{(p)}, \tag{6.98}$$

where $\beta_\parallel = \beta_{333}^{(1)} = \beta_{3'3'3'}^{(2)}$ and $\beta_\perp = \beta_{113}^{(1)} = \beta_{131}^{(1)} = \beta_{311}^{(1)} = \beta_{1'1'3'}^{(2)} = \beta_{1'3'1'}^{(2)} = \beta_{3'1'1'}^{(2)}$;

$$\gamma_{iikl}^{(p)} = \left(\gamma_{3311}^{(1)} + \frac{4}{3}\gamma_{1111}^{(1)} \right) \delta_{kl} + \left(\gamma_{3333}^{(1)} + \gamma_{3311}^{(1)} - \frac{4}{3}\gamma_{1111}^{(1)} \right) \ell_k^{(p)}\ell_l^{(p)}. \tag{6.99}$$

Substituting equations (4.77), (4.78), (4.79), (4.83), equations (4.85) to (4.87) and equations (6.97) to (6.99) into equations (6.67) to (6.87) results in terms containing $\ell_i^{(p)}$ and λ_i, which are eliminated using equations (4.92) to (4.94) of Section 4.4. This yields the following expressions for the terms in the integrand of B_K:

$$\alpha_2 = \frac{1}{15kT}\Delta a\Delta\alpha \left(3\cos^2\theta_{12} - 1 \right), \tag{6.100}$$

$$\alpha_3 = \frac{1}{15kT(4\pi\varepsilon_0)R^3}\left\{6a_\perp\Delta\alpha(a_\perp + \Delta a)\left(3\cos^2\theta_1 - 1\right)\right.$$

$$+\Delta a\left(\alpha_\perp(3\alpha_\perp + \Delta\alpha) - 2a_\perp\Delta\alpha\right)\left(3\cos^2\theta_1 + 3\cos^2\theta_2 - 2\right)$$

$$\left.-2\Delta\alpha\Delta a\left(2(\Delta\alpha + \Delta a) + 3(a_\perp + \alpha_\perp)\right)\cos\theta_{12}\left(3\cos\theta_1\cos\theta_2 + \cos\theta_{12}\right)\right\},$$

$$(6.101)$$

$$\alpha_4 = \frac{1}{15kT(4\pi\varepsilon_0)^2R^6}\left\{12\left[3\alpha_\perp a_\perp(\alpha_\perp^2 + \alpha_\perp a_\perp + a_\perp^2) - a_\perp^3(3\alpha_\perp + \Delta\alpha - \alpha_\perp^3(3a_\perp + \Delta a)\right]\right.$$

$$+6\Delta\alpha\Delta a(\alpha_\perp^2 + \alpha_\perp a_\perp + a_\perp^2)\cos\theta_{12}\left(\cos\theta_{12} - 3\cos\theta_1\cos\theta_2\right)$$

$$+\left[\Delta\alpha\Delta a\left(3a_\perp(\alpha_\perp - a_\perp) - 2\alpha_\perp^2 + a_\perp\Delta a(3\cos^2\theta_{12} - 1)\right)\right.$$

$$\left.+3\alpha_\perp\left(2a_\perp(\alpha_\perp\Delta a + a_\perp\Delta\alpha) + \alpha_\perp^2\Delta a\right)\right]\left(3\cos^2\theta_2 + 1\right)$$

$$+\left[\Delta\alpha\left(\Delta a[a_\perp(3a_\perp + 2\Delta a + 9\alpha_\perp) + \alpha_\perp(2\alpha_\perp + \Delta\alpha(1 + 3\cos^2\theta_{12}))]\right.\right.$$

$$\left.\left.+6a_\perp\left[a_\perp(\alpha_\perp + a_\perp) - \alpha_\perp\Delta a\right]\right) + 3\,\alpha_\perp^2\Delta a(2a_\perp + a_\perp)\right]\left(3\cos^2\theta_1 + 1\right)$$

$$+a_\perp\Delta\alpha\Delta a(3a_\perp + \alpha_\perp)\left(3\cos^2\theta_1 - 1\right)^2 + \alpha_\perp\Delta\alpha\Delta a(3\alpha_\perp + a_\perp)\left(3\cos^2\theta_2 - 1\right)^2$$

$$-4\alpha_\perp a_\perp\Delta\alpha\Delta a\left(3\cos^2\theta_1 - 1\right)\left(3\cos^2\theta_2 - 1\right)$$

$$-\Delta\alpha\Delta a\left[\alpha_\perp\Delta a + a_\perp\Delta\alpha + 6a_\perp\Delta a\right]\cos\theta_{12}\left(3\cos^2\theta_1 - 1\right)\left(3\cos\theta_1\cos\theta_2 + \cos\theta_{12}\right)$$

$$-\Delta\alpha\Delta a\left[\alpha_\perp\Delta a + a_\perp\Delta\alpha + 6\alpha_\perp\Delta\alpha\right]\cos\theta_{12}\left(3\cos^2\theta_2 - 1\right)\left(3\cos\theta_1\cos\theta_2 + \cos\theta_{12}\right)$$

$$+\left[6(\alpha_\perp^2\Delta a^2 + a_\perp^2\Delta\alpha^2) + \Delta\alpha\Delta a\left(2\alpha_\perp(\Delta\alpha + 3\Delta a) + 2a_\perp(\Delta a + 3\Delta\alpha)\right.\right.$$

$$\left.\left.+3\left(\alpha_\perp + a_\perp\right)^2 + (\Delta a^2 + \Delta\alpha^2)(1 + 3\cos^2\theta_{12}) + \Delta\alpha\Delta a(3 + \cos^2\theta_{12})\right)\right]$$

$$\left.\times\left(3\cos\theta_1\cos\theta_2 + \cos\theta_{12}\right)^2\right\},$$

$$(6.102)$$

$$\mu_2\alpha_1 = \frac{\mu_0^2\Delta\alpha}{15(kT)^2}\left\{3\cos^2\theta_{12} + 4\cos\theta_{12} - 1\right\},$$

$$(6.103)$$

$$\mu_2\alpha_2 = \frac{\mu_0^2}{15(kT)^2(4\pi\varepsilon_0)R^3}\left\{6a_\perp\Delta\alpha(1 + \cos\theta_{12})\left(3\cos^2\theta_1 - 1\right)\right.$$

$$+\left[3\alpha_\perp^2 + \alpha_\perp\Delta\alpha(1 + \cos\theta_{12}) - 2a_\perp\Delta\alpha\right]\left(3\cos^2\theta_1 + 3\cos^2\theta_2 - 2\right)$$

$$-\left[2\Delta\alpha(a_\perp + \Delta a) + 6\alpha_\perp(\alpha_\perp + \Delta\alpha) + 3\Delta\alpha^2\right.$$

$$+2\Delta\alpha(2(\Delta\alpha + 2\Delta a) + 3(a_\perp + \alpha_\perp))\cos\theta_{12}$$

$$+ \Delta\alpha \left(\Delta\alpha + 6\Delta a\right) \cos^2 \theta_{12} \big] \left(3 \cos\theta_1 \cos\theta_2 + \cos\theta_{12}\right) \Big\}, \tag{6.104}$$

$$\mu_2\alpha_3 = \frac{\mu_0^2}{15(kT)^2(4\pi\varepsilon_0)^2 R^6} \Big\{ -12\alpha_\perp^3 (1 + \cos\theta_{12}) + 6 \big[a_\perp\alpha_\perp\Delta\alpha + \alpha_\perp^2(\alpha_\perp + \Delta\alpha + 2a_\perp)$$

$$+ \Delta\alpha \left(\alpha_\perp^2 + \alpha_\perp a_\perp + a_\perp^2\right) \cos\theta_{12} \big] \left(\cos\theta_{12} - 3 \cos\theta_1 \cos\theta_2\right)$$

$$+ \big[3a_\perp\Delta\alpha(\alpha_\perp - a_\perp) - 2\Delta\alpha(\alpha_\perp^2 + a_\perp\Delta a) + 3\alpha_\perp^2(\alpha_\perp + 2a_\perp)$$

$$+ \Delta\alpha \left(4a_\perp\Delta a - 2\alpha_\perp^2 + 3\alpha_\perp a_\perp\right) \cos\theta_{12} + 6a_\perp\Delta\alpha\Delta a \cos^2\theta_{12} \big] \left(3\cos^2\theta_2 + 1\right)$$

$$+ \big[3\alpha_\perp^2(\alpha_\perp + 2a_\perp) + \alpha_\perp\Delta\alpha(2\alpha_\perp + \Delta\alpha) + 3a_\perp\Delta\alpha(a_\perp + \alpha_\perp) + 4a_\perp\Delta\alpha\Delta a$$

$$+ \Delta\alpha(2\alpha_\perp(\alpha_\perp + 2\Delta\alpha) + a_\perp(6a_\perp + 4\Delta a + 3\alpha_\perp)) \cos\theta_{12}$$

$$+ 3\alpha_\perp\Delta\alpha^2 \cos^2\theta_{12} \big] \left(3\cos^2\theta_1 + 1\right) + a_\perp\Delta\alpha(\alpha_\perp + 3a_\perp) \left(3\cos^2\theta_1 - 1\right)^2$$

$$+ \alpha_\perp\Delta\alpha(a_\perp + 3\alpha_\perp) \left(3\cos^2\theta_2 - 1\right)^2 - 4\alpha_\perp a_\perp\Delta\alpha \left(3\cos^2\theta_1 - 1\right) \left(3\cos^2\theta_2 - 1\right)$$

$$- \big[\Delta\alpha(2\alpha_\perp(a_\perp + \Delta a) + 3a_\perp(2a_\perp + \Delta\alpha)) + 2\Delta a(4a_\perp\Delta\alpha + 3\alpha_\perp^2)$$

$$+ \Delta\alpha(2\Delta a(\alpha_\perp + 6a_\perp) + a_\perp\Delta\alpha) \cos\theta_{12} \big] \left(3\cos^2\theta_1 - 1\right) \left(3\cos\theta_1\cos\theta_2 + \cos\theta_{12}\right)$$

$$- \big[\Delta\alpha(2\alpha_\perp(a_\perp + \Delta a + 3\Delta\alpha) + a_\perp(3\Delta\alpha - 4\Delta a)) + 6\alpha_\perp^2(\Delta\alpha + \Delta a)$$

$$+ \Delta\alpha(\Delta\alpha(a_\perp + 6\alpha_\perp) + 2a_\perp\Delta a) \cos\theta_{12} \big] \left(3\cos^2\theta_2 - 1\right) \left(3\cos\theta_1\cos\theta_2 + \cos\theta_{12}\right)$$

$$+ \big[3\alpha_\perp^2(4\Delta a + \Delta\alpha) + \Delta\alpha^2(\Delta\alpha + 2\alpha_\perp + 6(a_\perp + \Delta a)) + \Delta\alpha[\Delta a(4a_\perp + 12\Delta\alpha$$

$$+ 3\Delta a) + 3a_\perp(a_\perp + 2\alpha_\perp) + 2(6\Delta a(a_\perp + \alpha_\perp + \Delta a) + \Delta\alpha(2\Delta\alpha + 4\Delta a$$

$$+ a_\perp + \alpha_\perp)) \cos\theta_{12} + (3\alpha_\perp^2 + 2\Delta\alpha\Delta a + 9\Delta a^2) \cos^2\theta_{12}) \big]$$

$$\times \left(3\cos\theta_1\cos\theta_2 + \cos\theta_{12}\right)^2 \Big\}, \tag{6.105}$$

$$\mu_1\beta_1 = \frac{4\mu_0\beta}{9kT} \cos\theta_{12}. \tag{6.106}$$

Explicit expressions for the remaining terms defined in equations (6.67) to (6.87), are not given here, as they are very long. In order to calculate these terms, Macsyma's Fortran conversion facility was used to convert the expressions directly into Fortran to avoid programming errors. These terms are important as they establish convergence of B_K.

6.6 B_K for non-linear molecules

For non-linear gases the second Kerr-effect virial coefficient is given by

$$B_K = \frac{N_A^2}{216\pi^2(4\pi\varepsilon_0)} \int\limits_{R=0}^{\infty} \int\limits_{\alpha_1=0}^{2\pi} \int\limits_{\beta_1=0}^{\pi} \int\limits_{\gamma_1=0}^{2\pi} \int\limits_{\alpha_2=0}^{2\pi} \int\limits_{\beta_2=0}^{\pi} \int\limits_{\gamma_2=0}^{2\pi} \left\{ \frac{1}{2} \left(\frac{\partial^2 \overline{\pi^{(12)}}(\tau, E)}{\partial E^2} \right)_{E=0} \right.$$

$$\left. - \left(\frac{\partial^2 \bar{\pi}}{\partial E^2} \right)_{E=0} \right\} e^{-\frac{U_{12}}{kT}} R^2 \sin\beta_1 \sin\beta_2 \, dR \, d\alpha_1 d\beta_1 d\gamma_1 d\alpha_2, d\beta_2 d\gamma_2, \qquad (6.107)$$

where the integrand is given by (6.66). Explicit expressions for the terms of the integrand are obtained by substituting the relevant molecular property tensors, in terms of the the the interaction parameters described in Section 2.1.2, into equations (6.67) to (6.87). Since there are no hyperpolarizabilities, or higher-order polarizabilities, such as the A- or C-tensors, available for the non-linear gases under study, terms containing these tensors will not be evaluated. The exact form of the static polarizability tensors and the dipole and quadrupole moment tensors of molecules 1 and 2 for molecules with D_{2h} and C_{2v} symmetries, are given by equations (4.126) to (4.144) of Section 4.5. The form of the second and third rank T-tensors is given in equations (4.145) to (4.149).

The dynamic polarizability tensor has the same form as the static polarizability and is given by:

$$\alpha_{ij}^{(2)} = \mathrm{a}_\alpha^i \mathrm{a}_\beta^j \mathrm{a}_{i'}^\alpha \mathrm{a}_{j'}^\beta \alpha_{i'j'}^{(2)} = \begin{bmatrix} Z_{11} & Z_{12} & Z_{13} \\ Z_{12} & Z_{22} & Z_{23} \\ Z_{13} & Z_{23} & Z_{33} \end{bmatrix}, \quad \text{where } \alpha_{i'j'}^{(2)} = \alpha_{ij}^{(1)} = \begin{bmatrix} \alpha_{11} & 0 & 0 \\ 0 & \alpha_{22} & 0 \\ 0 & 0 & \alpha_{33} \end{bmatrix}$$

$$(6.108)$$

and the coefficients Z_{11}, Z_{12}, ., Z_{33} are exactly analogous to the coefficients W_{ij} of $\mathrm{a}_{ij}^{(2)}$ given by equations (4.139) to (4.144), with the static components a_{11}, a_{22} and a_{33} replaced by the dynamic components α_{11}, α_{22} and α_{33} respectively, so that

$$Z_{11} = \alpha_{11} \left[A_1^2 B_1^2 + A_4^2 B_4^2 + A_7^2 B_7^2 + 2A_1 A_4 B_1 B_4 + 2A_7 B_7 (A_4 B_4 + A_1 B_1) \right]$$

$$+ \alpha_{22} \left[A_1^2 B_2^2 + A_4^2 B_5^2 + A_7^2 B_8^2 + 2A_1 A_4 B_2 B_5 + 2A_7 B_8 (A_4 B_5 + A_1 B_2) \right] \qquad (6.109)$$

$$+ \alpha_{33} \left[A_1^2 B_3^2 + A_4^2 B_6^2 + A_7^2 B_9^2 + 2A_1 A_4 B_3 B_6 + 2A_7 B_9 (A_4 B_6 + A_1 B_3) \right],$$

$$Z_{22} = \alpha_{11} \left[A_2^2 B_1^2 + A_5^2 B_4^2 + A_8^2 B_7^2 + 2A_2 A_5 B_1 B_4 + 2A_8 B_7 (A_5 B_4 + A_2 B_1) \right]$$

$$+ \alpha_{22} \left[A_2^2 B_2^2 + A_5^2 B_5^2 + A_8^2 B_8^2 + 2A_2 A_5 B_2 B_5 + 2A_8 B_8 (A_5 B_5 + A_2 B_2) \right] \qquad (6.110)$$

$$+ \alpha_{33} \left[A_2^2 B_3^2 + A_5^2 B_6^2 + A_8^2 B_9^2 + 2A_2 A_5 B_3 B_6 + 2A_8 B_9 (A_5 B_6 + A_2 B_3) \right],$$

$$Z_{33} = \alpha_{11} \left[A_3^2 B_1^2 + A_6^2 B_4^2 + A_9^2 B_7^2 + 2A_3 A_6 B_1 B_4 + 2A_9 B_7 (A_6 B_4 + A_3 B_1) \right]$$

$$+ \alpha_{22} \left[A_3^2 B_2^2 + A_6^2 B_5^2 + A_9^2 B_8^2 + 2A_3 A_6 B_2 B_5 + 2A_9 B_8 (A_6 B_5 + A_3 B_2) \right] \qquad (6.111)$$

$$+ \alpha_{33} \left[A_3^2 B_3^2 + A_6^2 B_6^2 + A_9^2 B_9^2 + 2A_3 A_6 B_3 B_6 + 2A_9 B_9 (A_6 B_6 + A_3 B_3) \right],$$

$$Z_{12} = \alpha_{11} \left[A_1 A_2 B_1^2 + A_4 A_5 B_4^2 + A_7 A_8 B_7^2 + B_1 B_4 (A_1 A_5 + A_2 A_4) \right.$$

$$+ B_7 \left(B_4 (A_4 A_8 + A_5 A_7) + B_1 (A_1 A_8 + A_2 A_7) \right) \big] + \alpha_{22} \left[A_1 A_2 B_2^2 \right.$$

$$+ A_4 A_5 B_5^2 + A_7 A_8 B_8^2 + B_2 B_5 (A_1 A_5 + A_2 A_4) + B_8 \left(B_5 (A_4 A_8 + A_5 A_7) \right. \qquad (6.112)$$

$$+ B_2 (A_1 A_8 + A_2 A_7) \big) \big] + \alpha_{33} \left[A_1 A_2 B_3^2 + A_4 A_5 B_6^2 + A_7 A_8 B_9^2 \right.$$

$$+ B_3 B_6 (A_1 A_5 + A_2 A_4) + B_9 \left(B_6 (A_4 A_8 + A_5 A_7) + B_3 (A_1 A_8 + A_2 A_7) \right) \big],$$

$$Z_{13} = \alpha_{11} \left[A_1 A_3 B_1^2 + A_4 A_6 B_4^2 + A_7 A_9 B_7^2 + B_1 B_4 (A_1 A_6 + A_3 A_4) \right.$$

$$+ B_7 \left(B_4 (A_4 A_9 + A_6 A_7) + B_1 (A_1 A_9 + A_3 A_7) \right) \big] + \alpha_{22} \left[A_1 A_3 B_2^2 \right.$$

$$+ A_4 A_6 B_5^2 + A_7 A_9 B_8^2 + B_2 B_5 (A_1 A_6 + A_3 A_4) + B_8 \left(B_5 (A_4 A_9 + A_6 A_7) \right. \qquad (6.113)$$

$$+ B_2 (A_1 A_9 + A_3 A_7) \big) \big] + \alpha_{33} \left[A_1 A_3 B_3^2 + A_4 A_6 B_6^2 + A_7 A_9 B_9^2 \right.$$

$$+ B_3 B_6 (A_1 A_6 + A_3 A_4) + B_9 \left(B_6 (A_4 A_9 + A_6 A_7) + B_3 (A_1 A_9 + A_3 A_7) \right) \big],$$

$$Z_{23} = \alpha_{11} \left[A_2 A_3 B_1^2 + A_5 A_6 B_4^2 + A_8 A_9 B_7^2 + B_1 B_4 (A_2 A_6 + A_3 A_5) \right.$$

$$+ B_7 \left(B_4 (A_5 A_9 + A_6 A_8) + B_1 (A_2 A_9 + A_3 A_8) \right) \big] + \alpha_{22} \left[A_2 A_3 B_2^2 \right.$$

$$+ A_5 A_6 B_5^2 + A_8 A_9 B_8^2 + B_2 B_5 (A_2 A_6 + A_3 A_5) + B_8 \left(B_5 (A_5 A_9 + A_6 A_8) \right. \qquad (6.114)$$

$$+ B_2 (A_2 A_9 + A_3 A_8) \big) \big] + \alpha_{33} \left[A_2 A_3 B_3^2 + A_5 A_6 B_6^2 + A_8 A_9 B_9^2 \right.$$

$$+ B_3 B_6 (A_2 A_6 + A_3 A_5) + B_9 \left(B_6 (A_5 A_9 + A_6 A_8) + B_3 (A_2 A_9 + A_3 A_8) \right) \big].$$

The mean static and dynamic polarizabilities are:

$$a = \tfrac{1}{3} a_{ii} = \tfrac{1}{3} \left(a_{11} + a_{22} + a_{33} \right)$$

$$\text{and} \quad \alpha = \tfrac{1}{3}\alpha_{ii} = \tfrac{1}{3}\left(\alpha_{11} + \alpha_{22} + \alpha_{33}\right). \tag{6.115}$$

In addition, to simplify the final expressions, a tensor analogous to G_{il} in (4.150) is defined:

$$H_{il} = \alpha_{ij}^{(1)} T_{jk} \alpha_{kl}^{(2)} = \begin{bmatrix} H_{11} & H_{12} & H_{13} \\ H_{21} & H_{22} & H_{23} \\ H_{31} & H_{32} & H_{33} \end{bmatrix}, \tag{6.116}$$

where

$$\left. \begin{aligned} H_{11} &= \alpha_{11}(Z_{11}T_{11} + Z_{12}T_{12} + Z_{13}T_{13}), \\ H_{12} &= \alpha_{11}(Z_{12}T_{11} + Z_{22}T_{12} + Z_{23}T_{13}), \\ H_{13} &= \alpha_{11}(Z_{13}T_{11} + Z_{23}T_{12} + Z_{33}T_{13}), \\ H_{21} &= \alpha_{22}(Z_{11}T_{12} + Z_{12}T_{22} + Z_{13}T_{23}), \\ H_{22} &= \alpha_{22}(Z_{12}T_{12} + Z_{22}T_{22} + Z_{23}T_{23}), \\ H_{23} &= \alpha_{22}(Z_{13}T_{12} + Z_{23}T_{22} + Z_{33}T_{23}), \\ H_{31} &= \alpha_{33}(Z_{11}T_{13} + Z_{12}T_{23} + Z_{13}T_{33}), \\ H_{32} &= \alpha_{33}(Z_{12}T_{13} + Z_{22}T_{23} + Z_{23}T_{33}), \\ H_{31} &= \alpha_{33}(Z_{13}T_{13} + Z_{23}T_{23} + Z_{33}T_{33}). \end{aligned} \right\} \tag{6.117}$$

The tensor manipulation facilities of Macsyma may now be used to evaluate the terms of the integrand in equations (6.67) to (6.87), resulting in expressions which, when averaged over the interaction coordinates of the pair of molecules, yield their contribution to B_K.

The first term of the integrand, α_2, given by (6.88), becomes:

$$\alpha_2 = \frac{1}{5kT}\left(\alpha_{11}W_{11} + \alpha_{22}W_{22} + \alpha_{33}W_{33} - 3\alpha a\right), \tag{6.118}$$

while the term $\mu_2\alpha_1$ given by (6.103), becomes:

$$\mu_2\alpha_1 = \frac{\mu_0^2}{15(kT)^2}\left\{6\left(\alpha_{11}\mathcal{D}_1^2 + \alpha_{22}\mathcal{D}_2^2 + \alpha_{33}\mathcal{D}_3^2 + 2\alpha_{33}\mathcal{D}_3\right)\right.$$

$$\left. - \alpha\left(\mathcal{D}_1^2 + \mathcal{D}_2^2 + \mathcal{D}_3^2 + 2\mathcal{D}_3\right)\right\}. \tag{6.119}$$

The final expressions generated by Macsyma for the remaining terms α_3, α_4, ... are too large to be quoted here. Due to their size it is best to generate the expressions in Macsyma (or a similar symbolic manipulation package) and convert them directly to Fortran for integration, and thus avoid the introduction of errors which would certainly arise if such enormous terms were produced manually.

111

6.7 Summary of experimental work on the second Kerr-effect virial coefficient

A comprehensive list of the experimental second Kerr-effect virial coefficient data available is given in Tables 1.7 to 1.10. The data for the spherical gases is very sparse, usually with only one value, and at most three values, for a particular wavelength of the incident light. For the polar gases under study, only four have been measured and, although all the data sets contain a minimum of seven values at 632.8 nm, the experimental errors are large and the data points widely scattered, especially for the two fluoromethanes. Similarly, for the non-polar gases, B_K has been measured for a wide range of temperatures at 632.8 nm, but the errors and the scatter are large. For nitrogen, the sign of the second Kerr-effect virial coefficient is uncertain, as the errors exceed the measured values. Comparison of Tables 1.8,1.9 and 1.10 shows that, in general, B_K values for polar molecules are approximately a hundred times larger than those of non-polar molecules.

Experimental values of the second Kerr-effect virial coefficient are deduced from pressure-dependence measurements of the Kerr effect. The errors are often large because of the small density-dependence of K_m at the pressures used in the experiments, with additional systematic errors due to uncertainties in the pressure virial coefficients $B(T)$ and $C(T)$ used to obtain the molar volumes V_m of gas samples. B_K has been measured for the fluoromethanes by Buckingham and Orr [33], while Schaefer et al. [83] measured the effect for fluoromethane, trifluoromethane and chloromethane. Buckingham et al. [14] have measured the effect for the non-polar gases carbon dioxide, nitrogen, ethane, cyclopropane, and the non-linear gas ethene. B_K of carbon dioxide has also been measured more recently by Gentle et al. [15], who then measured B_K for the non-linear gas sulphur dioxide [21]. Values for the inert gases and sulphur hexafluoride have been obtained by Buckingham and Dunmur [82]. Bogaard et al. [179] measured the Kerr effect for the chloromethanes and deduced A_K, but due to the low pressures used were unable to obtain reliable values for B_K. Bogaard, Buckingham and Ritchie have measured B_K for the non-linear gases dimethyl ether [23] and hydrogen sulphide [180]. Recently, Tammer and Hüttner [25] investigated the Kerr effect of gaseous ethene and obtained values for the second Kerr-effect virial coefficient.

6.8 Summary of theoretical calculations of the second Kerr-effect virial coefficient

In 1955, Buckingham [174] developed a statistical mechanical theory of the second Kerr-effect virial coefficient, which was later extended by Buckingham and Orr [33] to include

the effects of polarizability and the shape of the molecule. Using this theory they calculated B_K for the fluoromethanes and obtained approximate agreement with their experimental values for fluoromethane, but found the calculated values of trifluoromethane were too small. They attributed this disagreement to short-range interaction effects on the polarizability and the potential energy, and argued that measurements of B_K for polar gases would probably not yield practical information about the nature of intermolecular potentials.

However, in 1983, Buckingham, Galwas and Fan-Chen [177] resolved the order of magnitude discrepancy between experiment and theory for the fluoromethanes, by extending their earlier theory [174] to include collision-induced polarizability, which was identified as the principal component of B_K. In this work, a simple Stockmayer potential [120] consisting of the dipole-dipole interaction together with a (6-12) Lennard-Jones potential was used, but the shape potential was not included. This new theory yielded calculated values which were in much better agreement with the experimental data, in spite of the fact that no attempt was made to optimise the Lennard-Jones parameters. However, although the fit between theory and experiment was improved, this was not conclusive due to the large uncertainty in the measured values. In our work, we include quadrupole-dipole, quadrupole-quadrupole and the induction potentials, as well as the shape potential, in the intermolecular potential. In addition, we include the effects of the quadrupole moment in the collision-induced polarizability for the first time. We have been careful to ensure that all the series in the calculation of B_K have converged.

Although B_K has been measured for several non-polar linear gases, it was only recently that theoretical values were first calculated by Couling and Graham [9] for nitrogen, carbon dioxide and ethane. Their calculated values for nitrogen and carbon dioxide are extremely small, which perhaps explains the poorly defined experimental values. For ethane, where B_K is an order of magnitude larger than nitrogen or carbon dioxide and the observed values are more clearly defined, their calculated values were in good agreement with the experimental data. However, they did not include the quadrupole series in their calculations and we will show that this series may be significant for polar and non-polar molecules.

In 1990, Gentle et al. [21] measured the Kerr effect of sulphur dioxide for temperatures ranging from 298.7 K to 490.3 K, and deduced fairly precise values for the second Kerr-effect virial coefficient. They then applied the theory of Buckingham et al. [177], which had proved relatively succesful for the fluoromethanes, to sulphur dioxide after approximating the molecule to be quasi-linear. However, although they optimised the Lennard-Jones parameters by fitting a simple Stockmayer potential to the experimental values for $B(T)$, most of the calculated B_K values were more than double the experimental values. Approximating a molecule to be quasi-linear involves setting $\alpha_{11} = \alpha_{22}$, while for sulphur

dioxide the actual values are $\alpha_{11} = 5.80 \times 10^{-40} \text{C}^2\text{m}^2\text{J}^{-1}$ and $\alpha_{22} = 3.30 \times 10^{-40} \text{C}^2\text{m}^2\text{J}^{-1}$ at $\lambda = 632$ nm [21]. This discrepancy might explain why the theory did not fit the experimental values. Recently, Couling and Graham [9] developed a molecular tensor theory of B_K for molecules with non-linear symmetry, to assess the extent to which the assumption of axial symmetry is responsible for the poor agreement between theory and experiment. They based their theory on the earlier work of Buckingham et $al.$ [177], extending it to molecules with low symmetry and including the effects of molecular shape. They optimised the Lennard-Jones force constants and their two shape factors D_1 and D_2, to obtain a very good fit of the $B(T)$, and the resulting set of parameters yielded calculated values of B_K in excellent agreement with the experimental data. The same procedure was followed for the non-linear gases dimethyl ether and ethene, with good results for polar dimethyl ether but poor agreement for non-polar ethene. Since the experimental values of B_K for ethene are very small, it was unclear whether the discrepancies were due to systematic errors arising from uncertainities in the pressure virial coefficients used to determine the molar volume V_m, or due to the failure of the model. It is, however, clear from their work that the effects of interacting non-linear molecules on molecular electromagnetic phenomena can only be comprehensively evaluated after due consideration of their molecular symmetry. We have extended this work by considering the effect on B_K of the dipole-quadrupole and quadrupole-quadrupole series, defined in equations (6.82), (6.83) and (6.85) to (6.87), resulting in a more complete theory.

Chapter 7

The Second Light-Scattering Virial Coefficient, B_ρ

The phenomenon of light-scattering was first studied in 1869 by Tyndall [181], who conducted a series of experiments on aerosols. He passed a strong beam of white light through a colloidal suspension of particles, and viewed the light scattered at right angles to the incident beam. The scattered light was observed to be linearly polarized blue light, providing some justification for the idea that the colour and polarization of skylight was due to the scattering of light from the sun by small particles suspended in the atmosphere. However, Tyndall still could not explain the mechanisms by which light was scattered, and was quoted by Kerker [182] as saying "The blue colour of the sky, and the polarization of skylight ... constitute, in the opinion of our most eminent authorities, the two great standing enigmas of meteorology."

In 1871 the enigma was explained by J. W. Strutt [183], the third Baron Rayleigh, in his theoretical discussion of the light-scattering phenomenon. He treated the incident light as vibrations in the ether which set up forced vibrations in the suspended particles. These particles scattered the incident light by acting as secondary sources of vibrations in all directions. Rayleigh also showed that, if a particle was assumed to be an isotropic sphere with a diameter much smaller than the wavelength λ of the incident light, the intensity of the light scattered by the particle was proportional to $\frac{1}{\lambda^4}$ and the component scattered at right angles to the incident beam was completely linearly polarized perpendicular to the plane of scattering. Thus, since blue light has a shorter wavelength than red light, the intensity of the scattered blue light is much greater than the red, resulting in the blue colour of the sky.

Lord Rayleigh [184] later refined his theory by proposing that the blue light of the sky was due to sunlight scattered from the *individual molecules of the air*, rather than from dust particles suspended in the atmosphere. In 1916, seventeen years later, Cabannes [185] confirmed this theoretical postulate experimentally. He passed a strong white light beam

through a pure, dust-free gas sample and observed that the light scattered at right angles to the incident beam was blue in colour and linearly polarized. As was to be expected, the light scattered by the gas molecules was far less intense than that scattered by the larger particles in the colliodal suspensions used by Tyndall.

However, the fourth Baron Rayleigh, R. J. Strutt, discovered that the 90° scattered light was not completely linearly polarized, and that the degree of depolarization was a characteristic constant of the gas under study [186]. His father's theory, which predicted complete linear polarization, had assumed that the scattering centres were *isotropic* spheres. Thus, R. J. Strutt extended this theory by considering the anisotropy of the gas molecules and relating the depolarization ratio to departures from spherical symmetry of the optical properties of the molecules [187].

Within the next ten years a large number of measurements were carried out for a wide variety of gases and vapours, in spite of the extreme difficulties involved in the experimental procedures. The Raman effect, in which the scattered light undergoes well defined frequency shifts, was discovered during this period and, subsequently, most workers concentrated on this new phenomenon. It was only in 1961 that the conventional Rayleigh scattering was seriously taken up again when Powers [188] produced new values for the depolarization ratio of several gases, which he measured using a photomultiplier to detect the scattered light rather than the visual or photographic detection techniques used by the earlier workers. He found that the results obtained in the 1920's were often as much as 10% too high. Then, in 1964, Bridge and Buckingham [189] were the first to employ the laser, with its intense parallel beam of monochromatic light, to measure the depolarisation ratio. This new technology allowed Bridge and Buckingham and subsequent workers [4, 17, 190–193] to make detailed and accurate measurements of the depolarization ratio of many gases and vapours. Their values were even lower than those measured by Powers, thus confirming the inadequacy of the experimental techniques used by the earlier workers.

7.1   General theory of light scattering

The scattering of light by a single molecule can be considered to arise when the oscillating multipole moments, induced in the molecule by the incident light wave, produce retarded scalar and vector potentials and therefore electric and magnetic fields at all points. These fields have been related to the electric and magnetic multipole moments of the system by Landau and Lifshitz [194] and Buckingham and Raab [195]. If an origin O is fixed within the molecule's system of oscillating charges, then at a point a distance R from the origin, where R is much greater than the dimensions of the molecule and the wavelegth of the radiated light, the scattered electric field $E_\alpha^{(s)}$ may be assumed to be a plane wave

given by [195]:

$$E_\alpha^{(s)} = -\frac{1}{(4\pi\varepsilon_0)Rc^2}\left[(\ddot{\mu}_\alpha - n_\alpha n_\beta \ddot{\mu}_\beta) - \frac{1}{c}\epsilon_{\alpha\beta\gamma}n_\beta\ddot{m}_\gamma + \frac{1}{3c}(n_\beta\dddot{\theta}_{\alpha\beta} - n_\alpha n_\beta n_\gamma\dddot{\theta}_{\beta\gamma}) + \cdots\right],$$

(7.1)

where n_α is a unit vector in the direction in which the wave is scattered, μ_α is the electric dipole moment tensor of the system of charges, $\theta_{\alpha\beta}$ is the *traceless* electric quadrupole moment tensor, and m_α is the magnetic dipole moment tensor, and each dot above these moments represents a partial derivative with respect to time. These multipole moments, as well as the primitive multipole moments, are defined in Appendix B. It must be noted that several workers [196–199] have demonstrated that electrodynamic situations exist for which it is necessary to retain the primitive multipole moments. In this work, however, the traditional traceless quadrupole moment is used, and this subtlety will need to be considered in future work.
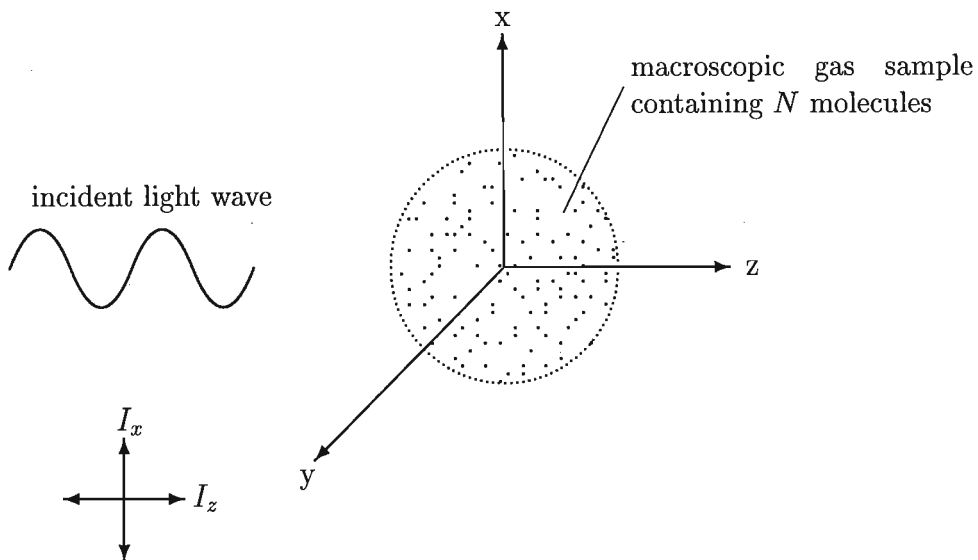
Figure 7.1: The space-fixed system of axes used to describe the scattering of light by a macroscopic gas sample containing N molecules.

In the arrangement shown in Figure 7.1 the origin of a space-fixed system of axes O(x,y,z) is placed within a macroscopic sample of gas containing a large number N of identical gas molecules. A uniform, parallel beam of light, linearly polarized in the xz plane and travelling in the z direction, is incident on the gas sample. The wavelength of the incident light is assumed to be very much larger than the dimensions of the gas molecules, and its frequency is assumed to lie far below the frequency of any electronic absorption transition. The depolarization ratio of the Rayleigh-scattered light observed

at a point on the y-axiz is given by:

$$\rho = \frac{I_z}{I_x}, \tag{7.2}$$

where I_x and I_z are the intensities of the light scattered with the electric vector parallel to the z and x axes respectively.

For light travelling along the y-axis the unit vector $n_\alpha = [0 \quad 1 \quad 0]$. Therefore, since ρ in (7.2) requires scattered intensities with the electric vector parallel to the x and z axes, the expression for the scattered electric field in (7.1), summed for the contributions from each molecule in the system of N molecules, becomes:

$$E_\alpha^{(s)} = -\frac{1}{(4\pi\varepsilon_0)Rc^2} \sum_{p=1}^{N} \ddot{\mu}_\alpha^{(p)}(t'), \tag{7.3}$$

where $\ddot{\mu}_\alpha^{(p)}$ is the dipole acceleration of the pth molecule, and only electric dipole radiation has been considered. The electric quadrupole and magnetic dipole are much smaller and are therefore neglected.

Now, μ_α is a function of the electrostatic field E, so that:

$$\frac{\partial\mu_\alpha}{\partial t} = \dot{\mu}_\alpha = \frac{\partial\mu_\alpha}{\partial E_\beta}\frac{\partial E_\beta}{\partial t} \tag{7.4}$$

and

$$\frac{\partial^2\mu_\alpha}{\partial t^2} = \ddot{\mu}_\alpha = \frac{\partial E_\beta}{\partial t}\frac{\partial E_\gamma}{\partial t}\frac{\partial^2\mu_\alpha}{\partial E_\beta\partial E_\gamma} + \frac{\partial\mu_\alpha}{\partial E_\beta}\frac{\partial^2 E_\beta}{\partial t^2}. \tag{7.5}$$

Even when intense laser beams are used, the term which is non-linear in the field in equation (7.5) can be safely neglected. Since:

$$E_\alpha = E_\alpha^{(0)}e^{-i\omega(t-\frac{R}{c})}, \tag{7.6}$$

we have

$$\frac{\partial^2 E_\beta}{\partial t^2} = -\omega^2 E_\beta. \tag{7.7}$$

It follows then from equations (7.3) and (7.5), that for a monochromatic incident light beam with a wavelength λ, the scattered electric field becomes:

$$E_\alpha^{(s)} = -\frac{1}{(4\pi\varepsilon_0)R}\left(\frac{2\pi}{\lambda}\right)^2 \sum_{p=1}^{N} \frac{\partial\mu_\alpha^{(p)}}{\partial E_\delta^{(p)}}E_\delta^{(p)}, \tag{7.8}$$

where $E_\delta^{(p)}$ implies the value of the electric field at the pth molecule. The differential

118

polarizability $\pi_{\alpha\beta}^{(p)}$ is defined as:

$$\pi_{\alpha\beta}^{(p)} = \frac{\partial \mu_{\alpha}^{(p)}}{\partial E_{\beta}^{(p)}}. \tag{7.9}$$

In general, the intensity I of a light wave with electric field vector $\mathbf{E}$ is given by the following expression:

$$I = \frac{1}{2\mu_0 c} \mathbf{E}.\mathbf{E}^*, \tag{7.10}$$

where the asterisk denotes the complex conjugate. Thus, from equation (7.2) and equations (7.8) to (7.10), we have:

$$\rho = \frac{I_z}{I_x} = \frac{\langle E_z E_z^* \rangle}{\langle E_x E_x^* \rangle} = \frac{\left\langle \sum_{p=1}^{N} \sum_{q=1}^{N} \pi_{zx}^{(p)} \pi_{zx}^{(q)} e^{i\chi_{pq}} \right\rangle}{\left\langle \sum_{p=1}^{N} \sum_{q=1}^{N} \pi_{xx}^{(p)} \pi_{xx}^{(q)} e^{i\chi_{pq}} \right\rangle}, \tag{7.11}$$

where χ_{pq} is the phase difference in the light scattered by molecules p and q, as seen at the observation point, and where the angular brackets indicate an average over all configurations of the specimen. This equation was first obtained by Buckingham and Stephen [35], and has been used a basis for the discussion of the effects of pair interactions on the depolarization ratio ρ from linear and quasi-linear molecules by Graham [200] and Couling and Graham [201], and for non-linear molecules by Couling and Graham [9, 36].

7.1.1 Non-interacting molecules

In a dilute gas molecular interactions are negligible and the oscillating dipole moment $\mu_{\alpha}^{(p)}$ of molecule p is induced only by the polarizing effect of the applied field $\mathcal{E}_0$, since there are no molecules close enough for their moments to set up significant fields and field gradients at molecule p. Thus, the differential polarizability $\pi_{\alpha\beta}$ is given simply by the molecular polarizability $\alpha_{\alpha\beta}$. In addition, there is no average phase relationship between the fields from any one pair of molecules and only self-correlations contribute to the summations in equation (7.11), which are therefore replaced by N times the contribution of an individual representative molecule 1. Thus, (7.11) simplifies to:

$$\rho_0 = \frac{N \left\langle \alpha_{zx}^{(1)} \alpha_{zx}^{(1)} \right\rangle}{N \left\langle \alpha_{xx}^{(1)} \alpha_{xx}^{(1)} \right\rangle}, \tag{7.12}$$

119

where the angular brackets now represent an average over all unbiased orientations of a molecule. The molecular tensors in (7.12) are referred to the space-fixed axes (x,y,z) and must be projected into the molecule-fixed axes (1,2,3), yielding:

$$\langle \alpha_{zx}^{(1)} \alpha_{zx}^{(1)} \rangle = \alpha_{ij}^{(1)} \alpha_{kl}^{(1)} \langle a_i^z a_k^z a_j^x a_l^x \rangle, \tag{7.13}$$

$$\langle \alpha_{xx}^{(1)} \alpha_{xx}^{(1)} \rangle = \alpha_{ij}^{(1)} \alpha_{kl}^{(1)} \langle a_i^x a_k^x a_j^x a_l^x \rangle. \tag{7.14}$$

Using the standard isotropic averages [34, 175]:

$$\langle a_i^z a_k^z a_j^x a_l^x \rangle = \tfrac{1}{30} \left(4\delta_{ik}\delta_{jl} - \delta_{ij}\delta_{kl} - \delta_{il}\delta_{kj} \right) \tag{7.15}$$

$$\text{and} \quad \langle a_i^x a_k^x a_j^x a_l^x \rangle = \tfrac{1}{15} \left(\delta_{ik}\delta_{jl} + \delta_{ij}\delta_{kl} + \delta_{il}\delta_{kj} \right), \tag{7.16}$$

equations (7.13) and (7.14) become:

$$\langle \alpha_{zx}^{(1)} \alpha_{zx}^{(1)} \rangle = \tfrac{1}{30} (3\alpha_{ij}^{(1)} \alpha_{ij}^{(1)} - \alpha_{ii}^{(1)} \alpha_{jj}^{(1)})$$

$$= \tfrac{2}{30} (\alpha_{11}^2 + \alpha_{22}^2 + \alpha_{33}^2 - \alpha_{11}\alpha_{22} - \alpha_{11}\alpha_{33} - \alpha_{22}\alpha_{33}), \tag{7.17}$$

$$\langle \alpha_{xx}^{(1)} \alpha_{xx}^{(1)} \rangle = \tfrac{1}{15} (2\alpha_{ij}^{(1)} \alpha_{ij}^{(1)} + \alpha_{ii}^{(1)} \alpha_{kk}^{(1)})$$

$$= \tfrac{1}{15} (3\alpha_{11}^2 + 3\alpha_{22}^2 + 3\alpha_{33}^2 + 2\alpha_{11}\alpha_{22} + 2\alpha_{11}\alpha_{33} + 2\alpha_{22}\alpha_{33}). \tag{7.18}$$

For linear molecules $\alpha_{ij}^{(1)}$ is diagonal with $\alpha_{11} = \alpha_{22} = \alpha_\perp$ and $\alpha_{33} = \alpha_\parallel$. The mean polarizability α is:

$$\alpha = \tfrac{1}{3}\alpha_{ii} = \tfrac{1}{3}(2\alpha_\perp + \alpha_\parallel), \tag{7.19}$$

while the anisotropy in the polarizability tensor is defined as:

$$\Delta\alpha = \alpha_\parallel - \alpha_\perp. \tag{7.20}$$

For non-linear molecules with D_{2h} and C_{2v} symmetries, α_{ij} is diagonal with three independent components, as shown in equation (6.108) of Section 6.6. The mean polarizability α is:

$$\alpha = \tfrac{1}{3}\alpha_{ii} = \tfrac{1}{3}(\alpha_{11} + \alpha_{22} + \alpha_{33}), \tag{7.21}$$

while the anisotropy in the polarizability tensor is often defined as [102, 202]:

$$\Delta\alpha = \frac{1}{\sqrt{2}} \sqrt{(\alpha_{11} - \alpha_{22})^2 + (\alpha_{22} - \alpha_{33})^2 + (\alpha_{33} - \alpha_{11})^2}. \tag{7.22}$$

For both linear and non-linear D_{2h} and C_{2v} gases, equations (7.17) and (7.18) simplify to:

$$\langle \alpha_{zx}^{(1)} \alpha_{zx}^{(1)} \rangle = \tfrac{1}{15}(\Delta\alpha)^2, \tag{7.23}$$

$$\langle \alpha_{xx}^{(1)} \alpha_{xx}^{(1)} \rangle = \alpha^2 + \tfrac{4}{45}(\Delta\alpha)^2. \tag{7.24}$$

Thus equation (7.12) may now be written:

$$\rho_0 = \frac{\tfrac{1}{15}(\Delta\alpha)^2}{\alpha^2 + \tfrac{4}{45}(\Delta\alpha)^2}. \tag{7.25}$$

The anisotropy in the molecular polarizability tensor was originally defined as the *dimensionless* quantity κ [190]:

$$\kappa^2 = \frac{(3\alpha_{ij}\alpha_{ij} - \alpha_{ii}\alpha_{jj})}{2\alpha_{ii}\alpha_{jj}}$$

$$= \frac{(\Delta\alpha)^2}{9\alpha^2} \tag{7.26}$$

and applies to both linear and non-linear molecules. From equations (7.25) and (7.26), it can easily be shown that ρ_o and κ are related by the expression:

$$\rho_0 = \frac{3\kappa^2}{5 + 4\kappa^2}, \tag{7.27}$$

first derived by Bridge and Buckingham [190]. This equation can be used to obtain values for κ^2 from measured values of ρ_0.

Since non-interacting spheres are isotropic, the anisotropy κ in equation (7.26) is zero. Therefore, from (7.27) we have $\rho_0 = 0$, confirming the well-known result that non-interacting spheres do not depolarize the light that they scatter.

7.1.2 Interacting molecules

If the pressure of a gas is increased to the extent where molecular interactions are significant, the depolarization ratio ρ_0 of the light scattered by a dilute gas sample of non-interacting *anisotropic* molecules is modified. The density dependence of the depolarization ratio may best be described by the virial expansion [35]:

$$\rho = \rho_0 + \frac{B_\rho}{V_m} + \frac{C_\rho}{V_m^2} + \cdots, \tag{7.28}$$

where B_ρ, C_ρ, ... are the second, third, ... light-scattering virial coefficients, and describe the contributions to ρ arising from interactions between pairs, triplets, ... of molecules,

respectively.

A complete molecular tensor theory of B_ρ, based on the treatment of Couling and Graham [9,36], is now presented.

In a gas the molecules are moving randomly relative to one another, so that the scattered light waves emitted by each of the molecules arrive at the distant observation point with different and randomly fluctuating phases. Therefore, the summation in equation (7.11), can be simplified considerably. Except for self-correlation, the only significant correlation of phase occurs when two molecules are involved in a close encounter. Benoît and Stockmayer [203] established that, apart from the term $\left\langle \pi_{xx}^{(1)} \pi_{xx}^{(2)} \cos \chi_{12} \right\rangle$, the interaction mechanism for all the terms in (7.11) is only significant at short ranges of approximately 0.5 nm to 2 nm, which are a small fraction of a typical wavelength of ~ 500 nm, and the phase differences χ_{12} between scattered waves from interacting molecules p and q are thus effectively zero. It is therefore not necessary to retain χ_{pq} for all the terms, and $e^{i\chi_{pq}}$ is set to unity in all but the abovementioned term. Thus, only allowing for self-correlation and pairwise contributions to the coherent fields, the summations in equation (7.11) are replaced by N times the contribution of a representative molecule, averaged over all pair encounters, yielding:

$$\rho = \frac{N \left\langle \pi_{zx}^{(1)} \pi_{zx}^{(1)} \right\rangle + N \left\langle \pi_{zx}^{(1)} \pi_{zx}^{(2)} \right\rangle}{N \left\langle \pi_{xx}^{(1)} \pi_{xx}^{(1)} \right\rangle + N \left\langle \pi_{xx}^{(1)} \pi_{xx}^{(2)} \cos \chi_{12} \right\rangle}, \qquad (7.29)$$

where the angular brackets now indicate an average of pair interactions. The probability $P(\tau)$ that molecule 1 has a neighbour in the range $d\tau$ at τ is given by equation (1.4) in Chapter 1.

The treatment of Graham [122] is used to obtain expressions for the differential polarizabilities in equation (7.29), as defined in equation (7.9). Graham [122] argued that the total oscillating dipole moment of molecule 1, $\mu_\alpha^{(1)}$, arises in part from the direct polarizing action of the incident light wave field $\mathcal{E}_0$, and in part from the fields and field gradients at molecule 1 due to the oscillating moments of a neighbouring molecule 2, so that [26]:

$$\mu_\alpha^{(1)}(\mathcal{E}_0) = \alpha_{\alpha\beta}^{(1)} \left(\mathcal{E}_{0\beta} + \mathcal{F}_\beta^{(1)} \right) + \tfrac{1}{3} A_{\alpha\beta\gamma}^{(1)} \left(\mathcal{E}_{0\beta\gamma} + \mathcal{F}_{\beta\gamma}^{(1)} \right), \qquad (7.30)$$

where $\mathcal{E}_{0\beta}$ and $\mathcal{E}_{0\beta\gamma}$ are the field and field gradient of the incident light wave at molecule 1, and $\mathcal{F}_\beta^{(1)}$ and $\mathcal{F}_{\beta\gamma}^{(1)}$ are the oscillating field and field gradient arising at molecule 1 due to the oscillating multipole moments of molecule 2.

In equation (7.30), the molecular polarizability tensor $\alpha_{\alpha\beta}^{(1)}$ is assumed to be independent of the field and field gradient at molecule 1. However, if molecule 2 possesses

permanent multipole moments, these may set up a strong electric field $F_\gamma^{(1)}$ and electric field gradient $F_{\gamma\delta}^{(1)}$ at molecule 1, which may modifiy its effective polarizability. In this case, the non-linear hyperpolarizability terms should be included in equation (7.30):

$$\mu_\alpha^{(1)}(\mathcal{E}_0) = \left(\alpha_{\alpha\beta}^{(1)} + \beta_{\alpha\beta\gamma}^{(1)}F_\gamma^{(1)} + \tfrac{1}{2}\gamma_{\alpha\beta\gamma\delta}^{(1)}F_\gamma^{(1)}F_\delta^{(1)} + \phi_{\alpha\beta\gamma\delta}^{(1)}F_{\gamma\delta}^{(1)} + \cdots\right)\left(\mathcal{E}_{0\beta} + \mathcal{F}_\beta^{(1)}\right)$$
$$+ \tfrac{1}{3}A_{\alpha\beta\gamma}^{(1)}\left(\mathcal{E}_{0\beta\gamma} + \mathcal{F}_{\beta\gamma}^{(1)}\right). \tag{7.31}$$

The field gradient $\mathcal{E}_{0\beta\gamma}$ of the incident light wave may be neglected since the dimensions of the molecules under study are very small compared with the wavelength of the light wave. In addition, proceeding on the precedent of the second refractivity virial coefficient of linear molecules for which Burns, Graham and Weller [62] showed the hyperpolarizability terms to be negligible, as well as our own observations for the second dielectric virial coefficient, the non-linear effects resulting from the intermolecular fields of permanent multipole moments will be neglected. Thus, equation (7.31) is now written as:

$$\mu_\alpha^{(1)}(\mathcal{E}_0) = \alpha_{\alpha\beta}^{(1)}\left(\mathcal{E}_{0\beta} + \mathcal{F}_\beta^{(1)}\right) + \tfrac{1}{3}A_{\alpha\beta\gamma}^{(1)}\mathcal{F}_{\beta\gamma}^{(1)}. \tag{7.32}$$

Similarly, the oscillating quadrupole moment of molecule 1 induced by the incident light wave field as well as the field and field gradient due to the oscillating multipole moments of moleule 2, is given by [26]:

$$\theta_{\alpha\beta}^{(1)}(\mathcal{E}_0) = A_{\gamma\alpha\beta}^{(1)}\left(\mathcal{E}_{0\gamma} + \mathcal{F}_\gamma^{(1)}\right) + C_{\alpha\beta\gamma\delta}^{(1)}\mathcal{F}_{\gamma\delta}^{(1)}. \tag{7.33}$$

If the oscillating octopoles and higher-order multipoles on molecule 2 are neglected then the field $\mathcal{F}_\beta^{(1)}$ at molecule 1 due to the oscillating dipole and quadrupole moments on molecule 2 has the form [26]:

$$\mathcal{F}_\beta^{(1)} = T_{\beta\gamma}^{(1)}\mu_\gamma^{(2)} - \tfrac{1}{3}T_{\beta\gamma\delta}^{(1)}\theta_{\gamma\delta}^{(2)}, \tag{7.34}$$

where the T-tensors are defined in equations (2.18) to (2.21) of Section 2.3. The field gradient $\mathcal{F}_{\gamma\delta}^{(1)}$ at molecule 1 due to the oscillating moments on molecule 2 is given by [26]:

$$\mathcal{F}_{\beta\gamma}^{(1)} = T_{\beta\gamma\delta}^{(1)}\mu_\delta^{(2)} - \tfrac{1}{3}T_{\beta\gamma\delta\varepsilon}^{(1)}\theta_{\delta\varepsilon\phi}^{(2)}. \tag{7.35}$$

Here $\mu_\gamma^{(2)}$ and $\theta_{\gamma\delta}^{(2)}$ are the oscillating dipole and quadrupole induced on molecule 2 by the fields and field gradients at 2 due to the incident light wave and the oscillating dipole and quadrupole moments of molecule 1. Using expressions analogous to equations (7.32) and

(7.33) for $\mu_\gamma^{(2)}$ and $\theta_{\gamma\delta}^{(2)}$, and substituting these expressions into equation (7.34), yields

$$\mathcal{F}_\beta^{(1)} = T_{\beta\gamma}^{(1)} \left[\alpha_{\gamma\delta}^{(2)} \left(\mathcal{E}_{0\delta} + \mathcal{F}_\delta^{(2)} \right) + \tfrac{1}{3} A_{\gamma\delta\varepsilon}^{(2)} \mathcal{F}_{\delta\varepsilon}^{(2)} \right] - \tfrac{1}{3} T_{\beta\gamma\delta}^{(1)} \left[A_{\varepsilon\gamma\delta}^{(2)} \left(\mathcal{E}_{0\varepsilon} + \mathcal{F}_\varepsilon^{(2)} \right) + C_{\gamma\delta\varepsilon\phi}^{(2)} \mathcal{F}_{\varepsilon\phi}^{(2)} \right].$$
(7.36)

The terms $\mathcal{F}_\delta^{(2)}$ and $\mathcal{F}_{\delta\varepsilon}^{(2)}$ refer to the field and field gradient at molecule 2 arising from the oscillating dipole and quadrupole moments of molecule 1, and are given by expressions analogous to equations (7.34) and (7.35), respectively. Substituting these expressions into equation (7.36), yields:

$$\mathcal{F}_\beta^{(1)} = T_{\beta\gamma}^{(1)} \alpha_{\gamma\delta}^{(2)} \mathcal{E}_{0\delta} + T_{\beta\gamma}^{(1)} \alpha_{\gamma\delta}^{(2)} \left(T_{\delta\varepsilon}^{(2)} \mu_\varepsilon^{(1)} - \tfrac{1}{3} T_{\delta\varepsilon\phi}^{(2)} \theta_{\varepsilon\phi}^{(1)} \right) + \tfrac{1}{3} T_{\beta\gamma}^{(1)} A_{\gamma\delta\varepsilon}^{(2)} \left(T_{\delta\varepsilon\phi}^{(2)} \mu_\phi^{(1)} + \cdots \right)$$

$$- \tfrac{1}{3} T_{\beta\gamma\delta}^{(1)} A_{\varepsilon\gamma\delta}^{(2)} \mathcal{E}_{0\varepsilon} - \tfrac{1}{3} T_{\beta\gamma\delta}^{(1)} A_{\varepsilon\gamma\delta}^{(2)} \left(T_{\varepsilon\phi}^{(2)} \mu_\phi^{(1)} - \tfrac{1}{3} T_{\varepsilon\phi\lambda}^{(2)} \theta_{\phi\lambda}^{(1)} \right)$$
(7.37)

$$- \tfrac{1}{3} T_{\beta\gamma\delta}^{(1)} C_{\gamma\delta\varepsilon\phi}^{(2)} \left(T_{\varepsilon\phi\lambda}^{(2)} \mu_\lambda^{(1)} + \cdots \right).$$

Substituting the equations (7.32) and (7.33) for $\mu_\alpha^{(1)}$ and $\theta_{\alpha\beta}^{(1)}$, respectively, yields:

$$\mathcal{F}_\beta^{(1)} = T_{\beta\gamma}^{(1)} \alpha_{\gamma\delta}^{(2)} \mathcal{E}_{0\delta} + T_{\beta\gamma}^{(1)} \alpha_{\gamma\delta}^{(2)} \left[T_{\delta\varepsilon}^{(2)} \left\{ \alpha_{\varepsilon\phi}^{(1)} (\mathcal{E}_{0\phi} + \mathcal{F}_\phi^{(1)}) + \tfrac{1}{3} A_{\varepsilon\phi\lambda}^{(1)} \mathcal{F}_{\phi\lambda}^{(1)} \right\} \right.$$

$$\left. - \tfrac{1}{3} T_{\delta\varepsilon\phi}^{(2)} \left\{ A_{\lambda\varepsilon\phi}^{(1)} (\mathcal{E}_{0\lambda} + \mathcal{F}_\lambda^{(1)}) + C_{\varepsilon\phi\lambda\eta}^{(1)} \mathcal{F}_{\lambda\eta}^{(1)} \right\} \right]$$

$$+ \tfrac{1}{3} T_{\beta\gamma}^{(1)} A_{\gamma\delta\varepsilon}^{(2)} T_{\delta\varepsilon\phi}^{(2)} \left[\alpha_{\phi\lambda}^{(1)} (\mathcal{E}_{0\lambda} + \mathcal{F}_\lambda^{(1)}) + \tfrac{1}{3} A_{\phi\lambda\eta}^{(1)} \mathcal{F}_{\lambda\eta}^{(1)} \right]$$

$$- \tfrac{1}{3} T_{\beta\gamma\delta}^{(1)} A_{\varepsilon\gamma\delta}^{(2)} \mathcal{E}_{0\varepsilon} - \tfrac{1}{3} T_{\beta\gamma\delta}^{(1)} A_{\varepsilon\gamma\delta}^{(2)} \left[T_{\varepsilon\phi}^{(2)} \left\{ \alpha_{\phi\lambda}^{(1)} (\mathcal{E}_{0\lambda} + \mathcal{F}_\lambda^{(1)}) + \tfrac{1}{3} A_{\phi\lambda\eta}^{(1)} \mathcal{F}_{\lambda\eta}^{(1)} \right\} \right.$$
(7.38)

$$\left. - \tfrac{1}{3} T_{\varepsilon\phi\lambda}^{(2)} \left\{ A_{\eta\phi\lambda}^{(1)} (\mathcal{E}_{0\eta} + \mathcal{F}_\eta^{(1)}) + C_{\phi\lambda\eta\nu}^{(1)} \mathcal{F}_{\eta\nu}^{(1)} \right\} \right]$$

$$- \tfrac{1}{3} T_{\beta\gamma\delta}^{(1)} C_{\gamma\delta\varepsilon\phi}^{(2)} T_{\varepsilon\phi\lambda}^{(2)} \left[\alpha_{\lambda\eta}^{(1)} (\mathcal{E}_{0\eta} + \mathcal{F}_\eta^{(1)}) + \tfrac{1}{3} A_{\lambda\eta\nu}^{(1)} \mathcal{F}_{\eta\nu}^{(1)} \right].$$

Successive substitution of $\mathcal{F}_\beta^{(1)}$ and $\mathcal{F}_{\beta\gamma}^{(1)}$, and of $\mathcal{F}_\beta^{(2)}$ and $\mathcal{F}_{\beta\gamma}^{(1)}$, leads to an extensive series of terms. It is difficult to know a priori when the series ought to be truncated, since it is impossible to be sure whether convergence has been reached until the terms are calculated. Thus the procedure is to calculate successively higher-order terms until the point is reached where the highest order term calculated makes a negligible contribution. Therefore, based on the observations of Couling and Graham for linear and quasi-linear gases [200, 201] and for non-linear gases [9], the series for $\mathcal{F}_\beta^{(1)}$ is truncated at a point

which will lead to scattered intensities in α^5, as well as all scattered intensities in $\alpha^2 A$, $\alpha^3 A$ and $\alpha^3 C$. Equation (7.38) then yields:

$$\mathcal{F}_\beta^{(1)} = T_{\beta\gamma}^{(1)}\alpha_{\gamma\delta}^{(2)}\mathcal{E}_{0\delta} + T_{\beta\gamma}^{(1)}\alpha_{\gamma\delta}^{(2)}T_{\delta\varepsilon}^{(2)}\alpha_{\varepsilon\phi}^{(1)}\mathcal{E}_{0\phi} + T_{\beta\gamma}^{(1)}\alpha_{\gamma\delta}^{(2)}T_{\delta\varepsilon}^{(2)}\alpha_{\varepsilon\phi}^{(1)}T_{\phi\lambda}^{(1)}\alpha_{\lambda\eta}^{(2)}\mathcal{E}_{0\eta}$$

$$- \tfrac{1}{3}T_{\beta\gamma\delta}^{(1)}A_{\varepsilon\gamma\delta}^{(2)}\mathcal{E}_{0\varepsilon} - \tfrac{1}{3}T_{\beta\gamma}^{(1)}\alpha_{\gamma\delta}^{(2)}T_{\delta\varepsilon\phi}^{(2)}A_{\lambda\varepsilon\phi}^{(1)}\mathcal{E}_{0\lambda} + \tfrac{1}{3}T_{\beta\gamma}^{(1)}A_{\gamma\delta\varepsilon}^{(2)}T_{\delta\varepsilon\phi}^{(2)}\alpha_{\phi\lambda}^{(1)}\mathcal{E}_{0\lambda} \qquad (7.39)$$

$$- \tfrac{1}{3}T_{\beta\gamma\delta}^{(1)}A_{\varepsilon\gamma\delta}^{(2)}T_{\varepsilon\phi}^{(2)}\alpha_{\phi\lambda}^{(1)}\mathcal{E}_{0\lambda} - \tfrac{1}{3}T_{\beta\gamma\delta}^{(1)}C_{\gamma\delta\varepsilon\phi}^{(2)}T_{\varepsilon\phi\lambda}^{(2)}\alpha_{\lambda\eta}^{(1)}\mathcal{E}_{0\eta} + \cdots .$$

Note that the term $-\tfrac{1}{3}T_{\beta\gamma}^{(1)}\alpha_{\gamma\delta}^{(2)}T_{\delta\varepsilon\phi}^{(2)}A_{\lambda\varepsilon\phi}^{(1)}\mathcal{E}_{0\lambda}$ was not included in the work by Couling and Graham [9, 201], but is included here for completeness.

To understand the physical interpretation of the terms in (7.39), consider the term $-\tfrac{1}{3}T_{\beta\gamma\delta}^{(1)}C_{\gamma\delta\varepsilon\phi}^{(2)}T_{\varepsilon\phi\lambda}^{(2)}\alpha_{\lambda\eta}^{(1)}\mathcal{E}_{0\eta}$, which represents the oscillating field at molecule 1 due to the quadrupole moment $C_{\gamma\delta\varepsilon\phi}^{(2)}T_{\varepsilon\phi\lambda}^{(2)}\alpha_{\lambda\eta}^{(1)}\mathcal{E}_{0\eta}$ on molecule 2 induced by the oscillating field gradient $T_{\varepsilon\phi\lambda}^{(2)}\alpha_{\lambda\eta}^{(1)}\mathcal{E}_{0\eta}$ at molecule 2 arising from the dipole moment $\alpha_{\lambda\eta}^{(1)}\mathcal{E}_{0\eta}$ induced in molecule 1 by the incident light wave field $\mathcal{E}_{0\eta}$.

Neglecting oscillating quadrupoles and higher order multipoles, and substituting for $\mu_\delta^{(2)}$ in equation (7.35) for the field gradient at molecule 1, yields only two terms whose contributions to B_ρ were found to significant enough for retention:

$$\mathcal{F}_{\beta\gamma}^{(1)} = T_{\beta\gamma\delta}^{(1)}\alpha_{\delta\varepsilon}^{(2)}\mathcal{E}_{0\varepsilon} + T_{\beta\gamma\delta}^{(1)}\alpha_{\delta\varepsilon}^{(2)}T_{\varepsilon\phi}^{(1)}\alpha_{\phi\lambda}^{(1)}\mathcal{E}_{0\lambda} + \cdots . \qquad (7.40)$$

Substituting equations (7.39) and (7.40) into (7.32) yields a final expression for the oscillating dipole moment induced on molecule 1 by the light wave field $\mathcal{E}_0$ in the presence of molecule 2:

$$\mu_\alpha^{(1)}(\mathcal{E}_0) = \alpha_{\alpha\eta}^{(1)}\mathcal{E}_{0\eta} + \alpha_{\alpha\beta}^{(1)}T_{\beta\gamma}\alpha_{\gamma\eta}^{(2)}\mathcal{E}_{0\eta} + \alpha_{\alpha\beta}^{(1)}T_{\beta\gamma}\alpha_{\gamma\delta}^{(2)}T_{\delta\varepsilon}\alpha_{\varepsilon\eta}^{(1)}\mathcal{E}_{0\eta} + \alpha_{\alpha\beta}^{(1)}T_{\beta\gamma}\alpha_{\gamma\delta}^{(2)}T_{\delta\varepsilon}\alpha_{\varepsilon\phi}^{(1)}T_{\phi\lambda}\alpha_{\lambda\eta}^{(2)}\mathcal{E}_{0\eta}$$

$$- \tfrac{1}{3}\alpha_{\alpha\beta}^{(1)}T_{\beta\gamma\delta}^{(1)}A_{\eta\gamma\delta}^{(2)}\mathcal{E}_{0\eta} + \tfrac{1}{3}\alpha_{\alpha\beta}^{(1)}T_{\beta\gamma}\alpha_{\gamma\delta}^{(2)}T_{\delta\varepsilon\phi}^{(1)}A_{\eta\varepsilon\phi}^{(1)}\mathcal{E}_{0\eta} - \tfrac{1}{3}\alpha_{\alpha\beta}^{(1)}T_{\beta\gamma}A_{\gamma\delta\varepsilon}^{(2)}T_{\delta\varepsilon\phi}^{(1)}\alpha_{\phi\eta}^{(1)}\mathcal{E}_{0\eta}$$

$$- \tfrac{1}{3}\alpha_{\alpha\beta}^{(1)}T_{\beta\gamma\delta}^{(1)}A_{\gamma\delta\varepsilon}^{(2)}T_{\varepsilon\phi}\alpha_{\phi\eta}^{(1)}\mathcal{E}_{0\eta} + \tfrac{1}{3}\alpha_{\alpha\beta}^{(1)}T_{\beta\gamma\delta}^{(1)}C_{\gamma\delta\varepsilon\phi}^{(2)}T_{\varepsilon\phi\lambda}^{(1)}\alpha_{\lambda\eta}^{(1)}\mathcal{E}_{0\eta}$$

$$+ \tfrac{1}{3}A_{\alpha\beta\gamma}^{(1)}T_{\beta\gamma\delta}^{(1)}\alpha_{\delta\eta}^{(2)}\mathcal{E}_{0\eta} + \tfrac{1}{3}A_{\alpha\beta\gamma}^{(1)}T_{\beta\gamma\delta}^{(1)}\alpha_{\delta\varepsilon}^{(2)}T_{\varepsilon\phi}\alpha_{\phi\eta}^{(1)}\mathcal{E}_{0\eta} + \cdots .$$

$$(7.41)$$

Differentiating equation (7.41) with respect to $\mathcal{E}_{0\eta}$ yields the following expression for the

differential polarizability, defined in equation (7.9):

$$\pi_{\alpha\eta}^{(p)} = \alpha_{\alpha\eta}^{(p)} + \alpha_{\alpha\beta}^{(p)}T_{\beta\gamma}\alpha_{\gamma\eta}^{(q)} + \alpha_{\alpha\beta}^{(p)}T_{\beta\gamma}\alpha_{\gamma\delta}^{(q)}T_{\delta\varepsilon}\alpha_{\varepsilon\eta}^{(p)} + \alpha_{\alpha\beta}^{(p)}T_{\beta\gamma}\alpha_{\gamma\delta}^{(q)}T_{\delta\varepsilon}\alpha_{\varepsilon\phi}^{(p)}T_{\phi\lambda}\alpha_{\lambda\eta}^{(q)}$$

$$- \frac{1}{3}\alpha_{\alpha\beta}^{(p)}T_{\beta\gamma\delta}^{(p)}A_{\eta\gamma\delta}^{(q)} + \frac{1}{3}\alpha_{\alpha\beta}^{(p)}T_{\beta\gamma}\alpha_{\gamma\delta}^{(q)}T_{\delta\varepsilon\phi}^{(p)}A_{\eta\varepsilon\phi}^{(p)} - \frac{1}{3}\alpha_{\alpha\beta}^{(p)}T_{\beta\gamma}A_{\gamma\delta\varepsilon}^{(q)}T_{\delta\varepsilon\phi}^{(p)}\alpha_{\phi\eta}^{(p)}$$

$$- \frac{1}{3}\alpha_{\alpha\beta}^{(p)}T_{\beta\gamma\delta}^{(p)}A_{\gamma\delta\varepsilon}^{(q)}T_{\varepsilon\phi}\alpha_{\phi\eta}^{(p)} + \frac{1}{3}\alpha_{\alpha\beta}^{(p)}T_{\beta\gamma\delta}^{(p)}C_{\gamma\delta\varepsilon\phi}^{(q)}T_{\varepsilon\phi\lambda}^{(p)}\alpha_{\lambda\eta}^{(p)} \tag{7.42}$$

$$+ \frac{1}{3}A_{\alpha\beta\gamma}^{(p)}T_{\beta\gamma\delta}^{(p)}\alpha_{\delta\eta}^{(q)} + \frac{1}{3}A_{\alpha\beta\gamma}^{(p)}T_{\beta\gamma\delta}^{(p)}\alpha_{\delta\varepsilon}^{(q)}T_{\varepsilon\phi}\alpha_{\phi\eta}^{(p)} + \cdots,$$

where the superscripts p and q indicate molecule p and q respectively. Using equation (7.42) in (7.29) yields:

$$\rho = \frac{a_2 + a_3 + a_4 + a_5 + a_2\mathcal{A}_1 + a_3\mathcal{A}_1 + a_3C_1 + \cdots}{b_2 + b_3}, \tag{7.43}$$

where

$$a_2 = \left\langle \alpha_{zx}^{(1)}\alpha_{zx}^{(1)} \right\rangle + \left\langle \alpha_{zx}^{(1)}\alpha_{zx}^{(2)} \right\rangle, \tag{7.44}$$

$$a_3 = 2\left\langle \alpha_{zx}^{(1)}\alpha_{z\beta}^{(1)}T_{\beta\gamma}\alpha_{\gamma x}^{(2)} \right\rangle + 2\left\langle \alpha_{zx}^{(1)}\alpha_{z\beta}^{(2)}T_{\beta\gamma}\alpha_{\gamma x}^{(1)} \right\rangle, \tag{7.45}$$

$$a_4 = \left\langle \alpha_{z\beta}^{(1)}T_{\beta\gamma}\alpha_{\gamma x}^{(2)}\alpha_{z\delta}^{(2)}T_{\delta\varepsilon}\alpha_{\varepsilon x}^{(1)} \right\rangle + \left\langle \alpha_{z\beta}^{(1)}T_{\beta\gamma}\alpha_{\gamma x}^{(2)}\alpha_{z\delta}^{(1)}T_{\delta\varepsilon}\alpha_{\varepsilon x}^{(2)} \right\rangle$$

$$+ 2\left\langle \alpha_{zx}^{(1)}\alpha_{z\beta}^{(2)}T_{\beta\gamma}\alpha_{\gamma\delta}^{(1)}T_{\delta\varepsilon}\alpha_{\varepsilon x}^{(2)} \right\rangle + 2\left\langle \alpha_{zx}^{(1)}\alpha_{z\beta}^{(1)}T_{\beta\gamma}\alpha_{\gamma\delta}^{(2)}T_{\delta\varepsilon}\alpha_{\varepsilon x}^{(1)} \right\rangle, \tag{7.46}$$

$$a_5 = 2\left\langle \alpha_{zx}^{(1)}\alpha_{z\beta}^{(1)}T_{\beta\gamma}\alpha_{\gamma\delta}^{(2)}T_{\delta\varepsilon}\alpha_{\varepsilon\phi}^{(1)}T_{\phi\lambda}\alpha_{\lambda x}^{(2)} \right\rangle + 2\left\langle \alpha_{zx}^{(1)}\alpha_{z\beta}^{(2)}T_{\beta\gamma}\alpha_{\gamma\delta}^{(1)}T_{\delta\varepsilon}\alpha_{\varepsilon\phi}^{(2)}T_{\phi\lambda}\alpha_{\lambda x}^{(1)} \right\rangle$$

$$+ 2\left\langle \alpha_{z\beta}^{(1)}T_{\beta\gamma}\alpha_{\gamma x}^{(2)}\alpha_{z\delta}^{(1)}T_{\delta\varepsilon}\alpha_{\varepsilon\phi}^{(2)}T_{\phi\lambda}\alpha_{\lambda x}^{(1)} \right\rangle + 2\left\langle \alpha_{z\beta}^{(1)}T_{\beta\gamma}\alpha_{\gamma x}^{(2)}\alpha_{z\delta}^{(2)}T_{\delta\varepsilon}\alpha_{\varepsilon\phi}^{(1)}T_{\phi\lambda}\alpha_{\lambda x}^{(2)} \right\rangle, \tag{7.47}$$

$$a_2\mathcal{A}_1 = -\frac{2}{3}\left\langle \alpha_{zx}^{(1)}\alpha_{z\beta}^{(1)}T_{\beta\gamma\delta}A_{x\gamma\delta}^{(2)} \right\rangle + \frac{2}{3}\left\langle \alpha_{zx}^{(1)}\alpha_{z\beta}^{(2)}T_{\beta\gamma\delta}A_{x\gamma\delta}^{(1)} \right\rangle$$

$$+ \frac{2}{3}\left\langle \alpha_{zx}^{(1)}A_{z\beta\gamma}^{(1)}T_{\beta\gamma\delta}\alpha_{\delta x}^{(2)} \right\rangle - \frac{2}{3}\left\langle \alpha_{zx}^{(1)}A_{z\beta\gamma}^{(2)}T_{\beta\gamma\delta}\alpha_{\delta x}^{(1)} \right\rangle, \tag{7.48}$$

$$a_3\mathcal{A}_1 = -\frac{2}{3}\left\langle \alpha_{zx}^{(1)}\alpha_{z\beta}^{(1)}T_{\beta\gamma}A_{\gamma\delta\varepsilon}^{(2)}T_{\delta\varepsilon\phi}\alpha_{\phi x}^{(1)}\right\rangle + \frac{2}{3}\left\langle \alpha_{zx}^{(1)}\alpha_{z\beta}^{(2)}T_{\beta\gamma}A_{\gamma\delta\varepsilon}^{(1)}T_{\delta\varepsilon\phi}\alpha_{\phi x}^{(2)}\right\rangle$$

$$-\frac{2}{3}\left\langle \alpha_{zx}^{(1)}\alpha_{z\beta}^{(1)}T_{\beta\gamma\delta}A_{\varepsilon\gamma\delta}^{(2)}T_{\varepsilon\phi}\alpha_{\phi x}^{(1)}\right\rangle + \frac{2}{3}\left\langle \alpha_{zx}^{(1)}\alpha_{z\beta}^{(2)}T_{\beta\gamma\delta}A_{\varepsilon\gamma\delta}^{(1)}T_{\varepsilon\phi}\alpha_{\phi x}^{(2)}\right\rangle$$

$$+\frac{2}{3}\left\langle \alpha_{zx}^{(1)}A_{z\beta\gamma}^{(1)}T_{\beta\gamma\delta}\alpha_{\delta\varepsilon}^{(2)}T_{\varepsilon\phi}\alpha_{\phi x}^{(1)}\right\rangle - \frac{2}{3}\left\langle \alpha_{zx}^{(1)}A_{z\beta\gamma}^{(2)}T_{\beta\gamma\delta}\alpha_{\delta\varepsilon}^{(1)}T_{\varepsilon\phi}\alpha_{\phi x}^{(2)}\right\rangle$$

$$\qquad (7.49)$$

$$+\frac{2}{3}\left\langle \alpha_{zx}^{(1)}\alpha_{z\beta}^{(1)}T_{\beta\gamma}\alpha_{gd}^{(2)}T_{\delta\varepsilon\phi}A_{x\varepsilon\phi}^{(1)}\right\rangle - \frac{2}{3}\left\langle \alpha_{zx}^{(1)}\alpha_{z\beta}^{(2)}T_{\beta\gamma}\alpha_{gd}^{(1)}T_{\delta\varepsilon\phi}A_{x\varepsilon\phi}^{(2)}\right\rangle$$

$$-\frac{2}{3}\left\langle \alpha_{z\beta}^{(1)}T_{\beta\gamma}\alpha_{\gamma x}^{(2)}\alpha_{z\delta}^{(1)}T_{\delta\varepsilon\phi}A_{x\varepsilon\phi}^{(2)}\right\rangle + \frac{2}{3}\left\langle \alpha_{z\beta}^{(1)}T_{\beta\gamma}\alpha_{\gamma x}^{(2)}\alpha_{z\delta}^{(2)}T_{\delta\varepsilon\phi}A_{x\varepsilon\phi}^{(1)}\right\rangle$$

$$+\frac{2}{3}\left\langle \alpha_{z\beta}^{(1)}T_{\beta\gamma}\alpha_{\gamma x}^{(2)}A_{z\delta\varepsilon}^{(1)}T_{\delta\varepsilon\phi}\alpha_{\phi x}^{(2)}\right\rangle - \frac{2}{3}\left\langle \alpha_{z\beta}^{(1)}T_{\beta\gamma}\alpha_{\gamma x}^{(2)}A_{z\delta\varepsilon}^{(2)}T_{\delta\varepsilon\phi}\alpha_{\phi x}^{(1)}\right\rangle,$$

$$a_3 C_1 = \frac{1}{3}\left\langle \alpha_{zx}^{(1)}\alpha_{z\beta}^{(1)}T_{\beta\gamma\delta}C_{\gamma\delta\varepsilon\phi}^{(2)}T_{\varepsilon\phi\lambda}\alpha_{\lambda x}^{(1)}\right\rangle + \frac{1}{3}\left\langle \alpha_{z\beta}^{(1)}T_{\beta\gamma\delta}C_{\gamma\delta\varepsilon\phi}^{(2)}T_{\varepsilon\phi\lambda}\alpha_{\lambda x}^{(1)}\alpha_{zx}^{(1)}\right\rangle$$

$$\qquad (7.50)$$

$$+\frac{1}{3}\left\langle \alpha_{zx}^{(1)}\alpha_{z\beta}^{(2)}T_{\beta\gamma\delta}C_{\gamma\delta\varepsilon\phi}^{(1)}T_{\varepsilon\phi\lambda}\alpha_{\lambda x}^{(2)}\right\rangle + \frac{1}{3}\left\langle \alpha_{z\beta}^{(1)}T_{\beta\gamma\delta}C_{\gamma\delta\varepsilon\phi}^{(2)}T_{\varepsilon\phi\lambda}\alpha_{\lambda x}^{(1)}\alpha_{zx}^{(2)}\right\rangle,$$

$$b_2 = \left\langle \alpha_{xx}^{(1)}\alpha_{xx}^{(1)}\right\rangle + \left\langle \alpha_{xx}^{(1)}\alpha_{xx}^{(2)}\cos\chi_{12}\right\rangle, \qquad (7.51)$$

$$b_3 = \left\langle \alpha_{xx}^{(1)}\alpha_{x\beta}^{(1)}T_{\beta\gamma}\alpha_{\gamma x}^{(2)}\right\rangle + \left\langle \alpha_{xx}^{(1)}\alpha_{x\beta}^{(2)}T_{\beta\gamma}\alpha_{\gamma x}^{(1)}\right\rangle. \qquad (7.52)$$

Here the notation $T_{\alpha\beta\gamma} = T_{\alpha\beta\gamma}^{(1)} = -T_{\alpha\beta\gamma}^{(2)}$ adopted in Section 2.3 has been used. In the $a_3\mathcal{A}_1$ term the last six components were not included in the work by Couling and Graham [9, 201], who first derived this term. The first two additional components are identically equal to components 5 and 6, which were evaluated by Couling and Graham, and the remaining four additional components, although not identical to the first four, are certainly similar and can be expected to have the same order of magnitude when evaluated. Thus, adding the six new terms is comparable to multiplying the original terms by a factor of two. We have included them at this point for completeness, but have not evaluated them numerically, since Couling and Graham showed the contribution of this term to be negligible, and included it only to establish convergence. In all our calculations we estimated the $a_3\mathcal{A}_1$ term by doubling the first six terms and found that the term remained negligible.

To proceed, the explicit forms of $T_{\alpha\beta}$, $T_{\alpha\beta\gamma}$, $\alpha_{\alpha\beta}$, $A_{\alpha\beta\gamma}$ and $C_{\alpha\beta\gamma\delta}$ are required.

7.1.3 B_ρ for linear molecules Check pg ?5

In molecule-fixed axes the polarizability α_{ij} is diagonal with $\alpha_{11} = \alpha_{22} = \alpha_\perp$ and $\alpha_{33} = \alpha_\parallel$. The component $\left\langle \alpha_{zx}^{(1)}\alpha_{zx}^{(1)}\right\rangle$ of the term a_2 in equation (7.44) has already been referred to molecule-fixed axes by the normal tensor-projection procedure in equation (7.23) of

Section 7.1.1. Similarly, the term $\left\langle \alpha_{xx}^{(1)}\alpha_{xx}^{(1)}\right\rangle$ in equation (7.51) has been referred to molecule-fixed axes in equation (7.24). Now, the remaining averages in equations (7.44) to (7.47), (7.51) and (7.52) must be referred to the diagonal elements of $\alpha_{ij}^{(1)}$ and $\alpha_{i'j'}^{(2)}$, and the interaction parameters described in Section 2.1.1. The A- and C- tensor components in equations (7.48) to (7.50) must also be referred to the independent elements of $A_{ijk}^{(1)}$ and $A_{i'j'k'}^{(2)}$, and $C_{ijkl}^{(1)}$ and $C_{i'j'k'l'}^{(2)}$ respectively.

Initially, all tensors are referred to the molecule-fixed axes of molecule 1 $O(1,2,3)$, including $\alpha_{ij}^{(2)}$ which is not generally diagonal. A projection from $O(1',2',3')$, where $\alpha_{i'j'}^{(2)}$ is diagonal, will be carried out later. The reason for initially referring all tensors to $O(1,2,3)$ is that for a given relative configuration of the pair of molecules the tensor product in $O(1,2,3)$ is fixed. By allowing the pair of molecules to rotate isotropically as a rigid whole in the space-fixed axes $O(x,y,z)$, the average projection of pair properties referred to $O(1,2,3)$ may be averaged into $O(x,y,z)$ over all orientations. Averaging over the interaction parameters τ of the pair may subsequently be performed.

The procedure for referring the terms to $O(1,2,3)$ is illustrated by a specific example: the term $\left\langle \alpha_{zx}^{(1)}\alpha_{z\beta}^{(1)}T_{\beta\gamma}\alpha_{\gamma\delta}^{(2)}T_{\delta\varepsilon}\alpha_{\varepsilon\phi}^{(1)}T_{\phi\lambda}\alpha_{\lambda x}^{(2)}\right\rangle$, which is the first term in a_5 given by equation (7.47). First the term must be projected from the space-fixed axes $O(x,y,z)$ into the molecule-fixed axes of molecule 1 as follows:

$$\left\langle \alpha_{zx}^{(1)}\alpha_{z\beta}^{(1)}T_{\beta\gamma}\alpha_{\gamma\delta}^{(2)}T_{\delta\varepsilon}\alpha_{\varepsilon\phi}^{(1)}T_{\phi\lambda}\alpha_{\lambda x}^{(2)}\right\rangle$$

$$= \left\langle \alpha_{ij}^{(1)}a_i^z a_j^x \alpha_{kl}^{(1)}a_k^z a_l^\beta T_{mn}a_m^\beta a_n^\gamma \alpha_{pq}^{(2)}a_p^\gamma a_q^\delta T_{rs}a_r^\delta a_s^\varepsilon \alpha_{tu}^{(1)}a_t^\varepsilon a_u^\phi T_{vw}a_v^\phi a_w^\lambda \alpha_{gh}^{(2)}a_g^\lambda a_h^x\right\rangle$$

$$= \left\langle \alpha_{ij}^{(1)}\alpha_{km}^{(1)}T_{mn}\alpha_{nr}^{(2)}T_{rs}\alpha_{sv}^{(1)}T_{vw}\alpha_{wh}^{(2)}\right\rangle \left\langle a_i^z a_k^z a_j^x a_h^x\right\rangle . \tag{7.53}$$

For a fixed interaction configuration the term $\left\langle \alpha_{ij}^{(1)}\alpha_{km}^{(1)}T_{mn}\alpha_{nr}^{(2)}T_{rs}\alpha_{sv}^{(1)}T_{vw}\alpha_{wh}^{(2)}\right\rangle$ is a constant, and if the rigid pair of molecules is allowed to rotate isotropically, then the standard isotropic average, given in equation (6.20), may be used to obtain the average projection:

$$\left\langle \alpha_{zx}^{(1)}\alpha_{z\beta}^{(1)}T_{\beta\gamma}\alpha_{\gamma\delta}^{(2)}T_{\delta\varepsilon}\alpha_{\varepsilon\phi}^{(1)}T_{\phi\lambda}\alpha_{\lambda x}^{(2)}\right\rangle$$

$$= \left\langle \alpha_{ij}^{(1)}\alpha_{km}^{(1)}T_{mn}\alpha_{nr}^{(2)}T_{rs}\alpha_{sv}^{(1)}T_{vw}\alpha_{wh}^{(2)}\right\rangle \frac{1}{30}(4\delta_{ik}\delta_{jh} - \delta_{ij}\delta_{kh} - \delta_{ih}\delta_{kj})$$

$$= \frac{1}{30}\left\langle 3\alpha_{ij}^{(1)}\alpha_{im}^{(1)}T_{mn}\alpha_{nr}^{(2)}T_{rs}\alpha_{sv}^{(1)}T_{vw}\alpha_{wj}^{(2)} - \alpha_{ii}^{(1)}\alpha_{km}^{(1)}T_{mn}\alpha_{nr}^{(2)}T_{rs}\alpha_{sv}^{(1)}T_{vw}\alpha_{wk}^{(2)}\right\rangle , \tag{7.54}$$

where the angular brackets now indicate an average over the pair interaction coordinates

R, θ_1, θ_2 and ϕ according to the general relationship:

$$\langle X \rangle = \int_\tau X P(\tau) \, d\tau, \tag{7.55}$$

in which the probability $P(\tau)$ that molecule 1 has a neighbour in the range $d\tau$ at τ has been related to the intermolecular potential in equation (1.4). Substituting into (7.55) yields:

$$\langle X \rangle = \frac{N_A}{2V_m} \int_{R=0}^{\infty} \int_{\theta_1=0}^{\pi} \int_{\theta_2=0}^{\pi} \int_{\phi=0}^{2\pi} X e^{-\frac{U_{12}}{kT}} R^2 \sin\theta_1 \sin\theta_2 \, dR d\theta_1 d\theta_2 d\phi. \tag{7.56}$$

Benoît and Stockmayer [203] were the first to establish the now familiar results:

$$\left\langle \alpha_{zx}^{(1)} \alpha_{zx}^{(2)} \right\rangle = \tfrac{1}{30} (\alpha_\parallel - \alpha_\perp)^2 \left\langle 3\cos^2\theta_{12} - 1 \right\rangle, \tag{7.57}$$

which is a contribution known as the angular correlation term; and

$$\left\langle \alpha_{xx}^{(1)} \alpha_{xx}^{(2)} \cos\chi_{12} \right\rangle = \tfrac{1}{15}\tfrac{2}{3} (\alpha_\parallel - \alpha_\perp)^2 \left\langle 3\cos^2\theta_{12} - 1 \right\rangle + \alpha^2 \left(\frac{-2B}{V_m} \right), \tag{7.58}$$

where B is the second pressure virial coefficient. Combining equations (7.23) and (7.57) and equations (7.24) and (7.58), yields the following expressions for the a_2 and b_2 terms defined in (7.44) and (7.51), respectively:

$$a_2 = \tfrac{1}{15}(\alpha_\parallel - \alpha_\perp)^2 + \tfrac{1}{30}(\alpha_\parallel - \alpha_\perp)^2 \left\langle 3\cos^2\theta_{12} - 1 \right\rangle, \tag{7.59}$$

$$b_2 = \alpha^2 + \tfrac{4}{45}(\alpha_\parallel - \alpha_\perp)^2 + \tfrac{2}{45}(\alpha_\parallel - \alpha_\perp)^2 \left\langle 3\cos^2\theta_{12} - 1 \right\rangle + \alpha^2 \left(\frac{-2B}{V_m} \right). \tag{7.60}$$

The property tensors of an linear molecule p may be expressed in terms of $\ell_i^{(p)}$, where $\ell_i^{(1)}$ and $\ell_i^{(2)}$ are the unit vectors along the principal axes of molecules 1 and 2, respectively [26].

Expressions for the A- and C- tensors and the T-tensors are given in equations (4.83), (4.84) and equations (4.85) to (4.87) of Section 4.4, respectively. The expression for the dynamic polarizability is expressed in equation (6.97) of Section 6.5.

Using these expressions for the molecular property tensors in equation (7.54) and similar equations for the other terms in the (7.43), yields lengthy expressions containing redundant interaction parameters $\ell_i^{(p)}$ and λ_i. Averaging according to equation (7.56) can only be performed after these interaction parameters have been eliminated using

equations (4.92) to (4.94) of Section 4.4. When this is done we find that:

$$a_3 = \frac{\alpha^3}{30(4\pi\varepsilon_0)} \left\langle R^{-3} \left\{ 36\kappa(\kappa-1) - 27\kappa(\kappa-1)(2\kappa+3)\cos^2\theta_1 + 27\kappa(\kappa-1)(2\kappa-1) \right. \right.$$

$$\left. \left. \times \cos^2\theta_2 - 324\kappa^2(\kappa+1)\cos\theta_1\cos\theta_2\cos\theta_{12} - 108\kappa^2(\kappa+1)\cos^2\theta_{12} \right\} \right\rangle, \qquad (7.61)$$

$$a_4 = \frac{\alpha^4}{30(4\pi\varepsilon_0)^2} \left\langle R^{-6} \left\{ 324\kappa^2(\kappa^2-2\kappa+1)\cos^4\theta_1 + 1944\kappa^3(\kappa-1)\cos^3\theta_1\cos\theta_2\cos\theta_{12} \right. \right.$$

$$+ \left((5103\kappa^4\cos^2\theta_{12} + 81\kappa^2(17\kappa^2+8\kappa+20))\cos^2\theta_2 + 405\kappa^3(\kappa-1)\cos^2\theta_{12}\right.$$

$$- 27\kappa\left(12\kappa^3-22\kappa^2+17\kappa-7\right)\right)\cos^2\theta_1 + \left(1944\kappa^3(\kappa-1)\cos^3\theta_2\cos\theta_{12}\right.$$

$$+ \left.(3402\kappa^4\cos^3\theta_{12} - 162\kappa^2(4\kappa^2-14\kappa-5)\cos\theta_{12})\cos\theta_2\right)\cos\theta_1$$

$$+ 324\kappa^2(\kappa^2-2\kappa+1)\cos^4\theta_2 + \left(405\kappa^3(\kappa-1)\cos^2\theta_{12} - 27\kappa(8\kappa^3-24\kappa^2\right.$$

$$+ \left. 21\kappa-5)\right)\cos^2\theta_2 + 567\kappa^4\cos^4\theta_{12} - 27\kappa^2(9\kappa^2-10\kappa-14)\cos^2\theta_{12}$$

$$+ \left. 18(2\kappa^4-9\kappa^3+11\kappa^2-6\kappa+2)\right\} \right\rangle, \qquad (7.62)$$

$$a_5 = \frac{9\alpha^5}{30(4\pi\varepsilon_0)^3} \left\langle R^{-9} \left\{ 243\kappa^3(\kappa^2-2\kappa+1)\cos^6\theta_1 + 1458\kappa^4(\kappa-1)\cos^5\theta_1\cos\theta_2\cos\theta_{12} \right. \right.$$

$$+ 9\kappa^2\left(27\kappa^2(9\kappa\cos^2\theta_2 + 2\kappa-2)\cos^2\theta_{12} - 9\kappa(7\kappa^2+25\kappa-23)\cos^2\theta_2\right.$$

$$- \left. 23\kappa^3+75\kappa^2-81\kappa+29\right)\cos^4\theta_1 + 27\kappa^3\cos\theta_2\cos\theta_{12}\left(54\kappa^2\cos^2\theta_{12}\right.$$

$$- \left.(54\kappa(2\kappa+5)\cos^2\theta_2 + 52\kappa^2-23\kappa-11)\right)\cos^3\theta_1 + 3\kappa\left(81\kappa^4\cos^4\theta_{12}\right.$$

$$- 3\kappa^2(243\kappa(2\kappa+3)\cos^2\theta_2 + 32\kappa^2-22\kappa-1)\cos^2\theta_{12} + 81\kappa^2(\kappa^2-7\kappa+6)\cos^4\theta_2$$

$$- \left. 3\kappa(\kappa^3-228\kappa^2+225\kappa-55)\cos^2\theta_2 + 36\kappa^4-115\kappa^3+159\kappa^2-117\kappa+37\right)\cos^2\theta_1$$

$$- 9\kappa^2\cos\theta_2\cos\theta_{12}\left(27\kappa^2(7\kappa+9)\cos^2\theta_{12} + 9\kappa(\kappa^2+3\kappa-4)\cos^2\theta_2 - (55\kappa^3+70\kappa^2\right.$$

$$- \left. 86\kappa-21)\right)\cos\theta_1 - 27\kappa^4(7\kappa+10)\cos^4\theta_{12} + 3\kappa^2(35\kappa^3+50\kappa^2-52\kappa-24)$$

$$\times \cos^2\theta_{12} - 27\kappa^2(5\kappa^3-14\kappa^2+13\kappa-4)\cos^4\theta_2 + 3\kappa(29\kappa^4-118\kappa^3+168\kappa^2$$

$$- \left. 98\kappa+19)\cos^2\theta_2 - 8\left(2\kappa^5-7\kappa^4+13\kappa^3-14\kappa^2+7\kappa-1\right)\right\} \right\rangle, \qquad (7.63)$$

$$a_2 \mathcal{A}_1 = -\frac{\alpha^2}{60(4\pi\varepsilon_0)} \Big\langle R^{-4} \Big\{ A_\perp \Big[180\kappa(\kappa-1)\cos^3\theta_2 + \cos\theta_1 \big((540\kappa^2 - 540\kappa(\kappa-1)) \Big.$$

$$\times \cos\theta_{12} + 216\kappa^2\cos^2\theta_{12} - 108\kappa(\kappa+1)\cos\theta_{12} - 216\kappa^2 + 108\kappa\big) - \big(216\kappa(\kappa+1)$$

$$\times \cos^2\theta_{12} - 108\kappa^2\cos\theta_{12} - 216\kappa\big)\cos\theta_2 + 540\kappa(\kappa\cos\theta_{12} - \kappa - 1)\cos^2\theta_1\cos\theta_2$$

$$+ 180\kappa(\kappa-1)\cos^3\theta_1\Big] + A_\parallel \Big[-135\kappa(\kappa-1)\cos^3\theta_2 + \big(405\kappa(\kappa+1)\cos^2\theta_2$$

$$\times \cos\theta_{12} + 324\kappa^2\cos^2\theta_{12} - 81\kappa(\kappa+1)\cos\theta_{12} - 162\kappa(\kappa-1)\big)\cos\theta_1$$

$$+ \big(162\kappa(\kappa+1)\cos^2\theta_{12} - 162\kappa^2\cos\theta_{12} + 81\kappa(\kappa-1)\big)\cos\theta_2$$

$$+ 810\kappa^2\cos^2\theta_1\cos\theta_2\cos\theta_{12} + 270\kappa(\kappa-1)\cos^3\theta_1\Big]\Big\}\Big\rangle, \tag{7.64}$$

$$a_3 \mathcal{A}_1 = -\frac{\alpha^3}{60(4\pi\varepsilon_0)^2} \Big\langle R^{-7} \Big\{ A_\perp \Big[12\kappa \big(135(\kappa-1)^2\cos^5\theta_1 + 810\kappa(\kappa-1)\cos^4\theta_1 \Big.$$

$$\times \cos\theta_2\cos\theta_{12} + (27\kappa(45\kappa\cos^2\theta_2 + 11(\kappa-1))\cos^2\theta_{12} - 45\kappa(\kappa+8)\cos^2\theta_2$$

$$- 182(\kappa-1)^2)\cos^3\theta_1 + 3(297\kappa^2\cos^3\theta_{12} - \kappa(236\kappa - 137)\cos\theta_{12}$$

$$+ (9\kappa^2(3\cos^2\theta_{12} + 1) + 2\kappa + 4)(15\cos^2\theta_2 - 7))\cos^2\theta_1\cos\theta_2 + 3(54\kappa^2\cos^4\theta_{12}$$

$$+ 27\kappa^2(11\cos^2\theta_2 - 2)\cos^3\theta_{12} - \kappa(189\kappa\cos^2\theta_2 + 5(13\kappa - 4))\cos^2\theta_{12}$$

$$+ (270\kappa(\kappa-1)\cos^4\theta_2 - (126\kappa^2 - 247\kappa - 44)\cos^2\theta_2 - 22\kappa - 8)\cos\theta_{12}$$

$$+ 7\kappa(\kappa+8)\cos^2\theta_2 + 20\kappa^2 - 30\kappa + 19)\cos\theta_1 + 162\kappa^2\cos\theta_2\cos^3\theta_{12}(\cos\theta_{12} - 1)$$

$$+ 3\big(99\kappa(\kappa-1)\cos^2\theta_2 - (45\kappa^2 - 40\kappa - 8)\big)\cos\theta_2\cos^2\theta_{12} + 6\kappa(10\kappa - 1)\cos\theta_2$$

$$\times \cos\theta_{12} + (\kappa-1)^2(135\cos^2\theta_2 - 190)\cos^3\theta_2 + 3(14\kappa^2 - 48\kappa + 19)\cos\theta_2\Big]$$

$$+ A_\parallel \Big[-9\kappa \big(135(\kappa-1)^2\cos^5\theta_1 + 810\kappa(\kappa-1)\cos^4\theta_1\cos\theta_2\cos\theta_{12}$$

$$+ (27\kappa(45\kappa\cos^2\theta_2 + 11\kappa(\kappa-1))\cos^2\theta_{12} + 45\kappa(5\kappa - 2)\cos^2\theta_2 - 2(85\kappa^2 - 146\kappa$$

$$+ 61))\cos^3\theta_1 + 3(297\kappa^2\cos^3\theta_{12} + 81\kappa^2(5\cos^2\theta_2 - 1)\cos^2\theta_{12} - \kappa(98\kappa - 131)$$

$$\times \cos\theta_{12} + 3(9\kappa^2 + 2\kappa + 4)(5\cos^2\theta_2 - 1))\cos^2\theta_1\cos\theta_2 + 3(54\kappa^2\cos^4\theta_{12} + 27\kappa^2$$

$$\times (11\cos^2\theta_2 - 1)\cos^3\theta_{12} - \kappa(81\kappa\cos^2\theta_2 + 35\kappa - 41)\cos^2\theta_{12} + (270\kappa(\kappa-1)$$

$$\times \cos^4\theta_2 - (54\kappa^2 - 175\kappa - 44)\cos^2\theta_2 - (11\kappa + 4))\cos\theta_{12} - 3(\kappa(5\kappa - 2)\cos^2\theta_2$$

$$- 3(\kappa - 1)^2)) \cos\theta_1 + (162\kappa^2 \cos^4\theta_{12} - 81\kappa^2 \cos^3\theta_{12} + 3(99\kappa(\kappa - 1) \cos^2\theta_2$$

$$- (27\kappa^2 - 49\kappa - 8)) \cos^2\theta_{12} + 3\kappa(4\kappa - 7) \cos\theta_{12} + (\kappa - 1)^2(135 \cos^4\theta_2$$

$$- 154 \cos^2\theta_2 + 27)) \cos\theta_2)]\}\rangle, \tag{7.65}$$

$$a_3 C_1 = \frac{\alpha^3}{10(4\pi\varepsilon_0)^2} \Big\langle R^{-8} \big\{ 6C_{3333}\kappa \big[150(\kappa - 1)^2 \cos^6\theta_1 + 900\kappa(\kappa - 1) \cos^5\theta_1 \cos\theta_2 \cos\theta_{12}$$

$$+ 5 \left(30\kappa(9\kappa \cos^2\theta_{12} - \kappa - 2) \cos^2\theta_2 + 72\kappa(\kappa - 1) \cos^2\theta_{12} - 35(\kappa - 1)^2 \right) \cos^4\theta_1$$

$$+ 30\kappa \cos\theta_{12}(36\kappa \cos^2\theta_{12} - 25\kappa + 13) \cos^3\theta_1 \cos\theta_2 + 3 \left(50(3\kappa^2 + 2\kappa + 1) \cos^4\theta_2 \right.$$

$$- 15(9\kappa^2 \cos^2\theta_{12} + 2\kappa^2 + 1) \cos^2\theta_2 + 72\kappa^2 \cos^4\theta_{12} - 5\kappa(13\kappa - 10) \cos^2\theta_{12} + 16\kappa^2$$

$$- 28\kappa + 15 \big) \cos^2\theta_1 + 6 \left(20(3\kappa^2 + 2\kappa + 1) \cos^2\theta_2 - 18\kappa^2 \cos^2\theta_{12} + (5\kappa^2 - 9\kappa \right.$$

$$- 2)) \cos\theta_1 \cos\theta_2 \cos\theta_{12} - 10(\kappa - 1)^2 \cos^4\theta_2 + 3 \left((33\kappa^2 + 16\kappa + 8) \cos^2\theta_{12} \right.$$

$$+ 2\kappa^2 + 1 \big) \cos^2\theta_2 + 27\kappa^2 \cos^4\theta_{12} - 3(7\kappa^2 - 1) \cos^2\theta_{12} - (2\kappa + 1)^2 \big]$$

$$- 24C_{1313}\kappa \big[75(\kappa - 1)^2 \cos^6\theta_1 + 450\kappa(\kappa - 1) \cos^5\theta_1 \cos\theta_2 \cos\theta_{12}$$

$$+ 5 \left(15\kappa(9\kappa \cos^2\theta_{12} - \kappa - 2) \cos^2\theta_2 + 2(18\kappa(\kappa - 1) \cos^2\theta_{12} - 11(\kappa - 1)^2) \right) \cos^4\theta_1$$

$$+ 30\kappa(18\kappa \cos^2\theta_{12} - 17\kappa + 11) \cos^3\theta_1 \cos\theta_2 \cos\theta_{12} + 3 \left(25(3\kappa^2 + 2\kappa + 1) \cos^4\theta_2 \right.$$

$$- 15(9\kappa^2 \cos^2\theta_{12} + 2\kappa^2 + 1) \cos^2\theta_2 + 36\kappa^2 \cos^4\theta_{12} - \kappa(55\kappa - 34) \cos^2\theta_{12}$$

$$+ 14\kappa^2 - 24\kappa + 13 \big) \cos^2\theta_1 + 12 \left(5(3\kappa^2 + 2\kappa + 1) \cos^2\theta_2 - 2(9\kappa^2 \cos^2\theta_{12} - \kappa^2 \right.$$

$$+ 3\kappa + 1)) \cos\theta_1 \cos\theta_2 \cos\theta_{12} - 5(\kappa - 1)^2 \cos^4\theta_2 - 3 \left(4(3\kappa^2 + 2\kappa + 1) \cos^2\theta_{12} \right.$$

$$- \kappa^2 - 6\kappa + 1 \big) \cos^2\theta_2 + 27\kappa^2 \cos^4\theta_{12} - 3(4\kappa^2 - 6\kappa - 1) \cos^2\theta_{12} + (\kappa - 1)^2 \big]$$

$$+ 6C_{1111}\kappa \big[75(\kappa - 1)^2 \cos^6\theta_1 + 450\kappa(\kappa - 1) \cos^5\theta_1 \cos\theta_2 \cos\theta_{12}$$

$$+ 5 \left(15\kappa(9\kappa \cos^2\theta_{12} - \kappa - 2) \cos^2\theta_2 + 36\kappa(\kappa - 1) \cos^2\theta_{12} - 31(\kappa - 1)^2 \right) \cos^4\theta_1$$

$$+ 60\kappa(9\kappa \cos^2\theta_{12} - 13\kappa + 10) \cos^3\theta_1 \cos\theta_2 \cos\theta_{12} + 3 \left(25(3\kappa^2 + 2\kappa + 1) \cos^4\theta_2 \right.$$

$$- 30(9\kappa^2 \cos^2\theta_{12} + 2\kappa^2 + 1) \cos^2\theta_2 + 36\kappa^2 \cos^4\theta_{12} - 4\kappa(25\kappa - 13) \cos^2\theta_{12}$$

$$+ 2 \left(25\kappa^2 - 22\kappa + 18 \right)) \cos^2\theta_1 + 30 \left(2(3\kappa^2 + 2\kappa + 1) \cos^2\theta_2 - 18\kappa^2 \cos^2\theta_{12} + 5\kappa^2 \right.$$

$$- 9\kappa - 2)) \cos\theta_1 \cos\theta_2 \cos\theta_{12} - 5(\kappa - 1)^2 \cos^4\theta_2 + 3 \left((57\kappa^2 + 8\kappa + 4) \cos^2\theta_{12} \right.$$

$$- 11\kappa^2 - 30\kappa + 2) \cos^2 \theta_2 - 108\kappa^2 \cos^4 \theta_{12} + 12(7\kappa^2 - 1) \cos^2 \theta_{12}$$

$$- 2 \ (\kappa^2 - 26\kappa + 7)]\}\rangle, \tag{7.66}$$

where the equation (7.65) describes the first six terms of $a_3 \mathcal{A}_1$ in (7.49), as derived by Couling and Graham [201].

By substituting equations (7.59) to (7.66) into equation (7.43), ρ takes the form:

$$\rho = \left[\frac{1}{15}(\Delta\alpha)^2 + \frac{1}{30}(\Delta\alpha)^2 \left\langle 3\cos^2 \theta_{12} - 1 \right\rangle + \frac{\alpha^3}{30(4\pi\varepsilon_0)} a_3' + \frac{\alpha^4}{30(4\pi\varepsilon_0)^2} a_4' + \frac{\alpha^5}{30(4\pi\varepsilon_0)^3} a_5' \right.$$

$$\left. + \frac{\alpha^2}{60(4\pi\varepsilon_0)} a_2 \mathcal{A}_1' + \frac{\alpha^3}{60(4\pi\varepsilon_0)^2} a_3 \mathcal{A}_1' + \frac{3\alpha^3}{30(4\pi\varepsilon_0)^2} a_3 C_1' + \cdots \right] \Bigg/$$

$$\left[\frac{1}{15} \left(15\alpha^2 + \frac{4}{3}(\Delta\alpha)^2 \right) + \frac{2}{45}(\Delta\alpha)^2 \left\langle 3\cos^2 \theta_{12} - 1 \right\rangle + \frac{\alpha^3}{30(4\pi\varepsilon_0)} b_3' + \alpha^2 \left(\frac{-2B}{V_m} \right) \right], \tag{7.67}$$

in which a_3' represents the part of a_3 in equation (7.61) contained within the angular brackets, with similar definitions for a_4', a_5', $a_2 \mathcal{A}_1'$, $a_3 \mathcal{A}_1'$ and $a_3 C_1'$ which occur in equations (7.62) to (7.66).

Equation (7.67) must now be expressed in the virial form of equation (7.103). We have from equation (7.25):

$$\rho_0 = \frac{3(\Delta\alpha)^2}{45\alpha^2 + 4(\Delta\alpha)^2}. \tag{7.68}$$

This allows equation (7.67) to be written in the form:

$$\rho = \rho_0 \left[1 + \frac{1}{2} \left\langle 3\cos^2 \theta_{12} - 1 \right\rangle + \frac{\alpha^3}{2(4\pi\varepsilon_0)(\Delta\alpha)^2} a_3' + \frac{\alpha^4}{2(4\pi\varepsilon_0)^2(\Delta\alpha)^2} a_4' + \frac{\alpha^5}{2(4\pi\varepsilon_0)^3(\Delta\alpha)^2} a_5' \right.$$

$$\left. + \frac{\alpha^2}{4(4\pi\varepsilon_0)(\Delta\alpha)^2} a_2 \mathcal{A}_1' + \frac{\alpha^3}{4(4\pi\varepsilon_0)^2(\Delta\alpha)^2} a_3 \mathcal{A}_1' + \frac{3\alpha^3}{2(4\pi\varepsilon_0)^2(\Delta\alpha)^2} a_3 C_1' + O\left(\frac{1}{V_m^2} \right) \right] \Bigg/$$

$$\left\{ 1 + \frac{4}{3}\rho_0 \left[\frac{1}{2} \left\langle 3\cos^2 \theta_{12} - 1 \right\rangle + \frac{3\alpha^3}{8(4\pi\varepsilon_0)(\Delta\alpha)^2} b_3' + \frac{2B}{V_m} + O\left(\frac{1}{V_m^2} \right) \right] \right\}, \tag{7.69}$$

133

which reduces to

$$\rho = \rho_0 + \rho_0(1 - \tfrac{4}{3}\rho_0)\left[\frac{2B}{V_m} + \tfrac{1}{2}\left\langle 3\cos^2\theta_{12} - 1\right\rangle + \frac{\alpha(1 + \tfrac{4}{5}\kappa^2)}{18(4\pi\varepsilon_0)\kappa^2}a_3' + \frac{\alpha^2(1 + \tfrac{4}{5}\kappa^2)}{18(4\pi\varepsilon_0)^2\kappa^2}a_4'\right.$$

$$+ \frac{\alpha^3(1 + \tfrac{4}{5}\kappa^2)}{18(4\pi\varepsilon_0)^3\kappa^2}a_5' + \frac{(1 + \tfrac{4}{5}\kappa^2)}{36(4\pi\varepsilon_0)\kappa^2}a_2\mathcal{A}_1' + \frac{\alpha(1 + \tfrac{4}{5}\kappa^2)}{36(4\pi\varepsilon_0)^2\kappa^2}a_3\mathcal{A}_1' + \frac{\alpha(1 + \tfrac{4}{5}\kappa^2)}{6(4\pi\varepsilon_0)^2\kappa^2}a_3C_1'$$

$$\left. - \frac{\alpha}{30(4\pi\varepsilon_0)}b_3' + O\left(\frac{1}{V_m^2}\right)\right]. \tag{7.70}$$

It follows from equations (7.103) and (7.70) that:

$$B_\rho = \rho_0(1 - \tfrac{4}{3})\left(2B + \mathsf{G} + \mathsf{a}_3 + \mathsf{a}_4 + \mathsf{a}_5 + \mathsf{a}_2\mathsf{A}_1 + \mathsf{a}_3\mathsf{A}_1 + \mathsf{a}_3\mathsf{C}_1 + \mathsf{b}_3 + \cdots\right), \tag{7.71}$$

where

$$\mathsf{G} = \tfrac{1}{2}\left\langle 3\cos^2\theta_{12} - 1\right\rangle V_m, \tag{7.72}$$

$$\mathsf{a}_3 = \frac{\alpha(1 + \tfrac{4}{5}\kappa^2)}{18(4\pi\varepsilon_0)\kappa^2}V_m a_3', \tag{7.73}$$

$$\mathsf{a}_4 = \frac{\alpha^2(1 + \tfrac{4}{5}\kappa^2)}{18(4\pi\varepsilon_0)^2\kappa^2}V_m a_4', \tag{7.74}$$

$$\mathsf{a}_5 = \frac{\alpha^3(1 + \tfrac{4}{5}\kappa^2)}{18(4\pi\varepsilon_0)^3\kappa^2}V_m a_5', \tag{7.75}$$

$$\mathsf{a}_2\mathsf{A}_1 = \frac{(1 + \tfrac{4}{5}\kappa^2)}{36(4\pi\varepsilon_0)\kappa^2}V_m a_2\mathcal{A}_1', \tag{7.76}$$

$$\mathsf{a}_3\mathsf{A}_1 = \frac{\alpha(1 + \tfrac{4}{5}\kappa^2)}{36(4\pi\varepsilon_0)^2\kappa^2}V_m a_3\mathcal{A}_1', \tag{7.77}$$

$$\mathsf{a}_3\mathsf{C}_1 = \frac{\alpha(1 + \tfrac{4}{5}\kappa^2)}{6(4\pi\varepsilon_0)^2\kappa^2}V_m a_3C_1', \tag{7.78}$$

$$\text{and} \qquad \mathsf{b}_3 = -\frac{\alpha}{30(4\pi\varepsilon_0)}V_m b_3'. \tag{7.79}$$

As with the normal second pressure virial coefficient B, the above eight coefficients are independent of the molar volume but dependent on temperature. The second light scattering virial coefficient is directly accessible from a plot of experimentally measured ρ versus $\frac{1}{V_m}$ values. If ρ_0 is known, then one may calculate:

$$B_\rho' = \left(2B + \mathsf{G} + \mathsf{a}_3 + \mathsf{a}_4 + \mathsf{a}_5 + \mathsf{a}_2\mathsf{A}_1 + \mathsf{a}_3\mathsf{A}_1 + \mathsf{a}_3\mathsf{C}_1 + \mathsf{b}_3 + \cdots\right). \tag{7.80}$$

The appearance of $2B$ in this expression for B'_ρ can mask the more interesting contributions from the remaining terms, which are summed to allow comparison with $2B$, giving

$$B'_\rho = (2B + \mathcal{S}_\rho),\qquad(7.81)$$

where the sum $\mathcal{S}_\rho$ arises purely from angular correlation, dipole-dipole, field-gradient, and induced quadrupole moment effects in the molecular interaction.

7.1.4 B_ρ for non-linear molecules

There are no literature values for the A- and C-tensor components for non-linear molecules, so that the contributions arising from the $a_2\mathcal{A}_1$, $a_3\mathcal{A}_1$ and a_3C_1 terms cannot be calculated. Calculations by Couling and Graham for linear and quasi-linear molecules [201], showed that the a_3C_1 term contributed less than 0.3% to the second light-scattering virial coefficient for *all* linear molecules studied, and our own calculations yield similar results (see Tables 8.8, 8.17 and 8.34). Thus, the omission of this term should not be significant. However, Couling and Graham [201] showed that the $a_2\mathcal{A}_1$ term, which only exists for polar molecules since the A-tensor is zero for non-polar molecules, can make significant contributions to B_ρ of as much as 9%. The contribution of the higher-order $a_3\mathcal{A}_1$ term was found to be less than 1% for the linear dipolar molecules investigated [201], and can thus be assumed to be negligible. The problem of the possible significance of the $a_2\mathcal{A}_1$ term cannot be solved until *ab initio* calculated estimates of the A-tensor components of non-linear polar molecules become available.

The averages in equations (7.44) to (7.47), (7.51) and (7.52) must be expressed in terms of the elements of the diagonal tensors $\alpha_{ij}^{(1)} = \alpha_{i'j'}^{(2)}$ as given in equation (6.108), and the seven interaction parameters R, α_1, β_1, γ_1, α_2, β_2 and γ_2, described in Section 2.1.2. As for linear molecules, all tensors must initially be referred to the molecule-fixed axes $O(1,2,3)$ of molecule 1, to ensure that for a given relative configuration of the pair of interacting molecules the tensor product in $O(1,2,3)$ is fixed. If the pair of molecules is allowed to rotate isotropically as a rigid whole in the space-fixed axes $O(x,y,z)$, the average projection of pair properties referred to $O(1,2,3)$ into $O(x,y,z)$ may be averaged over all orientations. Averaging over the interaction parameters τ of the pair may subsequently be carried out, the average $\langle X \rangle$ of the pair property X over the interaction coordinates following from the probability in equation (1.4):

$$\langle X \rangle = \frac{N_A}{16\pi^3 V_m} \int\limits_{R=0}^{\infty} \int\limits_{\alpha_1=0}^{2\pi} \int\limits_{\beta_1=0}^{\pi} \int\limits_{\gamma_1=0}^{2\pi} \int\limits_{\alpha_2=0}^{2\pi} \int\limits_{\beta_2=0}^{\pi} \int\limits_{\gamma_2=0}^{2\pi} X e^{-\frac{U_{12}}{kT}}$$

$$\times R^2 \sin\beta_1 \sin\beta_2 \, dR \, d\alpha_1 \, d\beta_1 \, d\gamma_1 \, d\alpha_2 \, d\beta_2 \, d\gamma_2.\qquad(7.82)$$

135

The term $\left\langle \alpha_{zx}^{(1)} \alpha_{zx}^{(2)} \right\rangle$ from equation (7.44) is now referred to molecule-fixed axes:

$$\left\langle \alpha_{zx}^{(1)} \alpha_{zx}^{(2)} \right\rangle = \left\langle \alpha_{ij}^{(1)} \alpha_{kl}^{(2)} \right\rangle \left\langle a_i^z a_k^z a_j^x a_l^x \right\rangle$$

$$= \tfrac{1}{30} \left\langle 3\alpha_{ij}^{(1)} \alpha_{ij}^{(2)} - 9\alpha^2 \right\rangle, \qquad (7.83)$$

where $\alpha_{ij}^{(2)}$, the polarizability tensor of molecule 2 expressed in the molecule-fixed axes of molecule 1, is given by equation (6.108) in Section 6.6. Thus, the angular brackets in equation (7.83) may be written as:

$$\left\langle 3\alpha_{ij}^{(1)} \alpha_{ij}^{(2)} - 9\alpha^2 \right\rangle = \left\langle 3(\alpha_{11}Z_{11} + \alpha_{22}Z_{22} + \alpha_{33}Z_{33}) - 9\alpha^2 \right\rangle, \qquad (7.84)$$

where Z_{11}, Z_{22} and Z_{33} are defined in equations (6.109), (6.110) and (6.111) of Section 6.6.

Couling and Graham [9, 36] referred the $\left\langle \alpha_{xx}^{(1)} \alpha_{xx}^{(2)} \cos \chi_{12} \right\rangle$ term from equation (7.51) to molecule-fixed axes using a procedure analogous to that of Benoît and Stockmayer [203] and Graham [200], to obtain:

$$\left\langle \alpha_{xx}^{(1)} \alpha_{xx}^{(2)} \cos \chi_{12} \right\rangle = \tfrac{2}{45} \left\langle 3\alpha_{ij}^{(1)} \alpha_{ij}^{(2)} - 9\alpha^2 \right\rangle + \alpha^2 \left(\frac{-2B}{V_m} \right)$$

$$= \tfrac{2}{45} \left\langle 3(\alpha_{11}Z_{11} + \alpha_{22}Z_{22} + \alpha_{33}Z_{33}) - 9\alpha^2 \right\rangle + \alpha^2 \left(\frac{-2B}{V_m} \right), \qquad (7.85)$$

where B is the second pressure virial coefficient.

The procedure for referring the higher-order terms to O(1,2,3), and averaging over all orientations of the average projection of the pair properties into O(x,y,z), is demonstrated in Section 7.1.3. This procedure yields terms of the form:

$$\left\langle \alpha_{zx}^{(1)} \alpha_{z\beta}^{(1)} T_{\beta\gamma} \alpha_{\gamma\delta}^{(2)} T_{\delta\varepsilon} \alpha_{\varepsilon\phi}^{(1)} T_{\phi\lambda} \alpha_{\lambda x}^{(2)} \right\rangle$$

$$= \tfrac{1}{30} \left\langle 3\alpha_{ij}^{(1)} \alpha_{im}^{(1)} T_{mn} \alpha_{nr}^{(2)} T_{rs} \alpha_{sv}^{(1)} T_{vw} \alpha_{wj}^{(2)} - \alpha_{ii}^{(1)} \alpha_{km}^{(1)} T_{mn} \alpha_{nr}^{(2)} T_{rs} \alpha_{sv}^{(1)} T_{vw} \alpha_{wk}^{(2)} \right\rangle, \qquad (7.86)$$

where the angular brackets indicate an average over the pair interaction coordinates R, α_1, β_1, γ_1, α_2, β_2 and γ_2 according to equation (7.82), and $\alpha_{ij}^{(1)}$, $\alpha_{ij}^{(2)}$ and T_{ij} are given by equation (6.108) in Section 6.6, and equation (4.145) in Section 4.5.

Once the Macsyma tensor manipulation facilities are invoked to evaluate the averages such as in equation (7.86), we obtain the following expressions for the terms in

136

equation (7.43):

$$b_3 = \frac{1}{15(4\pi\varepsilon_0)} \left\langle R^{-3} \left\{ \alpha_{11}(6\alpha + 4\alpha_{11})(Z_{11}T_{11} + Z_{12}T_{12} + Z_{13}T_{13}) + \alpha_{22}(6\alpha + 4\alpha_{22})(Z_{12}T_{12} \right. \right.$$

$$\left. \left. + Z_{22}T_{22} + Z_{23}T_{23}) + \alpha_{33}\ (6\alpha + 4\alpha_{33})(Z_{13}T_{13} + Z_{23}T_{23} + Z_{33}T_{33}) \right\} \right\rangle, \tag{7.87}$$

$$a_3 = \frac{1}{30(4\pi\varepsilon_0)} \left\langle R^{-3} \left\{ \alpha_{11}(3\alpha_{11} - 4\alpha)(Z_{11}T_{11} + Z_{12}T_{12} + Z_{13}T_{13}) + \alpha_{22}(3\alpha_{22} - 4\alpha)(Z_{12}T_{12} \right. \right.$$

$$+ Z_{22}T_{22} + Z_{23}T_{23}) + \alpha_{33}(3\alpha_{33} - 4\alpha)(Z_{13}T_{13} + Z_{23}T_{23} + Z_{33}T_{33}) + \alpha_{11}\left(T_{11}(Z_{11}^2\right.$$

$$\left. + Z_{12}^2 + Z_{13}^2) + T_{12}(Z_{11}Z_{12} + Z_{12}Z_{22} + Z_{13}Z_{23}) + T_{13}(Z_{11}Z_{13} + Z_{12}Z_{23} + Z_{13}Z_{33})\right)$$

$$+ \alpha_{22}\left(T_{12}(Z_{11}Z_{12} + Z_{12}Z_{22} + Z_{13}Z_{23}) + T_{22}(Z_{12}^2 + Z_{22}^2 + Z_{23}^2) + T_{23}(Z_{12}Z_{13}\right.$$

$$\left. + Z_{22}Z_{23} + Z_{23}Z_{33})\right) + \alpha_{33}\left(T_{13}(Z_{11}Z_{13} + Z_{12}Z_{23} + Z_{13}Z_{33}) + T_{23}(Z_{12}Z_{13}\right.$$

$$\left. \left. \left. + Z_{22}Z_{23} + Z_{23}Z_{33}) + T_{33}(Z_{13}^2 + Z_{23}^2 + Z_{33}^2)\right)\right\} \right\rangle, \tag{7.88}$$

$$a_4 = \frac{1}{30(4\pi\varepsilon_0)^2} \left\langle R^{-6} \left\{ 3\alpha_{11}\alpha_{22}\left(Z_{13}^2T_{23}^2 + 2T_{23}\left[Z_{12}Z_{13}T_{22} + T_{13}(Z_{12}Z_{33} + Z_{13}Z_{23})\right. \right. \right.$$

$$\left. + T_{12}(Z_{12}Z_{13} + Z_{13}Z_{22} + Z_{11}Z_{13}) + 2Z_{12}Z_{13}T_{11}\right] + Z_{12}^2T_{22}^2 + 2T_{22}\left[2Z_{12}Z_{23}T_{13}\right.$$

$$\left. + T_{12}(2Z_{12}Z_{22} + Z_{11}Z_{12}) + 2Z_{12}^2T_{11}\right] + Z_{23}^2T_{13}^2 + 2T_{13}\left[T_{12}(Z_{22}Z_{23} + Z_{11}Z_{23}\right.$$

$$\left. + Z_{12}Z_{13}) + Z_{12}Z_{23}T_{11}\right] + Z_{12}^2T_{11}^2 + T_{12}^2(Z_{22}^2 + 2Z_{11}Z_{22} + 2Z_{12}^2 + Z_{11}^2) + 2T_{11}T_{12}$$

$$\times (Z_{12}Z_{22} + 2Z_{11}Z_{12})\right) + 3\alpha_{11}\alpha_{33}\left(Z_{13}^2T_{33}^2 + 2T_{33}\left[Z_{12}Z_{13}T_{23} + T_{13}(2Z_{13}Z_{33}\right. \right.$$

$$\left. + Z_{11}Z_{13}) + 2Z_{13}Z_{23}T_{12} + 2Z_{13}^2T_{11}\right] + T_{13}^2(Z_{33}^2 + 2Z_{11}Z_{33} + 2Z_{13}^2 + Z_{11}^2) + Z_{12}^2T_{23}^2$$

$$+ 2T_{23}^2\left[T_{13}(Z_{12}Z_{33} + Z_{13}Z_{23} + Z_{11}Z_{12}) + T_{12}(Z_{12}Z_{23} + Z_{13}Z_{22}) + 2Z_{12}Z_{13}T_{11}\right]$$

$$+ Z_{23}^2T_{12}^2 + 2Z_{13}Z_{23}T_{11}T_{12} + Z_{13}^2T_{11}^2 + 2T_{13}\left[T_{12}(Z_{23}Z_{33} + Z_{11}Z_{23} + Z_{12}Z_{13})\right.$$

$$\left. \left. + T_{11}(Z_{13}Z_{33} + 2Z_{11}Z_{13})\right]\right) + 3\alpha_{22}\alpha_{33}\left(Z_{23}^2T_{33}^2 + 2T_{33}\left[T_{23}(2Z_{23}Z_{33} + Z_{22}Z_{23})\right. \right.$$

$$\left. + 2Z_{23}^2T_{22} + Z_{12}Z_{23}T_{13} + 2Z_{13}Z_{23}T_{12}\right] + T_{23}^2(Z_{33}^2 + 2Z_{22}Z_{33} + 2Z_{23}^2 + Z_{22}^2) + Z_{23}^2T_{22}^2$$

137

$$+ 2T_{23} \left[T_{22}(Z_{23}Z_{33} + 2Z_{22}Z_{23}) + T_{13}(Z_{12}Z_{33} + Z_{13}Z_{23} + Z_{12}Z_{22}) + T_{12}(Z_{13}Z_{33} \right.$$

$$\left. + Z_{12}Z_{23} + Z_{13}Z_{22}) \right] + Z_{12}^2 T_{13}^2 + Z_{13}^2 T_{12}^2 + 2T_{22}(2Z_{12}Z_{23}T_{13} + Z_{13}Z_{23}T_{12})$$

$$+ T_{12}T_{13}(Z_{11}Z_{23} + Z_{12}Z_{13}) \Big) + 3\alpha_{11}^2 \left(T_{13}^2(Z_{33}^2 + Z_{11}Z_{33} + Z_{23}^2 + 3Z_{13}^2) + 2T_{13} \right.$$

$$\times \left[T_{12}(Z_{23}Z_{33} + Z_{22}Z_{23} + Z_{11}Z_{23} + 3Z_{12}Z_{13}) + T_{11}(Z_{13}Z_{33} + Z_{12}Z_{23} + 4Z_{11}Z_{13}) \right]$$

$$+ T_{12}^2(Z_{23}^2 + Z_{22}^2 + Z_{11}Z_{22} + 3Z_{12}^2) + T_{11}T_{12}(Z_{13}Z_{23} + Z_{12}Z_{22} + 4Z_{11}Z_{12}) + T_{11}^2(Z_{13}^2$$

$$\left. + Z_{12}^2 + 4Z_{11}^2) \right) + 3\alpha_{22}^2 \left(T_{23}^2(Z_{33}^2 + Z_{22}Z_{33} + 3Z_{23}^2 + Z_{13}^2) + 2T_{23} \left[T_{22}(Z_{23}Z_{33} \right. \right.$$

$$\left. + 4Z_{22}Z_{23} + Z_{12}Z_{13}) + T_{12}(Z_{13}Z_{33} + 3Z_{12}Z_{23} + Z_{13}Z_{22} + Z_{11}Z_{13}) \right] + T_{22}^2(Z_{23}^2 + 4Z_{22}^2$$

$$\left. + Z_{12}^2) + 2T_{12}T_{22}(Z_{13}Z_{23} + 4Z_{12}Z_{22} + Z_{11}Z_{12}) + T_{12}^2(Z_{11}Z_{22} + Z_{13}^2 + 3Z_{13}^2 + Z_{11}^2) \right)$$

$$+ 3\alpha_{33}^2 \left(T_{33}^2(4Z_{33}^2 + Z_{23}^2 + Z_{13}^2) + 2T_{33} \left[T_{23}(4Z_{23}Z_{33} + Z_{22}Z_{23} + Z_{12}Z_{13}) + T_{13} \right. \right.$$

$$\times \left. (4Z_{13}Z_{33} + Z_{12}Z_{23} + Z_{11}Z_{13}) \right] + T_{23}^2(Z_{22}Z_{33} + 3Z_{23}^2 + Z_{22}^2 + Z_{12}^2) + 2T_{13}T_{23}$$

$$\times \left. (Z_{12}Z_{33} + 3Z_{13}Z_{23} + Z_{12}Z_{22} + Z_{11}Z_{12}) + T_{13}^2(Z_{11}Z_{33} + 3Z_{13}^2 + Z_{12}^2 + Z_{11}^2) \right) \right\} \right\rangle .$$

$$(7.89)$$

In spite of the compact notation employed, the a_5 term is exteremely large, so the tensor $H_{il} = \alpha_{ij}^{(1)} T_{jk} \alpha_{kl}^{(2)}$ defined in equation (6.116) is used to further compress the final expression [9, 36], yielding:

$$a_5 = \frac{1}{30(4\pi\varepsilon_0)^3} \left\langle R^{-9} \left\{ 9\alpha_{33} \left(T_{33}(H_{13}H_{31} + H_{23}H_{32} + 2H_{33}^2) + T_{23}(H_{33}(2H_{32} + H_{23}) \right. \right. \right.$$

$$+ H_{22}H_{32} + H_{12}H_{31}) + H_{23}H_{32}T_{22} + T_{13}(H_{33}(2H_{31} + H_{13}) + H_{21}H_{32} + H_{11}H_{31})$$

$$\left. + T_{12}(H_{13}H_{32} + H_{23}H_{31}) + H_{13}H_{31}T_{11} \right) + 9\alpha_{22} \left(H_{23}H_{32}T_{33} + T_{23}(H_{23}H_{33} + H_{22}H_{32} \right.$$

$$+ 2H_{22}H_{23} + H_{13}H_{21}) + T_{22}(H_{23}H_{32} + 2H_{22}^2 + H_{12}H_{21}) + T_{13}(H_{21}H_{32} + H_{12}H_{23})$$

$$\left. + T_{12}(H_{23}H_{31} + H_{22}(2H_{21} + H_{12}) + 9H_{11}H_{21}) + H_{12}H_{21}T_{11} \right) + 9\alpha_{11} \left(H_{13}H_{31}T_{33} \right.$$

$$+ T_{23}(H_{12}H_{31} + H_{13}H_{21}) + H_{12}H_{21}T_{22} + T_{13}(H_{13}H_{33} + H_{11}H_{31} + H_{12}H_{23} + 2H_{11}H_{13})$$

$$\left. + T_{12}(H_{13}H_{32} + H_{12}H_{22} + H_{11}H_{21} + 2H_{11}H_{12}) + T_{11}(H_{13}H_{31} + H_{12}H_{21} + 2H_{11}^2) \right)$$

$$+ 3T_{33} \left(Z_{33}(2H_{33}^2 + H_{23}H_{32} + H_{13}H_{31}) + Z_{23}(H_{33}(2H_{32} + H_{23}) + H_{22}H_{32} + H_{12}H_{31}) \right.$$

$$+ H_{23}H_{32}Z_{22} + Z_{13}(H_{33}(2H_{31} + H_{13}) + H_{21}H_{32} + H_{11}H_{31}) + Z_{12}(H_{13}H_{32} + H_{23}H_{31})$$

$$+ H_{13}H_{31}Z_{11} \Big) + 3T_{23} \left(Z_{33}(H_{33}(H_{32} + 2H_{23}) + H_{22}H_{23} + H_{13}H_{21}) + Z_{23}(H_{33}^2 \right.$$

$$+ 2H_{22}H_{33} + H_{32}^2 + 2H_{23}H_{32} + H_{13}H_{31} + H_{23}^2 + H_{22}^2 + H_{12}H_{21}) + Z_{22}(H_{32}H_{33}$$

$$+ 2H_{22}H_{32} + H_{12}H_{31} + H_{22}H_{23}) + Z_{13}(H_{33}(H_{21} + H_{12}) + H_{31}H_{32} + H_{23}H_{31}$$

$$+ H_{13}H_{23} + H_{21}H_{22} + H_{11}H_{21}) + Z_{12}(H_{31}H_{33} + H_{32}(H_{21} + H_{12}) + H_{31}(H_{22} + H_{11})$$

$$+ H_{21}H_{23} + H_{13}H_{22}) + Z_{11}(H_{12}H_{31} + H_{13}H_{21}) \Big) + 3T_{22} \left(H_{23}H_{32}Z_{33} + Z_{23}(H_{23}H_{33} \right.$$

$$+ H_{22}H_{32} + 2H_{22}H_{23} + H_{13}H_{21}) + Z_{22}(H_{23}H_{32} + 2H_{22}^2 + H_{12}H_{21}) + Z_{13}(H_{21}H_{32}$$

$$+ H_{12}H_{23}) + Z_{12}(H_{23}H_{31} + H_{22}(2H_{21} + H_{12}) + H_{11}H_{21}) + H_{12}H_{21}Z_{11} \Big) + 3T_{13}$$

$$\times \left(Z_{33}(H_{33}(H_{31} + 2H_{13}) + H_{12}H_{23} + H_{11}H_{13}) + Z_{23}(H_{33}(H_{21} + H_{12}) + H_{32}(H_{31} \right.$$

$$+ H_{13}) + H_{13}H_{23} + H_{12}H_{22} + H_{11}H_{12}) + Z_{22}(H_{21}H_{32} + H_{12}H_{23}) + Z_{13}(H_{33}^2 + 2H_{11}$$

$$\times H_{33} + H_{23}H_{32} + H_{31}^2 + 2H_{13}H_{31} + H_{12}H_{21} + H_{13}^2 + H_{11}^2) + Z_{12}(H_{32}H_{33} + H_{32}(H_{22}$$

$$+ H_{11}) + H_{31}(H_{21} + H_{12}) + H_{11}H_{23} + H_{12}H_{13}) + Z_{11}(H_{31}H_{33} + H_{21}H_{32} + 2H_{11}H_{31}$$

$$+ H_{11}H_{13}) \Big) + 3T_{12} \left(Z_{33}(H_{13}H_{32} + H_{23}H_{31}) + Z_{23}(H_{13}H_{33} + H_{12}H_{32} + H_{22}H_{31} \right.$$

$$+ H_{23}(H_{21} + H_{12}) + H_{13}H_{22} + H_{11}H_{13}) + Z_{22}(H_{13}H_{32} + H_{22}(H_{21} + 2H_{12})$$

$$+ H_{11}H_{12}) + Z_{13}(H_{23}H_{33} + H_{11}H_{32} + H_{21}H_{31} + H_{23}(H_{22} + H_{11}) + H_{13}H_{21}$$

$$+ H_{12}H_{13}) + Z_{12}(H_{23}H_{32} + H_{13}H_{31} + H_{22}^2 + 2H_{11}H_{22} + H_{21}^2 + 2H_{12}H_{21} + H_{12}^2$$

$$+ H_{11}^2) + Z_{11}(H_{23}H_{31} + H_{21}H_{22} + 2H_{11}H_{21} + H_{11}H_{12}) \Big) + 3T_{11} \left(H_{13}H_{31}Z_{33} \right.$$

$$+ Z_{23}(H_{12}H_{31} + H_{13}H_{21}) + H_{12}H_{21}Z_{22} + Z_{13}(H_{13}H_{33} + H_{11}H_{31} + H_{12}H_{23}$$

$$+ 2H_{11}H_{13}) + Z_{12}(H_{13}H_{32} + H_{12}H_{22} + H_{11}H_{21} + 2H_{11}H_{12}) + Z_{11}(H_{13}H_{31}$$

$$+ H_{12}H_{21} + 2H_{11}) \Big) - 12\alpha \left(T_{33}(H_{33}^2 + H_{23}H_{32} + H_{13}H_{31}) + T_{23}(H_{33}(H_{32} \right.$$

$$+ H_{23}) + H_{22}H_{32} + H_{12}H_{31} + H_{22}H_{23} + H_{13}H_{21}) + T_{22}(H_{23}H_{32} + H_{22}^2 + H_{12}H_{21})$$

$$+ T_{13}(H_{33}(H_{31} + H_{13}) + H_{21}H_{32} + H_{11}H_{31} + H_{12}H_{23} + H_{11}H_{13}) + T_{12}(H_{13}H_{32}$$

$$+ H_{23}H_{31} + H_{22}(H_{21} + H_{12}) + H_{11}H_{21} + H_{11}H_{12}) + T_{11}(H_{13}H_{31} + H_{12}H_{21} + H_{11}^2))$$

$$- (H_{11} + H_{22} + H_{33}) \Big(3\alpha_{33}(H_{33}T_{33} + H_{32}T_{23} + H_{31}T_{13}) + 3\alpha_{22}(H_{23}T_{23} + H_{22}T_{22}$$

$$+ H_{21}T_{12}) + 3\alpha_{11}(H_{13}T_{13} + H_{12}T_{12} + H_{11}T_{11}) + T_{33}(H_{33}Z_{33} + H_{32}Z_{23} + H_{31}Z_{13})$$

$$+ T_{23}(H_{23}Z_{33} + Z_{23}(H_{33} + H_{22}) + H_{32}Z_{22} + H_{21}Z_{13} + H_{31}Z_{12}) + T_{22}(H_{23}Z_{23}$$

$$+ H_{22}Z_{22} + H_{21}Z_{12}) + T_{13}(H_{13}Z_{33} + H_{12}Z_{23} + Z_{13}(H_{33} + H_{11}) + H_{32}Z_{12} + H_{31}Z_{11})$$

$$+ T_{12}(H_{13}Z_{23} + H_{12}Z_{22} + H_{23}Z_{13} + Z_{12}(H_{22} + H_{11}) + H_{21}Z_{11}) + T_{11}(H_{13}Z_{13}$$

$$+ H_{12}Z_{12} + H_{11}Z_{11}))\Big\}\Big\rangle. \tag{7.90}$$

Combining the results in equations (7.23), (7.24), (7.83) to (7.85), and (7.87) to (7.90), equation (7.43) can be written:

$$\rho = \left[\frac{1}{15}(\Delta\alpha)^2 + \frac{1}{30}g' + \frac{1}{30(4\pi\varepsilon_0)}a_3' + \frac{1}{30(4\pi\varepsilon_0)^2}a_4' + \frac{1}{30(4\pi\varepsilon_0)^3}a_5' + \cdots \right] \Big/$$

$$\left[\alpha^2 + \frac{4}{45}(\Delta\alpha)^2 + \frac{2}{45}g' + \frac{1}{15(4\pi\varepsilon_0)}b_3' + \alpha^2 \left(\frac{-2B}{V_m} \right) \right], \tag{7.91}$$

where g' is the expression for $\langle 3\alpha_{ij}^{(1)}\alpha_{ij}^{(2)} - 9\alpha^2 \rangle$ given in equation (7.84), while b_3' represents the part of b_3 in equation (7.87) contained in angular brackets, with similar definitions for a_3', a_4' and a_5' in equations (7.88) to (7.90), respectively.

Equation (7.67) must now be expressed in the virial form of equation (7.103). We have from equation (7.25):

$$\rho_0 = \frac{3(\Delta\alpha)^2}{45\alpha^2 + 4(\Delta\alpha)^2}, \tag{7.92}$$

where $\Delta\alpha$ is defined in equation (7.22). This allows equation (7.67) to be written in the form:

$$\rho = \rho_0 \left[1 + \frac{1}{2(\Delta\alpha)^2}g' + \frac{1}{2(4\pi\varepsilon_0)(\Delta\alpha)^2}a_3' + \frac{1}{2(4\pi\varepsilon_0)^2(\Delta\alpha)^2}a_4' + \frac{1}{2(4\pi\varepsilon_0)^3(\Delta\alpha)^2}a_5' \right.$$

$$\left. + \frac{2B}{V_m} + O\left(\frac{1}{V_m^2} \right) \right] \Big/ \left\{ 1 + \tfrac{4}{3}\rho_0 \left[\frac{1}{2(\Delta\alpha)^2}g' + \frac{3}{2(4\pi\varepsilon_0)(\Delta\alpha)^2}b_3' + \frac{2B}{V_m} \right] \right\}, \tag{7.93}$$

which simplifies to

$$\rho = \rho_0 + \frac{\rho_0(1 - \frac{4}{3}\rho_0)}{V_m} \left(2B + \mathsf{g} + \mathsf{a}_3 + \mathsf{a}_4 + \mathsf{a}_5 + \mathsf{b}_3 + \cdots\right), \tag{7.94}$$

where

$$\mathsf{g} = \frac{1}{2(\Delta\alpha)^2} V_m g', \tag{7.95}$$

$$\mathsf{a}_3 = \frac{1}{4\pi\varepsilon_0} \left\{ \frac{1}{2(\Delta\alpha)^2} + \frac{2}{48\alpha^2} \right\} V_m a'_3, \tag{7.96}$$

$$\mathsf{a}_4 = \frac{1}{(4\pi\varepsilon_0)^2} \left\{ \frac{1}{2(\Delta\alpha)^2} + \frac{2}{48\alpha^2} \right\} V_m a'_4, \tag{7.97}$$

$$\mathsf{a}_5 = \frac{1}{(4\pi\varepsilon_0)^3} \left\{ \frac{1}{2(\Delta\alpha)^2} + \frac{2}{48\alpha^2} \right\} V_m a'_5, \tag{7.98}$$

and

$$\mathsf{b}_3 = -\frac{1}{15(4\pi\varepsilon_0)\alpha^2} V_m b'_3. \tag{7.99}$$

It follows that

$$B_\rho = \rho_0(1 - \tfrac{4}{3}\rho_0)\left(2B + \mathsf{g} + \mathsf{a}_3 + \mathsf{a}_4 + \mathsf{a}_5 + \mathsf{b}_3 + \cdots\right). \tag{7.100}$$

The coefficients in equations (7.95) to (7.99) are independent of the molar volume, but dependent on temperature. As for linear molecules, measurements of B_ρ together with a measured value of ρ_0 yield values for:

$$B'_\rho = \left(2B + \mathsf{g} + \mathsf{a}_3 + \mathsf{a}_4 + \mathsf{a}_5 + \mathsf{b}_3 + \cdots\right). \tag{7.101}$$

The portion of B'_ρ which is of interest is the sum of the terms arising purely from angular correlation and collision-induced polarizability anisotropy:

$$\mathcal{S}_\rho = \mathsf{g} + \mathsf{a}_3 + \mathsf{a}_4 + \mathsf{a}_5 + \mathsf{b}_3 + \cdots. \tag{7.102}$$

In order to extract an experimental value of $\mathcal{S}_\rho$ from a value for B'_ρ, an $(\mathcal{S}_\rho/2B)$ ratio of the order of unity or greater is necessary.

7.2 Interacting spherical molecules

Since they are isotropic, isolated spherical molecules are unable to depolarize the light which they scatter. Nevertheless, a small depolarization ratio is observed in gases of spherical molecules at elevated pressures, since at these pressures the molecules can no longer be considered to be isolated. This depolarization of scattered light by interacting spherical molecules, which depends on the pressure of the sample, has been attributed to the alteration of the effective polarizability of the molecules resulting from the interaction between molecules when they collide or come into close contact with one another. The depolarization of light by spherical gases has been the subject of intensive investigation, both experimental and theoretical [89, 204, 205].

The pressure-dependent depolarization ratio is described by means of a virial-type expansion [96]

$$\rho = \frac{B_\rho}{V_m} + \frac{C_\rho}{V_m^2} + \cdots, \tag{7.103}$$

where B_ρ, C_ρ, ... are the second, third, ... light-scattering virial coefficients, and describe the contributions to ρ arising from interactions between pairs, triplets, ... of molecules, respectively. Note that since ideal gases do not depolarize the light they scatter, there is no first light-scattering virial coefficient. From dipole-induced-dipole theory [204], the second light-scattering virial coefficient may be written as:

$$B_\rho = \frac{4\pi N_A}{(4\pi\varepsilon_0)^2} \frac{6\alpha^2}{5} \int_0^\infty \frac{1}{R^4} e^{-\frac{U_{12}(R)}{kT}} \, dR, \tag{7.104}$$

where $U_{12}(R)$ is the intermolecular potential energy between interacting molecules 1 and 2 which are a distance R apart. Thus, if we consider only pair interactions, equation (7.103) becomes:

$$\rho = \frac{4\pi N_A}{(4\pi\varepsilon_0)^2 V_m} \frac{6\alpha^2}{5} \int_0^\infty \frac{1}{R^4} e^{-\frac{U_{12}(R)}{kT}} \, dR. \tag{7.105}$$

In early calculations, the integral in (7.105) was evaluated using Buckingham and Pople's H_k functions [96]:

$$\int_0^\infty \frac{1}{R^k} e^{-\frac{U_{LJ}(R)}{kT}} R^2 \, dR = \frac{R_o^{3-k}}{12y^4} H_k(y), \tag{7.106}$$

where $U_{LJ}(R)$ is the Lennard-Jones potential. Buckingham and Pople [96] tabulated

142

values of $H_k(y)$ for k ranging from 6 to 17 in integral steps.

Using equation (7.104), Watson and Rowell [89] calculated values for B_ρ, and compared them with their experimental values. They found that the ratio of $B_\rho^{\text{exp}}/B_\rho^{\text{calc}}$ showed a definite trend, with the ratio increasing from less than unity for the rare gases to values of approximately 2.5 and 7 for the large quasi-spherical molecules sulphur hexafluoride and neopentane, respectively. Other workers later confirmed Watson and Rowell's ratios of B_ρ^{exp} to B_ρ^{calc}, for argon and methane [206–209]. Watson and Rowell argued that the apparent breakdown of the DID theory of molecular interactions for larger molecules provides evidence of the inadequacy of the point-dipole approximation used in the DID theory. However, as discussed in Section 6.8, Dunmur, Manterfield and Robinson [88] have subsequently shown that at higher pressures the effects of triplet interactions contribute to the depolarization of light scattered from atoms and spherical molecules. For sulphur hexafluoride, which is a very large molecule, the evidence of three-body interactions manifests itself at much lower pressures. This is probably due to the fact that sulphur hexafluoride has a very low vapour pressure. Earlier measurements of the second light-scattering virial coefficient did not allow for the effects of three-body interactions, resulting in significant errors in the deduced values of B_ρ. Dunmur *et al.* [88] went on to show that the dipole-induced-dipole model for the collision-induced pair polarizability of atoms and spherical gases is successful for argon, krypton, xenon and methane, but appears to be inadequate for sulphur hexafluoride. This apparent inadequacy may be a result of collisions between four or more molecules, which have not been taken into account. Extremely precise measurements of the density dependence of the depolarization ratio would be necessary to determine these effects. Once again we note that for the molecules in this study, which are much smaller than sulphur hexafluoride, the measurements of the second virial coefficients are carried out at pressures well below their vapour pressures, so that the number of interactions between three or more molecules should be insignificant.

Chapter 8

Calculations of Second Virial Coefficients

8.1 Evaluation of the second virial coefficients by numerical integration

In order to calculate the various second virial coefficients discussed in this work it is necessary to integrate the relevant functions over the molecular interaction coordinates τ. In early calculations, the integrals were evaluated using Buckingham and Pople's H_k functions [96] which are described in Section 7.2. As computers became available, evaluation of the integrals either became simpler or, in some cases, became possible.

In 1969, Sutter [3] performed the numerical integration necessary to calculate B_ε by computer, since the series expansion of the H_k functions converged slowly and the higher-order terms were complicated. He used Simpson's rule for integration over four interaction coordinates to calculate B_ε and $B(T)$. Many subsequent second virial coefficient computations [2, 3, 40, 44, 95, 97, 98, 110] have been carried out using this method, which is simple to program. In 1980, Whitmore and Goodings [113] performed the integration calculations of $B(T)$ by Gaussian quadrature, but made no comment on the superiority of the method over that of Simpson's rule. Later, an extensive comparison of the two integration methods was undertaken by Weller [105] who showed that for a given precision the Gaussian method requires only half the number of intervals per integration variable, reducing the computer time necessary for a calculation by a factor of at least sixteen for linear molecules with four integration coordinates. Subsequently, Graham and Couling [9, 36, 200, 201] have used the method of Gaussian quadrature in all their computations of the second light-scattering and Kerr-effect virial coefficients for linear and non-linear molecules. Due to the success of the method, it has been adopted in this work.

In the integration procedure the ranges of the angles (θ_1, θ_2 and ϕ for linear molecules;

α_1, β_1, γ_1, α_2, β_2 and γ_2 for non-linear molecules) were divided into sixteen intervals, while the range of the separation R was taken from 0.1 nm to 3.0 nm and was usually divided into sixty four intervals. It was found that increasing the number of intervals for the angles from 16 to 32 yielded numerical values which agreed to at least seven significant figures, so that the lower number of intervals was used throughout to reduce computer time. For calculations of B_ε it was found that using 128 intervals for the range of R rather than 64 did change the results by up to 6%, so that for linear molecules 124 intervals were used. Although the difference can be significant it is still less than the experimental errors for B_ε for non-linear molecules, and in calculations of B_ε for these molecules the lower number of intervals was retained since the programs were already very time- and memory-consuming. For the other effects, increasing the number of intervals for the range changed the numerical values by less than 0.5%, and 64 intervals were used for all molecules.

The ability of the Macsyma package to translate expressions directly into Fortran code was utilised to effectively eliminate the introduction of errors in the integration arguments, which are often very long and complicated. Examples of the Fortran programs used are given in Appendix C. Many of the programs were run on the University of Natal Physics Department's IBM RISC system/6000 workstation with a 60 MHz processor, using the IBM Fortran compiler. Other programs were run on a 486 DX-2 66 MHz PC with 16 Mb of RAM, or a Pentium 133 MHz PC with 64 Mb of RAM, using the University of Salford FTN77 compiler. All of our programs were run in double precision. The basic format of the programs for the non-linear gases was designed by Couling [9]. Large arrays are used to store the numerical values of the intermolecular potentials for all the angular configurations required, which eliminates the repeated calculation of these values within the Gaussian quadrature routine and increases the speed by a factor of fifty. However, the arrays require large amounts of memory to store several million double-precision numbers, and it is necessary to make use of the facility to page to the hard disk. These non-linear programs each take several hours, as opposed to the linear programs which are only a few minutes in duration.

The aim of this work is to see if known molecular properties, either experimental or calculated, together with a self-consistent set of Lennard-Jones and shape parameters, combined with complete molecular theories of the second virial coefficients, will yield calculated values which agree with experiment for the full range of virial effects. To this end, as many molecular properties as possible have been collected, both measured and calculated. The theory for the second pressure virial coefficient presented in Chapter 3 has then been used to fit calculated values of $B(T)$ to the experimental values given in Appendix A over a range of temperatures, by optimising the values for the Lennard-Jones parameters R_0 and ε/k and the shape factors. Due to the sensitivity of the second

dielectric virial coefficient to the shape of the molecule, we have attempted to fine-tune the optimization of the molecular parameters by seeking a set of parameters which result in good agreement between theory and experiment for both $B(T)$ and B_ε, in the first instance.

A computer program was designed which calculates the values of $B(T)$ and B_ε over a range of temperatures for various sets of the Lennard-Jones parameters and the shape factor. For each set of parameters, the calculated values are compared with the experimental data available and the sum of the squares of the errors (SSE) for each effect is computed and the results stored in an array. When $B(T)$ is calculated for the next set of parameters, the elements of the array are sorted in ascending order of the SSE. As B_ε is calculated a running total of the SSE is compared with the SSE for B_ε of the data set in the preceding array element, and if the SSE of the current calculation exceeds that of preceding element the calculation is abandoned and the next set of parameters is processed. In this way, large amounts of data may be calculated and compared systematically allowing a very careful search over a fine grid for a set of parameters to optimize the fit of both $B(T)$ and B_ε. This program saves a substantial amount of time, particularly since it abandons the evaluation of a set of parameters immediately when it becomes clear that the SSE for B_ε is too large. This method of selective calculation was necessary since B_ε is so sensitive to the parameter set that the errors can increase very rapidly with small changes in the shape factor. A similar process was not feasible for non-linear gases since a single calculation of B_ε for a polar gas takes approximately 23 hours on a 133 MHz Pentium!

Even with the aid of this program, it was not always possible to find a set of parameters to fit both effects. For certain gases there appeared to be no common ground where reasonable calculated values existed for the two effects. In these cases our policy has been to select a set of parameters which satisfy the requirements for each effect separately and then to test these sets on the other second virial coefficients, where available.

For the non-linear gases, careful optimization of the Lennard-Jones force constants and the shape factors has been carried out by Couling and Graham [9], who fitted the calculated second pressure virial coefficient to experimental data, and then used these parameters in the calculations of the second light-scattering and Kerr-effect virial coefficients. For these gases we have used the their optimized parameters to calculate the second dielectric virial coefficient and the second refractivity virial coefficient, where available. Where these parameters yielded calculated values which disagreed with the measured values, we have attempted to find new parameters which improve the fit of B_ε without sacrificing the good fit of $B(T)$, which can then be tested on the remaining second virial coefficients.

As a double check of the fortran code of both the linear and non-linear programs, the

146

non-linear programs were used to calculate the various components contributing to the second virial coefficients for linear gases and these calculated values were compared with the values calculated by the relevant linear programs. In all cases the values were found to be equal to at least four or more significant figures.

8.2 Calculations for fluoromethane

8.2.1 Molecular properties of fluoromethane

Table 8.1 presents a list of the molecular properties of fluoromethane which have been used in these calculations. The dynamic properties, α, β, A and C are all for a wavelength of 632.8 nm. The A- and C-tensor components are estimated values. Since there are no values available for the components of the dynamic hyperpolarizability tensor β_{ijk}, components were estimated by setting the ratio $(\beta_{\parallel}/\beta_{\perp})$ equal to the ratio of the polarizability tensor components. Although this is obviously a crude approximation, it was adopted so the relative contribution of the hyperpolarizability to B_{ε} and B_R could be estimated. The optical-frequency values for $\beta_{\parallel}$ and $\beta_{\perp}$ were used in the calculations of B_{ε}. The contribution of the hyperpolarizability was found to be relatively insignificant, so that this approximation appears to be justified. The components $a_{\parallel}$ and $a_{\perp}$ of the static polarizability tensors were calculated using the mean static polarizability a determined by Sutter and Cole [2] and the static anisotropy Δa obtained by *ab initio* calculations at the MP2 level of theory by Spackman and Dougherty [202, 210]. Our optimized values of the Lennard-Jones force constants and the shape factor are given in Table 8.2, together with the fitted values of Couling and Graham [9].

8.2.2 Results of calculations of second virial coefficients for fluoromethane

For fluoromethane our attempt to optimize the Lennard-Jones force constants and the shape factor for both the second pressure and dielectric virial coefficients simultaneously met with some success. Our values of R_0, ε/k and D given in Table 8.2 resulted in calculated values of $B(T)$ which agreed with the measured values to within less than 3% over the temperature range from $T = 280$ K to 416.5 K, as shown in Table 8.3, which also shows the values of $B(T)$ calculated using parameter set (2). For our optimized set of parameters, the calculated values of B_{ε} fell within the experimental errors quoted by Sutter and Cole [2, 3], which are the most accurate measured values available. Table 8.4 shows the temperature dependence of the calculated values of B_{ε} for both sets of parameters, together with the measured values of Sutter and Cole [2, 3]. Figure 8.1 (a) shows graphically the relationship between the calculated curves and the experimental data. The solid curve represents the values calculated using parameter set (1), while the dotted line represents the values calculated using parameter set (2). Note that the measured values of Hamann *et al.* [52] are higher than those of Sutter and Cole, with larger experimental errors. From Tables 8.3 and 8.4, and Figure 8.1 (a) it is clear that our optimized parameter set offers the best fit to the measured values of both $B(T)$ and B_{ε}.

Table 8.1: Molecular parameters of fluoromethane used in the calculations ($\lambda = 632.8$ nm).

Molecular Parameter	Value	Reference
$10^{30}\mu$ (Cm)	6.170	[97]
$10^{40}\theta$ (Cm^2)	7.70	[97]
$10^{40}a$ (C^{2}m^{2}J^{-1})	3.305	[2]
$10^{40}\Delta a$ (C^{2}m^{2}J^{-1})	0.290	[202, 210]
$10^{40}a_{\parallel}$ (C^{2}m^{2}J^{-1})	3.498	
$10^{40}a_{\perp}$ (C^{2}m^{2}J^{-1})	3.208	
κ_a	0.0292	
$100\rho_0$	0.094	[4]
$10^{40}\alpha$ (C^{2}m^{2}J^{-1})	2.916	[44, 62]
$10^{40}\Delta\alpha$ (C^{2}m^{2}J^{-1})	0.345	[4]
$10^{40}\alpha_{\parallel}$ (C^{2}m^{2}J^{-1})	3.147	
$10^{40}\alpha_{\perp}$ (C^{2}m^{2}J^{-1})	3.498	
κ_{α}	0.0396	[4]
$10^{50}A_{\parallel}$ (C^{2}m^{3}J^{-1})	1.720	[211]
$10^{50}A_{\perp}$ (C^{2}m^{3}J^{-1})	2.767	[211]
$10^{60}C_{1111}$ (C^{2}m^{4}J^{-1})	0.85	[62]
$10^{60}C_{1313}$ (C^{2}m^{4}J^{-1})	0.67	[62]
$10^{60}C_{3333}$ (C^{2}m^{4}J^{-1})	1.06	[62]
$10^{50}\beta$ (C^{3}m^{3}J^{-2})	-0.19 ± 0.15	[33]
$10^{50}\beta_{\parallel}$ (C^{3}m^{3}J^{-2})	-0.11392	
$10^{50}\beta_{\perp}$ (C^{3}m^{3}J^{-2})	-0.10138	

Table 8.2: Lennard-Jones parameters and shape factors for fluoromethane.

		R_0 (nm)	ε/k (K)	D
(1)	Our fitted values	0.367	182	0.297
(3)	Fitted values of Couling and Graham [9]	0.380	199	0.254

149

Table 8.3: The temperature dependence of the calculated values of $B(T)$ for fluoromethane for two sets of parameters, and the best fit data of Dymond and Smith [1].

| T | $10^6 B^{exp}$ | (1) | | (2) | |
| | | $10^6 B^{calc}$ | % | $10^6 B^{calc}$ | % |
K	$m^3 mol^{-1}$	$m^3 mol^{-1}$	Error	$m^3 mol^{-1}$	Error
280	-244±3	-241.23	-1.14	-238.91	-2.09
300	-206±3	-203.92	-1.06	-206.53	-1.18
320	-174±3	-174.01	0.01	-171.65	0.97
340	-150±3	-150.38	0.25	-152.76	1.84
360	-129±3	-130.82	1.41	-126.11	4.22
380	-112±3	-114.99	2.67	-118.10	5.45
400	-99±2	-101.46	2.48	-104.66	5.72
420	-87±2	-89.53	2.91	-95.04	6.78

Table 8.4: Calculated values of B_ε for nitrogen for two sets of parameters, together with the measured values of Sutter and Cole [2,3].

| T | $10^{12} B_\varepsilon^{exp}$ | (1) | | (2) | |
| | | $10^{12} B_\varepsilon^{calc}$ | % | $10^{12} B_\varepsilon^{calc}$ | % |
K	$m^6 mol^{-2}$	$m^6 mol^{-2}$	Error	$m^6 mol^{-2}$	Error
323.15	-1307±37	-1327.41	1.56	-940.61	-28.03
369.45	-606±30	-604.48	-0.33	-421.95	-30.37
416.45	-331±66	-264.07	-20.22	-172.72	-47.82

150

A considerable number of terms was evaluated in order to establish convergence of each series. The relative contributions of the various terms used to calculate B_ε are given in Table 8.5. It is clear that the terms in the hyperpolarizability make a reasonably small contribution to the total, but the leading term $\beta_1\mu_1$ might be worth retaining if an accurate measured or calculated value for the static b_{ijk} was obtained. It is important to note the major contribution made by the leading $\mu_2\alpha_1\mathcal{A}_1$ term. However, the A-tensor components used in the calculations are only estimates, and it would be desirable to have more accurate values to compute such a significant term. Another important term to note is the leading $\alpha\mu\theta$ term which contributes 22.9% of the total calculated value of B_ε at 323.15 K. This term has never been considered before, and its inclusion here may partially account for the good fit obtained for B_ε.

Table 8.5: The relative contributions of the terms used to calculate B_ε for fluoromethane at 298.2 K.

Contributing Term	$10^{12} \times$ Value m^6mol^{-2}	% Contribution to B_ε
α_2	-1.089	0.08
α_3	18.623	-1.40
α_4	0.820	-0.06
β_1	7.821	-0.59
$\alpha_1\beta_1$	-0.096	0.01
$\alpha_1\mathcal{A}_1$	-0.445	0.03
$\alpha_2\mathcal{A}_1$	2.292	-0.17
$\mathcal{A}_2$	-0.796	0.06
$\alpha_1\mathcal{A}_2$	-0.711	0.05
α_2C_1	2.216	-0.17
$B_{\varepsilon_{ind}}$	28.635	-2.16
μ_2	-3815.794	287.46
$\alpha_1\mu_2$	1727.847	-130.17
$\alpha_2\mu_2$	494.765	-37.27
$\alpha_3\mu_2$	28.724	-2.16
$\mathcal{A}_1\mu_2$	-80.456	6.06
$\alpha_1\mathcal{A}_1\mu_2$	-8.413	0.61
$\beta_1\mu_3$	-17.266	1.30
$\beta_1\alpha_1\mu_3$	-2.529	0.19
$\alpha_1\mu_1\theta_1$	304.616	-22.95
$\alpha_2\mu_1\theta_1$	2.933	-2.93
$\beta_1\mu_1\theta_1$	-2.336	0.18
$\alpha_2\theta_2$	18.678	-1.41
$\alpha_3\theta_2$	5.465	-0.41
$B_{\varepsilon_{or}}$	-1356.045	102.16

$$B_\varepsilon = -1327.41 \times 10^{-12} m^6mol^{-2}$$

Figure 8.1: Temperature dependence of the calculated and measured values of the second (a) dielectric, and (b) Kerr-effect virial coefficients of fluoromethane. The solid curves represent our calculated values, the dotted lines represent the values calculated using the parameter set of Couling and Graham [9], and the dashed line is the calculated curve of Buckingham *et al.* [177].

The second Kerr-effect virial coefficient was then calculated using our optimized parameter set. The results compare reasonably well with the experimental data [33] which have very high uncertainties of approximately 50%, but are slightly higher than the values deduced from the measurements of Schaeffer *et al.* [83]. Figure 8.1 (b) shows how our theoretical curve passes within the error bars of most of the measured values. The dotted curve represents the calculated values of Couling and Graham [9], which are lower than ours by approximately 30%. They calculated B_K for fluoromethane, using the α series and the first three terms of the $\mu\alpha$ series. The additional terms we have used in our calculations make a positive contribution of approximately 15%, due chiefly to the leading $\mu_1\alpha_1\mathcal{A}_1$. Figure 8.1 (b) also shows the calculated curve of Buckingham *et al.* [177] as a dashed line. A more definitive test of the theory would be possible if more precise measured values were available.

From the relative magnitude of the terms contributing to the calculated value of B_K at $T=250.8$ K in Table 8.6 it is clear that all the different series have converged. The hyperpolarizability term $\mu_1\beta_1$ is obviously negligible and thus may justifiably be omitted. The large contribution from the leading term in the A-tensor is very interesting and highlights the need for accurate calculated values of the components $A_\parallel$ and $A_\perp$ for fluoromethane.

Table 8.6: The relative contributions of the terms used to calculate B_K for fluoromethane at 250.8 K, using parameter set (1).

Contributing Term	$10^{30} \times$ Value $C^2m^8J^{-2}mol^{-2}$	% Contribution to B_K
α_2	0.002	0.02
α_3	-0.014	-0.13
α_4	0.130	1.23
α_5	0.011	0.11
$\mu_2\alpha_1$	-3.686	-34.74
$\mu_2\alpha_2$	9.265	87.33
$\mu_2\alpha_3$	3.207	30.23
$\mu_2\alpha_4$	0.382	3.60
$\mu_2\beta_1$	-0.010	-0.09
$\mu_1\alpha_1\mathcal{A}_1$	1.019	9.61
$\mu_1\alpha_2\mathcal{A}_1$	0.181	1.71
$\mu_1\theta_1\alpha_1$	0.071	0.67

$$B_K = 10.609 \times 10^{-30} C^2m^8J^{-2}mol^{-2}$$

Although the second refractivity virial coefficient has been measured at three different wavelengths, values of the optical-frequency components of the molwecular parameters are only available at $\lambda = 632.8$ nm. Table 8.7 shows the contributions to the calculated

Table 8.7: The relative contributions of the terms used to calculate B_R for fluoromethane at 298 K for $\lambda = 632.8$ nm, using our optimized parameter set.

Contributing Term	$10^{12} \times$ Value $\mathrm{m^6mol^{-2}}$	% Contribution to B_R
α_2	-1.320	-23.34
α_3	13.698	242.24
α_4	0.532	9.41
β_1	-8.823	-156.03
$\alpha_1\beta_1$	-0.086	-1.52
$\alpha_1\mathcal{A}_1$	-0.666	-11.78
$\alpha_2\mathcal{A}_1$	2.067	36.55
$\mathcal{A}_2$	-0.919	-16.25
$\alpha_1\mathcal{A}_2$	-0.702	-12.41
$\alpha_2 C_1$	1.873	33.12

$$B_R^{\mathrm{calc}} = 5.65 \times 10^{-12}\mathrm{m^6mol^{-2}}$$
$$B_R^{\mathrm{exp}} = (4.32 \pm 1.80) \times 10^{-12}\mathrm{m^6mol^{-2}}$$

Table 8.8: The relative contributions of the terms used to calculate B_ρ for fluoromethane at 298.15 K and $\lambda = 632.8$ nm, using parameter set (1).

Contributing Term	$10^6 \times$ Value $\mathrm{m^3mol^{-1}}$	% Contribution to B_ρ
G	25.625	3.21
b_3	0.488	0.06
a_3	-135.625	-17.00
a_4	1309.982	164.28
a_5	93.658	11.75
$a_2\mathcal{A}_1$	-79.484	-9.97
$a_3\mathcal{A}_1$	-9.547	-1.20
$a_3 C_1$	0.151	0.02
$\mathcal{S}_\rho$	1205.249	151.15
$2B$	-407.840	-51.15

$$B_\rho' = 797.409 \times 10^{-6}\mathrm{m^3mol^{-1}}$$
$$B_\rho = 0.749 \times 10^{-6}\mathrm{m^3mol^{-1}}$$

value of B_R at $T = 298$ K, together with the measured value of Burns, Graham and Weller [62]. It can be seen that the α series is definitely converging, although it might be worth while to evaluate the α_5 term. The surprisingly large negative contribution of the β_1 term, shows that it not always justifiable to simply omit the hyperpolarizability effects. However, since the components $\beta_\parallel$ and $\beta_\perp$ are scaled estimates, and the value of β has a very large uncertainty, the calculated B_R is unacceptably imprecise. Accurate values for the components of the hyperpolarizability tensor β_{ijk} are neccessary to produce reliable calculated values.

Unfortunately, there are no measured values of B_ρ available for fluoromethane. However, we have calculated a value for the second light-scattering virial coefficient using our optimized parameter set. Table 8.8 shows the relative magnitudes of the various contributions to B_ρ for fluoromethane. It can be seen that the $\mathsf{a}\mathcal{A}_1$ series makes a negative contribution of more than 10% to the total, emphasizing the need for accurate measured or calculated values for the A-tensor components. The C-tensor term is negligible.

From the comparisons between our calculated values for $B(T)$, B_ε, B_R and B_K and the experimental data it would appear that our optimized set of parameters describe all the effects reasonably well. Although the values used for the hyperpolarizability, A- and C-tensors were only estimates they served to show the order of magnitude of the contributions arising from these tensors. Accurate measured or calculated values for these molecular tensor properties would further test the predictive merit of the DID model employed. In addition, measured values for the second light-scattering virial coefficient would allow a more comprehensive comparison of the agreement between the DID theory and experiment.

8.3 Calculations for trifluoromethane

8.3.1 Molecular properties of trifluoromethane

The molecular properties of trifluoromethane used in these calculations are given in Tables 8.9 and 8.10, together with our fitted values for R_0, ε/k and D. As for fluoromethane, the values of the components of the dynamic properties β_{ijk}, A_{ijk} and C_{ijkl} are all estimates which have been used to establish whether the terms of the various second virial coefficients containing these components are significant. Note that the same estimates were used for all wavelengths. The static polarizability anisotropy Δa in Table 8.10 was obtained by extrapolating the measured optical-frequency values of Bogaard et $al.$ [4] to zero frequency. Once again we assume that the static hyperpolarizability b_{ijk} is not very different from the dynamic value and use β as an estimate of b.

Table 8.9: Molecular parameters of trifluoromethane used in the calculations.

Molecular Parameter	Value	Reference
$10^{30}\mu$ (Cm)	5.50	[97]
$10^{40}\theta$ (Cm^2)	15.0	[97]
$10^{40}a$ (C^{2}m^{2}J^{-1})	3.970	[2]
$10^{40}\Delta a$ (C^{2}m^{2}J^{-1})	-0.190	[9]
$10^{40}a_{\parallel}$ (C^{2}m^{2}J^{-1})	3.843	
$10^{40}a_{\perp}$ (C^{2}m^{2}J^{-1})	4.033	
κ_a	-0.016	
$10^{50}A_{\parallel}$ (C^{2}m^{3}J^{-1})	1.80	
$10^{50}A_{\perp}$ (C^{2}m^{3}J^{-1})	3.57	
$10^{60}C_{1111}$ (C^{2}m^{4}J^{-1})	1.10	[62]
$10^{60}C_{1313}$ (C^{2}m^{4}J^{-1})	0.75	[62]
$10^{60}C_{3333}$ (C^{2}m^{4}J^{-1})	0.90	[62]
$10^{50}\beta$ (C^{3}m^{3}J^{-2})	-0.088	[212]
$10^{50}\beta_{\parallel}$ (C^{3}m^{3}J^{-2})	-0.0461	
$10^{50}\beta_{\perp}$ (C^{3}m^{3}J^{-2})	-0.0503	
D	-0.001	
R_0 (nm)	0.404	
ε/k (K)	166.0	

8.3.2 Results of calculations of second virial coefficients for trifluoromethane

Although the trifluoromethane is more plate-like than rod-shaped, the best fit for $B(T)$ and B_ε was obtained for a shape factor of $D = -0.001$ which is negligibly different from

Table 8.10: The components of the optical-frequency polarizability tensor α_{ij} of trifluoromethane, together with the values of ρ_0 [4] used in the calculations.

λ nm	$100\rho_0$	$10^{40}\alpha$ $(C^2m^2J^{-1})$		$10^{40}\Delta\alpha$ $(C^2m^2J^{-1})$		$10^{40}\alpha_{\parallel}$ $(C^2m^2J^{-1})$	$10^{40}\alpha_{\perp}$ $(C^2m^2J^{-1})$	κ_α
632.8	0.0504	3.097	[44,62]	-0.27	[4]	2.917	3.187	-0.029
514.5	0.07	3.139	[4]	-0.32	[4]	2.926	3.246	-0.034
488.0	0.07	3.145	[4]	-0.32	[4]	2.932	3.252	-0.034

zero, implying that the molecule is very nearly spherical in shape. This is however an improvement from the value of 0.26 obtained by Sutter [3] which is not physically reasonable. This fact led Sutter to conclude that the shape potential proposed by Buckingham and Pople [96] was inadequate. However these conclusions were based on a model which did not include the effects of the quadrupole moment or polarizability anisotropy. Calculations of $B(T)$ using our optimized parameters yielded values which agreed with the experimental values quoted in Appendix A to within less than 1% over almost the entire temperature range, as shown in Table 8.11. The same set of parameters resulted in calculated values of B_ε which differ from the measured values of Sutter and Cole [2] by less than 3%. Table 8.12 presents the temperature dependence of the calculated B_ε in comparison with the measured values of Sutter and Cole [2], while Table 8.13 lists the relative contributions of the terms of B_ε. It can be seen from Figure 8.2 (a) that the calculated values agree remarkable well with most of the experimental data, with the exception of the the early measurements of Lawley and Sutton [10], Turner [50] and Dymond and Smith [56], where the experimental errors are very large.

Table 8.11: The temperature dependence of the calculated values of the second pressure virial coefficient $B(T)$ for trifluoromethane, and smoothed values fitted to the combined experimental data of Sutter and Cole [5], and Lange and Stein [6].

Temperature K	$10^6 B^{exp}$ m^3mol^{-1}	$10^6 B^{calc}$ m^3mol^{-1}	% Error
243.15	-311.1±4	-310.75	-0.11
273.15	-234.9±4	-232.18	-1.16
298.15	-188.0±4	-187.33	-0.36
313.15	-165.8±4	-166.17	0.22
323.15	-153.0±4	-153.87	0.57
368.15	-110.4±4	-111.27	0.79
369.45	-109.4±4	-110.27	0.80
404.75	-84.6±3	-86.97	2.80

157

Table 8.12: The temperature dependence of the calculated values of B_ε for trifluoromethane, and the measured values of Sutter and Cole [2, 3].

Temperature K	$10^{12} B_\varepsilon^{\mathrm{exp}}$ $\mathrm{m^6mol^{-2}}$	$10^{12} B_\varepsilon^{\mathrm{calc}}$ $\mathrm{m^6mol^{-2}}$	% Error
323.15	1125±52	1149.92	2.22
369.45	903±20	896.27	-0.75
416.45	704±10	723.84	2.82

Table 8.13: The relative contributions of the terms used to calculate B_ε for trifluoromethane at 298.2 K.

Contributing Term	$10^{12} \times$ Value $\mathrm{m^6mol^{-2}}$	% Contribution to B_ε
α_2	-0.517	-0.04
α_3	17.703	1.54
α_4	0.662	0.06
β_1	-2.039	-0.17
$\alpha_1\beta_1$	-0.027	-0.002
$\alpha_1\mathcal{A}_1$	-2.069	-0.18
$\alpha_2\mathcal{A}_1$	2.420	0.21
$\mathcal{A}_2$	-0.006	-0.03
$\alpha_1\mathcal{A}_2$	-0.344	-0.001
$\alpha_2 C_1$	1.625	0.14
$B_{\varepsilon_{\mathrm{ind}}}$	17.408	1.51
μ_2	-894.734	-77.73
$\alpha_1\mu_2$	993.160	86.37
$\alpha_2\mu_2$	342.595	29.79
$\alpha_3\mu_2$	19.431	1.69
$\mathcal{A}_1\mu_2$	-95.024	-8.26
$\alpha_1\mathcal{A}_1\mu_2$	-7.412	-0.64
$\beta_1\mu_3$	-3.834	-0.33
$\beta_1\alpha_1\mu_3$	-0.508	-0.04
$\alpha_1\mu_1\theta_1$	676.121	58.80
$\alpha_2\mu_1\theta_1$	7.835	0.68
$\beta_1\mu_1\theta_1$	-1.503	-0.13
$\alpha_2\theta_2$	64.120	5.58
$\alpha_3\theta_2$	32.258	2.81
$B_{\varepsilon_{\mathrm{or}}}$	1132.512	98.49

$$B_\varepsilon = 1149.92 \times 10^{-12} \mathrm{m^6mol^{-2}}$$
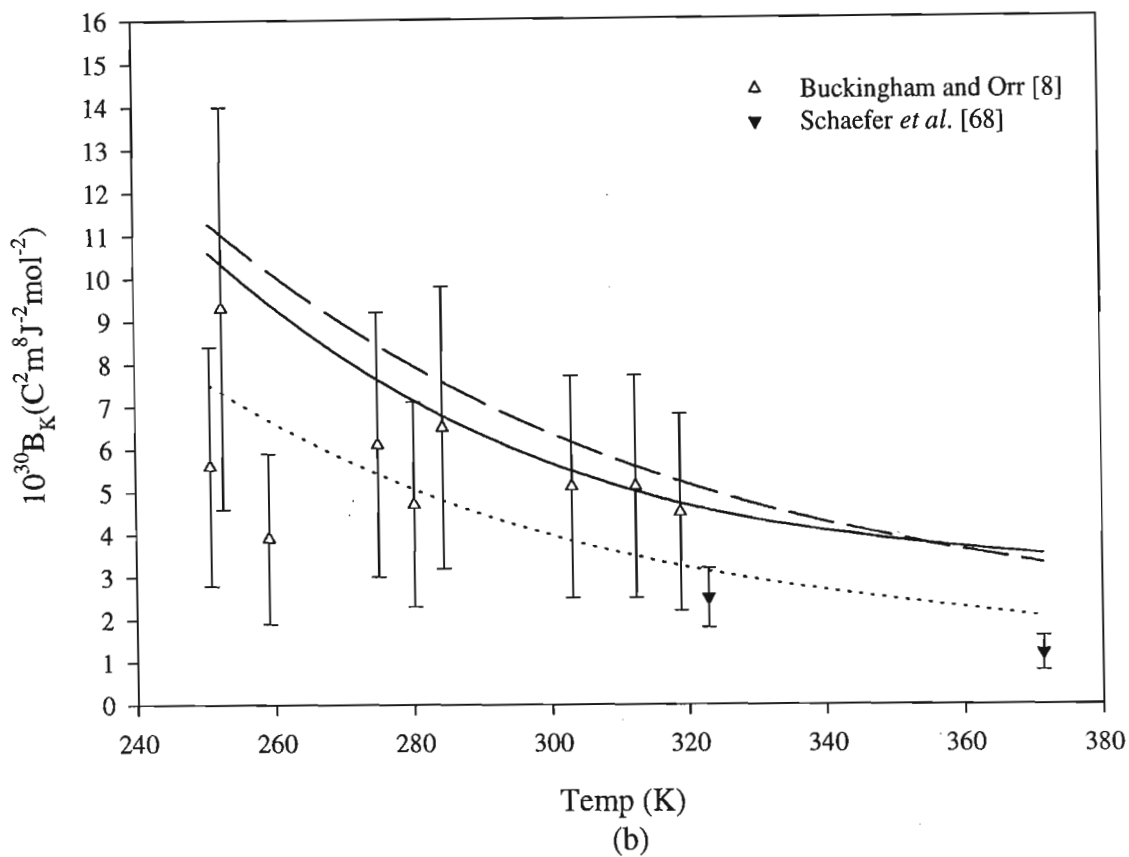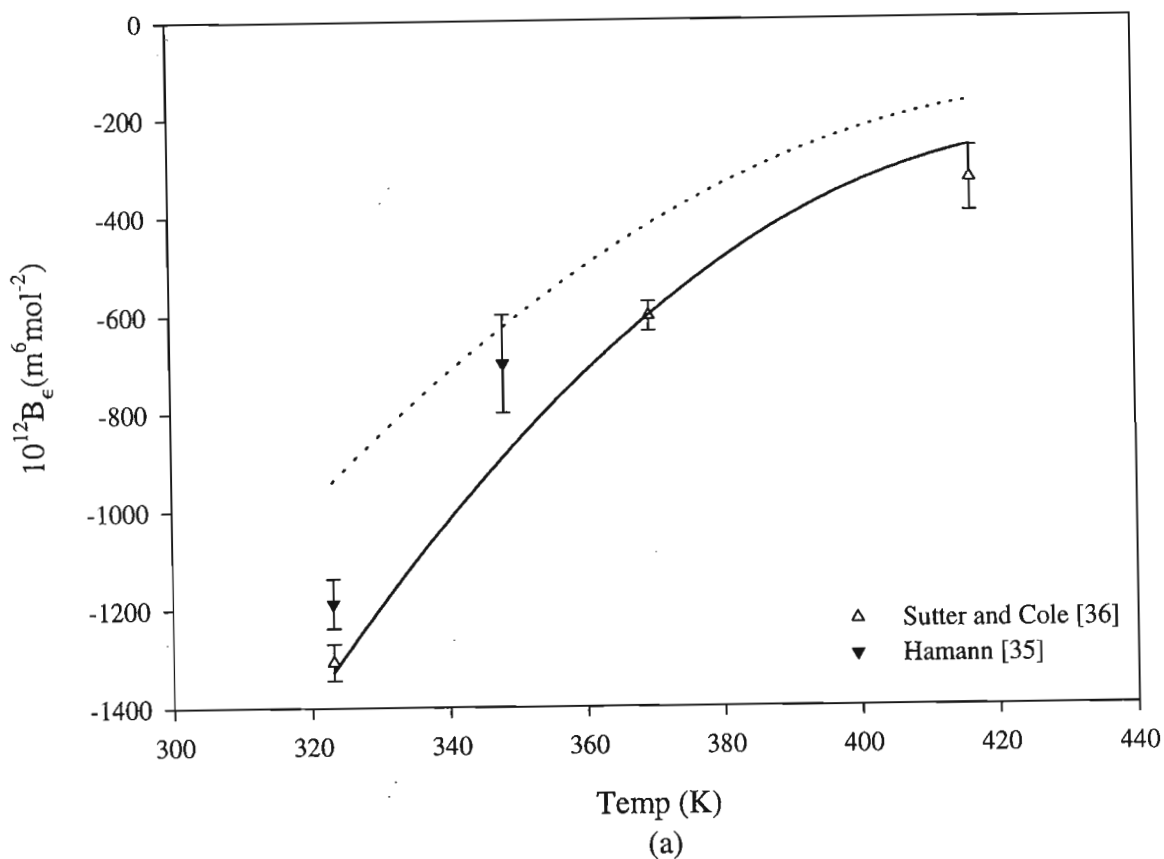
Figure 8.2: Temperature dependence of the calculated and measured values of the second (a) dielectric, and (b) Kerr-effect virial coefficients of trifluoromethane. The solid curves represent our calculated values, while in (b) the dotted line represents the curve calculated by Couling and Graham [9] and the dashed line is the calculated curve of Buckingham *et al.* [177].

159

It can be seen from Table 8.13 that, as for fluoromethane, the leading term in the A-tensor for the orientational term makes a significant contribution of -8.3%, which again draws our attention to the need for accurate values of the A-tensor components. The term $\alpha_1\mu_1\theta_1$, which makes a contribution of 23% to the calculated value of B_ε of fluoromethane, contributes 58.8% to B_ε of trifluoromethane. In addition, the $\alpha\theta$ series makes a smaller but still significant contribution of 8.4%. The most probable reason for the highly significant contribution of these term is the large quadrupole moment of this molecule. Previous workers [2,3,101] considered only the first three terms in the $\mu\alpha$ series, which in this case would yield a value of $B_\varepsilon = 441.02 \times 10^{-12}\text{m}^6\text{mol}^{-2}$ compared with our value of $B_\varepsilon = 1149.92 \times 10^{-12}\text{m}^6\text{mol}^{-2}$! These workers also omitted the contribution of $B_{\varepsilon_{\text{ind}}}$, but this is less significant, contributing only 1.5% to B_ε at 323.15 K. Thus, the importance of establishing convergence of all the series is demonstrated.

Table 8.14: The relative contributions of the terms used to calculate B_K for trifluoromethane at 245.5 K for $\lambda = 632.8$ nm.

Contributing Term	$10^{30} \times$ Value $\text{C}^2\text{m}^8\text{J}^{-2}\text{mol}^{-2}$	% Contribution to B_K
α_2	0.0003	0.003
α_3	-0.0082	0.08
α_4	0.1249	1.22
α_5	0.0113	0.11
$\mu_2\alpha_1$	0.8872	8.68
$\mu_2\alpha_2$	5.1436	50.33
$\mu_2\alpha_3$	2.2180	21.70
$\mu_2\alpha_4$	0.2520	2.47
$\mu_2\beta_1$	0.0339	0.33
$\mu_1\alpha_1\mathcal{A}_1$	1.4986	14.66
$\mu_1\alpha_2\mathcal{A}_1$	0.2423	2.37
$\mu_1\theta_1\alpha_1$	-0.1920	-1.88

$$B_K = 10.22 \times 10^{-30}\text{C}^2\text{m}^8\text{J}^{-2}\text{mol}^{-2}$$

Next, the second Kerr-effect virial coefficient was calculated for trifluoromethane using the molecular parameters listed in Table 8.9. The graph of the calculated curve and measure values is presented in Figure 8.2 (b). Couling and Graham [9] have also calculated B_K for trifluoromethane, using the parameter set: $R_0 = 0.440$ nm, $\varepsilon/k = 178.5$ K and $D = -0.050$; including the α series and the first three terms of the $\mu\alpha$ series. Their theoretical curve is shown as a dotted line. As for fluoromethane, their curve is lower than ours by almost a factor of two, due in part to the positive contribution of our additional terms, as shown in Table 8.14. These additional terms contribute approximately 18% to our theoretical values of B_K. Figure 8.2 (b) also shows the calculated curve of Buckingham

et al. [177] as a dashed line.

Considering the large experimental errors of the measured values the calculated values obtained using our parameter set constitute a reasonably good fit to the experimental data of Buckingham and Orr [33]. However, our calculated curve falls outside the experimental error range of the more precise values measured by Schaefer *et al.* [83].

The calculation of the second refractivity virial coefficient met with less success. Table 8.15 shows the wavelength dependence of the calculated values of B_R, together with experimental data of Buckingham and Graham [39] and Burns *et al.* [62]. It can be seen that the calculated values are much larger than the measured values and while the experimental values of B_R increase with increasing wavelength, the calculated values show the opposite trend. The contributions of the various terms in the calculation of B_R at $\lambda = 632.8$ nm is given in Table 8.16. It can be seen that both the $\alpha_1 \mathcal{A}_2$ and $\alpha_2 C_1$ terms are significant and it may be worth investigating the next term in each series.

Table 8.15: Calculated and measured values of B_R for trifluoromethane at $T = 298.2$ K.

λ	$10^{12}\ B_R^{\text{exp}}$	Ref.	$10^{12}\ B_R^{\text{calc}}$
nm	$\text{m}^6\text{mol}^{-2}$		$\text{m}^6\text{mol}^{-2}$
632.8	3.4±1.1	[39]	7.77
	2.54±1.35	[62]	
514.5	2.44±0.89	[62]	8.32
488.0	1.56±0.75	[62]	8.39

Table 8.16: The relative contributions of the terms used to calculate B_R for trifluoromethane at 632.8 nm.

Contributing Term	$10^{12} \times$ Value $\text{m}^6\text{mol}^{-2}$	% Contribution to B_R
α_2	-0.739	-9.51
α_3	9.762	125.60
α_4	0.289	3.72
β_1	-2.528	-32.53
$\alpha_1 \beta_1$	-0.027	-0.35
$\alpha_1 \mathcal{A}_1$	-1.842	-23.70
$\alpha_2 \mathcal{A}_1$	1.979	25.46
$\mathcal{A}_2$	0.039	0.50
$\alpha_1 \mathcal{A}_2$	-0.326	-4.19
$\alpha_2 C_1$	1.166	15.00

$$B_R = 7.773 \times 10^{-12} \text{m}^6\text{mol}^{-2}$$

As for fluoromethane, there is no experimental data for the second light-scattering virial coefficient for trifluoromethane. We have calculated B_ρ using our optimized parameter set and Table 8.17 shows the relative contributions of the various terms used to arrive at the calculated value. The contribution of the A-tensor terms amounts to less than 2% for this gas, but this value is obtained using estimated A-tensor components. Once again we note, that reliable measured or calculated values for the A-tensor are necessary to establish conclusively the relative importance of the A-tensor contribution to second virial coefficients. From the table it is clear that the C-tensor contribution is negligible.

Table 8.17: The relative contributions of the terms used to calculate B_ρ for trifluoromethane at 298.15 K and $\lambda = 632.8$ nm.

Contributing Term	$10^6 \times$ Value $\mathrm{m^3 mol^{-1}}$	% Contribution to B_ρ
G	7.189	0.56
b_3	0.254	0.02
a_3	-126.092	-9.81
a_4	1650.397	128.47
a_5	104.408	8.13
$a_2\mathcal{A}_1$	25.244	1.96
$a_3\mathcal{A}_1$	-2.275	-0.18
$a_3\mathcal{C}_1$	0.229	0.02
$\mathcal{S}_\rho$	1659.354	129.16
$2B$	-374.660	-29.16

$$B'_\rho = 1284.693 \times 10^{-6} \mathrm{m^3 mol^{-1}}$$
$$B_\rho = 0.647 \times 10^{-6} \mathrm{m^3 mol^{-1}}$$

Thus, we see that for trifluoromethane it was possible to find a parameter set which yielded excellent fits for both $B(T)$ and B_ε. Although the shape parameter of this set is less negative than one might expect, it is more reasonable than the positive value of Sutter [3]. The set of parameters chosen also yields a reasonably good fit to most of the experimental data for B_K, although the calculated values were larger than the measured values of Schaefer et $al.$ [83]. In addition, values of B_R calculated using the same set of Lennard-Jones and shape parameters were much larger than the available measured values. Thus, although our parameter set provides a good fit for $B(T)$, B_ε and a reasonable fit for B_K, it fails to explain the observed values of B_R. Measurements of B_ρ would be desirable, as they would allow a further test of the chosen parameters. It would also be of interest to study difluoromethane to see if the mean values for the parameters of fluoromethane and trifluoromethane would yield satisfactory results for second virial coefficients of difluoromethane.

162

8.4 Calculations for chloromethane

8.4.1 Molecular properties of chloromethane

Table 8.18 presents a list of the wavelenght-independent molecular properties of chloromethane which have been used in these calculations. The dynamic polarizability tensors α and the values of ρ_0 are given in Table 8.19. There are no β, A- and C-tensor components available.

Table 8.18: Wavelength-independent molecular parameters of chloromethane used in the calculations.

Molecular Parameter	Value	Reference
$10^{30}\mu$ (Cm)	6.32	[3]
$10^{40}\theta$ (Cm^2)	4.00	[213]
$10^{40}a$ (C^{2}m^{2}J^{-1})	5.25	[3]
$10^{40}\Delta a$ (C^{2}m^{2}J^{-1})	1.613	[4]†
$10^{40}a_{\parallel}$ (C^{2}m^{2}J^{-1})	6.325	
$10^{40}a_{\perp}$ (C^{2}m^{2}J^{-1})	4.712	
κ_a	0.102	

† Extrapolated from the dynamic values to zero frequency.

Table 8.19: The values of ρ_0 and the components of the optical-frequency polarizability tensor α_{ij} of chloromethane [4] used in the calculations.

λ nm	$100\rho_0$	$10^{40}\alpha$ (C^{2}m^{2}J^{-1})	$10^{40}\Delta\alpha$ (C^{2}m^{2}J^{-1})	$10^{40}\alpha_{\parallel}$ (C^{2}m^{2}J^{-1})	$10^{40}\alpha_{\perp}$ (C^{2}m^{2}J^{-1})	κ_α
632.8	0.755	5.04	1.71	6.18	4.47	0.113
514.5	0.779	5.10	1.75	6.27	4.52	0.114

Table 8.20: Lennard-Jones parameters and shape factors for chloromethane.

		R_0 (nm)	ε/k (K)	D
(1)	Our values fitted to $B(T)$	0.370	345	0.260
(2)	Our values fitted to B_ε	0.390	337	0.260
(3)	Fitted values of Couling and Graham [9]	0.395	350	0.210

For chloromethane we could not find a single set of parameters for which both $B(T)$ and B_ε fitted the experimental data available. Thus, we considered two different sets of parameters. The first set yields calculated values of $B(T)$ to within 0.5% of the

experimental values quoted in Table A.2 for temperatures in the range from $T = 280$ K to 400 K, while the values for B_ε, which are as much as 78% too high, are at least of the correct sign. The second set of parameters yield calculated values of B_ε which are within 50% of the measured values of Sutter and Cole [2], while the calculated values of $B(T)$ agreed with the experimental data to within less than 2.5%. Significantly better fits to B_ε could only be achieved if the calculated values of $B(T)$ were allowed to deviate from the observed values by percentages significantly in excess of the experimental precision of $B(T)$. Since the measured values of the second pressure virial coefficient are more precise and the theory better understood, this was considered to be unacceptable. These two sets of parameters are shown in Table 8.20, along with the fitted values quoted by Couling and Graham [7, 9]. It should be noted that the third significant figure in the values of D are significant.

8.4.2 Results of calculations of second virial coefficients for chloromethane

All three sets of parameters as shown in Table 8.20 were used to calculate values for the second pressure, dielectric and light-scattering virial coefficients. Table 8.21 shows the calculated values for $B(T)$ along with the smoothed values of Dymond and Smith [1]. It is clear that both of our optimized parameter sets yield better agreement with the experimental data for $B(T)$ than the parameter set used by Couling and Graham [9], due to the fact that we have included the induced-dipole-induced-dipole potential in the intermolecular potential (Chapter 2).

Table 8.21: Calculated values of $B(T)$ for chloromethane for three sets of parameters, together with the smoothed values of Dymond and Smith [1].

T	$10^6 B^{exp}$	(1) $10^6 B^{calc}$	%	(2) $10^6 B^{calc}$	%	(3) $10^6 B^{calc}$	%
K	m³mol⁻¹	m³mol⁻¹	Error	m³mol⁻¹	Error	m³mol⁻¹	Error
280	-470±10	-469.66	-0.07	-463.33	-1.42	-465.28	-1.00
300	-400±10	-398.47	-0.38	-397.02	-0.74	-401.03	0.26
320	-345±10	-343.62	-0.40	-345.12	0.03	-350.24	1.52
340	-300±5	-300.21	0.07	-303.47	1.16	-309.17	3.06
360	-264±5	-265.07	0.41	-269.37	2.03	-275.32	4.29
400	-212±5	-211.84	-0.08	-216.98	2.35	-222.92	5.15
SSE:		5.58		119.06		382.27	

Table 8.22 shows the relative importance of the various terms included in the calculation of the second dielectric virial coefficient. For this molecule the leading dipole series is by far the most important contribution, yielding approximately 107% of B_ε.

Table 8.22: The relative contributions of the terms used to calculate B_ε for chloromethane at 323.15 K for the parameter set (D=0.260, R_0=0.390, ε/k=337.0).

Contributing Term	$10^{12} \times$ Value $m^6 mol^{-2}$	% Contribution to B_ε
α_2	21.977	-0.75
α_3	73.964	-2.52
α_4	4.893	-0.17
$B_{\varepsilon_{ind}}$	100.834	-3.44
μ_2	-5837.051	198.56
$\alpha_1\mu_2$	1668.428	-56.75
$\alpha_2\mu_2$	985.353	-33.52
$\alpha_3\mu_2$	45.929	-1.56
$\alpha_1\mu_1\theta_1$	84.318	-2.87
$\alpha_2\mu_1\theta_1$	1.428	-0.05
$\alpha_2\theta_2$	8.906	-0.30
$\alpha_3\theta_2$	1.995	-0.07
$B_{\varepsilon_{or}}$	-3040.695	103.44

$$B_\varepsilon = -2939.861 \times 10^{-12} m^6 mol^{-2}$$

Table 8.23: Calculated values of B_ε for chloromethane for three sets of parameters, together with the measured values of Sutter and Cole [2].

		(1)		(2)		(3)	
T K	$10^{12}B_\varepsilon^{exp}$ $m^3 mol^{-1}$	$10^{12}B_\varepsilon^{calc}$ $m^6 mol^{-2}$	% Error	$10^{12}B_\varepsilon^{calc}$ $m^6 mol^{-2}$	% Error	$10^{12}B_\varepsilon^{calc}$ $m^6 mol^{-2}$	% Error
323.15	-4470±200	-2161.6	-51.6	-2939.9	-34.2	-1326.6	-70.3
369.45	-2517±50	-837.5	-66.7	-1430.1	-43.2	-506.6	-79.9
404.75	-1696±60	-361.2	-78.8	-846.4	-50.1	-201.3	-88.1

The only other terms to contribute significantly are the α_3 Kirkwood [127] term and the leading term in the dipole-quadrupole series which each amount to about 2.5%. Unfortunately, the A-tensor contribution, which has been shown to be significant for fluoro- and trifluoromethane, could not be calculated since no data is available for this molecule. The temperature dependence of B_ε for the three parameter sets is given in Table 8.23, while Figure 8.3 shows the relationship between the theoretical and experimental values graphically. In the figure, the solid line represents the curve calculated using the second parameter set, chosen to improve the B_ε fit. This curve lies closest to the experimental data, while the dashed curve, representing the calculated values of parameter set (1), is approximately 20% higher. The values calculated using the parameter set of Couling and Graham [9] are given by the dotted line, which lies furthest from the experimental data.
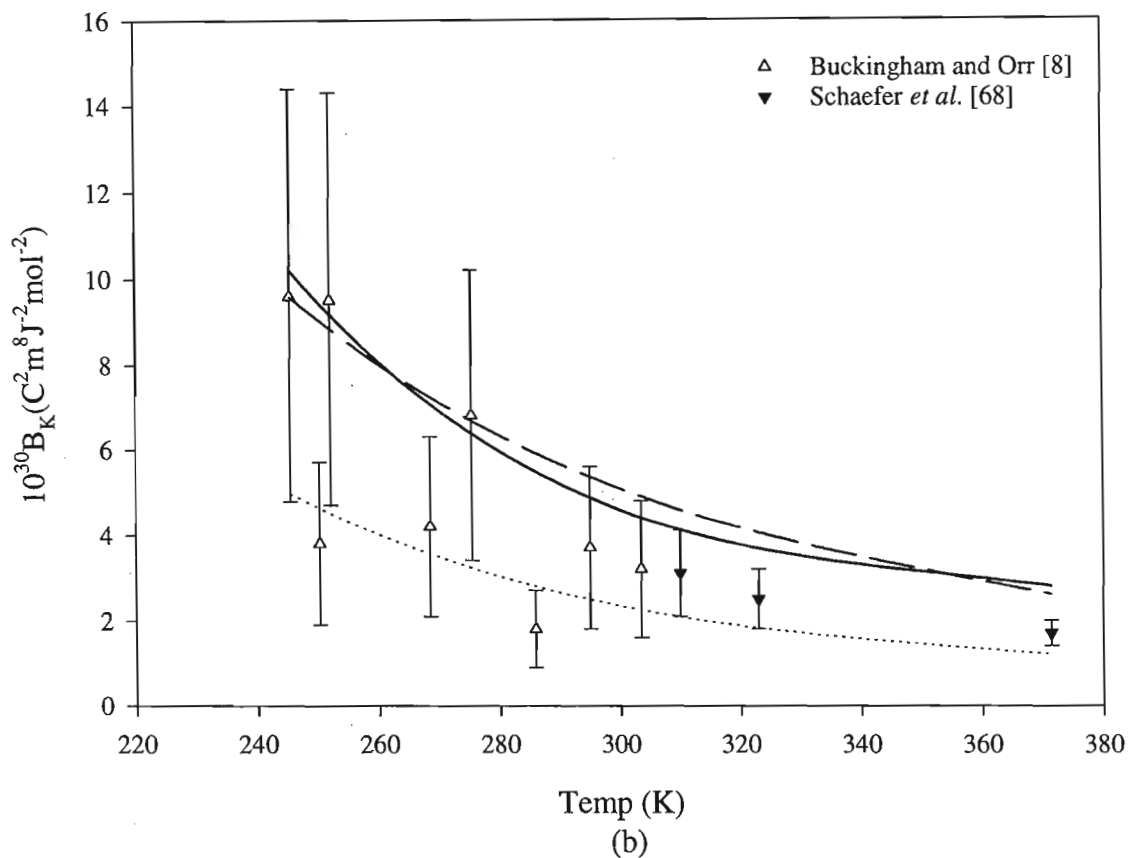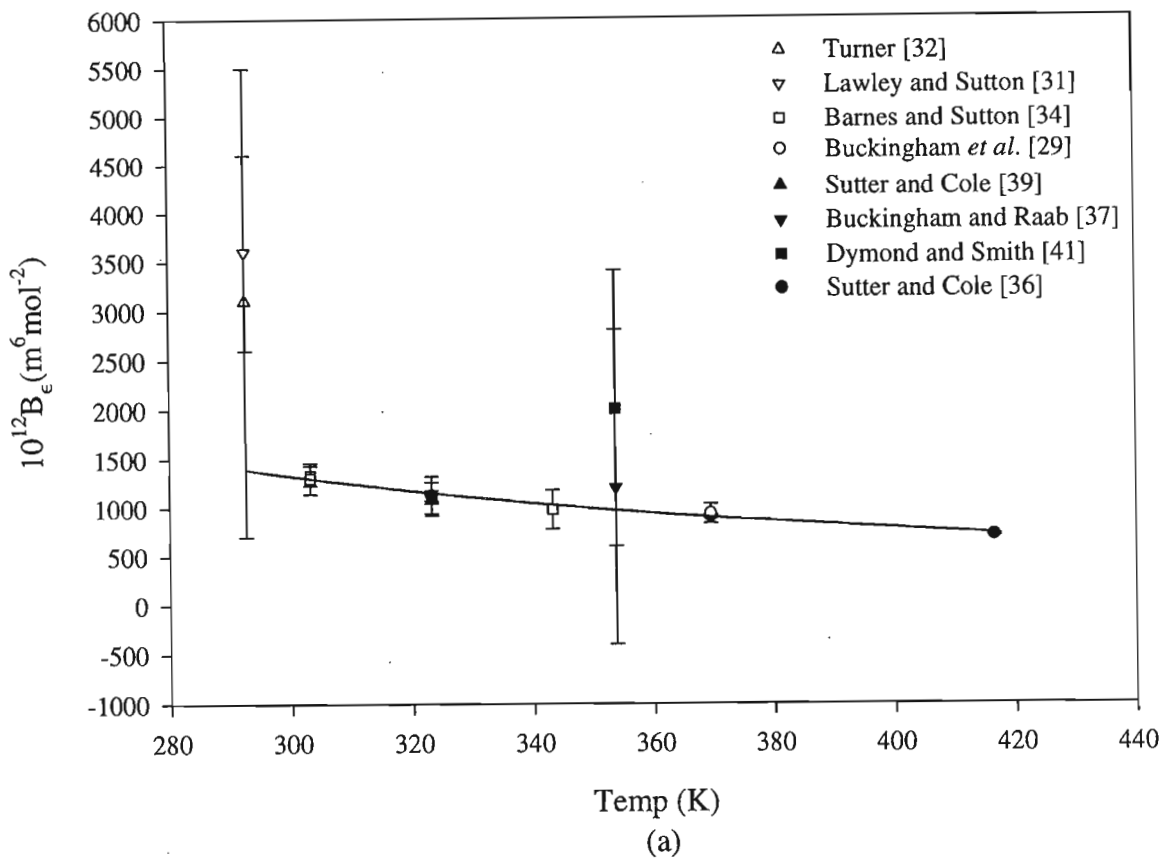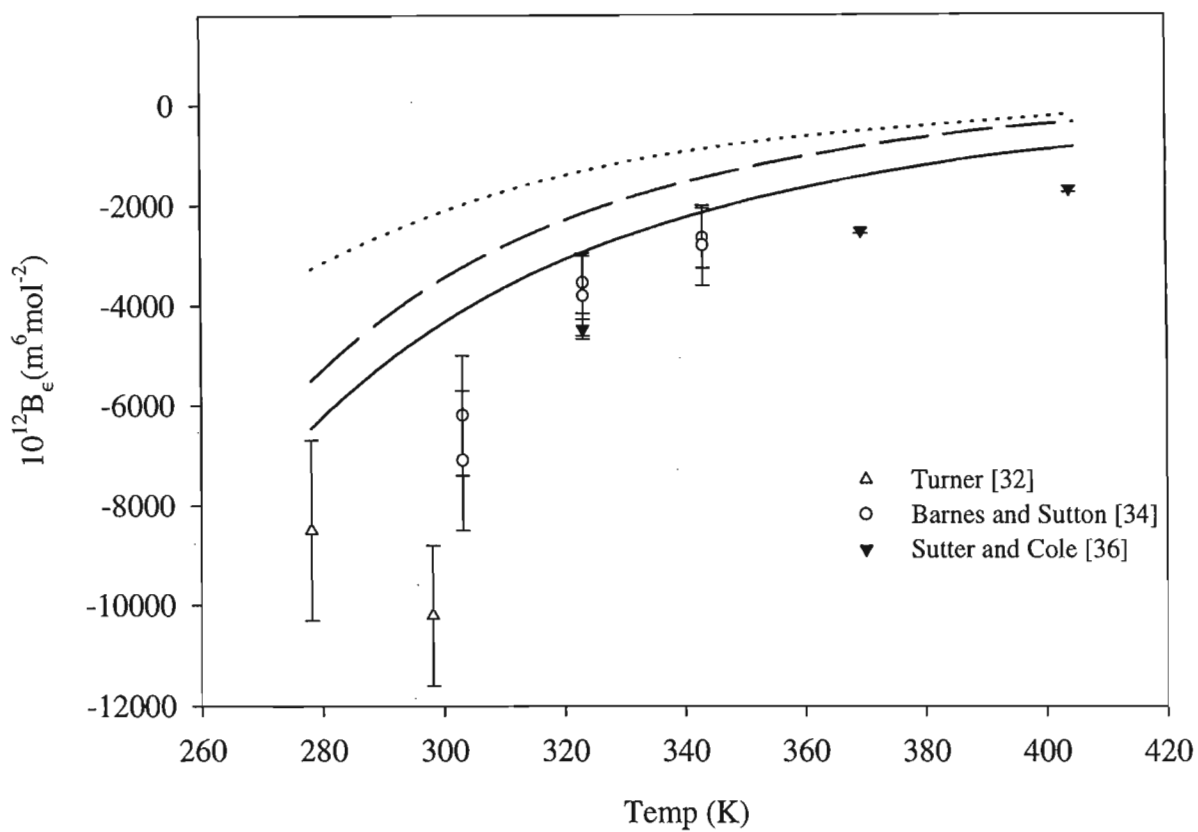
Figure 8.3: Temperature dependence of the calculated and measured values of the second dielectric virial coefficient of chloromethane. The solid line represents parameter set (2), the dashed line set (1), while the dotted line represents set (3), as given in Table 8.20.

166

It can be seen that a negative contribution from the A-tensor term, similar to that found for fluoromethane would improve the fit of all three parameter sets.

Although the second refractivity virial coefficients has not been measured for chloromethane, we have calculated values for B_R using all three parameter sets, for possible future comparison. Table 8.24 shows the relative contributions of the terms used to calculate B_R for a wavelength of 514.5 nm at 298.15 K. Note that, since no measured or estimated values are available for the hyperpolarizability, A- or C-tensor components, the contribution of these properties to B_R could not be calculated.

Table 8.24: The relative contributions of the terms used to calculate B_R for chloromethane at 298.15 K for $\lambda = 514.5$ nm.

	(1)		(2)		(3)	
Contrib.	$10^{12} \times$ Value	% of	$10^{12} \times$ Value	% of	$10^{12} \times$ Value	% of
Term	$m^6 mol^{-2}$	B_R	$m^6 mol^{-2}$	B_R	$m^6 mol^{-2}$	B_R
α_2	-27.233	-38.53	-26.038	-54.89	-15.833	-32.36
α_3	93.036	131.63	70.398	148.41	62.126	126.96
α_4	4.874	6.90	3.076	6.48	2.642	5.40
B_R	70.678		47.436		48.935	

Table 8.25: The relative contributions of the terms used to calculate B_K for chloromethane at 304.1 K for a wavelength of 632.8 nm.

	(1)		(2)		(3)	
	$10^{30} \times$ Value	% of	$10^{30} \times$ Value	% of	$10^{30} \times$ Value	% of
Term	$C^2 m^8 J^{-2} mol^{-2}$	B_K	$C^2 m^8 J^{-2} mol^{-2}$	B_K	$C^2 m^8 J^{-2} mol^{-2}$	B_K
α_2	0.0434	0.18	0.0398	0.27	0.0258	0.14
α_3	-0.2314	-0.98	-0.2202	-1.51	-0.1363	-0.74
α_4	0.7538	3.19	0.5739	3.94	0.5132	2.79
α_5	0.0780	0.33	0.0496	0.34	0.0434	0.24
$\mu_2\alpha_1$	-11.7648	-49.76	-11.1701	-76.60	-8.2259	-44.78
$\mu_2\alpha_2$	20.9010	88.41	15.3561	105.30	16.3967	89.25
$\mu_2\alpha_3$	11.8081	49.95	8.7531	60.02	8.5727	46.66
$\mu_2\alpha_4$	1.9779	8.37	1.1498	7.88	1.1288	6.14
$\mu_1\theta_1\alpha_1$	0.0752	0.32	0.0513	0.35	0.0528	0.29
B_K	23.6413		14.5833		18.3712	

$$B_K^{exp} = (1.97 \pm 0.29) \times 10^{-30} \, C^2 m^8 J^{-2} mol^{-2} \, [83]$$

There is only one measured value [83] of the second Kerr-effect virial coefficient for chloromethane. Table 8.25 gives the relative magnitudes of the various contributions to B_K for a wavelength of 632.8 nm at 304.1 K. As for B_R, the contribution of the hyperpolarizability, A- or C-tensor components to B_K could not be calculated. In the

calculation of B_K, the $\mu\alpha$ series makes the dominant contribution of more than 90%. All the values calculated are an order of magnitude larger than the measured value.

The only remaining test of the parameter sets is the second light-scattering virial coefficient. The sole measured value available is that of Couling and Graham [7,8] taken using a wavelength of 514.5 nm at room temperature. This measured value is given in Table 8.26, together with the theoretical values calculated using the three parameter sets. The best agreement is obtained with parameter set (2), which also yields the best fit for B_ε. The relative contributions of the terms used to calculate B_ρ for this parameter set are listed in Table 8.27.

Table 8.26: Calculated values of B_ρ for chloromethane for three sets of parameters, together with the measured value of Couling and Graham [7,8] at $\lambda = 514.5$ nm.

		(1)		(2)		(3)	
T	$10^6 B_\rho^{exp}$	$10^6 B_\rho^{calc}$	%	$10^6 B_\rho^{calc}$	%	$10^6 B_\rho^{calc}$	%
K	m^3mol^{-1}	m^3mol^{-1}	Error	m^3mol^{-1}	Error	m^3mol^{-1}	Error
299.65	-3.30±0.26	-2.42	26.7	-3.50	6.1	-3.68	11.5

Table 8.27: The relative contributions of the terms used to calculate B_ρ for chloromethane at 299.6 K and $\lambda = 514.5$ nm [9].

Contributing Term	$10^6 \times$ Value m^3mol^{-1}	% Contribution to B_ρ
G	37.60	-8.29
b_3	5.44	-1.20
a_3	-194.64	42.93
a_4	464.87	-102.54
a_5	29.74	-6.56
$\mathcal{S}_\rho$	343.01	-75.66
$2B$	-796.38	175.66

$$B_\rho' = -453.37 \times 10^{-6} m^3mol^{-1}$$
$$B_\rho = -3.495 \times 10^{-6} m^3mol^{-1}$$

In this work we are attempting to isolate a unique set of molecular parameters which will explain all of the second virial coefficient phenomena under study for each gas. The parameter set (2), chosen to optimize the B_ε fit, yields a value for B_ρ which lies within the experimental error of the measured value and fits $B(T)$ to within 2.5%. This set appears to be our best choice. Since all the parameter sets yield calculated values for B_K an order of magnitude larger than the experimental value, it is not possible to choose which of the sets provides the best fit, although the value calculated using set (2) is the closest

to the measured value. It would be of great interest if reliable measured or theoretical values were available for the A-tensor components, as well as more experimental values for the second Kerr-effect and light-scattering virial coefficients together with measured values for B_R. This would allow one to test the fit of the various parameter sets more rigourously. Until such time as this data becomes available, a more definitive conclusion is not possible.

8.5 Calculations for hydrogen chloride

8.5.1 Molecular properties of hydrogen chloride

Table 8.28 presents a list of the molecular properties of hydrogen chloride which have been used in these calculations. The dynamic polarizability α and hyperpolarizability β are at a wavelength of 632.8 nm. Since no experimental values for the components of C_{ijkl} for HCl are available, the estimated values of Burns, Graham and Weller [62] are used. These were obtained by scaling the values for HF quoted by Rivail and Cartier [214] in proportion to the relative values of the components of α_{ij} and A_{ijk} for HF and HCl. The values of R_0, ε/k and D are our fitted values, chosen to optimize the agreement between theory and experiment for both $B(T)$ and B_ε.

Table 8.28: Molecular parameters of hydrogen chloride used in the calculations ($\lambda = 632.8$ nm).

Molecular Parameter	Value		Reference
$10^{30}\mu$ (Cm)	3.646		[215]
$10^{40}\theta$ (Cm^2)	12.4		[215]
$10^{40}a$ (C^{2}m^{2}J^{-1})	2.867		[216]
$10^{40}\Delta a$ (C^{2}m^{2}J^{-1})	0.314		
$10^{40}a_\parallel$ (C^{2}m^{2}J^{-1})	3.076		
$10^{40}a_\perp$ (C^{2}m^{2}J^{-1})	2.762		
κ_a	0.0363$_9$		[4]
$100\rho_0$	0.079		[190]
$10^{40}\alpha$ (C^{2}m^{2}J^{-1})	2.893		[44, 62]
$10^{40}\Delta\alpha$ (C^{2}m^{2}J^{-1})	0.317		
$10^{40}\alpha_\parallel$ (C^{2}m^{2}J^{-1})	3.104		
$10^{40}\alpha_\perp$ (C^{2}m^{2}J^{-1})	2.787		
κ_α	0.0365		[4]
$10^{50}A_\parallel$ (C^{2}m^{3}J^{-1})	1.16		[216]
$10^{50}A_\perp$ (C^{2}m^{3}J^{-1})	0.133		[216]
$10^{60}C_{1111}$ (C^{2}m^{4}J^{-1})	0.8144		[62]
$10^{60}C_{1313}$ (C^{2}m^{4}J^{-1})	0.6588		[62]
$10^{60}C_{3333}$ (C^{2}m^{4}J^{-1})	1.0504		[62]
$10^{50}\beta$ (C^{3}m^{3}J^{-2})	0.0234	[216]	
$10^{50}\beta_\parallel$ (C^{3}m^{3}J^{-2})	0.009		[216]
$10^{50}\beta_\perp$ (C^{3}m^{3}J^{-2})	0.015		[216]
R_0 (nm)	0.355		
ε/k (K)	204.5		
D	0.028		

8.5.2 Results of calculations of second virial coefficients for hydrogen chloride

Unfortunately, there is a dearth of experimental second virial coefficient data for hydrogen chloride, due to its highly corrosive nature. The only effects which have been measured are the second pressure and dielectric virial coefficients. It was hoped that, since a more complete set of the molecular data necessary to calculate B_ϵ is available for hydrogen chloride than for the other gases under study, a good fit for the second dielectric virial coefficient would be possible. However, it was impossible to obtain values of B_ϵ of the correct order of magnitude, without altering the Lennard-Jones parameter to an unacceptable degree. The measured values are an order of magnitude higher than the highest calculated values found. The entire range of possible shape parameters was tested without success. The parameter set was optimized to obtain agreement for $B(T)$ to within 2%, with values of B_ϵ as high as possible. The temperature dependence of the second pressure virial coefficient is given in Table 8.29, while Table 8.30 shows measured values of B_ϵ along with our calculated values.

Table 8.29: Calculated values of $B(T)$ for hydrogen chloride, together with the experimental values [1].

T	$10^6 B(T)$ (exp)	$10^6 B(T)$	%
K	$m^3 mol^{-1}$	$m^3 mol^{-1}$	Error
190	-456±7	-454.5	0.32
200	-392±7	-392.6	0.15
225	-287±7	-287.0	0.00
250	-221±7	-221.1	0.05
275	-175±7	-176.5	0.86
295	-147±6	-150.1	2.04
300	-142±6	-144.5	1.40
330	-114±6	-116.3	2.02

Table 8.31 shows the relative contributions of the terms used to calculate B_ϵ for hydrogen chloride at 292.5 K. It can be seen that $B_{\epsilon_{ind}}$ makes a small but significant contribution to the total, due mainly to the α_3, or Kirkwood [127], term. The A-tensor series makes a significant contribution of approximately 4%, while apart from the leading μ_2 series the most important contribution is from the dipole-quadrupole $\mu_1\theta_1$ series, which yields 73% of the final value. The quadrupole series is also significant, contributing 16% to B_ϵ. Thus, once again, the importance of considering the quadrupole moment is demonstrated, since without these terms the calculated value would be considerably lower and thus the agreement with experiment even worse!

Table 8.30: Calculated values of B_ε for hydrogen chloride, together with the measured values of Lawley and Sutton[a] [10] and Powles and MacGrath[b] [11].

T	$10^{12} B_\varepsilon^{\text{exp}}$	$10^{12} B_\varepsilon^{\text{calc}}$
K	$\text{m}^6\text{mol}^{-2}$	$\text{m}^6\text{mol}^{-2}$
292.5	4000 ± 1000^a	559.86
	3600 ± 1000^b	
312.8	3600 ± 1000^a	486.93
	3200 ± 1000^b	

Table 8.31: The relative contributions of the terms used to calculate B_ε for hydrogen chloride at 292.5 K.

Contributing Term	$10^{12} \times$ Value $\text{m}^6\text{mol}^{-2}$	% Contribution to B_ε
α_2	0.632	0.11
α_3	11.885	2.12
α_4	0.473	0.08
β_1	0.415	0.07
$\alpha_1 \beta_1$	0.003	0.001
$\alpha_1 \mathcal{A}_1$	0.526	0.09
$\alpha_2 \mathcal{A}_1$	0.504	0.09
$\mathcal{A}_2$	-0.004	-0.001
$\alpha_1 \mathcal{A}_2$	-0.001	-0.000
$\alpha_2 C_1$	1.597	0.28
$B_{\varepsilon_{\text{ind}}}$	16.030	2.86
μ_2	-461.502	-82.43
$\alpha_1 \mu_2$	319.968	57.15
$\alpha_2 \mu_2$	151.477	27.06
$\alpha_3 \mu_2$	8.870	1.58
$\mathcal{A}_1 \mu_2$	20.436	3.65
$\alpha_1 \mathcal{A}_1 \mu_2$	3.778	0.67
$\beta_1 \mu_3$	0.578	0.10
$\beta_1 \alpha_1 \mu_3$	0.056	0.01
$\alpha_1 \mu_1 \theta_1$	404.636	72.27
$\alpha_2 \mu_1 \theta_1$	3.414	0.61
$\beta_1 \mu_1 \theta_1$	0.300	0.05
$\alpha_2 \theta_2$	58.164	10.39
$\alpha_3 \theta_2$	33.657	6.01
$B_{\varepsilon_{\text{or}}}$	543.832	97.14

$$B_\varepsilon = 559.862 \times 10^{-12} \text{m}^6\text{mol}^{-2}$$

No measured values for the second refractivity, Kerr-effect or light-scattering virial coefficients are available for hydrogen chloride. However, we have calculated values for B_R, B_K and B_ρ using our optimized parameter set.

Table 8.32 lists the relative significance of the terms used to calculate B_K at 298.15 K for a wavelength of 632.8 nm. The leading $\mu\alpha$ series makes the most significant contribution of 86%, while the $\mu\alpha\mathcal{A}$ series contributes 7%, emphasizing the importance of including the A-tensor terms.

Table 8.32: The relative contributions of the terms used to calculate B_K for hydrogen chloride at 298.15 K for a wavelength of 632.8 nm.

Contributing Term	$10^{30} \times$ Value $C^2m^8J^{-2}mol^{-2}$	% Contribution to B_K
α_2	0.0002	0.01
α_3	0.0029	0.21
α_4	0.0559	3.99
α_5	0.0045	0.32
$\mu_2\alpha_1$	-0.1277	-9.12
$\mu_2\alpha_2$	0.7597	54.24
$\mu_2\alpha_3$	0.5108	36.47
$\mu_2\alpha_4$	0.0579	4.13
$\mu_2\beta_1$	-0.0021	-0.15
$\mu_1\alpha_1\mathcal{A}_1$	0.0819	5.85
$\mu_1\alpha_2\mathcal{A}_1$	0.0201	1.44
$\mu_1\theta_1\alpha_1$	0.0366	2.61

$$B_K = 1.4007 \times 10^{-30} C^2m^8J^{-2}mol^{-2}$$

The relative contributions to the various terms used to calculate B_R for hydrogen chloride are given in Table 8.33. The $\alpha\beta$ series contributes 2.5% to B_R, while the A-tensor terms make a combined contribution of 6.3%. We note that the C-tensor term contributes almost 10%, and is thus highly significant. However, the C-tensor components used to calculate this term are values estimated by scaling the values of hydrogen fluoride [214]. Accurate measured or calculated C-tensor components would yield a more reliable value for this term.

Table 8.34 shows the relative magnitudes of the various contributions to our calculated value for B_ρ. It can be seen that, for hydrogen chloride, the A- and C-tensor terms together contribute less than a percent to the total and are thus negligible.

Table 8.33: The relative contributions of the terms used to calculate B_R for hydrogen chloride at 298.15 K for $\lambda = 632.8$ nm.

Contributing Term	$10^{12} \times$ Value $m^6 mol^{-2}$	% Contribution to B_R
α_2	0.621	3.83
α_3	12.067	74.40
α_4	0.490	3.02
β_1	0.404	2.49
$\alpha_1\beta_1$	0.003	0.02
$\alpha_1\mathcal{A}_1$	0.515	3.18
$\alpha_2\mathcal{A}_1$	0.509	3.14
$\mathcal{A}_2$	-0.004	-0.02
$\alpha_1\mathcal{A}_2$	-0.002	-0.01
$\alpha_2 C_1$	1.616	9.96

$$B_R = 16.219 \times 10^{-12} m^6 mol^{-2}$$

Table 8.34: The relative contributions of the terms used to calculate B_ρ for hydrogen chloride at 298.15 K and $\lambda = 632.8$ nm.

Contributing Term	$10^{6} \times$ Value $m^3 mol^{-1}$	% Contribution to B_ρ
G	5.640	0.45
b_3	-0.232	-0.02
a_3	75.378	5.97
a_4	1378.556	109.16
a_5	101.307	8.02
$a_2\mathcal{A}_1$	-11.461	-0.91
$a_3\mathcal{A}_1$	1.152	0.09
$a_3 C_1$	1.541	0.12
$\mathcal{S}_\rho$	1551.881	122.88
$2B$	-289.000	-22.88

$$B'_\rho = 1262.881 \times 10^{-6} m^3 mol^{-1}$$
$$B_\rho = 0.997 \times 10^{-6} m^3 mol^{-1}$$

Thus, although we have demonstrated that it is possible to find a good fit for $B(T)$, we were not able to obtain calculated values of B_ε of the correct order of magnitude. The measured values are large positive numbers and the best fit that we have presented here yielded values an order of magnitude smaller. We suggest that it is possible that the order of magnitude discrepancy may be due to problems with measuring B_ε experimentally, since hydrogen chloride is highly corrosive. Only new, precise experimental measurements can settle this question. Unfortunately, since no further data for second virial coefficients of hydrogen chloride exists, it is not possible to test our set of parameters more rigorously.

8.6 Calculations for nitrogen

8.6.1 Molecular properties of nitrogen

The static molecular properties of nitrogen are listed in Table 8.35, while Table 8.36 lists the values of the optical-frequency polarizability components and ρ_0. Since nitrogen is a non-polar molecule the dipole moment, first-order hyperpolarizability and the A-tensor components are all zero. No C-tensor data is available. Our optimized values for the Lennard-Jones and shape parameters are given in Table 8.37, together with the values used by Couling and Graham [7,9] to calculate the second Kerr-effect and light-scattering virial coefficients. We have used both sets of parameters to obtain theoretical values for all of the second virial coefficients under study.

Table 8.35: Wavelength-independent molecular parameters of nitrogen used in the calculations.

Molecular Parameter	Value	Reference
$10^{40}\theta$ (Cm^2)	-4.72	[217]
$10^{40}a$ (C^{2}m^{2}J^{-1})	1.936	[13]
$10^{40}\Delta a$ (C^{2}m^{2}J^{-1})	0.734	[9, 192]
$10^{40}a_{\parallel}$ (C^{2}m^{2}J^{-1})	2.425	
$10^{40}a_{\perp}$ (C^{2}m^{2}J^{-1})	1.691	
κ_a	0.1263	

Table 8.36: The components of the optical-frequency polarizability tensors α_{ij} of nitrogen, together with the values of ρ_0 used in the calculations.

λ nm	$100\rho_0$		$10^{40}\alpha$ C^{2}m^{2}J^{-1}		$10^{40}\Delta\alpha$ C^{2}m^{2}J^{-1}	$10^{40}\alpha_{\parallel}$ C^{2}m^{2}J^{-1}	$10^{40}\alpha_{\perp}$ C^{2}m^{2}J^{-1}	κ_{α}
632.8	1.042	[4]	1.961	[44, 62]	0.781	2.482	1.701	0.1327
514.5	1.0587	[8]	1.979	[4]	0.794	2.509	1.715	0.1338
488.0	1.05	[16]	1.984	[4]	0.793	2.513	1.720	0.1332

Table 8.37: Lennard-Jones parameters and shape factors for nitrogen.

		R_0 (nm)	ε/k (K)	D
(1)	Our fitted values	0.375	86.0	0.263
(2)	Fitted values of Couling and Graham [9]	0.368	91.5	0.112

8.6.2 Results of calculations of second virial coefficients for nitrogen

Both sets of parameters shown in Table 8.37 were used to calculate values for the second pressure, dielectric, refractivity, Kerr-effect and light-scattering virial coefficients. Table 8.38 shows the calculated values for $B(T)$ along with the smoothed values given by Dymond and Smith [1]. Our optimized parameter set yields calculated $B(T)$ values which agree to within 4.5% with the experimental data, while the values calculated using the second parameter set agree to within 6.8%. Both sets of calculated values fall within the range of the experimental errors.

Table 8.38: Calculated values of $B(T)$ for nitrogen for two sets of parameters, together with the smoothed values of Dymond and Smith [1].

		(1)		(2)	
T	$10^6 B^{\text{exp}}$	$10^6 B^{\text{calc}}$	%	$10^6 B^{\text{calc}}$	%
K	$\text{m}^3\text{mol}^{-1}$	$\text{m}^3\text{mol}^{-1}$	Error	$\text{m}^3\text{mol}^{-1}$	Error
200	-35.2 ± 1.0	-35.1	-0.3	-34.3	-2.6
250	-16.2 ± 1.0	-16.2	-0.0	-16.1	-0.6
300	-4.2 ± 0.5	-4.4	-4.5	-4.7	6.8
400	9.0 ± 0.5	9.3	3.3	8.6	-4.4
SSE:		0.14		1.23	

Since nitrogen is a non-polar gas, the values of the second dielectric virial coefficient are several orders of magnitude smaller than those of the polar gases. The experimental data available is very imprecise, with experimental uncertainties of between 25 and 170%, making it very difficult to distinguish the trend of the measured curve. Table 8.39 shows the relative importance of the terms used in the calculation of B_ε. It can been seen that, for nitrogen, the $B_{\varepsilon_{\text{ind}}}$ and $B_{\varepsilon_{\text{or}}}$ components are of similar magnitude, and thus the induction component cannot be omitted, as it sometimes is for polar molecules [3]. It must also be noted that it is not sufficient to calculate only the leading term in the quadrupole $\alpha\theta$ series, as the second and third terms contribute a total of 17.5% to B_ε. Unfortunately, since no C-tensor data is available, the $\alpha_2 C_1$ term could not be calculated. It is possible that this term may make a significant contribution to $B_{\varepsilon_{\text{ind}}}$.

The temperature dependence of the calculated values of B_ε for the two parameter sets are given in Table 8.40. The relationship between theory and experiment can be seen more clearly in Figure 8.4 (a), where the solid line represents the values of B_ε calculated using our optimized parameters, and the dotted line shows the curve obtained from the parameters of Couling and Graham [9]. It would appear that the experimental values decrease more rapidly with increasing temperature than the theoretical curves, although

this trend is not conclusive due to the large experimental errors. Since the solid curve passes through more of the error bars it could be said to fit the measured values slightly better than the dotted curve, so that our optimized parameter set would be preferred.

Table 8.39: The relative contributions of the terms used to calculate B_ε for nitrogen at 242.2 K for the parameter set (D=0.263, R_0=0.375, ε/k=86.0).

Contributing Term	$10^{12} \times$ Value $\mathrm{m^6mol^{-2}}$	% Contribution to B_ε
α_2	-0.629	-25.87
α_3	1.602	65.90
α_4	0.030	1.23
$B_{\varepsilon_\mathrm{ind}}$	1.003	41.26
$\alpha_2\theta_2$	1.002	41.22
$\alpha_3\theta_2$	0.361	14.85
$\alpha_4\theta_2$	0.065	2.67
$B_{\varepsilon_\mathrm{or}}$	1.428	58.74

$$B_\varepsilon = 2.431 \times 10^{-12} \mathrm{m^6mol^{-2}}$$

Table 8.40: Calculated values of B_ε for nitrogen for two sets of parameters, together with the measured values of Johnston *et al.*[a] [12] and Orcutt and Cole[b] [13].

T K	$10^{12}B_\varepsilon^{\mathrm{exp}}$ $\mathrm{m^3mol^{-1}}$	(1) $10^{12}B_\varepsilon^{\mathrm{calc}}$ $\mathrm{m^6mol^{-2}}$	(2) $10^{12}B_\varepsilon^{\mathrm{calc}}$ $\mathrm{m^6mol^{-2}}$
242.2	4.2 ± 1.0^a	2.64	3.43
296.2	2.0 ± 1.0^a	2.43	3.11
306.2	1.8 ± 1.0^a	2.40	3.07
322.2	0.6 ± 0.2^b	2.36	3.00
	1.0 ± 1.0^a		
344.2	0.0 ± 0.8^a	2.32	2.93
	-1.5 ± 2.5^a		

The contributions of the various terms in the calculation of B_R at $\lambda = 632.8$ nm for $T = 298$ K, using our optimized Lennard-Jones and shape parameters are given in Table 8.41. It is clear that α_3 is the dominant term and that the series is definitely converging. As was noted for B_ε, it is possible that the C-tensor term might make a significant contribution and experimental or theoretical values for the C-tensor components would allow a more complete calculation. Table 8.42 shows the measured values of B_R at three wavelengths. Although B_R has been measured at two different temperatures

Figure 8.4: Temperature dependence of the calculated and measured values of the second (a) dielectric, and (b) Kerr-effect virial coefficients of nitrogen. In both cases the solid and dotted lines represent the values calculated using parameter sets (1) and (2), respectively.

for a wavelength of 632.8 nm, the temperature dependence is not discernable, due to the scatter of the experimental data. All of the values calculated using both sets of parameters were larger than the measured values, with those obtained from our optimized set being slightly closer to experiment. As with the temperature dependence, it is unclear whether B_R depends on the wavelength. The data of Montixi et $al.$ [69] seem to indicate an increase of B_R with decreasing wavelength but the increase falls with the experimental error, so that a definitive conclusion is not possible. It should be noted, however, that both sets of theoretical data show a similar increase as the wavelength decreases.

Table 8.41: The relative contributions of the terms used to calculate B_R for nitrogen at 632.8 nm and 298 K for the parameter set (D=0.263, R_0=0.375, ε/k=86.0).

Contributing Term	$10^{12} \times$ Value $m^6 mol^{-2}$	% Contribution to B_R
α_2	0.0299	1.15
α_3	2.5166	96.61
α_4	0.0584	2.24
$B_R = 2.605 \times 10^{-12} m^6 mol^{-2}$		

Table 8.42: Calculated and measured values of B_R for nitrogen.

T K	λ nm	$10^{12} B_R^{exp}$ $m^6 mol^{-2}$	Ref.	(1) $10^{12} B_R^{calc}$ $m^6 mol^{-2}$	(2) $10^{12} B_R^{calc}$ $m^6 mol^{-2}$
298	632.8	0.74±0.65	[62]	2.61	3.62
		0.75±0.10	[69]		
		1.0±0.31	[39]		
323.2	633.0	0.89±0.06	[64]	2.47	3.38
		0.64±0.08	[65]		
298	514.5	0.62±0.78	[62]	2.68	3.73
		0.81±0.10	[69]		
	488.0	0.96±0.68	[62]	2.70	3.75
	488.1	0.85±0.10	[69]		

The second Kerr-effect virial coefficient has been measured for nitrogen by Buckingham et $al.$, but the results are very poorly defined, with no visible trend and such large percentage errors that the sign of the experimental values is not clear. The calculated values for B_K are very small, indicating that the pressure dependence of the molar Kerr constant K_m must be very slight and, therefore, extremely difficult to measure. The relationship between the experimental data and the values calculated from the two parameter sets is shown in Table 8.44 and Figure 8.4 (b), while the relative contributions

of the various terms making up B_K are listed in Table 8.43. In the graph, the solid line representing the curve calculated using our optimized parameters falls just above the error bars of the measured values, while the dotted line showing the values of obtained from the second parameter set are higher still. While the first set of parameters appears to yield a slightly better fit, the large uncertainties of the experimental values render it impossible to comment on the relative merits of the two parameter sets.

Table 8.43: The relative contributions of the terms used to calculate B_K for nitrogen at 248 K for $\lambda = 632.8$ nm for the parameter set ($D=0.263$, $R_0=0.375$, $\varepsilon/k=86.0$).

Contributing Term	$10^{32} \times$ Value $C^2 m^8 J^{-2} mol^{-2}$	% Contribution to B_K
α_2	0.0406	8.15
α_3	-0.3852	-77.30
α_4	0.7881	158.16
α_5	0.0280	5.62
$\theta_2\alpha_3$	0.0140	2.81
$\theta_2\alpha_4$	0.0101	2.03
$\theta_2\alpha_5$	0.0027	0.54

$$B_K = 0.4983 \times 10^{-32} C^2 m^8 J^{-2} mol^{-2}$$

Table 8.44: Calculated values of B_K for nitrogen for two sets of parameters, together with the measured values of Buckingham *et al.* [14], at a wavelength of $\lambda = 632.8$ nm.

T K	$10^{32} B_K^{exp}$ $C^2 m^8 J^{-2}$	(1) $10^{32} B_K$ $C^2 m^8 J^{-2}$	(2) $10^{32} B_K$ $C^2 m^8 J^{-2}$
248	-0.08±0.28	0.498	0.739
260	0.07±0.39	0.480	0.703
277	-0.21±0.33	0.456	0.658
286	-0.23±0.45	0.445	0.637
299	-0.30±0.59	0.430	0.609
315	0.04±0.30	0.412	0.578
334	-0.41±0.18	0.393	0.545

Finally, both parameter sets were used to calculate the second light-scattering virial coefficient for nitrogen at 514.5 nm and 488.0 nm. Table 8.45 shows the relative importance of the terms used to calculate B_ρ, while Table 8.46 shows the available measured values and the calculated values. Here it is clear that the second parameter set yields a far better fit to the experimental data.

Table 8.45: The relative contributions of the terms used to calculate B_ρ for nitrogen at 310 K and $\lambda = 514.5$ nm.

Contributing Term	$10^6 \times$ Value m^3mol^{-1}	% Contribution to B_ρ
G	1.155	10.69
b_3	0.443	4.10
a_3	-11.607	-107.42
a_4	26.328	243.66
a_5	0.666	6.16
$\mathcal{S}_\rho$	16.985	157.20
$2B$	-6.18	57.20

$$B'_\rho = 10.805 \times 10^{-6} m^3mol^{-1}$$
$$B_\rho = 0.123 \times 10^{-6} m^3mol^{-1}$$

Table 8.46: Calculated and measured values of B_ρ for nitrogen.

T K	λ nm	$10^{12} B_\rho^{exp}$ m^3mol^{-1}	Ref.	(1) $10^6 B_\rho^{calc}$ m^3mol^{-1}	(2) $10^6 B_\rho^{calc}$ m^3mol^{-1}
295.5	514.5	0.138±0.014	[7]	0.065	0.142
310		0.16	[91]	0.123	0.199
290	488.0	0.14	[16]	0.043	0.115

In conclusion, apart from the second light-scattering virial coefficient, our optimized Lennard-Jones and shape parameter set fits the experimental data better than the parameters used by Couling and Graham [9]. However, none of these fits can be said to be good, due in part to the large experimental errors and scatter in the measured values of B_ε, B_R and B_K. In order to make more a definitive conclusion, accurate experimental values would be necessary.

8.7 Calculations for carbon dioxide

8.7.1 Molecular properties of carbon dioxide

The molecular properties of carbon dioxide are listed in Table 8.47, while the wavelength-dependent parameters are given in Table 8.48. The dipole moment, first-order hyperpolarizability and the A-tensor components are all zero, since carbon dioxide is a non-polar molecule. As for the other non-polar molecules, no C-tensor components are available.

Table 8.47: Wavelength-independent molecular parameters of carbon dioxide used in the calculations

Molecular Parameter	Value	Reference
$10^{40}\theta$ (Cm^2)	-15.0	[218]
$10^{40}a$ $(C^2m^2J^{-1})$	3.245	[40]
$10^{40}\Delta a$ $(C^2m^2J^{-1})$	2.252	[9, 192]
$10^{40}a_\parallel$ $(C^2m^2J^{-1})$	4.387	
$10^{40}a_\perp$ $(C^2m^2J^{-1})$	2.134	
κ_a	0.2602	

Table 8.48: The components of the optical-frequency polarizability tensors α_{ij} of carbon dioxide, together with the values of ρ_0 used in the calculations.

λ nm	$100\rho_0$		$10^{40}\alpha$ $C^2m^2J^{-1}$		$10^{40}\Delta\alpha$ $C^2m^2J^{-1}$	$10^{40}\alpha_\parallel$ $C^2m^2J^{-1}$	$10^{40}\alpha_\perp$ $C^2m^2J^{-1}$	κ_α
632.8	4.049	[4]	2.907	[44, 62]	2.329	4.460	2.131	0.2671
514.5	4.085	[4]	2.957	[4]	2.380	4.544	2.164	0.2683
488.0	4.12	[4]	2.965	[4]	2.398	4.563	2.165	0.2696

Table 8.49: Lennard-Jones parameters and shape factors for carbon dioxide.

		R_0 (nm)	ε/k (K)	D
(1)	Our values fitted to $B(T)$	0.420	186	0.215
(2)	Our values fitted to B_ε	0.400	192	0.225
(3)	Fitted values of Couling and Graham [9]	0.400	190	0.250

Since it was not possible to find a set of Lennard-Jones and shape parameters which gave a good fit for both $B(T)$ and B_ε, we followed the same procedure adopted for chloromethane and selected two parameter sets. We first chose a set to improve the fit of $B(T)$, while maintaining physically reasonable values for B_ε, and then chose a set which yielded a good fit of the experimental data for B_ε, without sacrificing the fit of $B(T)$ too

much. These two sets of parameters are given in Table 8.49, together with the set used by Couling and Graham [9] to calculate B_ρ and B_K. All three parameter sets were used the calculate the full range of second virial coefficients.

8.7.2 Results of calculations of second virial coefficients for carbon dioxide

Table 8.50 shows the values of $B(T)$ calculated using the three parameter sets in Table 8.49, as well as the smoothed values taken from Dymond and Smith [1]. None of the parameter sets yield a very good fit to the experimental data, especially at the higher temperatures. However, the first set clearly fits better than the other two, with all the calculated values falling within 6.5% of the measured values.

Table 8.50: Calculated values of $B(T)$ for carbon dioxide for three sets of parameters, together with the smoothed values of Dymond and Smith [1].

T	$10^6 B^{\mathrm{exp}}$	(1)		(2)		(3)	
		$10^6 B^{\mathrm{calc}}$	%	$10^6 B^{\mathrm{calc}}$	%	$10^6 B^{\mathrm{calc}}$	%
K	$\mathrm{m^3mol^{-1}}$	$\mathrm{m^3mol^{-1}}$	Error	$\mathrm{m^3mol^{-1}}$	Error	$\mathrm{m^3mol^{-1}}$	Error
270	-155.4±2.0	-150.04	-3.45	-148.96	-4.14	-148.44	-4.48
280	-143.3±2.0	-139.71	-2.51	-138.74	-3.18	-138.25	-3.52
290	-132.5±2.0	-130.29	-1.67	-129.45	-2.30	-128.99	-2.65
300	-122.7±2.0	-121.67	-0.84	-120.98	-1.40	-120.55	-1.75
310	-113.9±2.0	-113.75	-0.13	-113.22	-0.59	-112.82	-0.95
320	-105.8±2.0	-106.46	0.62	-106.09	0.19	-105.72	-0.08
330	-98.5±2.0	-99.71	1.23	-99.52	1.04	-99.17	0.68
340	-91.7±2.0	-93.46	1.92	-93.44	1.90	-93.12	1.55
350	-85.5±2.0	-87.65	2.51	-87.80	2.69	-87.50	2.34
360	-79.7±2.0	-82.23	3.17	-82.56	3.59	-82.28	3.23
370	-74.4±2.0	-77.18	3.74	-77.68	4.41	-77.41	4.05
380	-69.5±2.0	-72.44	4.23	-73.12	5.21	-72.86	4.83
390	-64.8±2.0	-68.01	4.95	-68.84	6.23	-68.61	5.88
400	-60.5±2.0	-63.84	5.52	-64.84	7.17	-64.61	6.79
410	-56.5±2.0	-59.92	6.05	-61.07	8.09	-60.86	7.72
420	-52.8±2.0	-56.22	6.48	-57.53	8.96	-57.33	8.58
SSE:		124.83		194.89		196.47	

The second dielectric virial coefficient of carbon dioxide is an order of magnitude larger than that of nitrogen and the experimental values have correspondingly smaller percentage errors. This is due to the fact that, whereas for nitrogen $B_{\varepsilon_{\mathrm{ind}}}$ and $B_{\varepsilon_{\mathrm{or}}}$ contribute roughly the same amount to B_ε, for carbon dioxide the $B_{\varepsilon_{\mathrm{or}}}$ contribution is more than eight times larger than that of $B_{\varepsilon_{\mathrm{ind}}}$. This can be seen in Table 8.51, which

Table 8.51: The relative contributions of the terms used to calculate B_ε for carbon dioxide at 295.2 K for the parameter set ($D=0.225$, $R_0=0.400$, $\varepsilon/k=192.0$).

Contributing Term	$10^{12} \times$ Value $m^6 mol^{-2}$	% Contribution to B_ε
α_2	-3.835	-7.42
α_3	9.006	17.42
α_4	0.195	0.38
$B_{\varepsilon_{ind}}$	5.366	10.38
$\alpha_2 \theta_2$	30.937	59.83
$\alpha_3 \theta_2$	11.600	22.44
$\alpha_4 \theta_2$	3.799	7.35
$B_{\varepsilon_{or}}$	46.336	89.62

$$B_\varepsilon = 51.702 \times 10^{-12} m^6 mol^{-2}$$

shows the relative contribution of the various terms used in the calculation of B_ε. Here again we see the importance of including the first three terms of the $\alpha\theta$ series, as even the third term contributes more than 7% of B_ε. It is clear, however, that the series is converging and it should not be necessary to calculate any further terms.

Table 8.52: Calculated values of B_ε for carbon dioxide for three sets of parameters, together with the measured values.

T K	$10^{12} B_\varepsilon^{exp}$ $m^6 mol^{-2}$	Ref.	(1) $10^{12} B_\varepsilon^{calc}$ $m^6 mol^{-2}$	(2) $10^{12} B_\varepsilon^{calc}$ $m^6 mol^{-2}$	(3) $10^{12} B_\varepsilon^{calc}$ $m^6 mol^{-2}$
273.2	35.4±1.0	[41]	38.72	58.25	56.68
295.2	64±10	[48]	34.81	51.70	50.34
302.6	57.6±0.9	[40]	33.69	48.84	48.54
322.9	49.7±1.0	[45]	31.02	45.44	44.28
	50.7±0.9	[40]			
	41.4±2.4	[41]			
348.2	46.4±1.0	[45]	28.33	41.05	40.03
369.5	36±3	[49]	26.47	38.06	37.12
373.2	35.8±0.7	[41]	26.17	37.59	36.67
	33.5±0.4	[41]			
	34.8±0.7	[41]			
423.2	30.0±0.9	[41]	22.92	32.42	31.65

The temperature-dependence of the calculated and measured values of B_ε are tabulated in Table 8.52, and depicted graphically in Figure 8.5 (a). From the table we see that the values calculated from the first parameter set are much lower than the values obtained from the other two sets. This curve is represented in the figure by the dashed line, which
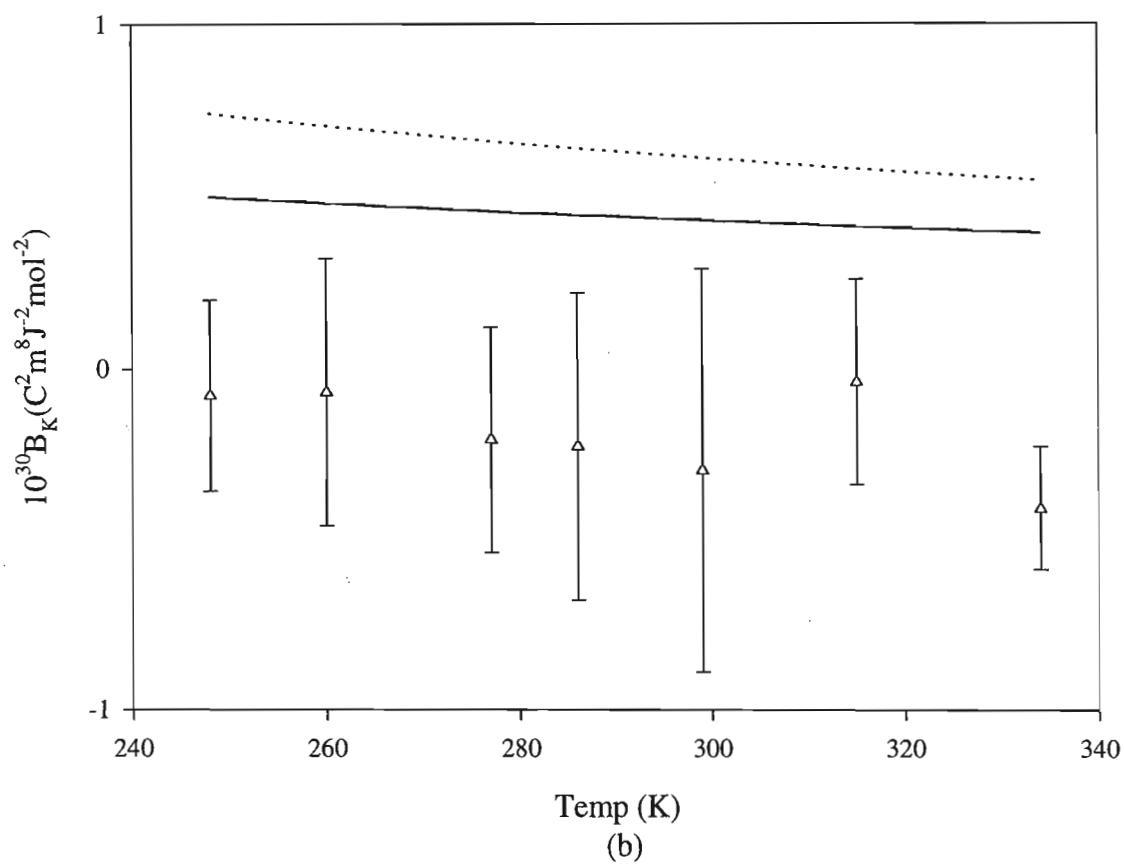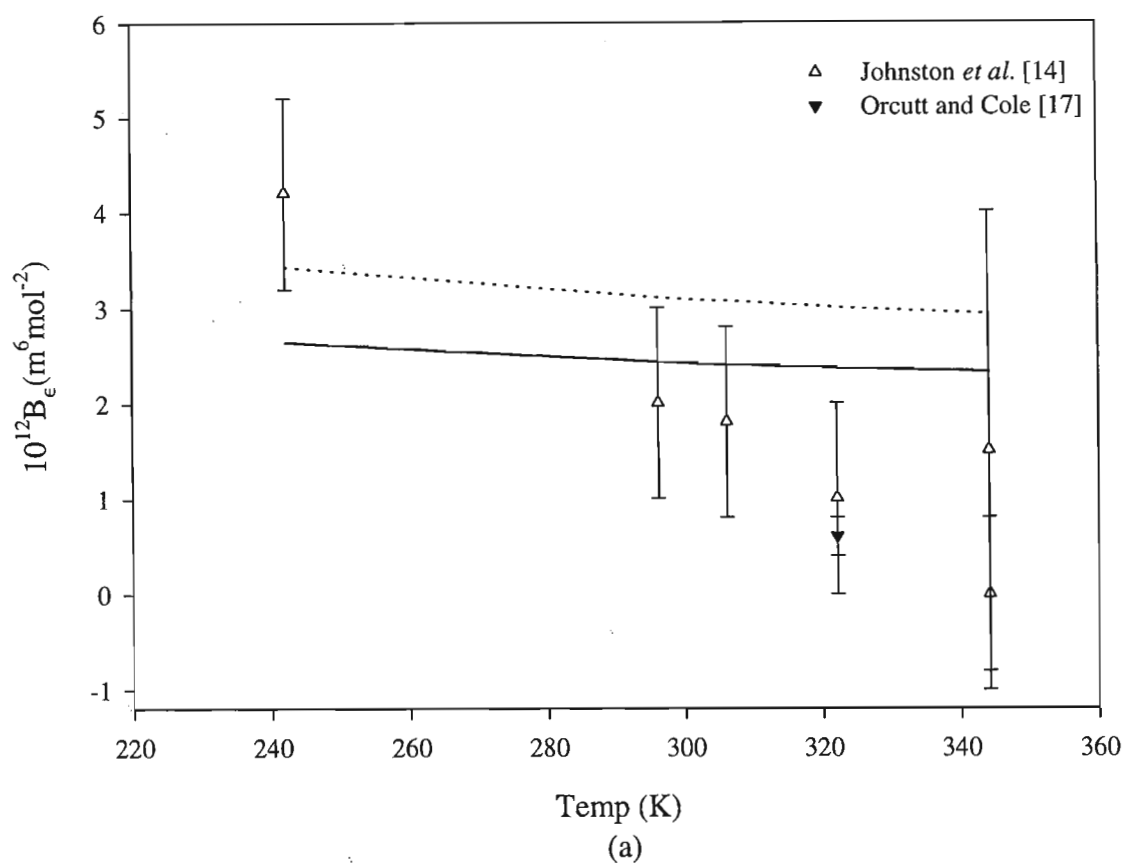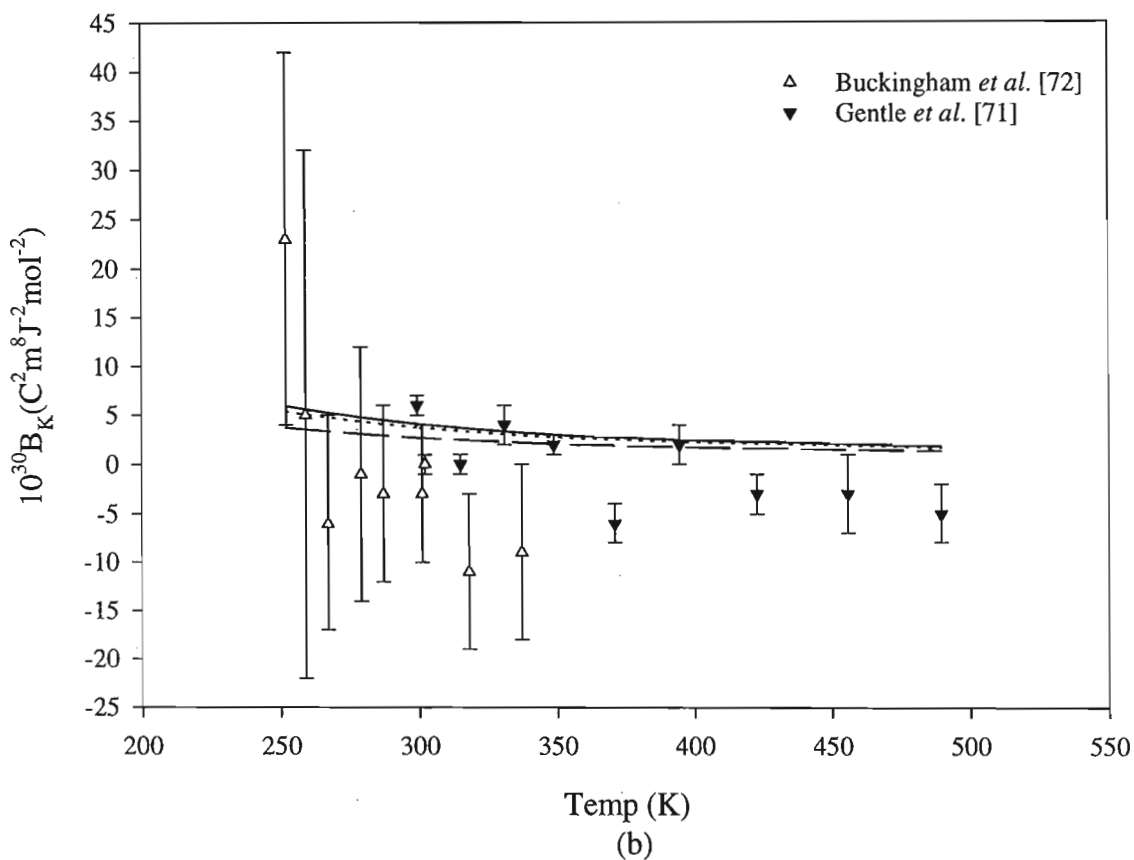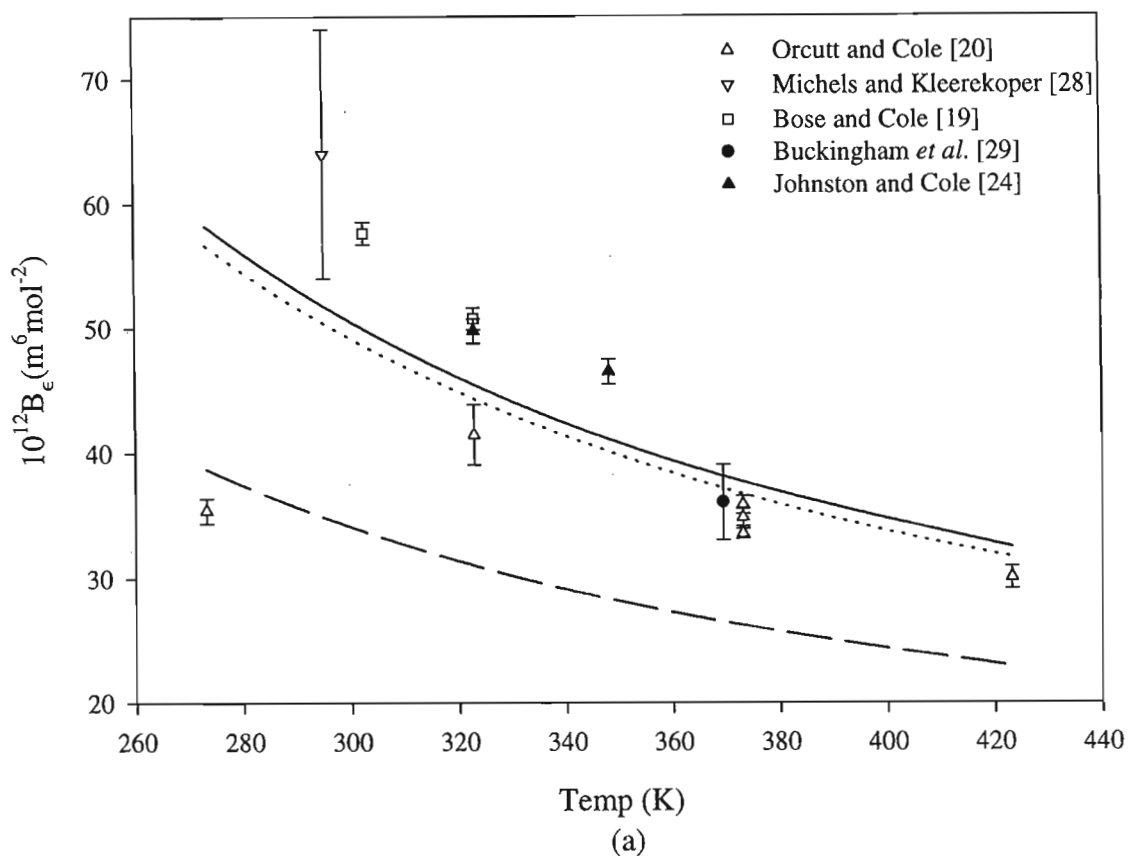
Figure 8.5: Temperature dependence of the calculated and measured values of the second (a) dielectric, and (b) Kerr-effect virial coefficients of carbon dioxide. The solid, dashed and dotted lines represent the values calculated using parameter set (2), (1) and (3) respectively.

186

falls below most of the experimental data. The solid and dotted lines, representing the theoretical values obtained from the second and third parameter sets respectively, fall between the various measured values, with the solid line giving the best fit.

As for nitrogen, the values of B_K measured by Buckingham et al. [14], and more recently by Gentle et al. [15] are very poorly defined, although the latter values are more precise than the earlier ones. This is not surprising, due to the difficulty involved in measuring such small pressure dependence. Our calculated values of B_K are shown, together with the measured values, in Table 8.53 and Figure 8.5 (b). It can be seen from the graph that the dashed line representing the values obtained from the first parameter set provide a marginally better fit than the solid and dotted lines, which represented the values calculated using the second and third parameter sets respectively. However, compared with the experimental errors and the scatter of the measured values, the difference between the three curves is very slight, with all of them providing an acceptable fit to experiment.

Table 8.53: Calculated values of B_K for carbon dioxide for three sets of parameters, together with the measured values of Gentle et al.[a] [15] and Buckingham et al.[b] [14].

T K	$10^{32}B_K^{exp}$ m^3mol^{-1}	(1) $10^{32}B_K^{calc}$ $C^2m^8J^{-2}mol^{-2}$	(2) $10^{32}B_K^{calc}$ $C^2m^8J^{-2}mol^{-2}$	(3) $10^{32}B_K^{calc}$ $C^2m^8J^{-2}mol^{-2}$
252	23 ± 19[b]	3.72	5.93	5.36
259	5 ± 27[b]	3.53	5.58	5.05
267	-6 ± 11[b]	3.34	5.23	4.74
279	-1 ± 13[b]	3.06	4.72	4.29
287	-3 ± 9[b]	2.92	4.48	4.07
299.2	6 ± 1[a]	2.70	4.09	3.71
301	-3 ± 7[b]	2.67	4.04	3.68
302	0 ± 10[b]	2.66	4.02	3.65
314.9	0 ± 1[a]	2.46	3.68	3.35
318	-11 ± 8[b]	2.43	3.63	3.30
330.9	4 ± 2[a]	2.26	3.32	3.03
337	-9 ± 9[b]	2.19	3.21	2.92
348.8	2 ± 1[a]	2.07	3.01	2.75
370.9	-6 ± 2[a]	1.91	2.75	2.52
394.5	2 ± 2[a]	1.74	2.47	2.26
422.8	-3 ± 2[a]	1.59	2.22	2.05
455.8	-3 ± 4[a]	1.47	2.05	1.89
489.5	-5 ± 3[a]	1.31	1.80	1.66

Table 8.54, which lists the relative contribution of the terms of B_K, shows the importance of including the quadrupole terms in the calculation of the second Kerr-effect virial coefficient. These terms, which have not been calculated before, contribute approx-

imately 30% to B_K. It should be noted that while the third term in the series $\theta_2\alpha_5$ makes a small but significant contribution, the series has clearly converged. The leading α series is converging rapidly, and no further terms are necessary.

Table 8.54: The relative contributions of the terms used to calculate B_K for carbon dioxide at 299.2 K for $\lambda = 632.8$ nm for the parameter set (D=0.225, R_0=0.400, ε/k=192.0).

Contributing Term	$10^{32} \times$ Value $C^2m^8J^{-2}mol^{-2}$	% Contribution to B_K
α_2	0.838	20.51
α_3	-2.113	-51.71
α_4	3.939	96.40
α_5	0.137	3.35
$\theta_2\alpha_3$	0.766	18.75
$\theta_2\alpha_4$	0.461	11.28
$\theta_2\alpha_5$	0.058	1.42

$$B_K = 4.086 \times 10^{-32} C^2m^8J^{-2}mol^{-2}$$

Table 8.55: Experimental and calculated values of B_R for carbon dioxide for three sets of parameters.

T K	λ nm	$10^{12}B_R^{exp}$ m^{6}mol^{-2}	Ref.	(1) $10^{12}B_R^{calc}$ m^{6}mol^{-2}	(2) $10^{12}B_R^{calc}$ m^{6}mol^{-2}	(3) $10^{12}B_R^{calc}$ m^{6}mol^{-2}
298.2	632.8	3.2±1.6	[39]	2.18	3.73	3.11
		4.75±1.30	[62]			
320		0.0±1.0	[72]	2.22	3.64	3.07
323		1.9±0.2	[64]	2.23	3.63	3.06
		5.3	[13]			
		3.31±3.6	[68]			
298	514.5	0.73±0.66	[62]	2.38	3.98	3.33
	488.0	1.03±0.66	[62]	2.39	4.01	3.36

Except for the measurements of Achtermann *et al.* [64], the experimental data for the second refractivity virial coefficient of carbon dioxide at 632.8 nm show wide scatter and large experimental errors. It is impossible to discern whether there is significant temperature dependence. At 514.5 nm and 488.0 nm, Burns *et al.* [62] measured B_R at room temperature, but the experimental errors are 90% and 65%, respectively, so any wavelength dependence is masked. B_R was calculated for carbon dioxide, using the three parameter sets, for all the temperatures and wavelengths where experimental data is available, and the calculated and measured values are given in Table 8.55. Although the

wide scatter and large errors in the experimental data make comparison with the theoretical values difficult, the more precise value of Achtermann *et al.* at 632.8 nm and 323 K is lower than any of the calculated values. At the other wavelengths, the experimental data is also lower than the theoretical values, leading to the tentative conclusion that the values calculated using parameter set (1) provide a better fit to the measured values.

Table 8.56 shows the relative contributions of the three α terms used to calculate B_R using the second parameter set for a wavelength of 632.8 nm at 298.2 K.

Table 8.56: The relative contributions of the terms used to calculate B_R for carbon dioxide at 298.2 K for λ=632.8nm for the parameter set (D=0.225, R_0=0.400, ε/k=192.0).

Contributing Term	$10^{12} \times$ Value $m^6 mol^{-2}$	% Contribution to B_ε
α_2	-3.360	-90.08
α_3	6.959	186.57
α_4	0.131	3.51

$$B_R = 3.730 \times 10^{-12} m^6 mol^{-2}$$

Table 8.57: Calculated values of B_ρ for carbon dioxide for three sets of parameters, together with the experimental data of Couling and Graham[a] [7] and Dayan *et al.*[b] [16].

			(1)		(2)		(3)	
T K	λ nm	$10^6 B_\rho^{exp}$ $m^3 mol^{-1}$	$10^6 B_\rho^{calc}$ $m^3 mol^{-1}$	% Err.	$10^6 B_\rho^{calc}$ $m^3 mol^{-1}$	% Err.	$10^6 B_\rho^{calc}$ $m^3 mol^{-1}$	% Err.
298.2	514.5	-8.29±0.16[a]	-9.21	11.1	-8.98	8.3	-8.92	7.6
300.0	488.0	-10[b]	-9.12	-8.8	-8.93	-10.7	-9	-10

Lastly, the second light-scattering virial coefficient was calculated at wavelengths of 514.5 nm and 488.0 nm, and compared with the measured values. The experimental data, together with the values calculated using the three parameter sets, are shown in Table 8.57, while the relative contributions of the various terms are given in Table 8.58. It can be seen in Table 8.58 that the second pressure virial coefficient contribution to B_ρ dominates the calculation. For this reason, all of the calculated values of B_ρ are very similar, so that it is difficult to choose which parameter set yields the best fit. Since the measured value of Couling and Graham [7,9] at 514.5 nm is more precise than that of Dayan *et al.* [16] at 488.0 nm, the third parameter set is most probably the best choice.

Table 8.58: The relative contributions of the terms used to calculate B_ρ for carbon dioxide at 298.2 K and $\lambda = 514.5$ nm for the parameter set (D=0.215, R_0=0.420, ε/k=186.0).

Contributing Term	$10^6 \times$ Value $\text{m}^3\text{mol}^{-1}$	% Contribution to B_ρ
G	3.477	-1.44
b_3	1.408	-0.58
a_3	-10.474	4.35
a_4	15.326	-6.36
a_5	0.103	-0.04
$\mathcal{S}_\rho$	9.840	-4.09
$2B$	-250.66	104.09

$$B'_\rho = -240.82 \times 10^{-6}\text{m}^3\text{mol}^{-1}$$
$$B_\rho = 8.98 \times 10^{-6}\text{m}^3\text{mol}^{-1}$$

Unfortunately, the results for carbon dioxide do not allow us to choose a unique parameter set which yields good fits for all of the second virial coefficient data available. Except for B_ε where the second and third parameter sets clearly provide at better fit to experiment, and for $B(T)$ where the first parameter set fits best, it is very difficult to choose which is best. In order to allow a definite conclusion, more accurate measured values for B_ε, B_R and B_K would be required. However, the variation between the Lennard-Jones parameters of the different sets is 5% or less and the shape factors are similar and physically reasonable, so that we can conclude that any of the sets would be acceptable.

8.8 Calculations for ethane

8.8.1 Molecular properties of ethane

The static molecular properties of ethane are listed in Table 8.59, while Table 8.60 lists the values of the optical-frequency polarizability components and ρ_0. Since ethane is a non-polar molecule there are no dipole moment, first-order hyperpolarizability and A-tensor components. No C-tensor data is available. Our optimized values for the Lennard-Jones and shape parameters are given in Table 8.61, together with the values used by Couling and Graham [7,9] to calculate the second Kerr-effect and light-scattering virial coefficients. We have used both sets of parameters to obtain theoretical values for all of the second virial coefficients under study.

Table 8.59: Wavelength-independent molecular parameters of ethane used in the calculations

Molecular Parameter	Value	Reference
$10^{40}\theta$ (Cm^2)	-3.34	[219]
$10^{40}a$ ($C^2m^2J^{-1}$)	4.870	[9, 140]
$10^{40}\Delta a$ ($C^2m^2J^{-1}$)	0.638	[9, 17]
$10^{40}a_{\parallel}$ ($C^2m^2J^{-1}$)	5.295	
$10^{40}a_{\perp}$ ($C^2m^2J^{-1}$)	4.657	
κ_a	0.0437	

Table 8.60: The components of the optical-frequency polarizability tensor α_{ij} of ethane as determined from the measured values of ρ_0 [17] and α [18].

λ nm	$100\rho_0$	$10^{40}\alpha$ $C^2m^2J^{-1}$	$10^{40}\Delta\alpha$ $C^2m^2J^{-1}$	$10^{40}\alpha_{\parallel}$ $C^2m^2J^{-1}$	$10^{40}\alpha_{\perp}$ $C^2m^2J^{-1}$	κ_{α}
632.8	0.149±0.006	4.9680	0.743	5.464	4.720	0.0499
514.5	0.168±0.006	5.0176	0.798	5.550	4.752	0.0530

Table 8.61: Lennard-Jones parameters and shape factors for ethane.

		R_0 (nm)	ε/k (K)	D
(1)	Our fitted values	0.420	208.3	0.375
(2)	Fitted values of Couling and Graham [9]	0.4418	230.0	0.200

8.8.2 Results of calculations of second virial coefficients for ethane

The second pressure virial coefficient of ethane was calculated using both sets of parameters given in Table 8.61, and the results are given in Table 8.62 together with the smoothed values of Dymond and Smith [1]. The values obtained using our best-fit parameters agree with the experimental data to within 1.5% over the temperature range 240 K to 350 K, and within 4% for the higher temperatures. The second parameter set yields values of $B(T)$ which differ from experiment by as much as 9.34% at 400 K.

Table 8.62: Calculated values of $B(T)$ for ethane for two sets of parameters, together with the smoothed values of Dymond and Smith [1].

T	$10^6 B^{exp}$	(1)		(2)	
		$10^6 B^{calc}$	%	$10^6 B^{calc}$	%
K	$m^3 mol^{-1}$	$m^3 mol^{-1}$	Error	$m^3 mol^{-1}$	Error
240	-282±3	-282.93	0.33	-278.39	-1.28
260	-243±2	-240.80	-0.91	-241.33	-0.69
280	-211±2	-207.70	-1.56	-211.07	0.03
300	-182±2	-181.01	-0.54	-185.89	2.14
325	-154±1	-154.13	0.08	-159.83	3.79
350	-130.5±1	-132.48	1.52	-138.33	6.00
375	-111.0±1	-114.68	3.32	-120.30	8.38
400	-96.0±1	-99.79	3.95	-104.97	9.34
SSE:		49.42		293.21	

Only one experimental value of B_ε is available. This was measured recently by St-Arnaud *et al.* [19] and has an experimental error of 5.5%. We used both parameter sets to calculate B_ε for ethane at 298.1 K and the results are given in Table 8.63. The value calculated using our optimized parameter set is 2% lower than the measured value and falls within the experimental error. The value obtained using the second parameter set is almost 30% lower than the experimental value, but is of the correct order of magnitude.

Table 8.63: Calculated values of B_ε for ethane for two sets of parameters, together with the measured value of St-Arnaud *et al.* [19].

T	$10^{12} B_\varepsilon^{exp}$	(1)		(2)	
		$10^{12} B_\varepsilon^{calc}$	%	$10^{12} B_\varepsilon^{calc}$	%
K	$m^6 mol^{-2}$	$m^6 mol^{-2}$	Error	$m^6 mol^{-2}$	Error
298.1	32.2±1.8	31.57	-1.96	23.01	-28.54

The relative contribution of the various terms used to calculate the second dielectric virial coefficient are given in Table 8.64. It can be seen that $B_{\varepsilon_{or}}$ contributes approximately one third of the total value of B_ε, demonstrating the importance of including the quadrupole moment terms, which have clearly converged. The dominant contribution comes from the α_3, or Kirkwood [127], term.

Table 8.64: The relative contributions of the terms used to calculate B_ε for ethane at 298.1 K.

Contributing Term	$10^{12} \times$ Value $m^6 mol^{-2}$	% Contribution to B_ε
α_2	-7.763	-24.59
α_3	27.317	86.53
α_4	1.064	3.37
$B_{\varepsilon_{ind}}$	20.618	65.31
$\alpha_2\theta_2$	4.769	15.11
$\alpha_3\theta_2$	5.879	18.62
$\alpha_4\theta_2$	0.304	0.96
$B_{\varepsilon_{or}}$	10.952	34.69

$$B_\varepsilon = 31.57 \times 10^{-12} m^6 mol^{-2}$$

Next, we calculated the second refractivity virial coefficient, for which two measured values are available for a wavelength of 633.0 nm. The contributions of the various terms in the calculation of B_R at $\lambda = 633.0$ nm for $T = 348$ K are given in Table 8.65 for our optimized parameter set. It is clear from the table that the series has converged. It is possible that the $\alpha_2 C_1$ term might make a significant contribution, but no measured or calculated values exist for the C-tensor components.

Table 8.65: The relative contributions of the terms used to calculate B_R for ethane at 632.8 nm and 348 K for the parameter set (D=0.375, R_0=0.420, ε/k=208.3).

Contributing Term	$10^{12} \times$ Value $m^6 mol^{-2}$	% Contribution to B_R
α_2	-8.440	-32.94
α_3	32.709	127.67
α_4	1.351	5.27

$$B_R = 25.620 \times 10^{-12} m^6 mol^{-2}$$

Table 8.66 shows the measure values of Jaeschke [72] and Achtermann et al. [64], together with the theoretical values calculated using both parameter sets. It can be seen that the first parameter set provides a better fit to experiment than the second set.

Table 8.66: Calculated and measured values of B_R for ethane.

T	λ	$10^{12}\,B_R^{\mathrm{exp}}$	Ref.	(1) $10^{12}\,B_R^{\mathrm{calc}}$	(2) $10^{12}\,B_R^{\mathrm{calc}}$
K	nm	$\mathrm{m^6 mol^{-2}}$		$\mathrm{m^6 mol^{-2}}$	$\mathrm{m^6 mol^{-2}}$
348	633.0	22.9±3.0	[72]	25.62	19.61
373		26.6±0.05	[64]	24.92	19.29

The second Kerr-effect virial coefficient has been measured for a range of temperatures from 255 K to 318 K at a wavelength of 623.8 nm by Buckingham *et al.* [14], with experimental errors of approximately 20%. We have calculated B_K over this temperature range using both parameter sets. Table 8.67 shows the relative contributions of the terms used to calculate B_K, while Table 8.68 shows the temperature dependence of the theoretical and experimental data. Figure 8.6 shows the relationship between the calculated and measured values graphically, with the solid and dotted lines representing the values obtained from the first and second parameter sets, respectively.

It can be seen from Table 8.67 that for ethane, the quadrupole moment series $\theta\alpha$ contributes negligibly to the second Kerr-effect virial coefficient.

Table 8.67: The relative contributions of the terms used to calculate B_K for ethane at 255 K for $\lambda = 632.8$ nm for the parameter set (D=0.375, R_0=0.420, ε/k=208.3).

Contributing Term	$10^{32} \times$ Value $\mathrm{C^2 m^8 J^{-2} mol^{-2}}$	% Contribution to B_K
α_2	0.696	2.34
α_3	-13.549	-45.64
α_4	39.075	131.64
α_5	3.384	11.40
$\theta_2\alpha_3$	0.026	0.09
$\theta_2\alpha_4$	0.047	0.16
$\theta_2\alpha_5$	0.005	0.02

$$B_K = 29.684 \times 10^{-32} \mathrm{C^2 m^8 J^{-2} mol^{-2}}$$

From Table 8.68 and Figure 8.6, it is clear that the second parameter set provides a far better fit of the theory to experiment, since it lies within the experimental error of the measured values. The values calculated from the first parameter set fall outside the experimental errors over the entire range of temperatures, but they are of the correct order of magnitude.

The only existing measurement of B_ρ for ethane is that of Couling and Graham [7,9], which was measured at room temperature for a wavelength of 514.5 nm. We calculated B_ρ for both parameter sets at this wavelength and temperature. Table 8.69 shows the
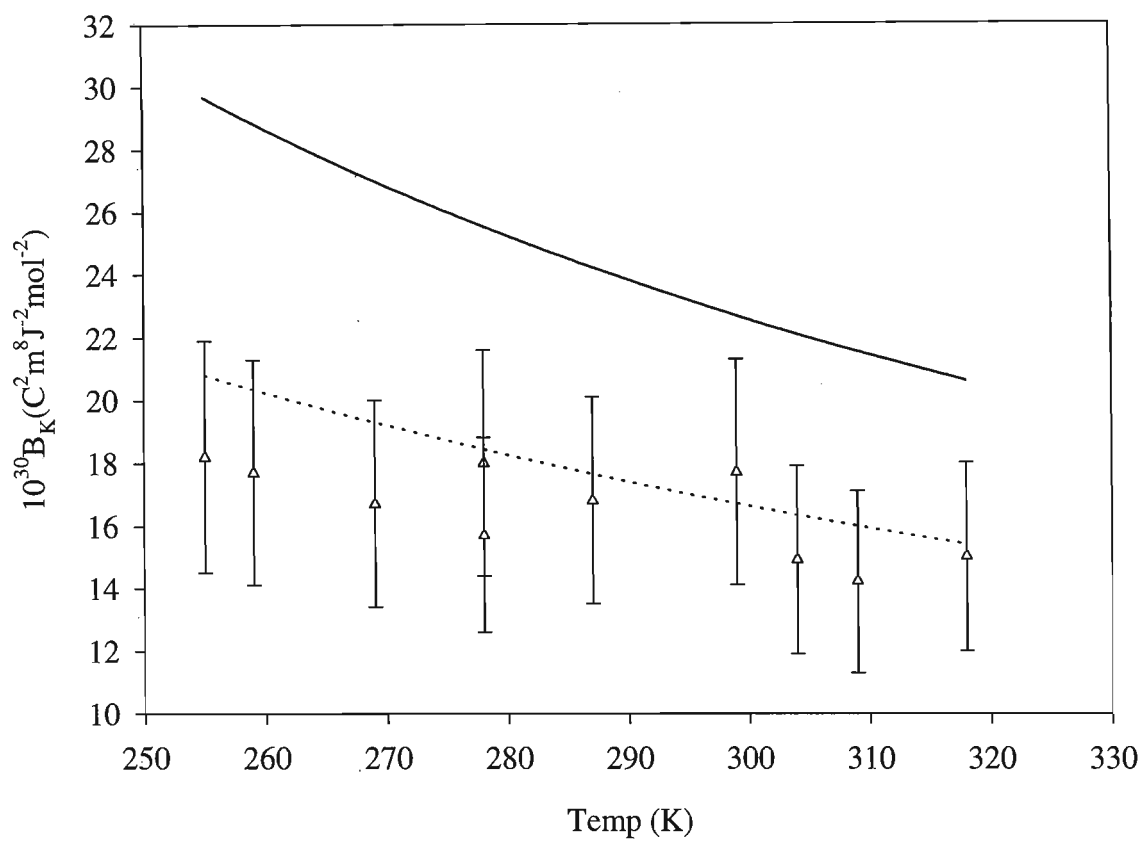
Figure 8.6: Temperature dependence of the calculated and measured values of the second Kerr-effect virial coefficient of ethane. The solid and dotted lines represent the values obtained using parameter sets (1) and (2), respectively.

Table 8.68: Calculated values of B_K for ethane for two sets of parameters, together with the measured values of Buckingham *et al.* [14], at a wavelength of $\lambda = 632.8$ nm.

T	$10^{32}B_K^{exp}$	(1)		(2)	
		$10^{32}B_K$	%	$10^{32}B_K$	%
K	$C^2m^8J^{-2}$	$C^2m^8J^{-2}$	Error	$C^2m^8J^{-2}$	Error
255	18.2±3.7	29.68	63.08	20.81	14.34
259	17.7±3.6	28.86	63.05	20.35	14.97
269	16.7±3.3	27.01	61.74	19.29	15.21
278	18.0±3.6	25.54	41.89	18.43	4.61
	15.7±3.1		62.68		17.39
287	16.8±3.3	24.22	44.17	17.64	5.00
299	17.7±3.6	22.68	28.14	16.69	-5.71
304	14.9±3.0	22.09	48.26	16.33	9.60
309	14.2±2.9	21.54	51.69	15.98	12.53
318	15.0±3.0	20.61	37.40	15.39	2.60

relative importance of the terms which contribute to B_ρ, while the calculated values are shown, together with the measured value, in Table 8.70. While both calculated values are larger than the experimental value and fall outside the experimental error, the value obtained from the second parameter set is in much better agreement with the measured value.

Table 8.69: The relative contributions of the terms used to calculate B_ρ for ethane at 295.9 K and $\lambda = 514.5$ nm for the parameter set ($D=0.375$, $R_0=0.420$, $\varepsilon/k=208.3$).

Contributing Term	$10^6 \times$ Value m^{3}mol^{-1}	% Contribution to B_ρ
G	20.52	10.69
b_3	2.69	4.10
a_3	-374.40	-107.42
a_4	1071.79	243.66
a_5	83.05	6.16
$\mathcal{S}_\rho$	803.65	157.20
$2B$	-372.88	57.20

$$B_\rho' = 403.77 \times 10^{-6} m^3 mol^{-1}$$
$$B_\rho = 0.722 \times 10^{-6} m^3 mol^{-1}$$

Our optimized parameter set yields good agreement with experiment for the second pressure, dielectric and refractivity virial coefficient data available, while the parameter set of Couling and Graham [9] yields much better agreement than ours for the second

Table 8.70: Calculated values of B_ρ for ethane for two parameter sets, together with the experimental value of Couling and Graham [7] at $\lambda = 514.5$ nm.

| T | $10^{12} B_\rho^{\text{exp}}$ | (1) $10^6 B_\rho^{\text{calc}}$ | (2) $10^6 B_\rho^{\text{calc}}$ |
K	$\text{m}^3\text{mol}^{-1}$	$\text{m}^3\text{mol}^{-1}$	$\text{m}^3\text{mol}^{-1}$
295.9	0.315 ± 0.018	0.722	0.381

Kerr-effect and light-scattering virial coefficients. Thus it is not possible, on the basis of the available experimental data, to choose a unique set of Lennard-Jones and shape parameters to describe all the effects under study adequately. However, the choice of fit for B_ε, B_R and B_ρ is hampered by the fact that only one or two values are available for comparison. Further experimental data would help to solve this problem.

8.9 Calculations for sulphur dioxide

8.9.1 Molecular properties of sulphur dioxide

The sulphur dioxide molecule has C_{2v} symmetry and is taken to lie in the 1-3 plane of the molecule-fixed axes (1,2,3). The 3 axis is taken as the principal molecular axis and the origin of the system is at the centre of mass of the molecule. The electric dipole moment tensor has one component, $[0 \ 0 \ \mu_3]$ while the traceless electric quadrupole moment tensor has two independent components θ_{11} and θ_{22}, with $\theta_{33} = -(\theta_{11} + \theta_{22})$. The optical-frequency polarizability tensor has three independent components α_{11}, α_{22} and α_{33} [26].

The values of the dipole moment, quadrupole moment, static and optical-frequency polarizability tensor components used in our the calculations are given in Table 8.71.

Table 8.71: Molecular parameters of sulphur dioxide used in the calculations

Molecular Parameter	Value	Reference
$10^{30}\mu_3$ (Cm)	-5.4262±0.0010	[220]
$10^{40}\theta_{11}$ (Cm^2)	-16.4±0.3	[221]
$10^{40}\theta_{22}$ (Cm^2)	12.9±0.2	
$10^{40}\theta_{33}$ (Cm^2)	3.5±0.1	
$10^{40}a_{11}$ (C^{2}m^{2}J^{-1})	5.661	[9]
$10^{40}a_{22}$ (C^{2}m^{2}J^{-1})	3.205	
$10^{40}a_{33}$ (C^{2}m^{2}J^{-1})	3.756	
$10^{40}\Delta a$ (C^{2}m^{2}J^{-1})	2.232	
$10^{40}\alpha_{11}$(632.8 nm) (C^{2}m^{2}J^{-1})	5.80±0.06	(a)
$10^{40}\alpha_{22}$(632.8 nm) (C^{2}m^{2}J^{-1})	3.30±0.04	
$10^{40}\alpha_{33}$(632.8 nm) (C^{2}m^{2}J^{-1})	3.88±0.06	
$10^{40}\Delta\alpha$(632.8 nm) (C^{2}m^{2}J^{-1})	2.27±0.06	
$10^{40}\alpha_{11}$(514.5 nm) (C^{2}m^{2}J^{-1})	5.928±0.01	(b)
$10^{40}\alpha_{22}$(514.5 nm) (C^{2}m^{2}J^{-1})	3.336±0.04	
$10^{40}\alpha_{33}$(514.5 nm) (C^{2}m^{2}J^{-1})	3.902±0.05	
$10^{40}\Delta\alpha$(514.5 nm) (C^{2}m^{2}J^{-1})	2.360±0.05	

(a) Experimental derivation from the Kerr effect [21] with
$\alpha_\nu = 4.326 \times 10^{-40}$ C^{2}m^{2}J^{-1} [4], $\rho_0 = 0.0179\pm0.0001$ [4]
(b) Experimental derivation from: $R_0 = 0.212\pm0.035$ [222]
$\alpha_\nu = 4.389 \times 10^{-40}$ C^{2}m^{2}J^{-1} [4], $\rho_0 = 0.0188\pm0.0001$ [9]

The equilibrium dipole moment is the value which Patel *et al.* [220] determined precisely by molecular beam electric resonance spectroscopy. In this work we have used the most precise set of experimental values for the electric quadrupole moment: those of Ellenbroek and Dymanus [221] obtained from magnetizability anisotropy measurements.

It must be noted that since the quadrupole moment of a polar molecule is dependent on the origin to which it is referred, it is necessary to specify that for these measurements the origin is fixed at the molecule's centre of mass. The optical-frequency polarizability tensor components at 514.5 nm are those obtained by Couling and Graham [9] from their measured value of ρ_0, the R_{20} value of Murphy [222] and the α_ν of Bogaard et al. [4], while the components at 632.8 nm are those deduced by Gentle et al. [21] from Kerr effect measurements. There are no experimental estimates of the individual components of the static polarizability tensor. However, Couling and Graham [9], scaled ab initio calculated values [223], by comparing their trace with the mean static polarizability extrapolated from experimental optical-frequency values [4]. The anisotropy of the scaled components agreed to within 4.5% with the value extrapolated from the experimental data of Bogaard et al. [4].

Table 8.72: Lennard-Jones parameters and shape factors for sulphur dioxide.

		R_0 (nm)	ε/k (K)	D_1	D_2
(1)	Our fitted values	0.388	210.0	0.1200	0.1386
(2)	Fitted values of Couling and Graham [9]	0.385	220.0	0.0873	0.1008

Since the computer programs to calculate the various second virial coefficients of non-linear gases take much longer to run than the equivalent programs for linear gases, it is not possible to test as many combinations of the Lennard-Jones and shape parameters when attempting to fit the theoretical values to the available experimental data. Since a parameter set which provided good agreement for the second pressure, Kerr-effect and light-scattering virial coefficients of sulphur dioxide had been found by Couling and Graham [9], we used this set of parameters to calculate the second dielectric virial coefficient. Since the value we calculated for B_ε was more than double the only available experimental value, we then attempted to find a new set of parameters which would improve the agreement with the measured value of B_ε without sacrificing the fit of the second pressure virial coefficient. We then used our new parameter set to calculate B_K and B_ρ, and compared our values with the available experimental data. Our new parameter set and the parameter set fitted to $B(T)$ by Couling and Graham [9] are given in Table 8.72

8.9.2 Results of calculations of second virial coefficients for sulphur dioxide

The values calculated for the second pressure virial coefficient of sulphur dioxide are listed in Table 8.73, together with the experimental values of Kang et al. [20], as quoted by Dymond and Smith [1]. The values calculated using the parameter set of Couling and

Graham [9] fit the experimental values to within approximately 2% over almost the entire temperature range. Our parameter set yielded calculated values for $B(T)$ which agree with the experimental values to within 2.6% over the temperature range from 283.15 K to 348.15 K, but are out by 6.32% at 398.15 K.

Table 8.73: Calculated values of $B(T)$ for sulphur dioxide for two sets of parameters, together with the experimental values of Kang *et al.* [20].

| T | $10^6 B^{\mathrm{exp}}$ | (1) | | (2) | |
| | | $10^6 B^{\mathrm{calc}}$ | % | $10^6 B^{\mathrm{calc}}$ | % |
K	$\mathrm{m^3 mol^{-1}}$	$\mathrm{m^3 mol^{-1}}$	Error	$\mathrm{m^3 mol^{-1}}$	Error
283.15	-500.0±20	-500.74	0.15	-501.32	0.26
293.15	-452.0±18	-453.15	0.25	-450.88	-0.24
303.15	-404.0±16	-411.32	1.81	-408.17	1.03
313.15	-367.5±15	-373.07	1.52	-371.62	1.12
323.15	-332.8±13	-340.01	2.16	-340.04	2.18
348.15	-279.0±11	-271.71	-2.61	-277.38	-0.58
373.15	-232.5±9	-223.98	-3.66	-231.04	-0.63
398.15	-201.0±8	-188.29	-6.32	-195.53	-2.72
423.15	-171.1±7	-162.33	-5.13	-167.55	-2.07
448.15	-144.1±7	-141.98	-1.47	-144.98	0.61
473.15	-125.8±7	-121.82	-3.16	-126.43	0.50
SSE:		531.79		141.90	

The second dielectric virial coefficient has only been measured once, at 292.7 K, by Lawley and Sutton [10] in 1963 and the experimental uncertainty is very large (60%). We have calculated B_ε at this temperature using both parameter sets and including as many terms as was necessary to ensure that the series were converging. Table 8.74 shows the relative contributions of the terms used to calculate B_ε. It is clear that $B_{\varepsilon_{\mathrm{ind}}}$ makes a small, but significant, contribution to B_ε of 4.5%, while all three of the series in $B_{\varepsilon_{\mathrm{or}}}$ are highly significant. In particular, we note that the dipole-quadrupole series $\alpha\mu\theta$ makes a contribution of 150%. In addition, the quadrupole series $\alpha\theta$ contributes 30% of B_ε. If the effects of the quadrupole moment were omitted then the calculated value would be a large negative number, rather than a large positive number! This demonstrates that effects of the quadrupole moment are not necessarily negligible in dipolar molecules, as we have already seen for the halogenated methanes.

The values of B_ε calculated using the two parameter sets are given in Table 8.75, together with the measured value. It can be seen that both the calculated values are higher than the measured value, but the value obtained using our new parameter set lies within the experimental error. We found that attempts to improve this value destroyed the fit obtained for $B(T)$. While the value obtained using parameter set (2), is more than

Table 8.74: The relative contributions of the terms used to calculate B_ε for sulphur dioxide at 292.7 K for the parameter set (D_1=0.1200, D_2=0.1386, R_0=0.388, ε/k=210.0).

Contributing Term	$10^{12} \times$ Value $m^6 mol^{-2}$	% Contribution to B_ε
α_2	29.417	1.29
α_3	68.668	3.00
α_4	4.272	0.19
$B_{\varepsilon_{ind}}$	102.357	4.48
μ_2	-4791.246	-209.48
$\alpha_1\mu_2$	1556.107	68.04
$\alpha_2\mu_2$	1070.891	46.82
$\alpha_3\mu_2$	91.401	4.00
$\alpha_1\mu_1\theta_1$	3107.603	135.87
$\alpha_2\mu_1\theta_1$	433.157	18.94
$\alpha_2\theta_2$	578.609	25.29
$\alpha_3\theta_2$	138.324	6.05
$B_{\varepsilon_{or}}$	2184.846	95.52

$$B_\varepsilon = 2287.20 \times 10^{-12} m^6 mol^{-2}$$

Table 8.75: Calculated values of B_ε for sulphur dioxide for two sets of parameters, together with the measured value of Lawley and Sutton [10].

| T | $10^{12} B_\varepsilon^{exp}$ | (1) | | (2) | |
| | | $10^{12} B_\varepsilon^{calc}$ | % | $10^{12} B_\varepsilon^{calc}$ | % |
K	$m^6 mol^{-1}$	$m^6 mol^{-2}$	Error	$m^6 mol^{-2}$	Error
292.7	1700±1000	2287.2	34.54	4020.9	136.47

double the measured value, it is at least of the correct order of magnitude.

The second Kerr-effect virial coefficient of sulphur dioxide has been measured by Gentle *et al.* [21], at a wavelength of 632.8 nm for a large temperature range. There is considerable scatter, but for most of measured values the experimental errors are approximately 5% and the temperature dependence is reasonably well defined. When Couling and Graham [9] developed the theory of the second Kerr-effect virial coefficient, they did not consider the quadrupole moment terms in the integrand, although they did include the dipole-quadrupole, quadrupole-quadrupole and quadrupole-induced-dipole potentials in the intermolecular potential (Chapter 2). However, due to the significant contributions of the quadrupole moment to B_ε, we extended the theory of B_K to include these terms and used them in our calculations of B_K. In Table 8.76 of the relative contributions

of the various terms in the calculated value of B_K, we see that the dipole-quadrupole $\mu\theta\alpha$ series contributes 8.24% to B_K, while the quadrupole series $\theta\alpha$ makes an additional contribution of 5.62%, so that the combined contribution is almost 14% of the total B_K. Thus, we see the importance of considering the effect of the quadrupole moment, even when dealing with dipolar molecules.

Table 8.76: The relative contributions of the terms used to calculate B_K for sulphur dioxide at 288.7 K for $\lambda = 632.8$ nm for the parameter set (D_1=0.1200, D_2=0.1386, R_0=0.388, ε/k=210.0).

Contributing Term	$10^{30} \times$ Value $C^2m^8J^{-2}mol^{-2}$	% Contribution to B_K
α_2	-0.079	-0.52
α_3	0.173	1.15
α_4	0.506	3.36
α_5	0.050	0.33
$\mu_2\alpha_1$	2.000	13.28
$\mu_2\alpha_2$	5.010	33.27
$\mu_2\alpha_3$	4.538	30.14
$\mu_2\alpha_4$	0.774	5.14
$\mu_1\theta_1\alpha_1$	-0.253	-1.68
$\mu_1\theta_1\alpha_2$	1.462	9.71
$\mu_1\theta_1\alpha_3$	0.031	0.21
$\theta_1\alpha_3$	0.178	1.18
$\theta_1\alpha_4$	0.482	3.20
$\theta_1\alpha_5$	0.186	1.24

$$B_K = 15.058 \times 10^{-30} C^2m^8J^{-2}mol^{-2}$$

The temperature dependence of calculated and measured values of the second Kerr-effect virial coefficient is shown in Table 8.77. It can be seen that values obtained from the two sets of parameters are very similar, although those calculated from our new parameter set are slightly higher. Figure 8.7 shows the measured values, together with the theoretical curves. The solid line and the dashed line, representing the values calculated using parameter sets (1) and (2) respectively, lie very close together and both provide a good fit of the experimental data. In order to demonstrate the effect of including the quadrupole series, the figure shows the values for B_K calculated by Couling and Graham [9] without any quadrupolar terms, as a dotted line. It can be seen that this dotted curve lies below the dashed curve, due to the postive contribution of the quadrupole terms.
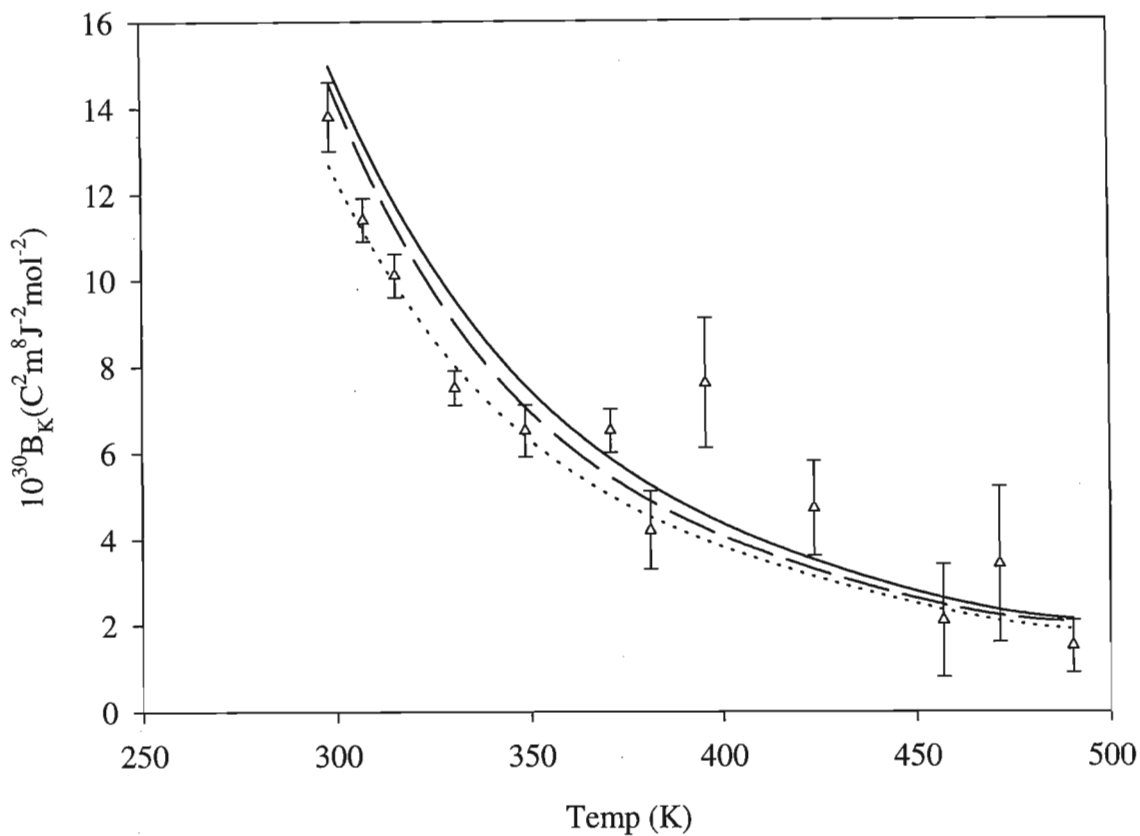
Figure 8.7: Temperature dependence of the calculated and measured values [21] of the second Kerr-effect virial coefficient of sulphur dioxide. The solid and dashed lined represent the values calculated using parameter sets (1) and (2), respectively. The dotted line represents the calculated values of Couling and Graham [9], which do not include quadrupole terms.

Table 8.77: Calculated values of B_K for sulphur dioxide for two sets of parameters, together with the measured values of Gentle *et al.* [21], at a wavelength of 632.8 nm.

		(1)		(2)	
T	$10^{32}B_K^{exp}$	$10^{32}B_K^{calc}$	%	$10^{32}B_K^{calc}$	%
K	$C^2m^8J^{-2}$	$C^2m^8J^{-2}$	Error	$C^2m^8J^{-2}$	Error
298.7	13.8±0.8	15.06	9.13	14.66	6.23
307.3	11.4±0.5	13.25	16.23	12.72	11.57
315.4	10.1±0.5	11.55	14.36	11.13	10.20
330.7	7.5±0.4	9.62	28.27	9.03	20.40
348.8	6.5±0.6	7.65	17.69	7.18	10.46
370.9	6.5±0.5	5.92	-8.92	5.40	-16.92
381.2	4.2±0.9	5.21	24.05	4.87	15.95
395.7	7.6±1.5	4.47	-41.18	4.18	-45.00
423.7	4.7±1.1	3.41	-27.45	3.27	-30.43
457.0	2.1±1.3	2.61	24.29	2.49	18.57
471.5	3.4±1.8	2.40	-29.41	2.21	-35.00
490.3	1.5±0.6	2.10	40.00	2.06	37.33

Although there are no experimental values for the second refractivity virial coefficient of sulphur dioxide, we have calculated B_R using both parameter sets. Table 8.78 shows the relative magnitude of the various contributions to B_R at 298.15 K, for a wavelength of 632.8 nm.

Table 8.78: The relative contributions of the terms used to calculate B_R for sulphur dioxide at 298.15 K for $\lambda = 632.8$ nm.

	(1)		(2)	
Contrib.	10^{12} × Value	% of	10^{12} × Value	% of
Term	m^6mol^{-2}	B_R	m^6mol^{-2}	B_R
α_2	21.584	22.27	20.114	21.57
α_3	70.842	73.11	68.942	73.94
α_4	4.480	4.62	4.180	4.49
B_R	96.906		93.236	

There is only a single measured value for B_ρ [9]. Thus, we calculated the second light-scattering virial coefficient at 514.5 nm for a temperature of 338.4 K, using our new parameter set and compared the result with the experimental value and the calculated value of Couling and Graham [9]. Table 8.79 shows the relative contributions of the terms used to calculate B_ρ, while Table 8.80 shows the calculated values, together with the measured value. Both of the calculated values fall outside the experimental error, but

the agreement is still good, with the value of Couling and Graham [9] yielding a slightly better fit.

Table 8.79: The relative contributions of the terms used to calculate B_ρ for sulphur dioxide at 338.4 K and $\lambda = 514.5$ nm for the parameter set (D_1=0.1200, D_2=0.1386, R_0=0.388, ε/k=210.0).

Contributing Term	$10^6 \times$ Value $m^3 mol^{-1}$	% Contribution to B_ρ
g	-17.798	10.69
b_3	-3.577	4.10
a_3	57.902	-107.42
a_4	195.399	243.66
a_5	23.111	6.16
S_ρ	255.036	157.20
$2B$	-594.820	57.20

$$B'_\rho = -339.784 \times 10^{-6} m^3 mol^{-1}$$
$$B_\rho = -6.225 \times 10^{-6} m^3 mol^{-1}$$

Table 8.80: Calculated values of B_ρ for sulphur dioxide for two parameter sets, together with the experimental value of Couling and Graham [7] at $\lambda = 514.5$ nm.

		(1)	(2)
T K	$10^6\,B_\rho^{exp}$ $m^3 mol^{-1}$	$10^6\,B_\rho^{calc}$ $m^3 mol^{-1}$	$10^6\,B_\rho^{calc}$ $m^3 mol^{-1}$
338.4	-6.96±0.49	-6.225	-6.328

The parameter set of Couling and Graham provides a much better fit to the experimental data of $B(T)$ than our new parameter set, as well as a slightly better fit for B_ρ. However, both parameter sets yield good agreement with the measured values of B_K, and our parameter set fits the experimental value of B_ε far better than parameter set (2). Unfortunately, the experimental data of Lawley and Sutton [10] for B_ε for other gases shows a large scatter, so that a single value is not a definitive test. Since the parameter set chosen by Couling and Graham provides a better fit for three of the effects and yields a value for B_ε which is the correct order of magnitude, we feel that it describes all of the available effects adequately. A precise set of B_ε values for a range of temperatures, would allow a more definite conclusion.

8.10 Calculations for dimethyl ether

8.10.1 Molecular properties of dimethyl ether

Dimethyl ether has the same C_{2v} symmetry as sulphur dioxide and is also taken to lie in the 1-3 plane with the 3-axis chosen to coincide with the principal molecular axis. The values of the molecular parameters used in our calculations are given in Table 8.81.

Table 8.81: Molecular parameters of dimethyl ether used in the calculations

Molecular Parameter	Value	Reference
$10^{30}\mu_3$ (Cm)	-4.37±0.03	[224]
$10^{40}\theta_{11}$ (Cm^2)	11.0±2.0	
$10^{40}\theta_{22}$ (Cm^2)	-4.3±2.0	[225]
$10^{40}\theta_{33}$ (Cm^2)	-6.7±1.7	
$10^{40}a_{11}$ (C^{2}m^{2}J^{-1})	6.584	
$10^{40}a_{22}$ (C^{2}m^{2}J^{-1})	5.195	
$10^{40}a_{33}$ (C^{2}m^{2}J^{-1})	5.399	[9, 226]
$10^{40}a$ (C^{2}m^{2}J^{-1})	5.726	
$10^{40}\Delta a$ (C^{2}m^{2}J^{-1})	1.299	
$10^{40}\alpha_{11}$(632.8 nm) (C^{2}m^{2}J^{-1})	6.69±0.17	
$10^{40}\alpha_{22}$(632.8 nm) (C^{2}m^{2}J^{-1})	5.46±0.14	
$10^{40}\alpha_{33}$(632.8 nm) (C^{2}m^{2}J^{-1})	5.28±0.13	[23]
$10^{40}\alpha$(632.8 nm) (C^{2}m^{2}J^{-1})	5.81±0.17	
$10^{40}\Delta\alpha$(632.8 nm) (C^{2}m^{2}J^{-1})	1.33±0.32	
$100\rho_0$(514.5 nm	0.371	[4]
$10^{40}\alpha_{11}$(514.5 nm) (C^{2}m^{2}J^{-1})	6.72	
$10^{40}\alpha_{22}$(514.5 nm) (C^{2}m^{2}J^{-1})	5.51	
$10^{40}\alpha_{33}$(514.5 nm) (C^{2}m^{2}J^{-1})	5.32	[226]
$10^{40}\alpha$(514.5 nm) (C^{2}m^{2}J^{-1})	5.85	
$10^{40}\Delta\alpha$(514.5 nm) (C^{2}m^{2}J^{-1})	1.32	

The electric dipole moment is that determined by Blukis *et al.* [224] from the Stark effect, while the electric quadrupole moment tensor components are those obtained by Benson and Flygare [225] from measurements of magnetizability anisotropy. It must be noted that the quadrupole moment depends on the origin of the molecular axes, and that for the values used here the origin is at the centre of mass of dimethyl ether. The static polarizability tensor components are the scaled *ab inito* values, determined by Couling and Graham [9] using the method described for sulphur dioxide in Section 8.9.1, from the MP2 values of Spackman and Ritchie [226]. The dynamic polarizability tensor components at $\lambda = 632.8$ nm, are the precise measured values of Bogaard *et al.* [23]. Since no measured values of the optical-frequency polarizability tensor components are

available for a wavelength of 514.5nm, the *ab initio* values calculated by Spackman and Ritchie [226] at the MP2 level of theory are used here.

Since a parameter set which provided good agreement for the second pressure and Kerr-effect virial coefficients of dimethyl ether had been found by Couling and Graham [9], we used this set of parameters to calculate the second dielectric virial coefficient for the range of temperatures for which measured values are available. The values we calculated for B_ε were much lower than the experimental values and, in most cases, negative and we consequently attempted to find a new set of parameters which would improve the agreement with the measured value of B_ε without sacrificing the fit of the second pressure virial coefficient. We used our new parameter set to calculate B_K and compared our values with the available experimental data. Our new parameter set and the parameter set fitted to $B(T)$ by Couling and Graham [9] are given in Table 8.82

Table 8.82: Lennard-Jones parameters and shape factors for dimethyl ether.

		R_0 (nm)	ε/k (K)	D_1	D_2
(1)	Our fitted values	0.390	400.0	0.1400	0.1556
(2)	Fitted values of Couling and Graham [9]	0.390	370.0	0.1923	0.2137

8.10.2 Results of calculations of second virial coefficients for dimethyl ether

Table 8.73 lists the values calculated for the second pressure virial coefficient of dimethyl ether, together with the experimental values of Haworth and Sutton [22] quoted by Dymond and Smith [1]. The values calculated using the parameter set of Couling and Graham [9] fit the experimental values to within 0.5%. Our parameter set yielded calculated values for $B(T)$ which agree with the experimental values to within 5.5%.

Table 8.83: Calculated values of $B(T)$ for dimethyl ether for two sets of parameters, together with the experimental values of Haworth and Sutton [22].

		(1)		(2)	
T	$10^6 B^{\mathrm{exp}}$	$10^6 B^{\mathrm{calc}}$	%	$10^6 B^{\mathrm{calc}}$	%
K	$\mathrm{m^3mol^{-1}}$	$\mathrm{m^3mol^{-1}}$	Error	$\mathrm{m^3mol^{-1}}$	Error
298.2	-456±10	-431.2	-5.44	-455.7	-0.07
313.2	-405±10	-389.5	-3.83	-406.4	0.35
328.2	-368±10	-354.3	-3.72	-366.1	0.52

B_ε has been measured by various workers over a range of temperature from 291.2 K to 343.2 K. The experimental errors are large and the values are not in very good agreement.

However, all of the values are large positive numbers of the same order of magnitude. When we used the parameter set of Couling and Graham, which provides a very good fit for $B(T)$, to calculate the second dielectric virial coefficient, we found that at the lower temperature the calculated values were large and negative, becoming less negative as the temperature increases and, for temperatures of 330 K and higher, small and positive. This can be seen in Table 8.84, which gives the measured values of B_ε, together with the values calculated using both parameter sets. Not only are these values far too low, but they also display the opposite trend to the measured values and the values calculated using our parameter set. This is shown clearly in Figure 8.8 (a), where the solid and dotted lines represent the values calculated using parameter sets (1) and (2), respectively. From the graph and the table, we see that the values obtained from our new parameter set are of the correct sign and order of magnitude, and decrease with increasing temperature. Although the solid curve lies below most of the experimental error bars, it is a reasonable fit, considering the scatter of the measured values. In addition, several of the experimental values have no quoted error, so that the fit may be better than it appears from the graph.

Table 8.84: Calculated values of B_ε for dimethyl ether for two sets of parameters, together with the available measured values.

		(1)	(2)
T	$10^{12}B_\varepsilon^{\text{exp}}$	$10^{12}B_\varepsilon^{\text{calc}}$	$10^{12}B_\varepsilon^{\text{calc}}$
K	$\text{m}^6\text{mol}^{-2}$	$\text{m}^6\text{mol}^{-2}$	$\text{m}^6\text{mol}^{-2}$
291.2	2800	1623.8	-1300.6
294.7	4000±1000	1590.6	-1121.5
303.2	2800±1000	1512.9	-734.1
311.5	2020	1441.4	-420.7
313.5	2600±1000	1424.7	-354.8
323.5	1600±400	1345.3	-81.1
334.7	2400±1000	1263.5	114.7
340.5	1540	1224.2	170.2
343.2	1600±400	1206.6	185.4

Table 8.85 shows the relative contribution of the various terms used to calculate B_ε for dimethyl ether. It can be seen that $B_{\varepsilon_{\text{ind}}}$ makes a significant contribution to B_ε of 7.1%, while all three of the series in $B_{\varepsilon_{\text{or}}}$ are significant. The most significant contribution of 57.3% is made by the dipole-quadrupole series $\alpha\mu\theta$, while the leading dipole-dipole $\alpha\mu$ series contributes 20% and the quadrupole series $\alpha\theta$ contributes 11% of B_ε. The combined effects of the terms containing the quadrupole moment make up more than two thirds of the total calculated value of B_ε.
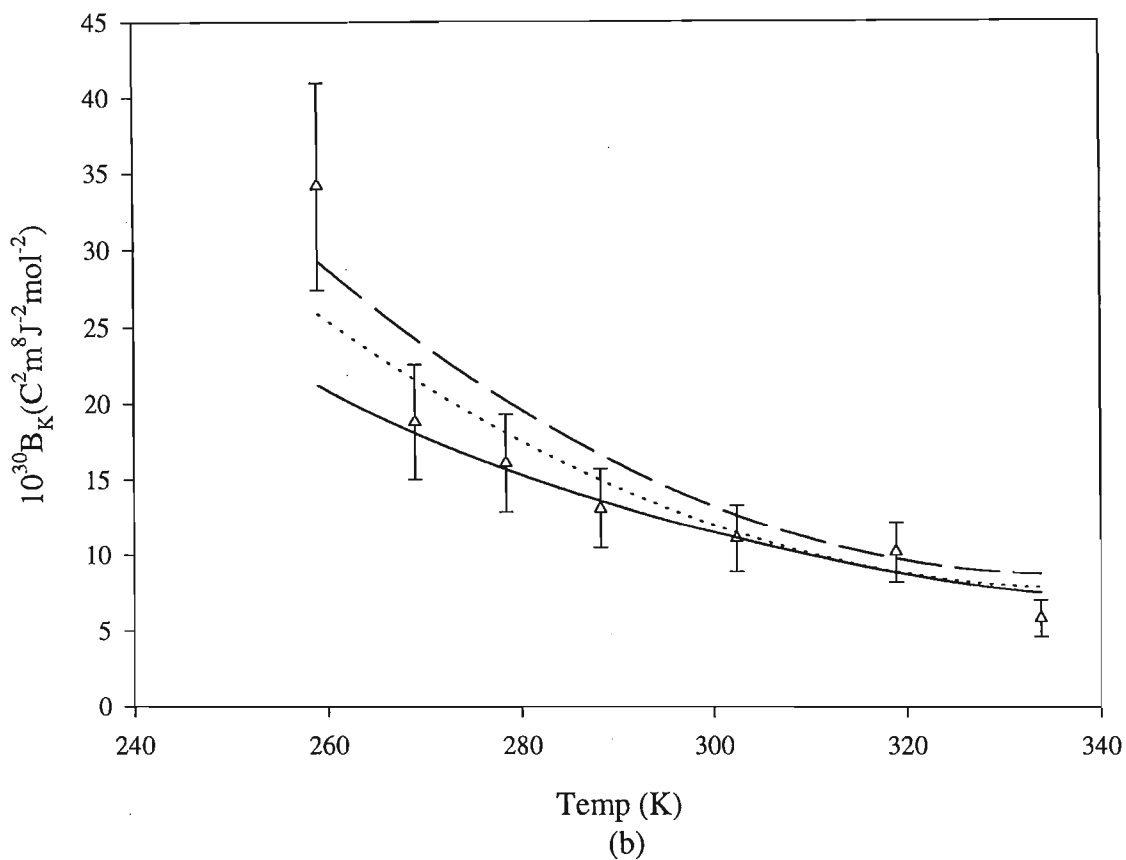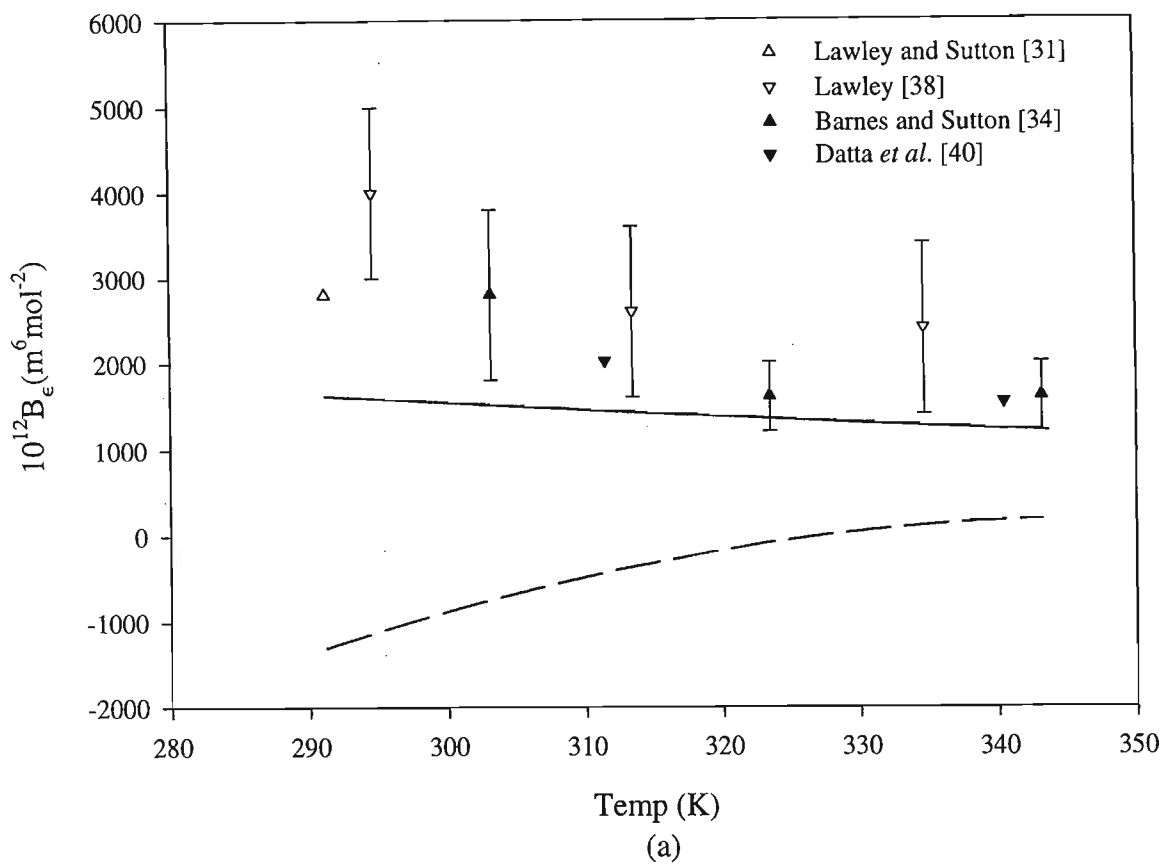
Figure 8.8: Temperature dependence of the calculated and measured values of the second (a) dielectric, and (b) Kerr-effect virial coefficients of dimethyl ether. The solid and dashed lines represent the values calculated using parameter sets (1) and (2), respectively, while the dotted line in (b) represents the curve calculated by Couling and Graham [9].

Table 8.85: The relative contributions of the terms used to calculate B_ε for dimethyl ether at 291.2 K for the parameter set (D_1=0.1400, D_2=0.1556, R_0=0.390, ε/k=400.0).

Contributing Term	$10^{12} \times$ Value $\text{m}^6\text{mol}^{-2}$	% Contribution to B_ε
α_2	7.191	0.44
α_3	102.284	6.30
α_4	6.254	0.39
$B_{\varepsilon_\text{ind}}$	115.729	7.13
μ_2	-1444.290	-88.94
$\alpha_1\mu_2$	932.999	57.46
$\alpha_2\mu_2$	835.188	51.43
$\alpha_3\mu_2$	75.106	4.63
$\alpha_1\mu_1\theta_1$	802.400	49.42
$\alpha_2\mu_1\theta_1$	128.551	7.92
$\alpha_2\theta_2$	153.130	9.43
$\alpha_3\theta_2$	25.015	1.54
$B_{\varepsilon_\text{or}}$	1508.099	92.87

$$B_\varepsilon = 1623.83 \times 10^{-12}\text{m}^6\text{mol}^{-2}$$

The second Kerr-effect virial coefficient has been measured by Bogaard *et al.* [23] at a wavelength of 632.8 nm. Although the experimental errors are approximately 20%, there is very little scatter, so that the temperature dependence is clearly discernible. Both parameter sets were used to calculate B_K and the relative contributions of the terms used in the calculation are shown in Table 8.86. It is clear that the leading dipole series $\mu\alpha$, which contributes 85% of the total value for B_ε, is the dominant contribution. The α series makes a significant contribution of 8.3%, while the dipole-quadrupole series $\mu\theta\alpha$ contributes 5%. The quadrupole series $\theta\alpha$ contributes less than 2% to the final value. Thus, the combined contribution of the terms containing the quadrupole moment is approximately 7%, which although small, is not negligible.

The calculated and measured values of B_K are listed in Table 8.87, and represented graphically in Figure 8.8 (b). The graph shows the values calculated using parameter sets (1) and (2) as solid and dashed curves, respectively. The dotted line represents the calculated values of Couling and Graham [9], which do not include the dipole-quadrupole $\mu\theta\alpha$ or quadrupole $\theta\alpha$ series. The experimental point at 259 K is much higher than the next point at 269 K, and it is not clear whether this is due to experimental scatter or if it is a true reflection of the temperature dependence of B_K. The solid line lies very near to and within the error bars of all the measured values in the temperature range from 269 K to 333.8 K, but is much lower than the experimental values at 259 K. The dashed line lies above most of the measured values, but falls within the experimental

Table 8.86: The relative contributions of the terms used to calculate B_K for dimethyl ether at 259.0 K for $\lambda = 632.8$ nm for the parameter set (D_1=0.1400, D_2=0.1556, R_0=0.390, ε/k=400.0).

Contributing Term	$10^{30} \times$ Value $C^2m^8J^{-2}mol^{-2}$	% Contribution to B_K
α_2	0.003	0.01
α_3	0.137	0.65
α_4	1.425	6.73
α_5	0.201	0.95
$\mu_2\alpha_1$	1.963	9.27
$\mu_2\alpha_2$	6.916	32.68
$\mu_2\alpha_3$	7.675	36.26
$\mu_2\alpha_4$	1.416	6.69
$\mu_1\theta_1\alpha_1$	-0.091	-0.43
$\mu_1\theta_1\alpha_2$	1.119	5.29
$\mu_1\theta_1\alpha_3$	0.045	0.21
$\theta_1\alpha_3$	0.039	0.18
$\theta_1\alpha_4$	0.215	1.02
$\theta_1\alpha_5$	0.103	0.49

$$B_K = 21.166 \times 10^{-30}C^2m^8J^{-2}mol^{-2}$$

Table 8.87: Calculated values of B_K for dimethyl ether for two sets of parameters, together with the measured values of Bogaard *et al.* [23], at a wavelength of $\lambda = 632.8$ nm.

| T | $10^{32}B_K^{exp}$ | (1) | | (2) | |
K	$C^2m^8J^{-2}$	$10^{32}B_K^{calc}$ $C^2m^8J^{-2}$	% Error	$10^{32}B_K^{calc}$ $C^2m^8J^{-2}$	% Error
259.0	34.2±6.8	21.17	-38.10	29.25	-14.47
269.0	18.8±3.8	18.20	-3.19	24.27	29.10
278.4	16.1±3.2	15.54	-0.56	20.22	25.59
288.2	13.1±2.6	13.62	3.97	16.65	27.10
302.4	11.1±2.2	11.21	0.99	12.65	13.69
318.9	10.2±2.0	8.79	-13.82	9.75	-4.41
333.8	5.8±1.2	7.49	29.14	8.75	50.86

uncertainty of the experimental point at 259 K. This makes it very difficult to decide which line represents the best fit of the experimental data. Above 259 K the values calculated using our new parameter set definitely fit the data best, but over the entire temperature range the values obtained from Couling and Graham's set of Lennard-Jones and shape parameters represent the best fit. An independent measurement in the lower

temperature range would enable a more definite conclusion. However, it can be said that both parameter sets yield reasonably good agreement with experiment.

The second refractivity and light-scattering virial coefficients have not been measured for dimethyl ether. However, in order to provide possible future comparison, we have calculated B_R and B_ρ using both parameter sets. Table 8.88 shows the relative magnitude of the various contributions to B_R, while Table 8.89 gives the relative contributions of the terms used to calculated B_ρ.

Table 8.88: The relative contributions of the terms used to calculate B_R for dimethyl ether at 298.15 K for $\lambda = 632.8$ nm.

Contrib. Term	(1) $10^{12} \times$ Value $m^6 mol^{-2}$	% of B_R	(2) $10^{12} \times$ Value $m^6 mol^{-2}$	% of B_R
α_2	8.122	6.90	21.514	11.76
α_3	103.185	87.65	148.356	81.12
α_4	6.416	5.45	13.022	7.12
B_R	117.723		182.892	

Table 8.89: The relative contributions of the terms used to calculate B_ρ for dimethyl ether at 328.15 K for $\lambda = 514.5$ nm.

Contrib. Term	(1) $10^6 \times$ Value $m^3 mol^{-1}$	% of B_ρ	(2) [9] $10^6 \times$ Value $m^3 mol^{-1}$	% of B_ρ
g	3.86	0.49	19.78	1.64
b_3	-1.12	-0.14	-2.50	-0.21
a_3	87.34	11.15	201.32	16.68
a_4	1273.99	162.66	1495.76	123.95
a_5	155.14	19.81	228.31	18.92
S_ρ	1519.21	193.97	1942.67	160.99
$2B$	-736.00	-93.97	-736.00	-60.99
B'_ρ	783.21		1206.67	
B_ρ	2.89		4.46	

In summary, we note that our new set of parameters yield calculated values of $B(T)$ which only agree with experiment to within approximately 5%, while parameter set (2) fits $B(T)$ to within 0.5% over the limited range of experimental data. Both sets agree reasonably well with experiment for B_K, but the values of B_ε calculated using parameter set (2) are of the wrong sign and are between 90% and 130% lower than the measured values, while our new parameter set yields calculated values for B_ε which agree to between

16% and 60% with experiment. Taking all of the results for dimethyl ether into account, it would appear that our new parameter set provides a slightly better fit of the available second virial coefficients than the parameter set of Couling and Graham [9].

8.11 Calculations for ethene

8.11.1 Molecular properties of ethene

The ethene molecule is taken to lie in the 1-3 plane of a system of coordinate axes O(1,2,3) with the C=C bond on the 3-axis and the origin of the molecule-fixed axes at the midpoint of the bond. Ethene is a non-polar molecule with D_{2h} symmetry, so that the traceless electric quadrupole moment tensor has two independent components: θ_{11} and θ_{22}, with $\theta_{33} = -(\theta_{11} + \theta_{22})$ and the polarizability tensor has three independent components: α_{11}, α_{22} and α_{33} [26].

Although the electric quadrupole moment of ethene has been the subject of extensive experimental and theoretical research, the experimental investigations are usually confined to partial determinations or combine various experimental data in order to estimate the two independent components. However, accurate theoretical estimates by Spackman [202] at the MP2 (second-order Møller-Plesset perturbation theory) level and Maroulis [103] at the MP4 level are available. These theoretical values are in excellent agreement with each other and are shown, together with the experimental data available, in Table 8.90.

Table 8.90: Selected experimental and theoretical values of the quadrupole moment tensor components of ethene.

Method	$10^{40}\theta_{11}$ Cm^2	$10^{40}\theta_{22}$ Cm^2	$10^{40}\theta_{33}$ Cm^2
Measurements of collision-induced absorption (CIA) spectra [227]	6.73	-13.33	6.60
Measurements of CIA spectra [228]	5.16	-10.41	5.52
Magnetizability anisotropy measurements [229]	4.67	-12.02	7.31
Measurements of induced birefringence + second dielectric virial coefficients + refractive index [74]	4.35	-10.99	6.68
MP2 theory [202]	5.43	-11.03	5.60
MP4 theory [103]	5.370 ± 0.22	-10.92 ± 0.45	5.549 ± 0.22

In this work we have used the theoretical values of Maroulis [103] which are in good

agreement with the estimates obtained by Dagg et al. [228] from collision-induced absorption spectra measurements in mixtures of ethene and rare gases.

For linear molecules the two independent components of the dynamic polarizability tensor can be deduced from the experimental values of ρ_0 and α [4,190]. However, since non-linear molecules have three independent components, an additional physical relationship connecting the components is necessary to evaulate the individual components. For this reason, there are very few experimentally-deduced polarizability components for non-linear molecules. Hills and Jones [230] measured the pure rotational Raman spectrum of ethene and compared it with the spectrum calculated using an asymmetric rotor computer simulation in order to deduce a value for the dimensionless quantity R_{20}, which is defined as:

$$R_{20} = -\frac{\sqrt{3}\,(\alpha_{11} - \alpha_{22})}{(\alpha_{11} + \alpha_{22} - 2\alpha_{33})}.$$
(8.1)

The polarizability anistropy defined in equation (7.22) may be determined from equation (7.25) if ρ_0 and α are known. Then, solving equations (7.21), (7.22) and (8.1) yields values for the polarizability tensor components α_{11}, α_{22} and α_{33}. Table 8.91 lists two sets of values for these components at 514.5 nm. The first set is obtained from the values for ρ_0 and α measured by Bogaard et al. [4] together with the value of R_{20} measured by Hills and Jones [230]. The second set was obtained using Couling and Graham's [9,36] measured value for ρ_0, the more precise value of R_{20} recently obtained by Barbès [231], and a value for α interpolated from Hohm's high-precision measurements of the frequency dependence of α for ethene [140]. In this work we will use the second set of values. Couling and Graham [9] showed that using the first set results in a decrease of less than 0.5% in their calculated value for $\mathcal{S}_\rho$ and it should have an equally negligible effect on the other second virial coefficients.

Table 8.91: Components of the dynamic polarizability tensor of ethene, at wavelengths of 514.5 nm and 632.8 nm.

	514.5 nm Set 1		514.5nm Set 2		632.8 nm	
$100\rho_0$	$1.247_5 \pm 0.005$	[4]	1.250 ± 0.002	[9]	1.207 ± 0.002	[4]
$10^{40}\alpha\,(\mathrm{C^2m^2J^{-1}})$	4.76	[4]	4.7871	[140]	4.7124	[140]
$10^{40}\Delta\alpha\,(\mathrm{C^2m^2J^{-1}})$	2.077		2.091		2.021_5	
R_{20}	0.22 ± 0.03	[230]	0.21 ± 0.01	[231]	0.21 ± 0.03	[231]
$10^{40}\alpha_{11}\,(\mathrm{C^2m^2J^{-1}})$	4.34_1		4.35_3		4.30_5	
$10^{40}\alpha_{22}\,(\mathrm{C^2m^2J^{-1}})$	3.82_6		3.85_7		3.80_4	
$10^{40}\alpha_{33}\,(\mathrm{C^2m^2J^{-1}})$	6.11_2		6.15_1		6.02_9	

Since there are no experimental estimates of the individual components of the static polarizability tensor a, Couling and Graham [9] scaled the *ab initio* calculated values of of Spackman [202] according to the mean static polarizability $a = (4.5717 \pm 0.0008) \times 10^{-40} C^2 m^2 J^{-1}$ extrapolated from measured dynamic values [140]. They then combined the dynamic values of α with values of ρ_0 [4] to obtain values for the dynamic polarizability anisotropy, which when extrapolated to infinite wavelength agreed with the anisotropy of the scaled static polarizability components to within 1.1%. Table 8.92 shows the static polarizability tensor components a_{ij}, mean static polarizability a and polarizability anisotropy Δa calculated by Spackman, as well as the scaled values.

Table 8.92: *Ab initio* calculated static polarizability tensor components, mean static polarizability and polarizability anisotropy of ethene, together with scaled values [9].

Polarizability property	$10^{40} \times$ MP2 calculated values [202] $C^2 m^2 J^{-1}$	$10^{40} \times$ Scaled values $C^2 m^2 J^{-1}$
a_{11}	4.092	4.245
a_{22}	3.534	3.666
a_{11}	5.594	5.803
a	4.407	4.571
Δa	1.845	1.914

For molecules with D_{2h} symmetry the dipole moment, first-order hyperpolarizability and the A-tensor are all zero. The second-order hyperpolarizability has six independent components. Maroulis [102] carried out *ab initio* SCF calculations of the static hyperpolarizability tensor components of ethene, and confirmed the assumption that these values are unlikely to differ from the optical frequency values. Couling and Graham [9] used these static values to determine the leading term in γ_{ijk} for the second Kerr-effect virial coefficient and found that it contributed only 0.04% to the total B_K. Thus, it seems reasonable to assume that the second-order hyperpolarizability will make a negligible contribution to the other second virial coefficients.

Table 8.93: Lennard-Jones parameters and shape factors for ethene.

R_0 (nm)	ε/k (K)	D_1	D_2	Reference
0.4232	205			[106]
0.4236	193.5			[232]
0.4232	190.0	0.22965	0.21383	[9]

Couling and Graham [9] determined values for the Lennard-Jones parameters R_0 and ε/k and their shape factors D_1 and D_2 by fitting values of the second pressure

virial coefficient $B(T)$ to the available experimental values [1] over the temperature range 238.15 K to 448.15 K. These fitted values are given in Table 8.93 along with the force constants quoted in the classic text of Hirschfelder *et al.*, which are obtained from viscosity data [106], and the more recent values of Das Gupta *et al.* [232] obtained from viscosity data and second pressure virial coefficients. Their optimized values yielded calculated values of $B(T)$ that fit the experimental values to within 1.0% over almost the entire range. The shape factors were chosen to reflect the molecular dimensions [9]. They then used the fitted parameters to calculate B_ρ and B_K. They found that the calculated B_ρ agreed very well with the measured values. The calculated B_K values were not in good agreement with the experimental values, with discrepancies of between 20% and 50%. It remains unclear whether this is due to the experimental uncertainties or the failure of the model.

The aim of this work is to attempt to find a set of molecular parameters which will adequately describe the second virial coefficients for as many of the effects under study as possible. With this in mind, the Lennard-Jones force constants and the shape factors determined by Couling and Graham [9] were used to calculate all the second dielectric and refractivity virial coefficients.

8.11.2 Results of calculations of second virial coefficients for ethene

The values of the second pressure virial coefficient calculated using the Lennard-Jones and shape parameters of Couling and Graham [9] are given in Table 8.94, together with the smoothed experimental values of Dymond and Smith [1]. It can be seen that the

Table 8.94: The temperature dependence of the calculated values of the second pressure virial coefficient $B(T)$ for ethene, and the best fit data of Dymond and Smith [1].

Temperature	$10^6 \, B^{\mathrm{exp}}$	$10^6 \, B^{\mathrm{calc}}$	%
K	$\mathrm{m^3 mol^{-1}}$	$\mathrm{m^3 mol^{-1}}$	Error
240.0	-218.5±2	-221.53	1.39
250.0	-201±2	-202.59	0.79
275.0	-166±1	-165.15	-0.51
300.0	-138±1	-137.25	-0.54
325.0	-117±1	-115.43	-1.34
350.0	-99±1	-97.86	-1.15
375.0	-84±1	-83.41	-0.70
400.0	-71.5±1	-71.36	-0.20
450.0	-51.7±1	-52.18	0.93

theoretical values agree with experiment to within 1.4% over the entire temperature range.

The second dielectric virial coefficient was then calculated using the same parameter set. The relative magnitudes of the terms contributing to B_ε, as defined in equations (4.152) to (4.154) and (4.160), are summarized in Table 8.95 for a temperature of 298.2 K. It is clear that the α_3 and $\theta_2 a_2$ terms are the most significant, although the α_2 term is not negligible. The α series of terms has evidently converged, while the $\theta\alpha$ series is converging rapidly.

Table 8.95: The relative contributions of the terms used to calculate B_ε for ethene at 298.2 K.

Contributing Term	$10^{12} \times$ Value $m^6 mol^{-2}$	% Contribution to B_ε
α_2	-10.640	-17.96
α_3	24.142	40.75
α_4	0.727	1.23
$B_{\varepsilon_{ind}}$	14.229	24.02
$\theta_2\alpha_2$	40.158	67.78
$\theta_2\alpha_3$	4.857	8.20
$B_{\varepsilon_{or}}$	45.015	75.98

$$B_\varepsilon = 59.244 \times 10^{-12} m^6 mol^{-2}$$

It can be seen from Table 1.2 that there are large variations in the experimental data. The fit of the calculated values to measured values is shown in Figure 8.9 (a). The solid line represents the values for B_ε calculated including the two quadrupole terms, while the dotted line shows the curve calculated using only the α series. From this graph it is clear that the solid curve fits the most recent measured values of Bose and Cole [24] very well. It can also be seen that the inclusion of the quadrupole series of terms improves the fit dramatically. Table 8.96 shows the temperature dependence of the calculated values of B_ε in comparison with the experimental data of Bose and Cole [24].

Table 8.96: The temperature dependence of the calculated values of B_ε for ethene, and the measured values of Bose and Cole [24].

Temperature K	$10^{12} B_\varepsilon^{exp}$ $m^6 mol^{-2}$	$10^{12} B_\varepsilon^{calc}$ $m^6 mol^{-2}$	% Error
298.2		59.24	
303.2	50.3±1.4	57.46	14.23
323.2	47.5±1.4	51.68	8.80
348.2		46.35	
373.2	42.0±2.8	42.49	1.17
423.2	37.6±2.4	37.23	-0.98
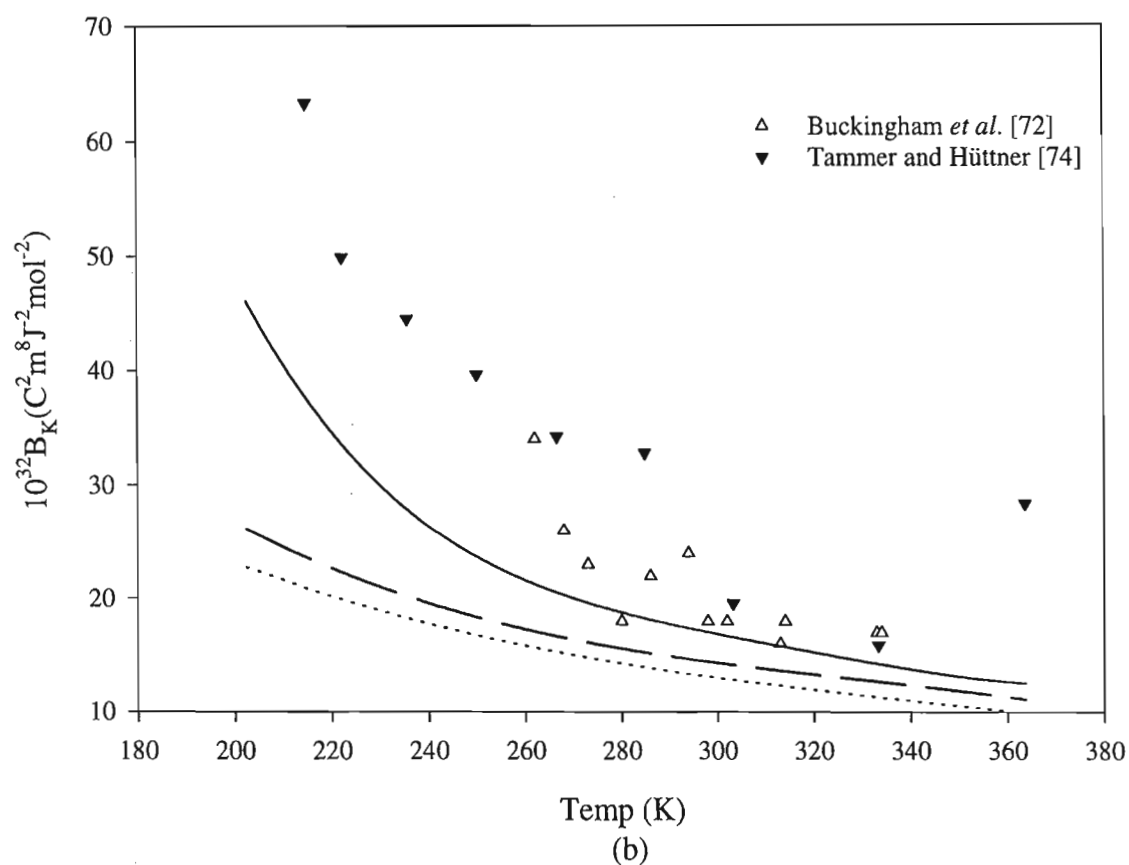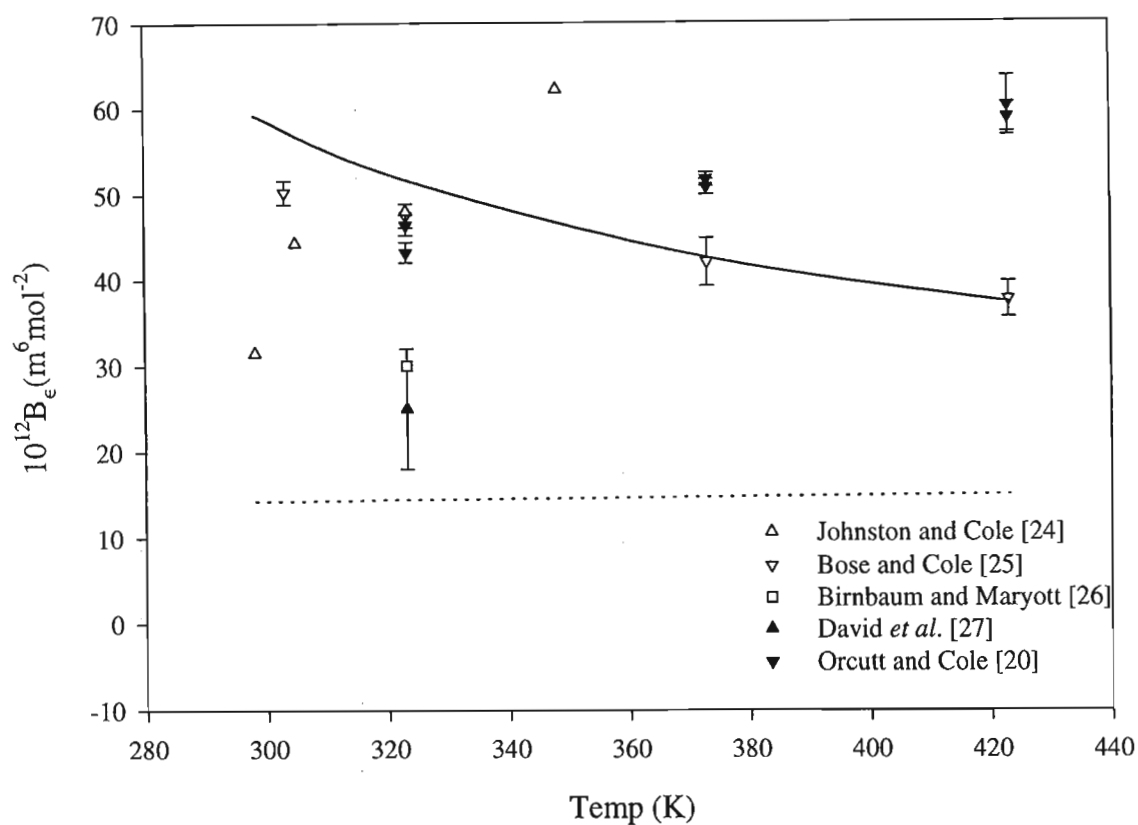
Figure 8.9: Temperature dependence of the calculated and measured values of (a) B_ε, and (b) B_K of ethene. The solid lines represent our calculated values. The dotted line in (a) shows values of B_ε calculated without quadrupole terms. The dashed and dotted lines in (b) represent the calculated values of Couling and Graham [9] and Tammer and Hüttner [25], respectively.

Couling and Graham [36] calculated the temperature dependence of B_K at $\lambda = 632\,\text{nm}$, which they found to be consistently lower than the experimental values of Buckingham et al. [14] by between 20% and 50%. The more recent measured values of Tammer and Hüttner [25] are generally higher than those of Buckinhgam et al. and cover a wider temperature range. We have recalculated B_K, including the new quadrupole terms $\theta_2\alpha_3$, $\theta_2\alpha_4$ and $\theta_2\alpha_5$. Table 8.97 shows the relative significance of the terms used to calculate B_K for ethene, including the new quadrupole series.

Table 8.97: The relative contributions of the terms used to calculate B_K for ethene at 202 K and 298 K.

Contributing Term	202 K		298K	
	$10^{32} \times$ Value $\text{C}^2\text{m}^8\text{J}^{-2}\text{mol}^{-2}$	% of B_K	$10^{32} \times$ Value $\text{C}^2\text{m}^8\text{J}^{-2}\text{mol}^{-2}$	% of B_K
α_2	25.990	56.36	3.516	20.64
α_3	-57.428	-124.54	-10.140	-59.54
α_4	54.801	118.84	19.905	116.88
α_5	2.926	6.35	1.139	6.69
$\theta_2\alpha_3$	-5.853	-12.69	0.135	0.80
$\theta_2\alpha_4$	17.765	38.53	1.782	10.46
$\theta_2\alpha_5$	7.910	17.15	0.693	4.07
B_K	46.112		17.031	

It can be seen from Table 8.97 that the α series has definitely converged, and that the hyperpolarizability makes a negligible contribution. Note that terms including the quadrupole moment make a significant contribution, clearly establishing the relative importance of the quadrupole series.

The temperature dependence of the measured values is given in Table 8.98 together with the calculated values of Tammer and Hüttner [25], Couling and Graham [9] and our new more complete calculations. Note that the errors quoted for the measured values [14] listed in Table 8.98 were obtained from a least-squares analysis of the experimental data. Thus, the uncertainties do not allow for systematic errors due to errors in the pressure virial coefficients which are used to deduce the molar volume. Figure 8.9 (b) shows a solid curve plotted through our calculated values. The dotted line shows the values calculated by Tammer and Hüttner using the theory of Buckingham and Dunmur [82,174] for spherical molecules. These values of B_K are even lower than those of Couling and Graham, which are indicated by a dashed line. It can be seen that although our solid curve lies below many of the experimental points, it clearly provides the best fit of the measured values.

Table 8.98: The temperature dependence of calculated values of B_K for ethene, and the measured values of Buckingham *et al.*[a] [14] and Tammer and Hüttner[b] [25].

T K	$10^{12} B_K^{exp}$ m⁶mol⁻²	I[b] Spherical Approx.		II Non-linear No θ		III Non-linear With θ	
		$10^{12} B_K^{calc}$ m⁶mol⁻²	% Err	$10^{12} B_K^{calc}$ m⁶mol⁻²	% Err	$10^{12} B_K^{calc}$ m⁶mol⁻²	% Err
202.4	103.0[b]	23	-77.67	26.28	-74.49	46.11	-55.23
211.4	90.1[b]	21	-76.69				
214.8	63.3[b]	21	-66.82				
222.2	49.9[b]	20	-59.92	22.06	-55.79	33.34	-33.19
235.6	44.5[b]	18	-59.55				
250.0	39.6[b]	17	-57.07				
262	34±7[a]			17.06	-49.82	21.47	-36.85
266.6	34.2[b]	15	-56.14				
268	26±6[a]			16.54	-36.38		
273	23±5[a]			16.13	-29.87		
280	18±3[a]			15.60	-13.33	18.94	5.22
284.9	32.8[b]	14	-57.32				
286	22±5[a]			15.18	-31.00		
294	24±5[a]			14.66	-38.92		
298	18±3[a]			14.42	-19.89	17.03	-5.399
302	18±3[a]			14.19	-21.17		
302.2	19.6[b]	13	-33.67				
313	16±3[a]			13.59	-15.06	15.78	-1.38
314	18±3[a]			13.53	-24.83		
333	17±3[a]			12.60	-25.88	14.39	-15.35
333.4	15.9[b]	11	-30.82				
334	17±3[a]			12.54	-26.23		
363.7	28.4[b]	10	-64.79	11.15	-60.74	12.52	-55.92

The second refractivity virial coefficient has been measured at several different wavelengths, but most of the experiments have been conducted at $\lambda = 633.0$ nm. The measured values at this wavelength are only available at two different temperatures, and the scatter at each is so large that it is not helpful to plot a graph of the experimental and theoretical values. Table 8.99 gives the relative magnitudes of the three calculated terms which contribute to B_R, and clearly shows that convergence has been established. Table 8.100 presents the calculated and measured values of the second refractivity virial coefficient of ethene for a wavelength of 633.0 nm.

Table 8.99: The relative contributions of the terms used to calculate B_R for ethene at 303 K.

Contributing Term	$10^{12} \times$ Value $m^6 mol^{-2}$	% Contribution to B_R
α_2	-11.916	-73.03
α_3	27.390	167.87
α_4	0.842	5.16
$B_R = 12.597 \times 10^{-12} m^6 mol^{-2}$		

Table 8.100: Calculated and measured values of B_R for ethene at $\lambda = 633.0$ nm.

Temperature K	$10^{12} B_R^{exp}$ $m^6 mol^{-2}$	Ref.	$10^{12} B_R^{calc}$ $m^6 mol^{-2}$
303	17.60±2.2	[74]	16.316
	40.8±2.0	[75]	
	6.0	[24]	
	17.7±0.4	[77]	
	20.3±0.8	[78]	
	17.4±0.4	[79]	
373	19.50±0.50	[64]	16.945
	17.8±0.3	[77]	
	20.1±0.5	[78]	
	17.8±0.3	[79]	

Couling and Graham [9,36] have calculated the second light-scattering virial coefficient at $\lambda = 514.5$ nm, compared the theoretical values with their measured value and the value of Berrue *et al.* [92] and found the theory and experiment to be in excellent agreement. The relative magnitudes of the various contributions to B_ρ at $T = 294.5$ K are given in Table 8.101. Although the α_5 term makes a significant contribution to $\mathcal{S}_\rho$ it is obvious that the series is converging very rapidly and the α_6 and higher-order terms in this series should contribute negligibly to B_ρ. Table 8.102 gives the experimental values of Couling

and Graham [9] and Berrue *et al.* [92], together with the values calculated by Couling and Graham allowing for the non-linearity of the molecule. They had previously calculated B_ρ for ethene treating it as an linear molecule [7] and found that the agreement of the calculated B_ρ with experiment improves when the low symmetry of the molecule is taken into account. In particular the calculated $\mathcal{S}_\rho$ increases by almost 50%, although this is masked by the much larger $2B$ contribution.

Table 8.101: The relative contributions of the terms used to calculate B_ρ for ethene at 294.92 K and $\lambda = 514.5$nm [9].

Contributing Term	$10^6 \times$ Value m^{3}mol^{-1}	% Contribution to B_ρ
g	23.42	-12.21
b$_3$	2.94	-1.53
a$_3$	-68.11	35.52
a$_4$	128.97	-67.26
a$_5$	7.14	-3.72
$\mathcal{S}_\rho$	94.36	-49.21
$2B$	-286.12	149.21

$$B'_\rho = -191.76 \times 10^{-6} \text{m}^3\text{mol}^{-1}$$
$$B_\rho = -2.357 \times 10^{-6} \text{m}^3\text{mol}^{-1}$$

Table 8.102: Measured and calculated values for $B\rho$ of ethene at $\lambda = 514.5$ nm.

Temperature K	$10^6\, B_\rho^{\text{exp}}$ m^{3}mol^{-1}	Ref.	$10^6\, B_\rho^{\text{calc}}$ m^{3}mol^{-1}	% Error
294.92	-2.384±0.027	[9]	-2.357	-1.13
328.0	-1.78±0.07	[92]	-1.671	-6.12

Thus it seems that by taking the non-linearity of ethene into account it is possible to find reasonable agreement between calculations based on the DID model and the available experimental data for the second virial coefficients considered here. In all cases, new precise measurements for a wide range of temperatures would allow a more rigorous comparison between experiment and theory.

8.12 Conclusions

The aim of this work has been to find a unique set of Lennard-Jones and shape parameters for each gas which, together with known molecular properties, either experimental or calculated, may be combined with complete molecular theories of the second virial coefficients to yield calculated values which agree with experiment for the full range of virial effects.

We have studied ten linear and non-linear gases, some dipolar and some non-polar, and have achieved mixed success. For the linear polar gas fluoromethane we were able to find a unique set of parameters which explained the available data reasonably well, while for trifluoromethane our set of parmaters provided good fits with experiment for all the available effects, except the second refractivity virial coefficient. For chloromethane we have presented the results for three slightly different sets of parameters and found that the set chosen to fit B_ε also yielded a good value of B_ρ and fits the experimental values for $B(T)$ to within 2%. The other linear polar gas which was studied is hydrogen chloride for which only values of $B(T)$ and B_ε have been measured. We were not able to find any set to yield measured values for B_ε as large as the experimental values, but the set of parameters which we chose fit the experimental data for $B(T)$ very well, and gave the closest fit to B_ε which we could find using physically reasonable Lennard-Jones parameters.

Of the linear non-polar gases under study, only for nitrogen could we find a set of parameters which yielded good values for all but one of the five effects available. For nitrogen we compared two different sets of parameters and found that our optimized set described all of the effects, except B_ρ, better than the set of Couling and Graham [9]. For carbon dioxide and ethane we were unable to choose a set of parameters which provided good agreement between theory and experiment for all of the effects. This is due in part to the fact that much of the experimental data available has large experimental errors and that for some of the effects only one or two measured values are available, making it difficult to select best-fit parameters.

We then studied three non-linear gases: the polar molecules sulpur dioxide and dimethyl ether, and the non-polar ethene. For all three molecules, we first considered the parameter set chosen for each by Couling and Graham [9] who extended the existing theory of B_ρ and B_K for linear molecules to the more general case of non-linear molecules and used the new theory to calculate B_ρ and B_K for these non-linear gases. Since their parameters yielded good fits for $B(T)$ we used these parameters in our new non-linear theory for the second dielectric virial coefficient to calculate values for B_ε to compare with experiment. For the ethene molecule we found that the calculated values of B_ε were in good agreement with experiment. We then re-calculated B_K including the quadrupole

terms and found that the agreement with experiment improved. Since these parameters also yield good agreement with the measured values of B_ρ and B_R, we conclude that this parameter set describes all of the available data reasonably well. For sulphur dioxide, we found that the value of B_ε calculated using Couling and Graham's parameter set was much larger than the single measured value. Thus, we found a new set of parameters which provided a reasonably good fit for $B(T)$ and yielded a value of B_ε which fell within the experimental error of the measured value. However, calculated values of B_K and B_ρ using this new set of values were not as good as those calculated with Couling and Graham's parameters. Thus, we concluded that since the parameter set chosen by Couling and Graham provides a better fit for three of the effects and yields a value for B_ε which is the correct order of magnitude, it describes all of the available effects adequately. Only a precise set of B_ε values for a range of temperatures, would allow a more definite conclusion. When we used Couling and Graham's parameter set to calculate B_ε for dimethyl ether, the results were very poor. As for sulphur dioxide, we found a new parameter set to optimize $B(T)$ and B_ε. This new set also yielded values for B_K which agree well with experiment, and thus we concluded that the new parameter set represents a better fit for all the available data than the original set.

A very important fact which has been clearly demonstrated by all our calculations is that, in general, quadrupole moment terms make a significant contribution to both the second dielectric and Kerr-effect virial coefficients, for both non-polar and polar molecules. No future calculations could be considered to be complete without the inclusion of these terms. An important point to note is that it is essential to establish convergence of the various sums to arrive at any meaningful conclusions. Many of the criticisms of the DID model have often erroneously stemmed from the failure to include sufficient terms and to obtain convergence. Before the advent of computers and computer algebraic manipulation packages this was completely understandable in view of the extreme complexity of the calculations. Even now, some of the larger terms demand large inputs of personal and computer time.

In overview, we found that for four of the gases, fluoromethane, chloromethane, dimethyl ether and ethene, a unique parameter set was found for each which described all of the available effects reasonably well. For the three gases, trifluoromethane, nitrogen and sulphur dioxide, one interaction parameter set explained all but one of the effects for which data was available to within the experimental uncertainty. For trifluoromethane the parameter set which yielded good agreement for $B(T)$, B_ε and B_K could not explain the observed values of B_R, while for nitrogen one parameter set produced reasonable agreement for all of the effects except B_ρ and a different set, which yielded good agreement for B_ρ, did not explain the remaining four effects as well as the first set. The parameter set which explained $B(T)$, B_K and B_ρ very well for sulphur dioxide,

yielded a value for B_ε which was much larger than the experimental value, although of the correct sign and order of magnitude. Hydrogen chloride posed a special problem as data was only available for two of the effects, $B(T)$ and B_ε. It was possible to find a set of interaction parameters in good agreement with the measured values of $B(T)$, but the experimental data for B_ε was an order of magnitude larger than the largest calculated values. Since the remaining effects have not been measured for this gas it was not possible to test the theory more rigorously. For the remaining gases carbon dioxide and ethane, it was impossible, based on the existing measured values, to select a unique parameter set which explained all of the effects. Definite conclusions are very often precluded by large scatter in one or more of the sets of observed data for some of the virial coefficients. A rigorous test of the various molecular theories for the different effects must await more precise measurements, but on general overview instances of complete failure in explaining experimental observations are few; and it would be fair to say that the mechanisms of the various second virial coefficients are fairly well understood, despite the daunting complexity and volume of the theories.

References

[1] DYMOND, J. H. and SMITH, E. B., 1980, *The Virial Coefficients of Gases and Mixtures*, (Oxford: Clarendon Press).

[2] SUTTER, H. and COLE, R. H., 1970, *J. chem. Phys.*, **52**, 132.

[3] SUTTER, H., 1970, Ph.D. thesis, Brown University.

[4] BOGAARD, M. P., BUCKINGHAM, A. D., PIERENS, R. K., and WHITE, A. H., 1978, *J. chem. Soc. Faraday Trans. I*, **74**, 3008.

[5] SUTTER, H. and COLE, R. H., 1967, *J. chem. Phys.*, **46**, 2014.

[6] LANGE, JR., H. B. and STEIN, F. P., 1970, *J. chem. Eng. Data*, **15**, 56.

[7] COULING, V. W., 1993, Master's thesis, University of Natal (Pietermaritzburg).

[8] COULING, V. W. and GRAHAM, C., 1994, *Molec. Phys.*, **82**, 235.

[9] COULING, V. W., 1995, Ph.D. thesis, University of Natal.

[10] LAWLEY, K. P. and SUTTON, L. E., 1963, *Trans. Faraday Soc.*, **59**, 2680.

[11] POWLES, J. G. and McGRATH, E. J., 1981, *Molec. Phys.*, **43**, 641.

[12] JOHNSTON, D. R., OUDEMANS, G. J., and COLE, R. H., 1960, *J. chem. Phys.*, **33**, 1310.

[13] ORCUTT, R. H. and COLE, R. H., 1967, *J. chem. Phys.*, **46**, 697.

[14] BUCKINGHAM, A. D., BOGAARD, M. P., DUNMUR, D. A., HOBBS, C. P., and ORR, B. J., 1970, *Trans. Faraday Soc.*, **66**, 1548.

[15] GENTLE, I. R., LAVER, D. R., and RITCHIE, G. L. D., 1989, *J. phys. Chem.*, **93**, 3035.

[16] DAYAN, E., DUNMUR, D. A., and MANTERFIELD, M. R., 1980, *J. chem. Soc. Faraday Trans. II*, **76**, 309.

[17] BAAS, F. and VAN DEN HOUT, K. D., 1979, *Physica A*, **95**, 597.

[18] HOHM, U., 1993, *Molec. Phys.*, **78**, 929.

[19] St-Arnaud, J. M., Okambawa, R., Bose, T. K., and Ingrain, D., 1995, *Int. J. Thermophys.*, **16**, 177.

[20] Kang, T. L., Hirth, L. J., Kobe, K. A., and McKetta, J. J., 1961, *J. chem. Eng. Data*, **6**, 220.

[21] Gentle, I. R., Laver, D. R., and Ritchie, G. L. D., 1990, *J. phys. Chem.*, **94**, 3434.

[22] Haworth, W. S. and Sutton, L. E., 1971, *Trans. Faraday Soc.*, **67**, 2907.

[23] Bogaard, M. P., Buckingham, A. D., and Ritchie, G. L. D., 1981, *J. chem. Soc. Faraday Trans. II*, **77**, 1547.

[24] Bose, T. K. and Cole, R. H., 1971, *J. chem. Phys.*, **54**, 3829.

[25] Tammer, R. and Hüttner, W., 1994, *Molec. Phys.*, **83**, 579.

[26] Buckingham, A. D., 1967, *Adv. chem. Phys.*, **12**, 107.

[27] Buckingham, A. D. and Pople, J. A., 1956, *Disc. Faraday Soc.*, **22**, 17.

[28] Buckingham, A. D. and Pople, J. A., 1955, *Trans. Faraday Soc.*, **51**, 1029.

[29] Lorentz, J. A., 1880, *Wiedem. Ann.*, **9**, 641.

[30] Lorenz, L., 1880, *Wiedem. Ann.*, **11**, 70.

[31] Buckingham, A. D., 1956, *Trans. Faraday Soc.*, **52**, 747.

[32] Kerr, J., 1875, *Phil. Mag.*, **50**, 337, 446.

[33] Buckingham, A. D. and Orr, B. J., 1969, *Trans. Faraday Soc.*, **65**, 673.

[34] Buckingham, A. D. and Pople, J. A., 1955, *Proc. phys. Soc. A*, **68**, 905.

[35] Buckingham, A. D. and Stephen, M. J., 1957, *Trans. Faraday Soc.*, **53**, 884.

[36] Couling, V. W. and Graham, C., 1996, *Molec. Phys.*, **87**, 779.

[37] Bose, T. K., Sochanksi, J. S., and Cole, R. H., 1972, *J. chem. Phys.*, **57**, 3592.

[38] Huot, J. and Bose, T. K., 1991, *J. chem. Phys.*, **95**, 2683.

[39] Buckingham, A. D. and Graham, C., 1974, *Proc. R. Soc. Lond. A*, **336**, 275.

[40] Bose, T. K. and Cole, R. H., 1970, *J. chem. Phys.*, **52**, 140.

[41] Orcutt, R. H. and Cole, R. H., 1965, *Physica*, **31**, 1779.

[42] Hosticka, C. and Bose, T. K., 1974, *J. chem. Phys.*, **60**, 1318.

[43] Nelson, R. D. and Cole, R. H., 1971, *J. chem. Phys.*, **54**, 4033.

[44] BURNS, R. C., 1978, Ph.D. thesis, University of Natal.

[45] JOHNSTON, D. R. and COLE, R. H., 1962, *J. chem. Phys.*, **36**, 318.

[46] BIRNBAUM, G. and MARYOTT, A. A., 1962, *J. chem. Phys.*, **36**, 2032.

[47] DAVID, H. G., HAMANN, S. D., and PEARSE, J. F., 1951, *J. chem. Phys.*, **19**, 1491.

[48] MICHELS and KLEEREKOPER, 1939, *Physica*, **6**, 586.

[49] BUCKINGHAM, A. D., COLE, R. H., and SUTTER, H., 1970, *J. chem. Phys.*, **52**, 5960.

[50] TURNER, D. J., 1966, D. Phil. thesis, Oxford.

[51] BARNES, A. N. M. and SUTTON, L. E., 1971, *Trans. Faraday Soc.*, **67**, 2915.

[52] HAMANN, S. D., 1970, *J. chem. Phys.*, **53**, 474.

[53] BUCKINGHAM, A. D. and RAAB, R. E., 1961, *J. chem. Soc.*, 5511.

[54] LAWLEY, K. P., 1962, D. Phil. thesis, Oxford.

[55] DATTA, K. K., SEAL, P., and BARUA, A. K., 1975, *J. chem. Phys.*, **62**, 227.

[56] DYMOND, J. H. and SMITH, E. B., 1964, *Trans. Faraday Soc.*, **60**, 1378.

[57] FOGG, P. G. T., HANKS, P. A., and LAMBERT, J. D., 1953, *Proc. R. Soc. Lond. A*, **219**, 490.

[58] OLSON, J. D., 1975, *J. chem. Phys.*, **63**, 474.

[59] HOHM, U., 1994, *Molec. Phys.*, **81**, 157.

[60] COULON, R., MONTIXI, G., and OCCELLI, R., 1981, *Can. J. Phys.*, **59**, 1555.

[61] MONTIXI, G. and COULON, R., 1983, *C. R. Acad. Sci.*, **296**, 135.

[62] BURNS, R. C., GRAHAM, C., and WELLER, A. R. M., 1986, *Molec. Phys.*, **59**, 41.

[63] ST-ARNAUD, J. M. and BOSE, T. K., 1976, *J. chem. Phys.*, **65**, 4854.

[64] ACHTERMANN, H. J., MAGNUS, G., and BOSE, T. K., 1991, *J. chem. Phys.*, **94**, 5669.

[65] ACHTERMANN, H. J., BOSE, T. K., JAESCHKE, M., and ST-ARNAUD, J. M., 1986, *Int. J. Thermophys.*, **7**, 357.

[66] ACHTERMANN, H. J., HONG, J. G., MAGNUS, G., AZIZ, R. A., and SLAMAN, M. J., 1993, *J. chem. Phys.*, **98**, 2308.

[67] BLYTHE, A. R., LAMBERT, J. D., PETTER, P. J., and SPOEL, H., 1960, *Proc. R. Soc. Lond. A*, **225**, 427.

[68] ST-ARNAUD, J. M. and BOSE, T. K., 1979, *J. chem. Phys.*, **71**, 4951.

[69] MONTIXI, G., COULON, R., and OCCELLI, R., 1983, *Can. J. Phys.*, **61**, 473.

[70] TIMOSHENKO, N. I., KOBELEV, V. P., and KHOLODOV, E. P., 1970, *Thermal Eng.*, **17**, 96.

[71] KHOLODOV, E. P., TIMOSHENKO, N. I., and YAMINOV, A. L., 1972, *Thermal Eng.*, **19**, 126.

[72] JAESCHKE, M., 1986, *Gas Quality*, edited by G. J. van Rossium, (Amsterdam: Elsevier).

[73] PHILLIPS, D., 1920, *Proc. R. Soc. Lond. A*, **97**, 225.

[74] BOSE, T. K., BOUDJARANE, K., HUOT, J., and ST-ARNAUD, J. M., 1988, *J. chem. Phys.*, **89**, 7435.

[75] ST-ARNAUD, J. M. and BOSE, T. K., 1978, *J. chem. Phys.*, **68**, 2129.

[76] MICHELS, A. and HAMERS, J., 1937, *Physica*, **4**, 995.

[77] ACHTERMANN, H. J. and BAEHR, H. D., 1988, *VDI Forschungsh.*, 649.

[78] ACHTERMANN, H. J., BAEHR, H. D., and BOSE, T. K., 1989, *J. chem. Therm.*, **21**, 1023.

[79] ACHTERMANN, H. J., BOSE, T. K., and MAGNUS, G., 1990, *Int. J. Thermophys.*, **11**, 133.

[80] SLIWINSKI, P., 1969, *Z. phys. Chem.*, **63**, 263.

[81] DUNMUR, D. A., HUNT, D. C., and JESSUP, N. E., 1979, *Molec. Phys.*, **37**, 713.

[82] BUCKINGHAM, A. D. and DUNMUR, D. A., 1968, *Trans. Faraday Soc.*, **64**, 1776.

[83] SCHAEFER, D. W., SEARS, R. E. J., and WAUGH, J. S., 1970, *J. chem. Phys.*, **53**, 2127.

[84] TAMMER, R., LÖBLEIN, K., PETING, K. H., and HÜTTNER, W., 1992, *Chem. Phys.*, **168**, 151.

[85] BÖTTCHER, C. J. F. and BORDEWIJK, P., 1978, *Theory of Electric Polarization*, vol. II, (Amsterdam: Elsevier).

[86] MÜLLER, H., KÖDER, H., and HÜTTNER, W., 1986, *Chem. Phys. Letters*, **125**, 473.

[87] VUKS, M. F., 1966, *Opt. Spect.*, **21**, 383.

[88] DUNMUR, D. A., MANTERFIELD, M. R., and ROBINSON, D. J., 1983, *Molec. Phys.*, **50**, 573.

[89] WATSON, R. C. and ROWELL, R. L., 1974, *J. chem. Phys.*, **61**, 2666.

[90] THIBEAU, M. and OKSENGORN, B., 1972, *J. Phys. (Paris)*, **33**, C1.

[91] BERRUE, J., CHAVE, A., DUMON, B., and THIBEAU, M., 1978, *J. Phys. (Paris)*, **39**, 815.

[92] BERRUE, J., CHAVE, A., DUMON, B., and THIBEAU, M., 1977, *Rev. Phys. Appl.*, **12**, 1743.

[93] BUCKINGHAM, A. D. and UTTING, B. D., 1970, *Annu. Rev. Phys. Chem.*, **21**, 287.

[94] MASON, E. A. and SPURLING, T. H., 1969, *The Virial Equation of State*, (Oxford: Pergamon).

[95] MAITLAND, G. C., RIGBY, M., SMITH, E. B., and WAKEHAM, W. A., 1981, *Intermolecular Forces, their Origin and Determination*, (Oxford: Clarendon Press).

[96] BUCKINGHAM, A. D. and POPLE, J. A., 1955, *Trans. Faraday Soc.*, **51**, 1173.

[97] COPELAND, T. G. and COLE, R. H., 1976, *J. chem. Phys.*, **64**, 1741.

[98] BROOKMEYER, B., 1993, Master's thesis, Brown University.

[99] MARGENAU, H. and MURPHY, G. M., 1992, *The Mathematics of Physics and Chemistry*, (New York: Van Nostrand).

[100] VARSHALOVICH, D. A., MOSKALEV, A. N., and KHARSONSKII, V. K., 1988, *Quantum Theory of Angular Momentum*, (Teaneck: World Scientific).

[101] BUCKINGHAM, A. D. and POPLE, J. A., 1955, *Trans. Faraday Soc.*, **51**, 1179.

[102] MAROULIS, G., 1992, *J. chem. Phys.*, **97**, 4188.

[103] MAROULIS, G., 1993, *J. Phys. B: Atom. Molec. Phys.*, **26**, 775.

[104] MAROULIS, G., 1992, *J. Phys. B: Atom. Molec. Phys.*, **25**, L77.

[105] WELLER, A. R. M., 1985, Master's thesis, University of Natal (Pietermaritzburg).

[106] HIRSCHFELDER, J. O., CURTISS, C. F., and BIRD, R. B., 1954, *Molecular Theory of Gases and Liquids*, (Chichester: Wiley).

[107] GARRETT, A. J. M., 1980, *J. Phys. A: Maths. Gen.*, **13**, 379.

[108] HOLBORN, L. and OTTO, Z., 1925, *Z. Physik.*, **33**, 1.

[109] POOL, R. A. H., SAVILLE, G., HERRINGTON, T. M., SHIELDS, D. D. C., and STAVELEY, L. A. K., 1962, *Trans. Faraday Soc.*, **58**, 1692.

[110] COPELAND, T. G. and COLE, R. H., 1976, *J. chem. Phys.*, **64**, 1747.

[111] McGLASHAN, M. L. and POTTER, D. J. B., 1962, *Proc. R. Soc. Lond. A*, **267**, 478.

[112] ISNARD, P. and GALATRY, L., 1980, *Molec. Phys.*, **39**, 501.

[113] WHITMORE, M. D. and GOODINGS, D. A., 1980, *Can. J. Phys.*, **58**, 820.

[114] SPURLING, T. H. and MASON, E. A., 1967, *J. chem. Phys.*, **46**, 322.

[115] ISNARD, P., ROBERT, D., and GALATRY, L., 1980, *Molec. Phys.*, **41**, 281.

[116] HARRIS, F. E. and ALDER, B. J., 1953, *J. chem. Phys.*, **21**, 1351.

[117] HARRIS, F. E. and ALDER, B. J., 1953, *J. chem. Phys.*, **21**, 1031.

[118] HARRIS, F. E. and ALDER, B. J., 1954, *J. chem. Phys.*, **22**, 1806.

[119] ONSAGER, 1936, *J. Am. chem. Soc.*, **58**, 1486.

[120] STOCKMAYER, W. H., 1941, *J. chem. Phys.*, **9**, 398.

[121] KIRKWOOD, J. G., 1939, *J. chem. Phys.*, **7**, 911.

[122] GRAHAM, C., 1971, Ph.D. thesis, Corpus Christi College (Cambridge).

[123] BUCKINGHAM, A. D., 1956, *Trans. Faraday Soc.*, **52**, 1035.

[124] KIELICH, S., 1962, *Acta Phys. Polon.*, **22**, 477.

[125] BUCKINGHAM, A. D. and ORR, B. J., 1967, *Quart. Rev.*, **21**, 195.

[126] DE GROOT, S. R. and TEN SELDAM, C. A., 1946, *Physica*, **12**, 669.

[127] KIRKWOOD, J. G., 1936, *J. chem. Phys.*, **4**, 592.

[128] BUCKINGHAM, A. D., MARTIN, P. H., and WATTS, R. S., 1973, *Chem. Phys. Letters*, **21**, 186.

[129] BUCKINGHAM, A. D. and WATTS, R. S., 1973, *Molec. Phys.*, **26**, 7.

[130] O'BRIEN, E. F., GUTSCHICK, V. P., McKOY, C., and McTAGUE, J. P., 1973, *Phys. Rev. A*, **8**, 690.

[131] LOGAN, D. E. and MADDEN, P. A., 1982, *Molec. Phys.*, **46**, 1195.

[132] BURNETT, E. S., 1936, *J. Appl. Mechanics A.*, **58**, 136.

[133] KIROUAC, S. and BOSE, T. K., 1976, *J. chem. Phys.*, **64**, 1580.

[134] KOSCHINE, A. and LEHMANN, J. K., 1992, *Meas. Sci. Technol.*, **3**, 411.

[135] ST-ARNAUD, J. M., HOURRI, A., OKAMBAWA, R., and BELANGER, M., 1995, *Rev. sci. Instrum.*, **66**, 5311.

[136] SUTTER, H. G., 1972, Dielectric and related molecular properties, Specialist periodical report, *Chem. Soc.*, **1**, 65.

[137] LENNARD-JONES, J. E., 1924, *Proc. R. Soc. Lond. A*, **104**, 441.

[138] LOGAN, D. E. and MADDEN, P. A., 1982, *Molec. Phys.*, **46**, 715.

[139] BULANIN, M. O., HOHM, U., LADVISHCHENKO, Y. M., and KERL, K., 1994, *Z. Naturforsch.*, **49**, 890.

[140] HOHM, U., 1993, *Z. Naturforsch.*, **48a**, 505.

[141] BUCKINGHAM, A. D. and POPLE, J. A., 1957, *J. chem. Phys.*, **27**, 820.

[142] LAWLEY, K. P. and SMITH, E. B., 1963, *Trans. Faraday Soc.*, **59**, 301.

[143] SPURLING, T. H. and MASON, E. A., 1967, *J. chem. Phys.*, **46**, 404.

[144] DATTA, K. K. and BARURA, A. K., 1973, *J. Phys. B: Atom. Molec. Phys.*, **6**, 1327.

[145] CASPARIAN, A. S. and COLE, R. H., 1974, *J. chem. Phys.*, **60**, 1106.

[146] HOSTICKA, C., BOSE, T. K., and SOCHANSKI, J. S., 1974, *J. chem. Phys.*, **61**, 2575.

[147] KIELPINSKI, A. L. and MURAD, S., 1987, *Molec. Phys.*, **61**, 1563.

[148] JOSLIN, C. and GOLDMAN, S., 1993, *Molec. Phys.*, **79**, 1351.

[149] MICHELS, A., LEBESQUE, H., LEBESQUE, L., and DE GROOT, S. R., 1947, *Physica*, **13**, 337.

[150] EVERETT, D. H. and MUNN, R. J., 1963, *Trans. Faraday Soc.*, **59**, 2486.

[151] BEAUME, R. and COULON, R., 1967, *C. R. hebd. Séanc. Acad. Sci., Paris B*, **265**, 309.

[152] BUCKINGHAM, A. D., 1956, *Proc. phys. Soc. B*, **69**, 344.

[153] YVON, J., 1936, *C. R. hebd. Séanc. Acad. Sci., Paris B*, **202**, 35.

[154] SILBERSTEIN, L., 1917, *Phil. Mag.*, **33**, 92, 521.

[155] JANSEN, L. and MAZUR, P., 1955, *Physica*, **21**, 193.

[156] HEINRICHS, J., 1969, *Chem. Phys. Letters*, **4**, 151.

[157] CERTAIN, P. R. and FORTUNE, P. J., 1971, *J. chem. Phys.*, **55**, 5818.

[158] MICHELS, A., DE BOER, J., and BIJL, A., 1937, *Physica*, **4**, 981.

[159] TEN SELDAM, C. A. and DE GROOT, S. R., 1952, *Physica*, **18**, 905.

[160] LIM, T.-K., LINDER, B., and KROMHOUT, R. A., 1970, *J. chem. Phys.*, **52**, 3832.

[161] HOHM, U., 1991, *Molec. Phys.*, **74**, 1233.

[162] BROWN, W. F., 1950, *J. chem. Phys.*, **18**, 1193.

[163] LEVINE, H. B. and McQUARRIE, D. A., 1968, *J. chem. Phys.*, **49**, 4181.

[164] BUCKINGHAM, A. D. and CLARKE, K. L., 1980, *Molec. Phys.*, **40**, 643.

[165] BUCKINGHAM, A. D. and CLARKE, K. L., 1978, *Chem. Phys. Letters*, **57**, 321.

[166] DACRE, P. D., 1982, *Molec. Phys.*, **45**, 17.

[167] DACRE, P. D., 1972, *Molec. Phys.*, **36**, 541.

[168] DACRE, P. D., 1982, *Molec. Phys.*, **45**, 1.

[169] DACRE, P. D., 1982, *Molec. Phys.*, **47**, 193.

[170] AZIZ, R. A. and SLAMAN, M. J., 1989, *Chem. Phys.*, **130**, 187.

[171] AZIZ, R. A. and SLAMAN, M. J., 1990, *J. chem. Phys.*, **92**, 1030.

[172] AZIZ, R. A. and CHEN, H. H., 1977, *J. chem. Phys.*, **67**, 5719.

[173] MEINANDER, N., 1994, *Chem. Phys. Letters*, **228**, 295.

[174] BUCKINGHAM, A. D., 1955, *Proc. phys. Soc. A*, **68**, 910.

[175] ANDREWS, A. L. and BUCKINGHAM, A. D., 1960, *Molec. Phys.*, **3**, 183.

[176] OTTERBEIN, G., 1934, *Phys. Z.*, **35**, 249.

[177] BUCKINGHAM, A. D., GALWAS, P. A., and FAN-CHEN, L., 1983, *J. Mol. Struct.*, **100**, 3.

[178] GRAY, C. G. and RALPH, H. I., 1970, *Phys. Lett. A*, **33**, 165.

[179] BOGAARD, M. P., ORR, B. J., BUCKINGHAM, A. D., and RITCHIE, G. L. D., 1978, *J. chem. Soc. Faraday Trans. II*, **74**, 1573.

[180] BOGAARD, M. P., BUCKINGHAM, A. D., and RITCHIE, G. L. D., 1982, *Chem. Phys. Letters*, **90**, 183.

[181] TYNDALL, J., 1869, *Phil. Mag.*, **37**, 384.

[182] KERKER, M., 1969, *The Scattering of Light*, (New York: Academic).

[183] STRUTT, J. W., (Third Baron Rayleigh), 1871, *Phil. Mag.*, **44**, 28.

[184] STRUTT, J. W., (Third Baron Rayleigh), 1899, Scientific Papers IV, 397.

[185] CABANNES, J., 1916, *Comptes Rendus*, **160**, 62.

[186] STRUTT, R. J., (Fourth Baron Rayleigh), 1918, *Proc. R. Soc. Lond. A*, **94**, 453.

[187] STRUTT, R. J., (Fourth Baron Rayleigh), 1918, *Proc. R. Soc. Lond. A*, **97**, 435.

[188] POWERS, J., 1961, *J. chem. Phys.*, **35**, 376.

[189] BRIDGE, N. J. and BUCKINGHAM, A. D., 1964, *J. chem. Phys.*, **40**, 2733.

[190] BRIDGE, N. J. and BUCKINGHAM, A. D., 1966, *Proc. R. Soc. Lond. A*, **295**, 334.

[191] ROWELL, R. L., AVAL, G. M., and BARRETT, J. J., 1971, *J. chem. Phys.*, **54**, 1960.

[192] ALMS, G. R., BURNHAM, A. K., and FLYGARE, W. H., 1975, *J. chem. Phys.*, **63**, 3321.

[193] BURNHAM, A. K., BUXTON, L. W., and FLYGARE, W. H., 1977, *J. chem. Phys.*, **67**, 4990.

[194] LANDAU, L. D. and LIFSHITZ, E. M., 1962, *The Classical Theory of Fields*, (Oxford: Pergamon).

[195] BUCKINGHAM, A. D. and RAAB, R. E., 1975, *Proc. R. Soc. Lond. A*, **345**, 365.

[196] RAAB, R. E., 1975, *Molec. Phys.*, **29**, 1323.

[197] LOGAN, D. E., 1982, *Molec. Phys.*, **46**, 271.

[198] IMRIE, D. A. and RAAB, R. E., 1991, *Molec. Phys.*, **74**, 833.

[199] GRAHAM, C., PIERRUS, J., and RAAB, R. E., 1992, *J. Phys. B: Atom. Molec. Phys.*, **25**, 4673.

[200] GRAHAM, C., 1992, *Molec. Phys.*, **77**, 291.

[201] COULING, V. W. and GRAHAM, C., 1993, *Molec. Phys.*, **79**, 859.

[202] SPACKMAN, M. A., 1989, *J. phys. Chem.*, **93**, 7594.

[203] BENOÎT, H. and STOCKMAYER, W. H., 1956, *J. Phys. Radium*, **17**, 21.

[204] McTAGUE, J. P. and BIRNBAUM, G., 1968, *Phys. Rev. Lett.*, **21**, 661.

[205] GELBART, W. M., 1974, *Adv. chem. Phys.*, **26**, 1.

[206] LALLEMAND, P., 1971, *J. Phys. (Paris)*, **32**, 119.

[207] McTague, J. P., Elleson, W. D., and Hall, L. H., 1972, *J. Phys. (Paris)*, **33**, C1.

[208] Barocchi, F. and McTague, J. P., 1975, *Phys. Lett. A*, **53**, 488.

[209] Berrue, J., Chave, A., Dumon, B., and Thibeau, M., 1979, *Opt. Comm.*, **31**, 317.

[210] Dougherty, J. and Spackman, M. A., 1994, *Molec. Phys.*, **82**, 193.

[211] Amos, R. D., 1982, *Chem. Phys. Letters*, **87**, 23.

[212] Shelton, D. P. and Buckingham, A. D., 1982, *Phys. Rev. A*, **26**, 2787.

[213] Vanderhart, D. L. and Flygare, W. H., 1970, *Molec. Phys.*, **18**, 77.

[214] Rivail, J. L. and Cartier, A., 1978, *Molec. Phys.*, **36**, 1085.

[215] De Leeuw, F. and Dynamus, A., 1973, *J. Mol. Spect.*, **48**, 427.

[216] Williams, J. H. and Amos, R. D., 1980, *Chem. Phys. Letters*, **70**, 162.

[217] Graham, C., Pierrus, J., and Raab, R. E., 1989, *Molec. Phys.*, **67**, 939.

[218] Battaglia, M. R., Buckingham, A. D., Neumark, D., Pierens, R. K., and Williams, J. H., 1981, *Molec. Phys.*, **43**, 1015.

[219] Buckingham, A. D., Graham, C., and Williams, J. H., 1983, *Molec. Phys.*, **49**, 703.

[220] Patel, D., Margolese, D., and Dyke, T. R., 1979, *J. chem. Phys.*, **70**, 2740.

[221] Ellenbroek, A. W. and Dymanus, A., 1976, *Chem. Phys. Letters*, **42**, 303.

[222] Murphy, W. F., 1981, *J. Raman Spect.*, **11**, 339.

[223] Bacskay, G. B., Rendell, A. P. L., and Hush, N. S., 1988, *J. chem. Phys.*, **89**, 5721.

[224] Blukis, U., Kasai, P. H., and Myers, R. J., 1963, *J. chem. Phys.*, **38**, 2753.

[225] Benson, R. C. and Flygare, W. H., 1970, *J. chem. Phys.*, **52**, 5291.

[226] Spackman, M. A. and Ritchie, G. L. D., Private Communication.

[227] Gray, C. G., Gubbins, K. E., Dagg, I. R., and Read, L. A. A., 1980, *Chem. Phys. Letters*, **73**, 278.

[228] Dagg, I. R., Read, L. A. A., and Smith, W., 1982, *Can. J. Phys.*, **60**, 1431.

[229] Kukolich, S. G., Aldrich, P. D., Read, W. G., and Campbell, E. J., 1983, *J. chem. Phys.*, **79**, 1105.

236

[230] HILLS, G. W. and JONES, W. J., 1975, *J. chem. Soc. Faraday Trans. II*, **71**, 812.

[231] BARBÈS, H., 1987, *J. Raman Spect.*, **18**, 507.

[232] GUPTA, A. D., SINGH, Y., and SINGH, S., 1973, *J. chem. Phys.*, **59**, 1999.

[233] ANGUS, S., ARMSTRONG, B., and DE REUCK, K. M., 1976, *International Thermodynamic Tables of the Fluid State of Carbon Dioxide*, (Oxford: Pergamon).

[234] BUCKINGHAM, A. D., 1959, *J. Q. Chem. Rev. Soc.*, **13**, 183.

Appendix A

Second Pressure Virial Coefficient Tables

Second pressure virial coefficients have been measured by many researchers for many gases and their mixtures. Tables A.1,A.2 and A.3 show the data used to fit the calculated and observed second virial coefficients of the gases considered in this study. Where available Dymond and Smith's [1] smoothed values have been used. For CO_2, no smoothed data is available,but the data of Angus et $al.$ [233] are recommended by Dymond and Smith [1]. No smoothed data is presented for CHF_3, so a curve was fitted to the combined data of Sutter and Cole [5], and Lange and Stein [6].

Table A.1: Temperature dependence of B(T) for spherical gases

Ar		Ne		Kr		Xe		CH$_4$		CF$_4$		SF$_6$	
T K	$10^6 B(T)$ m^{3}mol^{-1}	T K	$10^6 B(T)$ m^{3}mol^{-1}	T K	$10^6 B(T)$ m^{3}mol^{-1}	T K	$10^6 B(T)$ m^{3}mol^{-1}	T K	$10^6 B(T)$ m^{3}mol^{-1}	T K	$10^6 B(T)$ m^{3}mol^{-1}	T K	$10^6 B(T)$ m^{3}mol^{-1}
81	-276.0±5	60	-24.8±1	110	-364±10	160	-425±10	110	-330±10	225	-172.5±1	200	-685±15
85	-251.0±3	70	-17.9±1	115	-333±10	170	-378±10	120	-273±5	250	-137.5±1	210	-615±12
90	-225.0±3	80	-12.8±1	120	-306±5	180	-337±8	130	-235±5	275	-109.0±0.5	220	-555±12
95	-202.5±2	100	-6.0±1	130	-264±5	190	-306±8	140	-207±3	300	-87.0±0.5	240	-455±10
100	-183.5±1	125	-0.4±1	140	-229.5±5	200	-276±7	150	-182±3	325	-69.0±0.5	260	-380±8
110	-154.5±1	150	3.2±1	150	-200.7±2	210	-254±5	160	-161±3	350	-55.0±0.5	280	-323±7
125	-123.0±1	200	7.6±1	170	-159.0±2	225	-224±5	180	-129±2	400	-32.0±0.5	300	-277±5
150	-86.2±1	300	11.3±1	200	-116.9±1	250	-184±4	200	-105±2	450	-16.0±0.5	325	-226±5
200	-47.4±1	400	12.8±1	250	-75.7±1	275	-156±4	225	-83±2	500	-4.0±0.5	350	-190±5
250	-27.9±1	600	13.8±0.5	300	-50.5±1	300	-133±3	250	-66±1	600	14.0±0.5	375	-159±5
300	-15.5±0.5			400	-22.0±1	325	-109±2	275	-53±1	700	25.0±0.1	400	-135±4
400	-1.0±0.5			500	-8.1±0.5	350	-93.2±2	300	-42±1	800	33.0±0.1	425	-113±2
500	7.0±0.5			600	1.7±0.5	400	-69.4±2	350	-26±1			450	-97±2
600	12.0±0.5			700	8.2±0.5	450	-51.8±2	400	-15±1			475	-81±2
700	15.0±1					550	-28.0±2	500	-0.5±1			500	-67±2
800	17.7±1					650	-13.0±2	600	8.5±1			525	-56±2
900	20.0±1												
1000	22.0±1												

Table A.2: Temperature dependence of B(T) for non-polar gases

H$_2$		N$_2$		CO$_2$ [233]		C$_2$H$_6$		C$_2$H$_4$	
T	$10^6 B(T)$	T	$10^6 B(T)$	T	$10^6 B(T)$	T	$10^6 B(T)$	T	$10^6 B(T)$
K	m^{3}mol^{-1}	K	m^{3}mol^{-1}	K	m^{3}mol^{-1}	K	m^{3}mol^{-1}	K	m^{3}mol^{-1}
14	-274±5	75	-275±8	270	-155.4±2	200	-410±10	240	-218.5±2
15	-230±5	80	-243±7	273.15	-151.4±2	210	-370±5	250	-201±2
17	-191±5	90	-197±5	280	-143.3±2	220	-336±5	275	-166±1
19	-162±5	100	-160±3	290	-132.5±2	240	-282±3	300	-138±1
22	-132±5	110	-132±2	298.15	-124.5±2	260	-243±2	325	-117±1
25	-110±3	125	-104±2	300	-122.7±2	280	-211±2	350	-99±1
30	-82±3	150	-71.5±2	310	-113.9±2	300	-182±2	375	-84±1
40	-52±2	200	-35.2±1	320	-105.8±2	325	-154±1	400	-71.5±1
50	-33±2	250	-16.2±1	330	-98.5±2	350	-130.5±1	450	-51.7±1
75	-12±1	300	-4.2±0.5	340	-91.7±2	375	-111.0±1		
100	-1.9±1	400	9.0±0.5	350	-85.5±2	400	-96.0±1		
150	7.1±0.5	500	16.9±0.5	360	-79.7±2	450	-71.0±1		
200	11.3±0.5	600	21.3±0.5	370	-74.4±2	500	-52.0±0.5		
300	14.8±0.5	700	24.0±0.5	380	-69.5±2	550	-36.5±0.5		
400	15.2±0.5			390	-64.8±2	600	-24.5±0.5		
				400	-60.5±2				
				410	-56.5±2				
				420	-52.8±2				
				430	-49.3±2				

Table A.3: Temperature dependence of B(T) for polar gases

CH$_3$F		CHF$_3$		CH$_3$Cl		CHCl$_3$		HCl	
T	$10^6 B(T)$	T	$10^6 B(T)$	T	$10^6 B(T)$	T	$10^6 B(T)$	T	$10^6 B(T)$
K	m^{3}mol^{-1}	K	m^{3}mol^{-1}	K	m^{3}mol^{-1}	K	m^{3}mol^{-1}	K	m^{3}mol^{-1}
280	-244±3	243.15	-311.1±4	280	-470±10	320	-1000±50	190	-456.0±7
298.1	-209±3	273.15	-234.9±4	300	-400±10	340	-860±30	200	-392.0±7
300	-206±3	298.15	-188.0±4	320	-345±10	360	-740±30	225	-287.0±7
320	-174±3	313.15	-165.8±4	340	-300±5	380	-640±30	250	-221.0±7
323.1	-170±3	323.15	-153.0±4	360	-264±5	400	-560±30	275	-175.0±7
340	-150±3	368.15	-110.4±4	400	-212±5			295	-147.1±6
360	-129±3	369.45	-109.4±4	450	-155±5			300	-142.0±6
369.5	-121±3	404.75	-84.6±3	500	-111±3			330	-114.0±6
380	-112±3			550	-80±2			370	-90.0±6
400	-99±2			600	-57±2			400	-76.0±5
416.5	-89±2							420	-68.5±5
420	-87±2							450	-59.0±5
								480	-53.0±5

Appendix B

Electric Multipole Moments

A static distribution of electric charges q_i at positions $\mathbf{r}_i$ relative to an arbitrarily chosen origin O within the arrangement of charges, produces an electrical potential φ at all points in space. Buckingham [234] showed that if we consider any point P, with a displacement $\mathbf{R}$ from the origin, where $R \gg r_i$, then the electric potential is given by the multipole expansion:

$$\varphi = \frac{1}{4\pi\varepsilon} \left[\frac{1}{R} \sum_i q_i + \frac{R_\alpha}{R^3} \sum_i q_i r_{i\alpha} + \frac{(3R_\alpha R_\beta - R^2 \delta_{\alpha\beta})}{2R^5} \sum_i q_i r_{i\alpha} r_{i\beta} + \cdots \right], \qquad \text{(B.1)}$$

where the Greek subscripts denote Cartesian tensor components x, y or z, with a repeated subscript implying summation over these components, and $\delta_{\alpha\beta}$ is the Kronecker delta.

The summations in (B.1) are the electric multipole moments of the charge distribution, with the electric monopole, or the total charge of the distribution given by:

$$q = \sum_i q_i; \qquad \text{(B.2)}$$

the electric dipole moment given by:

$$\mu_\alpha = \sum_i q_i r_{i\alpha}; \qquad \text{(B.3)}$$

and the *primitive* electric quadrupole moment given by:

$$\theta_{\alpha\beta} = \sum_i q_i r_{i\alpha} r_{i\beta}. \qquad \text{(B.4)}$$

As for other multipole moments of higher order than the dipole moment, an alternative definition of the electric quadrupole moment has been adopted, called the *traceless*

quadrupole moment:

$$\theta_{\alpha\beta} = \tfrac{1}{2} \sum_i q_i \left(3 r_{i\alpha} r_{i\beta} - r_i^2 \delta_{\alpha\beta}\right), \tag{B.5}$$

which is often used by molecular physicists because it vanishes for a spherically-symmetric electric charge distribution, and therefore has intuitive appeal. However, Raab [196] has cautioned against using the traceless quadrupole moment indiscriminately, since there exist electrodynamic situations where it is necessary to retain the primitive definitions of multipole moments. The matter is controversial and we follow all earlier workers in the field by using the traceless quadrupole throughout.

Appendix C

Fortran programs

C.1 Example of a program to optimize $B(T)$ and B_ε for a linear non-polar molecule

```
      PROGRAM CO2OPT
C
C     PROGRAM TO CALCULATE B(E) AND B(T) FOR CO2 USING
C     GAUSSIAN INTEGRATION WITH 64 INTERVALS FOR RANGE AND 16
C     INTERVALS FOR ANGULAR VARIABLES, AND USING DOUBLE PRECISION.
C     DATE 01-08-95  VERSION CALCULATES BE FOR 8 TEMPERATURES AND
C     VARIOUS VALUES OF SHAPE, R(0) AND E/K, AND B(T) FOR 13 TEMPS.
C
      IMPLICIT DOUBLE PRECISION (A-H,O-Z)
      DIMENSION COEF2(128),COEF1(16),SEP(128),THETA1(16),
     + THETA2(16),PHI(16),C(3),CR(4),BETEMP(8),ABE(8),BE(8,1200),
     + BEEXP(8),BEEXPERR(8),BESSE(1200),BTTEMP(19),ABT(19),BT(19,1200),
     + BTEXP(19),BTEXPERR(19),BTSSE(1200),D(1200),R0(1200),EK(1200),
     + ULJ(128,16,16,16),USHAPE(128,16,16,16),UELEC(128,16,16,16)
C------------------------------------------
C     MOLECULAR DATA FOR CO2
C------------------------------------------
      ALPHA=3.24500
      ALFOP=2.90700
      AMU=0.00000
      THETA=-15.000
      BETA=0.0000
      BPERP=0.00000
      BPARA=0.00000
      APERP=0.000
      APARA=0.00
      CZZ=0.00000
      CXX=0.00000
      CXZ=0.00000
```

```
CAP=0.26000
AMIN1=0.10
AMAX1=3.0
AMIN=0.0
AMAX=3.14159265359

BTTEMP(1)=262.650
BTTEMP(2)=273.150
BTTEMP(3)=283.150
BTTEMP(4)=299.650
BTTEMP(5)=309.650
BTTEMP(6)=323.150
BTTEMP(7)=333.150
BTTEMP(8)=343.150
BTTEMP(9)=353.150
BTTEMP(10)=363.150
BTTEMP(11)=373.150
BTTEMP(12)=423.150
BTTEMP(13)=473.150

BTEXP(1)=-159.900
BTEXP(2)=-147.400
BTEXP(3)=-136.700
BTEXP(4)=-120.500
BTEXP(5)=-111.300
BTEXP(6)=-100.700
BTEXP(7)=-93.9000
BTEXP(8)=-87.1000
BTEXP(9)=-80.9000
BTEXP(10)=-75.3000
BTEXP(11)=-69.5000
BTEXP(12)=-46.3000
BTEXP(13)=-29.1000

BTEXPERR(1)=4.00
BTEXPERR(2)=4.00
BTEXPERR(3)=4.00
BTEXPERR(4)=3.00
BTEXPERR(5)=3.00
BTEXPERR(6)=3.00
BTEXPERR(7)=3.00
BTEXPERR(8)=3.00
BTEXPERR(9)=3.00
BTEXPERR(10)=2.00
BTEXPERR(11)=2.00
BTEXPERR(12)=2.00
BTEXPERR(13)=2.00

BETEMP(2)=295.15
```

```
          BETEMP(3)=302.55
          BETEMP(4)=322.85
          BETEMP(5)=348.15
          BETEMP(6)=369.45
          BETEMP(7)=373.15
          BETEMP(8)=423.15

          BEEXP(2)=64.0000
          BEEXP(3)=57.6000
          BEEXP(4)=47.2667
          BEEXP(5)=46.4000
          BEEXP(6)=36.0000
          BEEXP(7)=34.7000
          BEEXP(8)=30.0000

          BEEXPERR(2)=10.0000
          BEEXPERR(3)=6.00000
          BEEXPERR(4)=8.26667
          BEEXPERR(5)=5.00000
          BEEXPERR(6)=4.00000
          BEEXPERR(7)=3.50000
          BEEXPERR(8)=3.00000

          NLOW=1
          NSEP=128
          NANGLE=16

          CALL GAUSSPT(NLOW,NSEP,NSEP,AMIN1,AMAX1,SEP,COEF2)
          CALL GAUSSPT(NLOW,NANGLE,NANGLE,AMIN,AMAX,THETA1,COEF1)

          DO 180 N=1,NANGLE
           THETA2(N)=THETA1(N)
           PHI(N)=THETA1(N)
180       CONTINUE

          DO 7040 INDX4=1,NANGLE
             DO 7050 INDX3=1,NANGLE
                DO 7060 INDX2=1,NANGLE
                   DO 7070 INDX1=1,NSEP
C--------------------------------------------------------
C     CALCULATE QUADRUPOLE-QUADRUPOLE POTENTIAL
C--------------------------------------------------------
                E1=8.98758E-26*0.75*THETA**2*(1.-5.*(COS(THETA1(
     +          INDX2)))**2-5.*(COS(THETA2(INDX4)))**2+17.*(COS(
     +          THETA1(INDX2)))**2*(COS(THETA2(INDX4)))**2+2.*
     +          (SIN(THETA1(INDX2)))**2*(SIN(THETA2(INDX4)))**
     +          2*(COS(PHI(INDX3)))**2+16.*SIN(THETA1(INDX2))*
     +          COS(THETA1(INDX2))*SIN(THETA2(INDX4))*COS(THETA
     +          2(INDX4))*COS(PHI(INDX3)))/(SEP(INDX1)**5)
```

246

```
C------------------------------------------------------
C     CALCULATE QUADRUPOLE-INDUCED DIPOLE POTENTIAL
C------------------------------------------------------
              F1=8.07765E-29*(-9./8.)*ALPHA*THETA**2*(4.*COS
     +        (THETA1(INDX2))**4+4.*COS(THETA2(INDX4))**4+
     +        SIN(THETA1(INDX2))**4+SIN(THETA2(INDX4))**4)
     +        /(SEP(INDX1)**8)

              UELEC(INDX1,INDX2,INDX3,INDX4)=E1+F1

7070            CONTINUE
7060          CONTINUE
7050       CONTINUE
7040     CONTINUE


      N=0

      DO 200 ID=180,230
         SHAPE=ID*0.001
      DO 210 IR=390,410,5
         R=IR*0.001
      DO 220 IE=1860,1960,10
         PARAM2=IE*0.1+0.0

      M=0
      BTSSERR=0.00
      DO 6230 ITEMPK=1,11
        TEMPK=BTTEMP(ITEMPK)

      S1=0.000000
      S2=0.000000
      S3=0.000000
      S4=0.000000
C-------------------------------------
C     CALCULATION OF INTEGRAL
C-------------------------------------
      DO 6040 INDX4=1,NANGLE
         S3=0
         DO 6050 INDX3=1,NANGLE
            S2=0
            DO 6060 INDX2=1,NANGLE
               S1=0
               DO 6070 INDX1=1,NSEP
C------------------------------------
C     DETERMINE BT
C------------------------------------
     FI=(6.022E23/4.)*((SEP(INDX1))**2*SIN(THETA1(INDX2))*SIN(
     +  THETA2(INDX4)))
```

247

```
C-------------------------------------
C      CALCULATE LENNARD-JONES POTENTIAL
C-------------------------------------
          ULJ(INDX1,INDX2,INDX3,INDX4)=4.*PARAM2*1.380622E-23*
     +          ((R/SEP(INDX1))**12-(R/SEP(INDX1))**6)
C-------------------------------------
C      CALCULATE SHAPE POTENTIAL
C-------------------------------------
          USHAPE(INDX1,INDX2,INDX3,INDX4)=4.*SHAPE*PARAM2*
     +          1.380622E-23*(R/SEP(INDX1))**12*(3.*
     +          COS(THETA1(INDX2))**2+3.*COS(THETA2(INDX4))**2-2.)
C-------------------------------------
C      SUM ENERGY TERMS AND DIVIDE BY (-KT)
C-------------------------------------
               UTOT=ULJ(INDX1,INDX2,INDX3,INDX4)
     +             +USHAPE(INDX1,INDX2,INDX3,INDX4)
     +             +UELEC(INDX1,INDX2,INDX3,INDX4)
               G3=-1.*UTOT/(TEMPK*1.380622E-23)
               IF(G3.LT.-85) GO TO 6000
               G4=2.71828**G3
               GO TO 6010
6000           G4=0
6010           PROD=FI*(1.-G4)
               S1=S1+PROD*COEF2(INDX1)
6070              CONTINUE
            S2=S2+S1*COEF1(INDX2)*1.0E-09
6060           CONTINUE
         S3=S3+S2*COEF1(INDX3)
6050        CONTINUE
     S4=S4+S3*COEF1(INDX4)
6040    CONTINUE
     ABT(ITEMPK)=S4*2.E-12

     ERR=ABT(ITEMPK)-1.*BTEXP(ITEMPK)
     BTSSERR = BTSSERR + ERR**2

6230    CONTINUE

     IF (N .EQ. 1) THEN
       IF (BTSSERR .LT. BTSSE(1) ) THEN
         M=1
       ELSE
         M=2
       ENDIF
     ENDIF

     IF (N .GT. 1) THEN
       DO 400 IC=1,N
           IF(BTSSERR .LT. BTSSE(IC) ) THEN
```

248

```
              M=IC
              GOTO 410
           ENDIF
400     CONTINUE
        M=N+1
410     ENDIF

        BESSERR=0.0D0
        DO 4000 ITEMPK=2,8
          TEMPK=BETEMP(ITEMPK)

         S1=0.000000
         S2=0.000000
         S3=0.000000
         S4=0.000000
C-------------------------------
C     CALCULATION OF INTEGRAL
C-------------------------------
        DO 40 INDX4=1,NANGLE
           S3=0
           DO 50 INDX3=1,NANGLE
              S2=0
              DO 60 INDX2=1,NANGLE
                 S1=0
                 DO 70 INDX1=1,NSEP


C-----------------------------------
C     DETERMINE BE
C-----------------------------------
        ST1=SIN(THETA1(INDX2))
        ST2=SIN(THETA2(INDX4))
        CT1=COS(THETA1(INDX2))
        CT2=COS(THETA2(INDX4))
        CT12=-1.*COS(THETA1(INDX2))*COS(THETA2(INDX4))+SIN(THETA1(
     +     INDX2))*SIN(THETA2(INDX4))*COS(PHI(INDX3))
C-----------------------------------------------
C     DETERMINE DELTA EPSILON THETA 2 ALPHA 2
C-----------------------------------------------
        T2A2A = CT1**2*(CAP*(1350*CT2**4-540*CT2**2+54)+CAP**2*(675*CT2**4
     1    -270*CT2**2+27))+CAP**2*(45*CT2**4-18*CT2**2+9)+45*CT2**4+CAP*(
     2    -90*CT2**4+36*CT2**2-18)+CT1*CT12*(CAP*(1080*CT2**3-216*CT2)+CA
     3    P**2*(540*CT2**3-108*CT2))+CT12**2*(108*CAP**2*CT2**2+216*CAP*C
     4    T2**2)-18*CT2**2+9

        T2A2B=-(((675*CAP-675*CAP**2)*CT1**2+135*CAP**2-135*CAP)*CT2**4+((
     1    135*CAP**2+270*CAP)*CT1-2025*CAP**2*CT1**3)*CT12*CT2**3+((162*C
     2    AP**2-1620*CAP**2*CT1**2)*CT12**2+(675*CAP-675*CAP**2)*CT1**4+(
     3    855*CAP**2-900*CAP+45)*CT1**2-108*CAP**2+135*CAP-27)*CT2**2+(((
     4    135*CAP**2+270*CAP)*CT1**3+(207*CAP**2-252*CAP-36)*CT1)*CT12-32
```

249

```
5    4*CAP**2*CT1*CT12**3)*CT2+162*CAP**2*CT1**2*CT12**2+(135*CAP**2
6    -135*CAP)*CT1**4+(-108*CAP**2+135*CAP-27)*CT1**2+9*CAP**2-18*CA
7    P+9)

     C(1) = ALPHA**2*THETA**2/9.*(T2A2A+T2A2B)/SEP(INDX1)**6*ST1*ST2
     +       *0.24813987787284198000E-27/(3.0*TEMPK*1.380622E-23)
C------------------------------------------------
C    DETERMINE DELTA EPSILON THETA 2 ALPHA 3
C------------------------------------------------
     T2A3A = ((-54675*CAP**3-109350*CAP**2)*CT1**4+(6075*CAP**3+31590*C
1    AP**2-4860*CAP)*CT1**2+972*CAP**3-1944*CAP**2+972*CAP)*CT2**4+(
2    (-61965*CAP**3-123930*CAP**2)*CT1**3+(6075*CAP**3+19926*CAP**2-
3    1944*CAP)*CT1)*CT12*CT2**3+(((-23328*CAP**3-46656*CAP**2)*CT1**
4    2+1458*CAP**3+2916*CAP**2)*CT12**2+(15795*CAP**3+26730*CAP**2-9
5    720*CAP)*CT1**4+(-405*CAP**3-9720*CAP**2+5346*CAP-1782)*CT1**2-
6    486*CAP**3+1458*CAP**2-1458*CAP+486)*CT2**2+((-2916*CAP**3-5832
7    *CAP**2)*CT1*CT12**3+((9963*CAP**3+17982*CAP**2-3888*CAP)*CT1**
8    3+(-405*CAP**3-2430*CAP**2+972*CAP-324)*CT1)*CT12)*CT2+(1458*CA
9    P**3+2916*CAP**2)*CT1**2*CT12**2+(-972*CAP**3-972*CAP**2+1944*C
:    AP)*CT1**4+(-486*CAP**3+1458*CAP**2-1458*CAP+486)*CT1**2+162*CA
;    P**3-486*CAP**2+486*CAP-162

     T2A3B = CT1**2*(CAP**2*(54675*CT2**6-81405*CT2**4+27459*CT2**2-267
1    3)+CAP**3*(-54675*CT2**6+71685*CT2**4-20655*CT2**2+1701)+CAP*(9
2    720*CT2**4-6804*CT2**2+972))+CAP**3*(4860*CT2**6-4698*CT2**4+12
3    96*CT2**2-162)+CAP*(4860*CT2**6-8262*CT2**4+3888*CT2**2-486)+CA
4    P**2*(-9720*CT2**6+11178*CT2**4-3888*CT2**2+486)+CT12*(CT1*(CAP
5    **2*(25515*CT2**5-37422*CT2**3+7047*CT2)+CAP**3*(-25515*CT2**5+
6    38394*CT2**3-6075*CT2)+CAP*(-972*CT2**3-972*CT2))+CT1**3*(CAP**
7    3*(-164025*CT2**5+21870*CT2**3+2187*CT2)+CAP**2*(43740*CT2**3-8
8    748*CT2)))+CT1**4*(CAP**2*(54675*CT2**4-21870*CT2**2+2187)+CAP*
9    *3*(-54675*CT2**4+21870*CT2**2-2187))+CT12**2*(CAP**2*(1458*CT2
:    **4-3402*CT2**2)+CAP**3*(5346*CT2**2-1458*CT2**4)+CT1**2*(CAP**
;    3*(-185895*CT2**4+39366*CT2**2-2187)+8748*CAP**2*CT2**2)-1944*C
<    AP*CT2**2)+1782*CT2**4+CAP**3*CT1*CT12**3*(8748*CT2-69984*CT2**
=    3)-8748*CAP**3*CT12**4*CT2**2-1296*CT2**2+162

     C(2) = ALPHA**3*THETA**2/9.*(T2A3A+T2A3B)/SEP(INDX1)**9*ST1*ST2
     +       *0.22301700027584438200E-30/(3.0*TEMPK*1.380622E-23)
C------------------------------------------------
C    DETERMINE DELTA EPSILON THETA 2 ALPHA 4
C------------------------------------------------
     T2A4A1= ((492075*CAP**4+984150*CAP**3)*CT1**4+(131220*CAP**2-131
1    220*CAP**3)*CT1**2-3888*CAP**4+11664*CAP**3-11664*CAP**2+3888
2    *CAP)*CT2**6+((721710*CAP**4+1443420*CAP**3)*CT1**3+(96228*CA
3    P**2-96228*CAP**3)*CT1)*CT12*CT2**5+(((395847*CAP**4+791694*C
4    AP**3)*CT1**2-17496*CAP**3+17496*CAP**2)*CT12**2+(-251505*CAP
5    **4-448335*CAP**3+109350*CAP**2)*CT1**4+(-18225*CAP**4+59049*
6    CAP**3-91854*CAP**2+51030*CAP)*CT1**2+2592*CAP**4-10368*CAP**
```

```
7    3+15552*CAP**2-10368*CAP+2592)*CT2**4+((96228*CAP**4+192456*C
8    AP**3)*CT1*CT12**3+((-253692*CAP**4-463644*CAP**3+87480*CAP**
9    2)*CT1**3+(-14580*CAP**4+21870*CAP**3-34992*CAP**2+27702*CAP)
:    *CT1)*CT12)*CT2**3+((8748*CAP**4+17496*CAP**3)*CT12**4+((-831
;    06*CAP**4-157464*CAP**3+17496*CAP**2)*CT1**2-2916*CAP**4+2916
<    *CAP)*CT12**2+(41553*CAP**4+61236*CAP**3-43740*CAP**2)*CT1**4
=    +(7290*CAP**4-17496*CAP**3+34992*CAP**2-24786*CAP)*CT1**2-162
>    0*CAP**4+6480*CAP**3-9720*CAP**2+6480*CAP-1620)*CT2**2+((-874
?    8*CAP**4-17496*CAP**3)*CT1*CT12**3+((21870*CAP**4+34992*CAP**
@    3-17496*CAP**2)*CT1**3+(2916*CAP**4-4374*CAP**3+8748*CAP**2-7
1    290*CAP)*CT1)*CT12)*CT2+(2187*CAP**4+4374*CAP**3)*CT1**2*CT12
2    **2+(-2187*CAP**4-2187*CAP**3+4374*CAP**2)*CT1**4


     T2A4A2 = (-729*CAP**
3    4+2187*CAP**3-4374*CAP**2+2916*CAP)*CT1**2+324*CAP**4-1296*CA
4    P**3+1944*CAP**2-1296*CAP+324


     T2A4A = (T2A4A1+T2A4A2)
+       *ALPHA**4*THETA**2/9.*ST1*ST2*.20043766172607939427E-33
+       /SEP(INDX1)**12/(3.0*TEMPK*1.380622E-23)
C

     T2A4B1 = CAP**3*((-492075*CT1**4+207765*CT1**2-21870)*CT2**6+(76
1    545*CT1-360855*CT1**3)*CT12*CT2**5+((-54675*CT1**2-2187)*CT12
2    **2-492075*CT1**6+841995*CT1**4-262440*CT1**2+30618)*CT2**4+(
3    4374*CT1*CT12**3+(-426465*CT1**5+593406*CT1**3-76545*CT1)*CT1
4    2)*CT2**3+((-113724*CT1**4+137781*CT1**2+2187)*CT12**2+185895
5    *CT1**6-262440*CT1**4+82539*CT1**2-12636)*CT2**2+((13122*CT1-
6    8748*CT1**3)*CT12**3+(80919*CT1**5-98415*CT1**3+11826*CT1)*CT
7    12)*CT2+(4374*CT1**4-8748*CT1**2)*CT12**2-17496*CT1**6+21870*
8    CT1**4-8262*CT1**2+1296)+CAP**2*((10935-54675*CT1**2)*CT2**6-
9    21870*CT1*CT12*CT2**5+(-142155*CT1**4+136323*CT1**2-27702)*CT
:    2**4+(729*CT1**3+18225*CT1)*CT12*CT2**3+((43740*CT1**2-8748)*
;    CT12**2-43740*CT1**6+136323*CT1**4-85536*CT1**2+16767)*CT2**2
<    +(8748*CT1*CT12**3+(-17496*CT1**5+35721*CT1**3-13365*CT1)*CT1
=    2)*CT2+8748*CT1**6-18954*CT1**4+10206*CT1**2-1944)+CAP*((8262
>    -34020*CT1**2)*CT2**4-9234*CT1*CT12*CT2**3+(-20898*CT1**4+351
?    54*CT1**2-8262)*CT2**2+(5994*CT1-4860*CT1**3)*CT12*CT2+5346*C
@    T1**4-5346*CT1**2+1296)+(972-2592*CT1**2)*CT2**2+324*CT1*CT12
1    *CT2+972*CT1**2-324


     T2A4B2 = CAP**4*((492075*CT1**4-153090*CT1**2+10935)*CT2**6+(147
1    6225*CT1**5+65610*CT1**3-54675*CT1)*CT12*CT2**5+((2165130*CT1
2    **4-260253*CT1**2+2187)*CT12**2+492075*CT1**6-699840*CT1**4+1
3    60137*CT1**2-11178)*CT2**4+((1187541*CT1**3-115911*CT1)*CT12*
4    *3+(131220*CT1**5-535086*CT1**3+67554*CT1)*CT12)*CT2**3+((288
5    684*CT1**2-13122)*CT12**4+(-201204*CT1**4-142155*CT1**2+6561)
6    *CT12**2-142155*CT1**6+147015*CT1**4-29565*CT1**2+3159)*CT2**
7    2+(26244*CT1*CT12**5+(-102789*CT1**3-15309*CT1)*CT12**3+(-634
8    23*CT1**5+67554*CT1**3-4779*CT1)*CT12)*CT2-13122*CT1**2*CT12*
```

251

```
9     *4+(8748*CT1**2-4374*CT1**4)*CT12**2+8748*CT1**6-8262*CT1**4+
:     2430*CT1**2-324)


      T2A4B = (T2A4B1+T2A4B2)
+        *ALPHA**4*THETA**2/9.*ST1*ST2*.20043766172607939427E-33
+        /SEP(INDX1)**12/(3.0*TEMPK*1.380622E-23)
C

      T2A4C1 = CAP**3*((984150*CT1**6-503010*CT1**4+83106*CT1**2-4374)
1     *CT2**4+(1443420*CT1**5-507384*CT1**3+43740*CT1)*CT12*CT2**3+
2     ((791694*CT1**4-166212*CT1**2+4374)*CT12**2-87480*CT1**6+8310
3     6*CT1**4-34992*CT1**2+4374)*CT2**2+((192456*CT1**3-17496*CT1)
4     *CT12**3+(-64152*CT1**5+32076*CT1**3-8748*CT1)*CT12)*CT2+1749
5     6*CT1**2*CT12**4-11664*CT1**4*CT12**2-10368*CT1**4+6480*CT1**
6     2-1296)+CAP**2*((54675*CT1**4-21870*CT1**2+2187)*CT2**4+(4374
7     0*CT1**3-8748*CT1)*CT12*CT2**3+(8748*CT1**2*CT12**2+174960*CT
8     1**6-118827*CT1**4+42282*CT1**2-5103)*CT2**2+(128304*CT1**5-5
9     2488*CT1**3+11664*CT1)*CT12*CT2+(23328*CT1**4-2916*CT1**2)*CT
:     12**2-11664*CT1**6+15552*CT1**4-9720*CT1**2+1944)+CAP*((34020
;     *CT1**4-16524*CT1**2+1944)*CT2**2+(18468*CT1**3-4860*CT1)*CT1
<     2*CT2+1944*CT1**2*CT12**2+7776*CT1**6-10368*CT1**4+6480*CT1**
=     2-1296)+2592*CT1**4-1620*CT1**2+324


      T2A4C2 = CAP**4*((492075*CT1**6-142155*CT1**4-2187*CT1**2+2187)*
1     CT2**4+(721710*CT1**5-166212*CT1**3+4374*CT1)*CT12*CT2**3+((3
2     95847*CT1**4-65610*CT1**2+2187)*CT12**2-87480*CT1**6+1701*CT1
3     **4+9234*CT1**2-1215)*CT2**2+((96228*CT1**3-8748*CT1)*CT12**3
4     +(-64152*CT1**5+1944*CT1**3+1944*CT1)*CT12)*CT2+8748*CT1**2*C
5     T12**4+(972*CT1**2-11664*CT1**4)*CT12**2+3888*CT1**6+2592*CT1
6     **4-1620*CT1**2+324)


      T2A4C = (T2A4C1+T2A4C2)
+        *ALPHA**4*THETA**2/9.*ST1*ST2*.20043766172607939427E-33
+        /SEP(INDX1)**12/(3.0*TEMPK*1.380622E-23)
C

      T2A4D1 = CAP**3*((-492075*CT1**4+185895*CT1**2-17496)*CT2**6+(80
1     919*CT1-426465*CT1**3)*CT12*CT2**5+((4374-113724*CT1**2)*CT12
2     **2-492075*CT1**6+809190*CT1**4-260253*CT1**2+21870)*CT2**4+(
3     (-426465*CT1**5+584658*CT1**3-111537*CT1)*CT12-8748*CT1*CT12*
4     *3)*CT2**3+((-113724*CT1**4+113724*CT1**2-8748)*CT12**2+18589
5     5*CT1**6-260253*CT1**4+89100*CT1**2-8262)*CT2**2+((80919*CT1*
6     *5-111537*CT1**3+24948*CT1)*CT12-8748*CT1**3*CT12**3)*CT2+(43
7     74*CT1**4-8748*CT1**2)*CT12**2-17496*CT1**6+21870*CT1**4-8262
8     *CT1**2+1296)+CAP**2*((8748-43740*CT1**2)*CT2**6-17496*CT1*CT
9     12*CT2**5+(-142155*CT1**4+118827*CT1**2-18954)*CT2**4+(35721*
:     CT1-34263*CT1**3)*CT12*CT2**3+(26244*CT1**2*CT12**2-43740*CT1
;     **6+118827*CT1**4-70227*CT1**2+10206)*CT2**2+(8748*CT1*CT12**
<     3+(-17496*CT1**5+35721*CT1**3-17739*CT1)*CT12)*CT2+8748*CT1**
=     6-18954*CT1**4+10206*CT1**2-1944)+CAP*((5346-20898*CT1**2)*CT
>     2**4-4860*CT1*CT12*CT2**3+(-20898*CT1**4+24948*CT1**2-5346)*C
```

```
    ?    T2**2+(4536*CT1-4860*CT1**3)*CT12*CT2+5346*CT1**4-5346*CT1**2
    @    +1296)+(972-2592*CT1**2)*CT2**2+324*CT1*CT12*CT2+972*CT1**2-3
    1    24


      T2A4D2 = CAP**4*(((492075*CT1**4-142155*CT1**2+8748)*CT2**6+(1476
    1    225*CT1**5+131220*CT1**3-63423*CT1)*CT12*CT2**5+((2165130*CT1
    2    **4-201204*CT1**2-4374)*CT12**2+492075*CT1**6-667035*CT1**4+1
    3    62324*CT1**2-8262)*CT2**4+((1187541*CT1**3-102789*CT1)*CT12**
    4    3+(131220*CT1**5-491346*CT1**3+80676*CT1)*CT12)*CT2**3+((2886
    5    84*CT1**2-13122)*CT12**4+(-201204*CT1**4-100602*CT1**2+8748)*
    6    CT12**2-142155*CT1**6+162324*CT1**4-41229*CT1**2+2430)*CT2**2
    7    +(26244*CT1*CT12**5+(-102789*CT1**3-2187*CT1)*CT12**3+(-63423
    8    *CT1**5+80676*CT1**3-12069*CT1)*CT12)*CT2-13122*CT1**2*CT12**
    9    4+(8748*CT1**2-4374*CT1**4)*CT12**2+8748*CT1**6-8262*CT1**4+2
    :    430*CT1**2-324)


      T2A4D = (T2A4D1+T2A4D2)
    +       *ALPHA**4*THETA**2/9.*ST1*ST2*.20043766172607939427E-33
    +       /SEP(INDX1)**12/(3.0*TEMPK*1.380622E-23)
       C(3)=T2A4A+T2A4B+T2A4C+T2A4D
C------------------------------------------------
C    DETERMINE DELTA 2
C------------------------------------------------
      CR(2)=ALPHA**2*(-3.*CAP**2*ST1**2*COS(PHI(INDX
    1    3))**2*ST2**2-3.*CAP**2*CT1*ST1
    2    *COS(PHI(INDX3))*CT2*ST2
    3    +(6.*CAP**2*CT1**2-3.*CAP**2+3.*CAP)*CT2
    4    **2+(3.*CAP-3.*CAP**2)*CT1**2+2.*CAP**2-
    5    2.*CAP)/SEP(INDX1)*1.22708E-3*ST1*ST2
C------------------------------------------------
C    DETERMINE DELTA 3
C------------------------------------------------
      CR(3) = ALPHA**3*((3*CAP**3+6*CAP**2)*ST1**2*COS(PHI(INDX3))**2
    +    *ST2**2+(12*CAP**3+24*CAP**2)*CT1*ST1*COS(PHI(INDX3))*CT2*ST2
    +    +((12*CAP**3+24*CAP**2)*CT1**2+3*CAP**3-6*CAP**2+3*CAP)*CT2**2
    +    +(-3*CAP**3-3*CAP**2+6*CAP)*CT1**2-2*CAP**3+3*CAP**2-
    +    3*CAP+2)/SEP(INDX1)**4*1.102844E-06*ST1*ST2
C------------------------------------------------
C    DETERMINE DELTA 4
C------------------------------------------------
      CR(4) = ALPHA**4*(-27*CAP**4*CT12**4-243*CAP**4*CT1*CT2*CT12**3
    +    +(-729*CAP**4*CT1**2*CT2**2+24*CAP**4-12*CAP**3-12*CAP**2)*
    3    CT12**2+(((81*CAP**3-81*CAP**4)*CT1-729*CAP**4*CT1**3)*CT2**3
    +    +((81*CAP**3-81*CAP**4)*CT1**3+(135*CAP**4-108*CAP**3-27*CAP**
    6    2)*CT1)*CT2)*CT12+((243*CAP**3-243*CAP**4)*CT1**2+27*CAP**4
    +    -54*CAP**3+27*CAP**2)*CT2**4+((243*CAP**3-243*CAP**4)*CT1
    9    **4+(243*CAP**4-324*CAP**3+81*CAP**2)*CT1**2-18*CAP**4
    +    +54*CAP**3-54*CAP**2+18*CAP)*CT2**2+(27*CAP**4-54*CAP**3
    +    +27*CAP**2)*CT1**4+(-18*CAP**4+54*CAP**3-54*CAP**2+18*CAP)
```

```
     +     *CT1**2-8*CAP**3+18*CAP**2-12*CAP+2)/SEP(INDX1)**7*ST1*ST2
     +     *9.91187E-10
C-----------------------------------------------
C     SUM ENERGY TERMS AND DIVIDE BY (-KT)
C-----------------------------------------------
       UTOT=ULJ(INDX1,INDX2,INDX3,INDX4)+USHAPE(INDX1,INDX2,INDX3,INDX4)
     +          +UELEC(INDX1,INDX2,INDX3,INDX4)
             G3=-1.*UTOT/(TEMPK*1.380622E-23)
             IF(G3.LT.-85) GO TO 5000
             G4=2.71828**G3
             GO TO 5010
5000         G4=0

5010         CTOT=0.00
             DO 5011 NCTOT=2,4
               CTOT=CTOT+CR(NCTOT)
5011         CONTINUE
             DO 5012 NCTOT=1,3
               CTOT=CTOT+C(NCTOT)
5012         CONTINUE

             PROD=G4*CTOT
             S1=S1+PROD*COEF2(INDX1)

70           CONTINUE
           S2=S2+S1*COEF1(INDX2)*1.0E-09

60         CONTINUE
           S3=S3+S2*COEF1(INDX3)

50      CONTINUE
      S4=S4+S3*COEF1(INDX4)

40    CONTINUE
      ABE(ITEMPK)=S4*1.0E12

      ERR=ABE(ITEMPK)-BEEXP(ITEMPK)
      EXCESS=ABS(ERR)-BEEXPERR(ITEMPK)
      IF (EXCESS .LT. 0.0D0) EXCESS=0.0D0

      BESSERR=BESSERR+ERR**2+EXCESS**2

      IF (M .GT. 1) THEN
          IF (BESSERR .GT. BESSE(M-1) ) GOTO 220
      ENDIF
4000  CONTINUE

      IF (N .EQ. 0 ) THEN
        D(1)=SHAPE
```

```
          RO(1)=R
          EK(1)=PARAM2
          DO 470 ITEMPK=1,11
             BT(ITEMPK,1)=ABT(ITEMPK)
             IF (ITEMPK .LE. 8) BE(ITEMPK,1)=ABE(ITEMPK)
470       CONTINUE
          BTSSE(1)=BTSSERR
          BESSE(1)=BESSERR
          N=1
          GOTO 220
        ENDIF

        IF (M .LE. N) THEN
          DO 420 IC=M,N
             IF (BESSERR .GT. BESSE(IC)) THEN
                J=IC
                GOTO 430
             ENDIF
420       CONTINUE
          J=N+1
          N=M
          GOTO 500
430       IGAP=J-M-1
          IF (IGAP .EQ. -1) THEN
            DO 440 IC=N,M,-1
              D(IC+1)=D(IC)
              RO(IC+1)=RO(IC)
              EK(IC+1)=EK(IC)
              DO 480 ITEMPK=1,11
                BT(ITEMPK,IC+1)=BT(ITEMPK,IC)
                IF (ITEMPK .LE. 8) BE(ITEMPK,IC+1)=BE(ITEMPK,IC)
480           CONTINUE
              BTSSE(IC+1)=BTSSE(IC)
              BESSE(IC+1)=BESSE(IC)
440         CONTINUE
            N=N+1
          ELSEIF (IGAP .GT. 0) THEN
            DO 450 IC=M+1,(N-IGAP)
              NC=IC+IGAP
              D(IC)=D(NC)
              RO(IC)=RO(NC)
              EK(IC)=EK(NC)
              DO 490 ITEMPK=1,11
                BT(ITEMPK,IC)=BT(ITEMPK,NC)
                IF (ITEMPK .LE. 8) BE(ITEMPK,IC)=BE(ITEMPK,NC)
490           CONTINUE
              BTSSE(IC)=BTSSE(NC)
              BESSE(IC)=BESSE(NC)
450         CONTINUE
```

```fortran
          N=N-IGAP
        ENDIF
      ENDIF

500   D(M)=SHAPE
      RO(M)=R
      EK(M)=PARAM2
      DO 495 ITEMPK=1,11
        BT(ITEMPK,M)=ABT(ITEMPK)
        IF (ITEMPK .LE. 8) BE(ITEMPK,M)=ABE(ITEMPK)
495   CONTINUE
      BTSSE(M)=BTSSERR
      BESSE(M)=BESSERR

      IF (M .GT. N) N=M

220   CONTINUE
210   CONTINUE

      OPEN(UNIT=6,FILE='CO2BAD3',FORM='FORMATTED')
      WRITE(6,300)
300   FORMAT(1X,'CO2BAD3',/,'30/9/96',/)
C-------------------------------------------
C     OUTPUT OF INPUT DATA
C-------------------------------------------
      WRITE(6,2160)ALPHA
2160  FORMAT(1X,'ALPHA(STATIC):',F10.5)
      WRITE(6,2165)ALFOP
2165  FORMAT(1X,'ALPHA(OPTICAL):',F10.5)
      WRITE(6,2180)AMU
2180  FORMAT(1X,'MU:',F10.5)
      WRITE(6,2190)THETA
2190  FORMAT(1X,'THETA:',F10.5)
      WRITE(6,2191)BPARA
2191  FORMAT(1X,'BPARA:',F10.5)
      WRITE(6,2192)BPERP
2192  FORMAT(1X,'BPERP:',F10.5)
      WRITE(6,2193)APARA
2193  FORMAT(1X,'APARA:',F10.5)
      WRITE(6,2194)APERP
2194  FORMAT(1X,'APERP:',F10.5)
      WRITE(6,2195)CZZ
2195  FORMAT(1X,'C3333:',F10.5)
      WRITE(6,2196)CXX
2196  FORMAT(1X,'C1111:',F10.5)
      WRITE(6,2197)CXZ
2197  FORMAT(1X,'C1313:',F10.5)
      WRITE(6,2200)CAP
2200  FORMAT(1X,'KAPPA:',F10.5)
```

```
      WRITE(6,2235)AMIN1,AMAX1
2235  FORMAT(1X,'MIN AND MAX POINTS OF RANGE:',2(F10.5,3X),/)


      WRITE(6,310)NANGLE
310   FORMAT(1X,'ANGLES:',I3,' INTERVALS')
      WRITE(6,311)NSEP
311   FORMAT(1X,'SEP: ',I4,' INTERVALS')


      DO 460 IC=1,N
       WRITE(6,3220)D(IC)
3220    FORMAT(/,1X,'D:      ',F6.3)
       WRITE(6,3210)RO(IC)
3210    FORMAT(1X,'RO:    ',F6.3)
       WRITE(6,3230)EK(IC)
3230    FORMAT(1X,'E/K:    ',F8.3,/)


       DO 800 ITEMPK=1,11
          ERR=BT(ITEMPK,IC)-BTEXP(ITEMPK)
          PERCERR=ERR/BTEXP(ITEMPK)*100.00
          WRITE(6,6155)BTTEMP(ITEMPK),BT(ITEMPK,IC),ERR,PERCERR
6155      FORMAT(1X,'TEMPERATURE:',F10.1,'     B(T):',F10.2,
     +    F10.2,F10.2)
800    CONTINUE
       WRITE(6,3175)BTSSE(IC)
3175   FORMAT(1X,'SUM OF SQUARES OF ERRORS:',F20.2,/)
      BESSERR=0.0d0
       DO 810 ITEMPK=2,8
          ERR=BE(ITEMPK,IC)-BEEXP(ITEMPK)
          PERCERR=ERR/BEEXP(ITEMPK)*100.00
          WRITE(6,3155)BETEMP(ITEMPK),BE(ITEMPK,IC),ERR,PERCERR
3155      FORMAT(1X,'TEMPERATURE:',F10.1,'     B(E):',F10.2,
     +    F10.2,F10.2)
          BESSERR=BESSERR+ERR**2
810    CONTINUE
       WRITE(6,3175)BESSERR
      WRITE(6,3177)BESSE(IC)
3177   FORMAT(1X,'SS ERRORS + SS EXCESS:',F20.3,/)
460   CONTINUE

      CLOSE(UNIT=6)
200   CONTINUE

      END


C     Usage: Set NLOW=1
C               NDIM=no. of quadrature points required
C               NGAUSS=no. of quadrature points required
C               A=lower limit of integral
C               B=upper limit of integral
```

```fortran
C                    X=quadrature points (array of dimension NGAUSS)
C                    W=Weights (array of dimension NGAUSS)
C     The subroutine permits a little more generality than above, but you
C     almost certainly won't need it.
C-------------------------------------------------------------------------
      SUBROUTINE GAUSSPT(NLOW,NDIM,NGAUSS,A,B,X,W)
C-------------------------------------------------------------------------
C     IN X EN W KOMEN DE NGAUSS GAUSSPUNTEN EN GEWICHTEN, BEREKEND OP HET
C     INTERVAL (A,B);DIMENSIES VAN X EN W: NLOW:NDIM
C     EIS: NLOW<=1. DE ELEMENTEN VAN NLOW TOT 1 WORDEN NIET GEVULD
C-------------------------------------------------------------------------
      IMPLICIT DOUBLE PRECISION(A-H,O-Z)
      DIMENSION X(NLOW:NDIM),W(NLOW:NDIM)
C-------------------------------------------------------------------------
C     ZOEK STARTWAARDEN
C-------------------------------------------------------------------------
      GN=0.5/NGAUSS
      EXTRA=1.0/(.4*NGAUSS*NGAUSS+5.0)
      XZ=-GN
      NT=0
      NTEKEN=0
5     PNM2=1.0
      PNM1=XZ
      DO 10 I=2,NGAUSS
      PNM1XZ=PNM1*XZ
      PN=2.0*PNM1XZ-PNM2-(PNM1XZ-PNM2)/I
      PNM2=PNM1
10    PNM1=PN
      MTEKEN=1
      IF(PN.LE.0.0) MTEKEN=-1
      IF((MTEKEN+NTEKEN).EQ.0) GO TO 15
      GO TO 20
15    NT=NT+1
      X(NT)=XZ
20    NTEKEN=MTEKEN
      IF((1.0-XZ).LE.EXTRA) GO TO 30
      XZ=XZ+(1.-XZ*XZ)*GN+EXTRA
      GO TO 5
30    CONTINUE
C-------------------------------------------------------------------------
C     BEPAAL NULPUNTEN EN GEWICHTEN
C-------------------------------------------------------------------------
      DO 60 I=1,NT
      XZ=X(I)
      DELTA2=1.
35    PNM2=1.0
      PNM1=XZ
      PNM1AF=1.0
      Z=.5+1.5*XZ*XZ
```

```fortran
      DO 40 K=2,NGAUSS
      PNM1XZ=PNM1*XZ
      PN=2.0*PNM1XZ-PNM2-(PNM1XZ-PNM2)/K
      PNAF=XZ*PNM1AF+K*PNM1
      Z=Z+(K+0.5)*PN*PN
      PNM2=PNM1
      PNM1=PN
      PNM1AF=PNAF
40    CONTINUE
      DELTA1=PN/PNAF
      XZ=XZ-DELTA1
      IF(DELTA1.LT.0.0) DELTA1=-DELTA1
      IF((DELTA1.GE.DELTA2).AND.(DELTA2.LT.1.E-6)) GO TO 50
      DELTA2=DELTA1
      GO TO 35
50    X(I)=XZ
      W(I)=1.0/Z
60    CONTINUE
C--------------------------------------------------------------------
C     TRANSFORMATIE NAAR (A,B)
C--------------------------------------------------------------------
      NGHALF=NGAUSS/2
      NGP1=NGAUSS+1
      NTP1=NT+1
      APB=A+B
      BMAG2=(B-A)/2.0
      DO 90 I=1,NGHALF
      X(NGP1-I)=B-BMAG2*(1.0-X(NTP1-I))
  90  W(NGP1-I)=BMAG2*W(NTP1-I)
      IF(NGHALF.NE.NT) GO TO 100
      GO TO 110
 100  X(NT)=APB/2.0
      W(NT)=W(1)*BMAG2
 110  DO 120 I=1,NGHALF
      X(I)=APB-X(NGP1-I)
 120  W(I)=W(NGP1-I)
      RETURN
      END
```

C.2 Example of a program to calculate a component of B_ε for a non-linear molecule

```
      PROGRAM ESO2A2
C
C 19 JULY 1996.
C PROGRAM TO CALCULATE THE A2 TERM'S CONTRIBUTION TO B(epsilon) FOR SO2
C USING GAUSSIAN INTEGRATION WITH 64 INTERVALS FOR THE RANGE, AND
C 10 INTERVALS FOR ALL ANGULAR VARIABLES
C (I.E. ALPHA1, BETA1, GAMMA1, ALPHA2, BETA2 AND GAMMA2).
C DOUBLE PRECISION IS USED THROUGHOUT.
C
C --------------------
C SYSTEM INITIALIZATION:
C --------------------
      IMPLICIT DOUBLE PRECISION (A-H,O-Z)
      COMMON COEF1,DCTC
      DIMENSION COEF2(64,2),COEF1(10,2),SEP(64),AL1(10),BE1(10),GA1(10)
     + ,AL2(10),BE2(10),GA2(10),DCTC(9,10,10,10),FI(10,10,10,10,10),D1(6
     + 4),E1(10,10,10,10,10),F1(10,10,10,10,10),SE3(64),SE4(64),SE5(64),
     + SE6(64),SE8(64),SE12(64),G1(10,10,10),DDP(10,10,10,10,10),DQP(10,
     + 10,10,10,10),DIDP(10,10,10,10,10)
      INTEGER X1,X2,X3,X4,X5,X6,X7
C---------------------------------
C MOLECULAR DATA FOR SO2 (632.8 NM):
C---------------------------------
      SS1=0.000000
      SS2=0.000000
      SS3=0.000000
      SS4=0.000000
      SS5=0.000000
      SS6=0.000000
      SS7=0.000000
      DIP=-5.4262D0
      A11=5.80D0
      A22=3.30D0
      A33=3.88D0
      ALDYN=(A11+A22+A33)/3.0D0
      V11=5.6610D0
      V22=3.2050D0
      V33=3.7560D0
      ALSTAT=(V11+V22+V33)/3.0D0
      Q1=-16.40D0
      Q2=12.90D0
      AMIN1=0.1000
      AMAX1=3.0000
```

```
C-------------------------------------------------------------------
C READ THE GAUSSIAN COEFFICIENTS FROM THE DATAFILE GAUSS64.DAT:
C-------------------------------------------------------------------
        OPEN(UNIT=10,FILE='GAUSS64.DAT')
          DO 10 ICTR1=1,64
            DO 20 ICTR2=1,2
              READ(10,1010,END=11)COEF2(ICTR1,ICTR2)
1010          FORMAT(F18.15)
20          CONTINUE
10        CONTINUE
11      CLOSE(UNIT=10)
C---------------------------------------------------------
C CALCULATE THE INTEGRATION POINTS FOR THE RANGE:
C---------------------------------------------------------
        SEP1=(AMAX1-AMIN1)/2
        SEP2=(AMAX1+AMIN1)/2
        DO 30 INDX=1,64
          SEP(INDX)=SEP1*COEF2(INDX,1)+SEP2
30      CONTINUE
C-------------------------------------------------------------------
C READ THE GAUSSIAN COEFFICIENTS FROM THE DATAFILE GAUSS10.DAT:
C-------------------------------------------------------------------
        OPEN(UNIT=11,FILE='GAUSS10.DAT')
          DO 100 ICTR1=1,10
            DO 110 ICTR2=1,2
              READ(11,6000,END=12)COEF1(ICTR1,ICTR2)
6000          FORMAT(F18.15)
110        CONTINUE
100     CONTINUE
12      CLOSE(UNIT=11)
C---------------------------------------------------------
C CALCULATE THE INTEGRATION POINTS FOR ALPHA1:
C---------------------------------------------------------
        AMIN=0.0
        AMAX=2.*3.14159265358979323846

        AL11=(AMAX-AMIN)/2.
        AL12=(AMAX+AMIN)/2.
        DO 120 INDX=1,10
          AL1(INDX)=AL11*COEF1(INDX,1)+AL12
120     CONTINUE
C---------------------------------------------------------
C CALCULATE THE INTEGRATION POINTS FOR BETA1:
C---------------------------------------------------------
        AMIN=0.0
        AMAX=3.14159265358979323846

        BE11=(AMAX-AMIN)/2.
        BE12=(AMAX+AMIN)/2.
```

```
      DO 121 INDX=1,10
        BE1(INDX)=BE11*COEF1(INDX,1)+BE12
121   CONTINUE
C--------------------------------------------
C CALCULATE THE INTEGRATION POINTS FOR GAMMA1:
C--------------------------------------------
      AMIN=0.0
      AMAX=2.*3.14159265358979323846

      GA11=(AMAX-AMIN)/2.
      GA12=(AMAX+AMIN)/2.
      DO 122 INDX=1,10
        GA1(INDX)=GA11*COEF1(INDX,1)+GA12
122   CONTINUE
C--------------------------------------------
C CALCULATE THE INTEGRATION POINTS FOR ALPHA2:
C--------------------------------------------
      AMIN=0.0
      AMAX=2.*3.14159265358979323846

      AL21=(AMAX-AMIN)/2.
      AL22=(AMAX+AMIN)/2.
      DO 123 INDX=1,10
        AL2(INDX)=AL21*COEF1(INDX,1)+AL22
123   CONTINUE
C--------------------------------------------
C CALCULATE THE INTEGRATION POINTS FOR BETA2:
C--------------------------------------------
      AMIN=0.0
      AMAX=3.14159265358979323846

      BE21=(AMAX-AMIN)/2.
      BE22=(AMAX+AMIN)/2.
      DO 124 INDX=1,10
        BE2(INDX)=BE21*COEF1(INDX,1)+BE22
124   CONTINUE
C--------------------------------------------
C CALCULATE THE INTEGRATION POINTS FOR GAMMA2:
C--------------------------------------------
      AMIN=0.0
      AMAX=2.*3.14159265358979323846

      GA21=(AMAX-AMIN)/2.
      GA22=(AMAX+AMIN)/2.
      DO 125 INDX=1,10
        GA2(INDX)=GA21*COEF1(INDX,1)+GA22
125   CONTINUE
```

```
C ------------
C MAIN PROGRAM:
C ------------
        OPEN(UNIT=4,FILE='diel_so2_a2_10_292K_d8')
C---------------------------------
C INPUT MOLECULAR PARAMETERS
C---------------------------------
        TEMP=292.7
        TEMPK=TEMP*1.380622E-23

        R=0.3850D0
        PARAM2=220.0D0
        SHAPE1=0.11750D0
        SHAPE2=0.13570D0
C---------------------------------------------------------------
C CALCULATION OF THE LENNARD-JONES 6:12 POTENTIAL & STORAGE OF THE
C VALUES IN AN ARRAY:
C---------------------------------------------------------------
        DO 61 X1=1,64
          D1(X1)=4.*PARAM2*1.380622E-23*((R/SEP(X1))**12-(R/SEP(X1))**6)
          SE3(X1)=SEP(X1)**3
          SE4(X1)=SEP(X1)**4
          SE5(X1)=SEP(X1)**5
          SE6(X1)=SEP(X1)**6
          SE8(X1)=SEP(X1)**8
          SE12(X1)=SEP(X1)**12
61      CONTINUE
C---------------------------------------------------------------
C THE DIRECTION COSINE TENSOR COMPONENTS ARE STORED IN AN ARRAY:
C---------------------------------------------------------------
        DO 66 X4=1,10
          DO 77 X3=1,10
            DO 88 X2=1,10
C---------------------------------
C DIRECTION COSINE TENSOR COMPONENTS:
C---------------------------------
        A1=COS(AL1(X2))*COS(BE1(X3))*COS(GA1(X4))-1.*SIN(AL1(X2))*SIN(GA1
     +  (X4))
        A2=SIN(AL1(X2))*COS(BE1(X3))*COS(GA1(X4))+COS(AL1(X2))*SIN(GA1(X4
     +  ))
        A3=-1.*SIN(BE1(X3))*COS(GA1(X4))
        A4=-1.*COS(AL1(X2))*COS(BE1(X3))*SIN(GA1(X4))-1.*SIN(AL1(X2))*COS
     +  (GA1(X4))
        A5=-1.*SIN(AL1(X2))*COS(BE1(X3))*SIN(GA1(X4))+COS(AL1(X2))*COS(GA
     +  1(X4))
        A6=SIN(BE1(X3))*SIN(GA1(X4))
        A7=COS(AL1(X2))*SIN(BE1(X3))
        A8=SIN(AL1(X2))*SIN(BE1(X3))
        A9=COS(BE1(X3))
```

```
        DCTC(1,X2,X3,X4)=A1
        DCTC(2,X2,X3,X4)=A2
        DCTC(3,X2,X3,X4)=A3
        DCTC(4,X2,X3,X4)=A4
        DCTC(5,X2,X3,X4)=A5
        DCTC(6,X2,X3,X4)=A6
        DCTC(7,X2,X3,X4)=A7
        DCTC(8,X2,X3,X4)=A8
        DCTC(9,X2,X3,X4)=A9
88          CONTINUE
77        CONTINUE
66      CONTINUE
C----------------------------------------------------------
C THE MULTIPOLE INTERACTION ENERGIES ARE CALCULATED AND STORED
C IN ARRAYS:
C----------------------------------------------------------
        DO 939 X7=1,10
        WRITE(6,1000)X7
1000    FORMAT (1X, 'INDEX (IN RANGE 1 TO 10) IS CURRENTLY ',I2 )
          DO 40 X6=1,10
            DO 50 X5=1,10
C----------------------------------------------------------
C MOLECULE 2'S DIRECTION COSINE TENSOR COMPONENTS:
C----------------------------------------------------------
        B1=DCTC(1,X5,X6,X7)
        B2=DCTC(2,X5,X6,X7)
        B3=DCTC(3,X5,X6,X7)
        B4=DCTC(4,X5,X6,X7)
        B5=DCTC(5,X5,X6,X7)
        B6=DCTC(6,X5,X6,X7)
        B7=DCTC(7,X5,X6,X7)
        B8=DCTC(8,X5,X6,X7)
        B9=DCTC(9,X5,X6,X7)
              DO 60 X4=1,10
                DO 70 X3=1,10
                  DO 80 X2=1,10
C----------------------------------------------------------
C MOLECULE 1'S DIRECTION COSINE TENSOR COMPONENTS:
C----------------------------------------------------------
        A1=DCTC(1,X2,X3,X4)
        A2=DCTC(2,X2,X3,X4)
        A3=DCTC(3,X2,X3,X4)
        A4=DCTC(4,X2,X3,X4)
        A5=DCTC(5,X2,X3,X4)
        A6=DCTC(6,X2,X3,X4)
        A7=DCTC(7,X2,X3,X4)
        A8=DCTC(8,X2,X3,X4)
        A9=DCTC(9,X2,X3,X4)
```

264

```fortran
C---------------------------------------------------
C CALCULATION OF THE DIPOLE-DIPOLE POTENTIAL:
C---------------------------------------------------
      DDP(X2,X3,X4,X5,X6)=8.98758E-24*DIP**2*(-2*A9*B9+A6*B6+A3*B3)
C---------------------------------------------------
C CALCULATION OF THE DIPOLE-QUADRUPOLE POTENTIAL:
C---------------------------------------------------
      DQP(X2,X3,X4,X5,X6)=8.98758E-25*DIP*(Q2*(-2*A9*B9**2+(2*A6*B6+2*A
     + 3*B3+2*A9**2-2*A8**2-A6**2+A5**2-A3**2+A2**2)*B9+2*A9*B8**2+(-2*A
     + 6*B5-2*A3*B2)*B8+A9*B6**2+(2*A5*A8-2*A6*A9)*B6-A9*B5**2+A9*B3**2+
     + (2*A2*A8-2*A3*A9)*B3-A9*B2**2)+Q1*(-2*A9*B9**2+(2*A6*B6+2*A3*B3+2
     + *A9**2-2*A7**2-A6**2+A4**2-A3**2+A1**2)*B9+2*A9*B7**2+(-2*A6*B4-2
     + *A3*B1)*B7+A9*B6**2+(2*A4*A7-2*A6*A9)*B6-A9*B4**2+A9*B3**2+(2*A1*
     + A7-2*A3*A9)*B3-A9*B1**2))
C---------------------------------------------------
C CALCULATION OF THE DIPOLE-INDUCED DIPOLE POTENTIAL:
C---------------------------------------------------
      DIDP(X2,X3,X4,X5,X6)=-0.50*ALSTAT*8.07765E-27*DIP**2*(3*B9**2
     + +3*A9**2-2)
C---------------------------------------------------
C CALCULATION OF THE QUADRUPOLE-QUADRUPOLE POTENTIAL:
C---------------------------------------------------
      QUAD1=-16.*(A6*A9-A5*A8)*(B6*B9-B5*B8)-16.*(A3*A9-A2*A8)*(B3*B9-B
     + 2*B8)+4.*(2.*A9**2-2.*A8**2-A6**2+A5**2-A3**2+A2**2)*(B9-B8)*(B9+
     + B8)+(-4.*A9**2+4.*A8**2+3.*A6**2-3.*A5**2+A3**2-A2**2)*(B6**2-B5*
     + *2)+4.*(A3*A6-A2*A5)*(B3*B6-B2*B5)+(-4.*A9**2+4.*A8**2+A6**2-A5**
     + 2+3.*A3**2-3.*A2**2)*(B3**2-B2**2)

      QUAD2=-16.*(A6*A9-A4*A7)*(B6*B9-B4*B7)-16.*(A3*A9-A1*A7)*(B3*B9-B
     + 1*B7)+4.*(2.*A9**2-2.*A7**2-A6**2+A4**2-A3**2+A1**2)*(B9-B7)*(B9+
     + B7)+(-4.*A9**2+4.*A7**2+3.*A6**2-3.*A4**2+A3**2-A1**2)*(B6**2-B4*
     + *2)+4.*(A3*A6-A1*A4)*(B3*B6-B1*B4)+(-4.*A9**2+4.*A7**2+A6**2-A4**
     + 2+3.*A3**2-3.*A1**2)*(B3**2-B1**2)

      QUAD3=4.*(4.*A9**2-2.*(A8**2+A7**2+A6**2+A3**2)+A5**2+A4**2+A2**2
     + +A1**2)*B9**2-16.*(2.*A6*A9-A5*A8-A4*A7)*B6*B9-16.*(2.*A3*A9-A2*A8
     + -A1*A7)*B3*B9-4.*(2.*A9**2-2.*A7**2-A6**2+A4**2-A3**2+A1**2)*B8**
     + 2+16.*(A6*A9-A4*A7)*B5*B8+16.*(A3*A9-A1*A7)*B2*B8-4.*(2.*A9**2-2.
     + *A8**2-A6**2+A5**2-A3**2+A2**2)*B7**2+16.*(A6*A9-A5*A8)*B4*B7+16.
     + *(A3*A9-A2*A8)*B1*B7+(-8.*A9**2+4.*(A8**2+A7**2)+6.*A6**2-3.*(A5*
     + *2+A4**2)+2*A3**2-A2**2-A1**2)*B6**2+4.*(2.*A3*A6-A2*A5-A1*A4)*B3
     + *B6+(4.*A9**2-4.*A7**2-3.*A6**2+3.*A4**2-A3**2+A1**2)*B5**2-4.*(A
     + 3*A6-A1*A4)*B2*B5+(4.*A9**2-4.*A8**2-3.*A6**2+3.*A5**2-A3**2+A2**
     + 2)*B4**2-4.*(A3*A6-A2*A5)*B1*B4+(-8.*A9**2+4.*(A8**2+A7**2)+2.*A6
     + **2-A5**2-A4**2+6.*A3**2-3.*(A2**2+A1**2))*B3**2+(4.*A9**2-4.*A7*
     + *2-A6**2+A4**2-3.*A3**2+3.*A1**2)*B2**2+(4.*A9**2-4.*A8**2-A6**2+
     + A5**2-3.*A3**2+3.*A2**2)*B1**2

      E1(X2,X3,X4,X5,X6)=8.98758E-26*(1./3.)*(Q2**2*QUAD1+Q1**2*QUAD
```

```
      + 2+Q1*Q2*QUAD3)
C------------------------------------------------------------
C CALCULATION OF THE QUADRUPOLE-INDUCED DIPOLE POTENTIAL:
C------------------------------------------------------------
      QID1=Q2**2*(4.*A9**4+(-8.*A8**2+4.*A5**2+4.*A2**2)*A9**2+(-8.*A5*
     + A6-8.*A2*A3)*A8*A9+4.*A8**4+(4.*A6**2+4.*A3**2)*A8**2+A6**4+(-2.*
     + A5**2+2.*A3**2-2.*A2**2)*A6**2+A5**4+(2.*A2**2-2.*A3**2)*A5**2+A3
     + **4-2.*A2**2*A3**2+A2**4)+Q1**2*(4.*A9**4+(-8.*A7**2+4.*A4**2+4.*
     + A1**2)*A9**2+(-8.*A4*A6-8.*A1*A3)*A7*A9+4.*A7**4+(4.*A6**2+4.*A3*
     + *2)*A7**2+A6**4+(-2.*A4**2+2.*A3**2-2.*A1**2)*A6**2+A4**4+(2.*A1*
     + *2-2.*A3**2)*A4**2+A3**4-2.*A1**2*A3**2+A1**4)+Q1*Q2*(8.*A9**4+(-
     + 8.*A8**2-8.*A7**2+4.*A5**2+4.*A4**2+4.*A2**2+4.*A1**2)*A9**2+((-8
     + .*A5*A6-8.*A2*A3)*A8+(-8.*A4*A6-8.*A1*A3)*A7)*A9+(8.*A7**2+4.*A6*
     + *2-4.*A4**2+4.*A3**2-4.*A1**2)*A8**2+(8.*A4*A5+8.*A1*A2)*A7*A8+(4
     + .*A6**2-4.*A5**2+4.*A3**2-4.*A2**2)*A7**2+2.*A6**4+(-2.*A5**2-2.*
     + A4**2+4.*A3**2-2.*A2**2-2.*A1**2)*A6**2+(2.*A4**2-2.*A3**2+2.*A1*
     + *2)*A5**2+(2.*A2**2-2.*A3**2)*A4**2+2.*A3**4+(-2.*A2**2-2.*A1**2)
     + *A3**2+2.*A1**2*A2**2)

      QID2=Q2**2*(4.*B9**4+(-8.*B8**2+4.*B5**2+4.*B2**2)*B9**2+(-8.*B5*
     + B6-8.*B2*B3)*B8*B9+4.*B8**4+(4.*B6**2+4.*B3**2)*B8**2+B6**4+(-2.*
     + B5**2+2.*B3**2-2.*B2**2)*B6**2+B5**4+(2.*B2**2-2.*B3**2)*B5**2+B3
     + **4-2.*B2**2*B3**2+B2**4)+Q1**2*(4.*B9**4+(-8.*B7**2+4.*B4**2+4.*
     + B1**2)*B9**2+(-8.*B4*B6-8.*B1*B3)*B7*B9+4.*B7**4+(4.*B6**2+4.*B3*
     + *2)*B7**2+B6**4+(-2.*B4**2+2.*B3**2-2.*B1**2)*B6**2+B4**4+(2.*B1*
     + *2-2.*B3**2)*B4**2+B3**4-2.*B1**2*B3**2+B1**4)+Q1*Q2*(8.*B9**4+(-
     + 8.*B8**2-8.*B7**2+4.*B5**2+4.*B4**2+4.*B2**2+4.*B1**2)*B9**2+((-8
     + .*B5*B6-8.*B2*B3)*B8+(-8.*B4*B6-8.*B1*B3)*B7)*B9+(8.*B7**2+4.*B6*
     + *2-4.*B4**2+4.*B3**2-4.*B1**2)*B8**2+(8.*B4*B5+8.*B1*B2)*B7*B8+(4
     + .*B6**2-4.*B5**2+4.*B3**2-4.*B2**2)*B7**2+2.*B6**4+(-2.*B5**2-2.*
     + B4**2+4.*B3**2-2.*B2**2-2.*B1**2)*B6**2+(2.*B4**2-2.*B3**2+2.*B1*
     + *2)*B5**2+(2.*B2**2-2.*B3**2)*B4**2+2.*B3**4+(-2.*B2**2-2.*B1**2)
     + *B3**2+2.*B1**2*B2**2)

      F1(X2,X3,X4,X5,X6)=-0.5*8.07765E-29*ALSTAT*(QID1+QID2)
C------------------------------------------------------------
C CALCULATION OF THE INTEGRATION ARGUMENT:
C------------------------------------------------------------
      T11=2.*A7**2-A4**2-A1**2
      T22=2.*A8**2-A5**2-A2**2
      T33=2.*A9**2-A6**2-A3**2
      T12=2.*A7*A8-A4*A5-A1*A2
      T13=2.*A7*A9-A4*A6-A1*A3
      T23=2.*A8*A9-A5*A6-A2*A3

      W11 = V33*(A7**2*B9**2+(2*A4*A7*B6+2*A1*A7*B3)*B9+A4**2*B6**2+2*A
     + 1*A4*B3*B6+A1**2*B3**2)+V22*(A7**2*B8**2+(2*A4*A7*B5+2*A1*A7*B2
     + )*B8+A4**2*B5**2+2*A1*A4*B2*B5+A1**2*B2**2)+V11*(A7**2*B7**2+(2
     + *A4*A7*B4+2*A1*A7*B1)*B7+A4**2*B4**2+2*A1*A4*B1*B4+A1**2*B1**2)
```

266

```
      W22 = V33*(A8**2*B9**2+(2*A5*A8*B6+2*A2*A8*B3)*B9+A5**2*B6**2+2*A
     +    2*A5*B3*B6+A2**2*B3**2)+V22*(A8**2*B8**2+(2*A5*A8*B5+2*A2*A8*B2
     +    )*B8+A5**2*B5**2+2*A2*A5*B2*B5+A2**2*B2**2)+V11*(A8**2*B7**2+(2
     +    *A5*A8*B4+2*A2*A8*B1)*B7+A5**2*B4**2+2*A2*A5*B1*B4+A2**2*B1**2)

      W33 = V33*(A9**2*B9**2+(2*A6*A9*B6+2*A3*A9*B3)*B9+A6**2*B6**2+2*A
     +    3*A6*B3*B6+A3**2*B3**2)+V22*(A9**2*B8**2+(2*A6*A9*B5+2*A3*A9*B2
     +    )*B8+A6**2*B5**2+2*A3*A6*B2*B5+A3**2*B2**2)+V11*(A9**2*B7**2+(2
     +    *A6*A9*B4+2*A3*A9*B1)*B7+A6**2*B4**2+2*A3*A6*B1*B4+A3**2*B1**2)

      W12 = V33*(A7*A8*B9**2+((A4*A8+A5*A7)*B6+(A1*A8+A2*A7)*B3)*B9+A4*
     +    A5*B6**2+(A1*A5+A2*A4)*B3*B6+A1*A2*B3**2)+V22*(A7*A8*B8**2+((A4
     +    *A8+A5*A7)*B5+(A1*A8+A2*A7)*B2)*B8+A4*A5*B5**2+(A1*A5+A2*A4)*B2
     +    *B5+A1*A2*B2**2)+V11*(A7*A8*B7**2+((A4*A8+A5*A7)*B4+(A1*A8+A2*A
     +    7)*B1)*B7+A4*A5*B4**2+(A1*A5+A2*A4)*B1*B4+A1*A2*B1**2)

      W13 = V33*(A7*A9*B9**2+((A4*A9+A6*A7)*B6+(A1*A9+A3*A7)*B3)*B9+A4*
     +    A6*B6**2+(A1*A6+A3*A4)*B3*B6+A1*A3*B3**2)+V22*(A7*A9*B8**2+((A4
     +    *A9+A6*A7)*B5+(A1*A9+A3*A7)*B2)*B8+A4*A6*B5**2+(A1*A6+A3*A4)*B2
     +    *B5+A1*A3*B2**2)+V11*(A7*A9*B7**2+((A4*A9+A6*A7)*B4+(A1*A9+A3*A
     +    7)*B1)*B7+A4*A6*B4**2+(A1*A6+A3*A4)*B1*B4+A1*A3*B1**2)

      W23 = V33*(A8*A9*B9**2+((A5*A9+A6*A8)*B6+(A2*A9+A3*A8)*B3)*B9+A5*
     +    A6*B6**2+(A2*A6+A3*A5)*B3*B6+A2*A3*B3**2)+V22*(A8*A9*B8**2+((A5
     +    *A9+A6*A8)*B5+(A2*A9+A3*A8)*B2)*B8+A5*A6*B5**2+(A2*A6+A3*A5)*B2
     +    *B5+A2*A3*B2**2)+V11*(A8*A9*B7**2+((A5*A9+A6*A8)*B4+(A2*A9+A3*A
     +    8)*B1)*B7+A5*A6*B4**2+(A2*A6+A3*A5)*B1*B4+A2*A3*B1**2)

      F11=V11*(W11*T11+W12*T12+W13*T13)
      F12=V11*(W12*T11+W22*T12+W23*T13)
      F13=V11*(W13*T11+W23*T12+W33*T13)
      F21=V22*(W11*T12+W12*T22+W13*T23)
      F22=V22*(W12*T12+W22*T22+W23*T23)
      F23=V22*(W13*T12+W23*T22+W33*T23)
      F31=V33*(W11*T13+W12*T23+W13*T33)
      F32=V33*(W12*T13+W22*T23+W23*T33)
      F33=V33*(W13*T13+W23*T23+W33*T33)

      A2 = F33+F22+F11

      FI(X2,X3,X4,X5,X6)=A2/3.0*(SIN(BE1(X3))*SIN(BE2(X6)))
C----------------------------------
C CALCULATION OF THE SHAPE POTENTIAL:
C----------------------------------
      G1(X3,X4,X6)=4.*PARAM2*1.380622E-23*R**12*(SHAPE1*(3.*COS(BE1(X3)
     + )**2+3.*COS(BE2(X6))**2-2.)+SHAPE2*(3.*COS(GA1(X4))**2*SIN(BE1(X3
     + ))**2+3.*COS(GA2(X7))**2*SIN(BE2(X6))**2-2.))
```

```
80               CONTINUE
70                CONTINUE
60                 CONTINUE
50                  CONTINUE
40                   CONTINUE
C---------------------------------
C THE INTEGRAL IS CALCULATED:
C---------------------------------
          SS6=0.00
          DO 940 X6=1,10
            SS5=0.00
            DO 950 X5=1,10
              SS4=0.00
              DO 960 X4=1,10
                SS3=0.00
                DO 970 X3=1,10
                  SS2=0.00
                  DO 980 X2=1,10
                    SS1=0.00
                    DO 990 X1=1,64
C------------------------------------------------------------------
C SUMMATION OF THE ENERGY TERMS WITH SUBSEQUENT DIVISION BY (-kT):
C------------------------------------------------------------------
      G3=-1.*(D1(X1)+E1(X2,X3,X4,X5,X6)/SE5(X1)+F1(X2,X3,X4,X5,X6)/SE8(
     + X1)+G1(X3,X4,X6)/SE12(X1)+DDP(X2,X3,X4,X5,X6)/SE3(X1)+DIDP(X2,X3,
     + X4,X5,X6)/SE6(X1)+DQP(X2,X3,X4,X5,X6)/SE4(X1))/TEMPK

      IF(G3.LT.-85) GO TO 5000
      G4=2.71828**G3
      GO TO 5010
5000  G4=0
5010  SS1=SS1+FI(X2,X3,X4,X5,X6)/SEP(X1)*G4*COEF2(X1,2)
990                CONTINUE
      SS2=SS2+SS1*COEF1(X2,2)
980               CONTINUE
      SS3=SS3+SS2*COEF1(X3,2)
970              CONTINUE
      SS4=SS4+SS3*COEF1(X4,2)
960             CONTINUE
      SS5=SS5+SS4*COEF1(X5,2)
950            CONTINUE
      SS6=SS6+SS5*COEF1(X6,2)
940           CONTINUE
      SS7=SS7+SS6*COEF1(X7,2)
939          CONTINUE
      ANS=SS7*SEP1*AL11*BE11*GA11*AL21*BE21*GA21
     +                    *0.24734494511444167800E-14
```

```fortran
C-------------------------------------------------------------
C THE INTEGRAL IS PRINTED TOGETHER WITH MOLECULAR DATA USED
C-------------------------------------------------------------
      WRITE(4,2266)
2266  FORMAT(1X,'THE A2 TERM CONTRIBUTION TO B(epsilon) FOR SO2')
      WRITE(4,2268)
2268  FORMAT(1X,'AT THE WAVELENGTH 632.8 nm',/,/)
      WRITE(4,1140)ANS
1140  FORMAT(1X,'THE INTEGRAL IS',E15.7)
      WRITE(4,2150)
2150  FORMAT(1X,'INPUT DATA:    ')
      WRITE(4,2155)TEMP
2155  FORMAT(1X,'TEMPERATURE:          ',F10.5)
      WRITE(4,2156)DIP
2156  FORMAT(1X,'DIPOLE MOMENT:        ',F10.5)
      WRITE(4,2911)ALDYN
2911  FORMAT(1X,'MEAN DYNAMIC ALPHA:   ',F10.5)
      WRITE(4,2912)A11
2912  FORMAT(1X,'DYNAMIC ALPHA11:      ',F10.5)
      WRITE(4,2913)A22
2913  FORMAT(1X,'DYNAMIC ALPHA22:      ',F10.5)
      WRITE(4,2914)A33
2914  FORMAT(1X,'DYNAMIC ALPHA33:      ',F10.5)
      WRITE(4,2160)ALSTAT
2160  FORMAT(1X,'MEAN STATIC ALPHA:    ',F10.5)
      WRITE(4,2161)V11
2161  FORMAT(1X,'STATIC ALPHA11:       ',F10.5)
      WRITE(4,2162)V22
2162  FORMAT(1X,'STATIC ALPHA22:       ',F10.5)
      WRITE(4,2163)V33
2163  FORMAT(1X,'STATIC ALPHA33:       ',F10.5)
      WRITE(4,2190)Q1
2190  FORMAT(1X,'THETA11:              ',F10.5)
      WRITE(4,2241)Q2
2241  FORMAT(1X,'THETA22:              ',F10.5)
      WRITE(4,2210)R
2210  FORMAT(1X,'R(O):                 ',F6.5)
      WRITE(4,2220)SHAPE1
2220  FORMAT(1X,'SHAPE FACTOR 1:       ',F10.5)
      WRITE(4,2221)SHAPE2
2221  FORMAT(1X,'SHAPE FACTOR 2:       ',F10.5)
      WRITE(4,2230)PARAM2
2230  FORMAT(1X,'E/K:                  ',F9.5)
      WRITE(4,2235)AMIN1,AMAX1
2235  FORMAT(1X,'MIN AND MAX POINTS OF RANGE:',2(F10.5,3X))

      close(unit=4)
      END
```